



The Impact of the Chromatin Regulators, Abo1 and HIRA, on Global Nucleosome Architecture

Csenge Gál

Thesis submitted in partial fulfilment of the requirements for the
degree of Doctor of Philosophy

Faculty of Medical Sciences
Institute for Cell and Molecular Biosciences
Newcastle University

September 2014

Declaration

I certify that this thesis is my own work, except where acknowledged, and has not been previously submitted for a degree or any other qualification at this or any other university.

Some of the work in this thesis has been included in the following publications:

Gal, C., Moore, K.M., Paszkiewicz, K., Kent, N.A. and Whitehall, S.K. (2015). 'The impact of the HIRA histone chaperone upon global nucleosome architecture.' *Cell Cycle*, 14(1), pp. 123-134

Pai, C., Deegan, R.S., Subramanian, L., Gal, C., Sarkar, S., Blaikley, E.J., Walker, C., Hulme, L., Bernhard, E., Codlin, S., Bahler, J., Allshire, R., Whitehall, S., and Humphrey, T.C. (2014). 'A histone H3K36 chromatin switch coordinates DNA double-strand break repair pathway choice.' *Nature Communications*, 5, p. 4091.

Acknowledgements

Thank you to everyone who has supported me throughout the duration of this research project. I would especially like to thank my supervisor Dr Simon Whitehall for allowing me to grow as a research scientist. Your guidance, encouragement and patience over the past four years have been invaluable. I also would like to acknowledge Dr Nick Kent, for helping with all of the bioinformatics work carried out in this thesis, and for sharing and explaining the various scripts that I have had to use. In addition, I would like to thank all the members of the Yeast and Worm labs, past and present, for their continuous support and advice. In particular, Alessandra, Debbie, Ellen, Emma, Heather, Helen, Melanie and Monika thank you for your continuous assistance in the lab and your friendship outside of it. I couldn't have asked to be surrounded by a better group of people. Finally, I would like to thank my family for their love and support, in particular my parents, for their sacrifices over the years.

This project was funded by the Medical Research Council (MRC) and the National Institute for Health Research (NIHR).

Abstract

HIRA is an evolutionarily conserved histone H3-H4 chaperone that mediates replication-independent nucleosome deposition and is important in a variety of contexts such as transcription, the response to DNA damage and cellular quiescence. Here the genome-wide contribution of HIRA to nucleosome organization in *Schizosaccharomyces pombe* was determined using a chromatin sequencing approach. Cells lacking HIRA (*hip1* Δ) experience a global reduction in nucleosome occupancy over the 3' end of genes, consistent with the proposed role for HIRA in nucleosome re-assembly in the wake of RNA polymerase II. In addition, at HIRA-regulated promoters, it commonly maintains the proper occupancy of the -1 and +1 nucleosomes. Thus HIRA likely exerts its transcriptional regulatory roles through assembly/disassembly of specific target nucleosomes.

In addition to transcription-coupled functions, HIRA has been implicated in the DNA damage response pathway. Indeed HIRA deficient cells present with increased sensitivity to DNA damaging agents and experience delays to the repair of DNA double strand breaks. Furthermore, *hip1*⁺ exhibits interactions with components of both the homologous recombination (HR) and non-homologous end joining (NHEJ) repair pathways. HIRA has also been identified as a regulator of nitrogen-starvation induced quiescence in *S. pombe*. Cells lacking HIRA are defective in both their ability to maintain and exit quiescence. Consistent with this, quiescent *hip1* Δ cells fail to properly induce MBF-dependent gene transcription in response to the restoration of a nitrogen source.

During the course of this study Abo1, a bromodomain containing AAA-ATPase, was identified as a factor whose function potentially overlaps with histone chaperones such as HIRA. Therefore the contribution of Abo1 to global chromatin architecture was also assessed. Consistent with a nucleosome assembly function, *abo1* Δ cells have widespread changes to nucleosome occupancy and positioning in both euchromatic and heterochromatic regions of the genome. Furthermore, Abo1 physically interacts with the FACT histone chaperone and the distribution of Abo1 on chromatin is perturbed by loss of FACT subunits.

Abbreviations

AAA	ATPases associated with diverse cellular activities
Ac	Acetylation
ADMA	Asymmetric dimethylarginine
ADP	Adenosine di-phosphate
ANCCA	AAA Nuclear Coregulator Cancer-Associated Protein
Ar	ADP ribosylation
AR	Androgen receptor
ATAD2	ATPase family AAA domain containing 2
ATP	Adenosine tri-phosphate
bp	Base pairs
CDKI	Cyclin dependent kinase inhibitor
CENP-A	Centromere protein A
CHD	Chromodomain
ChIP	Chromatin immunoprecipitation
Co-IP	Co-immunoprecipitation
CTD	C-terminal domain
DAPI	4',6-diamidino-2-phenylindole
DD	Dimerization domain
DDR	DNA damage response
DEPC	Diethylpyrocarbonate
dH ₂ O	Deionised water
dHJ	Double Holliday junction
DIC	Differential interference contrast
DNA	Deoxyribonucleic acid
dNTPs	Deoxynucleotides
DSB	Double strand break
DSBR	Double strand break repair
E	Glutamate residue
ESCs	Embryonic stem cells
ER	Estrogen receptor
FACS	Fluorescence activated cell sorting
FACT	Facilitates chromatin transcription

GFP	Green fluorescent protein
GO	Gene ontology
H1	Histone H1
H2A	Histone H2A
H2A.Z	Histone variant H2A.Z
H2A.X	Histone variant H2A.X
H2B	Histone H2B
H3	Histone H3
H4	Histone H4
HAT	Histone acetyltransferases
HBD	Hormone binding domain
HDAC	Histone deacetylase
HKMT	Histone lysine methyltransferase
HIR	Histone cell cycle regulator
HIRA	Histone regulatory homologue A
HJ	Holliday junction
HMGB	High mobility group box
HML	Hidden MAT left
HMR	Hidden MAT right
HR	Homologous recombination
<i>imr</i>	Innermost repeat
IP	Immunoprecipitate
Iso	Isomerization
K	Lysine residue
KAT	Lysine acetyltransferase
Kb	Kilo base
kDa	Kilo Dalton
KDM	Lysine demethylase
LTR	Long terminal repeat
MD	Middle domain
Me	Methylation
me1	Monomethylation
me2	Dimethylation
me3	Trimethylation

MBT	Malignant brain tumour
MMA	Monomethylarginine
MMS	Methyl methanosulfate
MNase	Micrococcal nuclease
mRNA	Messenger RNA
MW	Molecular weight marker
NAD	Nicotinamide adenine dinucleotide
ncRNA	Non-coding RNA
NDR	Nucleosome depleted region
nH ₂ O	Nanopure water
NHEJ	Non-homologous end-joining
NTD	N-terminal domain
OD	Optical density
ORF	Open reading frame
<i>otr</i>	Outer repeat
P	Proline residue
PCR	Polymerase chain reaction
PFGE	Pulsed field gel electrophoresis
PGCs	Primary germ cells
Ph	phosphorylation
PHD	Plant homeodomain
PI	Propidium iodide
PRC	Polycomb repressor complex
PRMT	Arginine methyltransferase
PTM	Post translational modification
qRT-PCR	Quantitative real time polymerase chain reaction
Rb	Retinoblastoma protein
rDNA	Ribosomal deoxyribonucleic acid
RNA	Ribonucleic acid
RNA Pol I	RNA polymerase I
RNA Pol II	RNA polymerase II
RNA Pol III	RNA polymerase III
RNase A	Ribonuclease A
RT	Reverse transcriptase

RT-PCR	Reverse transcription polymerase chain reaction
S	Serine residue
SAHF	Senescence associated heterochromatin foci
SDMA	Symmetric dimethylarginine
SDSA	Synthesis-dependent strand annealing
SEM	Standard error of mean
Seq	Sequencing
ssDNA	Single-stranded DNA
STDEV	Standard deviation
SUMO	Small Ubiquitin-like Modifier
Su	SUMOylation
T	Threonine residue
TBZ	Thiabendazole
Tf	Transposon of fission yeast
tRNA	Transfer ribonucleic acid
TSH2B	Testis specific H2B
TSS	Transcription start site
TTS	Transcription termination site
Ty	Transposon of yeast
Ub	ubiquitination
UTR	Untranslated region
UV	Ultraviolet
WCE	Whole cell extract
wt	Wild type
Y	Tyrosine residue
YFP	Yellow fluorescent protein
Yta	Yeast Tat-binding analog

Table of Contents

Chapter 1 Introduction

1.1 The nucleosome and chromatin compaction.....	1
1.2 Histone Modifications.....	3
1.2.1 Acetylation.....	6
1.2.2 Methylation.....	10
1.2.2.1 Lysine Methylation.....	10
1.2.2.2 Arginine Methylation.....	13
1.2.3 Phosphorylation.....	14
1.2.4 Ubiquitination.....	15
1.3 Histone variant exchange.....	18
1.3.1 H2A variants.....	18
1.3.2 H3 variants.....	20
1.3.3 Other variants.....	20
1.4 ATP-dependent remodelers.....	21
1.4.1 SWI/SNF.....	23
1.4.2 ISWI.....	24
1.4.3 INO80/SWR-C.....	25
1.4.4 CHD.....	26
1.5 Histone chaperones.....	27
1.5.1 Histone H3-H4 chaperones.....	28
1.5.1.1 Asf1.....	30
1.5.1.2 CAF-1.....	31
1.5.1.3 HIR/HIRA.....	32
1.5.1.3.1 Characterization and composition.....	32
1.5.1.3.2 Nucleosome assembly through HIR/HIRA.....	35
1.5.1.3.3 Regulation of transcription by HIR/HIRA.....	36
1.5.1.3.4 HIRA in transcriptional elongation and repression of cryptic promoters.....	38
1.5.1.3.5 Role for HIR/HIRA in heterochromatin silencing....	38

1.5.1.3.6 HIRA in development	40
1.5.1.3.7 HIRA and senescence	43
1.5.1.3.8 HIRA in disease	45
1.5.1.4 Other H3-H4 chaperones	45
1.5.2 Histone H2A-H2B chaperones	46
1.5.2.1 FACT	48
1.5.2.1.1 FACT in transcription and nucleosome disassembly	48
1.5.2.1.2 FACT in nucleosome assembly	51
1.5.2.2 Other H2A-H2B chaperones.....	52
1.6 AAA-ATPases	53
1.6.1 ATAD2/Yta7.....	53
1.6.1.1 Characterization and composition.....	54
1.6.1.2 Regulation of gene expression by ATAD2.....	55
1.6.1.3 Yta7 as a boundary element.....	59
1.6.1.4 Further associated functions of Yta7	59
1.7 Project Aims.....	60

Chapter 2 Materials and Methods

2.1 General laboratory supplies	61
2.2 Strains and media	61
2.2.1 <i>Escherichia coli</i>	61
2.2.2 <i>Schizosaccharomyces pombe</i>	61
2.2.3 Growth of <i>S. pombe</i> strains	65
2.2.4 Genetic crosses and tetrad analysis.....	65
2.2.5 Analysis of cell viability	67
2.2.6 Yeast flow cytometry	67
2.3 DNA transformation	67
2.3.1 Transformation of <i>E. coli</i>	67
2.3.2 Transformation of <i>S. pombe</i>	68
2.4 DNA isolation	68
2.4.1 Plasmid isolation from <i>E. coli</i>	68
2.4.2 Isolation of <i>S. pombe</i> genomic DNA	68
2.5 DNA manipulation and analysis	69

2.5.1 Polymerase chain reaction (PCR)	69
2.5.2 Analysis of DNA by gel electrophoresis	69
2.5.2.1 Agarose gel electrophoresis	69
2.5.2.2 Contour-clamped homogeneous electric field (CHEF) pulse field gel electrophoresis (PFGE)	69
2.5.3 Micrococcal nuclease (MNase) digestion assay	70
2.5.3.1 MNase digestion	70
2.5.3.2 MNase dephosphorylation for sequencing.....	71
2.5.3.3 MNase sequencing	71
2.5.3.4 MNase-qPCR	72
2.5.4 Chromatin immunoprecipitation (ChIP)	74
2.5.5 Non-homologous end-joining (NHEJ) assay	77
2.6 RNA extraction, manipulation and analysis	77
2.6.1 RNA extraction	77
2.6.2 RNA clean-up and concentration	78
2.6.3 Quantification of RNA samples.....	78
2.6.4 DNase treatment of RNA.....	78
2.6.5 Reverse transcription and quantitative PCR	79
2.6.6 Microarray analysis.....	81
2.7 Protein extraction, manipulation and analysis	81
2.7.1 TCA protein extraction	81
2.7.2 Whole cell extracts.....	81
2.7.3 Co-immunoprecipitation.....	82
2.7.4 Western blotting.....	82
2.8 Bioinformatics.....	84

Chapter 3 Organization of chromatin by an ATAD2 homologue in *S. pombe*

3.1 Introduction.....	87
3.2 Results.....	88
3.2.1 Generating chromatin-seq samples	88
3.2.2 Abo1 plays a role in appropriate nucleosome organization at coding regions.....	91
3.2.3 Chromatin organization at Abo1 regulated genes.....	96

3.2.4 Abo1 is involved in proper nucleosome organization at pericentromeric heterochromatic regions	99
3.2.5 A role for Abo1 in nucleosome organization over Tf2 retrotransposons and retrotransposon remnants	104
3.2.6 Abo1 physically associates with the FACT histone chaperone	106
3.2.7 Enrichment of Spt16 is increased in the absence of <i>abo1</i> ⁺ at transcriptionally silent regions	108
3.2.8 Abo1 localization is deregulated at some genes in the absence of functional FACT complex	110
3.2.9 Requirement for Abo1 in nucleosome organization extends to replication origins	114
3.3 Discussion	117
3.3.1 Abo1 functions in the same pathway(s) as the FACT complex.....	117
3.3.2 Abo1 and nucleosome positioning.....	120
3.3.3 Abo1 function extends to heterochromatin	121
3.3.4 Further possible roles to address for Abo1	122

Chapter 4 Global chromatin organization and DNA damage repair by the HIRA histone chaperone in *S. pombe*

4.1 Introduction	124
4.2 Role for the HIRA complex in global nucleosome organization.....	125
4.2.1 MNase-seq analysis shows a reduction in nucleosome occupancy in <i>hip1</i> Δ cells	125
4.2.2 HIRA is necessary for nucleosome organization over the ORFs of protein coding genes	127
4.2.3 Chromatin structure of HIRA-repressed genes.....	132
4.2.4 Influence of HIRA on the <i>hht2</i> ⁺ - <i>hhf2</i> ⁺ promoter	134
4.2.5 Loss of <i>hip1</i> ⁺ results in a drop in histone H3 protein levels	136
4.2.6 Loss of HIRA function has a minor effect on pericentromeric heterochromatin	139
4.2.7 Loss of <i>hip1</i> ⁺ leads to a reduction in nucleosome occupancy over Tf2 LTR retrotransposons	141

4.2.8 The MNase maps of regions transcribed by Pol I and Pol III are not affected by loss of <i>hip1</i> ⁺	143
4.3 Role for the HIRA complex DNA damage response.....	146
4.3.1 HIRA function is required for appropriate DNA damage response	146
4.3.2 HIRA is required for efficient repair of broken chromosomes.....	148
4.3.3 Negative genetic interactions between <i>hip1</i> Δ and components of the HR repair pathway.....	150
4.3.4 Negative genetic interactions between <i>hip1</i> Δ and components of the NHEJ repair pathway	155
4.3.5 Genetic interactions between <i>hip1</i> Δ and the checkpoint pathways	160
4.3.6 Checkpoint release is comparable between wild type and <i>hip1</i> Δ cells.	164
4.4 Discussion	166
4.4.1 Global impact of HIRA upon nucleosome architecture.....	166
4.4.1.1 HIRA exerts its function through organizing the 3' end of genes	167
4.4.1.2 Possible role for HIRA, Set2 and CHD remodelers in preventing cryptic transcription through repressing histone <i>trans</i> exchange over the 3' end of genes.....	167
4.4.1.3 Possible nucleosome re-assembly role of HIRA independent to its function in transcriptional regulation.....	171
4.4.2 HIRA is required for appropriate DNA damage repair	172

Chapter 5 Maintenance of Quiescence by the HIRA Complex in *S. pombe*

5.1 Introduction.....	175
5.1.1 Cellular quiescence vs. senescence	175
5.1.2 Roles of cellular quiescence.....	177
5.1.3 Quiescence in <i>S. pombe</i>	178
5.2 Results.....	181
5.2.1 Loss of HIRA leads to diminished viability of <i>S. pombe</i> cells following G ₀ arrest	181
5.2.2 Cells lacking <i>hip1</i> ⁺ attempt to re-enter the cell cycle following 24 hours in G ₀	185
5.2.3 Chromatin remains intact in cells lacking HIRA.....	191

5.2.4 Over 850 genes are mis-transcribed in <i>hip1Δ</i> cells during quiescence.	196
5.2.5 Restoring HIRA function during quiescence exit rescues cell viability	198
5.2.6 Increased DNA DSBs in <i>hip1Δ</i> cells during quiescence exit	200
5.2.7 Loss of <i>hip1</i> ⁺ leads to diminished activation of cell cycle regulated genes following restoration of a nitrogen source	202
5.3 Discussion	208
5.3.1 HIRA deficient cells are unlikely to age rapidly due to a simple reduction in histone levels	208
5.3.2 Role for the HIRA complex in regulating MBF genes	209
5.3.3 Attempts to isolate suppressor mutations	210
5.3.4 HIRA and senescence	213

Chapter 6 General Discussion

6.1 Abo1 – A regulator of global chromatin architecture	215
6.2 Transcription through chromatin	216
6.3 HIRA and the DNA damage response pathway	217
6.4 Restart of the cell cycle following quiescence by HIRA	218
References	220
Appendix	256

List of Figures

Figure 1.1 Basic overview of assembly of higher order chromatin in a stepwise manner.....	2
Figure 1.2 Effects of histone modifications on each other	5
Figure 1.3 Opposing actions of HATs and HDACs in <i>S. cerevisiae</i>	9
Figure 1.4 Distribution of histone methylation over transcribed regions	12
Figure 1.5 Possible outcomes of histone ubiquitination	17
Figure 1.6 Outcomes of chromatin remodelling by ATP-dependent remodelers	22
Figure 1.7 Schematic diagram of histone deposition by replication-dependent and replication-independent histone H3-H4 chaperones	29
Figure 1.8 HIR complex homologues.....	34
Figure 1.9 Repression of <i>HTA1-HTB1</i> transcription by the HIR complex.....	37
Figure 1.10 Role for HIRA during development.....	42
Figure 1.11 SAHF formation is mediated by HIRA and ASF1a	44
Figure 1.12 Mechanism of transcription through chromatin by Pol II	47
Figure 1.13 Structure and function of the FACT complex	50
Figure 1.14 Structure and function of ATAD2/Yta7	57
Figure 1.15 The role of Yta7 over the <i>HTA1-HTB1</i> locus	58
Figure 3.1 MNase-seq datasets generated in this study correlate well with previously published results.....	90
Figure 3.2 Deletion of <i>abo1</i> ⁺ leads to perturbations of nucleosome organization over coding sequences	92
Figure 3.3 Loss of <i>abo1</i> ⁺ leads to a drop in histone H3 and H2A protein levels	94
Figure 3.4 Loss of <i>abo1</i> ⁺ results in “fuzzy” nucleosomes	95
Figure 3.5 Deletion of <i>abo1</i> ⁺ preferentially results in the de-repression of normally low level transcribed genes	97
Figure 3.6 Nucleosome depletion is visible over the promoter regions of Abo1-dependent genes.....	98
Figure 3.7 Heterochromatin is also affected by loss of <i>abo1</i> ⁺	101
Figure 3.8 Perturbations to nucleosomes are visible over heterochromatic regions in <i>abo1</i> Δ cells.....	102

Figure 3.9 Abo1-GFP enrichment over pericentromeric regions is unaffected by loss of <i>swi6</i> ⁺	103
Figure 3.10 Perturbations to nucleosomes are visible over <i>Tf2</i> retrotransposons and solo LTRs in <i>abo1</i> Δ cells	105
Figure 3.11 Abo1 physically interacts with components of the FACT complex	107
Figure 3.12 Loss of <i>abo1</i> ⁺ leads to an increase in Spt16-GFP levels at the <i>tlh1</i> ⁺ loci	109
Figure 3.13 Deletion of <i>pob3</i> ⁺ alters Abo1-GFP localization over several loci	111
Figure 3.14 Inactivation of <i>spt16</i> ⁺ alters Abo1-GFP enrichment on chromatin	112
Figure 3.15 Loss of FACT function does not affect Abo1-GFP localization on heterochromatin	113
Figure 3.16 Loss of <i>abo1</i> ⁺ leads to the over accumulation of nucleosomes over the NDR of replication origins.....	115
Figure 3.17 Loss of <i>abo1</i> ⁺ leads to an increase in Spt16-GFP levels at replication origins	116
Figure 4.1 Frequency distribution of MNase-seq generated chromatin species.....	126
Figure 4.2 Loss of <i>hip1</i> ⁺ leads to a drop in mononucleosome occupancy over coding regions, particularly towards the 3' end of genes	128
Figure 4.3 Loss of <i>hip1</i> ⁺ results in perturbations of mononucleosomes over the <i>hrp1</i> ⁺ locus	129
Figure 4.4 Loss of <i>hip1</i> ⁺ results in perturbations of mononucleosomes over the <i>dbp7</i> ⁺ locus	131
Figure 4.5 Nucleosomal arrays over HIRA-dependent genes are less distinctly organized	133
Figure 4.6 Nucleosomes are depleted over the promoter region of the <i>hht2</i> ⁺ - <i>hhf2</i> ⁺ histone gene pair	135
Figure 4.7 Histone H3 protein levels, but not H2A are significantly decreased in <i>hip1</i> Δ cells	137
Figure 4.8 Loss of both <i>hip1</i> ⁺ and <i>hrp3</i> ⁺ results in synthetic growth defects and severely abnormal cell morphology	138
Figure 4.9 Minor changes to chromatin are seen around heterochromatic regions in <i>hip1</i> Δ cells.....	140
Figure 4.10 Perturbations to nucleosomes are visible over <i>Tf2</i> retrotransposons and solo LTRs in <i>hip1</i> Δ cells.....	142

Figure 4.11 No changes to mononucleosomes over the tRNA genes in <i>hip1Δ</i> cells.	144
Figure 4.12 No changes to mononucleosomes over the rDNA genes and replication origins in <i>hip1Δ</i> cells	145
Figure 4.13 Conditional <i>hip1-HBD</i> strain demonstrates that HIRA is required for recovery following DNA damage.....	147
Figure 4.14 <i>hip1Δ</i> cells are severely delayed in repairing their chromosomes following DNA damage	149
Figure 4.15 Schematic diagram of homologous recombination mediated repair	152
Figure 4.16 Genetic analysis of <i>hip1Δ</i> cells with components of the homologous recombination repair pathway	154
Figure 4.17 Schematic representation of the non-homologous end-joining pathway in <i>S. pombe</i> cells.....	157
Figure 4.18 <i>hip1Δ</i> cells are severely delayed in repairing their chromosomes using NHEJ following DNA damage	158
Figure 4.19 Genetic analysis of <i>hip1Δ</i> cells with components of the non-homologous end-joining pathway.....	159
Figure 4.20 Genetic analysis of <i>hip1Δ</i> cells with components of the DNA damage checkpoint pathway	161
Figure 4.21 Checkpoints are triggered at comparable times in <i>hip1Δ</i> and wild type cells	163
Figure 4.22 Cell cycle arrest is of comparable length between <i>hip1Δ</i> and wild type cells	165
Figure 4.23 HIRA functions towards the 3' end of genes	170
Figure 4.24 Role of histone chaperones in histone dynamics in response to DNA damage.....	174
Figure 5.1 Schematic of proliferating vs. quiescent vs. senescent cells	176
Figure 5.2 Schematic of the vegetative cell cycle and G ₀ arrest upon nitrogen removal in <i>S. pombe</i>	179
Figure 5.3 Cells lacking HIRA lose viability following nitrogen starvation induced quiescence	182
Figure 5.4 Cells lacking HIRA remain slightly elongated following nitrogen starvation induced quiescence	183
Figure 5.5 Autophagy is induced appropriately in <i>hip1Δ</i> cells upon nitrogen removal from the media	184

Figure 5.6 The majority of <i>hip1Δ</i> cells attempt to re-enter the cell cycle after 24 hours in G ₀	186
Figure 5.7 Phloxine B staining of <i>hip1Δ</i> cells indicates that the majority of these cells are viable even following 9 days in quiescence	188
Figure 5.8 Cells lacking HIRA increase in cell length in response to restoration of nitrogen	190
Figure 5.9 MNase digestions of wild type and <i>hip1Δ</i> cells following 24 and 96 hours in quiescence.....	192
Figure 5.10 Histone gene transcription is upregulated, while histone H3 protein levels are reduced in <i>hip1Δ</i> cells compared to the wild type	194
Figure 5.11 Deletion of histone gene pairs does not phenocopy the HIRA quiescence phenotype.....	195
Figure 5.12 Restoring HIRA function during quiescence exit rescues cell viability	199
Figure 5.13 Cells lacking HIRA enter and exit quiescence with elevated levels of DSBs	201
Figure 5.14 Transcriptional induction of growth genes is appropriate in <i>hip1Δ</i> cells following exit from G ₀	203
Figure 5.15 Transcriptional induction of <i>cdc18⁺</i> and <i>cdt1⁺</i> is compromised in <i>hip1Δ</i> cells following exit from G ₀	204
Figure 5.16 Rum1 protein levels are degraded both in wild type and <i>hip1Δ</i> cells at comparable rates	206
Figure 5.17 Cig2 protein levels are induced to a lesser extent in <i>hip1Δ</i> cells than in the wild type	207
Figure 5.18 Deletion of <i>abo1⁺</i> partially rescues the viability of <i>hip1Δ</i> cells in quiescence	212

List of Tables

Table 1.1 Histone post-translational modifications (PTMs)	4
Table 1.2 Histone acetyltransferases (HATs)	8
Table 1.3 Histone methyltransferases (HKMTs)	12
Table 1.4 Lysine demethylases (KDMs)	13
Table 1.5 The human complement of H2A variants	19
Table 1.6 Histones and their respective histone chaperones	27
Table 1.7 HIRA complex subunits and function through evolution	33
Table 2.1 <i>S. pombe</i> strains.....	62
Table 2.2 PCR oligonucleotide primers for genotyping	66
Table 2.3 MNase-qPCR oligonucleotide primers	73
Table 2.4 ChIP-qPCR oligonucleotide primers	76
Table 2.5 Plasmids used in the NHEJ assay	77
Table 2.6 qRT-PCR oligonucleotide primers.....	80
Table 2.7 Antibodies	83
Table 2.8 Perl scripts.....	85
Table 4.1 Components of homologous recombination (HR) repair pathway.....	151
Table 5.1 GO terms of genes that are at least 2 fold down-regulated in the absence of <i>hip1</i> ⁺ relative to the wild type following 24 hours in quiescence	197

Chapter 1

Introduction

1.1 The nucleosome and chromatin compaction

Eukaryotic genomes are hierarchically packaged into a higher nucleoprotein complex termed chromatin. Chromatin is made up of nucleosomes, which are composed of ~146 base pairs (bp) of DNA wrapped around octamers of core histone variants; two copies of each of H2A, H2B, H3 and H4 (Kornberg, 1974; Luger *et al.*, 1997). Related histone variants also get incorporated into the nucleosome throughout the life of a cell and impact upon chromatin function (Felsenfeld and Groudine, 2003). The central 80 bp of the nucleosomal DNA are associated with histone (H3-H4)₂ heterotetramers, whereas about 40 bp of DNA in the periphery are loosely bound by two histone H2A-H2B dimers. The penultimate 10 bp are also assembled by the N-terminal tail of histone H3 (Ransom *et al.*, 2010). H1 linker histones are further incorporated into chromatin of higher eukaryotes, including humans. H1 linker histones help stabilize the chromatin structure and aid higher order compaction (Thoma *et al.*, 1979). Histone assembly and consequently disassembly is carried out in a stepwise manner, whereby histone (H3-H4)₂ heterotetramers are deposited first, followed by histone H2A-H2B dimers, and vice versa in disassembly (Fig 1.1) (Ransom *et al.*, 2010). This structure is likely to have evolved in order to overcome the problems created by a continuous increase in genome size. While this higher order compaction protects cells against genomic instability, it also restricts the access of DNA binding factors to their respective target sites. Since all cellular processes, including replication, transcription, and repair, take place within this context and require a range of proteins to interact directly with DNA, chromatin must be dynamic. It is essential that alternate chromatin states can be facilitated within any given cell for a range of cellular processes to take place simultaneously.

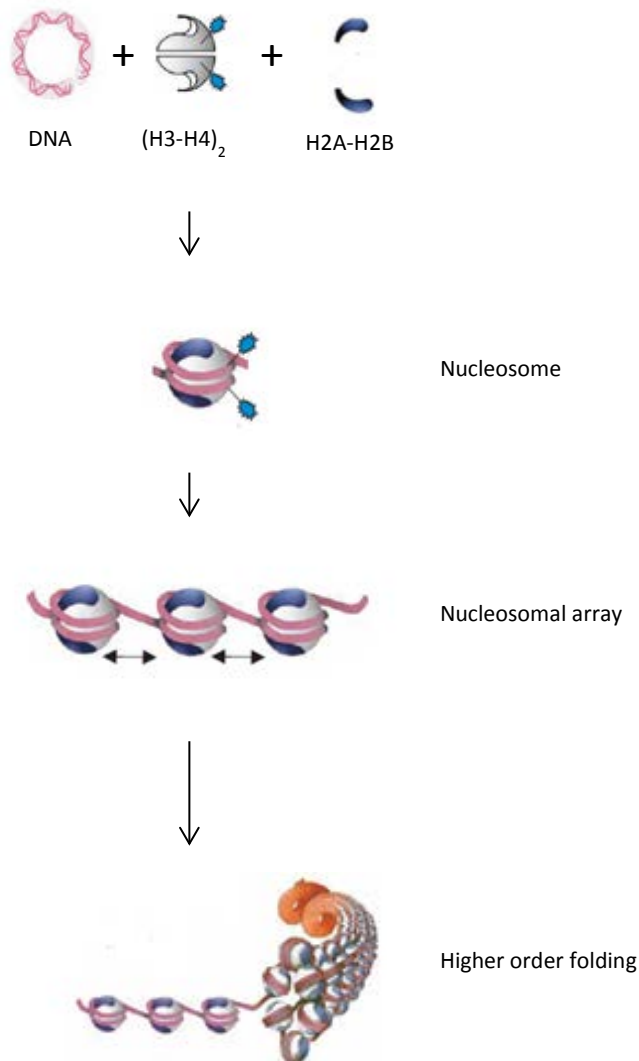


Figure 1.1 Basic overview of assembly of higher order chromatin in a stepwise manner.

Histone $(\text{H3-H4})_2$ tetramers are initially deposited onto DNA, followed by the rapid deposition of two H2A-H2B dimers, which form the nucleosome. Once several nucleosomes are assembled they are spaced to create phased nucleosomal arrays. Linker histones get incorporated and further folding takes place to generate higher order structures. Adapted from (Ridgway and Almouzni, 2000).

1.2 Histone modifications

Cells apply several mechanisms that help achieve the required alterations to chromatin. Some of the best studied of these are histone modifications. A wide range of histone modifications have now been identified and are the focus of numerous on-going studies. Histone proteins are mostly globular in structure but contain tails that protrude out (Kouzarides, 2007; Bannister and Kouzarides, 2011). These N-terminal tails are the targets for the majority of histone modifications (Bannister and Kouzarides, 2011). Table 1.1 illustrates the range of post-translational modifications (PTMs), along with their associated functions. PTMs can lead to dynamic chromatin changes due to their ability to directly perturb the electrostatic interactions between histones and DNA; in addition they can also provide a platform for docking proteins (Bannister and Kouzarides, 2011). These proteins coined ‘readers’ contain specific domains that allow recognition of the histone marks. For example, proteins containing bromodomains are able to recognize and bind histone acetylation marks, whereas those with chromo, tudor, PHD or MBT domains are able to recognize methylation marks (Bannister and Kouzarides, 2011). These proteins are often found in large complexes, containing several subunits with combinations of different domains that allow the simultaneous recognition of multiple histone marks. Furthermore, the binding of these proteins allows recruitment of additional factors, eliciting the desired changes to chromatin structure. For instance, triggering the relaxation of chromatin around transcriptionally active sites or allowing DNA ends to become accessible to repair proteins during DNA DSB repair.

In order to achieve such a tremendous variability in functional outcome, PTMs act in combination with each other, either synergistically or antagonistically, to recruit or destabilize varying protein complexes depending on the context. As many different types of modifications occur on lysines, some become mutually exclusive, resulting in antagonism. For example, H3K36 acetylation and methylation cannot occur concurrently as they require the same lysine residue. It has also been demonstrated that one modification can be dependent on another, for example methylation of H3K4 and H3K79 are entirely reliant on the preceding ubiquitination of H2BK123 (Lee *et al.*, 2007). This also demonstrates that modifications on different histone tails are too able to communicate. Furthermore, the binding of proteins can be disrupted by an adjacent modification, such as the case when H3S10 phosphorylation takes place, leading to the reduced binding of HP1 to methylated H3K9 (Fischle *et al.*, 2005). Interestingly, the

modified amino acids do not have to be adjacent to each other, for instance in *S. pombe*, acetylation of H3K4 prevents the binding of Chp1 to H3K9me2 and H3K9me3 (Xhemalce and Kouzarides, 2010). It is also possible that the catalytic activity of an enzyme becomes compromised by a modification of its substrate site, such as isomerisation of H3P38 which leads to the inability of Set2 to methylate H3K36 (Nelson *et al.*, 2006). In addition, some enzymes are better able to recognize their substrates in the presence of a second modification, such as in the case of GCN5 acetyltransferase, which is better able to identify and bind histone H3 when H3S10 is phosphorylated (Clements *et al.*, 2003). As a result of this cross-talk between modifications, the chromatin landscape is highly dynamic and regulated at multiple layers, making it incredibly complex and sophisticated, ultimately allowing a multitude of cellular processes to take place. Some of these examples are illustrated in Figure 1.2.

Table 1.1 Histone post-translational modifications (PTMs)

Histone Modifications	Residues Modified	Regulatory Functions
Acetylation	K-ac	Transcription, Repair, Replication, Condensation
Methylation (lysines)	K-me1 K-me2 K-me3	Transcription, Repair
Methylation (arginines)	R-me1 R-me2a R-me2s	Transcription
Phosphorylation	S-ph T-ph	Transcription, Repair, Condensation
Ubiquitylation	K-ub	Transcription, Repair
Sumoylation	K-su	Transcription
ADP ribosylation	E-ar	Transcription
Proline Isomerization	P-cis > P-trans	Transcription

Adapted from (Kouzarides, 2007).

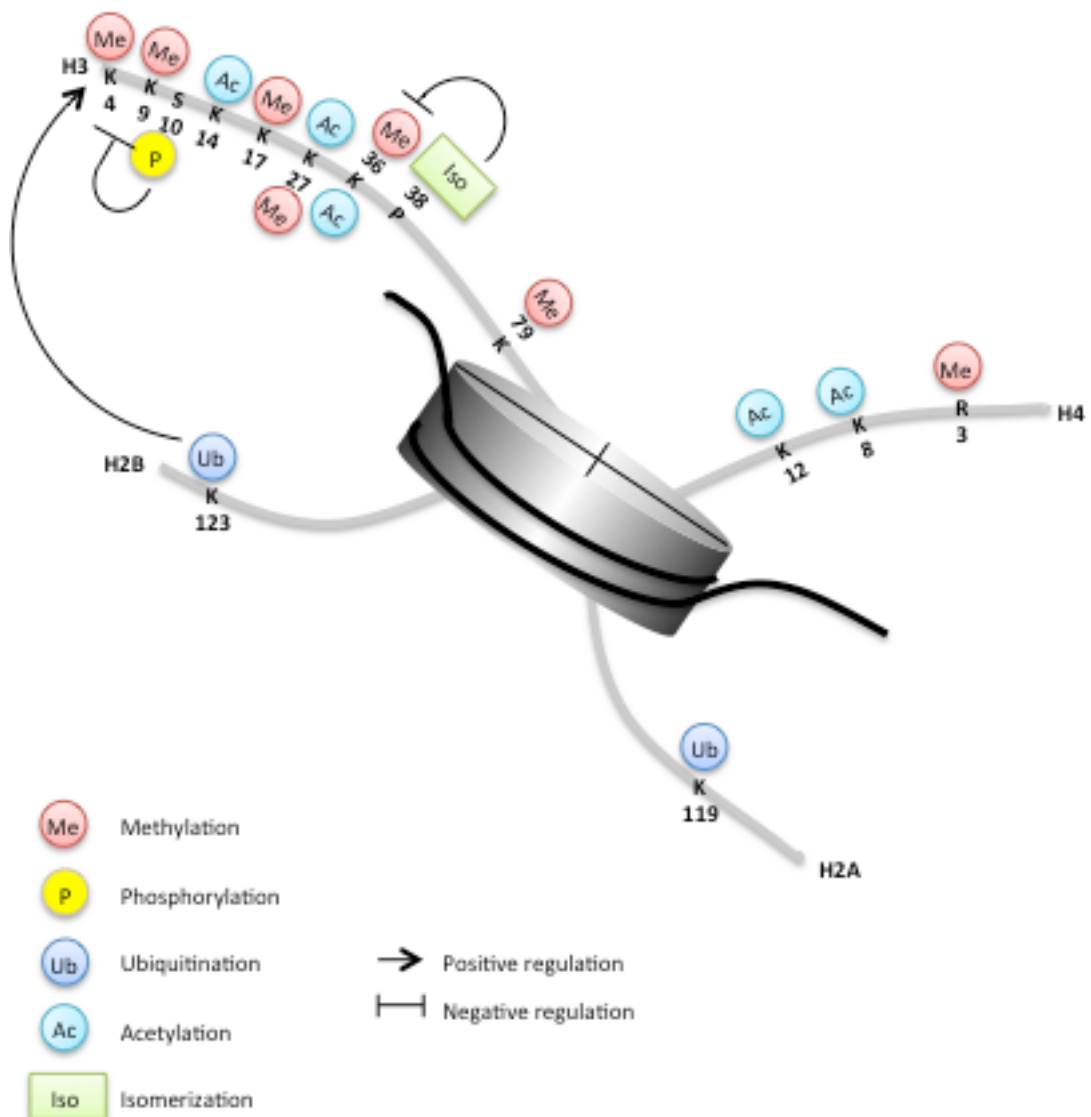


Figure 1.2 Effects of histone modifications on each other.

Histone PTMs co-operate to elicit the desired response. For example, ubiquitination of H2BK123 is essential for the methylation of H3K4, phosphorylation of H3S10 prevents binding of HP1 on H3K9 and proline isomerization of H3P38 prevents methylation of H3K36. In addition, several modifications take place on the same lysine, for instance H3K27 and H3K36 can both be methylated and acetylated leading to antagonism between the marks. Adapted from (Kouzarides, 2007; Bannister and Kouzarides, 2011).

1.2.1 Acetylation

Histone acetylation is perhaps the best studied covalent histone modification, with several decades' worth of extensive research on the subject. The acetylation of lysines leads to the neutralization of the lysine's positive charge, thus weakening the interaction between the histone tail and neighbouring molecules, such as adjacent linker DNA (Hong *et al.*, 1993) or acidic patches on histones in nucleosomes (Luger *et al.*, 1997). For example, acetylation of H4K16 alone is enough to disrupt the 30 nm fibre, leading to large structural changes (Shogren-Knaak *et al.*, 2006). In addition, acetylation of lysines serves as a docking site for bromodomain containing proteins (readers) which can recruit further remodelers to actively alter the structure of the local chromatin environment (Dhalluin *et al.*, 1999). Importantly, acetylation of lysines is highly dynamic and easily reversible, with acetyl groups having half-lives of only a couple of minutes (Waterborg, 2001). As a direct consequence of this, acetylation is highly associated with complex signal integration, primarily leading to transcriptional activation (Bannister and Kouzarides, 2011). For instance acetylation of H4K16, H3K9 and H3K14 are all important for appropriate transcription to take place, while their deacetylation is required for transcriptional repression (Owen *et al.*, 2000; Zentner and Henikoff, 2013). Additionally, acetylation has been shown to play a role in DNA replication and DNA damage repair (Zentner and Henikoff, 2013). Indeed, simultaneous acetylation of several lysines on histone H4 (K5ac8ac12ac16ac) by Gln is needed for the activation of the G₂/M checkpoint and for appropriate DNA DSB repair (Megee *et al.*, 1995).

The acetylation of lysines is catalyzed by a group of proteins termed histone acetyltransferases (HATs) or lysine acetyltransferases (KATs), the two terms are used interchangeably, which work by transferring the acetyl group from Acetyl coenzyme A (acetyl-CoA) to a lysine residue on histones. HATs are commonly categorized into two classes: type-A and type-B HATs. Type-A HATs are a diverse group of proteins that can be further classified into three categories based on amino acid sequence homology and structural similarities; these are GNAT, MYST and CNP/p300 (Hodawadekar and Marmorstein, 2007). These enzymes are generally involved in transcriptional activation and can modify numerous lysines on all N-terminal histone tails within the chromatin; although GCN5, p300 and Rtt109 (in yeast) can also acetylate the globular core, such as H3K56 (Masumoto *et al.*, 2005; Tsubota *et al.*, 2007; Das *et al.*, 2009; Tjeertes *et al.*,

2009). Acetylation of H3K56 in yeast is vital for replication-coupled nucleosome assembly and is required in response to DNA damage (Masumoto *et al.*, 2005). Type-A HATs are also often found as part of large multi-protein complexes, containing several other histone modifiers. This provides a further mechanism for regulating their activity. For instance, Gcn5 by itself is able to acetylate free histones but not those incorporated into nucleosomes, while as part of the SAGA complex it can acetylate nucleosomal histones too (Grant *et al.*, 1997). The type-B HATs on the other hand are a small group and highly conserved, with sequence similarity to *S. cerevisiae* HAT1, and are primarily involved in acetylating free histones (in particular H4K5, H4K12), prior to their incorporation into the chromatin (Parthun, 2007). Overall HATs constitute a large and well conserved family; a summary of HATs along with their respective histone modifications and functional outcomes is listed in Table 1.2.

Conversely to HATs, histone deacetylases (HDACs) remove the acetylation marks from lysines and are commonly associated with transcriptional silencing. A brief diagram of some of the well-known antagonisms between these two classes of enzymes is depicted in Figure 1.3. HDACs are currently grouped into four distinct categories, class I and II are considered “classical”, these proteins require Zn^{+} for activity, class III contains NAD^{+} dependent proteins (Sirtuins), and class IV is of “atypical” HDACs based on their underlying DNA sequence (Yang and Seto, 2007). The Sirtuin family, comprising of SIRT1-7 is of interest given as overexpression of Sirtuins is associated with lifespan extension in model organisms, as well as tumour development (Saunders and Verdin, 2007). Unlike HATs, most HDACs do not have high specificity for an individual histone mark, nor even for a single type of histone protein. Some exceptions to this are the *S. pombe* Sir2, and Clr3, which specifically remove acetyl groups from histone H4K16, H3K9, H3K14 and H3K4, and H3K14 (Shankaranarayana *et al.*, 2003; Kato *et al.*, 2013; Bjerling *et al.*, 2002; Wiren *et al.*, 2005). Finally, while HATs and HDACs are best known for acetylating and deacetylating histones, they also have a number of non-histone targets, such as p53, c-MYC, Rb1, NF-kB, just to name a few (Wagner *et al.*; Glozak *et al.*, 2005). HDACs are often misregulated during tumorigenesis; therefore a number of HDAC inhibitors are currently being investigated as therapeutic targets (West and Johnstone, 2014).

Table 1.2 Histone acetyltransferases (HATs)

HATs			Substrate Specificity	Functional Outcome
<i>S. cerevisiae</i>	<i>S. pombe</i>	Human		
Hat1	Hat1	HAT1	H4K5ac12ac	Histone deposition DNA repair
			H3K9ac14ac18ac23ac36ac H2B	Transcription activation DNA repair
Gcn5	Gcn5	hGCN5	H3K9ac14ac18ac H2B	Transcription activation
			H3K9ac14ac18ac H2B	Transcription activation
		PCAF	H4K5ac8ac H3K14ac18ac	Transcription activation, DNA repair
		CBP	H2AK5ac H2BK12ac15ac	Transcription activation
		p300	H2AK5ac H2BK12ac15ac	Transcription activation
Taf1	Taf1	TAF1	H3 and H4	Transcription activation
Esa1	Mst1	TIP60 (KAT5)	H4K5acK8ac12ac16ac H2AK4ac7ac	Transcription activation DNA repair
Sas3	Mst2*		H3K14ac23ac	Transcription activation and elongation DNA replication
		MYST3	H3K14ac	Transcription activation
		MYST4	H3K14ac	Transcription activation
	Mst2*	MYST2	H4K5ac8ac12ac	Transcription DNA replication Chromatin boundaries
Sas2	Mst2*	MYST1	H4K16ac	DNA repair Dosage compensation
Elp3	Elp3	ELP3	H3	
Hap2			H3K14ac	
Rtt109	Rtt109		H3K56ac	Transcription elongation Genome stability
		TFIIIC90	H3K9ac14ac18ac	Pol III transcription
		SRC1	H3 and H4	Transcription activation
		ACTR	H3 and H4	Transcription activation
		P160	H3 and H4	Transcription activation
		CLOCK	H3 and H4	Transcription activation

* Mst2 is homologous to MYST1-4 proteins found in humans.

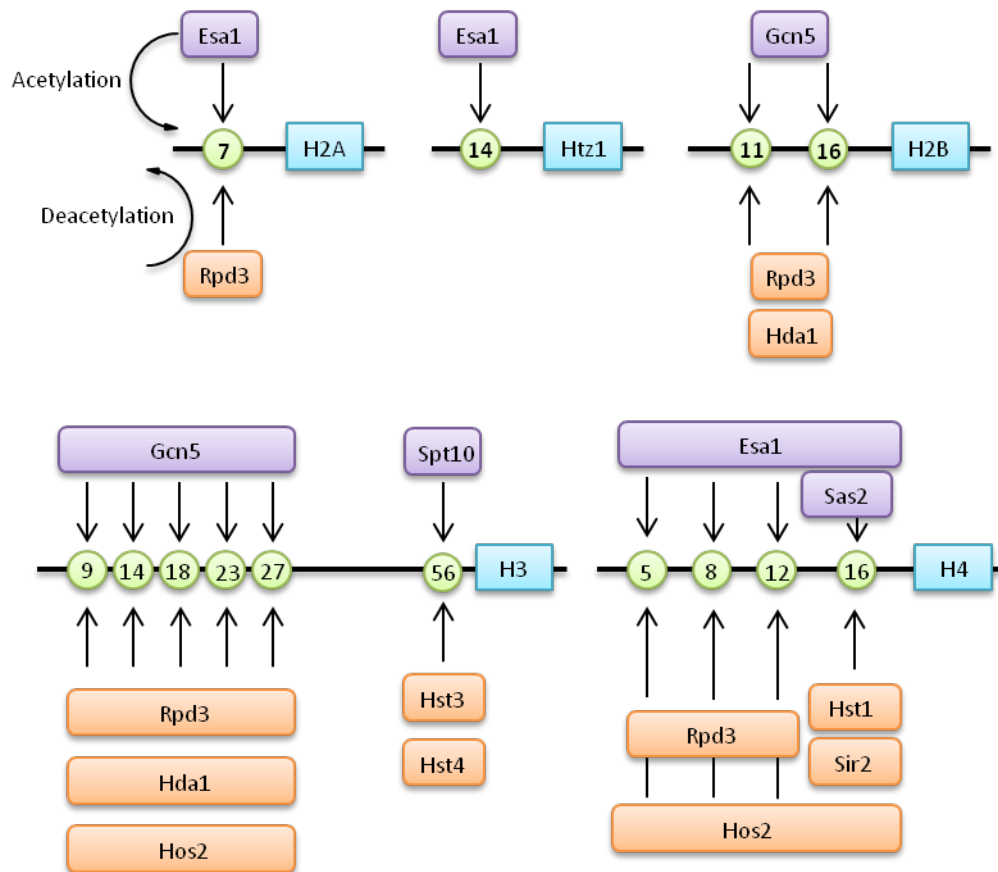


Figure 1.3 Opposing actions of HATs and HDACs in *S. cerevisiae*.

Diagram indicating some of the opposing actions of HATs (purple) and HDACs (orange) in *S. cerevisiae* where a wide range of substrates and modifying enzymes have been characterized. Adapted from (Millar and Grunstein, 2006).

1.2.2 Methylation

1.2.2.1 Lysine methylation

Unlike acetylation, which in addition to recruiting reader proteins can also directly affect chromatin structure through altering the charge of histones, methylation does not change the charges of the residues. Therefore, methyl marks are thought to act primarily as recruitment sites for reader proteins, which can facilitate transcriptional activation or repression (Bannister and Kouzarides, 2011; Black *et al.*, 2012). Lysine methylation is largely stable and is therefore involved in a wide range of maintenance roles, such as heterochromatic silencing and the maintenance of cell identity (Smith and Shilatifard, 2010). The methyl marks are placed upon histones by histone lysine methyltransferases (HKMTs), of which a large number have been identified (Table 1.3). The overwhelming majority of HKMTs contain a SET domain and methylate the N-terminal tail of histones by catalyzing the transfer of a methyl group from S-adenosylmethionine to a lysine residue (Bannister and Kouzarides, 2011). The single HKMT that is able to methylate the core globular domain of histones is Dot1 and this protein is without the conserved SET domain (Dlakic, 2001; Bannister and Kouzarides, 2011). Overall, HKMTs are highly specific enzymes, not only are they involved in the methylation of a specific residue but they are also able to mono-, di- or trimethylate the lysine to a varying degree, a phenomenon termed product specificity (Del Rizzo and Trievel, 2014). For example, the HKMTs DIM-5 in *Neurospora crassa* and the human G9a are able to mono-, di- and trimethylate H3K9, but an exchange of a single phenylalanine to a tyrosine residue changes their specificity to generate only H3K9me1 (Collins *et al.*, 2005). The converse can also be achieved; SET7/9 contains a tyrosine residue in the corresponding position where DIM-5 contains a phenylalanine, and upon replacement of the tyrosine with phenylalanine, SET7/9 is also able to di- and trimethylate H3K4 (Zhang *et al.*, 2003).

Lysine methylation is involved in regulating diverse cellular functions. Some marks are specifically associated with heterochromatic regions, like H3K27me and H3K9me. H3K27me3 is classically involved in the establishment and maintenance of facultative heterochromatin over the inactivated X chromosome (Trojer and Reinberg, 2007), through its role in recruitment of the Polycomb repressive complex 2 (PRC2), which contains the HKMT EZH2. EZH2 is able to maintain the repressive H3K27me3 mark leading to the epigenetic inheritance of repressive chromatin (Hansen *et al.*, 2008).

H3K9me on the other hand is associated with constitutive heterochromatin, such as the centromeric and telomeric regions. Methylation of H3K9me2 and H3K9me3 is primarily carried out by SUV39, and they are required for the recruitment of the heterochromatin protein HP1. HP1 specifically binds these methyl marks, coats the surrounding regions and establishes a transcriptionally silenced microenvironment (Bannister and Kouzarides, 2011). In addition to the above mentioned heterochromatin marks, methylation of H3K4, H3K36, and H3K79 are all associated with euchromatin and active transcription. H3K4 is primarily observed over promoter regions and at the TSSs of actively transcribed genes, overlapping with Pol II localization (Barski *et al.*, 2007; Shilatifard, 2012). H3K4me3 in particular is found to be enriched over the promoter regions, while H3K4me2 and H3K4me1 are enriched over the ORF, in addition to H3K36me (Fig 1.4) (Millar and Grunstein, 2006; Barski *et al.*, 2007; Soares *et al.*, 2014). Methylation of H3K4 is carried out by Set1 in yeast, while there are a number of human homologues that split this role between them. In *Drosophila* H3K4me2 and me3 methylation is primarily dependent on the Set1 protein (Wu *et al.*, 2008; Ardehali *et al.*, 2011; Hallson *et al.*, 2012), but MLL1/MLL2 have also been shown to be required for this methylation mark at *Hox* gene promoters (Wang *et al.*, 2009). In addition to marking promoter regions, H3K4me1 has been associated with functional enhancers in various cell types (Heintzman *et al.*, 2007), although its role over these regions is currently not understood. Methylation of H3K4 over enhancers is carried out by the monomethyltransferases MLL3 and MLL4 (*Drosophila Trr*) (Herz *et al.*, 2012). Thus methylation is not only required for appropriate transcriptional silencing, but can also play an activating role. Until relatively recently methylation was thought to be an irreversible event; however in 2004 the first lysine demethylase, LSD1, was identified (Shi *et al.*, 2004). LSD1 functions in conjunction with different complexes, to mediate the removal of mono- and dimethyl marks from either H3K4 or from H3K9. This allows LSD1 to switch between acting as a co-repressor to a co-activator, respectively (Klose and Zhang, 2007). Another group of proteins have been identified as able to demethylate histones, these all contain a Jumonji-C domain and have been named JHDMs (Klose and Zhang, 2007). The first of these to be characterized was JHDM1A, which specifically removes methyl marks from H3K36me2- and H3K36me1-modification states (Tsukada *et al.*, 2006). Finally, the JARID1 family of demethylases is responsible for removing methylation marks specifically from H3K4 (Liang *et al.*, 2007; Secombe *et al.*, 2007). Several JHDM and JARID1 family of demethylases exist, a list of which can be found in Table 1.4.

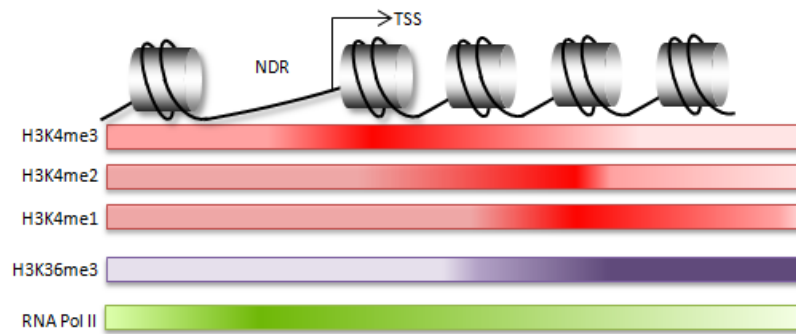


Figure 1.4 Distribution of histone methylation over transcribed regions.

Illustration of the prevalence of conserved methylation marks over transcribed regions. H3K4me3 is primarily observed over the promoter and the +1 nucleosome of the ORF, H3K4me2 is principally over the +2 nucleosome and downstream, while H3K4me1 is towards the 3' end of genes, as is H3K36me3. Adapted from (Millar and Grunstein, 2006).

Table 1.3 Histone methyltransferases (HKMTs)

HMTs			Substrate Specificity	Functional Outcome
<i>S. cerevisiae</i>	<i>S. pombe</i>	Human		
		SUV39H1	H3K9	Heterochromatin formation/silencing
	Clr4	SUV39H2	H3K9	Heterochromatin formation/silencing
		G9a	H3K9	Heterochromatin formation/silencing
		EuHMTase	H3K9	Heterochromatin formation/silencing
		ESET/SETDB1	H3K9	Transcription repression
		CLL8	H3K9	?
		MLL1	H3K4	Transcription activation
		MLL2	H3K4	Transcription activation
		MLL3	H3K4	Transcription activation
		MLL4	H3K4	Transcription activation
		MLL5	H3K4	Transcription activation
Set1	Set1	hSet1A	H3K4	Transcription activation
		hSet1B	H3K4	Transcription activation
		ASH1	H3K4	Transcription activation
Set2	Set2	SET2	H3K36	Transcription activation, DNA damage repair
		NSD1	H3K36	?
		SYMD2	H3K36	Transcription activation
Dot1		DOT1L	H3K79	Transcription activation
		Pr-SET7/8	H4K20	Transcription repression
	Set9	SUV4-20H1	H4K20	DNA damage response
		SUV4-20H2		
		EZH2	H3K27	Polycomb silencing
		SET7/9	H3K4	?
		RIZ1	H3K9	Transcription repression

Table 1.4 Lysine demethylases (KDMs)

KDMs			Substrate Specificity	Functional Outcome
<i>S. cerevisiae</i>	<i>S. pombe</i>	Human		
Jhd1			H3K36me1me2	Transcription elongation
Rph1			H3K9	Transcription elongation
			H3K36me2me3	
Jhd2	Jmj2		H3K4me2me3	
	SpLsd1/ Swm1/ Saf110	LSD1/BHC110	H3K4me1me2	Transcription activation and repression
			H3K9me1me2	Heterochromatin formation
		JHDM1a/FBXL 11	H3K36me1me2	
		JHDM1b/FBXL 10	H3K36me1me2	
		JHDM2a	H3K9me1me2	AR gene activation spermatogenesis
		JHDM2b	H3K9me	
		JMJD2A/ JHDM3A	H3K9me H3K36me2me3	Transcription repression
		JMJD2B	H3K9me H3K36me2me3	Heterochromatin formation
		JMJD2C	H3K9me H3K36me2me3	
		JMJD2D	H3K9me2me3	
		JARID1A	H3K4me2me3	Rb interacting protein
		JARID1B	H3K4me1me2me3	Transcription repression
		JARID1C	H3K4me2me3	
		JARID1D	H3K4me2me3	Male-specific antigen
		UTX	H3K27me2me3	Transcription activation
		JMJD3	H3K27me2me3	Transcription activation

1.2.2.2 Arginine Methylation

In addition to lysines, arginines can also be methylated, although to date these modifications have been less well characterized. There are three classes of protein arginine methyltransferases (PRMTs), type-I, type-II and type-III. Type-I are responsible for monomethylarginine (MMA) and asymmetric dimethylarginine (ADMA), type-II PRMTs catalyze the formation of MMA and symmetric dimethylarginine (SDMA), while type-III can only generate MMA (Wolf, 2009). In humans, there are 8 PRMTs, PRMT1, PRMT2, PRMT3, PRMT4/CARM1, PRMT6, and PRMT8 are type-I, PRMT5 is the only type-II and PRMT7 is the sole type-III enzyme

(Gayatri and Bedford, 2014). There are numerous histone arginine methylation sites; however the majority of them remain uncharacterized. One example of arginine methylation is that of H3R2me2a by PRMT6, which prevents the methylation of H3K4me3 (Hyllus *et al.*, 2007). Therefore it is likely that arginine methylation also forms a part in regulation of chromatin through histone (modification) cross-talk.

1.2.3 Phosphorylation

Histone phosphorylation takes place on serine (S), threonine (T) and tyrosine (Y) residues and is generally a transient modification that occurs in response to extracellular signals such as DNA damage (Zentner and Henikoff, 2013). Although initially characterized during the 1960s, the readers responsible for recognizing histone phosphorylation have only recently been identified. Members of the 14-3-3 family were demonstrated to specifically interact with the histone H3S10 phosphorylation mark, leading to transcriptional activation (MacDonald *et al.*, 2005). As phosphorylation is a transient mark and often occurs next to a methylated residue, it has been proposed that phosphorylation acts by affecting the stability of the readers and methyl marks adjacent to it. Indeed, there is some evidence that these “phospho-methyl” switches exist, as the mitotic release of HP1 from pericentromeric heterochromatin is the consequence of a H3S10 phosphorylation by the Aurora B kinase (Fischle *et al.*, 2005; Hirota *et al.*, 2005). Importantly this allows the dissociation of HP1 without a reduction in H3K9me, leading to the rapid establishment of heterochromatin within the daughter cells. Thus the “phospho-methyl” switch might contribute to the accurate propagation of epigenetic information.

Possibly the best-characterized phosphorylation event is that of serine 139 on H2A.X upon DNA damage induction leading to the formation of γ H2A.X (Rogakou *et al.*, 1998). γ H2A.X is formed upon DNA DSBs and is able to spread for kilo bases from the break site (Scully and Xie, 2013). It is thought to generate a highly specific chromatin environment that is able to recruit DNA DSB repair proteins (Stucki and Jackson, 2006; Scully and Xie, 2013), such as MDC1 which is a scaffolding protein and is required for the appropriate binding of the MRN complex (Chapman and Jackson, 2008). MRN is important for the initial response to DNA DSBs; it is implicated in the recruitment of the ATM checkpoint kinase (Lee and Paull, 2004), and its subunit, Mre11, is involved in

DNA end resection prior to repair (Stracker and Petrini, 2011). In addition, proteins involved in homologous recombination (HR) mediated repair and non-homologous end-joining (NHEJ) are also recruited by this phosphorylation event, such as Rad50, Rad51, BRCA1 (Paull *et al.*, 2000) and 53BP1 (Wang *et al.*, 2002).

1.2.4 Ubiquitination

Ubiquitination of histones was first identified some 30 years ago, however until recently not much has been known about its function. Broadly speaking ubiquitination of histones can lead to structural alterations, such as the eviction of a nucleosome, it can also act as a signalling molecule for recruitment of further proteins, and it can function to serve as a mark for degradation (Fig. 1.5) (Braun and Madhani, 2012). Perhaps the best studied ubiquitination event is the monoubiquitination of histone H2B on lysine 120 in metazoans (lysine 123 in *S. cerevisiae*). This ubiquitination event is dependent on RAD6 and RNF20/RNF40 (Bre1 in yeast) (Jentsch *et al.*, 1987; Robzyk *et al.*, 2000; Hwang *et al.*, 2003; Lee *et al.*, 2007) and is overwhelmingly associated with actively transcribed regions (Minsky *et al.*, 2008). H2Bub1 is also involved in facilitating both transcription initiation and elongation, possibly through mediating H2A-H2B dimer removal in front of Pol II (Belotserkovskaya *et al.*, 2003; Batta *et al.*, 2011). Recent work has demonstrated that *in vitro* ubiquitination of H2B favours disruption to chromatin (Fierz *et al.*, 2011), agreeing with a possible role for H2Bub1 in breaking nucleosomes in front of Pol II. H2Bub1 is also involved in mediating other histone modifications, such as H3K4 and H3K79 methylation by the HMTs COMPASS and Dot1 respectively (Briggs *et al.*, 2002; Sun and Allis, 2002). Importantly, this interaction is unidirectional, that is, methylation of either of these histone residues has no effect on the ubiquitination of H2B (Briggs *et al.*, 2002; Sun and Allis, 2002). Although, generally associated with transcription, like many other histone modifications, H2Bub1 can also facilitate gene repression. It has been demonstrated both in human cell lines and in yeast that H2Bub1 is required for the repression of lowly expressed, inducible genes (Batta *et al.*, 2011; Shema *et al.*, 2011). Moreover, recent work has proposed that ubiquitination of histones is not only needed for the recruitment of various factors, but might also play a role in modulating nucleosome occupancy. In *S. cerevisiae* loss of H2Bub leads to a global decrease in nucleosome occupancy, particularly at highly transcribed regions, while deubiquitylation mutants, such as

ubp8Δ, present with elevated histone levels and nucleosome overaccumulation (Batta *et al.*, 2011). Recent findings in *S. pombe* and in human cells have also demonstrated a role for H2Bub1 in the maintenance of transcription from within the core centromeric heterochromatin in a cell cyclical manner (G₂-M). In the absence of H2Bub1, centromeric transcription is reduced and a further elevation of H3K9me levels is seen, which leads to an increase in segregation defects (Sadeghi *et al.*, 2014). Finally, other residues besides K123 have recently been shown to be ubiquitinated on H2B, including K48 and K34 (Geng and Tansey, 2008; Wu *et al.*, 2011). H2BK34ub appears to act similarly to K123 that is promotes the methylation of H3K4 and H3K79 (Wu *et al.*, 2011), while the role of K48ub is not clear.

In addition to H2B, H2A and H2A.Z also undergo ubiquitination. H2AK119ub1 has not yet been identified in yeast, but it is conserved in metazoans, and is primarily associated with repressive functions. In *Drosophila* the Polycomb repressor complex (PRC1) is responsible for H2AK119ub1 and is required for the maintenance/repression of the developmentally regulated *Hox* genes. Ubiquitination of H2A119 by PRC1 leads to the recruitment of PRC2, which is able to read the H2A119ub1 mark, and facilitates the subsequent methylation of H3K27 leading to transcriptional silencing (Blackledge *et al.*, 2014; Cooper *et al.*, 2014; Kalb *et al.*, 2014). Importantly, the Polycomb complexes play an essential role in stem cell reprogramming and differentiation (Prezioso and Orlando, 2011; Onder *et al.*, 2012), as well as in cancer development (Ben-Porath *et al.*, 2008; Ernst *et al.*, 2010; McCabe *et al.*, 2012). Finally, H2A ubiquitination is important in DNA damage response pathways. In fact in mammalian cells, ubiquitination of H2A and H2AX by RNF168 at K13/15 (Gatti *et al.*, 2012; Mattioli *et al.*, 2012) and by RING1B/BMI1 on K118/119 (Chagraoui *et al.*, 2011; Ginjala *et al.*, 2011) mediate the association of 53BP1 and the repair protein BRCA1 with chromatin (Sobhian *et al.*, 2007; Fradet-Turcotte *et al.*, 2013). Therefore, specific ubiquitination events are also responsible for DNA damage repair in mammalian cells.

As mentioned above, further modifications also exist, including SUMOylation, ADP ribosylation, β -N-acetylglucosamination, proline isomerization and deimination (Bannister and Kouzarides, 2011); however their molecular functions are less well understood and will not be discussed here. Overall, PTMs, either individually or in combination with each other, can facilitate highly specific molecular responses to complex cellular requirements.

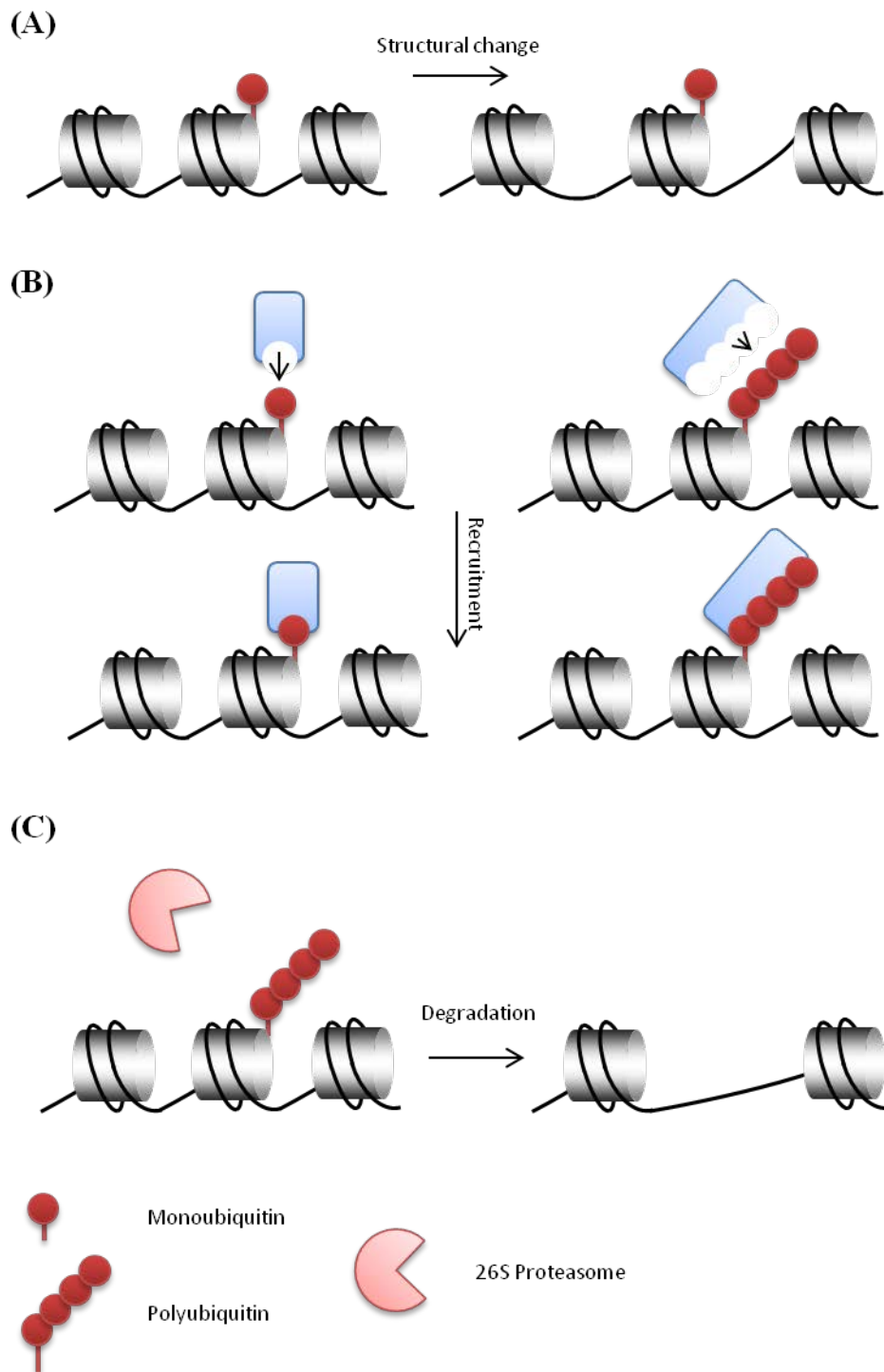


Figure 1.5 Possible outcomes of histone ubiquitination.

(A) Monoubiquitination can lead to structural changes, such as a more open chromatin. (B) Mono – and polyubiquitination can both serve as docking site for reader proteins, leading to further recruitment. (C) Polyubiquitination can lead to degradation via the 26S proteasome. Adapted from (Braun and Madhani, 2012).

1.3 Histone variant exchange

In addition to PTMs, replacing the canonical histones with variants provides an alternative mechanism for the regulation of chromatin (Jin *et al.*, 2005; Kamakaka and Biggins, 2005). Histone variant exchange takes place independently of replication and variants generally fulfil highly specialized roles (Jin *et al.*, 2005), leading to alterations of nucleosome structure, dynamics and ultimately accessibility to DNA (Weber and Henikoff, 2014).

1.3.1 H2A variants

Variants of H2A are the most numerous, although not all conserved between species (Table 1.5). H2A.Z is perhaps the best studied of these and is one that's highly conserved. It is distinct from H2A, with only about 60% sequence identity (Weber and Henikoff, 2014). Overall, replacement of H2A with H2A.Z leads to slight destabilization of nucleosomes *in vivo* (Weber and Henikoff, 2014). Therefore it might not be surprising that H2A.Z has been found to be particularly enriched over promoter regions and to an extent over the bodies of actively transcribed genes, especially over the +1 nucleosome (Weber and Henikoff, 2014; Weber *et al.*, 2014). In metazoans, enrichment of H2A.Z correlates with transcription levels, that is highly transcribed regions present with a relative increase in H2A.Z compared to the rest of the genome (Weber *et al.*, 2010). Furthermore, studies both in yeast and in humans have demonstrated a role for H2A.Z in helping to recruit RNA Pol II to promoter regions (Santisteban *et al.*, 2000; Adam *et al.*, 2001; Hardy *et al.*, 2009). In addition to a role in transcriptional activation, recent work has also proposed that H2A.Z facilitates elongation, as there has been an inverse correlation observed between H2A.Z levels and RNA Pol II stalling (Weber *et al.*, 2014). Reduction of H2A.Z led to an increase in RNA Pol II stalling, suggestive of a nucleosome barrier (Weber *et al.*, 2014). This suggests that H2A.Z-H2B dimers are more easily unwrapped and/or removed during transcriptional elongation than H2A-H2B dimers. Finally, a different role has also been proposed, in which yeast H2A.Z functions as a barrier between heterochromatin and euchromatin, preventing the spread of repressive chromatin into gene rich regions (Meneghini *et al.*, 2003).

H2A.X is mostly associated with the DNA damage response, and as a result not much is known about its other functions in genome organization, although H2A.X incorporation into the chromatin is widespread (Millar, 2013) (Section 1.2.3). Another distinct H2A variant is macroH2A. macroH2A is restricted to vertebrates where it is preferentially associated with transcriptionally silent domains, such as the inactivated X chromosome, senescence-associated heterochromatin foci (SAHF) and other large transcriptionally silenced euchromatic regions, where it co-localizes with the repressive H3K27me3 mark (Costanzi and Pehrson, 1998; Zhang *et al.*, 2005; Gamble *et al.*, 2010; Millar, 2013). Finally, H2A.B variants exist, although they appear to be restricted to mammals (Eirín-López *et al.*, 2008). The H2A.B1 homologue in mouse is H2A.Lap1, which has been shown to be highly expressed in the testis during meiosis and in post-meiotic round spermatids, and is particularly enriched over the TSSs of active genes in round spermatids (Soboleva *et al.*, 2012).

Table 1.5 The human complement of H2A variants.

Variant	Genes	Protein isoforms	Expression	Genomic locations
H2A.Z	H2A.Z.1	H2A.Z.1	Widespread	Promoters of Pol II genes and rRNA genes, flanking tRNA genes, enhancers, transposons, pericentromeric heterochromatin
	H2A.Z.2	H2A.Z.2.1 H2A.Z.2.2	Widespread Brain, skeletal muscle	
H2A.X	H2A.X	H2A.X	Widespread	Telomeric heterochromatin, XY body, sites of DNA damage, replication origins, Pol II genes.
mH2A	mH2A.1	mH2A.1.1	Differentiated cells	Xi, gene-coding sequences and distal upstream regions, large domains, TSS (differentiated cells).
		mH2A.1.2	Widespread	
	mH2A.2	mH2A.2	Widespread	
H2A.B	H2A.B1	H2A.B1	Testis and other tissues	–1 nucleosome (testis, H2A.Lap1), coding regions (HeLa, H2A.B).
	H2A.B2	H2A.B2		
	H2A.B3	H2A.B3		

Adapted from (Millar, 2013).

1.3.2 H3 variants

The best studied histone H3 variant is H3.3, which is incorporated into the chromatin in a replication-independent manner, in contrast to the canonical H3 (Weber and Henikoff, 2014). As a result of this, H3.3 make up a large proportion of histone H3 content in terminally differentiated cells, such as neurons; while only comprise a small fraction of the total H3 pool in actively dividing cells (Piña and Suau, 1987; McKittrick *et al.*, 2004). H3.3 is enriched primarily at promoters and the bodies of genes, both in active and inactive regions. It is also found in the subtelomeric and pericentromeric domains and so it is not restricted to highly transcribed regions (Weber and Henikoff, 2014). In addition to H3.3, H3.4 variant also exists, although so far it has only been found in the testis (Witt *et al.*, 1996). Finally, a centromeric form of H3 exists, CENP-A (CenH3). Importantly, in most organisms, it is the incorporation of this histone variant that leads to the establishment of the centromeric locus rather than the underlying DNA sequence (Müller and Almouzni, 2014). CENP-A is structurally different from the canonical H3, in fact they share only ~50% sequence identity. CENP-A presented with high specificity for kinetochore proteins, thereby facilitating appropriate chromosome segregation during cell division (Talbert and Henikoff, 2010).

1.3.3 Other variants

In addition to the above mentioned and relatively well studied histone variants, there are variants for H2B and H1 too. To date a H4 sequence variant has not been found, although in *Drosophila* a gene encoding H4 has been associated with expression patterns outside of S phase, characteristic of a variant (Akhmanova *et al.*, 1996). The H2B variant, TSH2B, is testis-specific and ChIP-seq analysis has shown is enriched in genes required for spermatogenesis (Hammoud *et al.*, 2009). Therefore, it has been proposed that this mark prevents the packaging of these regions into protamines (Talbert and Henikoff, 2010). Finally, the linker histone H1 has several variants (H1.1, H1.2, H1.3, H1.4, H1.5, H5), amongst them is an erythrocyte variant H5, which presents with a different structure, and is thought to be primarily involved in differentiation (Harshman *et al.*, 2013). Through the process of histone variant exchange another layer of control can be imposed on the chromatin structure, to fine-tune responses, whether affecting a specific cell type, a particular location in the genome, or exerting their effect during a particular cellular process.

1.4 ATP-dependent remodelers

Alongside histone modifications and histone variant exchange, ATP-dependent chromatin remodelling carried out by the Snf2-type ATPases provides an additional layer of control over the chromatin structure by modulating its accessibility. These chromatin remodelers utilize the energy generated from ATP-hydrolysis to disrupt nucleosome-DNA interactions, move nucleosomes along DNA (nucleosome phasing), remove or exchange nucleosomes/dimers or deposit newly synthesized nucleosomes (Clapier and Cairns, 2009; Hargreaves and Crabtree, 2011) (Fig. 1.6.A). Although there are several proteins involved in chromatin remodelling, often functioning in groups, they are generally classified into four categories based on their unique domains, these are SWI/SNF, INO80, ISWI and CHD (Fig 1.6.B). Common to them all is an ATPase domain, while the four classes contain motifs unique to each. Briefly, the SWI/SNF family of remodelers contain a bromodomain; the ISWI family a HAND-SANT-SLIDE (HSS) domain, the Ino80/Swr1 proteins contain an insertion in their ATPase domain, while CHD proteins contain a chromodomain and a DNA binding domain (Manning and Peterson, 2013).

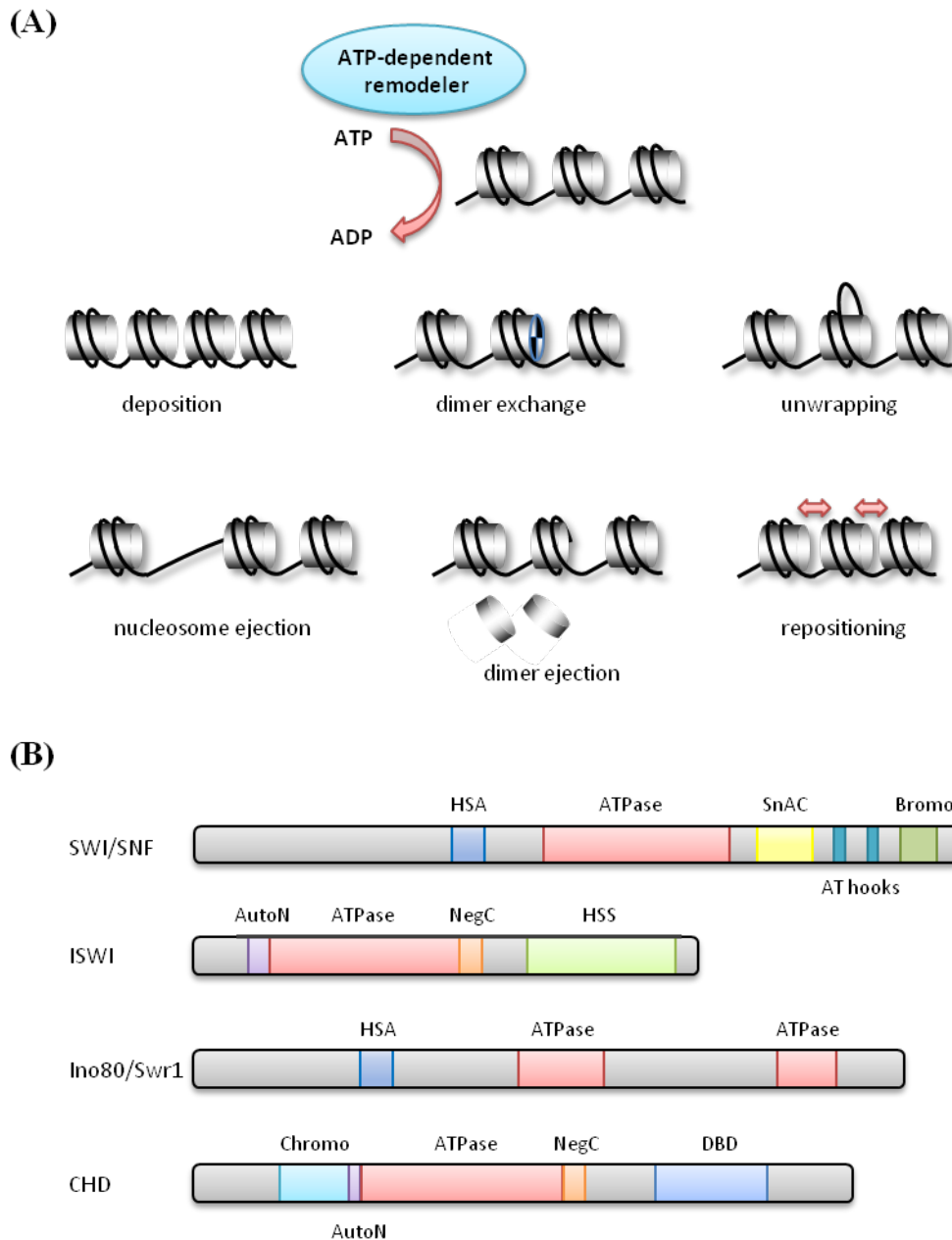


Figure 1.6 Outcomes of chromatin remodelling by ATP-dependent remodelers.

(A) Remodeler activities can lead to nucleosome deposition, dimer exchange, unwrapping, nucleosome ejection, dimer ejection and repositioning/spacing of nucleosomes. Adapted from (Clapier and Cairns, 2009). (B) **Domain structures of the four classes of ATP-dependent chromatin remodelers.** All ATP-dependent remodelers contain a highly conserved ATPase domain (red), while the four classes each contain domains unique to them. Briefly, the SWI/SNF family of remodelers contain a bromodomain; the ISWI family contains a HAND-SANT-SLIDE (HSS) domain, the Ino80/Swr1 proteins contain an insertion in their ATPase domain, while CHD proteins contain a chromodomain and a DNA binding domain. Adapted from (Manning and Peterson, 2013).

1.4.1 SWI/SNF (*Switch/Sucrose Non-Fermenting*)

The first chromatin-remodeler of the Snf2 family of ATPases to be characterized was SWI/SNF. The initial screens carried out in *S. cerevisiae* identified mutants that were defective in mating type switching, termed SWI (Stern *et al.*, 1984) and in sucrose fermentation, termed sucrose non-fermenting (SNF) (Neigeborn and Carlson, 1984). Since their characterization in budding yeast, homologues have been found in all model organisms, with a general composition of 8-14 subunits (Clapier and Cairns, 2009). The SWI/SNF family contains two complexes in yeast, RSC and SWI/SNF, in *Drosophila* it also includes the Brahma complex, and finally the human family also contain Brahma (BRM) and Brahma-related (BRG1) proteins. Characteristic of the SWI/SNF family of ATPases is their bromodomain, which allows recognition of acetylated lysines on histone tails (Hassan *et al.*, 2002). Overall SWI/SNF is associated with transcriptional activation, by generating a chromatin environment that is less compact and thereby easily accessible to Pol II (Clapier and Cairns, 2009). *Drosophila* Brahma localization in the polytene chromosomes, for example, coincides with transcriptionally active regions, and depletion of Brahma leads to a reduction in Pol II levels, suggesting that nucleosome remodelling by Brahma is important in facilitating transcription by Pol II (Armstrong *et al.*, 2002). The SWI/SNF complex has been shown to be required for the transcriptional activation of histone genes in *S. cerevisiae*, while the RSC complex is associated with repression of transcription outside of S phase (Eriksson *et al.*, 2012). The human SWI/SNF complex has also been shown to be involved in regulating the transcription of the Vitamin D gene, the estrogen receptor (ER), as well as a number of estrogen target genes (Zhang *et al.*, 2007a; Clapier and Cairns, 2009; Jeong *et al.*, 2009). Also, similarly to yeast, depending on the subunit composition of the human SWI/SNF complex, it can mediate both transcriptional activation and repression at the same set of gene promoters. For instance BAF170 has been demonstrated to be required for the SWI/SNF co-regulatory complex which mediates estrogen-induced activation of transcription but not repression; conversely BAF155 was involved in transcriptional repression but not activation (Zhang *et al.*, 2007a). Knockdown of the *Drosophila* Brahma also leads to global changes in nucleosome phasing over the ORFs of a subset of genes, particularly visible is a shift towards the 3' in the +3, +4, +5, etc. nucleosomes, as well as a decrease in global nucleosome occupancy (Shi *et al.*, 2014). In addition, *S. cerevisiae* RSC, but not SWI/SNF, has been shown to be required for phasing of nucleosomes on a global scale (Ganguli *et al.*, 2014). Depletion of RSC

results in nucleosome repositioning, with both + and – nucleosomal arrays shifting towards the NDR, resulting in a narrow and over occupied NDR (Ganguli *et al.*, 2014). Thus both Brahma and RSC are involved in global chromatin maintenance.

1.4.2 ISWI (*Imitation SWITCH*)

Protein complexes containing the ISWI ATPase were first identified in *Drosophila*, including the NURF, CHRAC and ACF complexes (Tsukiyama *et al.*, 1995; Tsukiyama and Wu, 1995; Ito *et al.*, 1997; Varga-Weisz *et al.*, 1997). Since then homologues in human and in yeast have too been characterized (Corona and Tamkun, 2004). Interestingly, ISWI lacks any domains that allow direct interaction with modified residues, such as a bromo or a chromo domain, rather it appears to be able to recognize nucleosomes (Corona and Tamkun, 2004). *In vitro* analysis has demonstrated that ISWI is able to generate nucleosome arrays from randomly synthesized nucleosomes, thus is has the ability to space nucleosomes (Whitehouse *et al.*, 2003). Furthermore, work carried out both *in vitro* and *in vivo* has demonstrated that all ISWI containing complexes can mediate transcriptional activation and repression. In *Drosophila* ISWI function is essential, homozygous mutants of *ISWI* die during larval or early pupal development and present with severe reduction in gene expression in the segmentation gene *en* and the homeotic gene *Ubx* (Deuring *et al.*, 2000). Furthermore *Drosophila* lacking the function of the NURF subunit, NURF301, showed reduced expression of *Ubx*, as well as an impairment of *hsp70* and *hsp26* gene induction (Badenhorst *et al.*, 2002). In addition, work *in vitro* has shown that the purified NURF complex is able to facilitate the transcription of *GAL4* from a chromatin template (Mizuguchi *et al.*, 1997). It has also been demonstrated that ISWI is not only able to facilitate active transcription, but is also required for the generation of silent chromatin. There are two ISWI homologues in *S. cerevisiae* *ISW1* and *ISW2*, and unlike in *Drosophila* these are not essential. Deletion of either of these genes results in de-repression at a number of loci as well as loss of silencing over the silent *HMR* mating type locus (Fazzio *et al.*, 2001; Cuperus and Shore, 2002). Recently it has also been demonstrated that the effect of ISWI on nucleosomes is on a global scale. Loss of activity of ISWI or NURF301 in *Drosophila* leads to decondensation of the male X chromosome, suggestive of a role in dosage compensation and global chromatin organization (Badenhorst *et al.*, 2002). Finally, nucleosome maps generated in *A. thaliana* have demonstrated that double

mutants of ISWI (*chr11* and *chr17*) lose global nucleosome spacing from the +1 nucleosome onwards over the body of protein coding genes (Li *et al.*, 2014), demonstrating that the nucleosome spacing function of ISWI is conserved.

1.4.3 INO80/SWR-C

INO80 and SWR-C are multi-subunit complexes that catalyze the deposition and removal of the histone variant H2A.Z from the +1 nucleosome over the ORFs of protein coding genes, and as a result, play an important role in transcriptional control. The incorporation of H2A.Z is carried out by the SWR-C complex, while removal of the variant is done by INO80 (Kobor *et al.*, 2004; Mizuguchi *et al.*, 2004; Papamichos-Chronakis *et al.*, 2011). The full INO80 complex is composed of ~15 subunits (Shen *et al.*, 2000), while SWR-C is made up of 14 (Mizuguchi *et al.*, 2004; Wu *et al.*, 2005). Interestingly, the two complexes share a number of the same subunits (Rvb1, Rvb2 and Arp4), with the Ino80 catalytic subunit being the core of the INO80 complex and Swr1 of the SWR-C complex (Shen *et al.*, 2000; Kobor *et al.*, 2004; Mizuguchi *et al.*, 2004). In agreement with their role in facilitating H2A to H2A.Z exchange, and *vice versa*, both SWR-C and INO80 complexes are enriched primarily over the +1 nucleosome (in >90% of protein coding genes) (Yen *et al.*, 2013). Previous work has demonstrated that SWR-C is able to deposit H2A.Z-H2B dimers directly into nucleosomes, while INO80 only has the ability to catalyze the exchange of H2A.Z for H2A specifically (Papamichos-Chronakis *et al.*, 2011). However, more recent work has suggested that not only is INO80 able to remove H2A.Z from these nucleosomes, it also promotes full nucleosome turnover (Yen *et al.*, 2013), possibly by exposing the H3-H4 core of the nucleosomes to other remodelers. In the absence of the functional INO80 complex in yeast, histone H3 turnover, which corresponds to full nucleosome turnover, is significantly reduced (Yen *et al.*, 2013). Thus, either directly or indirectly INO80 appears to play a role outside of H2A.Z-H2A exchange.

1.4.4 CHD

The CHD family of remodelers contain 9 members in higher eukaryotes, but just one in *S. cerevisiae* and two in *S. pombe* (Hargreaves and Crabtree, 2011). CHD proteins are characterized by tandem chromodomains located in the N-terminal region of the protein and a Snf2-like ATPase domain in the central region (Delmas *et al.*, 1993; Woodage *et al.*, 1997). The best studied member of the CHD family is Chd1, which has been associated with a wide variety of roles in general chromatin maintenance. Chd1 purified from *Drosophila* has been shown to be able to assemble nucleosomes *in vitro* in the absence of histone H1 proteins, suggestive of a role for CHD1 in active chromatin assembly (Lusser *et al.*, 2005). This agrees with further work in *Drosophila*, where Chd1 localization was found to coincide with transcriptionally active regions of chromatin. Furthermore, it has been demonstrated that loss of Chd1 function leads to an increase in the heterochromatin protein HP1a levels, while the converse is true when *CHD1* is overexpressed, resulting in perturbations to higher order chromatin structure (Bugga *et al.*, 2013). In addition to its ability to deposit nucleosomes, Chd1 has nucleosome spacing activity (Lusser *et al.*, 2005; Pointner *et al.*, 2012; Shim *et al.*, 2012). Deletion of both Chd1 encoding genes in *S. pombe*, *hrp1*⁺ and *hrp3*⁺, leads to a complete loss of the nucleosome periodicity over protein coding regions, as demonstrated by MNase-sequencing (Hennig *et al.*, 2012; Pointner *et al.*, 2012; Shim *et al.*, 2012). Thus CHD remodelers are particularly important in maintaining appropriate spacing of nucleosomes over coding regions. In addition to roles in nucleosome spacing, Chd1 in yeast has been demonstrated to play a role in suppressing histone H3 turnover over the 3' end of long genes (>1000 bp), essentially stabilizing nucleosomes (Radman-Livaja *et al.*, 2012). It has recently been suggested that it does this by preventing histone exchange following transcription, that is, it restricts the incorporation of histones from the free pool. Indeed, loss of *S. cerevisiae* *CHD1* leads to an increase in histone exchange from mid-ORF to the 3' end, and to a redistribution of nucleosomes towards the 5' end of genes (Smolle *et al.*, 2012). In agreement with a role in maintaining nucleosome towards the 3' end of ORFs, loss of *hrp1*⁺ and *hrp3*⁺ leads to an increase in cryptic antisense transcripts that largely originate from the 3' end of long genes (Hennig *et al.*, 2012; Pointner *et al.*, 2012; Shim *et al.*, 2012).

1.5 Histone chaperones

In addition to ATP-dependent remodelers, a distinct group of proteins function in the assembly and disassembly of nucleosomes. These proteins have been termed histone chaperones. Histone chaperones have initially been described by Laskey *et al.* (1978), and were thought of as acidic proteins that can prevent non-specific interactions between DNA, RNA and positively charged proteins, such as histones. However, over the years a number of well conserved histone chaperones have been identified, with essential roles in cellular processes such as replication, DNA damage repair, transcription, and senescence (Burgess and Zhang, 2013). There are diverse groups of chaperones that function with the different histone pairs and their roles can vary depending on the context, i.e. the same chaperone can function in both assembly and disassembly of nucleosomes, as well as in histone variant exchange. Table 1.6 depicts some of the well characterized histone chaperones with their respective histone partners and brief function.

Table 1.6 Histones and their respective histone chaperones

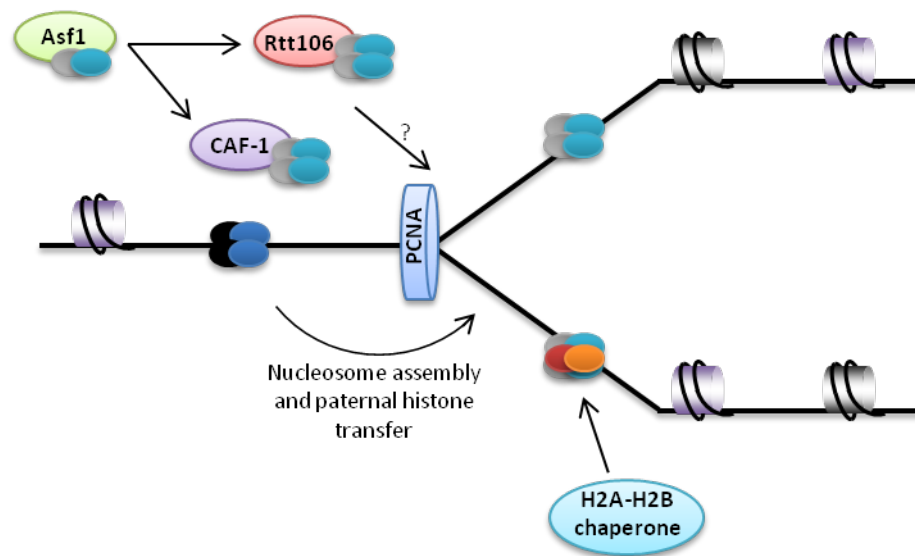
Histones	Chaperone	Nuclear processes
H2A-H2B	FACT	Replication, Repair, Transcription
	Nap1	Transcription
	Chz1	Transcription
H2A.X-H2B	FACT	Repair
H2A.Z-H2B	Nap1	Transcription
	Chz1	Transcription
H3-H4	Asf1	Replication, Repair, Transcription
	CAF1	Replication, Repair
	FACT	Transcription
	Vps75	Replication
	Rtt106	Replication
	Spt6	Transcription
	Nap1	Transcription
	HIRA	Transcription, Repair
H3.3-H4	Daxx	Transcription

Adapted from (Burgess and Zhang, 2013).

1.5.1 Histone H3-H4 chaperones

The process of nucleosome assembly depends on the initial deposition of the core (H3-H4)₂ heterotetramers, followed by the rapid deposition of H2A-H2B dimers. Since (H3-H4)₂ tetramers make up the core of the nucleosome, their initial assembly is likely to be rate-limiting. Their assembly is largely dependent on histone chaperones and as a result of this a number of H3-H4 histone chaperones have been identified and well characterized to date. Some of these include Asf1, CAF1, DAXX, Rtt106, HIRA, Vps75 and Spt6. A further way of classification is based on their role in replication-coupled or uncoupled nucleosome assembly. CAF1, Vps75, Rtt106 are all known to function in replication-dependent assembly, while HIRA, DAXX and Spt6 are restricted to replication-independent nucleosome deposition only. Asf1 functions in both pathways, primarily through partnering with either CAF1 or HIRA (Fig 1.7).

Replication-coupled nucleosome assembly



Replication-independent nucleosome assembly

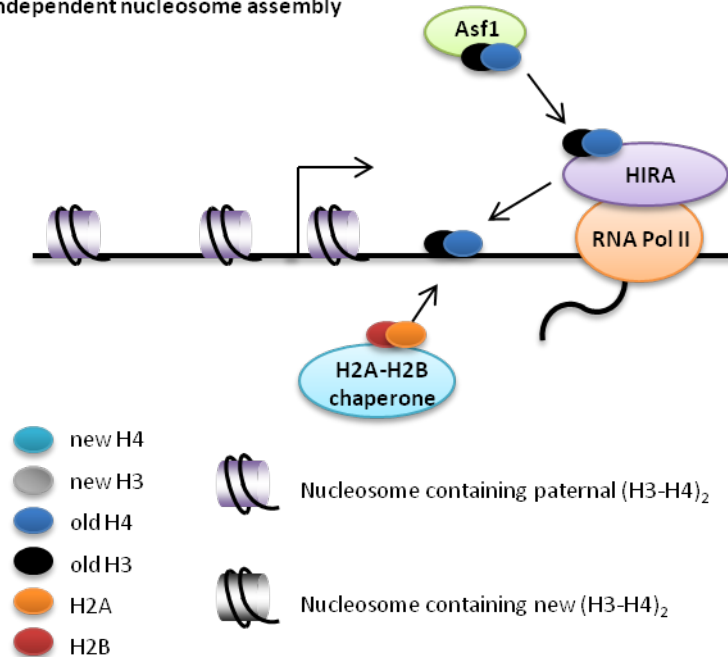


Figure 1.7 Schematic diagram of histone deposition by replication-dependent and replication-independent histone H3-H4 chaperones.

During replication-dependent nucleosome assembly newly synthesized histone H3-H4 dimers are bound by Asf1, which transfers the dimers to CAF-1 or Rtt106, leading to the formation of $(H3-H4)_2$, which gets deposited onto newly synthesized DNA. Paternal H3-H4 also gets incorporated onto the newly synthesized DNA strand however the mechanism behind that is still unclear. During transcription, replication-independent nucleosome assembly is primarily mediated by the HIRA complex, which is possibly associated with RNA Pol II. Adapted from (Burgess and Zhang, 2013).

1.5.1.1 Asf1 (*Anti-silencing function 1*)

Asf1 was first identified in *S. cerevisiae*, where deletion of the gene resulted in de-repression of genes near the telomeric regions, as well as sensitivity to a number of DNA damaging agents (Le *et al.*, 1997). While Asf1 function is not essential in *S. cerevisiae*, it has proven to be critical in other species, including *S. pombe*, *Drosophila* and chicken DT-40 cells (Sanematsu *et al.*, 2006; Tanae *et al.*, 2012). A temperature sensitive *asf1* mutant, *asf1-33*, in *S. pombe* presents with slow growth, an increase in DNA DSBs and sensitivity to DNA damaging agents (Tanae *et al.*, 2012). In addition, *asf1-33* cells lose silencing over the pericentromeric heterochromatin, and MNase digestions resulted in a significantly greater proportion of mononucleosomes compared to the wild type, suggestive of a large scale defect in chromatin structure (Tanae *et al.*, 2012).

Asf1 is thought of as the central histone H3-H4 chaperone, as it is essential in both replication-coupled and replication-uncoupled nucleosome assembly. It partners with the CAF-1 and HIRA histone chaperones to carry out the specific processes. While yeast contains a single Asf1 protein, two paralogs exist in most metazoans, ASF1a and ASF1b. Previous work has demonstrated that the majority of CAF-1 and H3.1 containing complexes interact with ASF1b, while HIRA and H3.3 complexes preferentially contain ASF1a (Tagami *et al.*, 2004). However, neither ASF1a nor ASF1b has any preferential binding activity to either H3.1 or H3.3, suggesting that the specificity comes from CAF-1 and the HIRA/UBN1 complex, respectively (Tagami *et al.*, 2004). Importantly, Asf1 has no affinity for binding H3-H4 tetramers; therefore it is possible that the major function of Asf1 is to supply histone dimers to CAF-1 and HIRA in nucleosome assembly. Indeed, it has been demonstrated that Asf1 binds to histone dimers, which get passed to CAF-1 and HIRA respectively, which have the ability to assemble them into tetramers prior to incorporation into the chromatin (Liu *et al.*, 2012).

In addition to a role in nucleosome assembly, Asf1 has also recently been shown to be required for appropriate induction of heat stress response genes in *A. thaliana*. Deletion of both of the ASF1 homologues, ASF1a and ASF1b, leads to a severe reduction of heat stress response gene induction (Weng *et al.*, 2014). They are both required for promoter nucleosome remodelling, as ASF1a/b levels correlate with nucleosome loss and RNA

Pol II recruitment. Furthermore, agreeing with previously published work, ASF1Aa/b facilitates H3K56ac, which stimulates transcriptional activation (Weng *et al.*, 2014). Acetylation of H3K56 in yeast is through the co-operation of Asf1 with the HAT Rtt109, and is important for transcriptional elongation, particularly through heterochromatin (Lu and Kobor, 2014). The yeast Asf1 protein has also been demonstrated to play a role in repressing histone gene transcription outside of S phase (Sutton *et al.*, 2001), while it is also required for appropriate *PHO5* and *PHO8* gene induction and repression, by mediating both nucleosome disassembly and reassembly, respectively (Adkins *et al.*, 2004).

1.5.1.2 CAF-1 (Chromatin assembly factor-1)

The CAF-1 histone chaperone complex is associated with nucleosome deposition during replication. The CAF-1 complex is evolutionarily conserved from yeast to humans, with 3 highly preserved subunits (p150, p60 and p48 in humans, and Cac1, Cac2 and Cac3 in *S. cerevisiae*, respectively) (Kaufman *et al.*, 1995; Verreault *et al.*, 1996). The p48/Cac3 subunit of the complex is able to directly interact with histones and has been found in a number of chromatin-related complexes, outside of CAF-1 (Loyola and Almouzni, 2004).

The complex was first purified from human cells and was demonstrated to have nucleosome assembly activity on replicating SV40 DNA *in vitro* (Smith and Stillman, 1989). Furthermore, *in vivo* analysis has demonstrated that CAF-1 is primarily associated with the H3.1 variant, which is deposited during S phase, making it a bone fide replication-dependent chaperone (Tagami *et al.*, 2004). During replication, CAF-1, through its p150 subunit gets recruited by the Proliferating Cell Nuclear Antigen (PCNA) to sites of DNA synthesis (Shibahara and Stillman, 1999). CAF-1 is then able to load newly synthesized, H3K56 acetylated, histone (H3-H4)₂ tetramers onto the chromatin (Shibahara and Stillman, 1999; Liu *et al.*, 2012; Winkler *et al.*, 2012). During its role in histone deposition, CAF-1 co-operates with the Asf1 histone chaperone (Asf1b in metazoans) (Sanematsu *et al.*, 2006) and as expected, knockdown of CAF-1 function leads to a decrease in H3.1 containing nucleosome incorporation (Nabatiyan and Krude, 2004).

CAF-1 has also been shown to play a role in heterochromatin formation and maintenance, as loss of any of the CAF-1 subunits in a number of organisms, including *S. cerevisiae*, *S. pombe*, *Drosophila*, and mice, leads to perturbations and loss of silencing over heterochromatic regions (Houlard *et al.*, 2006; Song *et al.*, 2007; Dohke *et al.*, 2008). The mechanism appears to be similar between the species; in the absence of functional CAF-1 complex, HP1 protein association with chromatin is decreased, thus leading to perturbed silencing over these regions (Dohke *et al.*, 2008; Huang *et al.*, 2010). Evidence from *S. pombe* suggests that CAF-1 functions by recruiting dislocated HP1 from heterochromatin during replication and redistributing it to sites of newly synthesized heterochromatic regions (Dohke *et al.*, 2008). Therefore, CAF-1 function is also important in epigenetic maintenance of heterochromatin.

1.5.1.3 HIR/HIRA (Histone cell cycle regulator)

1.5.1.3.1 Characterization and composition

Initial identification and characterization of the *HIR* genes (*HIR1*, *HIR2*, *HIR3* and *HPC2*) have come from genetic screens in *S. cerevisiae* for factors required for repression of three out of the four histone gene pairs, *HTA1-HTB1*, *HHT1-HHF1* and *HHT2-HHF2*, outside of S phase (Xu *et al.*, 1992; Spector *et al.*, 1997). It was also in budding yeast that all subunits of HIR were co-purified in a single complex, with a stoichiometry of one copy of Hir1 and Hir3, and two copies of Hir2 and Hpc2 respectively (Green *et al.*, 2005; Prochasson *et al.*, 2005). Since the initial findings in budding yeast, HIR homologues have also been identified in multiple other species, including in *S. pombe*, *Drosophila*, mice, and humans. Importantly, the single human HIRA protein also co-purifies with histone H3.3, as well as three other proteins homologous to HIR subunits, Ubinuclein-1 (UBN1), Ubinuclein-2 (UBN2), and Cabin1 (Tagami *et al.*, 2004). Recent work has also demonstrated that a single HIRA protein, similarly to metazoans, is also conserved in *A. thaliana* along with homologues for Cabin1, UBN1 and UBN2 (Nie *et al.*, 2014). Furthermore, similarly to metazoans, the *A. thaliana* HIRA complex has particular affinity to the histone variant H3.3 (Nie *et al.*, 2014). Thus it appears that the function of the HIRA complex is highly conserved throughout evolution. A diagram of HIRA complex composition in some model organisms is depicted in Figure 1.8 while Table 1.7 summarizes the key roles of HIRA. The single HIRA protein in metazoans is a homologue of the two budding yeast Hir1

and Hir2 proteins, while Cabin1 is thought to be the orthologue of Hir3, and Ubinuclein (UBN1/UBN2) that of Hpc2 (Balaji *et al.*, 2009; Banumathy *et al.*, 2009). As expected, recent work confirmed that HIRA and UBN1 largely co-localize on the chromatin, although regions do exist where only the HIRA protein binds (Pchelintsev *et al.*, 2013). The function of HIRA upon these regions is not understood; however a report from budding yeast suggests that the Hir1 subunit alone is enough to repress the *HTA1* promoter when it's artificially recruited (Spector *et al.*, 1997), so perhaps the subunits or a proportion of them can function independently of the extended HIRA complex.

Table 1.7 HIRA complex subunits and function through evolution.

Species	HIR complex subunits	Main functions
<i>S. cerevisiae</i>	Hir1, Hir2, Hir3, Hpc2	Regulation of histone gene expression Maintenance of heterochromatin silencing Suppression of spurious transcription Nucleosome assembly (replication-independent)
<i>S. pombe</i>	Hip1, Slm9, Hip3, Hip4	Regulation of histone gene expression Maintenance of heterochromatin silencing Suppression of spurious transcription Transcriptional regulation of inducible genes
<i>Drosophila</i>	dHIRA, yemenuclein- α	Histone H3.3 deposition in the male pronucleus during sperm decondensation
human	HIRA, UBN1, UBN2, Cabin1	Incorporation of histone H3.3 into nucleosomes SAHF formation Telomere length maintenance via ALT

Adapted from (Amin *et al.*, 2012).

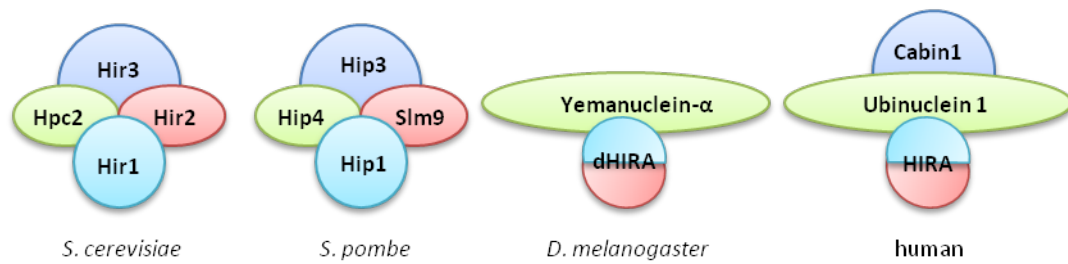


Figure 1.8 HIR complex homologues.

The HIR complex in *S. cerevisiae* comprises of four subunits. These are Hir1, Hir2, Hir3 and Hpc2. *S. pombe* also consists of four subunits, with Hip1, SIm9, Hip3 and Hip4 respectively. In *Drosophila* there is a single HIRA protein, which appears to be a fusion between the yeast Hir1 and Hir2 proteins, and it interacts with a Hpc2-like protein, called Yemanuclein- α . Similarly to *Drosophila*, the human HIRA complex consists of a single HIRA protein and a Hpc2-like homologue Ubinuclein1 and a Hir3-like protein Cabin1. Adapted from (Amin *et al.*, 2012).

1.5.1.3.2 Nucleosome assembly through HIR/HIRA

In vitro assays have demonstrated that the purified HIR complex can assemble nucleosomes independently of replication and that it most likely carries this out through binding histone H3-H4 pairs, not H2A-H2B (Ray-Gallet *et al.*, 2002; Green *et al.*, 2005; Prochasson *et al.*, 2005). In higher eukaryotes the HIRA protein preferentially binds the histone H3 variant H3.3 (Tagami *et al.*, 2004), which is associated with transcription over replication, demonstrating that HIRA is a replication independent chaperone also in these organisms. Further weight is added by the fact that HIRA does not only co-purify with histone H3.3 but also with ASF1a (Ray-Gallet *et al.*, 2002; Tagami *et al.*, 2004; Green *et al.*, 2005; Nie *et al.*, 2014), which in higher eukaryotes is the replication-independent ASF1 homologue. This is conserved throughout evolution. In *S. cerevisiae* loss of any of the four HIR subunits disrupts HIR and Asf1 binding, and *in vitro* Asf1 increases the ability of HIR to assemble nucleosomes (Green *et al.*, 2005). Partial inactivation of Asf1 function, which specifically reduces the physical association between Asf1 and HIR, also reduces the ability of the HIR complex to deposit nucleosomes *in vivo* (Green *et al.*, 2005). In addition, *asf1Δhir1Δ* double mutants in *S. cerevisiae* present with defects in incorporating histone H3 at the *PHO5* promoter to a similar degree than either single mutants, further confirming that these two genes act in the same pathway (Schermer *et al.*, 2005). Interestingly, recent work has demonstrated that when the human histone variants, H3.1 and H3.3 are introduced into yeast, which has only a single histone H3 protein, the yeast HIR complex preferentially incorporates H3.3 into the chromatin in a transcription dependent manner (Song *et al.*, 2013). H3.1 is almost completely excluded from transcriptionally active chromatin (Song *et al.*, 2013). The authors have also demonstrated that the choice between H3.1 and H3.3 variants is entirely dependent on the HIR complex, as Asf1 allows the indiscriminate deposition of both H3.1 and H3.3 (Song *et al.*, 2013). Therefore, the ability of the HIRA complex to distinguish between different histone variants is conserved from yeast to humans.

1.5.1.3.3 Regulation of transcription by HIR/HIRA

The best studied example of the HIRA complex in regulating gene transcription comes from budding yeast, where HIR is amongst the factors required for appropriate regulation of histone gene transcription (Amin *et al.*, 2012). Previous work has shown that a number of chromatin associated factors are involved in modulating the appropriate expression of histone genes, and that it is the interplay between these different proteins that leads to appropriate repression and activation. In particular Asf1, Rtt106, and HIR have been demonstrated to play a repressive role by creating a chromatin environment that prevents Pol II association (Sutton *et al.*, 2001; Fillingham *et al.*, 2009). HIR is thought to first bind to the centre of the *HTA1-HTB1* promoter region and physically associate with Asf1, then recruit Rtt106 (Fillingham *et al.*, 2009; Silva *et al.*, 2012). Loss of any of these three factors creates a nucleosome free region over the *HTA1-HTB1* promoter and leads to inappropriate histone gene transcription outside of S phase to a similar extent (Sutton *et al.*, 2001; Fillingham *et al.*, 2009; Silva *et al.*, 2012; Zunder and Rine, 2012). HIR in co-operation with Rtt106 is believed to be involved in the recruitment of RSC or SWI/SNF to facilitate the repression or activation of histone gene transcription respectively (Dimova *et al.*, 1999; Ng *et al.*, 2002; Ferreira *et al.*, 2011; Zunder and Rine, 2012). Therefore, the HIR complex is not only involved in repressing histone gene transcription, but through recruitment of Rtt106 and SWI/SNF it also facilitates appropriate transition leading to histone gene transcription (playing a co-activator role) (Fig 1.9). The role of the HIR complex in regulating histone gene expression has also been recapitulated in *S. pombe*, where it was shown that deletion of *hip1*⁺ leads to transcription of core histone genes outside of S phase (Blackwell *et al.*, 2004). Finally, recent work has demonstrated that the HIR complex in *C. albicans* is also involved in repressing histone gene expression outside of S phase (Stevenson and Liu, 2013). In addition to studies linking the HIRA complex to histone gene transcription, work carried out in *S. pombe* and in *A. thaliana* have both demonstrated a need for HIRA in appropriate induction of responsive, environmentally regulated genes (Chujo *et al.*, 2012; Nie *et al.*, 2014). In the absence of the functional HIRA complex, environmental stress response (ESR) genes *ctt1*⁺, *gpx1*⁺, *gpd1*⁺ and *tps1*⁺ fail to get induced in *S. pombe* upon heat stress (Chujo *et al.*, 2012). Therefore, it is possible that the HIRA complex plays a role in general transcriptional regulation.

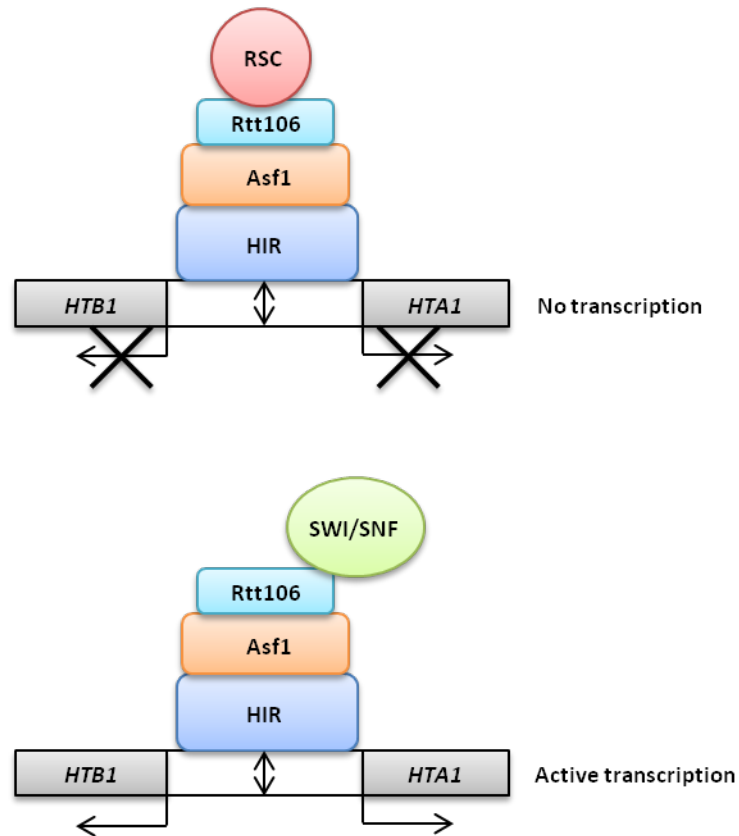


Figure 1.9 Repression of *HTA1-HTB1* transcription by the HIR complex.

The HIR complex in *S. cerevisiae* is involved in binding the histone gene *HTA1-HTB1* promoter, which is required for the appropriate (and sequential) recruitment of Asf1, Rtt106 and RSC. The presence of these complexes maintains repression of histone genes outside of S phase. Conversely, during S phase RSC is removed and the SWI/SNF complex is recruited to remodel the nucleosomes surrounding the promoter regions, leading to histone gene transcription. Adapted from (Zunder and Rine, 2012).

1.5.1.3.4 HIRA in transcriptional elongation and repression of cryptic promoters

Genetic analysis of the HIR complex in *S. cerevisiae* indicated that it is required not only for transcriptional activation, but also for transcriptional elongation. Mutations in the *HIR* genes alongside mutations in either *POB3* or *SPT16* lead to either synthetic lethality or extremely poor growth (Formosa *et al.*, 2002). Pob3 and Spt16 have previously been shown to be components of the yeast FACT complex, which is associated with facilitating transcriptional elongation. In addition, combining *HIR* mutants with mutants of *SPT4/5/6* or *PAF1*, transcription elongation components, also leads to synthetic lethality (Formosa *et al.*, 2002). Therefore, it appears that HIR is not only important in transcriptional activation but might also facilitate transcriptional elongation.

Loss of *HIR* function leads to the accumulation of cryptic/antisense transcripts (Nourani *et al.*, 2006). These transcripts arise from the 3' end of genes, from so called cryptic promoters, which are normally repressed. However, mutations in a number of chromatin maintenance genes, where nucleosomes are not properly reassembled over these regions, lead to antisense transcription. Cryptic transcription is also observed in *S. pombe* HIRA mutants (Blackwell *et al.*, 2004; Greenall *et al.*, 2006; Anderson *et al.*, 2009; Anderson *et al.*, 2010); therefore it is possible that HIRA is generally involved in the suppression of spurious transcription, most likely through facilitating the re-assembly of nucleosomes in the wake of RNA Pol II.

1.5.1.3.5 Role for HIR/HIRA in heterochromatin silencing

As mentioned previously, assembly and disassembly of nucleosomes throughout a variety of cellular processes is essential, and the HIR complex has been demonstrated to be a key histone chaperone in nucleosome assembly. One of its roles is maintaining heterochromatin structure and silencing. Initial work in *S. cerevisiae* has found that deletion of any of the *HIR* genes by themselves has no effect on heterochromatin silencing over the *HM* (*HMR* and *HML*) loci or over the telomeric regions. However, genetic interaction studies have demonstrated that loss of the *HIR* genes in the absence of CAF-1 leads to loss of position-dependent gene silencing that is severely exacerbated compared to the *cac* mutants by themselves (Kaufman *et al.*, 1998). Thus in the absence

of a functional CAF-1 nucleosome deposition pathway, HIR becomes necessary for heterochromatin maintenance. In heterochromatic silencing, like in other activities, the HIR complex functions through the same pathway as Asf1. Loss of *HIR* genes alongside *ASF1* does not exacerbate the phenotype of the single mutants, while deletion of *ASF1* alongside components of the CAF-1 complex, leads to similar phenotypes to those observed in the *hir cac* double mutants (Sharp *et al.*, 2001). Not surprisingly, Rtt106 has also been shown to play a role through the HIRA/Asf1 pathway in heterochromatin silencing (Huang *et al.*, 2005; Huang *et al.*, 2007). In addition to maintaining heterochromatin over the *HM* loci and telomeric regions, HIR has also been implicated in preventing the transposition of Ty elements. A screen carried out in a *cac* mutant background has identified *HIR* genes as important for the repression of Ty transposition (Qian *et al.*, 1998). Since, work has also identified both Asf1 and Rtt106 as being important for repression of retrotransposition in *cac* mutants (Amin *et al.*, 2012).

In addition, work carried out in *S. pombe* has shown that loss of any of the HIR/HIRA subunits leads to loss of silencing within the pericentromeric heterochromatin, the mating type locus and over *Tf2* retrotransposons (Blackwell *et al.*, 2004; Greenall *et al.*, 2006; Anderson *et al.*, 2009; Anderson *et al.*, 2010; Yamane *et al.*, 2011), even in the presence of functional CAF-1. Hence, in *S. pombe* the HIRA complex alone plays a more central role in heterochromatin maintenance than it does in *S. cerevisiae*. Finally, the *A. thaliana* HIRA complex is required for the silencing of *knox* genes, possibly through the establishment of heterochromatin (Phelps-Durr *et al.*, 2005). Therefore, the HIRA complex is likely to be important in maintaining repressive chromatin structures in eukaryotes.

1.5.1.3.6 HIRA in development

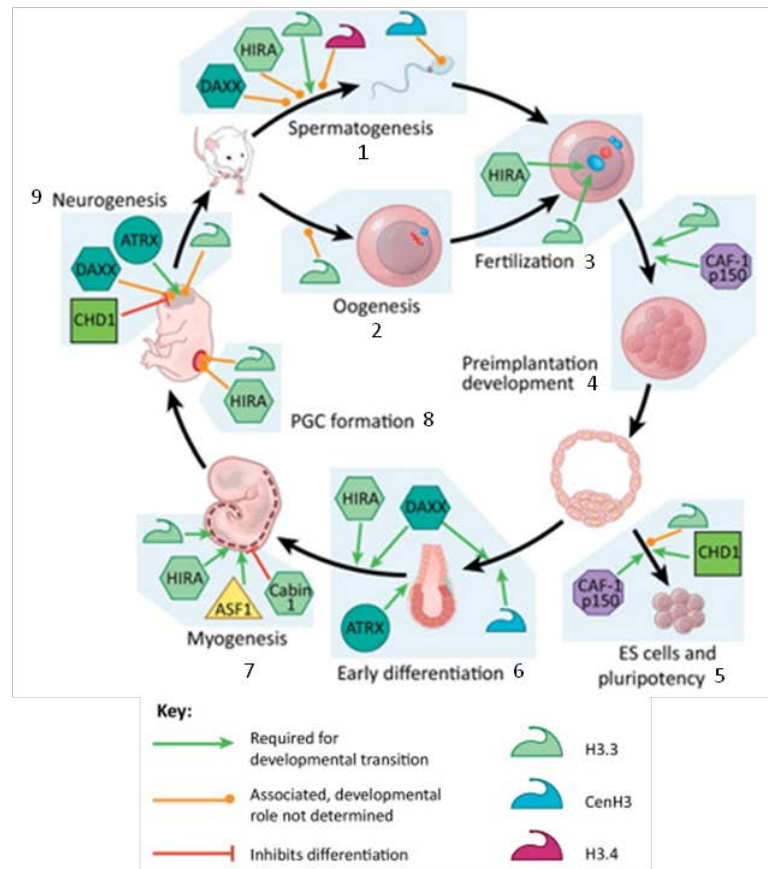
HIRA is essential in early development, a role which has been found to be conserved across species. HIRA protein and mRNA levels were found to be at their peak during early stages of development in mice, chicken, *Drosophila*, zebra fish, *Xenopus*, *A. thaliana* and gibel carp too (Amin *et al.*, 2012). Mutations of HIRA in mice lead to gastrulation defects, abnormal mesodermal development and embryonic lethality by day 11 (Roberts *et al.*, 2002). HIRA is also essential in the gibel carp, where knockdown of HIRA by morpholinos leads to death either during embryogenesis or during larval development (Wang *et al.*, 2014). The role of HIRA during the indicated developmental stages, along with other histone chaperones is depicted in Figure 1.10.A (Filipescu *et al.*, 2013).

The function of HIRA is perhaps best understood during sperm decondensation in the male pronucleus in *Drosophila* (Fig 1.10.B). This is essential for male fertility and for embryonic development (Kirov *et al.*, 1998; Llevadot *et al.*, 1998; Loppin *et al.*, 2005; Bonnefoy *et al.*, 2007). A point mutation in the *Drosophila* HIRA gene, termed *sesame* (*ssm*), leads to sterility in females, suggesting that HIRA is essential for the assembly of the paternal chromatin during fertilization. Indeed, *ssm* mutants are defective in their ability to deposit maternal histone H3.3 into the male pronucleus, which remains abnormally condensed and fails to assemble on the mitotic spindle (Loppin *et al.*, 2000). As a result of this haploid maternal embryos fail to develop, hence the *ssm* mutation is embryonic lethal (Loppin *et al.*, 2000). Similarly to *Drosophila*, depletion of HIRA in both the gibel carp and colour crucian carp leads to a failure in sperm decondensation (Zhao *et al.*, 2011). Finally, work in mice has also demonstrated a need for HIRA in sperm decondensation and appropriate fertility through its role in histone H3.3 deposition (Lin *et al.*, 2014). In addition, this study has demonstrated that HIRA mediated H3.3 deposition is not restricted to the paternal genome, as when HIRA was not functional depletion was also observed in the oocyte (Lin *et al.*, 2014). This suggests that remodelling also takes place in the maternal chromosomes and that this is also HIRA mediated.

Recently, identification of a *Yemanuclein-α* mutation in *Drosophila*, has also demonstrated a role for HIRA mediated chromatin maintenance during meiosis. The *yem*¹ allele presents with disruptions to chromosome organization on the meiotic

spindle, possibly as a result of inappropriate kinetochore function (Meyer *et al.*, 2010). In support of this model, Yem1- α localized to the kinetochores during meiosis, while *yem*¹ flies were shown to produce diploid eggs following meiosis, indicative of non-disjunction (Meyer *et al.*, 2010). Consequently, it is possible that the HIRA complex is involved in meiosis through a role in the assembly/maintenance of kinetochores. Finally, while histone H3.3 and the HIRA complex are generally associated with marking active transcription, recent work has demonstrated that in embryonic stem cells (ESCs) the HIRA complex and H3.3 are required for the maintenance of repressive chromatin over developmentally regulated bivalent genes. Bivalent genes are important in ESC differentiation, as they are able to respond rapidly to developmental signals. In HIRA depleted cells, H3.3 levels are down and consequently so are H3K27me and PRC2 levels, while H3K4me levels remain unchanged (Banaszynski *et al.*, 2013). In addition, HIRA physically associates with PRC2 over these regions in ESCs, hence not only is HIRA and H3.3 are important for maintaining active transcription but they might also play a role in the maintenance of repressive states (Banaszynski *et al.*, 2013)

(A)



(B)

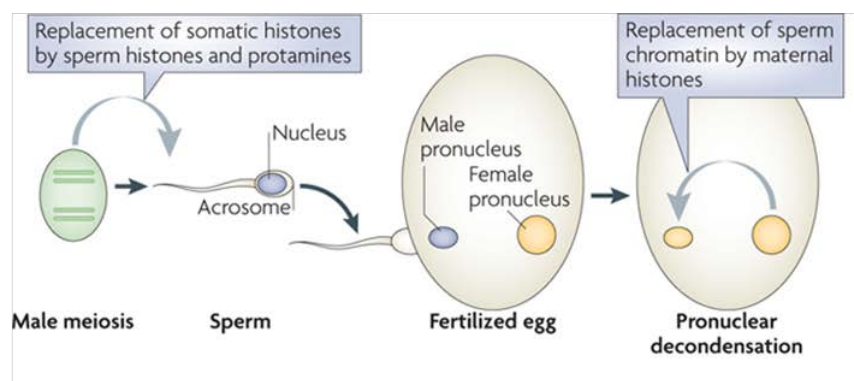


Figure 1.10 Role for HIRA during development

(A) Role of histone chaperones and their respective histone variants during mouse development. Mouse reproduction begins with the fusion of the two gametes (1,2) into a zygote (3). This cell acquires totipotency and starts dividing (4,5) giving rise to daughter cells that are able to further specialize (6). The diverse cell lineages they establish differentiate into the array of tissues in the adult organism (7,8). Among these lineages, primary germ cells (PGCs) undergo reprogramming to establish the germline of the adult (9), allowing it to produce either male or female gametes. Taken from (Filipescu *et al.*, 2013). **(B) Condensation and decondensation of sperm chromosomes.** During the male meiosis sperm gets condensed by replacing the canonical histones with variants, as well as protamines. However, following fertilization in order for appropriate mitosis to take place pronuclear decondensation must occur. During this process, maternal histones replace the variants and protamines are also removed. Taken from (Talbert and Henikoff, 2010).

1.5.1.3.7 HIRA and senescence

The HIRA complex, alongside ASF1a, has been shown to also play a role in modulating cellular senescence in human tissue cultures. Their roles are thought to be through the formation of senescence-associated heterochromatin foci (SAHF) (Zhang *et al.*, 2005; Zhang *et al.*, 2007b; Banumathy *et al.*, 2009). SAHF, distinct to senescent cells, contain a number of heterochromatic features, including high levels of H3K9me, the heterochromatin protein, HP1, and the histone H2A variant, macroH2A (Adams, 2007). When senescent cells are observed under the microscope in the presence of a nuclear stain, clear, punctuate foci are visible. Remarkably, each individual focus represents a highly condensed chromosome (Zhang *et al.*, 2005). There have been several proposals as to how SAHF maintains senescence; one of the more popular ones is that it silences proliferation promoting genes, such as cyclin A (Zhang *et al.*, 2005; Zhang *et al.*, 2007b). HIRA and ASF1a are both rate-limiting in SAHF formation, with ASF1a, but not HIRA, being required for macroH2A deposition (Zhang *et al.*, 2005). SAHF formation is thought to occur in a temporal manner, in which signals such as shortened telomeres, oncogenic activation, or persistent DNA damage, provide the initial trigger, leading to chromosome condensation. Chromosome condensation requires HIRA and ASF1a, and it takes place prior to H3K9me enrichment and HP1 recruitment (Fig 1.11) (Zhang *et al.*, 2005).

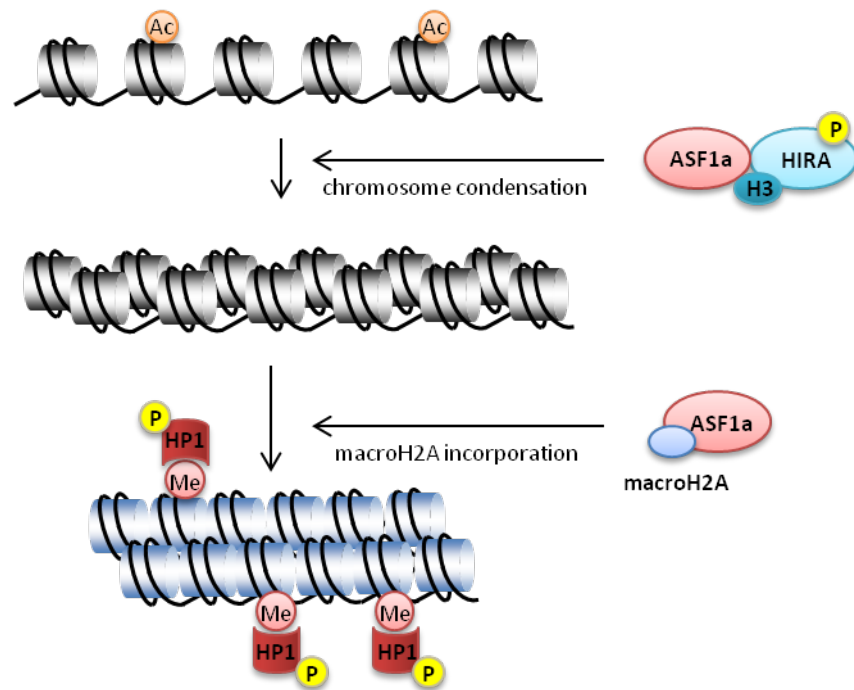


Figure 1.11 SAHF formation is mediated by HIRA and ASF1a.

Following signals to trigger senescence, the HIRA/ASF1a proteins drive chromosome condensation. Chromatin gets hypoacetylated, and H3 methylated on lysine 9. This in turn leads to recruitment of HP1, which is dependent on HP1 phosphorylation. Also incorporated into condensed chromatin is macroH2A, which does not rely on the HIRA complex. Adapted from (Adams, 2007).

1.5.1.3.8 HIRA in disease

Previous work has implicated the HIRA complex, in addition to FACT, Asf1, Spt6, and Chd1, in maintenance of HIV latency through nucleosome assembly over the HIV promoter region. This creates a repressive environment which blocks the access of transcription factors to DNA (Gallastegui *et al.*, 2011). In addition, work has implicated HIRA in angiogenesis through its role in regulating endothelial genes. Following angiogenic signals, HIRA expression is induced in endothelial cells, where it mediates the incorporation of K56ac H3.3 over several endothelial genes, such as *Vegfr1*, *Cxcl1*, *Cxcl5*, *Ereg* and *Plxdc1* (Dutta *et al.*, 2010). These genes are involved in vascularisation and have been demonstrated to play a role in angiogenesis. In the absence of HIRA, transcription of these genes is down regulated and so is vascularisation (Dutta *et al.*, 2010). Therefore, it is possible that inappropriate upregulation of HIRA can lead to angiogenesis, hence promoting tumour formation.

1.5.1.4 Other H3-H4 chaperones

Rtt106 is a fungal specific histone chaperone and is best characterized in its role in mediating histone gene expression in *S. cerevisiae*, as described in Section 1.5.1.3.3 and Figure 1.9. In addition, Rtt106 has been demonstrated to play a role in nucleosome assembly coupled to DNA synthesis in a manner similar to CAF-1 (Figure 1.7). It was recently shown that Rtt106 is able to bind (H3-H4)₂ heterotetramers *in vivo*, thus similarly to CAF-1, it is able to assemble tetramers prior to deposition onto chromatin (Fazly *et al.*, 2012).

DAXX is a histone chaperone unique to metazoans that has a role in specifically depositing the H3.3 variant making it a replication-independent chaperone (Drané *et al.*, 2010). However, while HIRA is mainly responsible for nucleosome assembly over genic loci, DAXX's activity appears to be restricted to the pericentromeric and telomeric regions (Drané *et al.*, 2010).

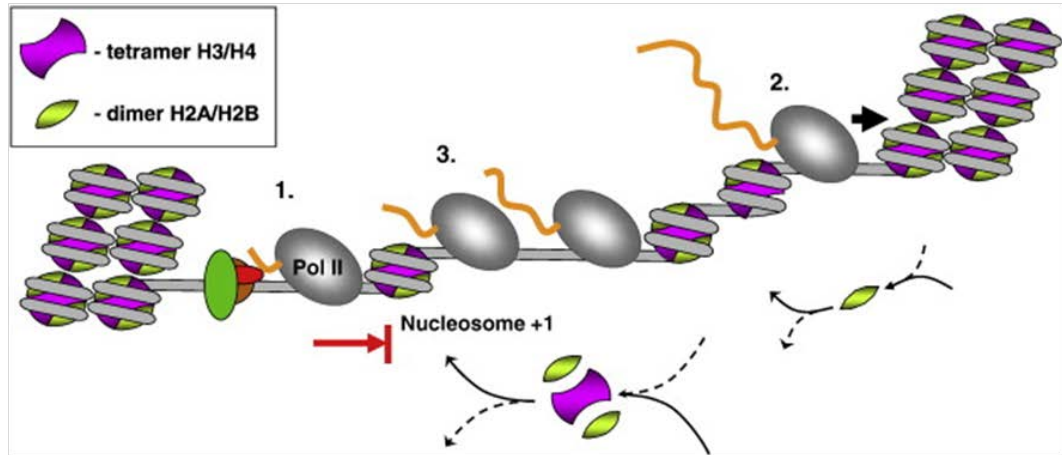
Spt6 in *S. cerevisiae* is essential for reassembly of promoter nucleosomes following transcription over the *PHO5*, *PHO8*, *ADH2*, *ADY2*, and *SUC2* genes, facilitating transcriptional repression (Adkins and Tyler, 2006). Recent work has also demonstrated

that in *spt6-1004* mutants, nucleosome loss occurs over coding regions, with highly transcribed regions being particularly affected (Ivanovska *et al.*, 2011). Finally, deletion of *spt6*⁺ in *S. pombe* leads to a significant reduction in the heterochromatin mark, H3K9me2 and in turn to decreased association of the HP1 protein, Swi6 (Kato *et al.*, 2013). As a result *spt6*Δ cells present with loss of silencing over the pericentromeric regions, a decrease in nucleosomes over the *dh-dg* repeats, and an increase in Pol II occupancy over these regions (Kato *et al.*, 2013). Therefore, the nucleosome reassembly function of Spt6 is important globally.

1.5.2 H2A-H2B histone chaperones

H2A-H2B dimers are incorporated into the nucleosomes following the deposition of (H3-H4)₂ heterotetramers. As a result of this, H2A-H2B dimers are more dynamic than H3-H4 and are involved in fine tuning transcriptional responses. H2A-H2B dimers are exchanged more often than H3-H4 for variants and are also differentially remodelled/disassembled during transcription. For example, in low to moderately transcribed genes, H2A-H2B dimer loss is more likely to occur, maintaining a hexameric nucleosome, while in housekeeping genes and those with high rates of transcription, entire nucleosomes get disassembled (Fig 1.12.A and B) (Kulaeva *et al.*, 2013). As a result, histone chaperones facilitating H2A-H2B assembly, disassembly and exchange are extremely important in facilitating proper transcription. There are a handful of conserved H2A-H2B chaperones, but perhaps the best studied one is the FACT complex.

(A)



(B)

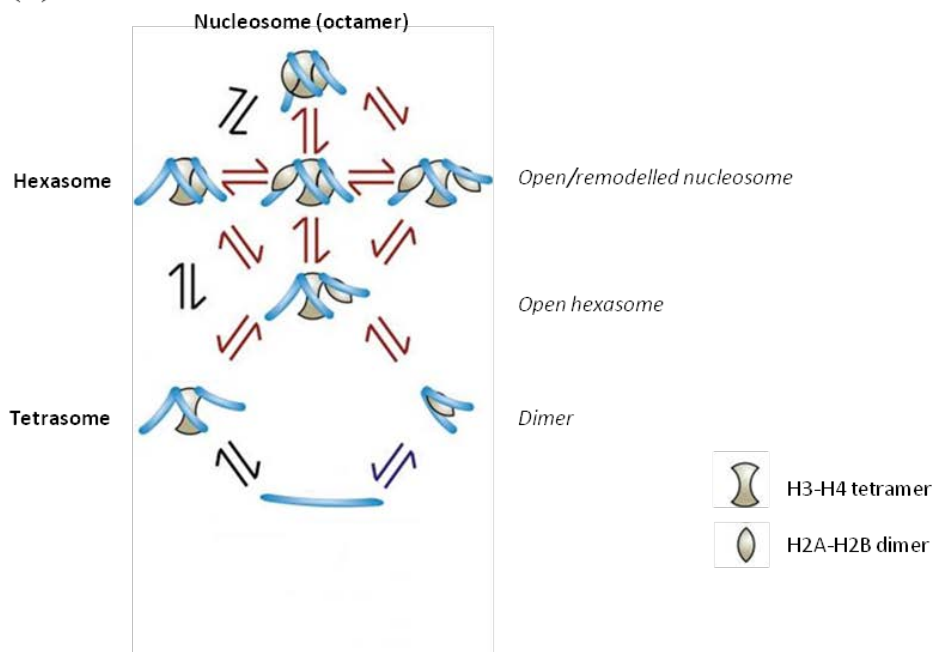


Figure 1.12 Mechanism of transcription through chromatin by Pol II.

(A) Following transcription initiation, Pol II undergoes pausing at the +1 nucleosome (1), the length of the pause is determined by the ability of enzymes to remodel the nucleosome, making it more accessible. This can be achieved by displacement of the H2A-H2B dimer or by exchange. It is often here that the H2A.Z variant is incorporated in the place of H2A, which leads to reduced Pol II pausing (2). At low to moderately transcribed regions, it is likely that dimer exchange will take place and nucleosomes will be fully re-assembled before the next round of transcription. (3) Over highly transcribed regions, it is possible that several Pol II enzymes are in close proximity of each other, therefore the second Pol II will encounter hexasomes that are already less stable than a full nucleosome, leading to nucleosome eviction (instead of dimer displacement). Adapted from (Kulaeva *et al.*, 2013). (B) **The possible states of assembly/disassembly of the nucleosome.** The black arrows indicate established reversible steps involved in chromatin assembly and disassembly. The red and purple arrows indicate more speculative steps. The respective histone chaperones and ATP dependent remodelers have been removed for the sake of simplicity. Adapted from (Das and Tyler, 2013).

1.5.2.1 FACT (*Facilitates Chromatin Transcription*)

The FACT histone chaperone is extremely well conserved amongst eukaryotes, with two subunits in metazoans, SSRP1 and Spt16. In yeast there are two homologous proteins, Pob3 and Spt16. However, while the metazoan SSRP1 contains a HMGB DNA binding domain, in yeast a third protein, Nhp6, provides that function to the FACT complex (Fig 1.13.A). (*S. cerevisiae* actually contains two Nhp6 proteins, Nhp6a and Nhp6b.) Activity of the FACT complex is essential in most organisms, with *S. pombe* being one of the few where viable *pob3*⁺ knockouts can be constructed. FACT has initially been characterized as a H2A-H2B chaperone; however emerging evidence now suggests that it is also able to bind H3-H4 (Belotserkovskaya *et al.*, 2003; Stuwe *et al.*, 2008). Thus, it is one of the few chaperones with affinity for all histone pairs. Furthermore, FACT has been proposed to act in both replication-coupled and replication-independent nucleosome assembly.

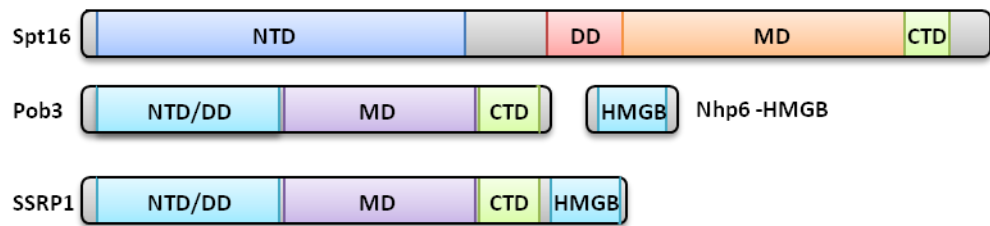
1.5.2.1.1 FACT in transcription and nucleosome disassembly

There are two models as to how FACT functions during transcription. First, the dimer displacement model proposes that FACT is able to evict H2A-H2B dimers from the nucleosome, thus making it accessible to Pol II. The second model is the global accessibility model, which suggests that rather than displacing the dimers, FACT is able to remodel the nucleosome whilst holding onto the dimers, consequently making the nucleosome dynamic and open to Pol II, without loss of H2A-H2B (Fig 1.13.B). Recent evidence suggests that the global accessibility model is likely to be correct, although it is probable that at highly transcribed regions, with increased Pol II presence, dimers and/or nucleosomes are entirely displaced (Hsieh *et al.*, 2013; Kulaeva *et al.*, 2013). It was demonstrated *in vitro* that in the presence of FACT, a single round of transcription produces little free DNA and an inverse amount of hexasomes, while transcription without FACT produces an increase in histone free DNA with very little intact hexasomes (Hsieh *et al.*, 2013). FACT complex purified from yeast was also found to enhance accessibility to endonucleases and hydroxyl radicals, while partially protecting DNA, and this can occur without displacement of dimers from the nucleosome (Xin *et al.*, 2009). Therefore, FACT remodels nucleosomes in such a way that they mimic nucleosome free type accessibility to nucleases, without the loss of nucleosomes. Furthermore, *S. cerevisiae spt16-11* mutants present with a reduced ability to remodel

nucleosomes, a phenotype which is suppressed by histone H2A mutants that contain mutations affecting their binding to H3-H4 tetramers (McCullough *et al.*, 2011). Hence, *spt16-11* is rescued by histones that are easier to remodel and spend more time in an open conformation, once again suggesting that the major role of FACT is to create accessible chromatin for Pol II.

Although FACT is principally thought to remodel nucleosomes during Pol II passage, it is also able to evict them. For example, FACT is required for appropriate transcription of inducible and cell cycle regulated genes in *S. cerevisiae*, through its role in nucleosome eviction over the promoter regions (Takahata *et al.*, 2009a; Takahata *et al.*, 2009b; Xin *et al.*, 2009). Some mutations in FACT reduce nucleosome eviction over these regions and consequently lead to a decrease in gene expression (Takahata *et al.*, 2009a).

(A)



(B)

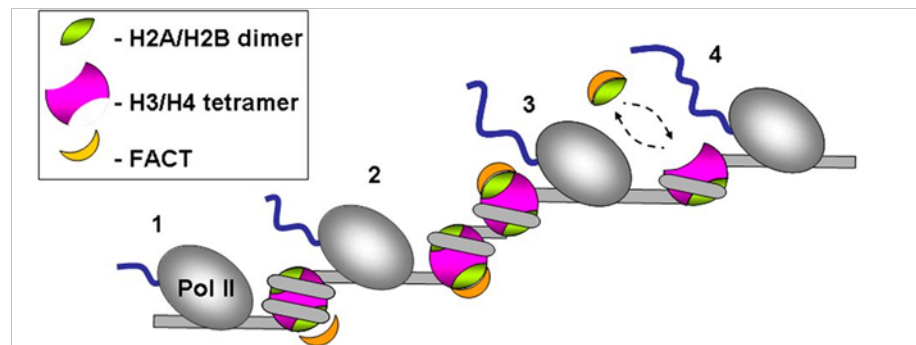


Figure 1.13 Structure and function of the FACT complex.

(A) Domains of the FACT complex. Spt16 is characterized by a N-terminal domain (NTD), a dimerization domain (DD), which facilitates heterodimer formation with Pob3/SSRP1, a middle domain (MD) and a C-terminal domain (CTD). Similarly, Pob3 and SSRP1 have highly conserved DD, MD and CTD, with SSRP1 containing an extra HMGB domain, which facilitates DNA binding. In yeast, the Nhp6 protein contains the homologues HMGB domain. Adapted from (Winkler and Luger, 2011; Formosa, 2012).

(B) Role of FACT in Pol II transcription. The model proposed by Hsieh *et al.* (2013) suggests that during moderate level transcription, FACT destabilizes the nucleosome in front of RNA Pol II (1), then as Pol II enters the nucleosome, it partially unwinds nucleosomal DNA, while FACT sequentially binds to promoter-proximal (2) and promoter-distant H2A-H2B dimers (3). The FACT-dimer interactions allow nucleosome survival during transcription, possibly through FACT mediating dimer replacement following elongating Pol II (4). Adapted from (Hsieh *et al.*, 2013).

1.5.2.1.2 FACT in nucleosome assembly

While both *in vitro* and *in vivo* experiments have clearly identified a role for the FACT complex in nucleosome disassembly or reorganization leading to a more accessible chromatin state, it has also been implicated in nucleosome reassembly following Pol II progression (Belotserkovskaya *et al.*, 2003; Jamaï *et al.*, 2009; Voth *et al.*, 2014). *In vitro* analysis has demonstrated that FACT has the ability to deposit nucleosomes (Belotserkovskaya *et al.*, 2003), and *in vivo* measurements of histone turnover in *S. cerevisiae* have also shown that FACT depleted cells lose histones at a significantly higher rate (Jamaï *et al.*, 2009). The loss of nucleosomes is transcription dependent and does not affect the incorporation of newly synthesized histones into the nucleosome (Jamaï *et al.*, 2009). Therefore, FACT plays an important role in the re-assembly of nucleosomes in the wake of Pol II. Importantly, the study has found that the *spt16-197* mutants incorporate newly synthesized histone H3 inappropriately, in addition to failing to replace old histone H3-H4 tetramers (Jamaï *et al.*, 2009). *S. pombe* FACT mutants have also been shown to be depleted of H3 in a transcription-dependent manner, with increased loss of H3 seen over highly transcribed regions in a *spt16-18* mutant (Choi *et al.*, 2012). Hence, FACT is not only a chaperone involved in H2A-H2B assembly/disassembly but also has a role to play in H3-H4 reassembly. In addition, FACT depleted cells present with an increase in cryptic/antisense and alternate transcripts, a finding which has been observed in both budding and fission yeast (Kaplan *et al.*, 2003; Cheung *et al.*, 2008; Choi *et al.*, 2012).

FACT has also been associated with the assembly of newly synthesized histones, thus acting in a replication-dependent manner. There have been several lines of evidence for this; firstly FACT physically associates with a number of replication complex proteins, it is essential in almost all eukaryotes, and importantly it can assemble core nucleosomes *in vitro* (VanDemark *et al.*, 2006; Xin *et al.*, 2009; Formosa, 2012). Mutants of the FACT complex are sensitive to mutations that affect histone H4K5 and H4K12 acetylation, which are marks of newly synthesized histones, as well as to mutations in *GCN5*, which has also been shown to be important in replication (VanDemark *et al.*, 2006). Therefore, it is possible that the FACT complex functions in nucleosome assembly during replication too.

1.5.2.2 Other H2A-H2B chaperones

Nap1 is a chaperone that preferentially binds H2A-H2B *in vivo* and is involved in multiple steps of H2A-H2B deposition onto the nucleosome. Nap1 is a nucleocytoplasmic shuttling protein, which is important for the initial import of histones into the nucleus. *In vitro* assays have further demonstrated that Nap1 is able to reconstitute nucleosomes, and functions alongside ACF to assemble properly spaced arrays (Burgess and Zhang, 2013). Nap1 is also able to chaperone H2A.Z-H2B dimers and it is responsible for their import into the nucleus and in maintaining a soluble pool of the H2A.Z variant (Straube *et al.*, 2010).

In addition to Nap1, Chz1 is a chaperone specifically associated with H2A.Z-H2B dimers (Luk *et al.*, 2007). It is thought that Chz1 functions with the SRW-C complex in variant exchange, by presenting the H2A.Z-H2B dimers to SWR-C, which is then able to place them into the nucleosome in exchange for a H2A-H2B dimer (Luk *et al.*, 2007; Straube *et al.*, 2010).

Finally, Nucleolin is an H2A-H2B chaperone that has primarily been associated with rDNA transcription via eviction of the H2A-H2B dimers (Durut and Saez-Vasquez, 2015). It is also recruited to DNA double strand breaks, where it displaces H2A-H2B dimers to facilitate proper repair (Kobayashi *et al.*, 2011; Goldstein *et al.*, 2013).

1.6 AAA-ATPases

Although the classical Snf2-family of ATP-dependent remodelers has been extensively studied, recently another family of proteins, AAA (ATPases Associated with diverse cellular Activities) ATPases have been linked to possess some chromatin associated functions. AAA-ATPases are a very large and diverse group of proteins that are conserved in all organisms (Ogura and Wilkinson, 2001; Snider and Houry, 2008). These proteins are characterized by two conserved ATP-binding domains, so-called AAA motifs. Each of these contains a Walker A and Walker B motif, which are generally associated with nucleic acid binding. These proteins often form ring shaped hexamers and use the energy from ATP hydrolysis to induce conformational changes to a wide range of substrates (Bar-Nun and Glickman, 2012). As a result of this, they function in a wide variety of cellular contexts and fulfil many essential roles, including, but not limited to, protein degradation, DNA replication, membrane fusion events and signal transduction (Davey *et al.*, 2002; Bar-Nun and Glickman, 2012). Some of the best studied members are linked to protein degradation, such as components of the 19S and 26S proteasome, and Cdc48/p97 (Bar-Nun and Glickman, 2012). Over the years a small number of these proteins have been found to be involved in chromatin associated processes, including Cdc48, ATAD2/Yta7, Pontin/Rvb1, and Reptin/Rvb2. However to date ATAD2/Yta7, and its homologues, alone have been shown to be capable of direct physical interaction with chromatin subunits and have been demonstrated to fulfil roles strikingly similar to histone chaperones.

1.6.1 ATAD2/Yta7

Human ATAD2 (also known as ANCCA) is an evolutionarily conserved AAA ATPase. These proteins function under diverse cellular contexts with only a minor subset involved in nuclear functions. The human homologues, ATAD2 and ATAD2B, have primarily been of interest for their association with cancer development and progression; however they appear to exert their effect through chromatin maintenance roles. Over-expression of ATAD2 is a strong indicator of poor prognosis in various cancers, including breast, prostate, lung, liver, and ovarian cancers (Zou *et al.*, 2009; Fouret *et al.*, 2012; Salhia *et al.*, 2014; Wan *et al.*, 2014; Wu *et al.*, 2014; Zou *et al.*, 2014). Recently, the up-regulation of ATAD2 has also been linked to resistance to

current cancer therapies (Murakami *et al.*, 2013).

1.6.1.1 Characterization and Composition

ATAD2B is primarily expressed in the testis and the brain, principally during development, and has also been demonstrated to be misregulated during tumorigenesis (Leachman *et al.*, 2010). An increased expression of ATAD2B, particularly in the cytoplasm, has been detected in astrocytomas, glioblastomas and oligodendrogliomas, all of which are brain tumours (Leachman *et al.*, 2010). However, there is nothing known about the molecular function of ATAD2B, nor is there evidence at this time that it directly contributes to tumorigenesis.

Mice, like humans, have two isoforms of ATAD2, which differ by 300 amino acids. The shorter version lacks 300 bp from its N-terminal region (Caron *et al.*, 2010). This difference might also account for their differential localization; the longer isoform, which corresponds to the human ATAD2, is primarily associated with chromatin while the shorter one is soluble and can be found in the cytoplasmic fractions (Caron *et al.*, 2010). ATAD2 contains a bromodomain, which in mammals has been shown to be important for binding to acetylated H3 and H4 tails (Ciró *et al.*, 2009; Caron *et al.*, 2010). In addition to its bromodomain, ATAD2 possesses two ATPase domains, which aid protein multimerization (Caron *et al.*, 2010) (Fig 1.14.A). ATAD2 without an active ATPase domain is unable to form multimers and in turn can not bind acetylated H4 peptides *in vitro* (Caron *et al.*, 2010).

ATAD2 is conserved throughout evolution, in fact *Drosophila* appears to be the only model organism without a homologue. In *S. cerevisiae* there is a single ATAD2 protein, termed Yta7. Unlike the mouse and human ATAD2, Yta7 does not require its bromodomain for recognizing specific acetyl lysine histone marks; rather the Yta7 N-terminal can recognize the histone backbone, which might allow it to carry out general chromatin maintenance functions. Initial biochemical and genetic analysis carried out in *S. cerevisiae* identified Yta7 as a component of a large molecular weight complex that interacts with chromatin around the *HMR* boundary region. It was found to co-purify with the Pol ϵ subunit Dbp4, with various chromatin remodelers such as Dls1, Itc1 and Iswi2, as well as histone proteins (Tackett *et al.*, 2005). In a more recent study, Yta7 was shown to further co-purify with members of the FACT complex (Spt16 and Pob3), the

histone chaperone Rtt106, members of the RSC complex, subunits of the CK2 complex as well as further subunits of RNA Pol II (Kurat *et al.*, 2011).

1.6.1.2 Regulation of gene expression by ATAD2/Yta7

Current understanding in cancer biology is that genes which are normally expressed in a tissue-specific manner are especially potent in causing malignant transformations. Furthermore, genes that drive germline differentiation are particularly enriched within this group. ATAD2 fits both of these criteria as its normal expression is predominantly limited to male germ cells (Caron *et al.*, 2010). ATAD2 has been shown to be a transcriptional regulator of estrogen responsive genes as well as of the estrogen receptor $E\alpha$ (Zou *et al.*, 2007). This function of ATAD2 is dependent on its ATPase domain, as mutations in this region render ATAD2 defective as a co-activator of estrogen (Zou *et al.*, 2007). On the other hand, ATAD2 is also amongst estrogen responsive genes. Therefore, up-regulation of ATAD2 leads to a positive feedback loop; resulting in amplification of ATAD2 mRNA and protein levels (Fig 1.14.B).

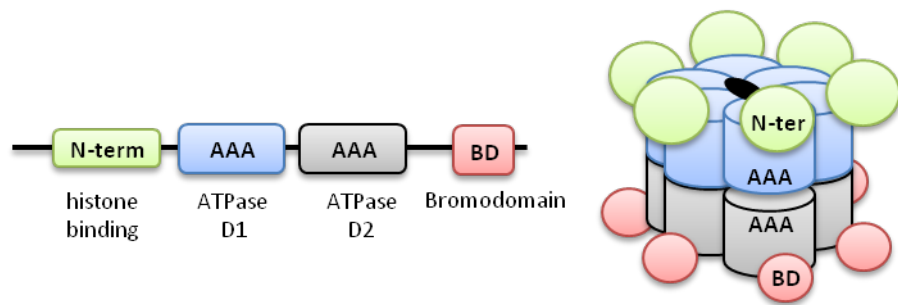
ATAD2 is also responsible for the regulation and activation of androgen responsive genes (Zou *et al.*, 2009). Additionally, ATAD2 has been shown to interact with E2F transcription factors and is required for the induction of E2F target genes (Revenko *et al.*, 2010). Finally, ATAD2 has been shown to interact with MYC and to act as a co-factor alongside MYC in transcriptional activation (Ciró *et al.*, 2009). Thus, ATAD2 is not only required in response to hormonal signals, agreeing with its role in development, but is also needed for general regulation of transcription. This makes the scope of ATAD2 targets extremely large and diverse, allowing plenty of opportunity for malignant transformations.

In addition to studies of cancer cell lines, several groups have demonstrated that the *S. cerevisiae* Yta7 acts both to repress and activate transcription of a variety of genes. Initial genetic analysis indicated that YTA7 acts through a functionally overlapping pathway with members of the HIR complex, as well as Spt16 (component of FACT) and Asf1 (Gradolatto *et al.*, 2008) to suppress histone gene transcription outside of S phase (Gradolatto *et al.*, 2008; Fillingham *et al.*, 2009). Yta7 binds to regions of the *HTA1-HTB1* locus, alongside RSC and Rtt106. During S phase Yta7 gets hyperphosphorylated

by the cyclin-dependent kinase catalytic subunit Cdk1 and by the casein kinase CK2 (Ubersax *et al.*, 2003; Kurat *et al.*, 2011). This phosphorylation event leads to the dissociation of Yta7 from the chromatin, which in turn destabilizes RSC. RNA Pol II gets recruited and transcription of the loci takes place (Fig 1.15.A). In the absence of Yta7 phosphorylation, dissociation of Yta7 is compromised and histone gene transcription levels are decreased as a result. Also, in a *yta7*Δ mutant or in the absence of a functional AAA-ATPase domain, positioning of both Rtt106 and RSC is altered, leading to the formation of repressive chromatin and once again reduced levels of histone gene transcripts (Kurat *et al.*, 2011) (Fig. 1.15.B).

In addition to regulating histone gene induction, Yta7 has been shown to be required for optimal induction of non-constitutively expressed genes (Lombardi *et al.*, 2011). Microarray analysis of *yta7*Δ cells grown in rich media revealed a down regulation of genes which are required under inducible conditions, such as meiosis and sporulation (Lombardi *et al.*, 2011). Furthermore, Yta7, as well as H2A.Z, were required for proper *GAL* gene induction. It is likely that Yta7 acts by removing histone H3 from nucleosomes, a hypothesis supported by the fact that *yta7*Δ cells are sensitive to changes to histone dosage. *yta7*Δ mutants grow better upon deletion of one of the two copies of the histone H3-H4 gene pair (Lombardi *et al.*, 2011), indicating that histone H3-H4 levels are increased in this mutant. Indeed, H3 chip at the *GAL* promoter as well as digestions of bulk chromatin by MNase suggest that *yta7*Δ cells are over-accumulating nucleosomes (Lombardi *et al.*, 2011).

(A)



(B)

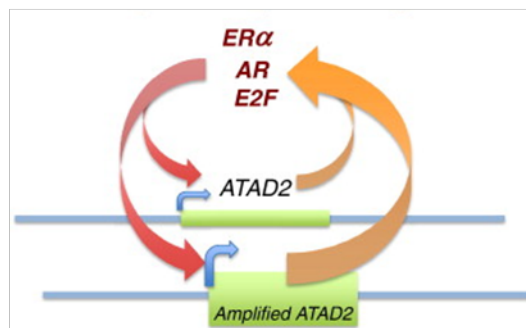


Figure 1.14 Structure and function of ATAD2/Yta7.

(A) Diagram of ATAD2/Yta7 protein domains and folding. Yta7/ATAD2 proteins contain a N-terminal domain, which recognizes the histone backbone, two AAA-ATPase domains and a bromodomain. ATAD2/Yta7 is likely to form a homohexameric ring, with the N-terminal and bromodomain facing the opposite direction, and a nuclear pore in the middle. **(B) Feedback loop of ATAD2 upregulation in tumours.** ATAD2 mediates the expression of estrogen receptor alpha (ER α), the androgen receptor (AR) and a number of E2F target genes. It is also regulated by the same factors. Therefore, upregulation of ATAD2 leads to a positive feedback loop, increasing the levels of proteins that are responsible for its induction, thus leading to amplification of ATAD2 itself. Taken from (Boussouar *et al.*, 2013).

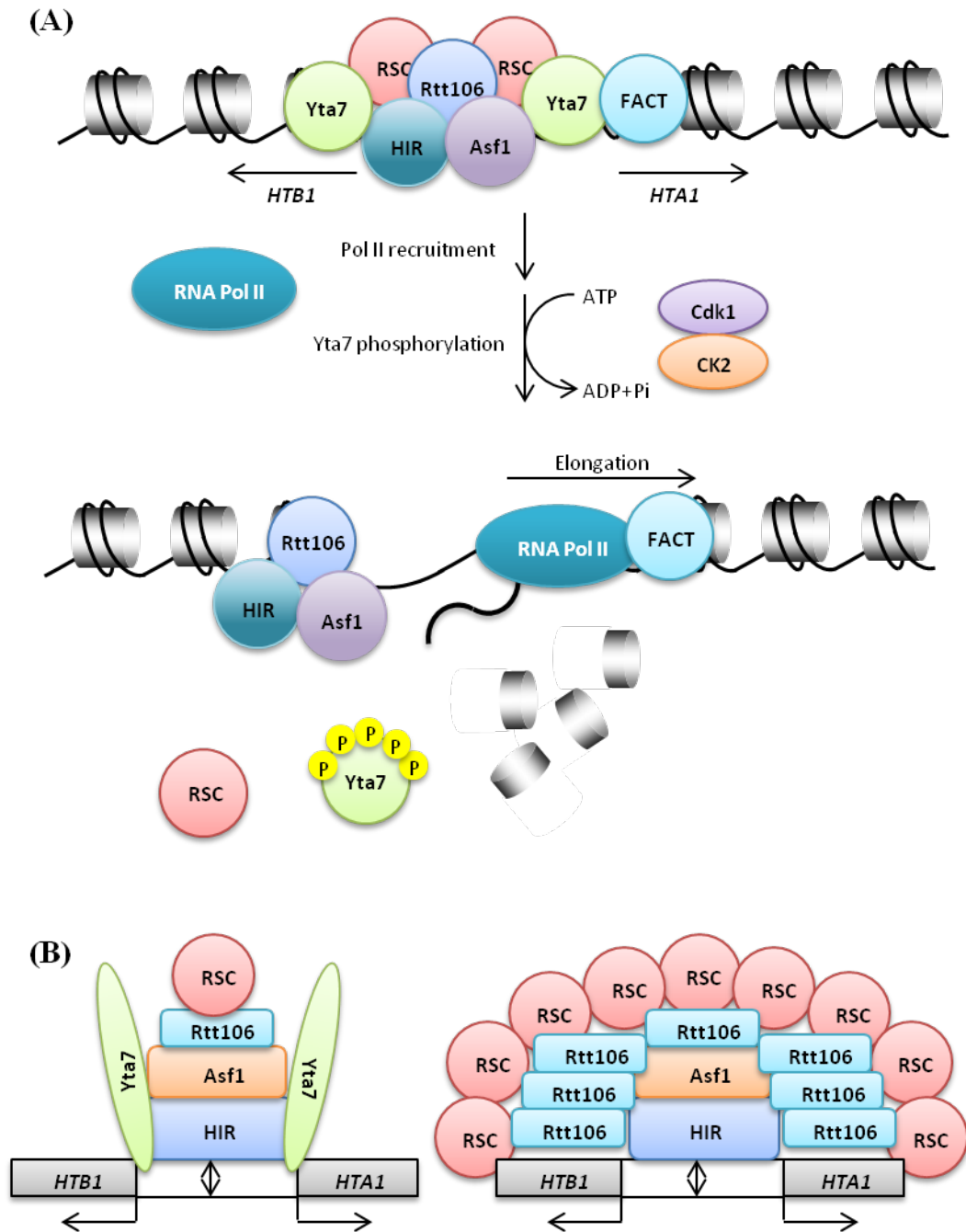


Figure 1.15 The role of Yta7 over the *HTA1-HTB1* locus

(A) The presence of Yta7 over the *HTA1-HTB1* locus prevents histone gene transcription outside of S phase. In S phase, Yta7 is phosphorylated by Cdk1 and CK2, which allows proper recruitment and elongation by RNA Pol II. **(B)** Outside of S phase, Yta7 acts as a boundary element over the histone gene promoter *HTA1-HTB1*, preventing the spreading of repressive chromatin. In the absence of Yta7, increased recruitment of Rtt106 and RSC takes place, and heterochromatin-like silencing spreads. Adapted from (Kurat *et al.*, 2011; Zunder and Rine, 2012).

1.6.1.3 Yta7 as a boundary element

Yta7 was initially identified as a boundary element, restricting the spread of heterochromatin independently of the HMR-tRNA genes (Jambunathan *et al.*, 2005). In the absence of *YTA7*, silencing was shown to have increased around the boundary region of the *HMR* locus, suggesting that Yta7 is required to maintain active transcription on, and adjacent, to the boundary (Jambunathan *et al.*, 2005; Tackett *et al.*, 2005). The ATPase domain of Yta7 is essential for its boundary function (Kurat *et al.*, 2011), and although its bromodomain isn't required for association of Yta7 with chromatin barriers, it is required for proper barrier activity (Gradolatto *et al.*, 2009).

1.6.1.4 Further associated functions of Yta7

In addition to its role in regulating transcription and maintaining appropriate heterochromatin boundaries, Yta7 has been implicated in telomere maintenance too (Askree *et al.*, 2004). Loss of *YTA7* leads to a shortening of the telomeres by about 50-100 bp (Askree *et al.*, 2004). Finally, Yta7 physically interacts with the checkpoint kinase Rad53 upon MMS induced DNA damage (Smolka *et al.*, 2005). Hence, it might play a role in the DNA damage response pathway. Although the molecular function of ATAD2 is not particularly well characterized, the fact that the *S. cerevisiae* homologue both physically and genetically interacts with histone chaperones, as well as a number of chromatin associated factors, indicates that it is likely to play a role in general chromatin maintenance.

Recent work carried out in our lab has also identified two Yta7 homologues in *S. pombe*, termed Abo1 and Abo2 (Murton, 2012). Viable single mutants can be generated; however the *abo1Δabo2Δ* double mutant is inviable (Murton, 2012). Loss of *abo1*⁺, but not *abo2*⁺ results in a mild cell cycle delay, as evident by an elongated phenotype (Murton, 2012). In addition Abo1, but not Abo2 is required for repression of transcription of Tf2 elements and solo LTRs (Murton, 2012). Similarly, *abo1Δ* cells but not *abo2Δ* are sensitive to DNA damaging agents, and produce antisense transcripts from the *hrp1*⁺ loci. Also, Abo1 is required for proper silencing of pericentromeric heterochromatin, and silencing of the mating type loci (Murton, 2012). Finally, loss of *abo1*⁺ leads to segregation defects and reduced spore viability following meiosis

(Murton, 2012) Interestingly, the barrier activity that is attributed to Yta7 in *S. cerevisiae* is provided by Abo2 alone, as loss of *abo1*⁺ has no effect on the spread of heterochromatin (Murton, 2012). Therefore, some of the chromatin maintenance functions associated with Yta7 have clearly diverged between the two *S. pombe* proteins. Finally, the phenotypes associated with loss of *abo1*⁺ are very similar to that of HIRA deficient *S. pombe* cells. Therefore, it is possible that like HIR and Yta7 in *S. cerevisiae*, HIRA and Abo1 in *S. pombe* participate in similar pathways.

1.7 Project Aims

The conserved AAA-ATPase, ATAD2/Yta7 has previously been associated with chromatin regulatory roles; however the precise contribution of this protein to global chromatin architecture has not yet been determined. In addition, the HIRA histone chaperone has been studied for a number of years and has been well characterized in its role in heterochromatin maintenance; nonetheless it is still not clear to what extent it contributes to global chromatin architecture. Therefore, the initial aim of the work presented here was to determine the nucleosome profiles of *S. pombe* cells in the absence of ATAD2/Yta7 homologue, Abo1, and in cells lacking HIRA. Further characterization of the function of Abo1 in chromatin maintenance was undertaken, while the role of HIRA in the DNA damage response was characterized. In addition, previous work has hinted at a role for HIRA in quiescence exit, therefore the mechanism behind HIRA-mediated quiescence maintenance was further explored.

Chapter 2

Materials and Methods

2.1 General laboratory supplies

General laboratory chemicals, including those that were used to make media were purchased from Sigma-Aldrich, Fisher Scientific, BD Biosciences, VWR, Melford, and Formedium.

2.2 Strains and media

2.2.1 *Escherichia coli*

Cultures of *E. coli* SURE cells (*e14*⁻ [*mcrA*] Δ [*mcrB*-*hsdSMR*-*mrr*] 171 *endA1 supE44 thi-1 gyrA96 relA1 lac recB recJ sbcC umuC::Tn5[kan^r] ucrC [F'*proAB lac*^q Δ *mis Tn10 (Tet^rO)*]) were grown in Luria-Bertani (LB) medium (2% [w/v] Bacto-tryptone, 1% [w/v] Bacto-yeast extract, 1% [w/v] NaCl [pH 7.2]). Bacto-agar (2% [w/v]) was added for solid media. When required, Ampicillin (Sigma) was added to a final concentration of 0.1 mg/ml.*

2.2.2 *Schizosaccharomyces pombe*

S. pombe cells were grown in rich YE5S media (0.5% [w/v] yeast extract, 3% [w/v] glucose and 225 mg/L adenine, histidine, leucine, uracil and lysine hydrochloride). When required 500 μ g/ml Geneticin (G418) was added to the media post sterilisation. For selection based on amino acid auxotrophy, cells were grown in Edinburgh minimal medium (EMM) (3 g/L potassium hydrogen phallate, 2.2 g/L Na₂HPO₄, 5 g/L NH₄Cl, 2% [w/v] glucose, 20 ml/L salts [52.5 g/L MgCl₂·6H₂O, 0.735 g/L CaCl₂·2H₂O, 50 g/L KCl and 2 g/L NaSO₄], 1 ml/L vitamins [1 g/L pantothenic acid, 10 g/L nicotinic acid, 10 g/L inositol and 10 mg/L biotin], 0.1 ml/L minerals [5 g/L boric acid, 4 g/L MnSO₄, 4 g/L ZnSO₄·7H₂O, 2 g/L FeCl₂·6H₂O, 0.4 g/L molybdic acid, 1 g/L KI, 0.4 g/L CuSO₄·5H₂O and 10 g/L citric acid] supplemented with the appropriate amino acids. Solid media were prepared by the addition of bacto-agar (2% [w/v]). For long-term storage cells were kept in 40% glycerol in YE5S and stored at -80°C. *S. pombe* strains used in this study are listed in table 2.1.

Table 2.1 *S. pombe* strains

Identification Number	Strain Name	Genotype	Source
CsG156	<i>abo1</i> Δ	<i>h⁻ abo1::kanMX</i>	This study
EL313	<i>spt16-GFP</i>	<i>h⁺ Spt16-L-GFP-kanMX ade6-M210 arg3-D4 his3-D1 leu1-32 ura4-DS/E</i>	Robin Allshire
EL306	<i>pob3-HA</i>	<i>h⁺ FPH-Pob3 otr1R(dg-glu) Sph1:ade6⁺ ade6-M210 leu1-32 ura4-D18</i>	Robin Allshire
EL130	<i>pob3-GFP</i>	<i>h⁻ pob3-L-GFP-kanMX otr1R(Sph1):ura4⁺ arg3-D4 his3-D1 leu1-32 ura4-DS/E</i>	Robin Allshire
SW921	<i>abo1-GFP</i>	<i>h⁺ ade6-M210 ard3D4 his3-D1 leu1-32 ura4-D18 abo1-GFP::kanMX6</i>	Lab stock
SW865	<i>abo1-PK</i>	<i>h⁻ ade6-M216 leu1-32 ura4-D18 abo1-PK::ura4⁺</i>	Lab stock
CsG338	<i>sp16-GFP</i> <i>abo1-PK</i>	<i>h⁺ spt16-L-GFP-kanMX abo1-PK::ura4⁺ ade6-M^x ura4^x leu1-32</i>	This study
CsG345	<i>abo1</i> Δ <i>spt16-GFP</i>	<i>h⁻ spt16-L-GFP::kanMX abo1::kanMX ade6-M21^x leu1-32 ura4D^x his^x arg^x</i>	This study
CsG346	<i>abo1</i> Δ <i>pob3-GFP</i>	<i>h⁻ pob3-L-GFP-kanMX abo1::kanMX leu1-32 ura4D^x ade6^x his3^x arg3^x</i>	This study
CsG351	<i>pob3-GFP</i> <i>abo1-PK</i>	<i>h^x pob3-L-GFP-kanMX abo1-PK::ura4⁺</i>	This study
CsG352	<i>abo1-GFP</i> <i>pob3</i> Δ	<i>h^x abo1-GFP::kanMX pob3::natMX</i>	This study
CsG360	<i>spt16-18</i> <i>abo1-GFP</i>	<i>h^x abo1::kanMX6 spt16-18::kanMX le1-32 ura4^x his3^x</i>	This study
CsG354	<i>clr4</i> Δ <i>imr1R</i>	<i>h^x clr4::kanMX imr1R(NcoI)::ura4⁺ ori1 ura4-DS/E leu1-32 ade6-M21^x</i>	This study
CsG356	<i>clr4</i> Δ <i>otr1R</i>	<i>h^x clr4::kanMX otr1R(SphI)::ura4⁺ ura4-DS/E leu1-32 ade6-M210</i>	This study
SW235	<i>otr1R</i>	<i>h⁺ otr1R(SphI)::ura4⁺ leu1-32 ade6-M210 ura4-DS/E</i>	Lab stock
SW232	<i>imr1R</i>	<i>h⁺ imr1R(NcoI)::ura4⁺ ori1 ade6-M210 leu1-32 ura4-DS/E</i>	Lab stock
HM489	<i>abo1</i> Δ <i>otr1R</i>	<i>h⁺ otr(SphI)::ura4⁺ leu1-32 ade6-M216 ura4^x abo1::kanMX</i>	Lab stock
SW873	<i>abo1</i> Δ <i>imr1R</i>	<i>h⁺ imr1R(NcoI)::ura4⁺ ori1 ade6-M210 leu1-32 ura4-DS/E abo1::kanMX</i>	Lab stock

Identification Number	Strain Name	Genotype	Source
CsG363	<i>abo1-GFP</i>	<i>h^x abo1-GFP::kanMX6 swi6-kanMX</i>	This study
	<i>swi6Δ</i>		
SW577	<i>hip1Δ</i>	<i>h⁻ hip1::ura4⁺ ura4-D18</i>	Lab stock
CsG141	<i>set2Δ</i>	<i>h⁻ set2::kanMX</i>	This study
CsG142	<i>hip1Δ set2Δ</i>	<i>h⁻ set2::kanMX hip1::ura4⁺ ura4-D18</i>	This study
CsG1	<i>rad22-YFP</i>	<i>h⁻ rad22-YFP::kanMX</i>	This study
CsG2	<i>hip1Δ</i>	<i>h⁻ hip1::ura4⁺ ura4-D18 rad22-</i>	This study
	<i>rad22-YFP</i>	<i>YFP::kanMX</i>	
CsG25	<i>hip1-HBD</i>	<i>h⁺ hip1-HBD(est)::ura4⁺ ura4-D18</i>	This study
CsG74	<i>chk1-HA</i>	<i>h⁺ ade6-M704 leu1-32 ura4-D18 chk1-HA</i>	Lab stock
CsG83	<i>hip1Δ</i>	<i>h^x hip1::ura4⁺ chk1-HA</i>	This study
	<i>chk1-HA</i>		
CsG103	<i>chk1Δ</i>	<i>h^x chk1::ura4⁺ ura4-D18</i>	This study
CsG104	<i>cds1Δ</i>	<i>h^x cds1::ura4⁺ ura4-D18</i>	This study
CsG89	<i>hip1Δ rad3Δ</i>	<i>h^x hip1::kanMX rad3::ura4⁺ ura4-D18</i>	This study
CsG91	<i>hip1Δ chk1Δ</i>	<i>h^x hip1::kanMX chk1::ura4⁺ ura4-D18</i>	This study
CsG93	<i>hip1Δ cds1Δ</i>	<i>h^x hip1::kanMX cds1::ura4⁺ ura4-D18</i>	This study
SW201	<i>hip1-GFP</i>	<i>h⁺ ade6-M210 leu1-32 ura4-D18</i>	Lab stock
		<i>hip1GFP::ura4⁺</i>	
CsG136	<i>rad57Δ</i>	<i>h⁺ rad57::ura4⁺ ura4-D18 leu1-32 his7-</i>	Tim
		<i>366 ade6-M216</i>	Humphrey
SW751	<i>rad51Δ</i>	<i>h⁺ rad51::kanMX ade6-M^x leu1-32 ura4-</i>	Lab stock
		<i>D18</i>	
CsG135	<i>rad50Δ</i>	<i>h⁺ smt0 rad50::kanMX ura4-D18</i>	Tim
			Humphrey
CsG264	<i>exo1Δ</i>	<i>h⁺ exo1::kanMX ura4-D18 ade6^x leu1-32</i>	David
			Lydall
CsG260	<i>hip1Δ rad51Δ</i>	<i>h^x hip1::ura4⁺ ura4-D18 rad51::kanMX</i>	This study
CsG158	<i>hip1Δ rad50Δ</i>	<i>h⁻ rad50::kanMX hip1::ura4⁺ ura4-D18</i>	This study
CsG275	<i>hip1Δ exo1Δ</i>	<i>h^x exo1::kanMX hip1::ura4⁺ ura4-D18</i>	This study
CsG189	<i>ku70Δ</i>	<i>h⁻ ku70::ura4⁺ ura4-D18 ade6^x leu1^x</i>	This study
CsG195	<i>ku80Δ</i>	<i>h⁺ ku80::kanMX</i>	This study
CsG204	<i>lig4Δ</i>	<i>h^x lig4::ura4⁺ ura4-D18 leu1-32</i>	This study
CsG249	<i>hip1Δ ku80Δ</i>	<i>h^x ku80::kanMX hip1::ura4⁺ ura4-D18</i>	This study
CsG198	<i>hip1Δ ku70Δ</i>	<i>h^x ku70::ura4⁺ hip1::kanMX</i>	This study

Identification Number	Strain Name	Genotype	Source
CsG262	<i>hip1Δ lig4Δ</i>	<i>h^x hip1::ura4⁺ lig4::ura4⁺ ura4-D18</i>	This study
CsG46	<i>rad3Δ</i>	<i>h⁺ rad3::ura4⁺ ura4-D18</i>	This study
FP4	<i>yox1-PK</i>	<i>h⁻ yox1::3PK::ura4⁺ leu1-32 ura4-D18</i>	Brian
		<i>his7-366 ade6-M216</i>	Morgan
FP34	<i>yox1-PK</i>	<i>h⁻ yox1::3PK::ura4⁺ leu1-32 ura4-D18</i>	Brian
	<i>rad3Δ</i>	<i>ade6^x rad3::ura4⁺</i>	Morgan
CsG265	<i>yox1-PK</i>	<i>h⁻ yox1::3PK::ura4⁺ leu1-32 ura4-D18</i>	This study
	<i>hip1Δ</i>	<i>his7-366 ade6-M216 hip1::kanMX</i>	
CsG268	<i>yox1-PK</i>	<i>h⁻ yox1::3PK::ura4⁺ leu1-32 ura4-D18</i>	This study
	<i>hip1Δ rad3Δ</i>	<i>ade6^x rad3::ura4⁺ hip1::kanMX</i>	
AW046	<i>hrp3Δ</i>	<i>h⁺ hrp3::kanMX ade6-M21^x ura4-D18</i>	Lab stock
		<i>leu1-32</i>	
CsG349	<i>hrp3Δ hip1Δ</i>	<i>h⁻ hip1::ura4⁺ hrp3::kanMX</i>	This study
CsG168	<i>hip1Δ abo1Δ</i>	<i>h⁻ hip1::ura4⁺ abo1::kanMX ura4-D18</i>	This study
CsG116	<i>atg8-GFP</i>	<i>h⁻ atg8-GFP</i>	This study
CsG124	<i>atg8-GFP</i>	<i>h^x hip1::kanMX atg8-GFP</i>	This study
	<i>hip1Δ</i>		
CsG243	<i>hip1Δ hht2Δ</i>	<i>h⁻ hip1::kanMX hht2/hhf2::ura4⁺</i>	This study
	<i>hhf2Δ</i>		
CsG300	<i>rum1-HA</i>	<i>h⁻ rum1-HA</i>	Lab stock
CsG301	<i>rum1-HA</i>	<i>h^x hip1::kanMX rum1-HA</i>	This study
	<i>hip1Δ</i>		
SW7	<i>cig2-HA</i>	<i>h^x cig2-HA</i>	Lab stock
CsG328	<i>cig2-HA</i>	<i>h^x cig2-HA hip1::kanMX</i>	This study
	<i>hip1Δ</i>		
CsG14	<i>hht1Δ hhf1Δ</i>	<i>h⁻ hht1/hhf1::ura4⁺ hht2/hhf2::ura4⁺</i>	This study
	<i>hht3Δ hhf3Δ</i>	<i>(otr1R (Sph1):ade6⁺)</i>	
CsG15	<i>hht2Δ hhf2Δ</i>	<i>h⁺ hht2/hhf2::ura4⁺ hht3.3/hhf3::ura4⁺</i>	This study
	<i>hht3Δ hhf3Δ</i>	<i>(otr1R (Sph1):ade6⁺)</i>	
CsG22	<i>hht1Δ hhf1Δ</i>	<i>h⁻ hht1/hhf1::ura4⁺</i>	This study
CsG23	<i>hht2Δ hhf2Δ</i>	<i>h⁻ hht2/hhf2::ura4⁺</i>	This study
CsG24	<i>hht3Δ hhf3Δ</i>	<i>h⁻ hht3/hhf3::ura4⁺</i>	This study

(ura4^x = ura4-D/SE or ura4-D18) (M^x = ade6-M210 or ade6-M216) (his3^x = histidine marker not determined) (ade6^x = adenine marker not determined) (leu1^x = leucine marker not determined) (h^x = mating type not determined)

2.2.3 Growth of *S. pombe* strains

Cells were cultured in either non-selective, nutrient rich YE5S media or Edinburgh minimal media (EMM) with the required supplements. Strains were grown on the appropriate agar plates at 30°C for 2-3 days and then stored at room temperature. Liquid cultures were prepared by inoculating a single colony or a loop of cells, taken from a fresh agar plate, into ~ 5 ml medium. Cultures were grown overnight with shaking at the appropriate temperature. Cell number was estimated by measuring the OD₅₉₅ (OD₅₉₅ 0.1 \approx 2 x 10⁷ cells/ml).

To induce quiescence entry, exponentially growing cells were harvested by centrifugation (3000 rpm for 2 minutes), washed three times in an equal volume of EMM-N (EMM medium lacking NH₄Cl) and resuspended in EMM-N at an OD₅₉₅ ~ 0.3. Cultures were further incubated at 30°C for the indicated times.

2.2.4 Genetic crosses and tetrad analysis

For genetic crosses freshly cultured strains of opposite mating types were mixed on EMMG agar plates (as EMM but 0.5 g/L sodium glutamate used in place of NH₄Cl) and incubated at 25°C for 48-72 hours. Light microscopy was used to check for spores and the correct genotype identified using tetrad analysis. Tetrad dissection was performed by micromanipulation of the asci onto YE5S agar plates using a Singer micro-manipulator. The spores were incubated at 30°C until colonies were visible and genotypes were determined by growth on selective media and/or PCR analysis. Table 2.2 contains the PCR primers used for genotyping in this study.

Table 2.2 PCR oligonucleotide primers for genotyping

Primer Name	DNA Sequence 5'-3'
MP	ACG GTA GTC ATC GGT CTT CC
MT1	AGA AGA GAG AGT AGT TGA AG
MM	TAC GTT CAG TAG ACG TAG TG
hht1_for	TGC ATA CCA ACT TGT ATC TAC
hht1_rev	GTA TAA TAC AGG CAA GCA GTC
hht2_for	CCA GAG TAA GTC AGA CAC AAG
hht2_rev	GAA TAA GTC AAG TGA GAA AGC
hht3_for	TAC ATT CCA CAA CAC TCA AGG
hht3_rev	GTA TTC AGC CGT GAT ACA ACG
abo1_up	AAC ACC CTA TAG TTA TCA GGC
abo1_down	AAT AAG CCA AGA GTC GGC TAG
hip1_inF	AAG ACT GCT CTA TTT ACT GCC
hip1_rev	CTA ATA TTC ACA GTG GAA GAC
lig4_inF	TCAGTCATTTGTTTCGTGTAGG
lig4_outR	CTGCAGCTTTAATATTACAAC

2.2.5 Analysis of cell viability

Cells were grown in liquid culture at 30°C with shaking until the culture reached an OD₅₉₅ of ~ 0.3. Cell concentration was adjusted to OD₅₉₅ 0.3 in 300 µl of YE5S and then cells were subjected to 5-fold serial dilutions in nanopure water. Cells were then transferred to agar plates using a 48 pin tool (Sigma). To test for sensitivity to genotoxic agents, the dilution series was transferred to YE5S plates supplemented with the appropriate agent at the appropriate concentration. To test for UV sensitivity plates were irradiated following spotting using a UV Stratalinker with the appropriate dose. Plates were incubated for 2-4 days at 30°C.

2.2.6 Yeast flow cytometry

Approximately 10⁷ cells were harvested and then resuspended in 1 ml ice cold 70% ethanol. A 0.3 ml aliquot was transferred into 3 ml of sodium citrate (pH 7.2) in a 15 ml Falcon tube, mixed and centrifuged at 2000 rpm in a bench top centrifuge for 5 minutes. Pellet was resuspended in 0.5 ml 50 mM sodium citrate (pH 7.2) supplemented with 0.1 mg/ml RNase A and was incubated at 37°C for 2 hours. Nuclei were stained by addition of propidium iodide to a final concentration of 4 µg/ml. Cells were analysed using a FACS Canto II flow cytometer (BD Biosciences), data was collected using FACSDiva and analyzed using Cyflogic.

2.3 DNA transformation

2.3.1 Transformation of *E. coli*

Competent *E. coli* cells were prepared as previously described (Dainty, 2007) and stored at -80°C. An aliquot of the prepared cells (50-100 µl) was defrosted and mixed with the transforming DNA. Cells were incubated on ice for 30 minutes, heat shocked at 42°C for 45 seconds, then were placed back on ice for a further 2 minutes. 300 µl of LB was added to tubes, which were incubated at 37°C for 30-60 minutes. Cells were plated onto LB agar plates supplemented with Ampicillin and incubated at 37°C overnight.

2.3.2 Transformation of *S. pombe*

Cells were cultured in YE5S at 30°C until they reached an OD₅₉₅ 0.5. A 50 ml aliquot of cells was centrifuged for 3 minutes at 2000 rpm in a bench top centrifuge. The resulting pellet was washed sequentially in 1 ml nH₂O, 1 ml LiAc/TE (0.1 M lithium acetate, 10 mM Tris-HCl [pH 7.5], 1 mM EDTA [pH 8.0]) and resuspended in 1 ml LiAc/TE. A 100 µl aliquot of cells was mixed with 2 µl of sonicated salmon sperm DNA (10 mg/ml) and 5-10 µl of the transforming DNA (up to ~1 µg) and was incubated at room temperature for 10 minutes. 260 µl of PEG/LiAc/TE was added (40% PEG-4000 [v/v], 0.1 M lithium acetate, 10 mM Tris-HCl [pH 7.5], 1 mM EDTA [pH 8.0]) to the mixture and cells were incubated at 30°C for a further 30-60 minutes. 43 µl of DMSO was added to the cells, which were heat shocked at 42°C for 5 minutes. Cells were washed once in 1 ml nH₂O, resuspended in 250 µl nH₂O and then plated onto appropriately supplemented EMM agar plates.

2.4 DNA isolation

2.4.1 Plasmid isolation from *E. coli*

An LB culture (5 ml) with ampicillin was inoculated with a single colony and grown at 37°C overnight. DNA isolation was performed using GelElute Plasmid Miniprep (Sigma) kit according to manufacturer's instructions.

2.4.2 Isolation of *S. pombe* genomic DNA

A 1 ml aliquot of a saturated overnight YE5S culture was centrifuged at 8000 rpm and the resulting pellet was washed with 1 ml dH₂O and resuspended in Breakage Buffer (10 mM Tris-HCl [pH 8.0], 1 mM EDTA [pH 8.0], 100 mM NaCl, 1% SDS (w/v), 2% Triton-X100). 200 µl of glass beads (0.5 mm Biospec) and an equal volume of phenol:chloroform:isoamyl alcohol (25:24:1) (pH 8.0) was added to the cells which were then disrupted using a mini bead beater (Biospec Products) for 20 seconds on full power. 500 µl of Breakage Buffer was added and cells were centrifuged at 13300 rpm for 5 minutes. The supernatant was added into a fresh tube containing 0.1 volume of 3 M sodium acetate (pH 5.2) and two volumes of 100% ethanol. Tubes were incubated at -20°C for at least an hour, pelleted and then centrifuged at 13300 rpm for 15 minutes.

Supernatant was removed and the pellet was washed in 70% ethanol, dried and resuspended in 100 μ l of nH_2O .

2.5 DNA manipulation and analysis

2.5.1 Polymerase chain reaction (PCR)

The oligonucleotide primers used in this study are shown above in table 2.2.

S. pombe genomic DNA was extracted as described in section 2.4.2 and approximately 1 μ l (50 ng) was used per 25 μ l reaction. A typical reaction consisted of 1x Phusion GC buffer (NEB), 20 μ M dNTPs, 0.5 μ M forward and reverse primers, 50 ng template DNA, 1 μ M DMSO and 1 U Phusion polymerase (NEB). Standard PCR conditions were 95°C for 30 seconds, 35 cycles (95°C for 30 seconds, X°C for 30 seconds, 68°C for Y minutes), 68°C for 5 minutes. Where, X was generally set at 4°C below the lowest melting temperature of the forward and reverse primers, and Y, the extension time, was calculated based upon approximately 30 seconds/kb.

2.5.2 Analysis of DNA by gel electrophoresis

2.5.2.1 Agarose gel electrophoresis

Generally DNA was separated on 1-1.5% agarose 1% TAE (40 mM Tris Base, 20 mM acetic acid, and 1 mM EDTA [pH 8.0]) gels, unless specified otherwise. DNA was stained using 500 ng/ml ethidium bromide. Fermentas 1 kb ladder and NEB low molecular weight ladders were used to help determine the size of the DNA products. The DNA was then observed using a UV transilluminator and an image captured using Quantity-One (BioRad).

2.5.2.2 Contour-clamped homogeneous electric field (CHEF) pulsed field gel electrophoresis (PFGE)

Buffers, enzymes and the agarose were provided in the CHEF Yeast Genomic DNA Plug Kit (Bio-Rad). Cultures were grown to about 6×10^6 cells/ml in 50 ml YE5S cultures. Cell number was measured using a Scharfe cell counter (Casy® Cell Counter and Analyzer TT). 4×10^8 cells/ml were washed and resuspended in 1 ml of 0.5 M ice cold EDTA (pH 8.0), centrifuged at 6000 rpm for 2 minutes at 4°C, and resuspended in

146 µl cell suspension buffer at room temperature. 7 µl lyticase stock was added and immediately mixed.* 84 µl 2% clean-cut agarose at 60°C was added to the mixture, cells were vortexed for 5 seconds and pipetted into two plug moulds and were allowed to solidify for 30-60 minutes at 4°C. Once the plugs had solidified, they were transferred to 2 ml Eppendorfs and 188 µl lyticase buffer as well as 7 µl lyticase per plug was added. Plugs were incubated overnight at 37°C without agitation. Plugs were washed with 1 ml nH₂O and digested overnight in 188 µl proteinase K buffer and 7.5 µl proteinase K per plug at 50°C. Proteinase K solution was removed and plugs were washed three times in 330 µl 1x Wash buffer supplemented with 1 mM PMSF. Plugs were stored at 4°C until chromosome fractionation. DNA was separated on 0.6% Megabase agarose gel prepared in 1 x TAE (40 mM Tris Base, 20 mM acetic acid, and 1 mM EDTA [pH 8.0]) using a CHEF DR III system (BioRad). Gels were run on a voltage gradient of 2 Vcm⁻¹ for 48 hours at 14°C, with an induced angle of 106° and initial and final switch times of 1200 seconds and 1800 seconds respectively. Visualization of the DNA was achieved by staining with 250 ml 1 x TAE containing 1 µg/ml ethidium bromide for 1-2 hours. Images were obtained using the UV transilluminator and were captured using Quantity-One (BioRad).

*For nitrogen starved (G₀) cells Sigma lyticase (L2524) at 5 mg/ml in CES buffer (20mM citrate/phosphate [pH 5.6], 40 mM EDTA [pH 8.0], 1.2 M sorbitol) was used instead. A 10 µl aliquot was added to plugs during overnight incubation in lyticase buffer.

2.5.3 Micrococcal Nuclease digestion (MNase) assay

2.5.3.1 MNase digestion

Cells were grown to an OD₅₉₅ =0.75-0.8 in 100 ml YE5S at 30°C, crosslinked with a final concentration of 1% formaldehyde (Sigma F8775) for 20 minutes at 30°C and quenched by the addition of glycine to 125 mM. Cells were washed with CES buffer (20 mM citrate/phosphate [pH 5.6], 40 mM EDTA [pH 8.0], 1.2 M sorbitol) supplemented with 10 mM β-mercaptoethanol and resuspended in 500 µl CES buffer with 0.5-1.0 mg Zymolyase-100T*. Cells were spheroplasted by gentle shaking at 30°C for up to 45 minutes, washed with ice cold 1.2 M sorbitol and resuspended in 800 µl NP-S buffer (1.2 M sorbitol, 10 mM CaCl₂, 100 mM NaCl, 1 mM EDTA [pH 8.0], 14 mM β-mercaptoethanol, 50 mM Tris-HCl [pH 8.0], 0.075% NP-40, 5 mM spermidine, 0.1 mM

PMSF, 1% Sigma protease inhibitor cocktail [Sigma P8215]). Spheroplasts were divided up into four 200 µl aliquots, each mixed with 300 µl of NP-S buffer. MNase was added at the indicated concentrations and samples were digested for 10 minutes at 37°C. MNase activity was terminated by the addition of EDTA (pH 8.0) and SDS to the final concentrations of 50 mM and 0.2% (w/v) respectively. Samples were incubated at 65°C overnight with 0.2 mg/ml proteinase K and 10 µg RNase A. DNA was subsequently purified by phenol:chloroform extraction followed by ethanol precipitation. Samples were resuspended in 30-50 µl nH₂O and analyzed on 1.2% 1 x TBE gels (89 mM Tris-HCl, 89 mM boric acid, 2 mM EDTA [pH 8.0]).

* Nitrogen starved (G₀) cells were incubated in 500 µl of 7 mg/ml lyticase (Sigma L-5263-200KU) (in CES buffer) and 500 µl of 5 mg/ml lysing enzymes (Sigma L-1412) (in CES buffer) on a shaker at 30°C for between 2-2.5 hours.

2.5.3.2 MNase dephosphorylation for sequencing

A set of three MNase treated samples were pooled and the volume adjusted to 80 µl with nH₂O. 10 µl of T4 polynucleotide kinase buffer (NEB) and 10 µl of native T4 polynucleotide kinase (NEB MO201S/L 10x) were added. Samples were incubated at 37°C for 30 minutes, before the addition of 300 µl of TE (pH 8.0) and an equal volume of phenol:chloroform:isoamyl alcohol (pH 8.0). Samples were vortexed for 10 seconds then centrifuged for 5 minutes at 13 000 rpm. DNA was precipitated with 0.1 volume of sodium acetate (pH 5.2) and 2 volumes of 100% ethanol followed by incubation at -20°C for at least 30 minutes. Samples were resuspended in 70 µl of TE (pH 7.5). DNA concentration was measured using a Nanodrop Spectroph and samples were analyzed on a 1.2% 1 x TBE agarose gels in order to provide a picture for the sequencing service. 11 µg of DNA was transferred to 52 µl TE (pH 7.5). These samples were used for sequencing and used to generate information on nucleosome positioning and occupancy.

2.5.3.3 MNase-sequencing

Preparation for sequencing was performed by the University of Exeter sequencing service. Briefly, DNA fragments were end repaired, 3'-adenylated, and ligated to indexed adapters without size selection using Nextflex reagents (Newmarket Scientific, UK). Libraries were amplified with 8 cycles PCR using Kapa HiFi PCR master mix (Anachem), primers removed with GeneRead size selection protocol (QIAGEN) before

quantification by Bioanalyser DNA 7500 assay. Libraries were pooled, denatured, diluted to 6 nM before clustering in a single lane of a high output Illumina flowcell. Sequencing (100 nt) was undertaken on a HiSeq 2500 using TruSeq SBS v3 reagents (Illumina).

2.5.3.4 MNase-qPCR

MNase digests of wild type and *hip1*Δ cells were performed as described above (Section 2.5.3.1). For each strain three biological replicate samples were pooled and analysed on 1% TAE agarose gels. Gel slices containing mononucleosomal DNA were excised, frozen at -80°C and spun through 0.45 μM Spin-X columns (Costar). Samples were phenol extracted and ethanol precipitated and resuspended in TE (pH7.5). dsDNA concentration was measured using a Qubit fluorometer (Life Technologies). 20 ng of mononucleosomal DNA was used in qPCR reactions using the PrimerDesign Mastermix kit. Reactions using genomic DNA were included as a control. 10 μl Mastermix, 1 μl Primermix (1:10 dilution), 1 μl DNA, 8 μl PCR grade nH₂O were added per reaction. Reactions were analyzed using a Rotor Gene 6000 Real-Time thermocycler with the following settings: Step 1 10 minutes at 95°C, Step 2 15 sec at 95°C, Step 3 60 sec at 5°C, steps 2 and 3 are repeated for 50 cycles. A melt curve was generated at the end of each run to assess primer specificity. The primers used for this analysis are listed in Table 2.3.

Table 2.3 MNase-qPCR oligonucleotide primers

Primer name	DNA sequence 5'-3'
dg_rep_nuc_3759432_for	AAT TCG GGT CAT ACT TCG TG
dg_rep_nuc_3759372_rev	CAA TCA TAC TCG AAA AAA AAG AAA TC
dh_rep_nuc1_3755019_for	GTT AAA AGT GGC AGA AAG TG
dh_rep_nuc1_3755069_rev	ATA TGC GTT GGG TTA TCT CA
dh_rep_nuc2_3756009_for	TTC GTT CAA ATG ATA TTA AT
dh_rep_nuc2_3756069_rev	GTG TTT TTT ATA CCT ATT TG
hht2_-120_for	GTA GCG GGG AAG CCG AAA TC
hht2_-80_rev	CAA TCA CAA CCC TAA CCC TG
Tf2_nuc_85_for	GAA CAT TTA ATA AAC CTT TTT GC
Tf2_nuc_140_rev	ATC GAA TTT CCC TAT CTC TG
hrp1_Nuc_peak_314_for	AAT CAT GAA AAT TCT TTC GC
hrp1_Nuc_peak_371_rev	ATC ATC AAA GGC AGA AGA CG
dbp7_10-80bp_for	ACC ATT GCT TCT CAA TTT TG
dbp7_10-80bp_rev	CGA CTA GAC TTC AAG GCT TC
dbp7_1927-1985_for	ATG CGT GAC CTT CAT TTG GG
dbp7_1927-1985_rev	GCG CTT CTC GCA AAG CGA AG
hrp1_5137-5225_for	CTG AGT TAA AAT ACA CAT CTG
hrp1_5137-5225_rev	TAA TAT TCG TCG ACC AAA GG

2.5.4 Chromatin immunoprecipitation (ChIP)

For each ChIP reaction, a 50 ml culture was grown to approximately 5×10^6 cells/ml and fixed by the addition of formaldehyde (Sigma F8775) to a final concentration of 1% and incubated at room temperature for 15 minutes. Fixation was stopped by the addition of glycine to 125 mM. Cells were washed twice with 50 ml ice cold 1 x PBS (137 mM NaCl, 2.7 mM KCl, 10 mM Na_2HPO_4 , and 1.8 mM KH_2PO_4), were transferred to ribolyzer tubes in 1 ml 1 x PBS, were pelleted and snap frozen in liquid nitrogen. Pellets were thawed on ice and 350 μl of ChIP lysis buffer (50 mM Hepes-KOH [pH 7.5], 140 mM NaCl, 1 mM EDTA [pH 8.0], 1% [v/v] Triton X-100 and 0.1% [w/v] sodium deoxycholate) supplemented with 1% yeast protease inhibitors (Sigma P8215) and 1 mM PMSF was added to the samples, along with 500 μl of glass beads (0.5 mm). Cells were disrupted using a mini-beadbeater (Biospec) with 2 x 2 minute pulses with 1 minute on ice in between. The bottom of the tubes was pierced and lysate was collected in a fresh Eppendorf tube by centrifuging at 1000 rpm for 1 minute at 4°C. Lysates were quickly vortexed and sonicated using a cooled Diagenode Twin sonicating waterbath with 6 x 5 minute pulses of 30 sec ON/OFF cycle. Following sonication samples were cleared by centrifuging at 13000 rpm for 10 minutes at 4°C; the supernatant was transferred to a fresh tube and centrifuged again at 13000 rpm for 10 minutes at 4°C. The supernatant was transferred to a fresh tube and was pre-cleared by incubating with rotation at 4°C for 1 hour using 50:50 slurry of Sepharose protein A beads along with ChIP lysis buffer. Beads were pelleted by low speed centrifugation for 2 minutes at 4°C and 300 μl from the supernatant was transferred to a fresh tube. 30 μl of this was transferred to another Eppendorf as the whole cell extract (WCE) and was frozen at -20°C. To the remaining sample, 25 μl of protein A beads were added along with the appropriate antibody (1.5 μl histone H3, 1 μl anti-GFP, 1 μl H3K9me2) and samples were incubated overnight with rotation at 4°C. Beads were pelleted by centrifugation at 4°C for 2 minutes in a microfuge. Supernatant was removed and beads were washed with 1 ml of each of the following buffers in this order: ChIP lysis buffer for 5 minutes at 4°C with rotation, ChIP lysis buffer with 0.5 M NaCl for 10 minutes at 4°C with rotation, Wash buffer (10 mM Tris-HCl [pH 8.0], 0.25 M LiCl, 0.5% NP-40, 0.5% [w/v] SDS, 1 mM EDTA [pH 8.0]) for 10 minutes at 4°C with rotation and finally TE (pH 8.0) for 5 minutes at 4°C with rotation. Between each wash beads were pelleted at low speed and kept cold. On the final wash all supernatant was removed and 100 μl 10% Chelex-100 resin was added to each IP and 10 μl to each WCE. All samples were incubated at

100°C for 12 minutes, cooled at room temperature, 1.5 µl of 25 mg/ml Proteinase K was added to each tube, following which all samples were incubated at 55°C for 30 minutes and then were once more incubated at 100°C for 10 minutes. Following final incubation samples were quickly centrifuged and supernatant was moved into a fresh Eppendorf. All IP samples were diluted 1:5 in nH₂O, whilst all WCE were diluted 1:400 in nH₂O. Quantitative-PCR reactions for analysis of ChIP DNA samples were carried out using Primerdesign PrecisionFast qPCR Mastermix using the following volumes: 10 µl Mastermix, 1 µl Primermix (1:10 dilution), 2 µl DNA, 7 µl PCR grade nH₂O. Reactions were analyzed using a Rotor Gene 6000 Real-Time thermocycler with the following settings: Step 1 10 minutes at 95°C, Step 2 15 sec at 95°C, Step 3 60 sec at 60°C, steps 2 and 3 are repeated for 50 cycles. A melt curve was generated at the end of each run to assess primer specificity. ChIP-qPCR primers used in this study are shown in table 2.4.

Table 2.4 ChIP-qPCR oligonucleotide primers

Primer name	DNA sequence 5'-3'
act1_For	GGC ATC ACA CTT TCT ACA ACG
act1_Rev	GAG TCC AAG ACG ATA CCA GTG
cen_dh_F	CCA GAC CAT TAC AAG CAC TAC ATA CG
cen_dh_R	GAA TCT TCT CTT GAA TAA AAC CGC C
qimr_for	CTA ATG CGG AGT AAG GCT AAT C
qimr_rev	TGG ACA GAA TGG ATG GAT ATT G
qdg_for	AAT TGT GGT GGT GTG GTA ATA C
qdg_rev	GGG TTC ATC GTT TCC ATT CAG
pot1_for	GAA GAA CGC ATT CAG CAT CA
pot1_rev	CAA TTT TCG TGC CAA ATC CT
msh1_for	ACA GGA TTT TGT CCG TCC AG
msh1_rev	AGC TGG AAC AAA GCT TCC AA
tlh1_for	TCG TGG TCA TAA ACG CAC AT
tlh1_rev	ATA CTC GGC GAA ATG AAT GG
adh1_for	AAC GTC AAG TTC GAG GAA GTC C
adh1_rev	AGA GCG TGT AAA TCG GTG TGG
ura4_for	TAC CTT TGG GAC GTG GTC TC
ura4_rev	CCC GTC TCC TTT AAC ATC CA
cnt1_for	CAG ACA ATC GCA TGG TAC TAT C
cnt1_rev	AGG TGA AGC GTA AGT GAG TG
tip41_for	CAC GCC TTG TCG TAC GTT TA
tip41_rev	ACG GCA GTC CTT CAA GAG AA
prm1_for	GAT TCG CTG GAG AAA GTT GC
prm1_rev	CGG AGA GAC TGG ATT TCA GG
tdh1_for	TGG CCA AGC CTA CCA ACT AC
tdh1_rev	GAA AGT TGG ATA CCG GCA GA
ars2004_for	CTT TTG GGT AGT TTT CGG ATC C
ars2004_rev	ATG AGT ACT TGT CAC GAA TTC
ars727_for	AAC ATA TAC GGT GAG ATG GGA T
ars727_rev	ATT CGT ATT TTC CAA TGC TT

2.5.5 Non-homologues end-joining (NHEJ) assay

Plasmids based on the pAL19 backbone but containing either two *PstI* sites (plasmid PS) or two *EcoRI* sites (plasmid PI) were linearized with the appropriate enzymes leading to the excision of a linear ~500 bp or ~540 bp DNA fragment respectively (Manolis *et al.*, 2001; Pai *et al.*, 2014). The now linear vector was gel purified and 1 µg was transformed into logarithmically growing cells (20 ml of OD₅₉₅ ~ 0.5) as described previously (Section 2.3.2), along with an undigested control plasmid (pAL19). All of the plasmids contain a *LEU2* marker, so NHEJ frequency was calculated as the percentage of *leu*⁺ colonies arising from cells transformed with the linear plasmid over those transformed with undigested DNA. At least three experiments were performed for each strain, and the average percentage rejoining calculated. Plasmids used in this study are listed in Table 2.5.

Table 2.5 Plasmids used in the NHEJ assay

Plasmid	Description	Source
PS	Based on pAL19 plasmid, contains a 500 bp linker fragment between two <i>PstI</i> sites	Tim Humphrey
PI	Based on pAL19 plasmid, contains a 540 bp linker fragment between two <i>EcoRI</i>	Tim Humphrey
pAL19	Contains a pUC backbone with <i>arsI</i> and <i>S. cerevisiae LEU2</i> .	Tony Carr

2.6 RNA extraction, manipulation and analysis

2.6.1 RNA extraction

Cells were cultured in the indicated medium to an OD₅₉₅ ~0.3, then a 50 ml aliquot was centrifuged and the pellet snap frozen in liquid nitrogen and stored at -80°C until required. Pellets were thawed on ice for 5 minutes, resuspended in 750 µl of TES (10 mM Tris-HCl, 10 mM EDTA [pH 8.0], 0.5% SDS [w/v]) and an equal volume of acidic phenol:chloroform (pH 5.2) (Sigma P1944), vortexed for 10 seconds and then incubated at 65°C for 1 hour. Samples were vortexed at 10 minute intervals for 10 seconds. Following the 1 hour incubation, samples were placed on ice for 1 minute, vortexed for 20 seconds and were centrifuged for 15 minutes at 14 000 rpm at 4°C. The aqueous layer was removed into heavy phase lock tubes (5Prime-2302810) containing 700 µl of

acidic phenol:chloroform, centrifuged for 5 minutes at 14 000 at 4°C. The top layer was removed and added to light phase lock tubes (5Prime-2302800) containing phenol:chloroform:isoamyl alcohol 25:24:1 (pH 6.4) (Sigma P3803) and was centrifuged for 5 minutes at 14 000 at 4°C. The top layer was added to tubes containing 1.5 ml of 100% ethanol and 50 µl of 3 M sodium acetate (pH 5.2). RNA was precipitated at -80°C for 1 hour or at -20°C overnight. Samples were centrifuged at room temperature for 15 minutes at 13 000 rpm in a microfuge. The supernatant was discarded, pellets were washed in 70% ethanol, allowed to air dry then resuspended in 100 µl of DEPC treated H₂O.

2.6.2 RNA Clean-up and concentration

RNA was extracted as previously described in Section 2.6.1 and was checked for degradation by analysis of 5 µl on a 1% TAE agarose gel. Samples were processed by using either the Quiagen RNeasy Mini Kit or the Zymo Research RNA Clean & ConcentratorTM – 25 according to the manufacturer's instructions.

2.6.3 Quantification of RNA samples

RNA concentration was determined using a Nanodrop 1000 spectrophotometer (Thermo Scientific). Samples were diluted in DEPC treated H₂O to a suitable concentration and read at an absorbance at 260 nm and 280 nm. Concentration was calculated in ng/µl.

2.6.4 DNase treatment of RNA

RNA was extracted and cleaned up as previously described in sections 2.6.1 and 2.6.2 then was DNase treated either using the Ambion TURBO DNA-freeTM Kit or using the Primerdesign Precision DNase kit (DNASE-50). Using the Ambion TURBO DNA-freeTM Kit, digestions were carried out under the following conditions: 10 µg RNA, 5 µl DNase I Buffer and 1 µl DNase were added, incubated at 37°C for 30 minutes, a further 1 µl DNase was added to the mix then samples were left to incubate at 37°C for another 30 minutes. 10 µl DNase Inhibitor was added, mixed and incubated for another 2-3 minutes at room temperature; centrifuged and clear layer was removed to a fresh 500 µl PCR grade Eppendorf tube. In case of the Primerdesign Precision DNase method digestions were carried out by the addition of 3 µl 10x Precision DNase reaction buffer to 30 µl of RNA and 1 µl of Precision DNase. Samples were incubated at 30°C for 30

minutes and DNase was deactivated by incubation at 55°C for 5 minutes.

2.6.5 Reverse transcription and quantitative PCR (RT-qPCR)

RNA was extracted and purified as previously described in sections 2.6.1 and 2.6.2 then was DNase treated as described in section 2.6.3. Reverse transcription and quantitative PCR were carried out as either a one-step reaction using the Primerdesign Precision OneStep qRT-PCR Mastermix or were carried out as two-step reactions using Invitrogen SuperScript® II Reverse Transcriptase followed by qualitative PCR using Roche LightCycler® DNA Master SYBR Green I. Following the Primerdesign Precision OneStep qRT-PCR method, 10 µl Precision OneStep™ qRT-PCR Mastermix, 1 µl primer mix (1:10 dilution each), 2 µl RNA, 7 µl RNase-free H₂O were added per reaction and mixed. SYBR green detection was recorded using a Rotor Gene 6000 Real-Time PCR machine with the following settings: Step 1 (Reverse Transcription) 10 minutes at 55°C, Step 2 (Enzyme activation – Hotstart) 8 minutes at 95°C, Step 3 (Denaturation) 10 seconds at 95°C, Step 4 (Data Collection) 60 seconds at 60°C. Steps 3-4 were repeated 50 times, and at the finish a melt curve was generated to help confirm primer specificity. When the two-step method was applied, reverse transcription was set up by addition of the following: 6 µl DEPC treated H₂O, 10 µl Reaction mix (Invitrogen SuperScript® II), 2 µl RNA, 2 µl Enzyme mix (Invitrogen SuperScript® II Reverse Transcriptase). PCR settings were the following: 25°C for 10 minutes, 50°C for 50 minutes and 85°C for 5 minutes. When finished 1 µl RNase H was added to mixture and samples were incubated at 37°C for 20 minutes. qPCR was set up by addition of the following: 8.8 µl nH₂O, 3.2 µl MgCl₂, 4 µl primer mix (1:10 dilution of each primer), 2 µl enzyme mix and 2 µl DNA. SYBR green detection was recorded using a Rotor Gene 6000 Real-Time PCR machine with the following settings: 10 min 95°C then 36 cycles of (15 sec at 95°C, 10 sec at 55°C, 15 sec at 72°C). qRT-PCR primers used in this study are listed in Table 2.6. Expression levels were normalized to *act1*⁺ unless stated otherwise.

Table 2.6 qRT-PCR oligonucleotide primers

Primer	DNA sequence 5'-3'
act1_For	GGC ATC ACA CTT TCT ACA ACG
act1_Rev	GAG TCC AAG ACG ATA CCA GTG
htt2_F	ATG GCT CGT ACC AAG CAA AC
htt2_R	AAA TCT TGG GCA ATT TCA CG
hhf2_F	TAA GCC TGC TAT CCG TCG TC
hhf2_R	CCA TAA ATG GTA CGG CCT TG
hta_for	ATC TGC TCA ATC CCG TTC TG
hta_rev	AGA TGA CGG GGA ATG ATA CG
htb_for	GTT GAA GCA AGT TCA CCC TG
htb_rev	TCA AAC GAA CAG CAG TCT GG
cdc18_F	GTT GCA GCT TCA AGT GGT GA
cdc18_R	TTG GCT CAT AGC AGA TGT CG
sde2_for	GCG AAG AAA CCT GCT GAA AC
sde2_rev	AAG TTG AGC CCC TTC GGT AT
cdt1_for	TCA ACA AGT CGC GAG TTA CG
cdt1_rev	CGC GAT GAA TTT TGA ACA GA
ura3_for	ACC CCT GGT CTT CGT AAC CT
ura3_rev	CAA CGA TCA CAC CGT CAA TC
mis3_for	GAA GCG TTC CAT TTC CTC AG
mis3_rev	ATA ACG GCG ACA GTT GTT CC

2.6.6 Microarray analysis

Microarray analysis was performed by Babis Rallis and Sandra Codlin from the group of Jürg Bähler, UCL. In brief, Alexa 555- or 647-labeled cDNA was produced from the RNA (extracted as described in Section 2.6.1) using a Superscript direct cDNA labelling system (Invitrogen) and Alexa 555 and 647 dUTP label mix. The 58 cDNA was then purified using an Invitrogen PureLink PCR Purification system. The cDNA was hybridized to the array using a Gene Expression Hybridization kit (Agilent). The array was an Agilent custom-designed array containing 60-mer oligonucleotides synthesized in situ on the array and contained 4x44000 probes. Following hybridization for at least 17 hours, the array was washed using a Gene Expression Wash Buffer kit (Agilent) and scanned in an Agilent Array Scanner. The microarray signal was extracted using GenePix. The list of genes 2 fold up or down regulated in *hip1Δ* cells compared to the wild type during quiescence can be found in Appendix A.

2.7 Protein extraction, manipulation and analysis

2.7.1 TCA protein extraction

Approximately $\sim 4 \times 10^7$ cells were harvested following addition of trichloroacetic acid (TCA) to a final concentration of 10%. Cells were resuspended in 200 μ l 10% TCA and then disrupted using a mini beadbeater (Biospec) with 0.75 ml glass beads (0.5 mm) using two pulses of 15 sec with 1 min on ice in between. A further 500 μ l 10% TCA was added and the lysate was recovered from the beads which was then clarified by spinning at 13 000 rpm in a microcentrifuge. The resulting pellet was washed three times in acetone, dried and resuspended in 30 μ l TCA buffer (100 mM Tris-HCl [pH 8.0], 1% [w/v] SDS, and 1 mM EDTA [pH 8.0]). Protein concentration was measured using the Pierce BCA Protein Assay Kit (Thermoscientific) as per the manufacturer's instructions.

2.7.2 Whole cell protein extracts

Cells were cultured in 50 ml YE5S to an OD₅₉₅ ~ 0.3 then were centrifuged and washed with 1 ml dH₂O, snap frozen and resuspended in 100 μ l of ice cold Western lysis buffer (50 mM Tris-HCl [pH 7.5], 150 mM NaCl, 10 mM Imidazole, 0.5% [v/v] NP-40 [IGEPAL]) supplemented with 1 mM PMSF, 54 mM NaF, 5 μ M NaVO₄, 1 μ l/ml aprotinin, 5 μ g/ml pepstatin A and 5 μ g/ml leupeptin. Added all to screw capped 2 ml

tubes containing 1 ml pre-chilled glass beads and disrupted cells with beadbeater (Biospec) using two pulses of 30 sec with 1 minute on ice in between. 400 µl of the Western lysis buffer mix was added to each sample, then the bottom of the tubes was pierced and lysate was collected in fresh Eppendorf by centrifuging at 2000 rpm for 1 minute at 4°C. Cell lysate was further cleared by centrifuging in a microfuge at 13 000 rpm for 10 minutes at 4°C. The supernatant was removed and protein concentrations were measured using Coomassie protein detection reagent (Pierce) as per the manufacturer's instructions.

2.7.3 Co-Immunoprecipitation (Co-IP)

Cells were cultured in 50 ml YE5S to an OD₅₉₅ ~0.3 then whole cell extracts were prepared as described in section 2.9.2 with the following modification: the Western lysis buffer was supplemented with 1% yeast protease inhibitors (Sigma P8215) and 1 mM PMSF. Whole cell extracts were pre-cleared with 40 µl pre-washed Sepharose A beads for 1-2 hours at 4°C on rotating wheel. Protein extracts were centrifuged at 2000 rpm for 2 minutes at 4°C and 400 µl supernatant was transferred into fresh Eppendorfs, leaving the beads behind. A 40 µl aliquot was removed as a control WCE and stored at -20°C while 40 µl pre-washed Sepharose A beads and 1.5 µl anti-GFP antibody were added to the remaining sample and incubated overnight at 4°C on a rotating wheel. Samples were washed 3-6 times in 500 µl of Western Lysis Buffer supplemented with 1 mM PMSF and 1% protease inhibitors (Sigma P8215). After final wash all buffer was removed using a syringe and beads were resuspended in 40 µl 1x Lamelli buffer (0.1% β-mercaptoethanol, 0.0005% Bromophenol blue, 10% glycerol, 2% [w/v] SDS and 63 mM Tris-HCl [pH 6.8]). In the meantime 4 µl of the WCE were mixed with an equal volume of 1x Lamelli buffer and all samples were boiled at 100°C for 3 minutes. 40 µl of IP and 8 µl of WCE were analyzed on 9% SDS-polyacrylamide gels (Section 2.7.4).

2.7.4 Western blotting

Protein extracts were prepared as described in Sections 2.7.1, 2.7.2 and 2.7.3. Protein samples were denatured by heating to 100°C for 2-3 minutes and were resolved by SDS PAGE gel electrophoresis. Samples were then transferred onto nitrocellulose membranes, were blocked for 10-30 minutes using 10% BSA in TBST (1 mM Tris-HCl [pH 8.0], 15 mM NaCl, 0.1% [v/v] Tween 20) and were incubated for either 1 hour or overnight at 4°C with the appropriate primary antibody. The primary antibodies and

their relevant secondary antibodies used in this study are shown in Table 2.7. Primary antibodies were all diluted in 5% (w/v) BSA in TBST. Following incubation, membranes were washed three times in TBST; the appropriate secondary antibody was added at a dilution of 1:2000 and the membranes were incubated for up to 1 hour at room temperature with shaking. All secondary antibodies were diluted in 5% (w/v) BSA in TBST. The membranes were then washed three times in TBST and were developed using the Pierce™ ECL 2 Western Blotting Substrate (Thermoscientific) on a Typhoon (GE Healthcare) according to the manufacturer's instructions. For histone H3 and H2A western blots 2.5 to 5 µg of protein was loaded, while for Atg8, Cig2 and Rum1 blots 20 µgs were used.

Table 2.7 Antibodies

Primary Antibodies	Manufacturer (CAT #)	Dilution	Secondary Antibody
HA	Thermoscientific (26183)	1:1000	mouse
PK	Serotec	1:1000	mouse
Tubulin	TAT1 from CRUK	1:2000	mouse
GFP	Invitrogen (A11122)	1:1000	rabbit
Histone H3	Abcam (ab1791)	1:1000	rabbit
Histone H3K9me2	Abcam (ab1220)	Not diluted	mouse
Histone H2A	Abcam (ab13923)	1:1000	rabbit

2.8 Bioinformatics

Bioinformatic analysis was carried out during analysis of chromatin-sequencing data. Initial processing of sequence reads was performed by Dr Nick Kent from Cardiff University. All scripts used in this study were written by Dr Nick Kent, including those used for subsequent analysis in Newcastle. The list of scripts used in this study and their functions are briefly described in Table 2.7. Briefly, all initial paired reads were aligned to the ASM294v1.17 reference genome using Bowtie 0.12.7 (Kent *et al.*, 2011) with command line flags: `-n 0 --trim3 75 --maxins 5000 --fr -k 1 --sam`. Aligned read pairs were sorted according to chromosome and then into a range of size classes based on the SAM format ISIZE value (difference between 5' end of the mate read and the 5' end of the first mapped read) plus or minus 20%. Mono-nucleosome-sized reads are, therefore, represented as 150 bp \pm 30 bp. In order to define the genomic position of MNase-resistant chromatin species the mid-point position of the read pairs in a particular size class were mapped. Frequency distributions of the mid-point positions were then calculated using 10 bp bins. To provide a direct comparison with previously published wild-type nucleosome position data set, mono-nucleosome position frequency distributions were smoothed by plotting an Epanechnikov kernel density estimate (KDE) with $h = 30$. For all other analyses, frequency distributions were more lightly smoothed by taking a 3-bin moving average. All frequency distributions were output in the zero-referenced, chromosome base, three-column .sgr format (chromosome number, feature/bin position, mid-point frequency value) for rendering with the Integrated Genome Browser and for further processing. Average cumulative chromatin particle position frequency distributions at, and surrounding, genomic features were calculated using the script SiteWriter_CFD, with values for each bin normalised to the average cumulative frequency value obtained for all bins within the feature window. To provide the comparison of our data with the smoothed nucleosome position map of Shim and co-workers the positions of 33874 unambiguous peak summit bins were marked in our wild-type KDE mono-nucleosome data set (Table 2.8 script peakmarkerEpKDE_lite) and compared with GSM994397_WT.wig replicate data (converted to 10bp binned .sgr format). Protein-coding gene transcription start sites (TSS) positions were taken from the previously described dataset (Lantermann *et al.*, 2009) and too were replication origin positions (Givens *et al.*, 2012). Nucleosome positions were analysed using a simple heuristic peak marking process (Table 2.8 script Pom_di_nuc_PeakMarkCompare_10bin). Peak summit positions were marked in read-

depth-normalised wild type, *abo1Δ* and *hip1Δ* chromatin particle position frequency distribution data sets and then filtered into a list of those that match between data-sets and two lists of those that do not. The mutant_NOT_WT lists contain peaks that occur in different genomic positions, and peaks that exceed a two-fold difference in peak height in either data set with processing to exclude threshold artefacts. The scripts used in this thesis are available from Dr Nick Kent, Cardiff University. Genic loci used for nucleosome alignment of genes described as highly and lowly expressed and solo LTRs can be viewed in Appendix B. Also in Appendix B is a list of genes that have come out as containing “highly disorganized” dinucleosomes in *abo1Δ* cells.

Table 2.8 Perl scripts

Script name	Brief Description of Function
Chrgrep.sh	Script to group individual chromosome records from bowtie-aligned SAM files
SAMparser.plx	This script takes the chrn_info.txt files from chrgrep.sh and calculates the centre positions of the paired reads for each chromosome within user-defined size classes (+/- a user-defined window)
Spombe_Chrg_changer.plx	This script takes chr1, chr2 format .sgr files that display in IGB using the S_pombe_Sep_2007 Genome Version, and converts the chromosome format to I, II etc allowing you to display the sgr files in IGB using the S_pombe_May_2012 Genome Version
peakmarkerEpKDE_lite.pl	This script takes a sgr file as an input, and calls peak centre/summit bins above a single, but scalable, threshold. It then lists these bin positions with a y-axis value proportional to the scaled read frequency. The scaling value can be chosen to reflect differences in read depth between two experiments - either based on total depth or a SiteWriter-derived local depth. For simple peak counts, just leave at 1.00
Negativity.plx	This script takes any .sgr file and turns all the read frequency (col[2]) values negative so that you can easily compare them in another state using the IGB

SiteWriter_CFD.plx	This script takes .txt files containing a list of sites/genomic features (these could be TSSs or TF sites or whatever you want) and compares it with whole-genome, partn .sgr files. It then outputs cumulative frequency distribution values over a user-specified bin range centered on, and surrounding the sites
Trend_Compare_Stats.plx	This script performs a SiteWriter-style cumulative frequency calculation over each bin in the specified window surrounding each feature, but it also outputs a range of values including p-values for paired T and Wilcoxon Mann-Whitney tests between the two scaled/normalized samples at each bin
Di_nuc_spotter.plx	Marks genes or transcripts within which "disorganised" tracts of nucleosomes occur in a mutant relative to a wild-type condition or similar
Pom_di_nuc_PeakMarkCompare_10bin.pl	This script takes two EQUAL BIN No. Part300 .sgr files (A and B) and uses various criteria to mark peaks and to describe those peak bins that match and do not match between the data sets

Chapter 3

Organization of chromatin by an ATAD2 homologue in *S. pombe*

3.1 Introduction

Abo1 is a conserved bromodomain AAA-ATPase, with homology to both the *S. cerevisiae* Yta7 and to the human ATAD2 and ATAD2B proteins. ATAD2 has been linked to cancer development and its overexpression in tumour cells is a strong indicator of poor survival (Boussouar *et al.*, 2013; Raeder *et al.*, 2013). Therefore, establishing its precise mode of action is of considerable importance. Despite this, there is little information regarding the molecular function of bromodomain AAA-ATPases. Work carried out using *S. cerevisiae* has revealed roles in regulation of gene expression, boundary function, and nucleosome disassembly (Lombardi *et al.*, 2011), but there is little evidence that these functions are conserved. Fission yeast provides an attractive model for the study of these factors as like humans, it contains two ATAD2 homologues; Abo1 and Abo2, which show high levels of sequence similarity to their human counterparts. Previous work from our lab has demonstrated that loss of *abo1*⁺ leads to numerous phenotypes that overlap with those of histone chaperone mutants, such as an increase in antisense transcription, loss of silencing within heterochromatic regions and a cell cycle delay (Murton, 2012). These phenotypes are consistent with an important role for Abo1 in global regulation of chromatin. Therefore, the predominant aim of the work described in this chapter was to determine whether Abo1 has an effect on global nucleosome organization in *S. pombe*.

3.2 Results

3.2.1 Generating Chromatin-Seq Samples

In order to better understand the chromatin architecture of *abo1Δ* cells, a sequencing methodology was applied which can determine both the occupancy and positioning of multiple nucleosome size classes (Kent *et al.*, 2011), thus permitting a high-resolution view of chromatin. Chromatin was digested with micrococcal nuclease (MNase), an enzyme that preferentially cuts linker DNA and therefore allows the identification of nucleosome occupied sequences. MNase digests resulted in pools of DNA, representing the different nucleosome size classes, which were visualized on agarose gels (Fig 3.1.A). Digests derived from wild type and *abo1Δ* cells presented with highly similar molecular weight distributions. Three biological replicates from wild type and *abo1Δ* cells were pooled and sequenced, resulting in 56.3 and 52.7 million aligned paired-end reads respectively. The datasets were stratified according to paired read end-to-end distance into ranges representing the expected sizes of MNase-resistant DNA species (nucleosome particles) in eukaryotic chromatin (Fig 3.1.B). DNA fragments of 150 bp \pm 20% derive primarily from mononucleosomes, whereas those of 300 bp \pm 20% originate from dinucleosomes and DNA species smaller than 100 bp would represent subnucleosomal particles, including unwrapped nucleosomes and transcription factors (Kent *et al.*, 2011). Frequency distributions, of the mid-points between paired reads for each end-to-end distance class, were then determined across the genome, and peaks in these distributions were taken to imply the presence of a positioned chromatin particle.

The quality and reliability of the sequencing data was determined by direct comparison to a previously published data set (Shim *et al.*, 2012). Fig 3.1.C illustrates the distribution of frequency read peaks at specific loci using the Integrated Genome Browser (IGB), where a peak represents a nucleosome. Comparisons of the average distribution of nucleosomes from the Shim *et al* wild type dataset to the samples generated in this study are shown in Fig 3.1.D. In this analysis, nucleosome positions were defined as the locations of peak summits in mononucleosome position distributions. A cumulative frequency distribution of nucleosome positions at, and surrounding these wild type nucleosome positions was plotted for each set. All datasets resolve into a periodic pattern with an average repeat length of 156 bp arising from arrays of *S. pombe* mononucleosomes. The average amplitude of the nucleosome peaks

decays over distance, consistent with statistical positioning of yeast chromatin, and agreeing with previously published work (Shim *et al.*, 2012). However, while the two wild type datasets overlap, the height of the nucleosome peaks in *abo1* Δ cells was decreased, suggesting that some aspect of chromatin organization is impaired in this mutant.

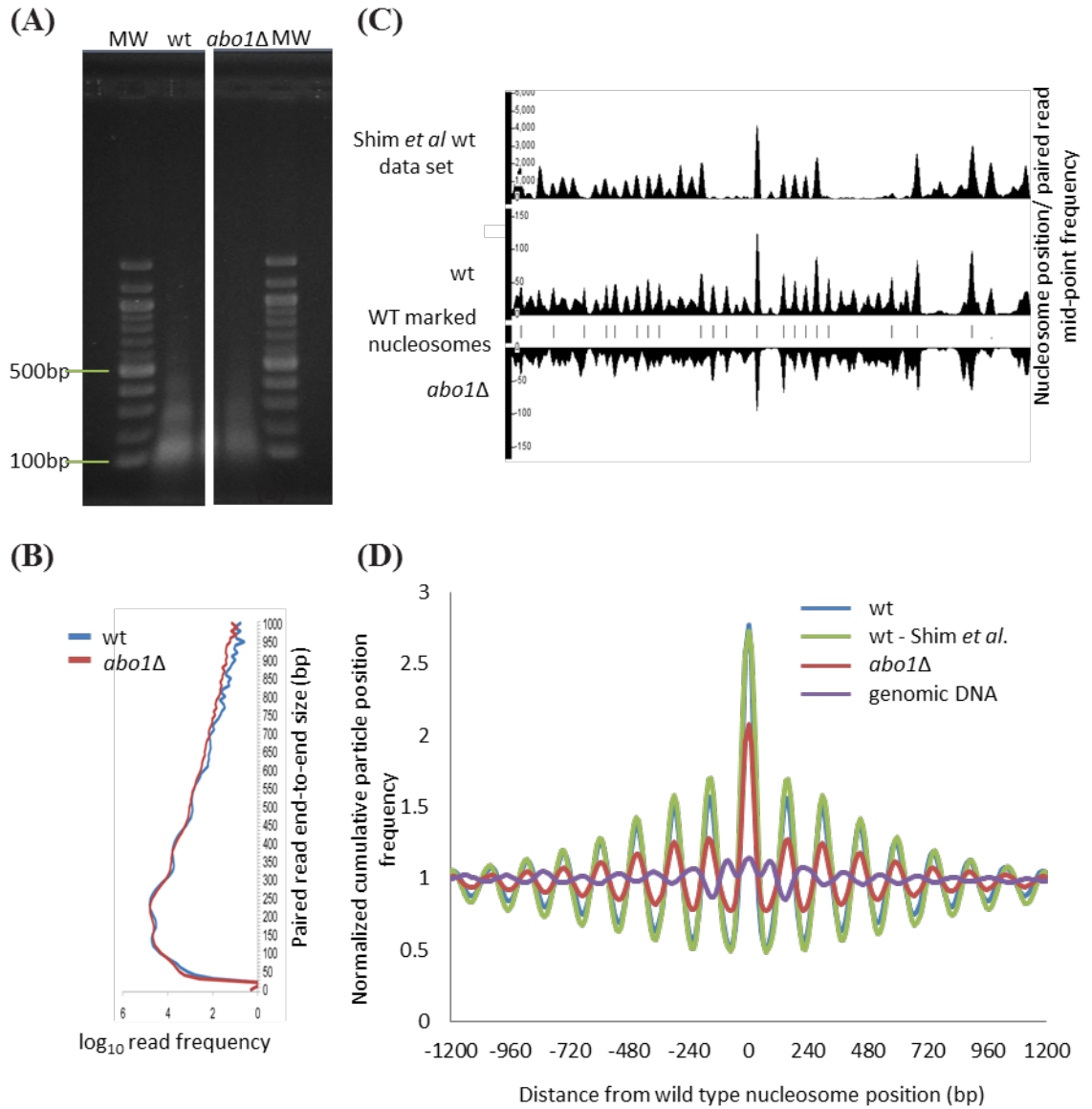


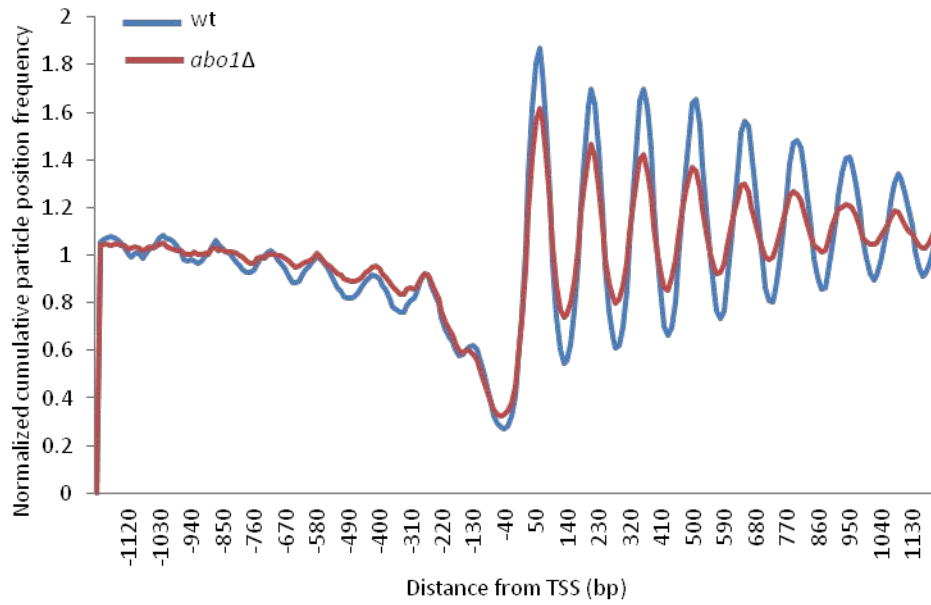
Figure 3.1 MNase-seq datasets generated in this study correlate well with previously published results.

(A) Ethidium bromide-stained agarose gels of DNA pools extracted from MNase digested wild type and *abo1Δ* chromatin and used for MNase-sequencing in this study. Visible below the 500 bp mark are the mono-, di- and tri-nucleosome bands for each set. (B) Frequency distribution of paired read end-to-end size values following MNase-seq of DNA shown in Figure A. (C) Genome browser view of (Shim *et al.*, 2012) wild type nucleosome occupancy data set plotted in relation to the mononucleosomal (150 bp) paired-read mid-point frequency data obtained in this study (all smoothed using an Epinechnikov kernel density estimate). (D) Comparison of cumulative frequency distributions of mid-point nucleosome (150 bp) positions from Shim *et al.* (2012) wild type, as well as the wild type and *abo1Δ* datasets generated in this study.

3.2.2 *Abo1 plays a role in appropriate nucleosome organization at coding regions*

Next, 4013 protein coding genes were aligned by their transcription start sites (TSS) as identified by Lantermann *et al.* (2009) and nucleosome architecture was determined in wild type and *abo1* Δ cells. Nucleosomes surrounding the TSSs are organized into a nucleosome depleted region (NDR) just upstream, and into an ordered array over the open reading frame (ORF), downstream of the TSS. The average nucleosome profiles of wild type and *abo1* Δ cells were similar over the NDR and the promoter regions but not over the ORF. Cells lacking *abo1*⁺ presented with a reduction in amplitude height over the nucleosomal peaks throughout the ORF. Conversely, an increase in nucleosome occupancy was observed over the linker regions. These distributions suggest that proper nucleosome organization over coding sequences is dependent upon *abo1*⁺ (Fig 3.2.A). In order to determine whether a specific group of genes was disrupted upon loss of *abo1*⁺, K-means clustering was used to define 9 arbitrary nucleosome peak profiles in the *abo1* Δ dataset. Comparison of the wild type and *abo1* Δ datasets revealed that no one group is dependent upon *abo1*⁺, rather that all protein coding gene profiles resolve more clearly in the wild type sample (Fig 3.2.B), suggesting that Abo1 impacts upon correct nucleosome placement to some extent over the majority of coding regions.

(A)



(B)

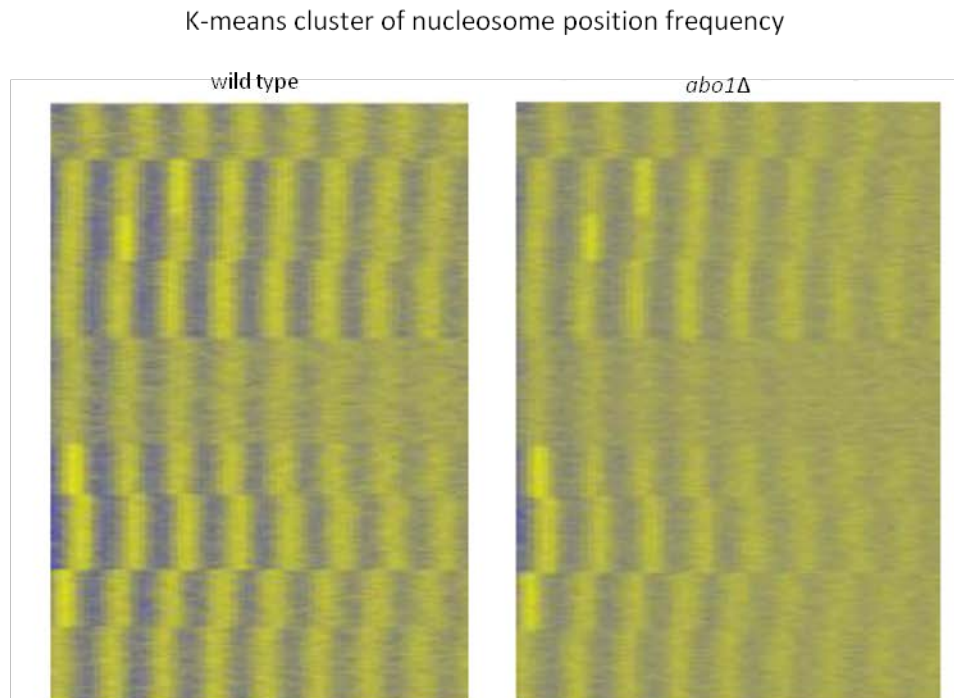


Figure 3.2 Deletion of *abo1*⁺ leads to perturbations of nucleosome organization over coding sequences.

(A) Wild type and *abo1Δ* MNase-seq generated mononucleosomal (150 bp) DNA fragments were aligned over 4013 *S. pombe* protein coding genes, using the TSSs identified by Lantermann *et al.* (2009). (B) Nucleosome position frequency values for the coding regions of 4013 *S. pombe* genes (Lantermann *et al.*, 2009) were k-means clustered ($k = 9$) and displayed with positive values coloured yellow and other values coloured blue on the left hand panel. The cluster order was then used to display the equivalent wild type frequency values in the right-hand panel.

Since the MNase profiles suggested a reduction in global nucleosome occupancy, histone protein levels were quantified. Histone H3 and H2A levels were significantly decreased in *abo1Δ* cells compared to the wild type (Fig 3.3). This is not a result of an impact of Abo1 upon histone gene transcription as previous analyses have shown that histone gene mRNA levels are unaffected by *abo1*⁺ deletion (Murton, 2012). In addition, when a heuristic algorithm was employed to mark nucleosome peaks, of the 30021 nucleosome positions that coincided between wild type and *abo1Δ* cells, 1036 were at least 2-fold higher in the wild type than *abo1Δ*, while the converse was true for only 14. Overall, the data indicates that loss of *abo1*⁺ results in a global reduction in nucleosome occupancy.

In addition to a drop in nucleosome occupancy, the initial nucleosome alignments suggested an effect on positioning. While nucleosome peaks are lower in *abo1Δ* cells, the number of reads corresponding to linker regions increased. This could indicate that in addition to a reduction in nucleosome occupancy, a proportion of nucleosomes shifted from their preferential sites. To address this issue, dinucleosome peaks were compared over coding regions (Fig 3.4.A). A dinucleosome peak will only arise if the constituent mononucleosomes are well positioned with respect to each other, therefore a shift and/or loss of either mononucleosome will impact greatly upon the dinucleosome maps. Indeed, the differences between wild type and *abo1Δ* dinucleosome maps were slightly more pronounced than those seen over mononucleosomal alignments. Figure 3.4.C illustrates a locus, over the *cufI*⁺ gene, where nucleosomes have become particularly disorganized. A heuristic peak finder identified 466 of these loci, where *abo1Δ* cells presented with over 60% 'fuzzy' nucleosomes. Running these genes through the Princeton GO term-finder found no functional relationship between them, nor was it possible to find a connection based on chromosomal location. Removal of these genes and re-aligning the dinucleosome peaks also did not yield a better fit (Fig 3.4.B), suggesting that like its role in nucleosome occupancy, Abo1 also has a global effect on nucleosome positioning.

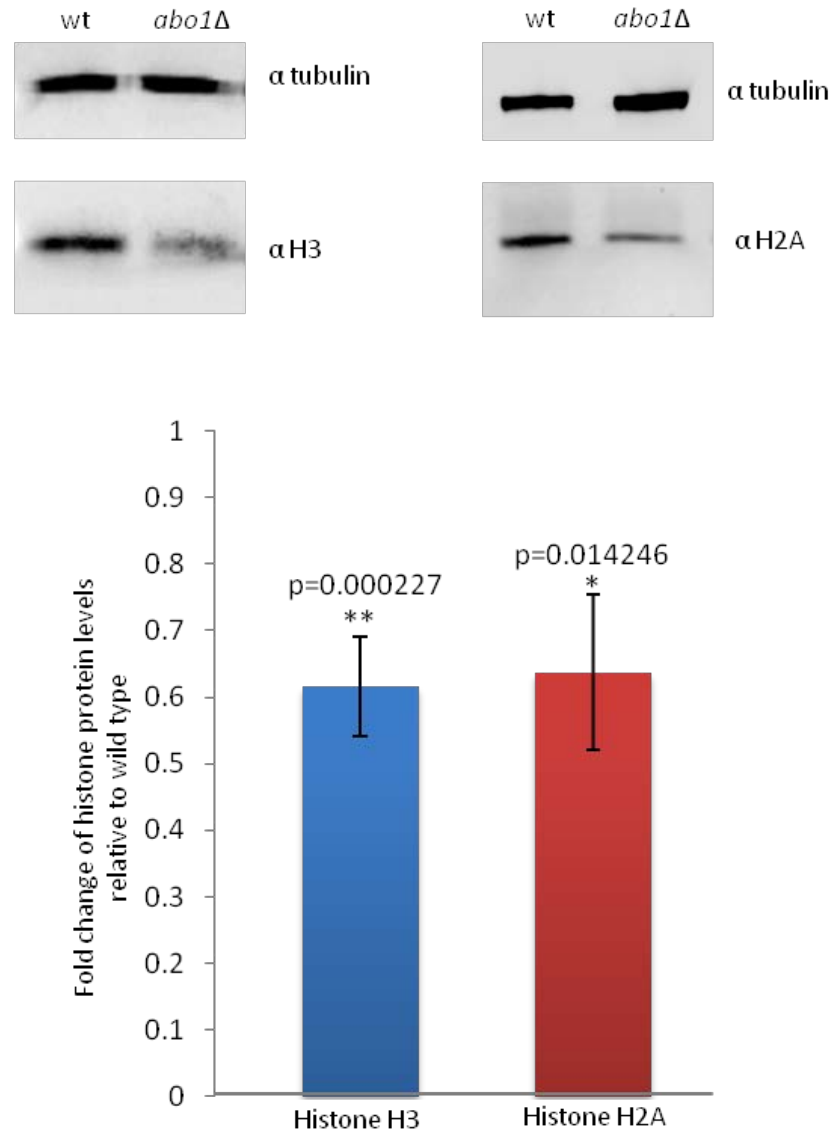


Figure 3.3 Loss of *abo1*⁺ leads to a drop in histone H3 and H2A protein levels.

Whole cell protein extracts were subjected to western blotting probed with histone H3 (Abcam) or histone H2A (Abcam) and tubulin antibodies. Histone protein levels were normalized to tubulin and fold change shown is of *abo1* Δ cells relative to the wild type. Data are the mean of at least three independent biological replicates; error bars represent \pm SEM (* denotes $p < 0.05$ and ** $p < 0.001$).

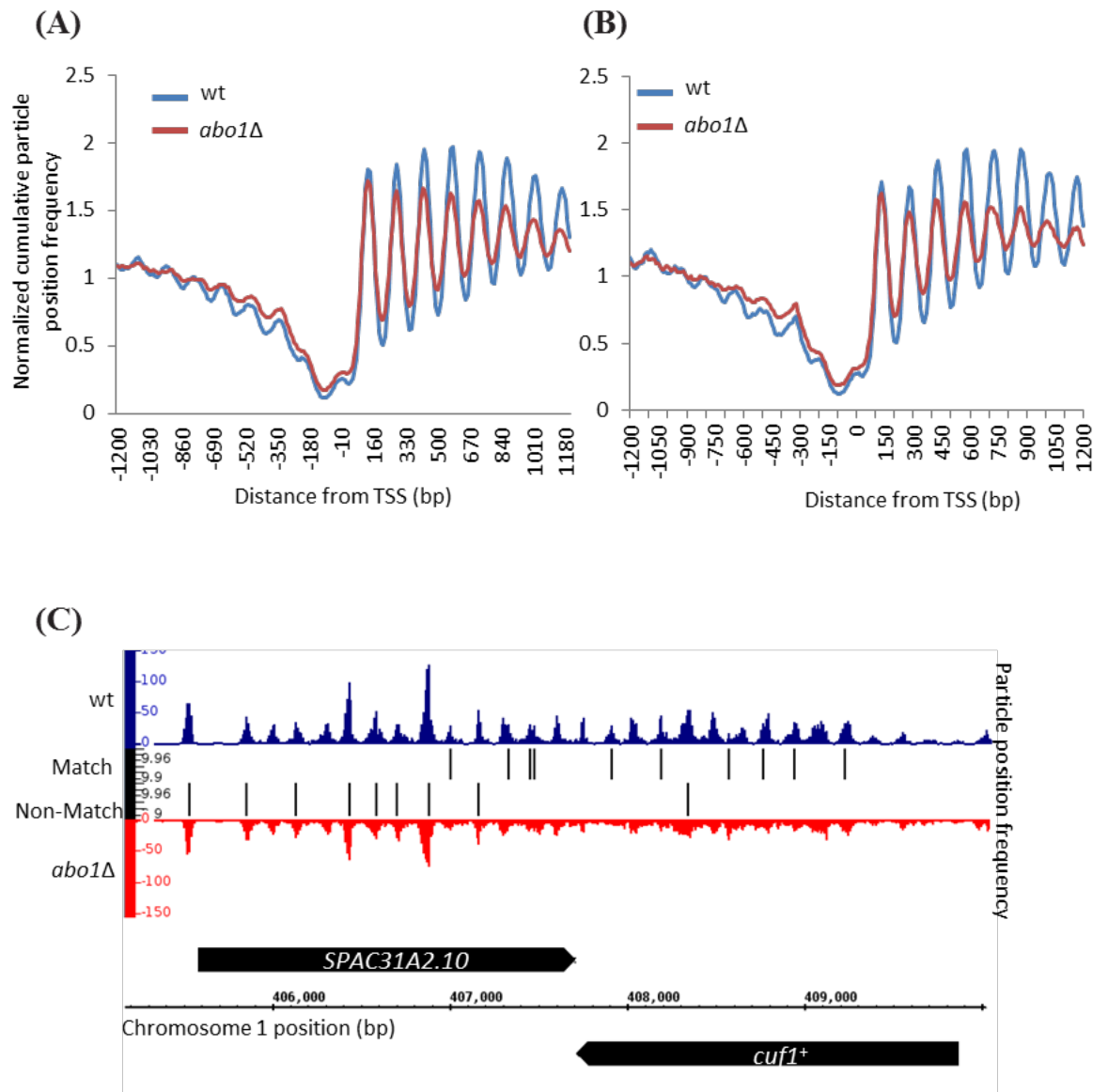


Figure 3.4 Loss of *abo1*⁺ results in “fuzzy” nucleosomes.

(A) Average dinucleosome (300 bp) sequence read frequency profiles generated by MNase-seq for 4013 *S. pombe* protein coding genes aligned at the TSSs as described by Lantermann *et al.* (2009). (B) The 466 genes identified previously as possessing particularly disorganized dinucleosomes upon loss of *abo1*⁺ function were removed from the 4013 *S. pombe* protein coding genes and the MNase-seq generated dinucleosome particles (300 bp) were realigned by TSS (Lantermann *et al.*, 2009). (C) Comparison of sequence read frequency for dinucleosome particles (300 bp) following MNase-seq in wild type and *abo1Δ* across the indicated region of Chromosome 1. The position of matching and non-matching dinucleosome peaks is indicated.

3.2.3 Chromatin organization at *Abo1* regulated genes

A recent study by Marguerat *et al.* (2012) identified the absolute transcript levels of genes in *S pombe*. Based on their measurements of transcript abundance, protein-coding genes in the top 10% and the bottom 10% were taken and their nucleosome profiles compared to all protein coding genes (Fig 3.5.A). Not unexpectedly, a wider NDR is seen in highly expressed genes when compared to the other two datasets, while genes with low-level expression had less well-organized nucleosomal arrays over their coding regions in addition to a shallow NDR. Microarray analysis comparing *abo1* Δ cells to wild type found that Abo1 typically plays a repressive role in transcriptional regulation. In the absence of *abo1*⁺, 281 RNAs are upregulated with only 8 down regulated compared to the wild type (Jürg Bähler, personal communications). Genes that are significantly upregulated overlap with those identified as up in the absence of the histone deacetylase *clr6*⁺ and in the absence of the *hip1*⁺ subunit of the HIRA complex (Fig 3.5.B), both of which are associated with repressive functions. Overall, the genes that are regulated in an Abo1-dependent manner are mostly expressed at low levels and accordingly present with a shallow NDR and less well defined nucleosomal arrays (Fig 3.5.C). Comparison of wild type and *abo1* Δ mutant cells revealed that there is nearly a complete loss of the +1 nucleosome in *abo1* Δ cells at Abo1-dependent genes and there is also some reduction in the -1 nucleosome over the promoter regions (Fig 3.6.A). The depletion of nucleosome occupancy over the promoter region can be confirmed when individual genes are inspected. For example, transcription from the *grt1*⁺ and the *aes1*⁺ loci is 2-fold upregulated in *abo1* Δ cells, and there is a reduction of nucleosomes that affect both the -1 and the +1 nucleosomes (Fig 3.6.B and C), demonstrating that Abo1 also plays a role in nucleosome assembly over specific promoter regions. It is however unclear what directs Abo1 involvement in promoter nucleosome assembly in this subset of genes.

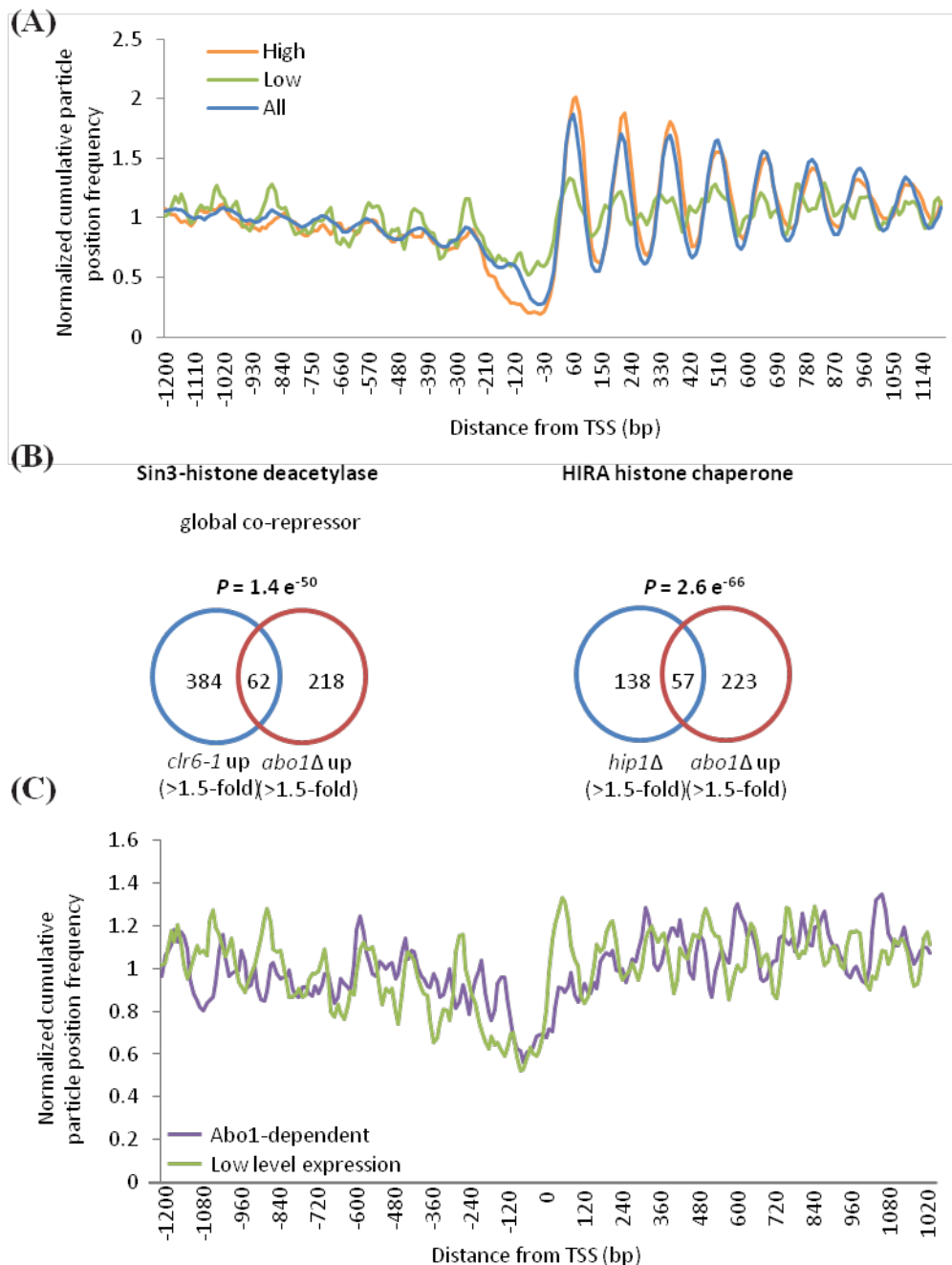


Figure 3.5 Deletion of *abo1*⁺ preferentially results in the de-repression of normally low level transcribed genes.

(A) Mononucleosomal particles (150 bp) following MNase-seq were aligned by their TSSs for all 4013 *S. pombe* protein coding genes identified by Lantermann *et al.* (2009) as well as those identified as the top 10% of highly and top 10% lowly transcribed protein coding genes described by Maraguet *et al.* (2012). (B) Microarray data of midlog phase growing *abo1Δ* cells shows over 280 genes that are upregulated compared to wild type. Venn diagrams show overlap between genes that are up-regulated (≥ 1.5 fold) in *abo1Δ* mutants with genes that are up-regulated under the indicated condition, along with the significance of the overlaps (based on hypergeometric distribution). (C) Comparison of MNase-seq generated mononucleosome particle maps (150 bp) of genes transcribed to low-levels as described by Maraguet *et al.* (2012) and of Abo1-dependent genes as identified by microarray analysis aligned by their TSSs as identified by Lantermann *et al.* (2009).

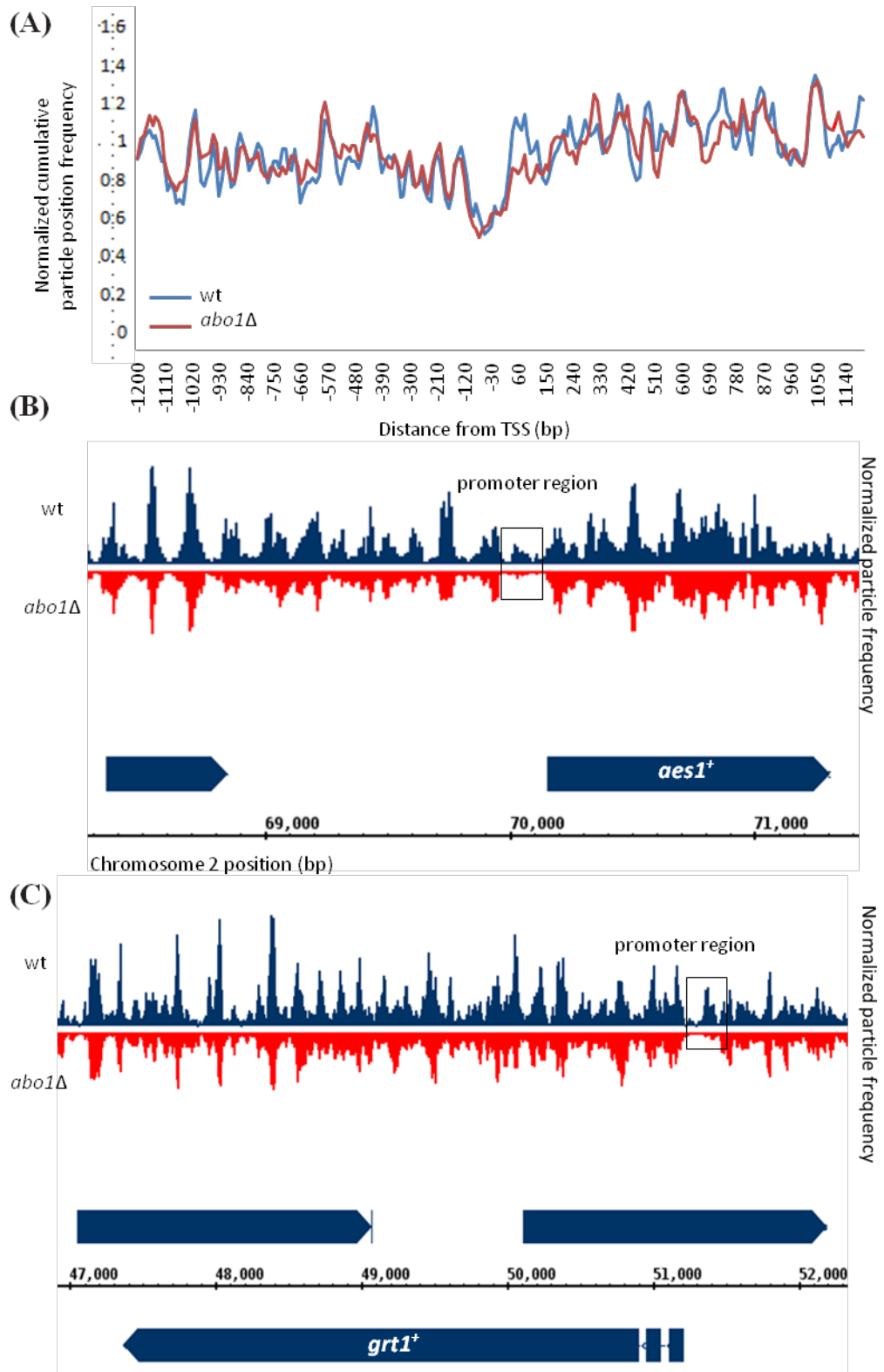


Figure 3.6 Nucleosome depletion is visible over the promoter regions of Abo1-dependent genes.

(A) Mononucleosome particle maps (150 bp) generated by MNase-seq of Abo1-dependent genes as identified by microarray analysis in wild type and *abo1Δ* cells aligned by their TSSs as described by Lantermann *et al.* (2009). (B) and (C) Integrated Genome Browser view of MNase-seq generated mononucleosomes (150 bp) over individual genes that are Abo1-dependent in wild type and *abo1Δ* cells.

3.2.4 Abo1 is involved in proper nucleosome organization at pericentromeric heterochromatin

Nucleosome organization was also investigated at heterochromatic domains in both wild type and *abo1* Δ cells. There are three large heterochromatic regions in *S. pombe*: the pericentromeric regions, telomeres, and the mating type locus (Buscaino *et al.*, 2010). Centromeres are organized into two distinct transcriptionally silenced domains, the inner domain comprises the central core and the inner portion of the *imr* repeats. This region is associated with CENP-A chromatin and is the site of kinetochore assembly. The outer domain flanks the inner region and comprises the outer portion of the *imr* as well as the *otr* (*dg-dh* repeats) (Buscaino *et al.*, 2010). This region is assembled into heterochromatin that is dependent upon methylation of histone H3 on lysine 9 (carried out by the histone methyltransferase Clr4), which in turn is required for the recruitment of the HP1 homologue Swi6.

Previous assays from our lab have demonstrated that upon loss of *abo1*⁺, silencing of the inserted marker gene over these regions is disrupted (Murton, 2012). In the absence of *abo1*⁺ non-coding centromeric (*dg-dh*) transcripts accumulate (Murton, 2012). Since deletion of *abo1*⁺ leads to loss of silencing, histone H3 and histone H3K9me2 levels were measured by ChIP-qPCR. Histone H3 levels at *dh* repeats were slightly but significantly decreased in an *abo1* Δ mutant, while no significant change was observed in H3K9me2 levels (Fig 3.7.A and B). It was also possible to assay the spread of H3K9me2 by using strains with the *ura4*⁺ marker gene inserted into the *imr* or *otr* regions, in order to determine whether loss of silencing is due to failure of H3K9me2 to spread into the marker gene (Fig 3.7.C). It was not possible to detect a significant difference between wild type and *abo1* Δ cells in H3K9me2 enrichment at either *dh* repeats or over the *ura4*⁺ marker gene. It should however be noted that H3K9me2 enrichment was highly variable in *abo1* Δ cells. Taken together, these results would indicate that loss of H3K9 methylation is not the reason for loss of silencing. Nevertheless, Abo1 is enriched at heterochromatic regions as demonstrated by ChIP-qPCR analysis (Fig 3.8.A) and nucleosome maps reveal changes within the outer repeats in *abo1* Δ cells compared to the wild type (Fig 3.8 B), suggesting that Abo1 is involved in appropriate assembly and/or maintenance of nucleosomes within pericentromeric heterochromatin.

The association of Abo1-GFP with heterochromatin in the absence of *swi6*⁺ was also determined, and it is recruited and/or maintained independently of Swi6 levels at the *dh* repeats and over the *imr* region (Fig 3.9). The converse is also true; collaborators (Janet Partridge, personal communications) have found that loss of *abo1*⁺ does not affect Swi6-GFP enrichment over the *dg-dh* repeats, nor does it affect the number of Swi6-GFP loci visible in the nucleus as demonstrated by fluorescent microscopy examinations (Murton, 2012).

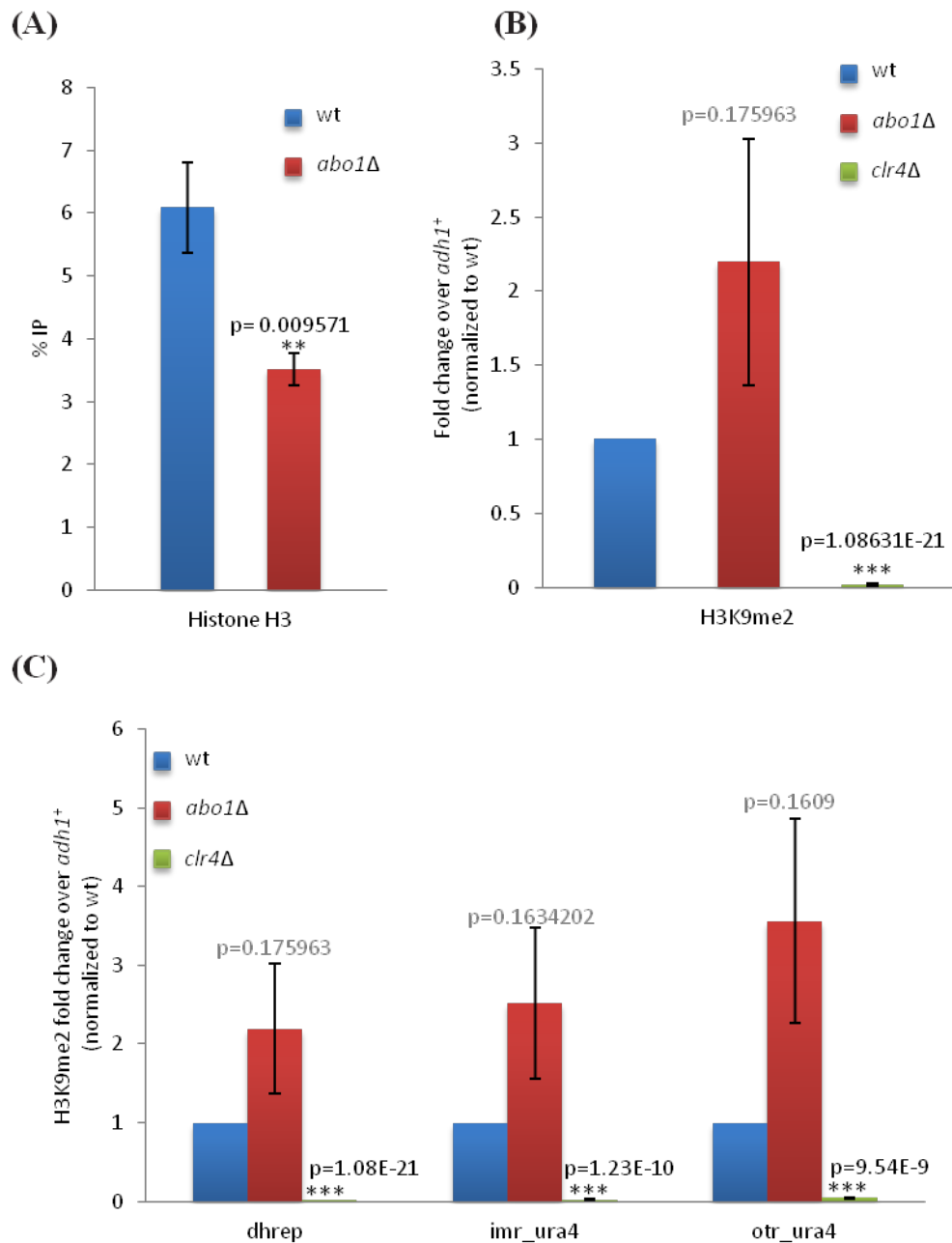


Figure 3.7 Heterochromatin is also affected by loss of *abo1*⁺.

(A) Histone H3 levels at *otr* repeats were determined by ChIP-qPCR. IP relative to input was determined. Data are the mean of three independent biological replicates and error bars represent \pm SEM (** indicates $p < 0.01$). (B) H3K9me2 levels at *otr* repeats were determined by ChIP-qPCR. IP relative to input was determined and mutants were normalized to the wild type. Data are the mean of six independent biological replicates and error bars represent \pm SEM (***) $p < 0.001$). (C) H3K9me2 levels at *otr* repeats and over the inserted *ura4*⁺ marker gene were determined by ChIP-qPCR. IP relative to input was determined and mutants were normalized to the wild type. Data are the mean of at least three independent biological replicates and error bars represent \pm SEM (***) $p < 0.001$).

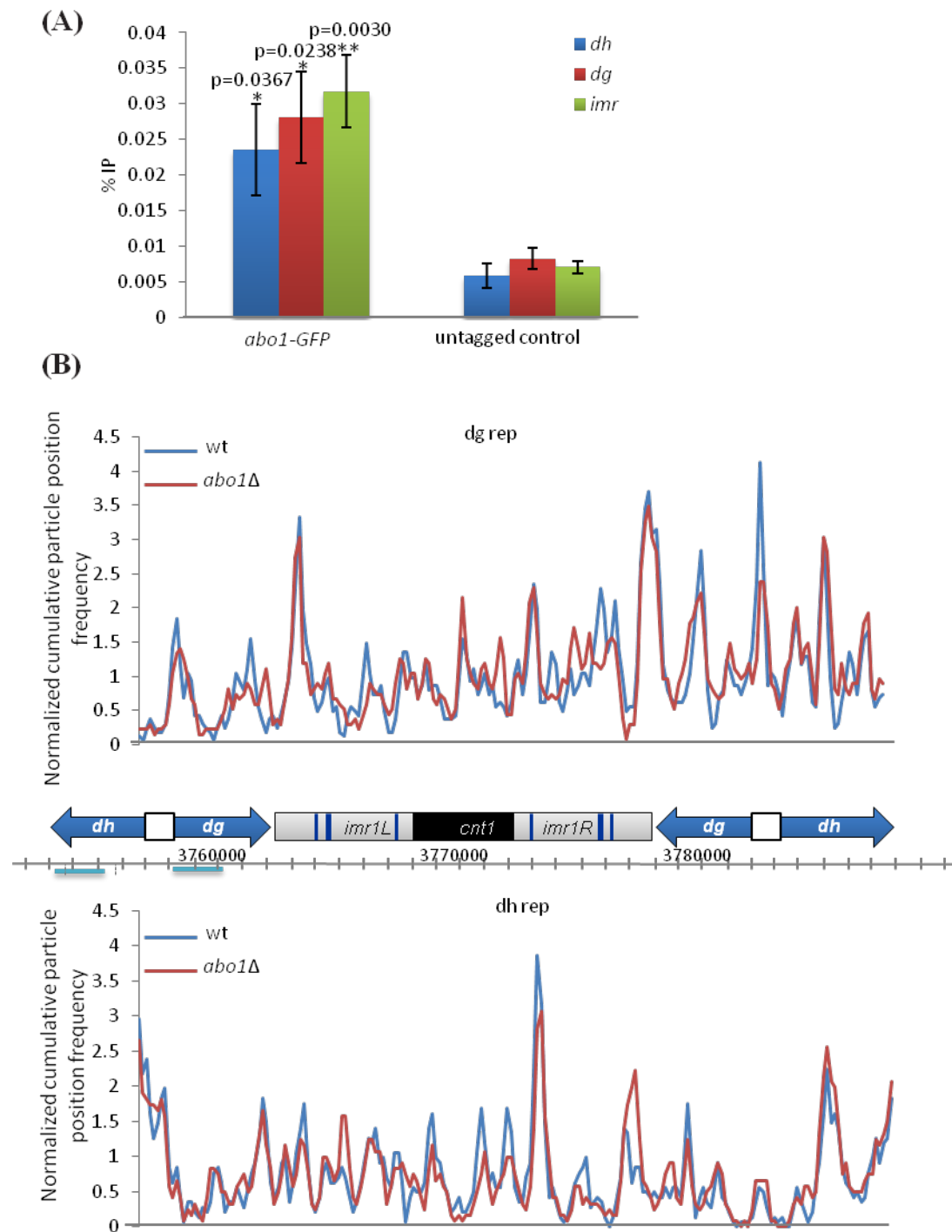


Figure 3.8 Perturbations to nucleosomes are visible over heterochromatic regions in *abo1Δ* cells.

(A) Abo1-GFP levels were determined as IP relative to input at the indicated strains over the indicated regions by ChIP-qPCR analysis. Data are the mean of four independent biological replicates and error bars denote \pm SEM. P values were calculated relative to the untagged control (* $p < 0.05$; ** $p < 0.01$). **(B)** Alignment of mononucleosomes (150 bp) generated by MNase-seq over the indicated regions of centromere 1.

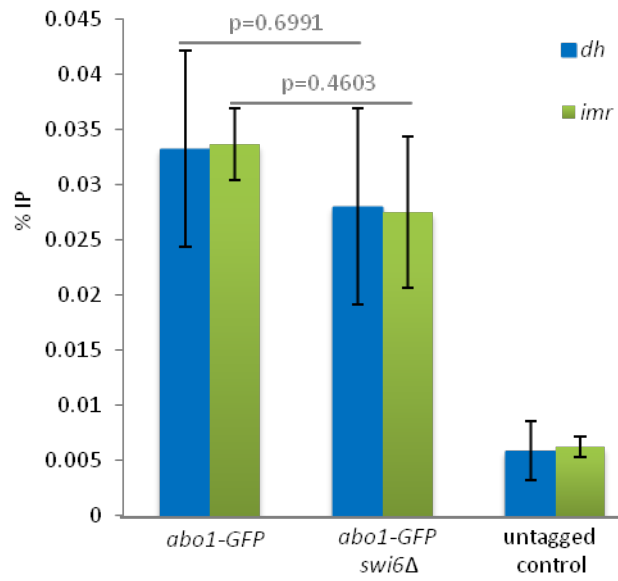


Figure 3.9 Abo1-GFP enrichment over pericentromeric regions is unaffected by loss of *swi6*⁺.

Abo1-GFP levels were determined as IP relative to input at the indicated strains over the indicated regions by ChIP-qPCR analysis. Data are the mean of three independent biological replicates and error bars denote \pm SEM. (All tagged strains are significantly enriched over the untagged control with a p-value of less than 0.05.)

3.2.5 A role for *Abo1* in nucleosome organization over *Tf2* retrotransposons and retrotransposon remnants

Next, the chromatin at *S. pombe* *Tf2* LTR retrotransposons was examined. As well as the classic heterochromatic regions, distinctly silenced domains exist in *S. pombe* over LTRs and retrotransposons. These elements are transcriptionally silent, but lack both H3K9 methylation and Swi6 recruitment. Instead, they rely on CENP-B proteins, HDACs and histone chaperones (Hansen *et al.*, 2005; Greenall *et al.*, 2006; Cam *et al.*, 2008). The *S. pombe* genome contains 13 full length *Tf2* long terminal repeat retrotransposons, which present with an increase in expression in the absence of *abo1* Δ as revealed by both microarray analysis and reporter gene measurement of individual elements (Murton, 2012). Nucleosome alignments of *Tf2* elements have revealed a single nucleosome over the 5' LTR, a nucleosome over the UTR and a nucleosomal array over the element ORF. Distinct from most transcribed gene sequences, these retrotransposons have a NDR downstream of the TSS. Comparisons of wild type and *abo1* Δ cells showed a reduction in peak height over the LTR, the UTR and the coding regions of *Tf2* elements suggesting that Abo1-mediated nucleosome assembly occurs in all three regions (Fig 3.10.A). In addition to the full length *Tf2* elements, *S. pombe* contains ~250 solo LTRs (Bowen *et al.*, 2003). Mononucleosome read sequences over 95 of these regions were also aligned and compared. This revealed a single nucleosome over the LTR with a largely nucleosome free region downstream (Fig 3.10.B). Once again, in the absence of *abo1*⁺ the height of the nucleosome peak was reduced, demonstrating that Abo1-mediated chromatin maintenance takes place at these retrotransposon remnants.

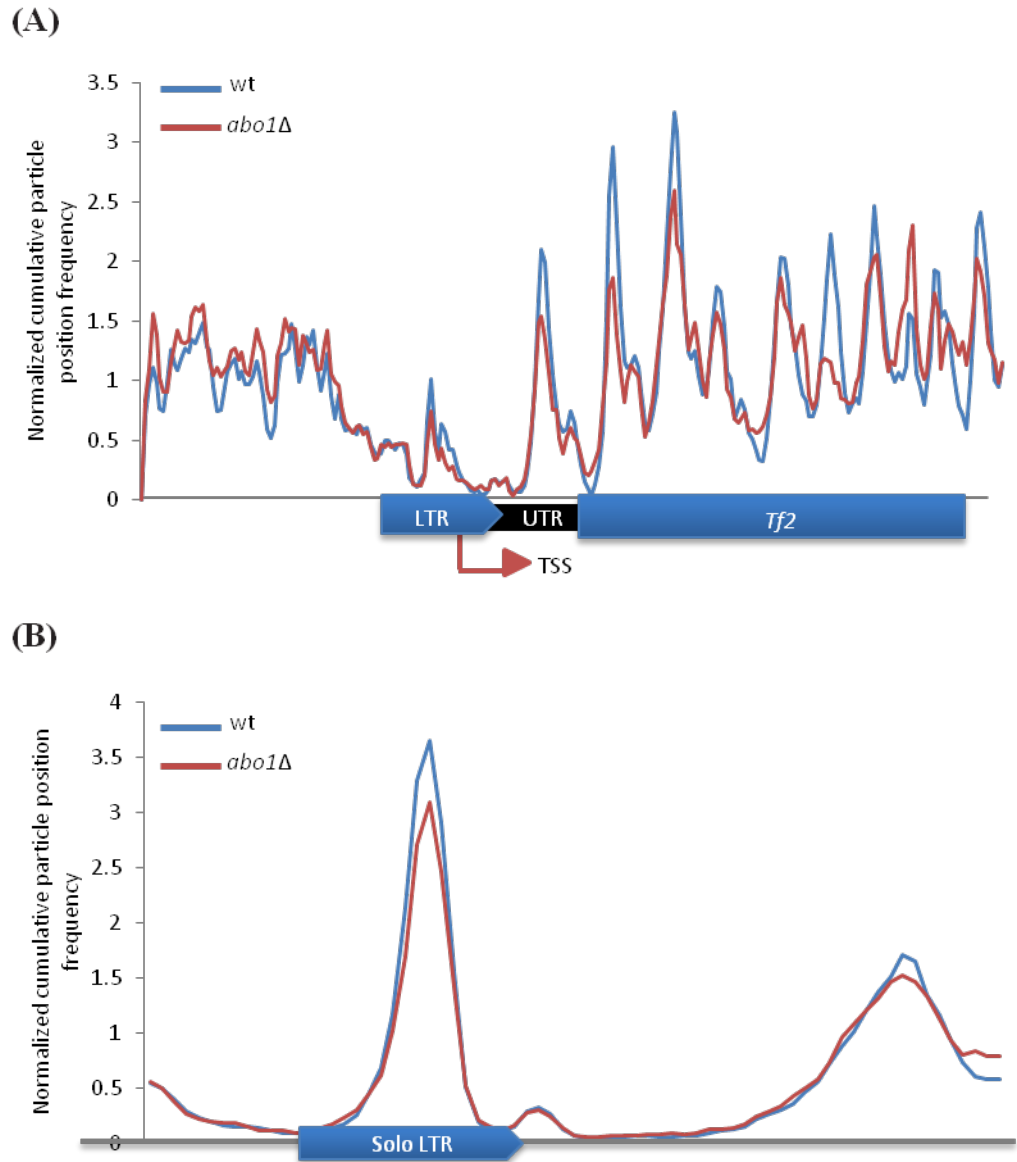


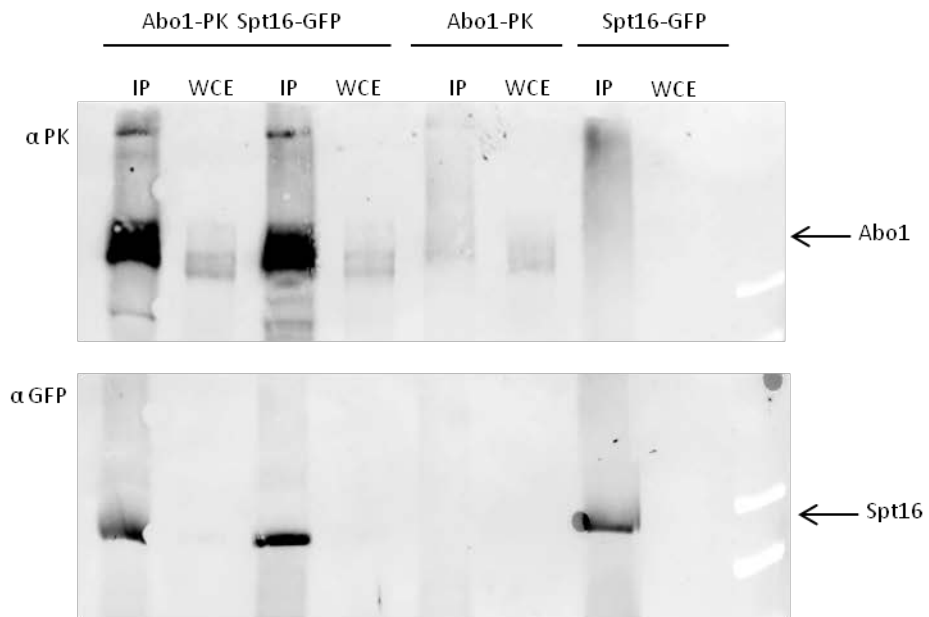
Figure 3.10 Perturbations to nucleosomes are visible over *Tf2* retrotransposons and solo LTRs in *abo1Δ* cells.

(A) Mononucleosomal particles (150 bp) following MNase-seq were aligned over the 13 full length *S. pombe Tf2* elements by their ATG site as described in *pombase*. (B) Mononucleosomal particles (150 bp) generated by MNase-seq were aligned over 95 solo LTRs identified in the *S. pombe* genome by their start sites as described previously (Bowen *et al.*, 2003).

3.2.6 Abo1 physically associates with the FACT histone chaperone

The MNase profiles suggest that Abo1 functions as a histone chaperone and evidence from *S. cerevisiae* indicates that Yta7 physically and genetically interacts with histone chaperones. Preliminary mass spectrometry analysis of Abo1 interacting proteins revealed the two subunits of the FACT complex, Spt16 and Pob3, as physically associating with Abo1 (L. Subramanian & R. Allshire, personal communications). In order to confirm this finding, co-immunoprecipitation analysis of Abo1 with either Spt16 or Pob3 was carried out. Strains expressing Spt16-GFP and Abo1-PK or Pob3-GFP and Abo1-PK were analyzed. In each case the pull-down step was carried out using Sepharose A beads coupled to the anti-GFP antibody, then samples were analyzed by western blotting, with the anti-PK antibody. The presence of Abo1 was detected only in the relevant immunoprecipitated samples indicating that Abo1 physically interacts with both Spt16 and Pob3 (Fig 3.11.A and B).

(A)



(B)

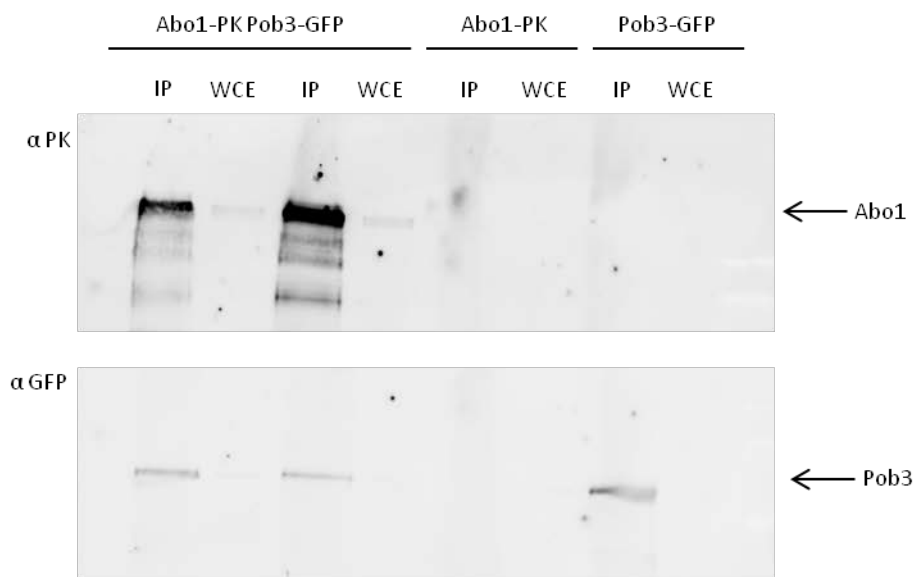


Figure 3.11 Abo1 physically interacts with components of the FACT complex.

(A) and (B) Whole cell protein extracts of the indicated strains were immunoprecipitated using Sepharose A beads coupled to the α GFP antibody. WCE contains 2% of that used in the immunoprecipitation (IP). The presence of tagged proteins was analyzed by western blotting using α PK and α GFP antibodies. The data shown here is representative of two biological replicates.

3.2.7 Enrichment of Spt16 is increased in the absence of $abo1^+$ at transcriptionally silent regions

Next, the effect of loss of $abo1^+$ upon Pob3 and Spt16 chromatin binding was examined. Pob3-GFP and Spt16-GFP ChIP-qPCR was carried out in the presence and absence of $abo1^+$. No significant difference was noted at actively transcribed regions; however there was a small but significant increase of Spt16 levels at the $tlh1/2^+$ genes upon deletion of $abo1^+$ (Fig 3.12). $tlh1/2^+$ are located within the subtelomeric regions of chromosomes and in the absence of $abo1^+$ $tlh1/2^+$ transcript levels are significantly increased (A. J. Whale, personal communications). Therefore, it is likely that FACT levels increase at $tlh1/2^+$ loci as a result of corresponding increase in RNA Pol II levels. Overall, deletion of $abo1^+$ does not seem to have an impact upon Spt16 and Pob3 localization at actively transcribed genes.

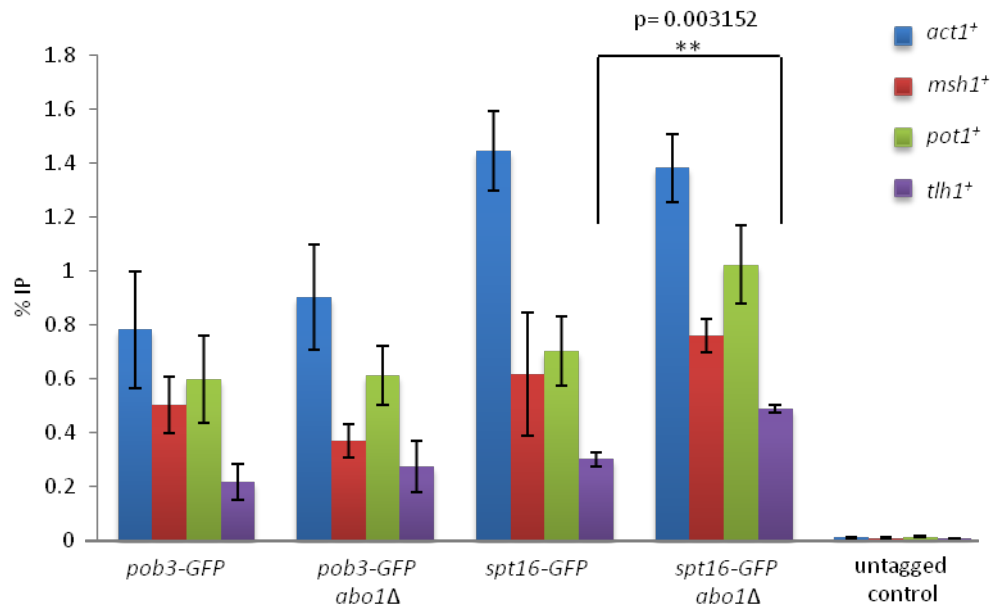


Figure 3.12 Loss of *abo1*⁺ leads to an increase in Spt16-GFP levels at the *tlh1*⁺ loci. Enrichment of Pob3-GFP and Spt16-GFP in midlog phase growing cells was detected using ChIP-qPCR analysis at the indicated loci. Data are the mean of at least three independent repeats and error bars represent \pm SEM (** denotes $p < 0.01$).

3.2.8 *Abo1* localization is deregulated at some genes in the absence of functional FACT complex

Next, the role of FACT in regulating Abo1 recruitment and localization at transcribed genes was probed. Abo1-GFP levels were measured by ChIP-qPCR in the presence and absence of *pob3*⁺. Upon loss of *pob3*⁺, Abo1-GFP levels significantly decreased at the *act1*⁺ locus, hinting at a role for *pob3*⁺ in appropriate Abo1 localization (Fig 3.13). On the other hand, further loci inspected, *pot1*⁺ and *msh1*⁺, showed a small but significant increase in Abo1-GFP enrichment, while *tlh1/2*⁺ loci displayed no change upon deletion of *pob3*⁺ (Fig 3.14). As *spt16*⁺ is an essential gene in *S. pombe*, a *ts* allele (*spt16-18*) (Choi *et al.*, 2012) was utilized to determine the impact of Spt16 upon Abo1 chromatin binding. Even at the permissive temperature (30°C) the *spt16-18* strain has phenotypes, such as slow growth and an elongated cell shape, suggesting that Spt16 protein function is somewhat compromised (data not shown). Abo1-GFP enrichment on the chromatin was assayed by ChIP-qPCR again, and its enrichment was significantly reduced at the *act1*⁺ locus while there was a small but significant increase at *pot1*⁺ (Fig 3.14.A), similarly to that observed in *pob3*Δ cells, suggesting that overall Abo1 distribution is perturbed. Next, midlog phase growing cells were incubated at the non-permissive temperature (37°C) for 2 hours, as described previously (Choi *et al.*, 2012), and ChIP-qPCR analysis was carried out to determine whether further loss of FACT function would lead to any further changes in Abo1 chromatin association. At the *act1*⁺ locus Abo1 enrichment was significantly reduced in the *spt16-18* mutant compared to the wild type (Fig 3.14.B), however there was not a significant change at the *pot1*⁺ loci, like that observed previously, nor were there any significant changes at a number of other loci tested. These results suggest that Spt16 is needed for appropriate Abo1 localization to some but not all transcribed regions.

Abo1-GFP enrichment was also probed at heterochromatic regions in the absence of *pob3*⁺ and in the *spt16-18* mutant incubated at the non-permissive temperature. Abo1 levels did not change significantly over the centromeric region (*cnt1*), nor over the *dh* repeats and the *imr* regions (Fig 3.15). Thus it would appear that Abo1 localization is FACT dependent only at actively transcribed sequences and more likely at specific loci.

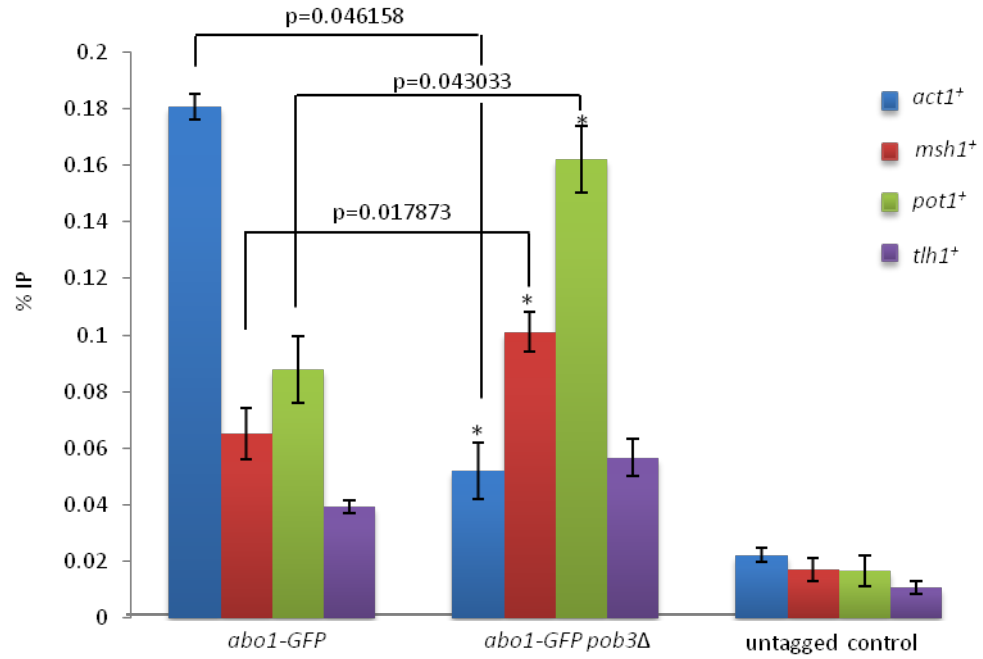
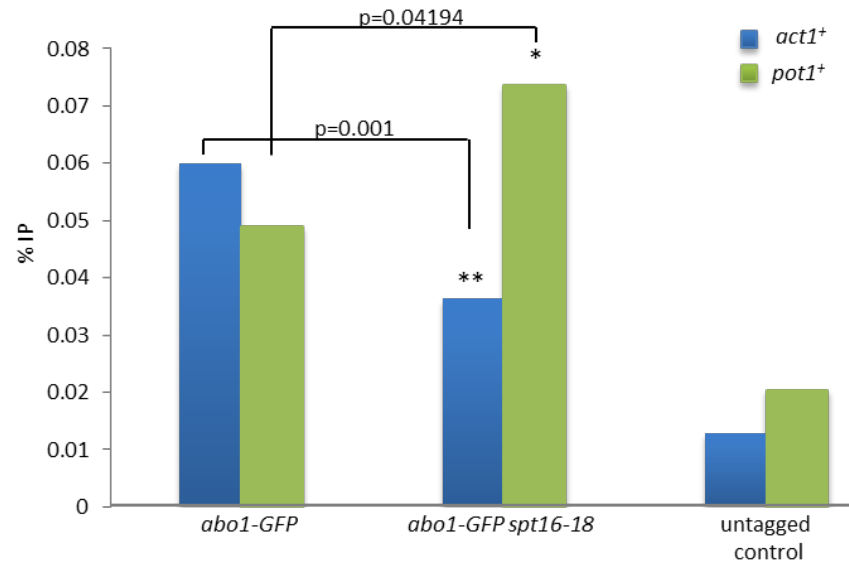


Figure 3.13 Deletion of *pob3*⁺ alters Abo1-GFP localization over several loci.

Enrichment of Abo1-GFP in midlog phase growing cells was detected using ChIP-qPCR analysis at the indicated loci. Data are the mean of three independent biological replicates. Error bars represent \pm SEM (* denotes $p < 0.05$). All tagged samples are significantly enriched ($p < 0.05$) compared to the untagged control with the exception of *abo1-GFP pob3Δ* over the *act1*⁺ loci ($p = 0.09686$).

(A)



(B)

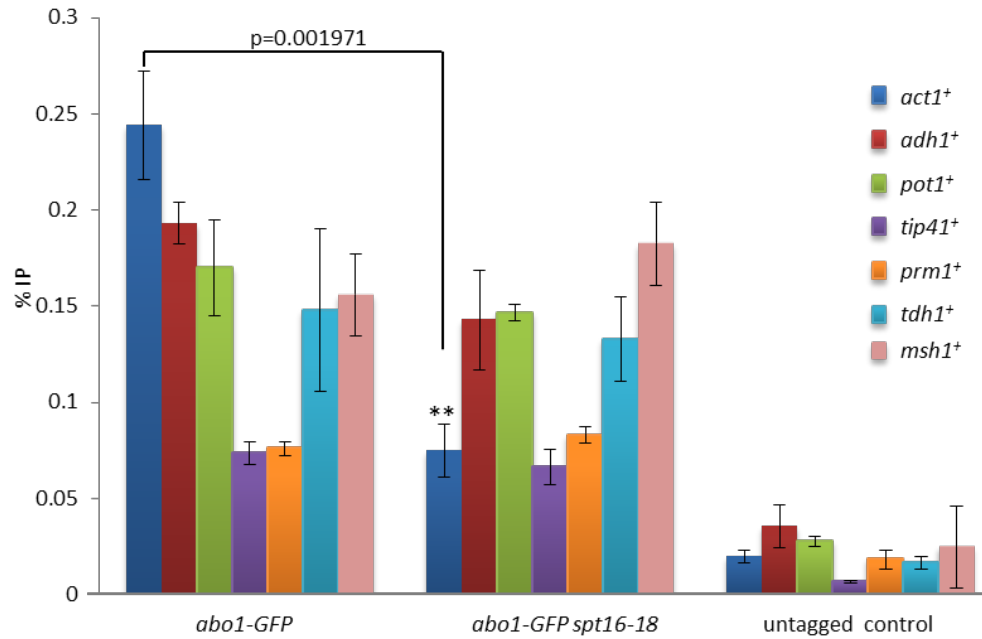


Figure 3.14 Inactivation of *spt16*⁺ alters Abo1-GFP enrichment on chromatin.

(A) ChIP-qPCR analysis was used to detect Abo1-GFP enrichment at the indicated loci in midlog phase growing cells. Data are the mean of at least three independent repeats and error bars denote \pm SEM (* $p < 0.05$; ** $p < 0.01$). All tagged strains are significantly different from the untagged control ($p < 0.05$). All tagged strains are significantly different from the untagged control ($p < 0.05$). (B) Midlog phase growing cells were placed at 37°C for 2 hours, following growth at 30°C, in order to further reduce Spt16 function as described previously by Choi *et al.* (2012). ChIP-qPCR analysis was used to detect Abo1-GFP enrichment at the indicated loci. Data are the mean of at least three independent repeats and error bars represent \pm SEM (** denotes $p < 0.01$). All tagged strains are significantly different from the untagged control ($p < 0.05$).

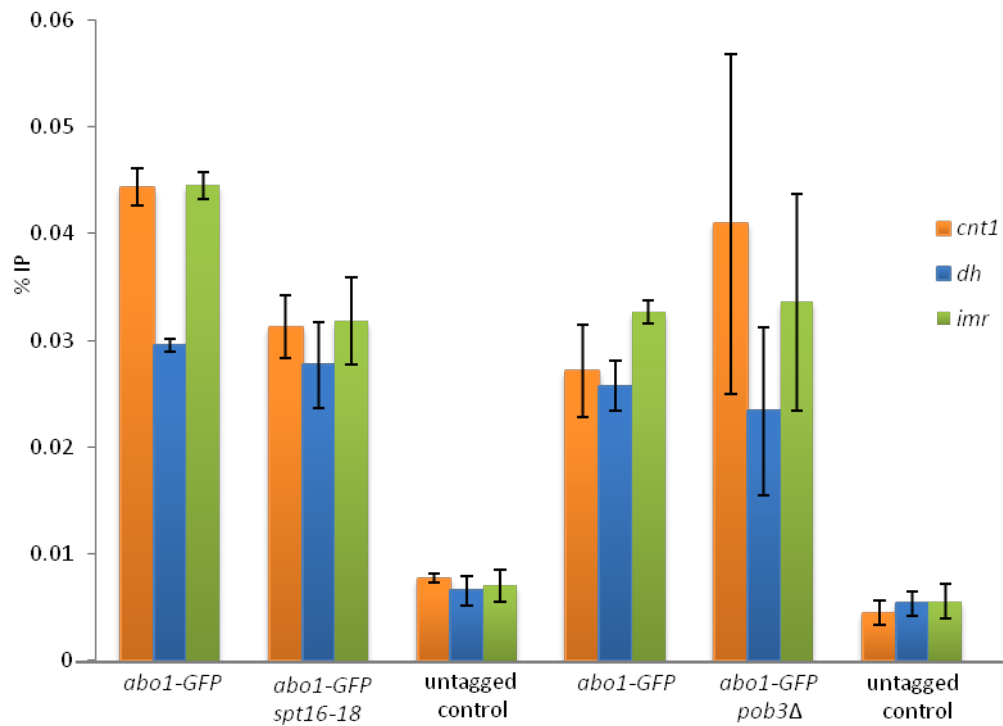


Figure 3.15 Loss of FACT function does not affect Abo1-GFP localization on heterochromatin.

ChIP-qPCR analysis was used to detect Abo1-GFP enrichment at the indicated loci in midlog phase growing cells. Data are the mean of at least two independent repeats and error bars denote \pm SEM. All tagged strains are significantly enriched compared to the untagged control ($p < 0.05$).

3.2.9 Requirement for Abo1 in nucleosome organization extends to replication origins

Based on the connection with FACT, which is known to function both as a replication-independent and replication-dependent histone chaperone, the role of *abo1*⁺ surrounding replication origins was examined. Replication origins were aligned either by the 217 origin of replication complex (ORC) binding sites or by their AT islands as described previously (Givens *et al.*, 2012). In agreement with previous observations, a broad NDR is observed over replication of origin sites. Loss of *abo1*⁺ resulted in increased nucleosome occupancy over the NDRs while a reduction in nucleosome occupancy was observed over the flanking regions independent of the alignment feature used (Fig 3.16). These findings suggest another overlap of function between Abo1 and FACT and hint at a possible role for Abo1 in replication initiation.

Spt16-GFP and Pob3-GFP enrichment over two replication origins, *ars2004* and *ars727* was assayed next. *ars2004* is an early-firing replication origin, that is thought to be highly active, while *ars727* is late firing, with lower activity (Hayashi *et al.*, 2007; Givens *et al.*, 2012). ChIP-qPCR analysis of non-synchronous midlog phase populations showed that both Pob3 and Spt16 localize to these sites. Upon deletion of *abo1*⁺, not Pob3, but Spt16 levels are significantly increased at both replication origins tested (Fig 3.17.A). This would suggest that Abo1 functions to keep Spt16 (FACT) away from replication origins; possibly to limit unwanted reorganization around these sites until the appropriate time.

Next, Abo1-GFP levels were measured over *ars2004* and *ars727*. ChIP-qPCR analysis of these regions showed that Abo1-GFP enriches at both with relative similar levels (Fig 3.17.B). To determine, whether this is also FACT dependent, *spt16-18* cells grown at the non-permissive temperature were utilized. Abo1-GFP levels were not significantly altered over the replication origins inspected (Fig 3.17.C). Abo1-GFP *pob3*Δ cells were also inspected for Abo1 enrichment over these regions and once again there wasn't a significant alteration in Abo1-GFP levels. Thus Abo1 recruitment to replication origins is not dependent upon the FACT complex.

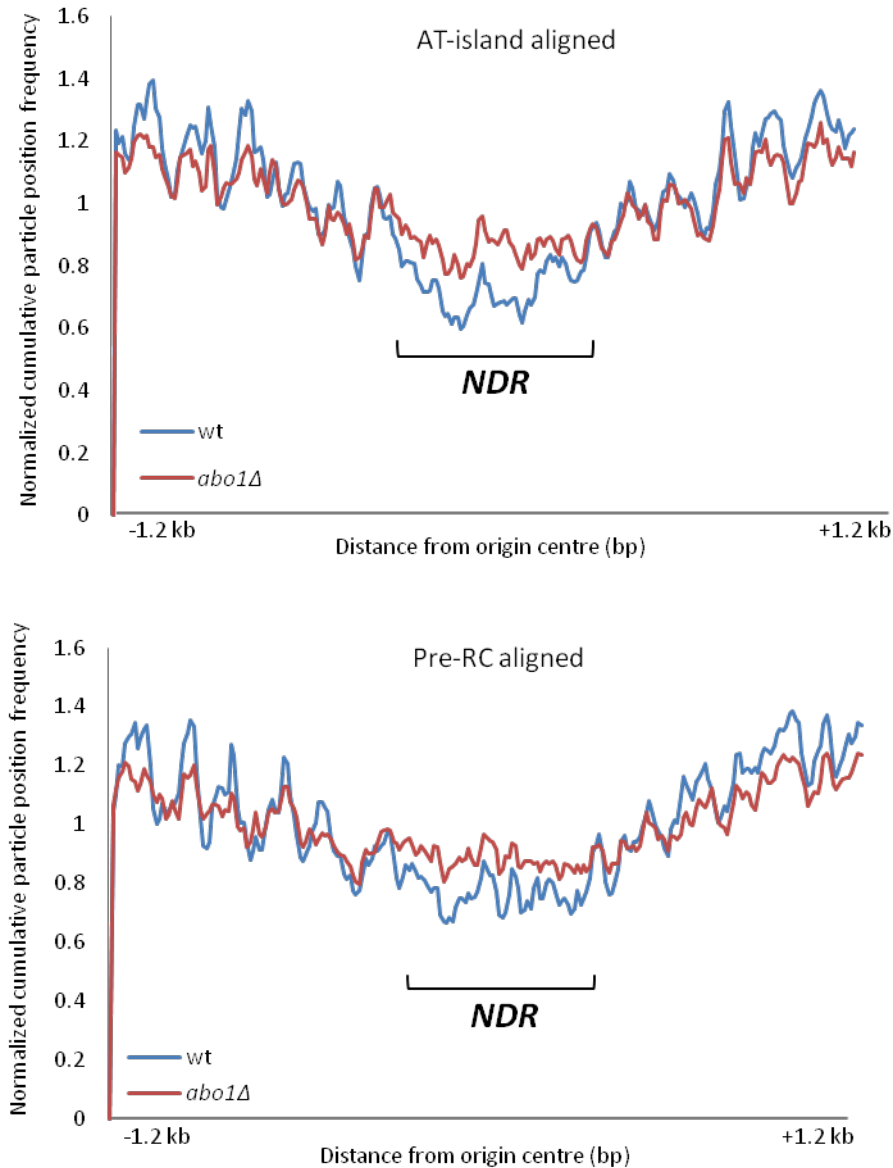


Figure 3.16 Loss of *abo1*⁺ leads to the over accumulation of nucleosomes over the NDR of replication origins.

Mononucleosomal particles (150 bp) following MNase-seq were aligned over 217 replication origins either by their AT islands or by binding sites of the pre-replication complex previously described (Givens *et al.*, 2012).

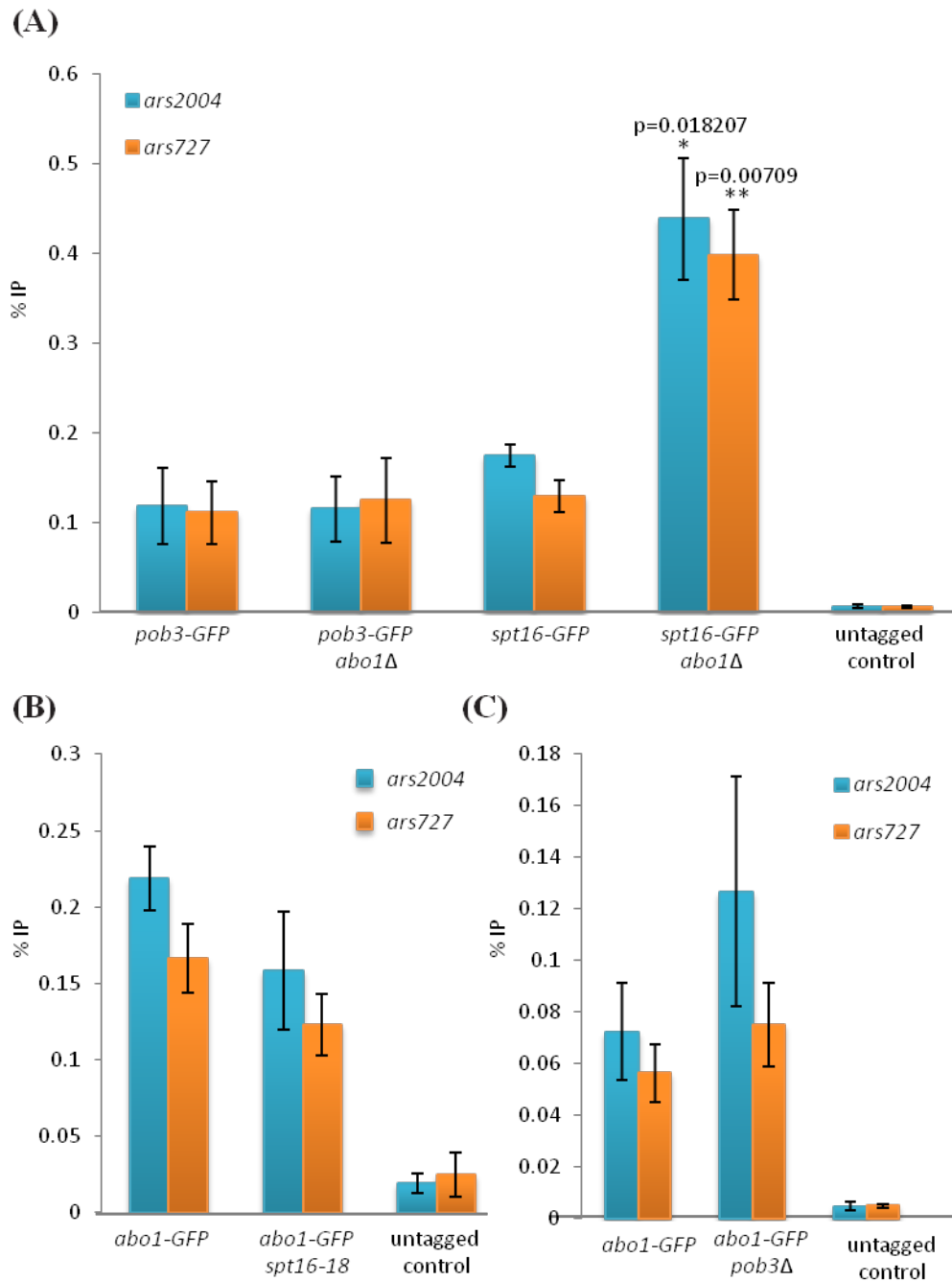


Figure 3.17 Loss of *abo1*⁺ leads to an increase in Spt16-GFP levels at replication origins.

(A) ChIP-qPCR of Pob3-GFP and Spt16-GFP was carried out over two replication origins, *ars2004* and *ars727*, in midlog phase growing cells. The data are the mean of three independent repeats and error bars denote \pm SEM (* denotes $p < 0.05$; ** $p < 0.01$). (B) ChIP-qPCR analysis of Abo1-GFP in *spt16-18* cells over two replication origins, *ars2004* and *ars727*, in midlog phase growing cells. The data are the mean of at least three independent repeats and error bars denote \pm SEM. (C) ChIP-qPCR analysis of Abo1-GFP in *pob3Δ* cells over two replication origins, *ars2004* and *ars727*, in midlog phase growing cells. The data are the mean of four independent repeats and error bars denote \pm SEM. All tagged strains are significantly enriched compared to the untagged control ($p < 0.05$).

3.3 Discussion

The findings described in this chapter demonstrate a requirement for the ATAD2 homologue, Abo1, in the global regulation of nucleosome organization and suggest a role in nucleosome assembly. Chromatin sequencing revealed that *abo1*⁺ is required in both coding and intergenic sequences for the appropriate occupancy and positioning of nucleosomes, a finding which agrees with previous data demonstrating that loss of *abo1*⁺ leads to the accumulation of both coding and non-coding transcripts (Murton, 2012). The function of Abo1 extends to heterochromatic regions and accordingly, previous findings have demonstrated that it is required for appropriate silencing within these regions, as well as for chromosome segregation and meiosis (Murton, 2012).

3.3.1. *Abo1 Functions in the same pathway(s) as the FACT complex*

Nucleosome eviction and deposition are important processes coupled to transcription (in addition to replication). Several ATP-dependent remodelers (CHD1, SWI/SNF) and histone chaperones (HIRA, Asf1, FACT, Spt6, and Rtt106) have now been shown to function in these processes. The requirement for Abo1 in silencing spurious transcription as well as in the maintenance of nucleosome organization over genic regions would suggest that it also acts in the wake of elongating Pol II, most likely in concert with other histone chaperones. The distribution and enrichment of Abo1 would also support its role in transcription-coupled nucleosome disassembly/assembly, since it is readily enriched at actively transcribed regions. Previous work using *S. cerevisiae* as a model has also found that *YTA7* genetically interacts with a number of histone chaperones, such as HIRA, FACT, Asf1 and Rtt106, and also co-purifies with several chromatin interacting proteins, such as FACT, Rtt106, and RNA Pol II (Gradolatto *et al.*, 2008; Gradolatto *et al.*, 2009). The work presented here adds further evidence that the interaction between histone chaperones and Abo1 is evolutionarily conserved, as Abo1 also co-purifies with the components of the *S. pombe* FACT complex, Spt16 and Pob3. Furthermore, in the absence of *pob3*⁺ and *spt16*⁺ function, Abo1 enrichment on the chromatin is significantly reduced at the *act1*⁺ loci, consistent with FACT being required for the correct recruitment and/or localization of Abo1 at some actively transcribed genes. In contrast, Abo1-GFP levels have increased over the *pot1*⁺ and *msh1*⁺ loci, while there was no change observed over heterochromatic regions,

suggesting that Abo1 depends on FACT for appropriate localization primarily over sequences with 'active' nucleosome turnover. Overall, it would be highly informative to obtain a high resolution view of both histone H3 levels and Abo1 binding in wild type cells as well as in the *pob3Δ* and *spt16-18* mutants in order to further address this issue.

There are further suggestions that FACT and Abo1 function in the same pathway, as deletions of *abo1*⁺ and *pob3*⁺ are non-additive. Sensitivity assays of DNA damaging and oxidative stress inducing agents show that the *abo1Δ pob3Δ* double mutant is no more sensitive than the *pob3Δ* single mutant (A. J. Whale, personal communications). Moreover, deletion of *abo1*⁺ and reduced levels of Spt16 lead to the production of the same set of intergenic transcripts (A. J. Whale, personal communications) (Choi *et al.*, 2012). This along with the ChIP data suggests that Abo1 functions downstream of FACT and/or that its proper chromatin localization is dependent on the FACT complex. This model suggests one of two things; one that FACT and Abo1 co-operate in remodeling nucleosomes in front of an elongating Pol II, and that in the absence of either nucleosomes are not appropriately remodeled or disassembled, impeding Pol II progression, or that Abo1 along with FACT plays a role in nucleosome reassembly following Pol II passage. There are arguments for both models and it is also possible that like FACT, Abo1 also functions in both assembly and disassembly of nucleosomes.

There are several mechanisms by which Abo1 could function in either or both of these processes. Abo1 is a member of the AAA-ATPase family of proteins, which are generally accepted to act as molecular motors that can facilitate the folding/unfolding of substrate proteins. Therefore it is possible that Abo1 acts upon the histone octamers and uses the energy from ATP hydrolysis to destabilize the nucleosome and consequently facilitate nucleosome breathing which in turn allows FACT to remove or remodel histone H2A-H2B dimers. Of course by the same mechanism, it would also be able to help re-assemble entire nucleosomes or stabilize the partially unfolded nucleosome during Pol II progression, and while FACT is thought of as a chaperone involved in breaking nucleosomes (Orphanides *et al.*, 1998; Belotserkovskaya *et al.*, 2003; Formosa, 2012; Hsieh *et al.*, 2013), it has also been shown to promote the reassembly of old histones behind RNA pol II (Jamai *et al.*, 2009), and so it would be interesting to determine whether any of these processes are compromised in the absence of *abo1*⁺. Histone turnover could be measured, which would shed some light on the ability of Abo1 to replace nucleosomes following Pol II progression.

Interestingly, deletion of the two *S. cerevisiae* *nhp6*⁺ genes (*nhp6a* and *nhp6b*) results in strikingly similar phenotypes to those described upon *abo1*⁺ loss, such as a global reduction of occupancy and the fuzziness of nucleosomes (Celona *et al.*, 2011). Nhp6a and Nhp6b are high-mobility group (HMG) non-histone chromatin proteins that act in conjunction with the FACT complex, although are not essential for all FACT activity (Formosa *et al.*, 2001; Ruone *et al.*, 2003). It is thought to act as a factor that catalyzes the first of a two-step destabilization of nucleosomes, which allows FACT to bind and remove the histone H2A-H2B dimers (Formosa *et al.*, 2001; Ruone *et al.*, 2003). However, it is also involved in nucleosome stabilization and assembly following Pol II progression and it also acts to modulate the activities, sliding and binding to nucleosomes, of other ATP-dependent remodelers, like SWI/SNF (Hepp *et al.*, 2014). Deletion of *abo1*⁺ along with *nhp6*⁺ is synthetically negative, suggesting some functional interplay between the two (A.J. Whale, personal communications). It is possible that both Abo1 and Nhp6 act to stabilize/destabilize partially unwound nucleosomes and although they are functionally similar, loss of both would cause greater perturbations. It is also possible that they can both modulate FACT function. To this end, it would be possible to measure FACT levels in either of the single mutants and in the double mutant to determine whether it is altered in an additive manner. It would also be possible to assay FACT activity in nucleosome assembly *in vitro* with and without these proteins present, or *in vivo* by measuring histone turnover.

Finally, deletion of *abo1*⁺ leads to increased levels of Spt16 over replication origins. This would suggest that Abo1 is actually involved in prohibiting Spt16 from amassing over these regions, either by directly preventing FACT-nucleosome interactions, or indirectly, as a result of Abo1 occupying these sites normally. The fact that Abo1 is also enriched over replication origins and that in its absence replication origins have altered nucleosome profiles hints at a role for Abo1 in replication coupled chromatin organization too. Perhaps, by assaying histone H3K56 acetylation patterns, a mark which is associated with newly synthesized nucleosomes, in an *abo1Δ* mutant background; it would be possible to determine whether Abo1 has a role to play in regulating replication-coupled nucleosome assembly as well.

Deletion of *abo1*⁺ also leads to changes to replication origins, and Abo1 itself is phosphorylated in a cell cycle dependent manner (A. J. Whale, personal communications), further suggesting that it functions in the context of replication.

Interestingly, there is evidence that the *Drosophila* FACT is phosphorylated by CK2 and this event prohibits FACT binding nucleosomal DNA, thus weakening its interaction with nucleosomes (Tsunaka *et al.*, 2009). As Abo1 is also phosphorylated by CK2 (A. J. Whale, personal communications), it would be interesting to determine the outcome of this CK2-dependent phosphorylation. There are initial suggestions that Abo1 is also removed from the chromatin upon replication fork stalling, an event which is correlated with an increase in Abo1 phosphorylation, although this is dependent upon the checkpoint kinases Rad3 and Cds1 (A. J. Whale, personal communications). Whether this is due to a role in replication or due to a response to a DNA damaging agent is difficult to determine. There have also been previous observations that the human ATAD2 is removed from the chromatin upon DNA damage induction, in order for repair to take place (Kyle Miller, personal communications). It is possible that the general principles of protein recruitment and removal on the chromatin are similar between DNA damage repair mechanisms and that of replication origins, as has been demonstrated with histone chaperone recruitment to both replication forks and DNA damage repair sites. Indeed, remodelling of chromatin is required in both scenarios. Finally, there is evidence that the *S. cerevisiae* Yta7 is removed from histone gene promoters during transcription, but it is not simply involved in gene repression, as in the absence of *YTA7*, histone gene induction is reduced (Kurat *et al.*, 2011; Zunder and Rine, 2012). Thus, it appears that the role of Yta7 (and indeed Abo1 and ATAD2) is not simply repressing or activating but rather is context dependent and is regulated through different layers.

3.3.2 *Abo1* and nucleosome positioning

Global mapping of nucleosomes has also revealed a role for Abo1 in correct nucleosome positioning over coding sequences. Loss of *abo1*⁺ leads to nucleosomes becoming disorganized, shifting from their preferred sites, and leading to “fuzzy” nucleosomes. This was particularly interesting, as spacing of nucleosomes over coding sequences is depleted upon loss of the CHD chromatin remodeling complex subunits, Hrp1 and Hrp3. It is unlikely that Abo1 works as a nucleosome 'spacer', as AAA-ATPases are distinct from the Snf2-family of helicases. However, it is possible that it contributes to the localization of these CHD remodelers or other chromatin interacting proteins. Preliminary mass spectrometry analysis does indeed indicate that Abo1

physically associates with Hrp1. Also in support of this hypothesis, previous work carried out using *S. cerevisiae* demonstrated that Yta7 blocks the inappropriate spread of the RSC remodeler into the *HTA1* coding sequence (Jambunathan *et al.*, 2005), and the human ATAD2 protein mediates the loading of the MLL histone methyltransferase complex onto the chromatin (Revenko *et al.*, 2010).

3.3.3 *Abo1* function extends to heterochromatin

Abo1 is also required for silencing within heterochromatin. Appropriate heterochromatin formation and maintenance is essential for the recruitment of cohesin proteins to ensure proper chromosome segregation during mitosis (Murton, 2012). Mutations that affect heterochromatin exhibit a variety of defects in chromosome segregation, a high loss rate of a non-essential minichromosome, and an increased sensitivity to the microtubule-destabilizing agent thiabendazole (TBZ). Indeed, loss of *abo1*⁺ leads to all of the aforementioned phenotypes, as well as to loss of marker gene silencing within the *imr* and *otr* regions of centromeric repeat sequences, and to an increase in Pol II mediated non-coding RNA transcription that arises from within the *dg-dh* repeats of the *otr* (Murton, 2012). These domains are characterized by high levels of H3K9Me2 and the association of the HP1 homologue, Swi6. Abo1 is also enriched over these regions suggesting that it is directly involved in heterochromatin maintenance, furthermore Swi6 has been identified as a physical interacting partner for Abo1 (Motamedi *et al.*, 2008), although, in this study this was not addressed. However, deletion of *swi6*⁺ had no effect on Abo1-GFP localization at the *dh* repeats nor the *imr* regions. Quantification of H3K9me2 levels by ChIP-qPCR in wild type and *abo1Δ* cells also showed no significant alterations. The fact that H3K9me2 levels were not reduced in *abo1Δ* cells correlates well with findings from collaborators which suggest that Swi6 levels remain normal and with previous findings from our group which show that Swi6 localization is also normal in *abo1Δ* cells (Murton, 2012). On the other hand, histone H3 levels at these regions are decreased in *abo1Δ* cells and nucleosome mapping revealed marked changes in some nucleosomes over these regions, suggesting that loss of *abo1*⁺ leads to changes in nucleosome occupancy, which apparently is enough to cause loss of silencing, despite an increase in H3K9me2 levels and a normal distribution of Swi6. It could be useful to determine whether there is a global change in histone H3K9 methylation in *abo1Δ* cells, and also in other histone modification marks. A

further connection with respect to heterochromatin maintenance is that FACT has also been demonstrated to maintain heterochromatin fidelity. Loss of *pob3*⁺ alleviates gene silencing at the pericentromeric repeats and at the silent mating-type locus, but not at telomeres (Lejeune *et al.*, 2007), similarly to what has been observed in *abo1*Δ cells. Therefore, it is possible that Abo1 functions alongside FACT in heterochromatin maintenance too; although based on our ChIP assays it is unlikely to be through FACT recruitment of Abo1.

3.3.4 Further possible roles to address for Abo1

While this study has largely been focused on the global nucleosome architecture of *abo1*Δ cells, a future direction could be to address its capacity for histone binding and exchange. Due to time constraints, it was not possible to measure histone turnover in *abo1*Δ cells, nor was it possible to appropriately assess the relative abundance of all histone species in the absence of *abo1*⁺. While, it seems likely that total histone H3 and H2A levels are decreased in *abo1*Δ cells, it is not clear whether histone H4, H2B and H2A.Z behave the same. Interestingly, previous work carried out in tissue culture found that depletion of ATAD2 led to an increase of histone H2A turnover (Caron *et al.*, 2010). Although highly speculative, it is possible that a reduction in H2A levels would lead to an increase in the histone H2A variant H2A.Z to assemble H2A.Z-H2B dimers, and consequently nucleosomes. Therefore loss of ATAD2, and perhaps Abo1, might also affect the ratio between H2A and H2A.Z. What is quite fascinating with respect to this connection is that H2A.Z is primarily found in the promoter regions and in the +1 nucleosome of genes and that H2B-H2A.Z containing nucleosomes tend to be loosely bound and less stable, impeding Pol II progression to a lesser degree than H2B-H2A containing nucleosomes (Weber *et al.*, 2014). Therefore, it might be possible that an over accumulation of H2A.Z, in the absence of H2A, would lead to similar nucleosome arrays as seen in an *abo1*Δ mutant, of course this is only speculation. With respect to this an increase in H2A.Z could also lead to its mis-incorporation, as in the case in the *S. cerevisiae ino80*Δ mutant, which was found to have spurious incorporation of H2A.Z-H2B dimers, leading to genomic instability (Papamichos-Chronakis *et al.*, 2011). Preliminary mass spectrometry data has indicated that Abo1 physically interacts not only with histones H3-H4 but also with H2A, H2B and H2A.Z, as well as with a number of H2A interacting factors. Therefore, another avenue of investigation could be

the connection between Abo1 and regulation of H2A-H2A.Z levels.

Finally, another connection between Yta7 and H2A.Z comes from evidence in *S. cerevisiae*, which has suggested that Yta7, along with H2A.Z (Wan *et al.*, 2009) and Spt16, is required for the induction of inducible genes, indeed Yta7 enriches at the 5' end of these genes (Lombardi *et al.*, 2011). In agreement with these findings, loss of *abo1*⁺ affects the ability of stress response genes *ctt1*⁺, *gpx1*⁺ and *hsp9*⁺ to become fully induced following heat stress (A. J. Whale, personal communications). And so, there are several possible roles for Abo1 in chromatin maintenance and the work for the future will have to involve teasing out the direct versus indirect consequences of *abo1*⁺ loss.

Chapter 4

Global chromatin organization and DNA damage repair by the HIRA histone chaperone in *S. pombe*

4.1 Introduction

HIRA has previously been implicated in genome-wide chromatin maintenance through a role in replication-independent nucleosome assembly. However, its precise contribution to nucleosome organization is yet to be determined. Previous work has revealed that the absence of functional HIRA results in increased cryptic antisense transcription, loss of silencing at heterochromatic regions, and a decrease in viability following exposure to a range of DNA damaging agents (Anderson *et al.*, 2009). These results are consistent with a general role for HIRA in chromatin maintenance, and also suggest that this histone chaperone plays a role in the response to DNA damage. Therefore the aim of the work described in this chapter was firstly to determine the impact of HIRA upon global chromatin organization, and secondly to characterize the role of the HIRA complex in the response to DNA damage.

4.2 Role for the HIRA complex in global nucleosome organization

4.2.1 MNase-seq analysis shows a reduction in nucleosome occupancy in *hip1Δ* cells

As discussed previously, the HIRA histone chaperone in *S. pombe* comprises of four subunits, (Hip1, Slm9, Hip3 and Hip4) and loss of any of them leads to inactivation of the HIRA complex (Blackwell *et al.*, 2004; Greenall *et al.*, 2006; Anderson *et al.*, 2009; Anderson *et al.*, 2010). Therefore, all subsequent work was carried out using a *hip1Δ* mutant strain. In order to characterize the contribution of HIRA to nucleosome organization genome-wide, the previously described MNase sequencing technology was implemented (Section 3.2.1). Three biological replicates from *hip1Δ* cells, containing mono-, di-, and trinucleosomes (Fig 4.1.A), were pooled and sequenced, resulting in 49.6 million aligned paired-end reads. The data was stratified and particles size selected as described previously (Section 3.2.1) and compared to the wild type dataset (Fig 4.1.B). The average distribution of mononucleosome reads was mapped in both the wild type and *hip1Δ* samples (Fig 4.1.C). Both wild type and *hip1Δ* mononucleosome reads resolved into a periodic pattern with an average repeat length of 156 bp. However *hip1Δ* cells presented with slight changes to nucleosome peak heights similarly to that observed in *abo1Δ* cells (Section 3.2.1), suggesting that some aspect of global nucleosome organization is disrupted.

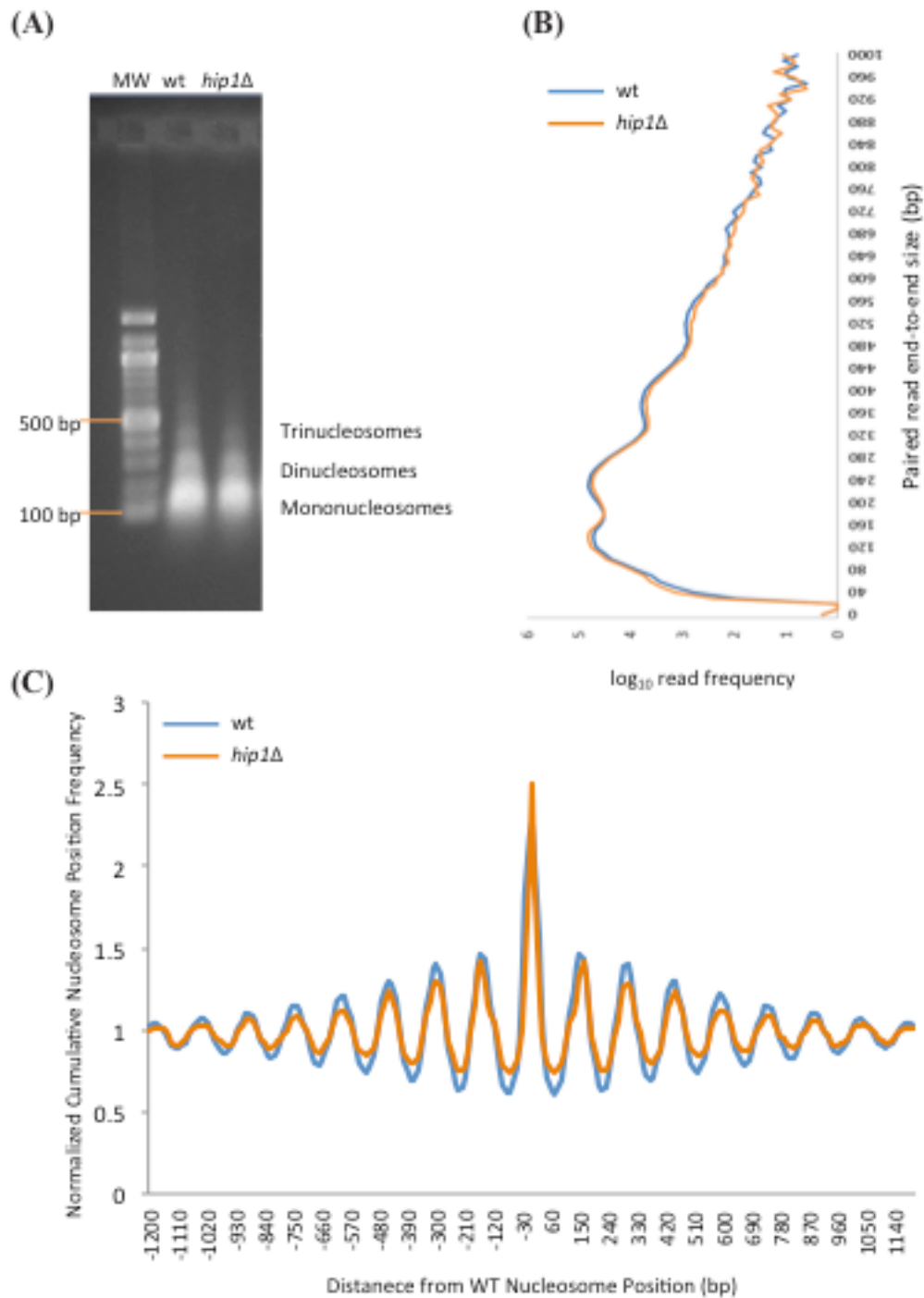


Figure 4.1 Frequency distribution of MNase-seq generated chromatin species.

(A) Ethidiumbromide-stained agarose gels of DNA pools extracted from MNase digested wild type and *hip1Δ* chromatin used for chromatin sequencing in this study. Below the 500 bp mark are the mono-, di- and tri-nucleosome bands for each set. (B) Frequency distribution of paired read end-to-end size values after MNase-seq of DNA shown in figure A. (C) Frequency distributions of mid-point nucleosome positions following MNase-seq of wild type and *hip1Δ* cells.

4.2.2 HIRA is necessary for nucleosome organization over the ORFs of protein coding genes

Nucleosome organization of wild type and *hip1Δ* cells was determined over protein coding regions as described previously (Section 3.2.2). The average nucleosome profiles of wild type and *hip1Δ* cells were similar over the NDR and the promoter region but not over the ORF. *hip1Δ* cells presented with a reduction in peak height over the ORF, particularly toward the 3' end of genes (+4 nucleosome onwards). Overall, these findings suggest that HIRA is involved in appropriate nucleosome organization only over the ORF of protein coding regions (Fig 4.2.A), particularly towards the transcription termination sites (TTS). In agreement with a role for HIRA in nucleosome maintenance over coding regions, Hip1-GFP is readily enriched at the *act1*⁺ ORF (Fig 4.2.B).

The finding that HIRA is required for proper nucleosome organization over ORFs is consistent with the finding that HIRA suppresses cryptic antisense transcription from within the 3' end of genes (Anderson *et al.*, 2009). To further investigate this, nucleosome profiles over some genes where antisense transcription is known to take place were compared (Anderson *et al.*, 2009). A widespread perturbation in nucleosome architecture was observed over the gene body of the *hrp1*⁺ locus, which extended into neighboring regions, including *atg12*⁺ (Fig 4.3.A). In order to confirm some of the differences in the nucleosome profiles observed in Fig 4.3.A, mononucleosomal DNA was isolated from independent pools of MNase digests and a previously described quantitative PCR (MNase-qPCR) approach was used to compare the occupancy of some specific nucleosomes in the wild type (Infante *et al.*, 2012). The area amplified overlaps the center of the peak generated by MNase-seq and the location and name of the amplified regions is indicated in Figure 4.3.A. Using two regions, one within the *hrp1*⁺ gene and one over *atg12*⁺, it was possible to independently verify that these nucleosome peaks are reproducibly decreased in *hip1Δ* cells (Fig 4.3.B).

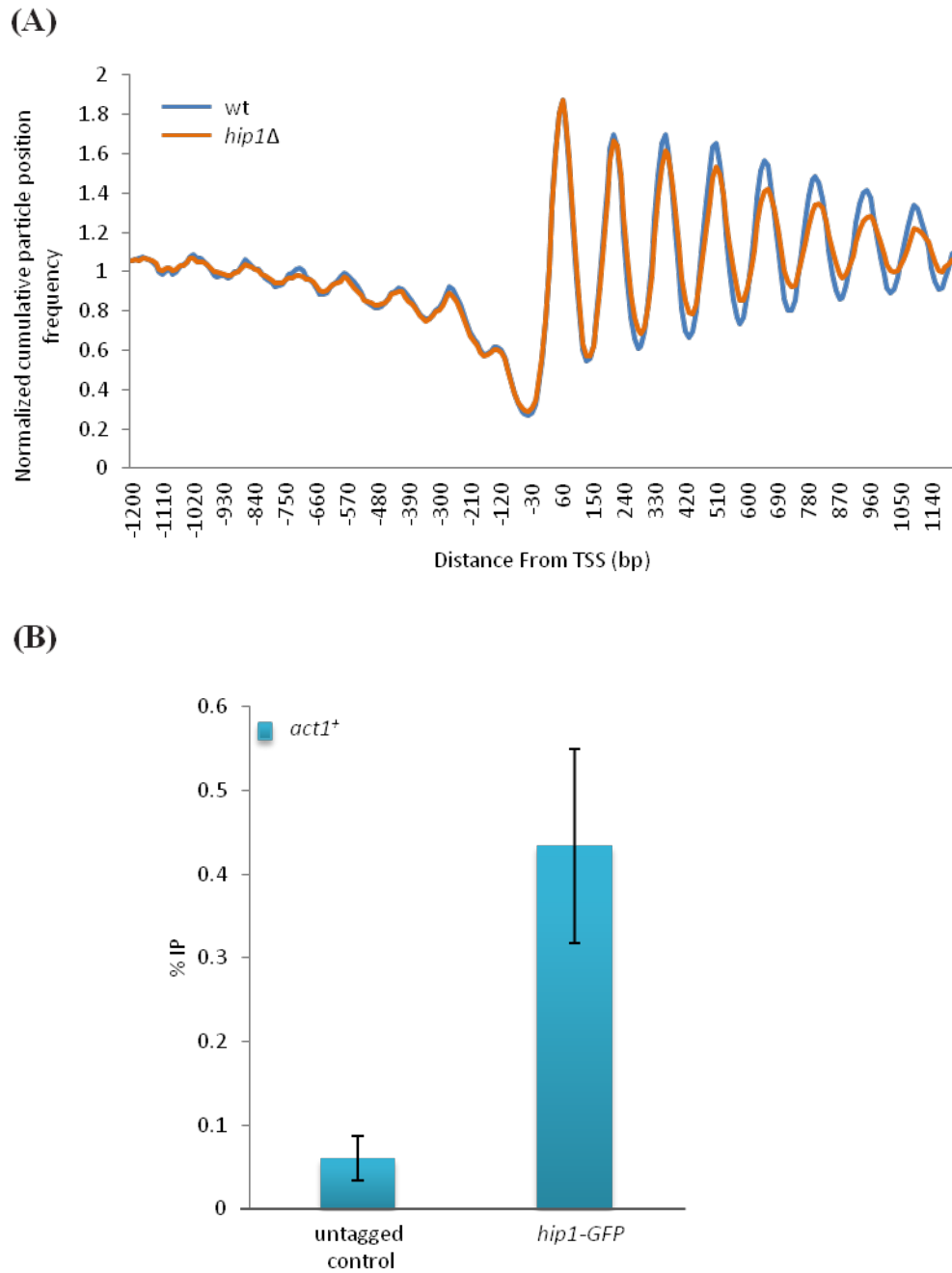


Figure 4.2 Loss of *hip1⁺* leads to a drop in mononucleosome occupancy over coding regions, particularly towards the 3' end of genes.

(A) Mononucleosomal fragments (150 bp) following MNase-seq for 4013 protein-coding genes were aligned by their transcription start sites (TSSs) as identified by Lantermann *et al.* (2009). (B) ChIP-qPCR analysis of Hip1-GFP enrichment over the *act1⁺* loci.

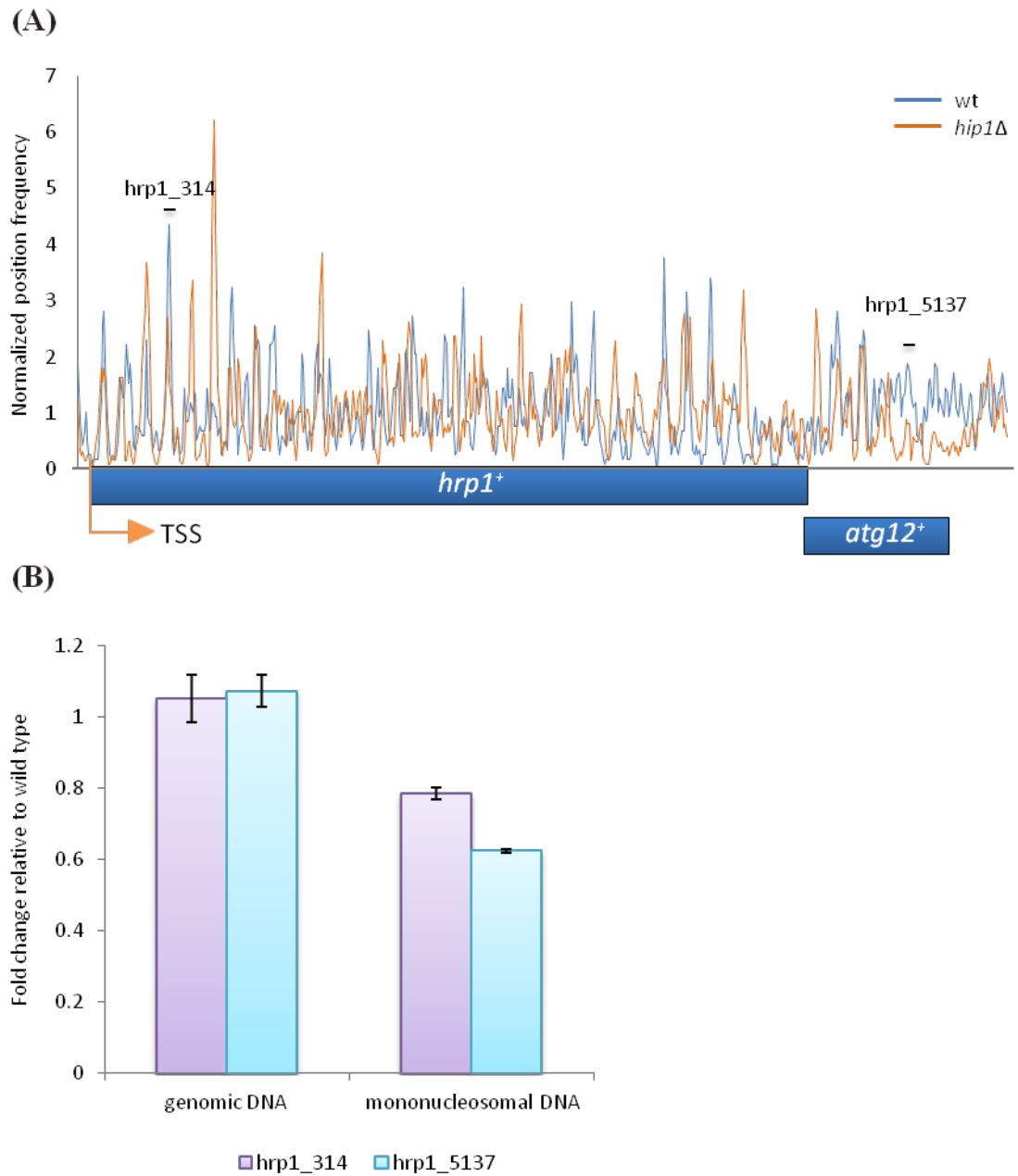


Figure 4.3 Loss of *hip1*⁺ results in perturbations of mononucleosomes over the *hrp1*⁺ locus.

(A) Alignment of mononucleosomes (150 bp) following MNase-seq over the *hrp1*⁺ loci for wild type and *hip1*Δ cells (B) qPCR validation of the sequencing data. Mononucleosomes were excised from an agarose gel and qPCR was implemented to measure sequence reads over the indicated loci from Figure (A). Genomic DNA was included as a control. Data is the mean of three technical repeats for a biological replicate to the sequenced dataset. Error bars represent ± STDEV.

At other genes the influence of *hip1*⁺ deletion was much more subtle; however reductions in the occupancy of some nucleosomes were detectable at the 3' end of genes, such as *dbp7*⁺ (Fig 4.4.A). Once again, MNase-qPCR was implemented to measure in an independent biological replicate the relative mononucleosomal DNA over the indicated peaks in Figure 4.4.A. In this case, two peaks were picked for qPCR analysis, one where no change was suggested by the initial MNase-seq generated map and one where a decrease was expected in *hip1*Δ cells compared to the wild type. Indeed the MNase-qPCR results suggest that the amount of DNA was very similar over the *dbp7*_10 region, while a severe reduction in amplification was observed over the *dbp7*_1927 region (Fig 4.4.B). Overall, these findings suggest that relatively subtle perturbations of nucleosome occupancy towards the 3' can be sufficient to allow cryptic antisense transcription. These findings are also consistent with other evidence which suggests that HIRA functions to restore chromatin that has been disrupted by RNA Pol II elongation.

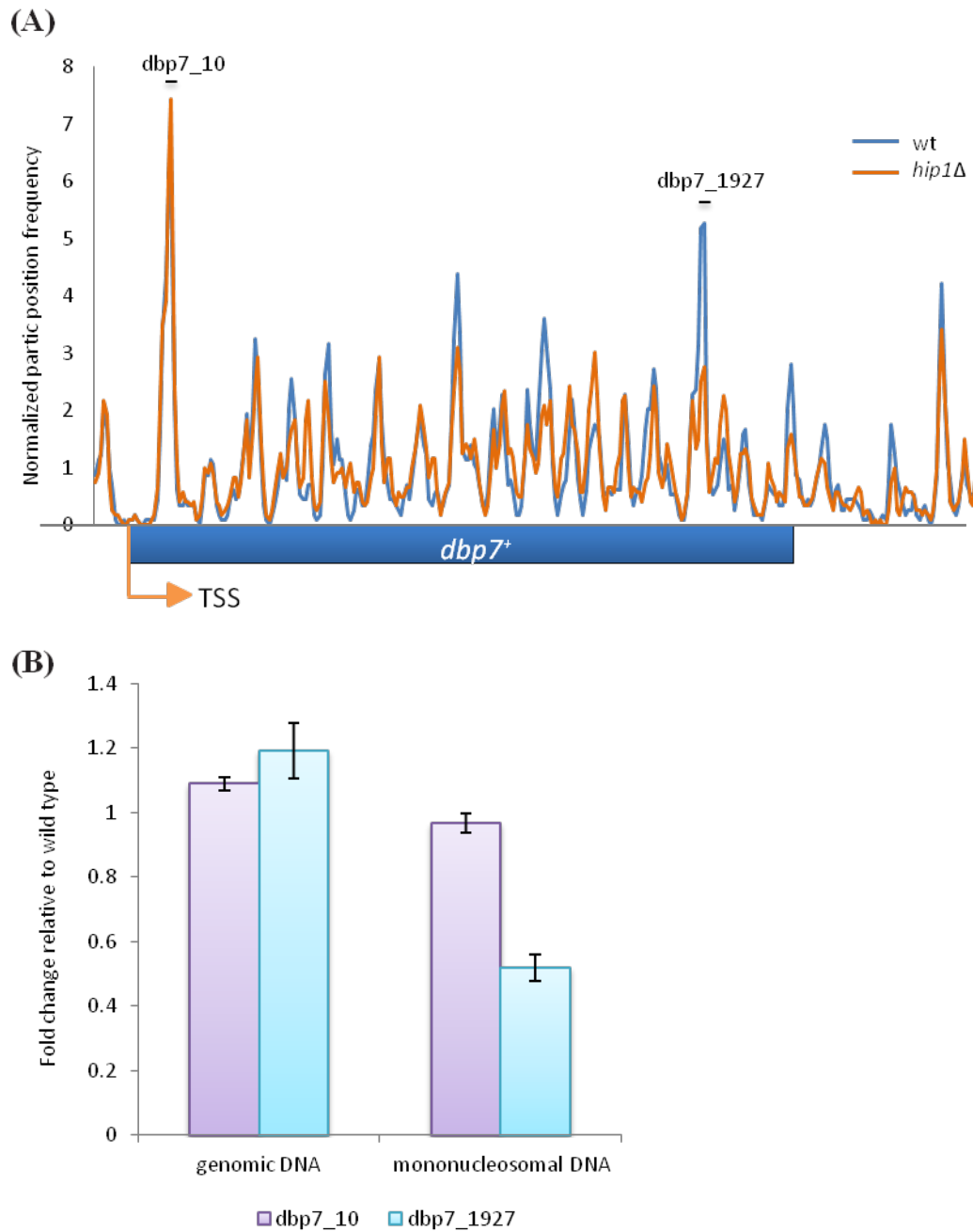


Figure 4.4 Loss of *hip1*⁺ results in perturbations to mononucleosomes over the *dbp7*⁺ locus.

(A) Alignment of mononucleosomes (150 bp) following MNase-seq over the *dbp7*⁺ loci for wild type and *hip1*Δ cells (B) qPCR validation of the sequencing data. Mononucleosomes were excised from an agarose gel and qPCR was implemented to measure sequence reads over the indicated loci from Figures (A). Genomic DNA was included as a control. Data are the mean of three technical repeats for a biological replicate to the sequenced dataset. Error bars represent ± STDEV.

4.2.3 Chromatin structure of HIRA-repressed genes

At a global level HIRA does not appear to influence promoter chromatin (Fig 4.2.A). However, previous microarray analysis has identified numerous Pol II genes that are repressed by HIRA (Anderson *et al.*, 2009). To analyze their chromatin structure, mononucleosome maps of 106 protein coding genes that are at least two-fold up-regulated in the absence of *hip1*⁺ were compared to the complete gene set (4013 protein coding genes). HIRA-regulated genes are often transcribed at low levels (Anderson *et al.*, 2009) and accordingly, their average nucleosome map presented with a shallow NDR and poorly defined nucleosomal peaks (Fig 4.5.A). The average peak of these genes is also low, suggesting that HIRA regulated genes are generally associated with low nucleosome occupancy. This again is characteristic of poorly expressed/silenced genes (Lantermann *et al.*, 2009). Next, wild type and *hip1*Δ nucleosomal maps were compared for HIRA-regulated genes, and in the absence of *hip1*⁺, the height of the nucleosome peak over the promoter is also reduced (Fig 4.5.B). A reduction in the +1 nucleosome peak was also evident, suggesting that HIRA is more likely to be involved in the maintenance of occupancy of the +1 and -1 nucleosomes at these specific loci.

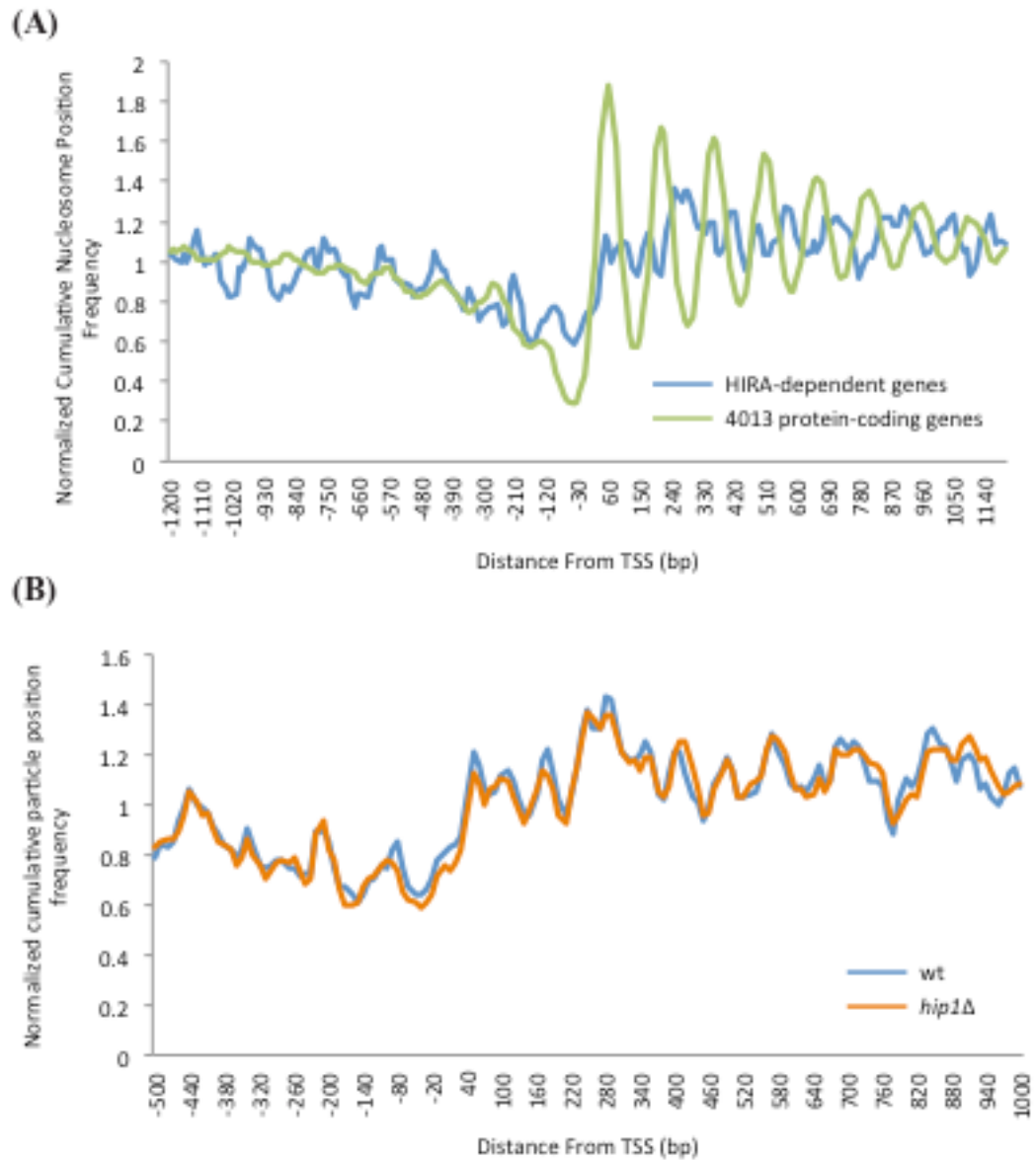


Figure 4.5 Nucleosomal arrays over HIRA-dependent genes are less distinctly organized.

(A) Comparison of MNase-seq generated mononucleosome maps over all 4013 protein-coding genes aligned by their TSSs, as identified by Lantermann *et al.* (2009) and of HIRA-dependent genes, as identified by previous microarray data analysis (Anderson *et al.*, 2009). (B) Alignment of mononucleosomes of HIRA-dependent genes by their TSSs in wild type and *hip1Δ* cells.

4.2.4 Influence of HIRA on the *hht2⁺-hhf2⁺* promoter

HIRA is known to regulate the transcription of histone genes, as examination of a synchronous population shows that histone gene expression is upregulated in *hip1Δ* cells outside of S phase (Blackwell *et al.*, 2004; Takayama and Takahashi, 2007). *S. pombe* has three copies of H3-H4 gene pairs but HIRA mediated repression is thought to operate predominantly through *hht2⁺-hhf2⁺* (Takayama and Takahashi, 2007). Therefore nucleosome organization over the region of the *hht2⁺-hhf2⁺* gene pair was compared. In *hip1Δ* cells a reduction in the nucleosome peak is observed over the promoter region, which is where key transcriptional regulators, Ams2 and Teb1 bind (Fig 4.6.A) (Takayama and Takahashi, 2007; Valente *et al.*, 2013). MNase-qPCR was used to measure in an independent biological replicate the mononucleosome levels over this peak, and in agreement with the MNase-seq data, this too indicates that there is a reduction in nucleosome occupancy over the promoter region in *hip1Δ* cells compared to the wild type (Fig 4.6.B). It is possible that HIRA regulates nucleosome assembly over the promoter sequence of *hht2⁺-hhf2⁺* which is most likely unstable so that during S-phase it can be removed, allowing Teb1 binding, which in turn recruits Ams2, leading to an increase of histone gene transcription (Takayama and Takahashi, 2007; Valente *et al.*, 2013). In the absence of *hip1⁺* this nucleosome is more likely to be absent, allowing for constitutive Teb1 binding and leading to an increase in histone gene transcription.

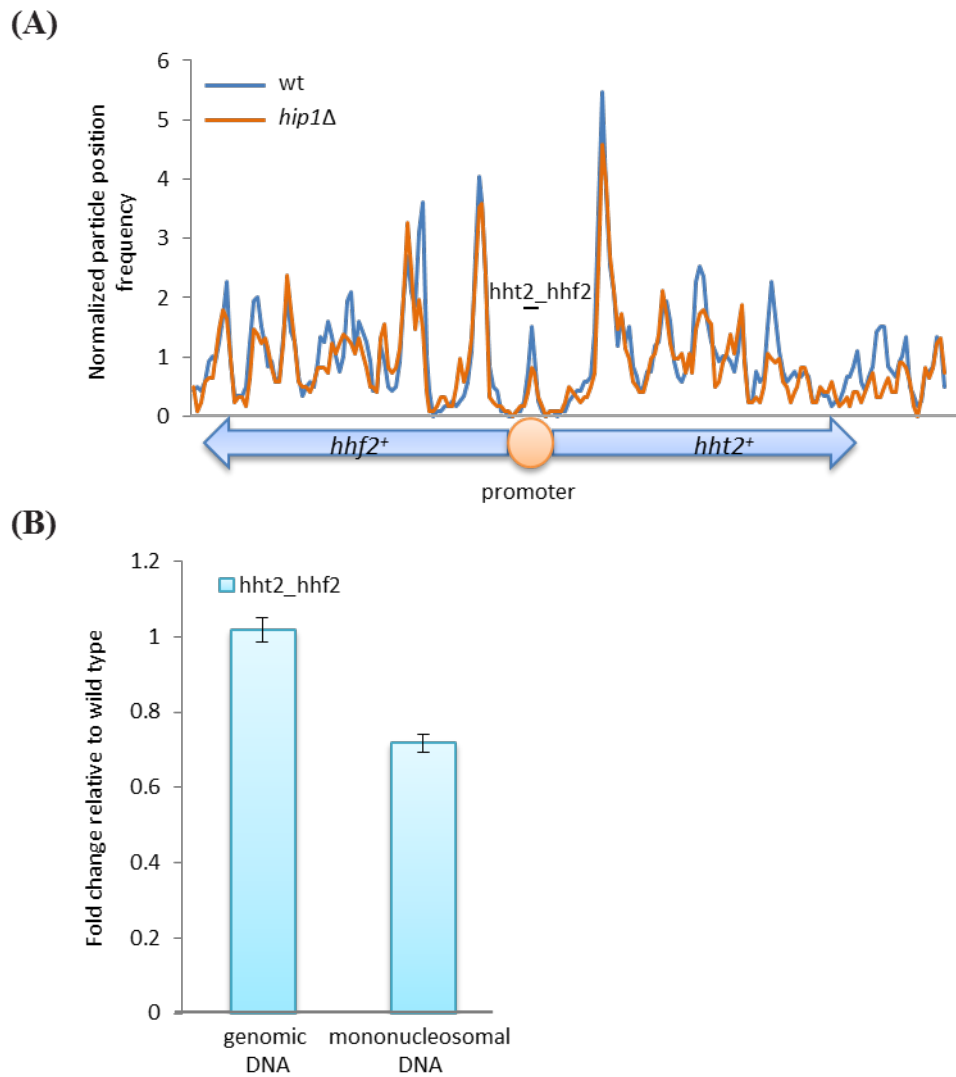


Figure 4.6 Nucleosomes are depleted over the promoter region of the *hht2*⁺-*hhf2*⁺ histone gene pair.

(A) Comparison of MNase-seq generated mononucleosome maps over the coding regions of *hht2*⁺ and *hhf2*⁺ (histone H3.2-H4.2) gene pair in wild type and *hip1*Δ cells. (B) qPCR validation of the sequencing data. Mononucleosomes were excised from an agarose gel and qPCR was implemented to measure sequence reads over the indicated loci from Figure (A). Genomic DNA was included as a control. Data are the mean of two technical repeats for a biological replicate to the sequenced dataset. Error bars represent \pm STDEV.

4.2.5 Loss of *hip1*⁺ results in a drop in histone H3 protein levels

Although histone H3 transcription is derepressed in *hip1*Δ cells (Blackwell *et al.* 2004), the MNase mapping studies suggest a global decrease in nucleosome occupancy. Therefore, the impact of *hip1*⁺ deletion on histone H3 levels was determined by western blotting (Fig 4.7.A). Histone H3 protein levels were significantly reduced in *hip1*Δ cells, supporting the proposed role of HIRA in histone H3-H4 placement onto the chromatin. Not surprisingly, loss of *hip1*⁺ has also affected histone H2A levels, but rather than a decrease a small but significant increase was observed (Fig 4.7.A). It is therefore plausible that some of the phenotypes of *hip1*Δ cells are a result of histone protein imbalance. However, due to time constraints this was not pursued further. Since, *hip1*Δ cells have lower nucleosome occupancy and a reduction in histone H3 protein levels it could be predicted that they would be sensitive to further reductions in histone H3-H4 dosage. Indeed, deletion of the histone H3.2-H4.2 gene pair, *hht2*⁺-*hhf2*⁺, along with *hip1*⁺ leads to a slight reduction in fitness. *hht2*Δ *hhf2*Δ *hip1*Δ cells present with an increased sensitivity to the spindle poison thiabendazole (Fig 4.7.B).

Since HIRA appears to play a role in establishing or maintaining appropriate occupancy of nucleosomal sites, another prediction could be that the loss of nucleosome positioning in conjunction with the loss of *hip1*⁺ would lead to the worsening of phenotypes. *S. pombe* contains two ATP-dependent remodelers of the CHD family, Hrp1 and Hrp3, which are responsible for nucleosome spacing and upon deletion of both the clearly defined nucleosome arrays over the ORFs are lost (Hennig *et al.*, 2012; Pointner *et al.*, 2012; Shim *et al.*, 2012; Touat-Todeschini *et al.*, 2012). Indeed, the combination of deletions of *hip1*⁺ and *hrp3*⁺ led to extremely slow growing cells, with severely abnormal cell morphology (Fig 4.8.A and B).

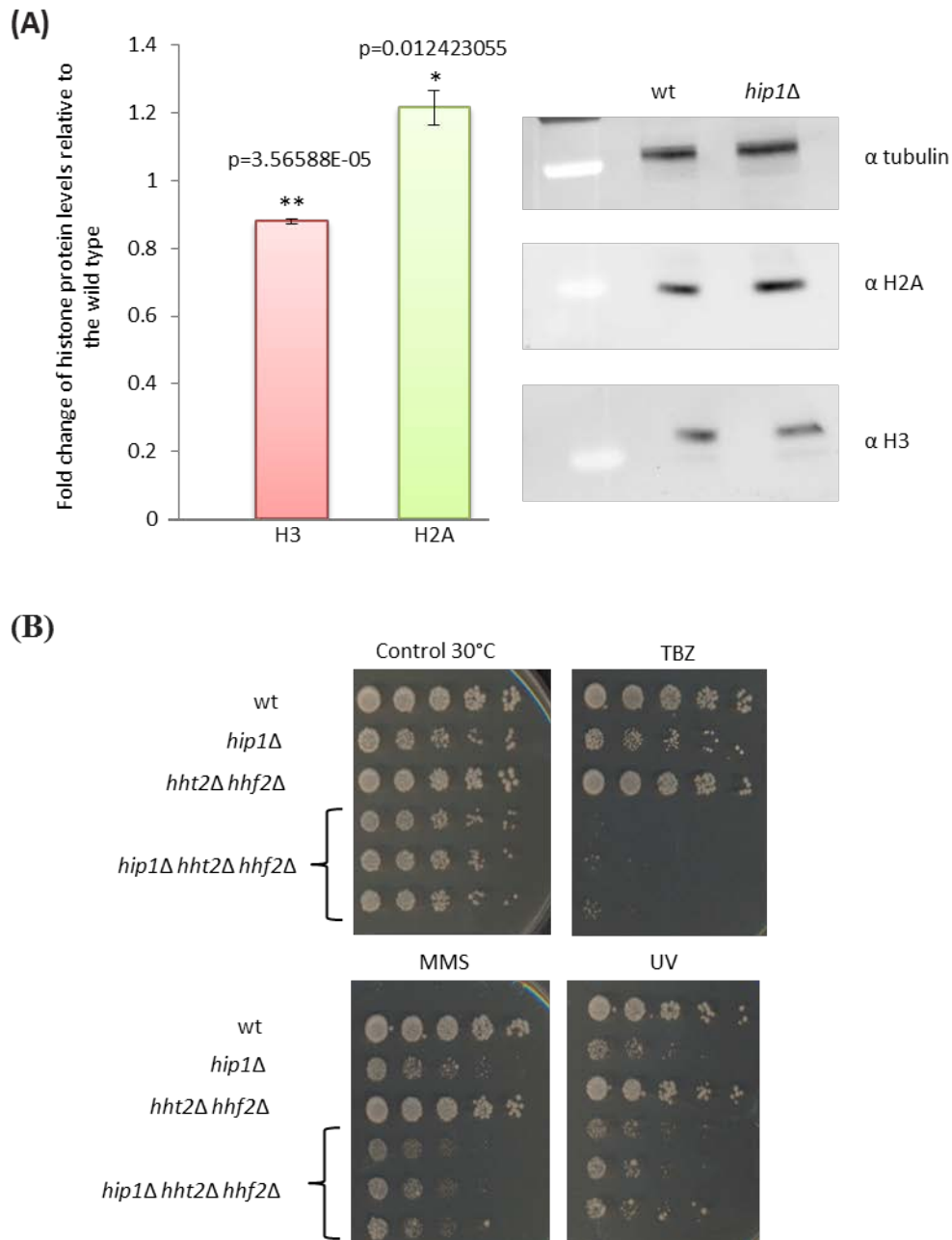


Figure 4.7 Histone H3 protein levels, but not H2A are significantly decreased in *hip1Δ* cells.

(A) Histone H3 and H2A protein levels were measured in TCA extracted whole cell lysates by western blotting. Histone protein levels were normalized to tubulin and fold change shown is of *hip1Δ* cells relative to the wild type. Data are the mean of at least three independent replicates, error bars represent \pm SEM (* denotes $p < 0.05$; ** denotes $p < 0.001$) **(B)** Spot tests onto YE5S plates + the indicated damaging agent (12.5 $\mu\text{g/ml}$ TBZ, 0.005% MMS, 150 J/m^2 UV) of 5-fold serial diluted midlog phase growing cells.

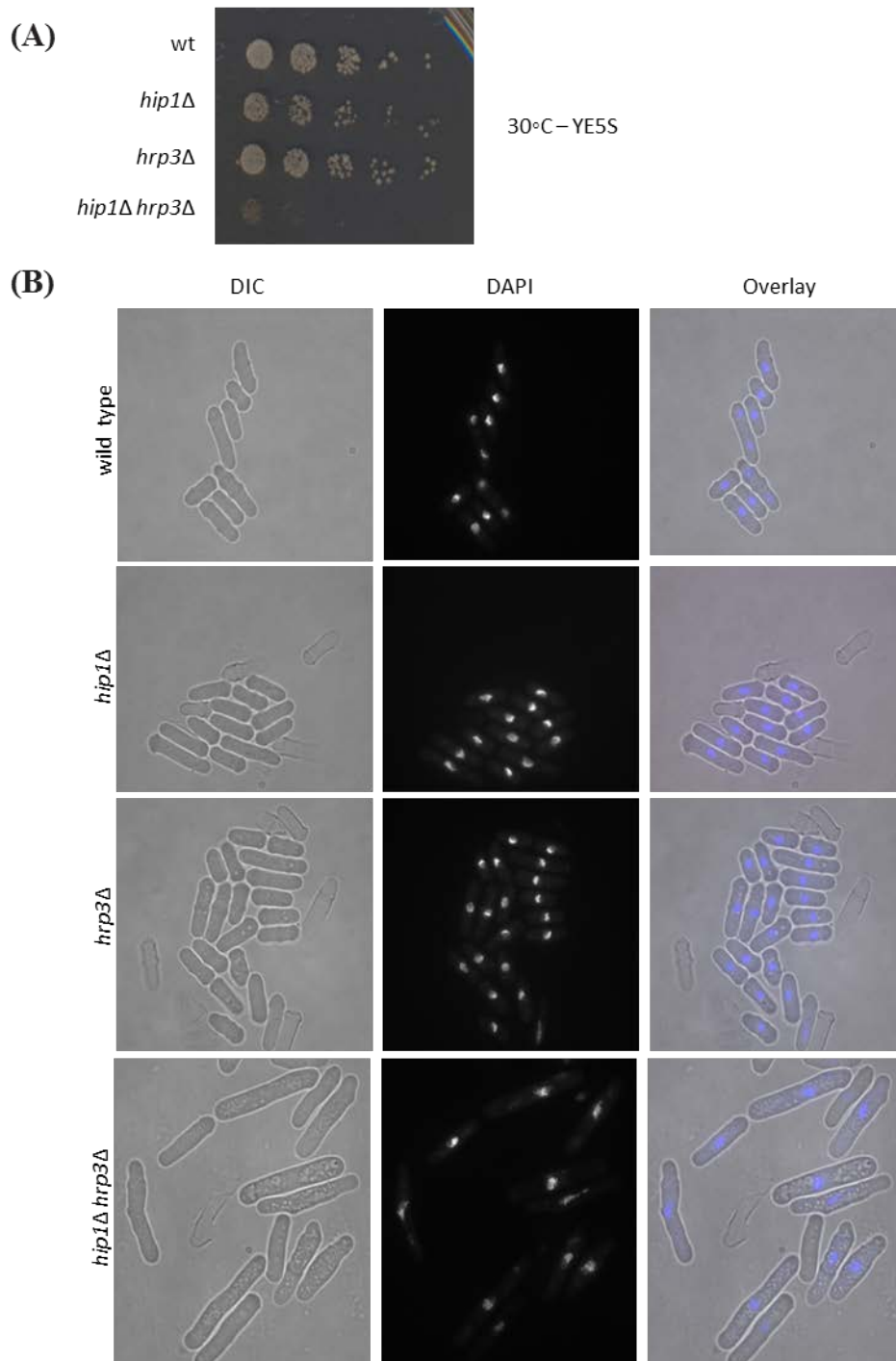


Figure 4.8 Loss of both *hip1*⁺ and *hrp3*⁺ results in synthetic growth defects and severely abnormal cell morphology.

(A) Spot tests of midlog phase growing cells at 30°C onto YE5S plates following a 5-fold serial dilution. Plates were further incubated at 30°C for 3 nights. (B) Cells were grown to mid-log phase in YE5S medium at 30°C then DIC, DAPI and merged images were taken using a Zeiss Axiovert microscope under the 100x oil-immersion lens.

4.2.6 Loss of HIRA function has a minor effect on pericentromeric heterochromatin

Previously published work demonstrated that HIRA is involved in the silencing of the pericentromeric repeats (Blackwell *et al.*, 2004; Greenall *et al.*, 2006; Anderson *et al.*, 2009; Anderson *et al.*, 2010). Comparison of nucleosome organization over the pericentromeric repeats has demonstrated only subtle alterations (Fig 4.9.A). However, the reductions and gains in occupancy appear to be specific. An independent pool of triplicate MNase digests were used for MNase-qPCR and it was possible to confirm some of the changes seen in the mapping data (Fig 4.9.B). This was also the case by carrying out histone H3 ChIP-qPCR, which, as expected, over the indicated region of the *dh* repeat (Fig 4.9.A) did not show any differences between the wild type and the *hip1Δ* mutant (Fig 4.9.C). Hence it appears that loss of HIRA affects only a subset of nucleosomes rather than leading to a widespread reduction in nucleosome occupancy. However, HIRA does interact with these regions, as demonstrated by the enrichment of Hip1-GFP over the *dh* repeats compared to the untagged control (Fig 4.9.D).

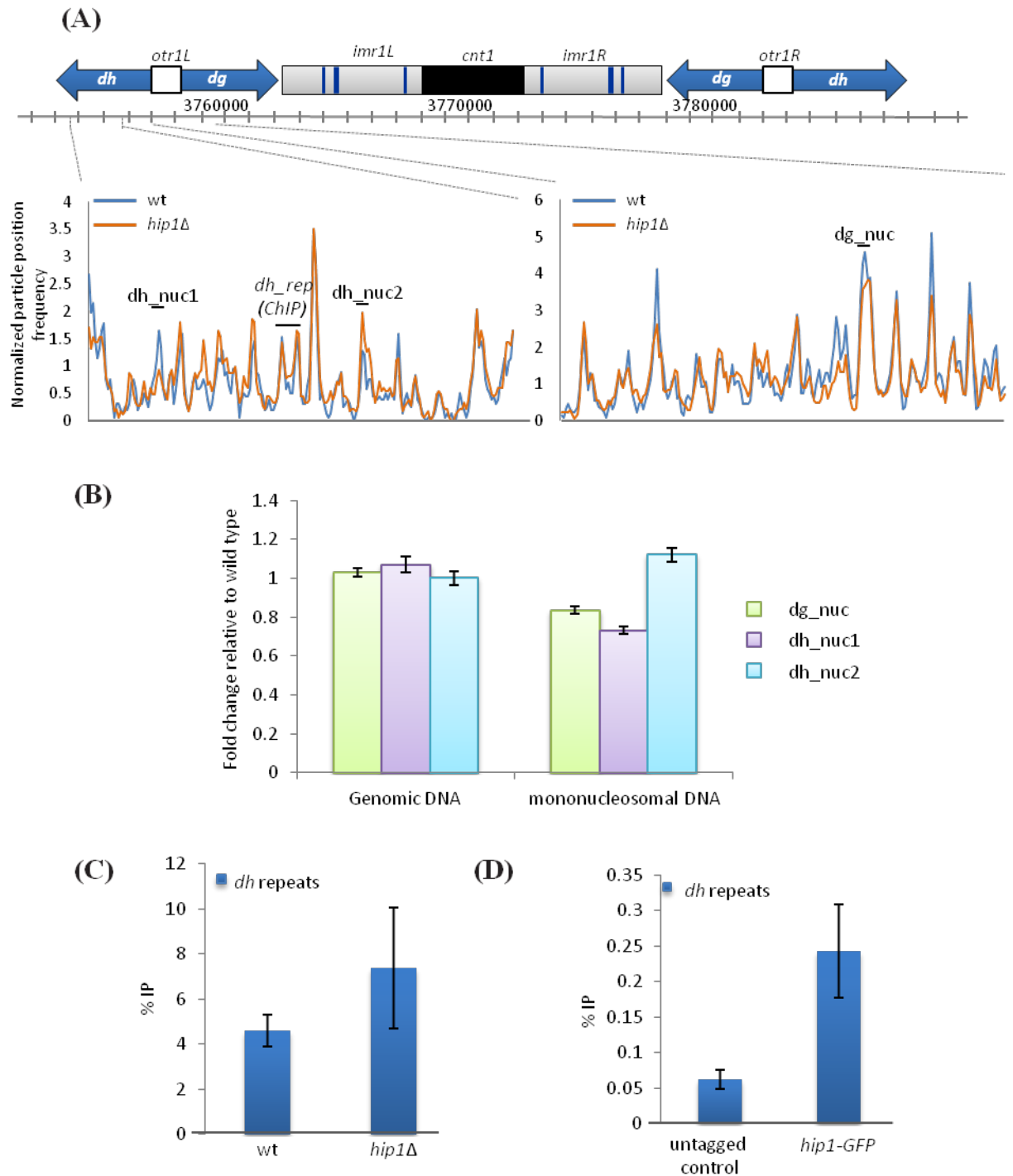


Figure 4.9 Minor changes to chromatin are seen around heterochromatic regions in *hip1Δ* cells.

(A) MNase-seq generated mononucleosome maps of wild type and *hip1Δ* cells over the left outer repeat of centromere 1. (B) qPCR validation of the sequencing data. Mononucleosomes were excised from an agarose gel and qPCR was implemented to measure sequence reads over the indicated loci from Figure (A). Genomic DNA was included as a control. Data are the mean of two technical repeats for a biological replicate to the sequenced dataset. Error bars represent \pm STDEV. (C) Histone H3 ChIP-qPCR analysis of wild type and *hip1Δ* cells over the *dh* repeats in exponentially growing cells. (D) Hip1-GFP ChIP-qPCR analysis of midlog phase cells over the *dh* repeats.

4.2.7 Loss of $hip1^+$ leads to a reduction in nucleosome occupancy over Tf2 LTR retrotransposons

It has previously been demonstrated that components of the HIRA complex are also required for silencing of Tf2 retrotransposons (Greenall *et al.*, 2006; Anderson *et al.*, 2009). Comparison of mononucleosome maps over the Tf2 long terminal repeat retrotransposons in wild type and *hip1* Δ cells revealed a modest drop in peak height over the UTR and the coding regions in *hip1* Δ cells suggesting that HIRA-mediated histone deposition occurs in these regions too (Fig 4.10.A). Once again, MNase-qPCR was used to confirm the drop in nucleosome occupancy over the indicated region, and once more it was possible to show that the reduction is reproducible using an independently generated set of mononucleosomal DNA (Fig 4.10.B).

In addition, a single mononucleosome peak is visible over the solo LTRs in the *S. pombe* genome, which is also reduced upon loss of *hip1* $^+$ (Fig 4.10.C), implying that HIRA contributes to nucleosome assembly both at retrotransposons and at their remnants.

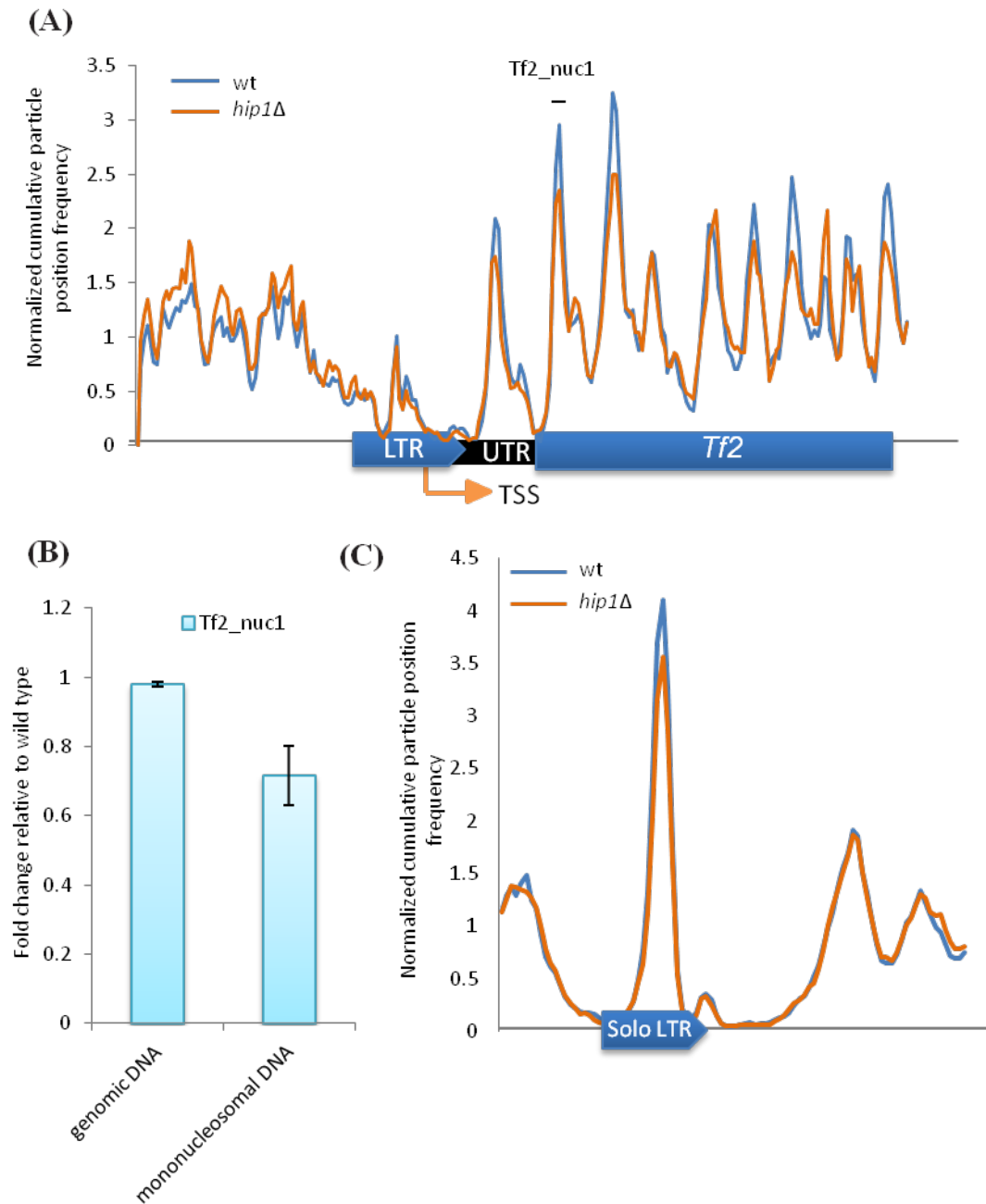


Figure 4.10 Perturbations to nucleosomes are visible over *Tf2* retrotransposons and solo LTRs in *hip1Δ* cells.

(A) Mononucleosomal particles (150 bp) following MNase-seq were aligned over the 13 full length *S. pombe* *Tf2* elements by their ATG site as described in *pombase*. (B) qPCR validation of the sequencing data. Mononucleosomes were excised from an agarose gel and qPCR was used to measure sequence reads over the indicated loci from Figure (A). Genomic DNA was included as a control. Data are the mean of two technical repeats. Error bars represent \pm STDEV. (C) Mononucleosomal particles (150 bp) generated by MNase-seq were aligned over 95 solo LTRs identified in the *S. pombe* genome by their start sites as described previously (Bowen *et al.* 2003).

4.2.8 The MNase maps of regions transcribed by Pol I and Pol III are not affected by loss of *hip1*⁺

Other regions of the genome were also inspected to determine whether HIRA is required for chromatin maintenance at loci outside of Pol II transcriptional control. tRNA genes are transcribed by Pol III and so 171 *S. pombe* tRNA genes were aligned by their TSS and mononucleosome maps were compared between wild type and *hip1*Δ cells. In *S. pombe* tRNA genes are characterized by a prominent upstream nucleosome (centred at -160), another peak over the NDR, a nucleosomal peak over the gene and a disorganized array downstream of the transcription termination site (TTS). This structure is different from *S. cerevisiae* where, two well positioned nucleosomes are visible both upstream and downstream of the TSS (Kumar and Bhargava, 2013). There were no dramatic changes to tRNA MNase peaks in the *hip1*Δ mutant compared to the wild type (Fig 4.11.A). The internal promoter regions of tRNA genes are bound by TFIIC which in itself is unstable but can recruit TFIIB to create a stably bound complex to tRNA promoter regions (Hamada *et al.*, 2001). Therefore, it is possible that the prominent peak upstream of the TSS results from TFIIB binding with TFIIC downstream of it. In order to explore this possibility the 75 bp size classes were aligned over the same region. This group should include reads generated by transcription factors stably binding DNA rather than nucleosomes (Kent *et al.*, 2011). Comparison of the 75 bp particles showed a single prominent peak over the NDR, which was present at similar levels in both wild type and *hip1*Δ mutant samples (Fig 4.11.B), therefore it looks like HIRA does not play a role in nucleosome organization over Pol III loci.

Next rDNA repeat sequences were compared to determine whether Pol I transcribed regions are affected by loss of *hip1*⁺. rDNA repeats are characterized by apparently nucleosome depleted regions over ribosomal RNA genes with well-organized nucleosomes in-between (Fig 4.12.A). Similarly to nucleosomes over tRNA genes, rDNA repeats were not obviously affected by deletion of *hip1*⁺, suggesting that HIRA function is not required at these regions.

Finally, replication origins were compared between wild type and *hip1*Δ cells, as described in Section 3.2.9. Deletion of *hip1*⁺ has no effect upon nucleosome organization over replication origins (Fig 4.12.B), which is consistent with HIRA being a replication-independent histone chaperone.

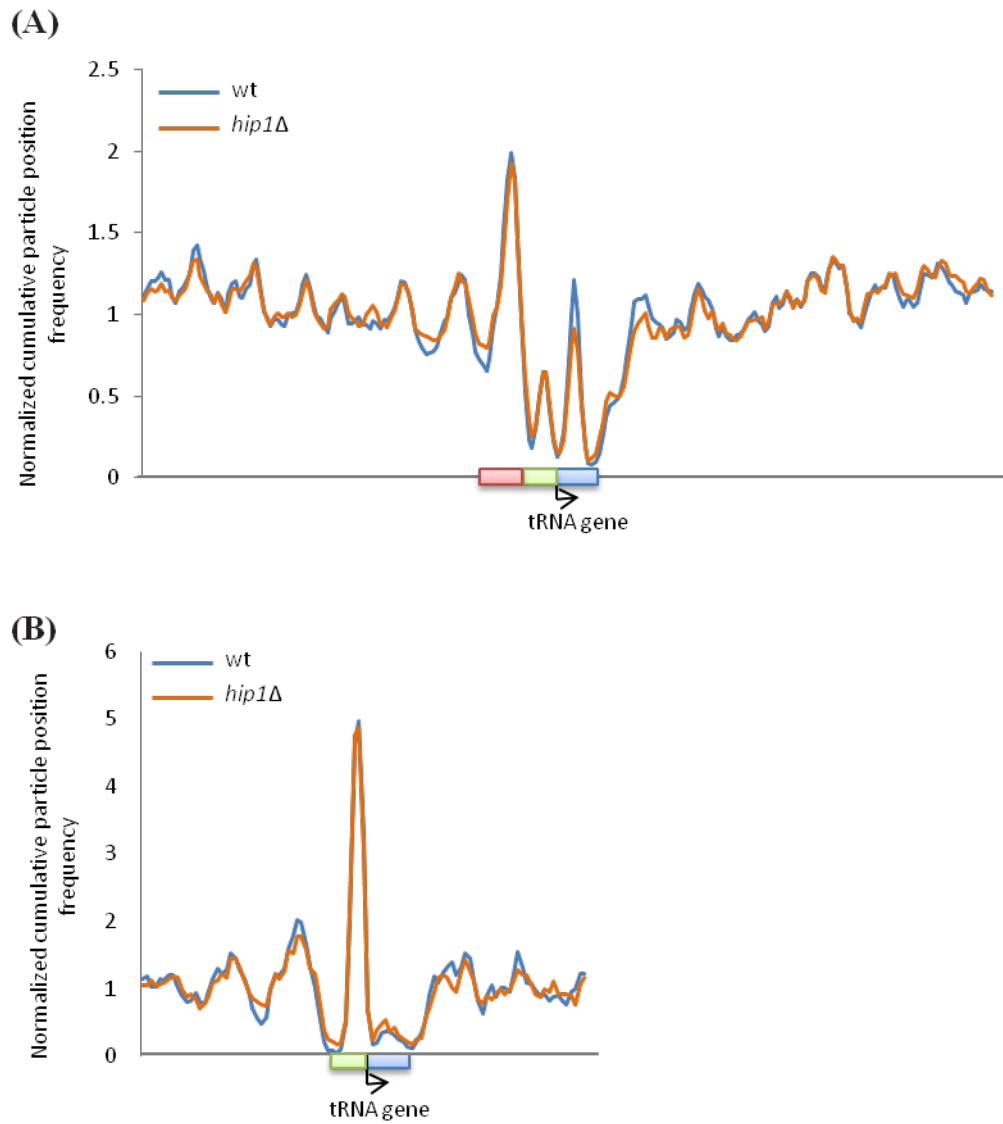


Figure 4.11 No changes to mononucleosomes over the tRNA genes in *hip1Δ* cells
(A) Mononucleosomes (150 bp) generated by MNase-seq were aligned over 171 *S. pombe* tRNA genes in wild type and *hip1Δ* cells. tRNA gene is illustrated by a blue box, the NDR with a green box, while the upstream (US) nucleosome is highlighted by a red box. **(B)** TFIIIB at tRNA genes in wild type and *hip1Δ* cells (75 bp particles).

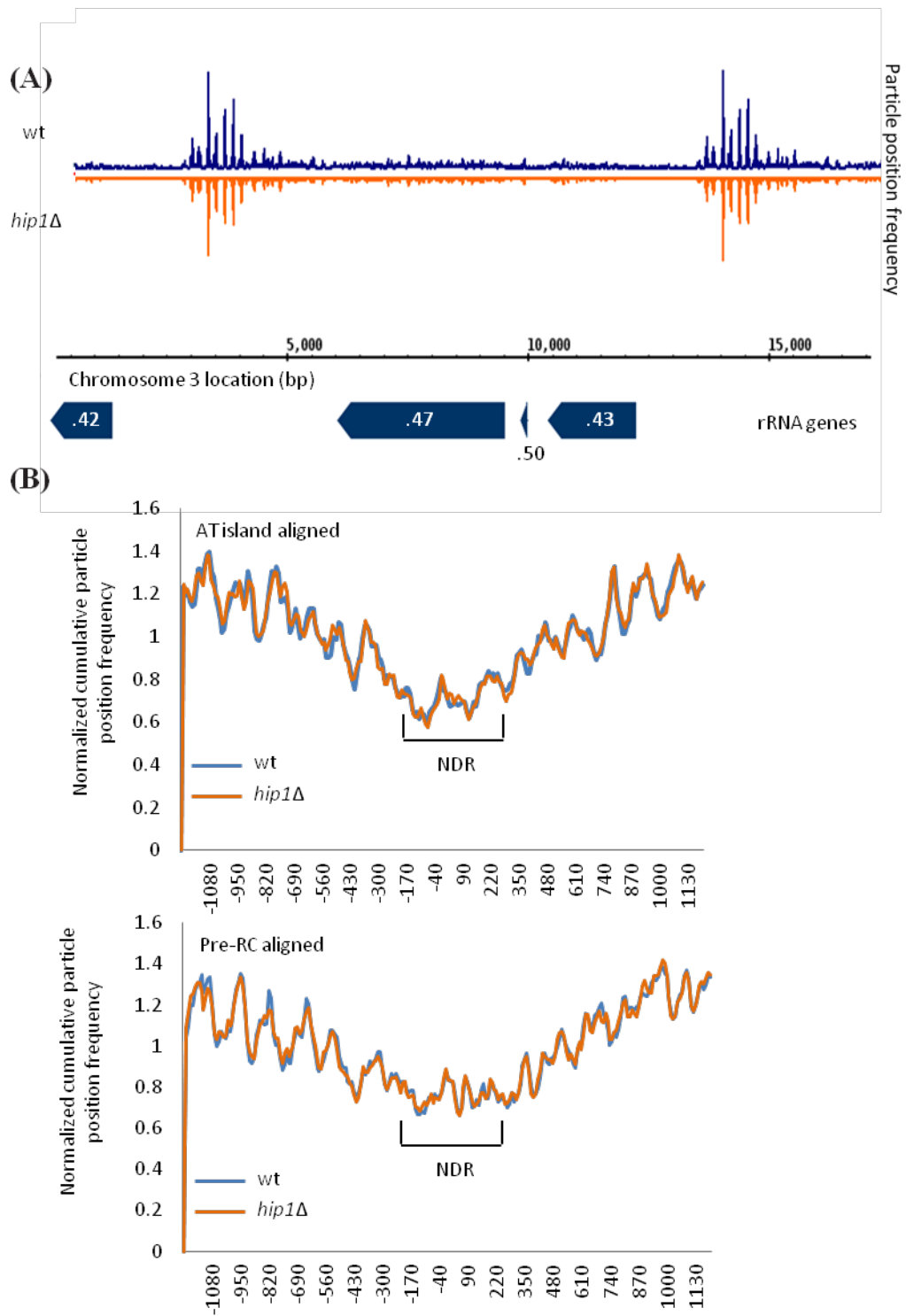


Figure 4.12 No changes to mononucleosomes over rDNA genes and replication origins in *hip1Δ* cells

(A) View of the complete rDNA repeat sequence using the Integrated Genome Browser (IGB). (B) Mononucleosomal particles (150 bp) following MNase-seq were aligned over 217 replication origins either by their AT islands or by binding sites of the pre-replication complex as described by (Givens *et al.*, 2012).

4.3 Role for the HIRA complex in DNA damage response

4.3.1 HIRA function is required for appropriate DNA damage response

Previous work has indicated that the HIRA complex is required for resistance to DNA damaging agents (Anderson *et al.*, 2009). Moreover, the genomic DNA of *hip1Δ* cells has higher levels of DNA strand breaks following bleomycin treatment (Anderson *et al.*, 2009). However, it has not been shown whether HIRA through its role in chromatin organization, simply shields the DNA from damaging agents or also plays a role in the DNA damage response (DDR). In order to address this, a strain expressing Hip1 fused to a hormone binding domain (HBD) was constructed (Boe *et al.*, 2008). In the absence of the hormone β -estradiol, Hip1-HBD is sequestered by Hsp90, however upon addition of β -estradiol into the medium Hsp90 releases Hip1-HBD, thus leading to rapid induction of HIRA function (Fig 4.13.A) (Boe *et al.*, 2008). Utilizing this conditional allele, it was possible to determine whether the role of the HIRA complex is primarily in protecting from DNA damage (protection) or is also required for the DNA damage repair processes (recovery). Midlog phase wild type, *hip1Δ*, and *hip1-HBD* cells were treated with 0.01% of the alkylating agent methyl methanesulfonate (MMS), which induces double strand breaks (DSBs) for 40 minutes either in the presence or absence of β -estradiol, following which 5-fold serial dilutions onto YE5S plates +/- β -estradiol were carried out and the results analyzed (Fig 4.13.B). As expected, the ability of *hip1Δ* cells to form visible colonies following MMS treatment was severely compromised. *hip1-HBD* cells behaved like *hip1Δ* cells when β -estradiol was not present in the media and also when β -estradiol was supplemented only during MMS treatment but not during recovery. In contrast, when β -estradiol was present only on the YE5S plates (i.e. during recovery from DNA damage), *hip1-HBD* cells had comparable growth to wild type cells. Overall, these results suggest that HIRA function is not simply required to protect the cells from DNA damage, but is also important to allow recovery from DNA damage.

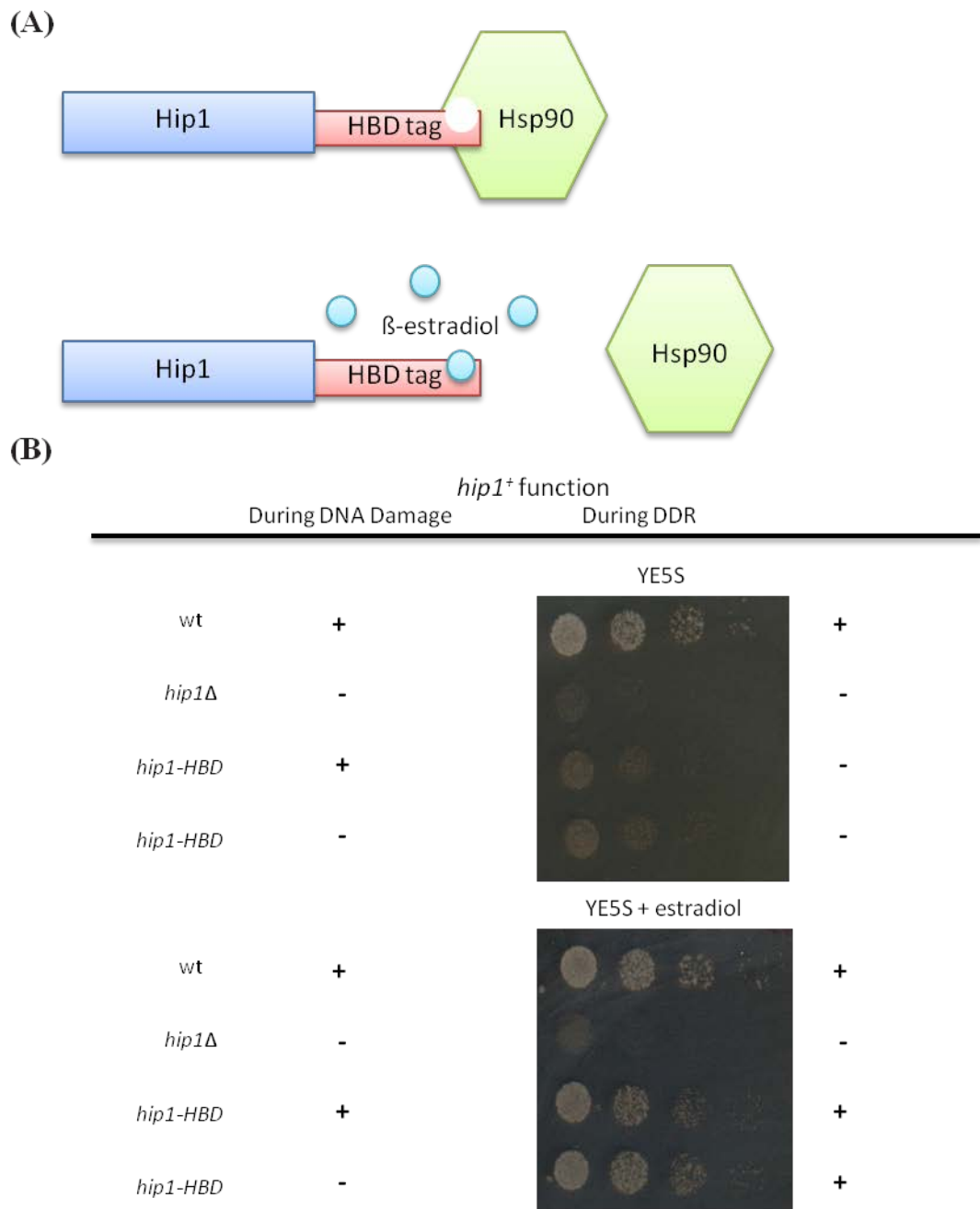


Figure 4.13 Conditional *hip1-HBD* strain demonstrates that HIRA is required for recovery during the DNA damage response (DDR)

(A) Hip1 is fused to a β -estradiol responsive hormone-binding domain (HBD), which in the absence of β -estradiol forms a complex with heat-shock protein 90 (Hsp90), which leads to the inactivation of Hip1 by steric hindrance. Addition of β -estradiol leads to the displacement of Hsp90, thus to reactivation of the tagged Hip1 protein. Adapted from (Boe *et al.*, 2008). (B) Cultures were grown to midlog phase in the absence or presence of β -estradiol as indicated. Each culture was then treated with 0.01% MMS for 40 minutes following which cells were 5-fold serial diluted and spotted onto YE5S plates either in the absence or presence of β -estradiol. Plates were incubated for 3 nights at 30°C.

4.3.2 HIRA is required for efficient repair of broken chromosomes

To further characterize the role of HIRA in the repair of DSBs, pulsed field gel electrophoresis (PFGE) was employed to visualize the repair of broken chromosomes. Chromosomal DNA was prepared at various time points after MMS treatment to follow chromosome repair. Both wild type and *hip1* Δ cells were able to repair their chromosomes, although in *hip1* Δ cells repair was delayed. Indeed, even following 24 hours of damage induction *hip1* Δ cells harboured unrepaired chromosomes (Figure 4.14.A). In order to check that the difference between wild type and *hip1* Δ cells was not simply due to the number of cells surviving MMS treatment, total cell number was measured during the experiment. Importantly, after 8 hours similar numbers of cells were present in the wild type and *hip1* Δ cultures (Fig 4.14.B). Therefore, the delay in repair observed in *hip1* Δ cells is unlikely to be simply due to reduced viability.

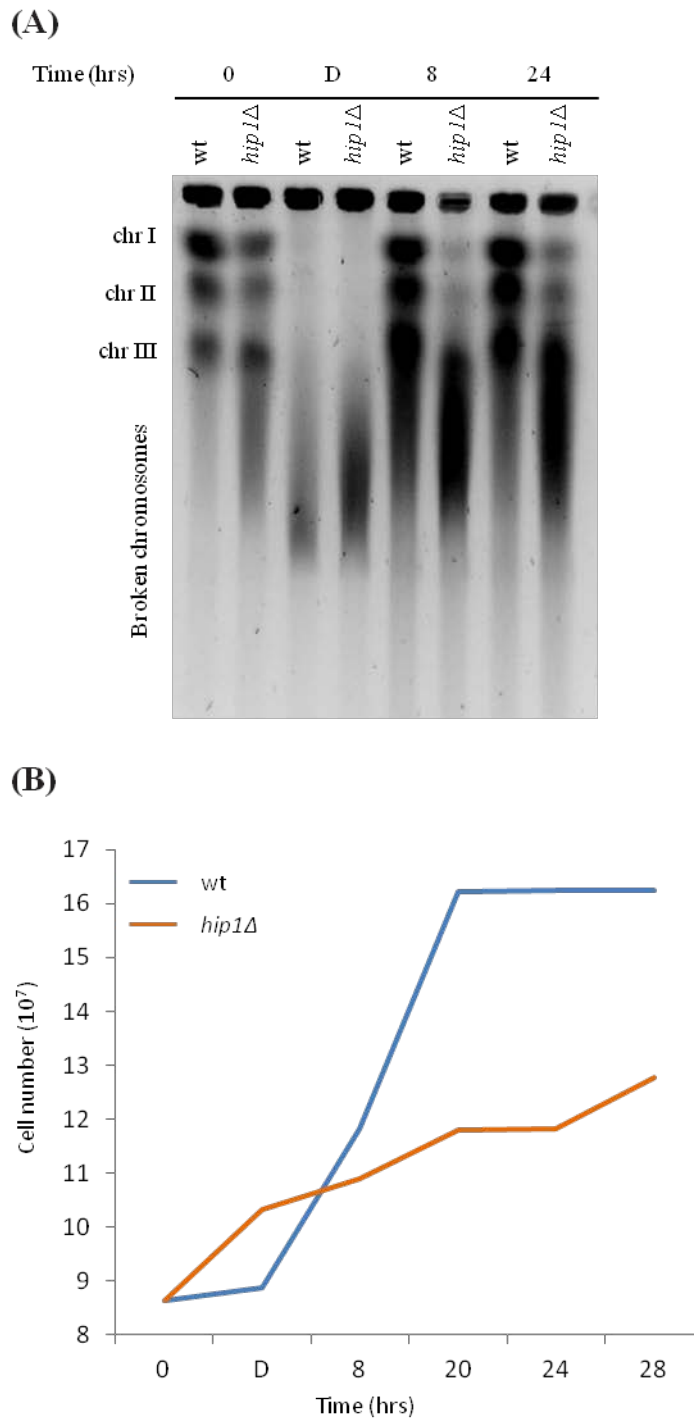


Figure 4.14 *hip1Δ* cells are severely delayed in repairing their chromosomes following DNA damage.

(A) Cultures were grown to midlog phase at 30°C in YE5S, were treated with 0.01% MMS for 40 minutes then chromosomal DNA integrity was analyzed by pulse-field gel electrophoresis (PFGE) at the indicated times. Data shown are representative of three independent biological replicates. **(B)** Measurements of total cell number for the experiment shown in Fig A.

4.3.3 Negative genetic interactions between *hip1*Δ and components of the HR repair pathway

Homologous recombination (HR) mediated repair is a conserved DSB repair pathway and is the preferred choice of repair for *S. pombe* cells due to the fact that they spend the majority of the cell cycle in G₂ (Ferreira and Cooper, 2004). A list of HR components and their homologues in both *S. cerevisiae* and in human are listed in Table 4.1, while a basic overview of the steps of HR and the respective proteins catalysing them are depicted in Figure 4.15. HR is initiated by extensive resection of the 5' end of the DSBs to generate a 3' single-stranded DNA (ssDNA) overhang, which is recognized and bound by RPA. Rad51 binds to the ssDNA, creating a nucleofilament, and initiates strand invasion of the sister chromatid or homologous chromosome. Strand invasion initiates formation of a D-loop, within which DNA synthesis takes place, and DNA repair can either take place by synthesis-dependent strand annealing (SDSA) or through the formation of a Holliday Junction (HJ). In the event of SDSA, the invading strand is expelled and anneals to the broken chromosome end, and no cross-over occurs between the chromosomes. If repair takes place through formation of a HJ then the free 3' end anneals to the D-loop, resulting in a double HJ (dHJ). The resulting dHJs can either be dissolved through the action of helicases, such as Rqh1 and Top3, resulting in non-crossover product formation, or resolved by resolvases, such as Eme1 and Mus81, leading to the formation of either crossover or non-crossover products (Li and Heyer, 2008).

Table 4.1 Components of homologous recombination (HR) repair pathway

	<i>S. pombe</i>	<i>S. cerevisiae</i>	Humans
Resection	Mre11-Rad50-Nbs1 (MRN Complex) Ctp1 Exo1 Rqh1 Dna2	Mre11-Rad50-Xrs2 (MRX Complex) Sae2 Exo1 Sgs1 Dna2	MRE11-RAD50-NBS1 (MRN Complex) CTP1 EXO1 BLM1 DNA2
ssDNA Binding	RPA (lrg su Rad11)	RPA (lrg su Rfa1)	RPA (lrg su RPA70)
Homologous pairing and strand exchange	Rad51 Rad52 Rad54 Rti1 Rad55-Rad57 (Rlp1, Rd11, Sws1) ? Mnd1-Hop2 Swi5-Sfr1	Rad51 Rad52 Rad54 Rad59 Rad55-Rad57 ? Mnd1-Hop2 Sea3-Mei5	RAD51 RAD52 RAD54 ? RAD51B-RAD51C RAD51D-XRCC2 BRCA2 MND1-HOP2 SWI5-MEI5
Inhibition of Rad51 Filament Formation	Fbh1 Srs2	? Srs2	FBH1 RTEL
DNA Synthesis	PCNA, Pol δ , Pol ϵ	PCNA, Pol δ , Pol ϵ	PCNA, Pol δ , Pol ϵ
HJ Dissolution	Rqh1-Top3	Sgs1-Top3	BLM-TOPIII α
HJ Resolution	Mus81-Eme1 ? Slx1-4	Mus81-Mms4 YEN1 Slx1-4	MUS81-EME1 GEN1 SLX1-4

Taken from (Deegan, 2012).

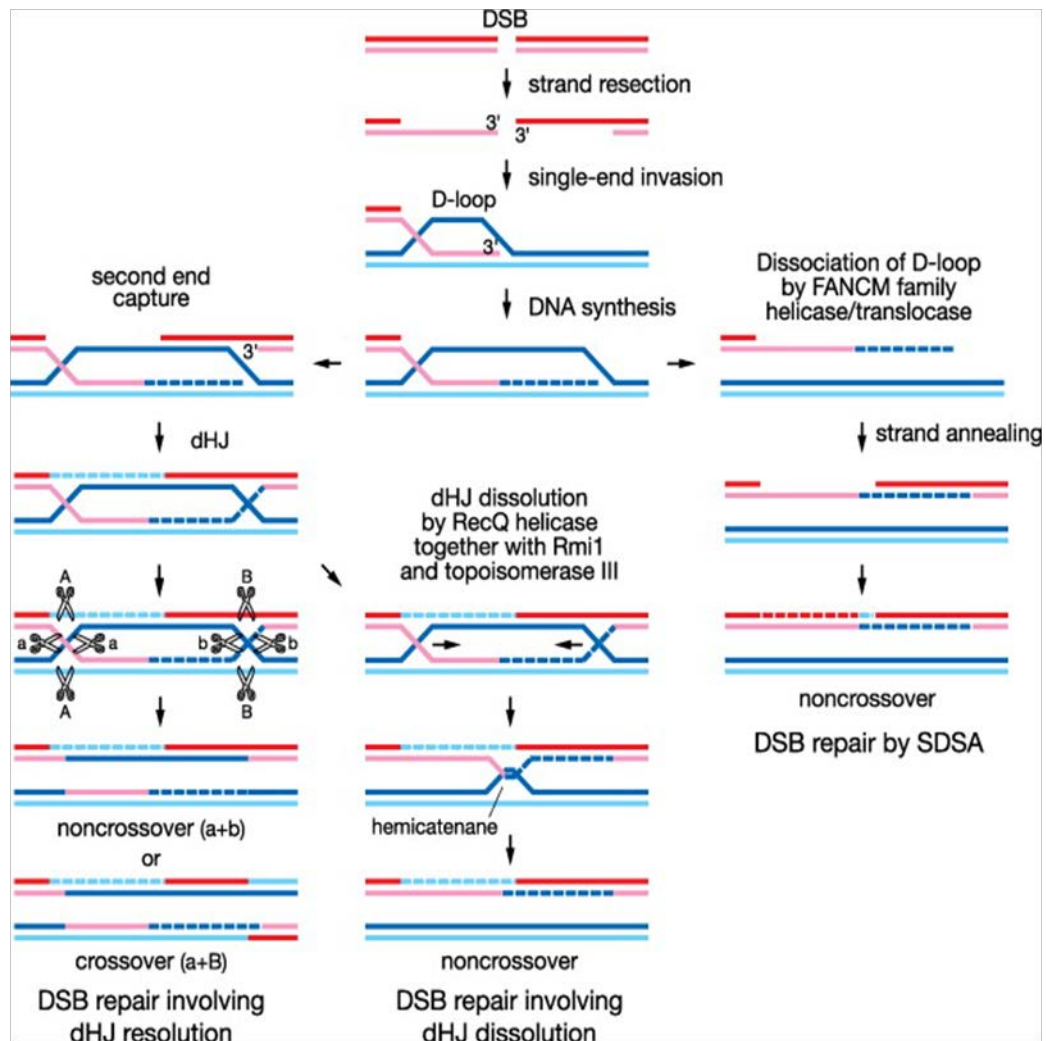


Figure 4.15 Schematic diagram of homologous recombination (HR) mediated repair.

Schematic representation of homologous recombination mediated DNA damage repair in *S. pombe*. Following formation of a DSB, the DNA ends are resected to form 3' ssDNA overhangs. This ssDNA is bound by RPA, followed by replacement with Rad51 to form a nucleofilament. The nucleofilament invades the homologous DNA template and forms a D-loop. DNA synthesis is primed within the D-loop, by the invading strand. When repair proceeds by SDSA, the invading strand is expelled from the homologous duplex DNA and re-anneals to the second end of the break, resulting in a non-crossover product. If repair proceeds by DSBR, the second end of the break anneals to the D-loop forming a double Holliday junction (dHJ). This can either be dissolved through the action of helicases resulting in non-crossover product formation, or resolved by resolvases resulting in the formation of either crossover or non-crossover products. Taken from (Lorenz and Whitby, 2006).

In order to assay whether HIRA plays a role in HR the *hip1Δ* allele was combined with mutations in genes involved in HR. Single *hip1Δ*, *rad50Δ*, *exo1Δ* and *rad51Δ* mutants along with *hip1Δrad50Δ*, *hip1Δexo1Δ*, and *hip1Δrad51Δ* double mutants were exposed to a range of DNA damaging agents (UV, MMS, bleocin) following growth to mid log phase. UV induced DNA damage causes the formation of pyrimidine dimers, which lead to distortion of the DNA structure impeding transcription and replication. Bleocin is a radiomimetic, which similarly to ionizing radiation, causes DNA DSBs. In agreement with previous reports, loss of resection components *exo1*⁺ and *rad50*⁺ leads to mild DNA damage sensitivities, while deletion of *rad51*⁺ leads to high sensitivity even at very low doses of DNA damaging agents. However, loss of *exo1*⁺, *rad50*⁺ and *rad51*⁺ all exacerbated the *hip1Δ* phenotype (Fig 4.16). In fact, generating a *hip1Δrad51Δ* double mutant was particularly challenging; the cells were severely elongated, slow growing and a large portion of the population inviable. That the phenotypes of HR deficient mutants are exacerbated by *hip1*⁺ deletion suggests that HIRA function is separate from, or at least not restricted to, HR-mediated DSB repair.

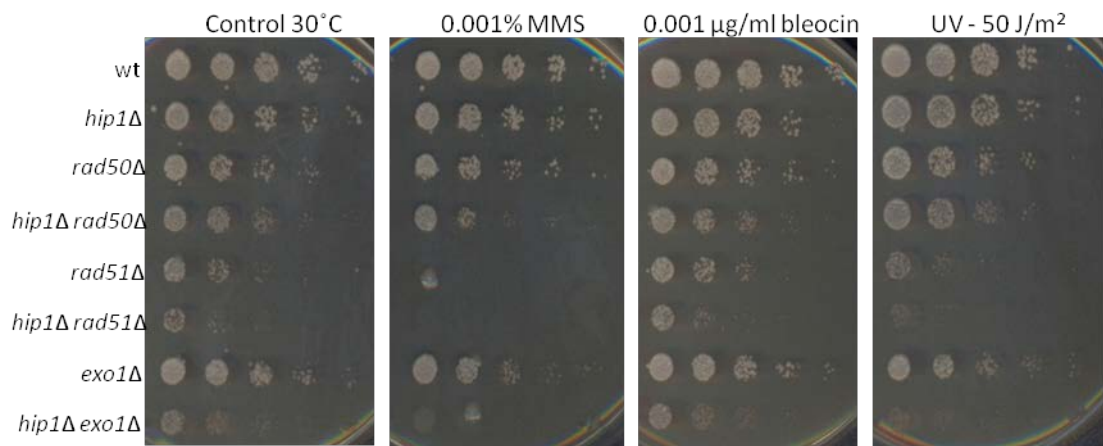


Figure 4.16 Genetic analysis of *hip1Δ* cells with components of the homologous recombination repair pathway.

Cells were grown in liquid YE5S to mid-log phase at 30°C then undergone 5-fold serial dilutions and were spotted onto YE5S plates with the indicated DNA damaging agents at the indicated concentrations. Plates were incubated at 30°C for 3 nights.

4.3.4 Negative genetic interactions between *hip1Δ* and components of the NHEJ repair pathway

The genetic interactions between *hip1Δ* and components of the HR pathway suggest a role for HIRA in DNA damage repair by non-homologues end-joining (NHEJ). In *S. pombe* NHEJ is predominantly restricted to the G₁/G₀ phases of the cell cycle (Mochida and Yanagida, 2006). NHEJ is activated by binding of the Ku proteins, Ku70-Ku80 heterodimers, to sites of DNA DSBs, thereby protecting DNA ends from resection. The localization of Ku dimers facilitates processing of DNA ends and subsequent ligation by the Ligase 4 (Lig4), Xlf1 and XRCC4 complex. A basic representation of NHEJ in *S. pombe* is depicted in Figure 4.17.

The ability of *hip1Δ* cells to complete NHEJ was measured next. Cultures were grown to mid-log phase then starved for nitrogen for 24 hours. This causes cells to round up and arrest with 1C DNA content. In this state *S. pombe* cells are dependent upon NHEJ for DSB repair (Ferreira and Cooper, 2004). Following the arrest cells were treated with UV, as described previously (Mochida and Yanagida, 2006), and their ability to mediate chromosome repair was observed by PFGE. DNA damage repair takes longer when cells are in this G₀ state, agreeing with previous findings (Mochida and Yanagida, 2006), but wild type cells restored their chromosomes within 24 hours, while *hip1Δ* cells did not (Fig. 4.18.A). This suggests that HIRA is important for efficient NHEJ. Next, a plasmid rejoining approach was also implemented to measure NHEJ efficiency (Barbet *et al.*, 1992; Pai *et al.*, 2014). In this assay a plasmid carrying the *S. cerevisiae* *LEU2* marker gene is linearized by restriction digestion as described in Section 2.5.5. Logarithmically growing cells are then transformed with either the linearized or the uncut plasmid and the NHEJ frequency determined by calculating the percentage of *leu*⁺ colonies arising from cells transformed with the linear plasmid over those transformed with the uncut plasmid (Fig 4.18.B). A control for this assay was the *lig4Δ* strain, which is unable to complete NHEJ. Percentage re-joining was calculated in wild type, *hip1Δ*, and *lig4Δ* cells. *hip1Δ* cells had only about 30-40% re-joining efficiency of wild type cells suggesting a role in NHEJ. *lig4Δ* cells, as expected, had around 5-10% percentage re-joining of the wild type (Fig. 4.18.C).

In order to further investigate the relationship between the NHEJ repair pathway and HIRA, the *hip1Δ* allele was combined with mutations in NHEJ genes. While NHEJ

mutants are not particularly sensitive to DNA damaging agents, combining the *ku70Δ*, *ku80Δ*, and *lig4Δ* mutants with the *hip1Δ* allele, led to the enhancement of *hip1Δ* DNA damage sensitivity (Fig. 4.19). This suggests that the function of HIRA is not restricted to the NHEJ repair pathway. Overall, these results indicate that HIRA is required for recovery from DSBs irrespective of whether the lesions are repaired by HR or NHEJ. Therefore it is possible that HIRA is common to both of these repair pathways, or that it acts independently of both and functions in checkpoint activation/maintenance or in chromatin assembly and/or disassembly around the damage sites.

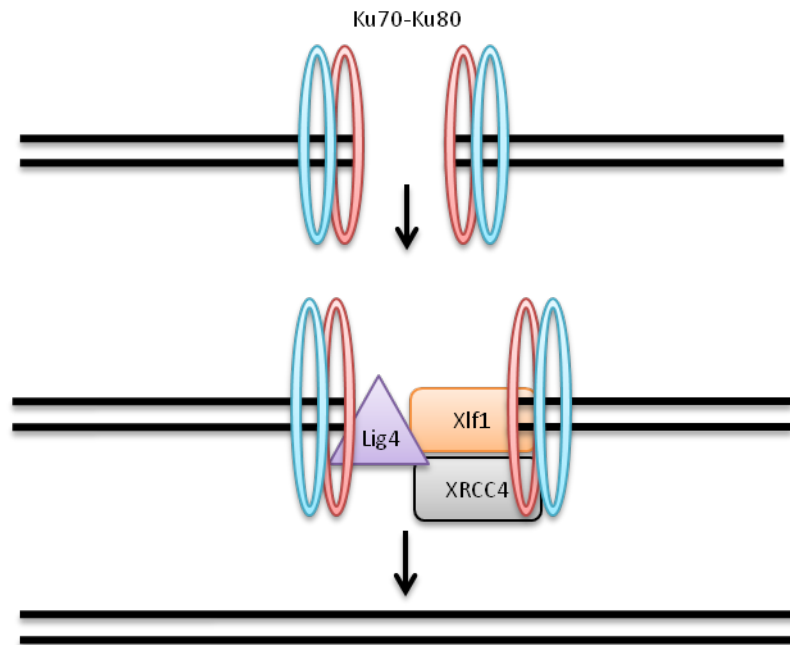


Figure 4.17 Schematic representation of the non-homologous end-joining pathway in *S. pombe* cells.

Ku70-Ku80 heterodimers bind break sites and retain chromosome ends in close proximity to each other. DNA ligase 4 and XRCC4, with the help of Xlf1, ligate the broken DNA ends together. Adapted from (Deegan, 2012).

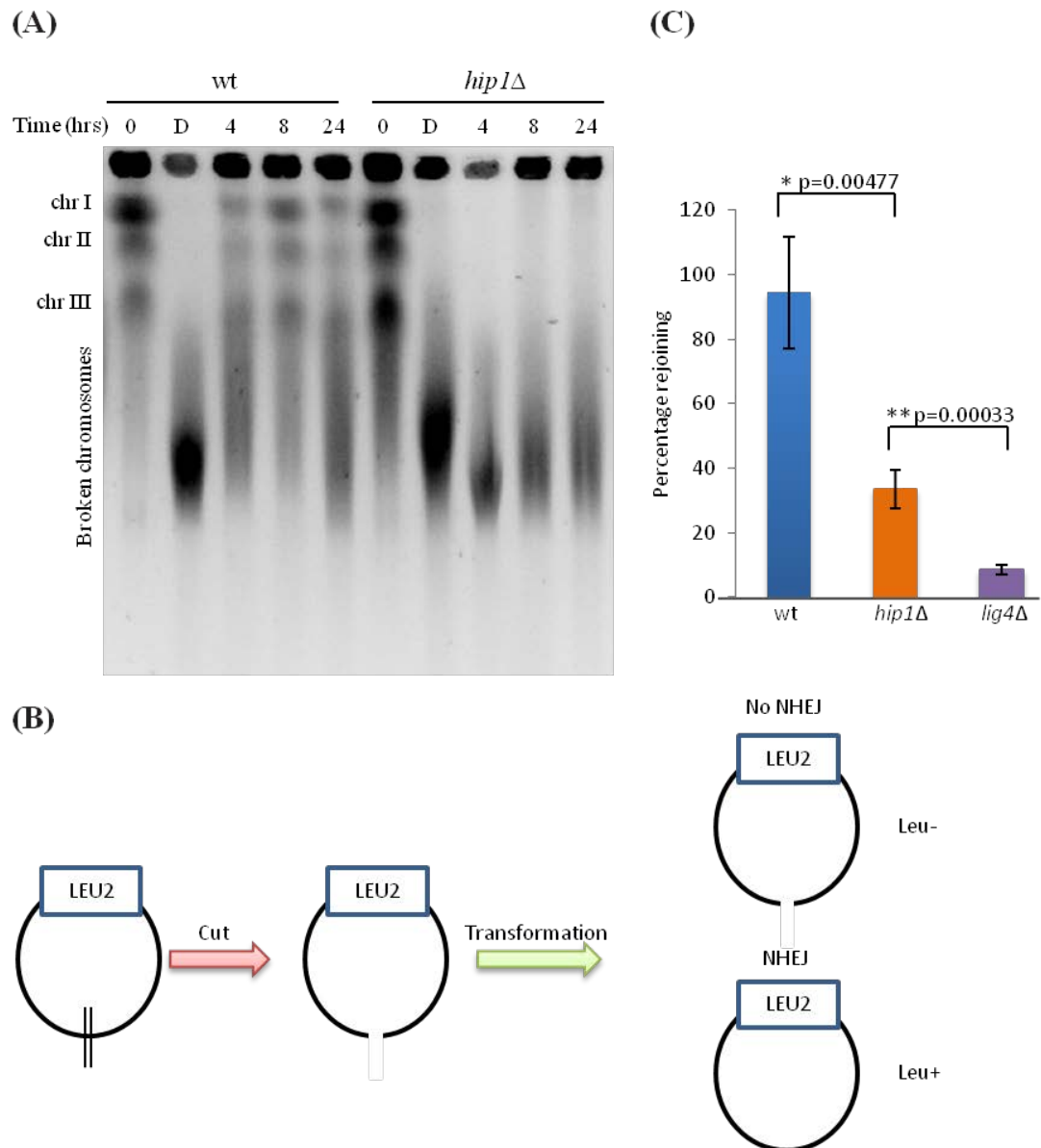


Figure 4.18 *hip1Δ* cells are severely delayed in repairing their chromosomes using NHEJ following DNA damage.

(A) Quiescent cells were treated with 150 J/m² dose of UV then chromosomal DNA integrity was analyzed by PFGE at the indicated times. The image shown here is representative of two biological replicates. (B) Diagram of plasmid re-joining assay adapted from (Deegan, 2012). A LEU2 containing plasmid was linearized with the EcoRI or PstI restriction enzymes. Midlog phase cells were transformed with either 1 μg of uncut control plasmid or the linearized plasmid. NHEJ frequency was calculated as the percentage of *leu*⁺ colonies arising from cells transformed with linear plasmids over those transformed with the undigested DNA. (C) NHEJ assay was performed and percentages of *leu*⁺ colonies were calculated as described in Section 2.5.5. Data are the meant of at least 5 independent biological replicates and error bars represent ± SEM (* denotes $p < 0.05$; ** denotes $p < 0.001$).

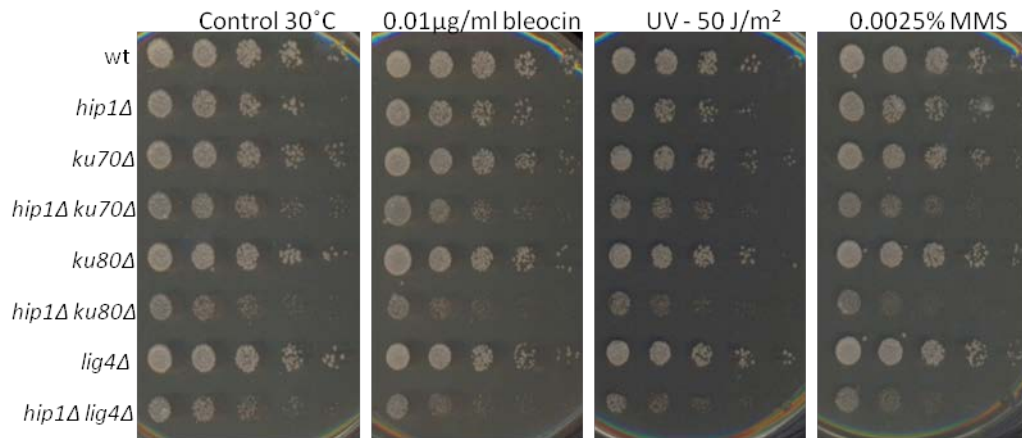


Figure 4.19 Genetic analysis of *hip1Δ* cells with components of the non-homologous end-joining pathway.

Cells were grown in liquid YE5S to mid-log phase at 30°C then undergone 5-fold serial dilutions and were spotted onto YE5S plates with the indicated DNA damaging agents at the indicated concentrations. Plates were incubated at 30°C for 3 nights.

4.3.5 Genetic interactions between *hip1*Δ and the checkpoint pathways

Previous work has shown that the DNA damage checkpoint pathway is important in cells in which the Asf1 histone chaperone is defective (Sharp *et al.*, 2005). As HIRA interacts with Asf1, the interaction between HIRA and the checkpoint pathways was explored. The major checkpoint pathways in *S. pombe* are illustrated in Figure 4.20.A. Upon DNA double strand breaks (DSBs) and replication fork collapse, Rad17 helps to recruit the 9-1-1 complex, composed of Rad9, Rad1, and Hus1, to sites of DNA strand breaks. Two phosphatidylinositol 3' kinase-like kinases, Tel1 and Rad3, also localize to these sites. The recruitment of Rad3 is thought to be through its interaction with Rad26 and is essential for triggering checkpoint arrest. Rad3 (ATR) is the central sensor kinase, which leads to the phosphorylation of the effector kinases, Chk1 and Cds1. Chk1 activation is mediated by the protein kinase Crb2 upon DNA damage, while Cds1 phosphorylation depends on Mrc1 in response to replication stress (Harrison and Haber, 2006). There is however some redundancy between Chk1 and Cds1, as in the absence of Chk1, Cds1 becomes phosphorylated in response to DNA damage and vice versa; Chk1 becomes activated upon replication stress in the absence of Cds1 (Boddy *et al.*, 1998; Zeng *et al.*, 1998; Froget *et al.*, 2008). Phosphorylation of either Chk1 or Cds1 leads to the phosphorylation of Cdc25, which results in the binding of Rad24, a 14-3-3 protein, involved in the nuclear export of Cdc25. Removal of Cdc25 stops Cdc2 from becoming active and leads to a G₂-phase cell cycle arrest (Rhind and Russell, 2000). Furthermore, both can phosphorylate Mik1, which is most likely necessary for extended cell cycle arrest (Baber-Furnari *et al.*, 2000). Since HIRA appears to play a role in DDR, genetic interactions between *hip1*Δ and multiple components of the checkpoint pathways were assayed by constructing double mutant strains and performing sensitivity assays. Spot tests were carried out on plates containing either hydroxyurea (HU), which causes replication stress, or containing the DNA damaging agent MMS. While the phenotypes of the *hip1*Δ*cds1*Δ and *hip1*Δ*chk1*Δ strains were reminiscent of the *hip1*Δ single mutant, loss of *rad3*⁺ was additive with loss of *hip1*⁺. *hip1*Δ *rad3*Δ cells were particularly slow growing and sensitive to both MMS and HU (Fig 4.20.B). Therefore, loss of HIRA exacerbates some problems associated with an impaired checkpoint pathway.

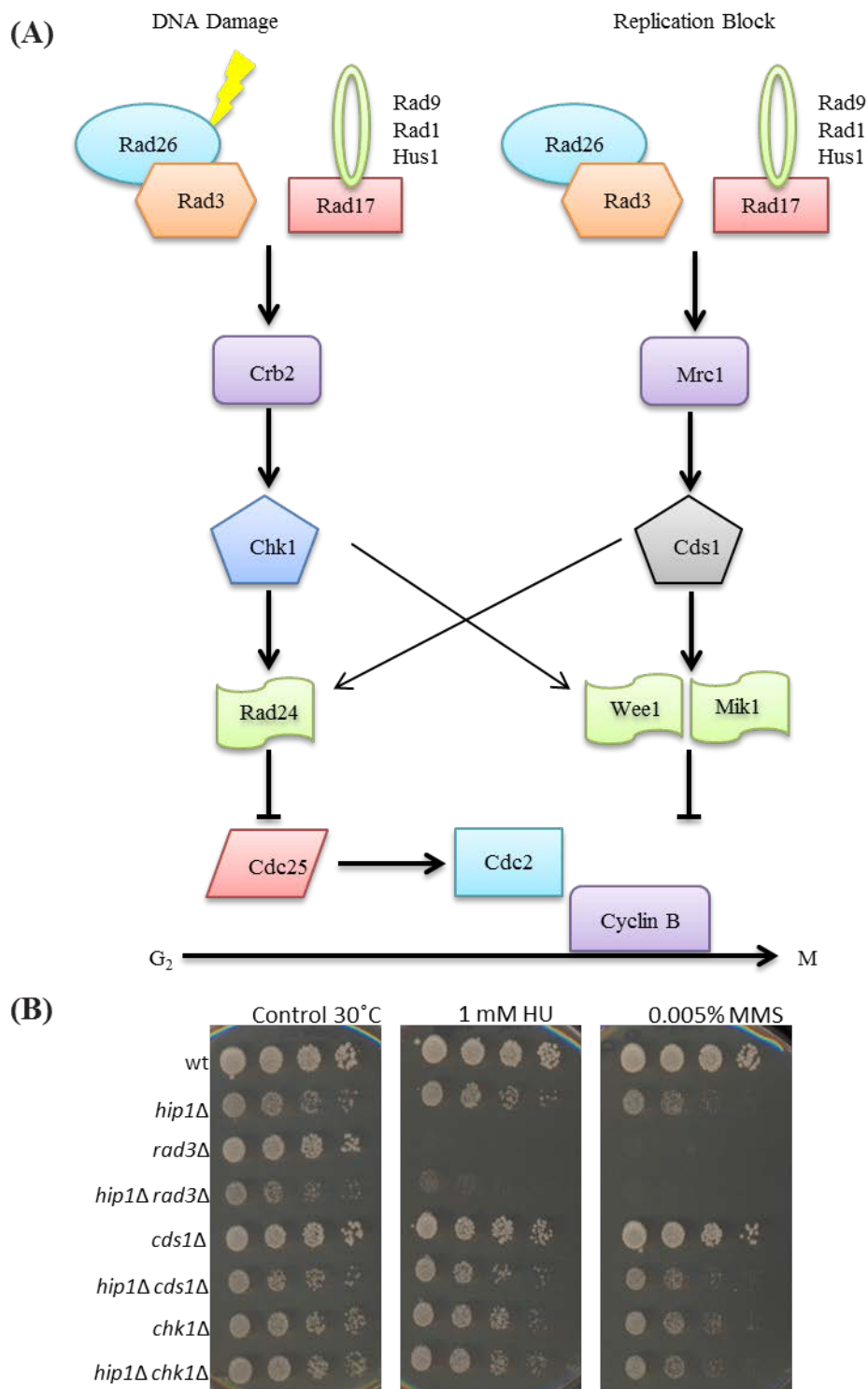


Figure 4.20 Genetic analysis of *hip1Δ* cells with components of the DNA damage checkpoint pathway.

(A) Diagram of the DNA damage checkpoint pathways in *S. pombe*. Adapted from (Deegan, 2012) (B) Cells were grown in liquid YE5S to mid-log phase at 30°C then undergone 5-fold serial dilutions and were spotted onto YE5S plates with the indicated agents at the indicated concentrations. Plates were incubated at 30°C for 3 nights.

Since *hip1Δ* cells display some sensitivity to DNA damaging agents that are similar to those of checkpoint mutants, and since the loss of checkpoints reduces the fitness of *hip1Δ* cells, checkpoint activation was next investigated. In response to DNA damage, Chk1 is phosphorylated by Rad3, which leads to the inhibition of cell cycle progression. Chk1 phosphorylation was measured by western blotting following MMS induced DNA damage. Both wild type and *hip1Δ* cells were able to phosphorylate Chk1 following MMS treatment, thus HIRA is not required for DNA damage checkpoint activation (Fig. 4.21.A). However, it was still possible that the phosphorelay is compromised downstream, and so a downstream target of Rad3 was also investigated. Yox1 has previously been shown to regulate MBF-dependent genes and is phosphorylated in response to DNA damage, which is dependent on Rad3 and Cds1 (Purtill *et al.*, 2011). Deletion of *hip1Δ* had no effect on Yox1 phosphorylation, confirming that the DNA damage checkpoint response is efficient in the absence of HIRA (Fig. 4.21.B).

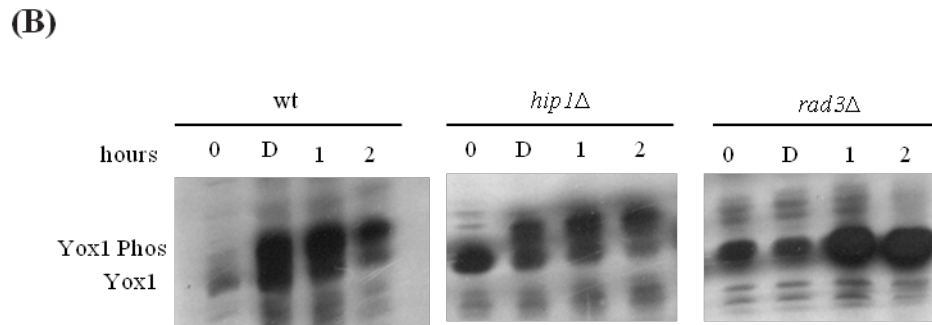
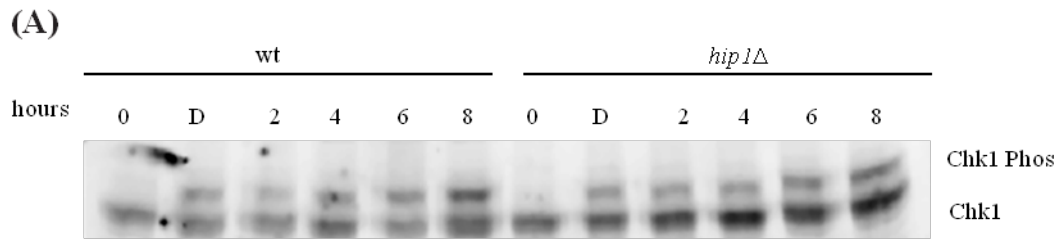


Figure 4.21 Checkpoints are triggered at comparable times in *hip1Δ* and wild type cells.

(A) Mid-log phase cultures at 30°C growing in YE5S were treated with 0.01% MMS for 40 minutes then pellets were collected at the indicated times for protein extractions. Chk1-HA was detected using α HA antibody. Western blots presented above are representative of three biological replicates. (B) Cells were treated as described above. Following western blotting Yox1-PK was detected using α PK antibody. *rad3Δ* cells were included as a control. Data presented above are representative of two biological replicates.

4.3.6 Checkpoint release is comparable between wild type and *hip1* Δ cells

Since HIRA function is not required for checkpoint activation, its role in checkpoint maintenance and release was investigated next. Release from the checkpoint was monitored in wild type, *hip1* Δ and *rad3* Δ cells. Cells were treated with a low dose of UV, in order to avoid cell death, and septation was monitored for up to 3 hours at 15 minute intervals. Previous work has shown that wild type cells stop dividing following 30 minutes and remain arrested for up to 2-3 hours (Wang *et al.*, 1999). On the other hand *rad3* Δ cells do not arrest and level of septated cells in the population doesn't drop. It was possible to see a clear reduction in septation index in both wild type and *hip1* Δ cells following 60 minutes which lasted for ~120-150 minutes. In contrast *rad3* Δ cells did not arrest (Fig 4.22). Therefore, the kinetics of checkpoint trigger and release appear to be highly similar in wild type and *hip1* Δ cells. Given that *hip1* Δ cells appear to repair DNA more slowly than wild type, it is possible that cells lacking HIRA are released from the checkpoint arrest without completing DNA repair.

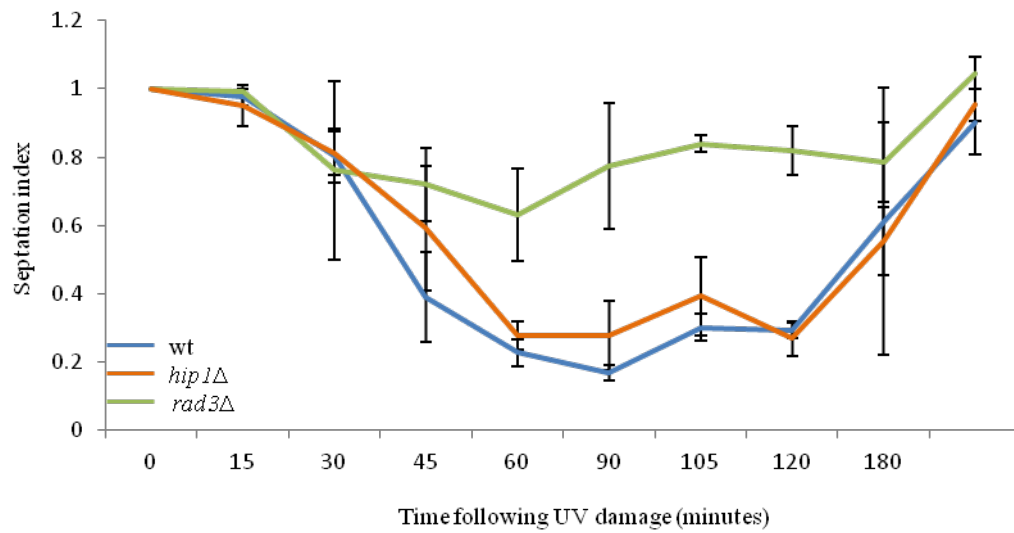


Figure 4.22 Cell cycle arrest is of comparable length between *hip1Δ* and wild type cells.

Midlog phase growing cultures were treated with a 100 J/m² UV dose, following which septation index was determined as the proportion of calcofluor white stained septa within cells over the total number of cells. This value was then normalized to the untreated samples. Data are the mean of three independent biological repeats and error bars represent \pm SEM.

4.4 Discussion

The findings described in this chapter demonstrate that the HIRA complex plays a role in the maintenance of nucleosome occupancy, particularly towards the 3' ends of genes, thereby in agreement with a possible role in nucleosome re-assembly coupled to transcription. In addition, the role HIRA plays during DNA damage was explored, and findings presented in this chapter hint at a role in chromatin re-establishment following DNA damage repair too.

4.4.1 *Global impact of HIRA upon nucleosome architecture*

Here a high resolution sequencing methodology was implemented to assess the impact of HIRA on global chromatin architecture. It was demonstrated, in agreement with previous findings, that HIRA plays a role in nucleosome maintenance in both euchromatic and heterochromatic regions. Cells lacking the *hip1*⁺ subunit of the HIRA complex have reduced histone H3 protein levels and a global reduction in nucleosome occupancy. Unexpectedly, given the phenotype of HIRA mutants the mapping did not reveal drastic changes to nucleosome organization; rather a decrease in occupancy was visible towards the 3' end of ORFs. HIRA, in *S. pombe* at least, is likely to be required for nucleosome re-assembly over transcribed regions but is unlikely to play a role in determining the sites of occupancy, which is consistent with the mapping data. Interestingly, of all remodeler and histone chaperone mutants whose nucleosomes have been mapped in the past, none were found to alter the position of the +1 or +2 nucleosomes hinting at the biological importance of these sites.

As discussed in Section 1.5.2 and summarized in Figure 1.11, the overwhelming majority of nucleosomes do not get disassembled during transcription; however it is important to remember that a small proportion do. An estimated 10% of nucleosomes get completely disassembled during transcription, independently of replication, of which 5% get turned over independently of both transcription and replication (Jackson, 1990). In light of this, it is perhaps less surprising that the impact of HIRA on transcriptionally active sites is relatively little. It is still worth to keep in mind, that HIRA could facilitate the re-assembly of nucleosomes in the 5-10% of the population where disassembly does take place.

4.4.1.1 HIRA exerts its function through organizing the 3' end of genes

Consistent with the suggestions that HIRA plays a role in nucleosome maintenance are previous reports, which have demonstrated an overall more “open” genome in HIRA mutants (Anderson *et al.*, 2009). The data presented here suggests that HIRA is responsible primarily for nucleosome organization over the ORF, following the +5 nucleosome onwards, which corresponds to approximately 700 bp and downstream in the gene. Given that the average gene in *S. pombe* is between 1,407–1,446 bp in length (Wood *et al.*, 2002), HIRA exerts its function primarily in the middle to the 3' end of genes. This observation also fits with data demonstrating that cells lacking HIRA present with increased cryptic antisense transcription, a phenotype associated with failure to re-assemble nucleosomes (Anderson *et al.*, 2009; Yamane *et al.*, 2011). Thus, the genome wide mapping of *hip1Δ* cells presented here adds further evidence to the notion that HIRA functions during transcription elongation. It would be possible to implement ChIP-seq and measure HIRA levels at genic regions, as it would be interesting to determine whether there is an enrichment of HIRA over the 3' end of genes relative to the 5'. It would also be possible to measure the transcript levels towards the 5' and the 3' end of genes in *hip1Δ* cells to determine whether there is any particular dependency on HIRA towards the 3', as our data suggests.

4.4.1.2 Possible role for HIRA, Set2 and CHD remodelers in preventing cryptic transcription through repressing histone trans exchange over the 3' end of genes

Histone *trans* exchange is the process of replacing nucleosomal ‘parental’ histones with histones from the free pool. This process is thought to be limited during transcription, as an increase in new histone incorporation would lead to loss of paternal PTMs that are associated with specific modifications, and could result in disturbances to chromatin structure (Li *et al.*, 2007; Das and Tyler, 2013). There has been some evidence from *S. cerevisiae* that promoter regions and the surrounding nucleosomes undergo high turnover, whereby histones from the free pool get incorporated (termed H3 *trans* exchange), which is facilitated by Asf1, not HIRA (Rufiange *et al.*, 2007). It might be possible that this feature is conserved in *S. pombe* and the nucleosomes closest to the NDR are reliant on Asf1 (and possibly another histone chaperone, like Rtt106) for

assembly. This would also suggest, and agree with a lot of previous findings, that the major role of HIRA during transcription in *S. pombe* is through the re-assembly or maintenance of parental nucleosomes over the bodies of genes. With regards to this point, several groups have now illustrated that H3 *trans* exchange is dependent on transcription, whereby an increase in H3 *trans* exchange is more likely to occur over highly transcribed regions (Dion *et al.*, 2007; Rufiange *et al.*, 2007). If HIRA played a role in H3 *trans* exchange during transcription than one would expect more of a disruption over highly transcribed regions compared to all others. However, if the role of HIRA during transcription is generally restricted to re-assembly of old nucleosomes over the gene bodies, then the effect of loss of HIRA would be no worse than observed over all TSS. Indeed, the latter is true, there is no more of a reduction in nucleosome occupancy over the top 10% highly transcribed genes as defined by (Marguerat *et al.*, 2012), than already observed over all TSS (Fig 4.23) (if anything there is less of an effect). I would rather propose that HIRA plays a role in the prevention of histone *trans* exchange, either directly or indirectly.

Interestingly, in co-operation with HIRA, Chd1 has also been implicated in the assembly of H3.3 containing nucleosomes in a replication-independent manner in *Drosophila* (Radman-Livaja *et al.*, 2012). In addition, there have been numerous implications that the *S. cerevisiae* Chd1 protein also functions in the suppression of cryptic transcripts, in addition to or through, its nucleosome spacing activity; the mechanism is currently unknown (Pointner *et al.*, 2012; Radman-Livaja *et al.*, 2012). It has been demonstrated however that it's involved in suppressing histone *trans* exchange during Pol II elongation, and that this appears to be through Set2 mediated trimethylation of H3K36, which recruits Chd1 (Smolle *et al.*, 2012). Set2 is essential for the methylation of H3K36, which in turn is necessary for appropriate function of the Rpd3S histone deacetylase complex, *S. pombe* Clr6, which is required to maintain nucleosomes in a hypoacetylated state following Pol II progression. In the absence of Set2, methylation of H3K36 is lost, nucleosomes become hyperacetylated, chromatin organization becomes disrupted, leading to the accumulation of cryptic transcripts (Smolle *et al.*, 2012). Loss of *CHD1* led to an overall redistribution of nucleosomes towards the 5' end of genes, suggesting that normally Chd1 plays a role in maintenance of nucleosomes towards the 3' end (Smolle *et al.*, 2012). Also, Set2 was demonstrated to exert its function in preventing cryptic transcription primarily over lowly expressed long genes (Li *et al.*, 2007). This suggests that Chd1 and Set2, similarly to HIRA,

primarily function to maintain nucleosome organization towards the 3' end of genes, at least in budding yeast. If Set2 and Chd1 function in the prevention of histone *trans* exchange, through H3K36 methylation, and HIRA functions in the re-assembly of paternal nucleosomes, then deletion of either *set2*⁺ or one of the CHD1 homologues, *hrp1*⁺ or *hrp3*⁺, alongside *hip1*⁺ would be expected to exacerbate the HIRA phenotypes. Indeed, double mutants of both *hrp3Δhip1Δ* and *set2Δhip1Δ* (Figure 4.8 and 4.23.C) were considerably less fit than either of the single mutants, suggesting that Set2 and Hrp3 become central when HIRA is not functional. Also, while deletion of *set2*⁺ exacerbated the growth defect of *hip1Δ* cells in rich media, loss of *gcn5*⁺, which acetylates H3K36, has previously been suggested to improve it (Roguev *et al.*, 2008). Indeed, in the absence of DNA damaging agents, *hip1Δgcn5Δ* cells behaved the same as either of the single mutants (data not shown). It would be interesting to confirm this by measuring cryptic transcripts, in the double mutants and compare them to the respective singles. However, it is difficult to say to what extent the increase in cryptic transcription is responsible for the reduction of cellular fitness that has been observed in the double mutants. It is possible that loss of both HIRA and Hrp3 activity affects a region outside of the 3' end of genes, as mentioned in Section 4.2.5. It could therefore be informative to determine whether the double mutants present with any pronounced defects in the nucleosome ladders generated by MNase digestions. However, it is possible that either directly or indirectly HIRA prevents histone *trans* exchange.

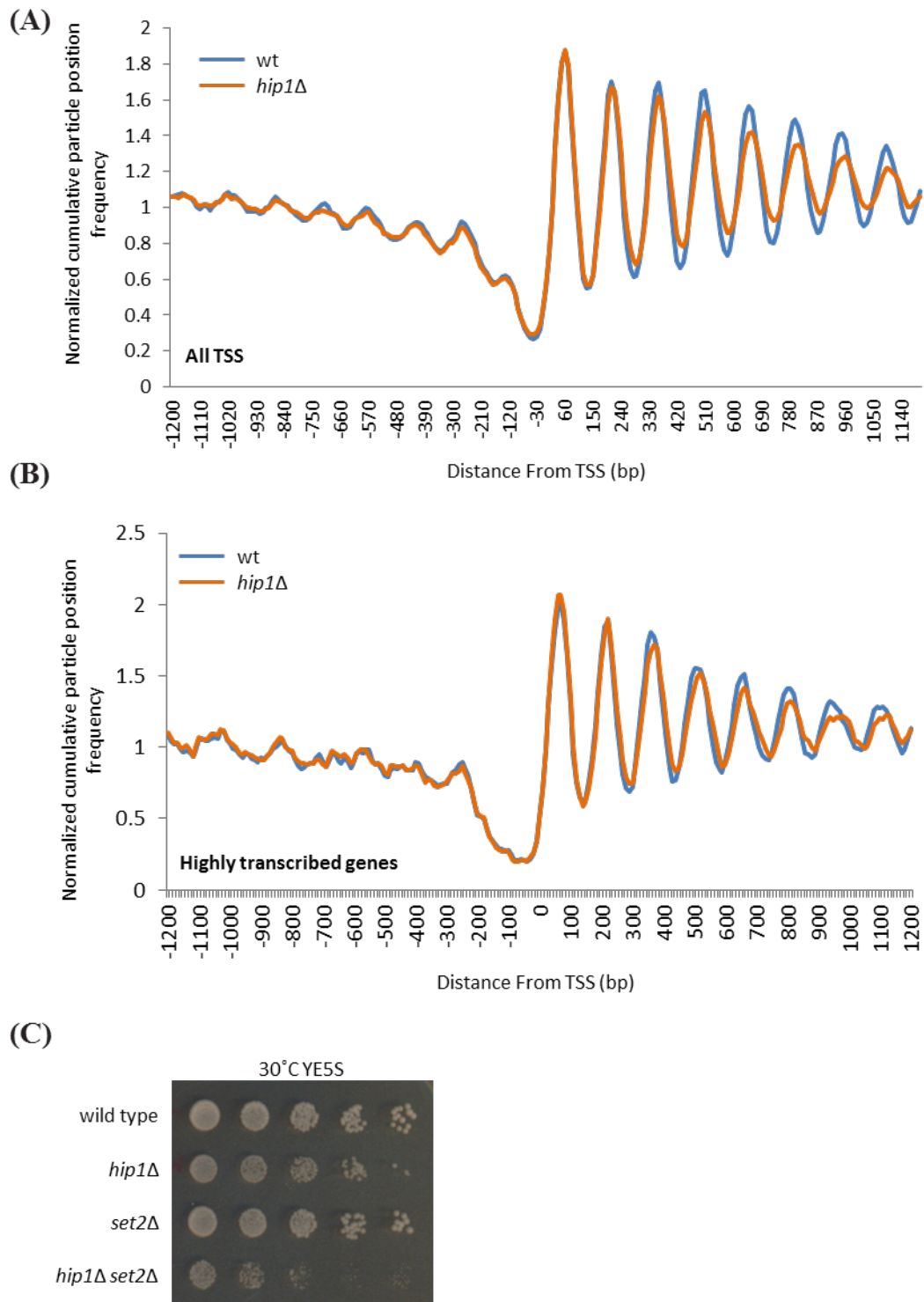


Figure 4.23 HIRA functions towards the 3' end of genes.

(A) Mononucleosomal fragments (150 bp) following MNase-seq for 4013 protein-coding genes were aligned by their transcription start sites (TSSs) (Lantermann *et al.*, 2009). (B) Mononucleosomal fragments (150 bp) following MNase-seq for top 10% highly expressed protein-coding genes were aligned by their transcription start sites (TSSs) (Lantermann *et al.*, 2009; Marguerat *et al.*, 2012). (C) Spot tests of the indicated strains were carried out following 5-fold serial dilutions of cells grown in YE5S to exponential phase. Plates were incubated for a further 3 nights at 30°C.

4.4.1.3 Possible nucleosome re-assembly role of HIRA independent to its function in transcriptional regulation

Also, worth noting, that previous work on the histone chaperone Spt6 has demonstrated that its role in nucleosome assembly over the bodies of genes is independent of its role in transcription regulation at promoters. That is, loss of *SPT6* though altered the nucleosome maps generated over the bodies of genes, did not correlate with steady state transcriptional increases (Ivanovska *et al.*, 2011). Rather, transcriptional changes were a result of the effect of Spt6 over specific promoter regions and/or the +1 nucleosome (Ivanovska *et al.*, 2011). This once again, is what has been observed upon loss of HIRA function. While on the global scale it wasn't possible to detect any changes to the -1 nucleosome, the NDR, and the +1 nucleosome, we did see them in a subset of genes that are transcriptionally upregulated in HIRA mutants, as previously demonstrated by microarray analysis (Blackwell *et al.*, 2004; Anderson *et al.*, 2009). Thus, HIRA function in promoter remodelling and therefore regulating transcription, is distinct from its role in nucleosome remodelling throughout transcription elongation. Both of these roles have been characterized independently in the past, but here is an actual read-out provided for the structural differences, supporting this notion.

4.4.2. HIRA is required for appropriate DNA damage repair

At the start of this study, there was little evidence linking the HIRA complex to DNA damage repair directly. However, there have been numerous reports demonstrating a role for the CAF-1 histone chaperone in appropriate restoration of chromatin following DNA damage repair (Gaillard *et al.*, 1996). Subsequently to DNA damage induction, nucleosomes are evicted from the chromatin, possibly to allow repair proteins to sites of damage (Berkovich *et al.*, 2007; Ikura *et al.*, 2007). While eviction of nucleosomes is important in appropriate repair, replacement of the displaced nucleosomes is equally imperative for proper resumption of transcription. Studies carried out both *in vitro* and *in vivo* have demonstrated that following DNA damage repair, a higher than usual proportion of newly synthesized histones get incorporated into the nucleosomes compared to the parental histones (Polo *et al.*, 2006). As expected therefore the incorporation of newly synthesized histones is dependent on the histone chaperone CAF-1. In CAF-1 knockdown cells *in vivo*, H3.1 deposition is lost, while checkpoint activation, transcription of repair factors and DNA double strand break repair completion are appropriate. Hence, the function of CAF-1 is following DNA damage repair completion, in re-establishing the chromatin environment (Polo *et al.*, 2006).

During the course of this study, it has been demonstrated that indeed HIRA also functions in DNA damage repair in mammalian cells (Polo, 2014). HIRA was shown to function independently of the repair machinery, and was demonstrated to be necessary for transcription restart following UVC damage (Adam *et al.*, 2013). The study revealed that HIRA localizes to sites of UVC irradiation along with CAF-1, but not ASF1, NAP and DAXX (Adam *et al.*, 2013). Furthermore, in addition to histone H3.1, H3.3 is also deposited at sites of DNA DSBs, an action that is carried out principally by HIRA.

Similarly to the results obtained from studies in tissue culture, the work presented here suggests a role for HIRA in the DNA damage response independently of DNA damage repair and checkpoint activation. In *hip1Δ* cells both checkpoint activation, as demonstrated by Chk1 phosphorylation, and repair of chromosomal DNA, as measured by PFGE, has taken place, albeit restoration of chromosomes with slower kinetics. It is possible that the HIRA complex in yeast is also required for appropriate disassembly of nucleosomes following DNA damage, thus allowing rapid access to repair proteins. It would be possible to address this issue by measuring the recruitment of repair proteins

following DNA damage induction. A rapidly inducible system is now available in *S. pombe*, which could help facilitate future work on the subject (Pai *et al.*, 2014).

It is also possible that HIRA is required for the transcription of repair genes, similarly to its role in transcriptional activation of stress-response genes (Chujo *et al.*, 2012). To address this point, it would be possible to measure transcript levels of repair genes known to be induced upon DNA damage repair, either by microarray analysis or by qRT-PCR. However, genetic analysis of *hip1Δ* with a range of repair mutants would suggest that it isn't a failure to induce these genes that's required from HIRA in repair. *hip1Δ* in combination with all mutants tested, including checkpoint, was significantly more sensitive to a range of DNA damaging agents than any of the single mutants, which isn't necessarily what would be expected if HIRA is required for the transcription of these genes.

Based on the results obtained throughout this study, as well as the recently published data on the role of HIRA in the DDR pathway, it is rather likely that the function of HIRA is through its role in nucleosome assembly (Fig 4.24). In order to confirm this, the association of Hip1 to sites of damage could be assayed by ChIP to establish its pattern of localization. Histone H3 could also be measured following repair completion in wild type and *hip1Δ* cells, which would help to determine whether nucleosomes have been replaced properly in *hip1Δ* cells.

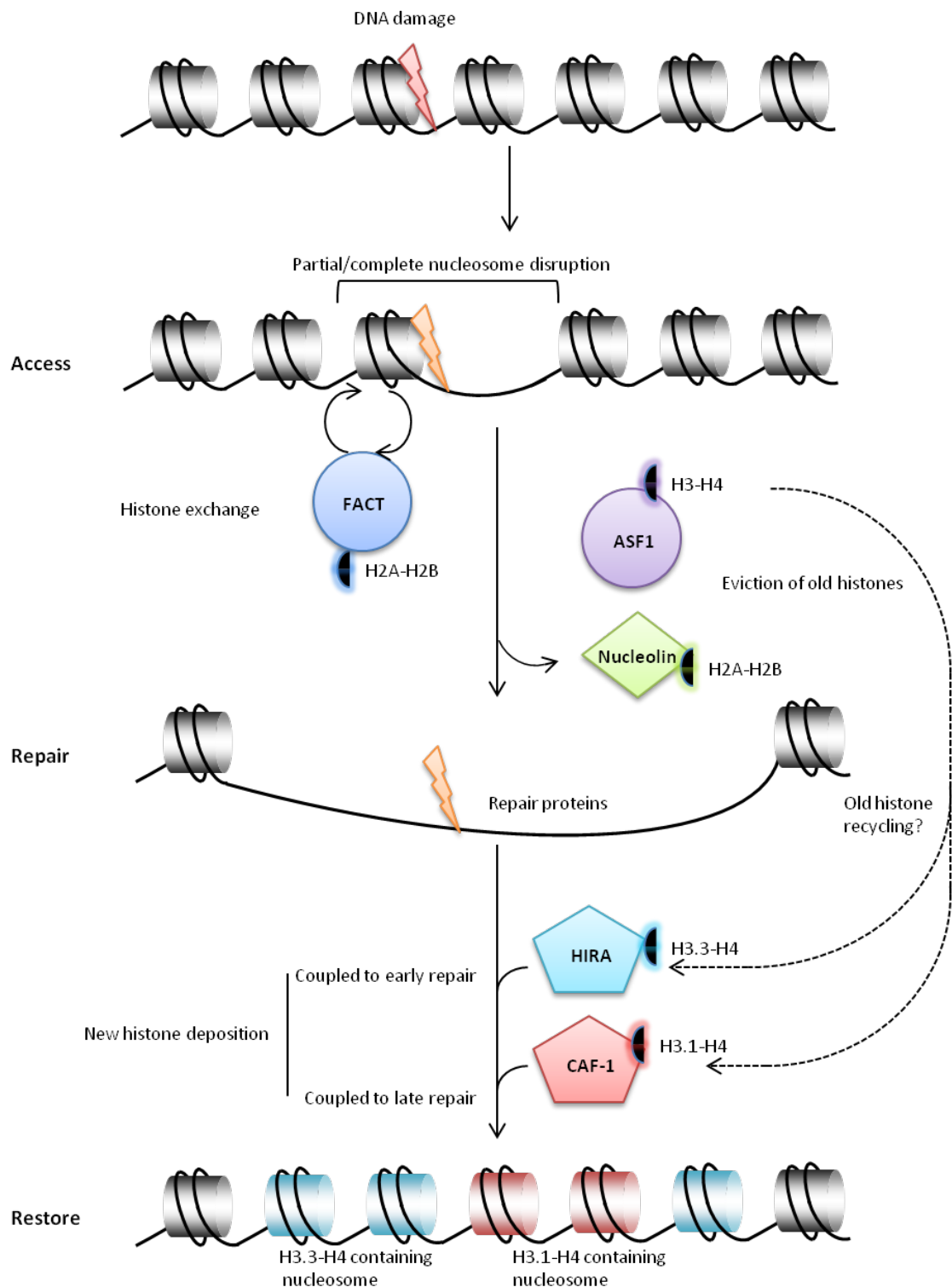


Figure 4.24 Role of histone chaperones in histone dynamics in response to DNA damage. Nucleosome disorganization after DNA damage is followed by nucleosome re-assembly with *de novo* histone deposition and potential recycling of displaced histones. FACT, ASF1 and Nucleolin have so far been demonstrated to promote histone exchange and histone eviction while *de novo* deposition following repair completion is thought to be mediated by CAF-1 and HIRA. ASF1 is possibly involved in recycling old histones and presenting them to CAF-1 and HIRA for deposition, although this mechanism remains unclear. Adapted from (Polo, 2014).

Chapter 5

Maintenance of Quiescence by the HIRA Complex in *S. pombe*

5.1 Introduction

5.1.1 Cellular Quiescence vs. Senescence

Cells that have exited the cell cycle into G₀ may exist in one of two alternative states, quiescence or senescence. The difference between these states is not always obvious, and often is inadequately defined. However, there is one essential difference, which is that the cell cycle arrest is reversible in quiescent cells while it is not in senescent cells (Heinrichs, 2008; Blagosklonny, 2011; van Deursen, 2014). When referring to the G₀ phase, quiescence is possibly the more appropriate term, as the majority of cells in complex multicellular organisms are believed to be quiescent rather than senescent (Heinrichs, 2008; Blagosklonny, 2011; van Deursen, 2014). Figure 5.1 shows a simplified diagram of the differences between proliferating, quiescent and senescent cells. In tissue culture, quiescence can occur as a result of serum, growth factor or nutrient withdrawal, and the arrest takes place in the absence of growth promoting pathways (Demidenko and Blagosklonny, 2008). On the contrary, senescence appears to take place in the presence of growth stimulation, for example an active mTOR pathway, coupled with cell cycle arrest for example through the activity of cyclin dependent kinase inhibitors (CDKIs) (Dulić *et al.*, 1993; Wong and Riabowol, 1996; Demidenko and Blagosklonny, 2008). Two of the most common CDKIs upregulated in senescent cells are p21 and p16 (Campisi, 2001; Braig and Schmitt, 2006). Fibroblasts or retinal pigment epithelial cells which have been arrested by serum starvation are quiescent as they can be stimulated to re-enter the cell cycle by inactivation of p21. In contrast, inactivation of p21 does not stimulate cell cycle re-entry for these cells if they have been arrested in the presence of serum. In this case these cells are senescent (Demidenko and Blagosklonny, 2008). Also it has been shown that cell cultures arrested by ectopic overexpression of p21 are quiescent for the initial 3-4 days of arrest (reversible) but become senescent following that (irreversible arrest), a transition which has been measured by proliferative potential (PP) (Chang *et al.*, 2000; Demidenko *et al.*, 2009). Overall, there are clear biochemical differences between quiescent and senescent cells, some of which include the hyperactivation of proliferation promoting genes plus genes responsible for cell cycle arrest in senescent cells, while proliferation promoting

genes are down regulated during quiescence (Campisi and d'Adda di Fagagna, 2007; Blagosklonny, 2011).

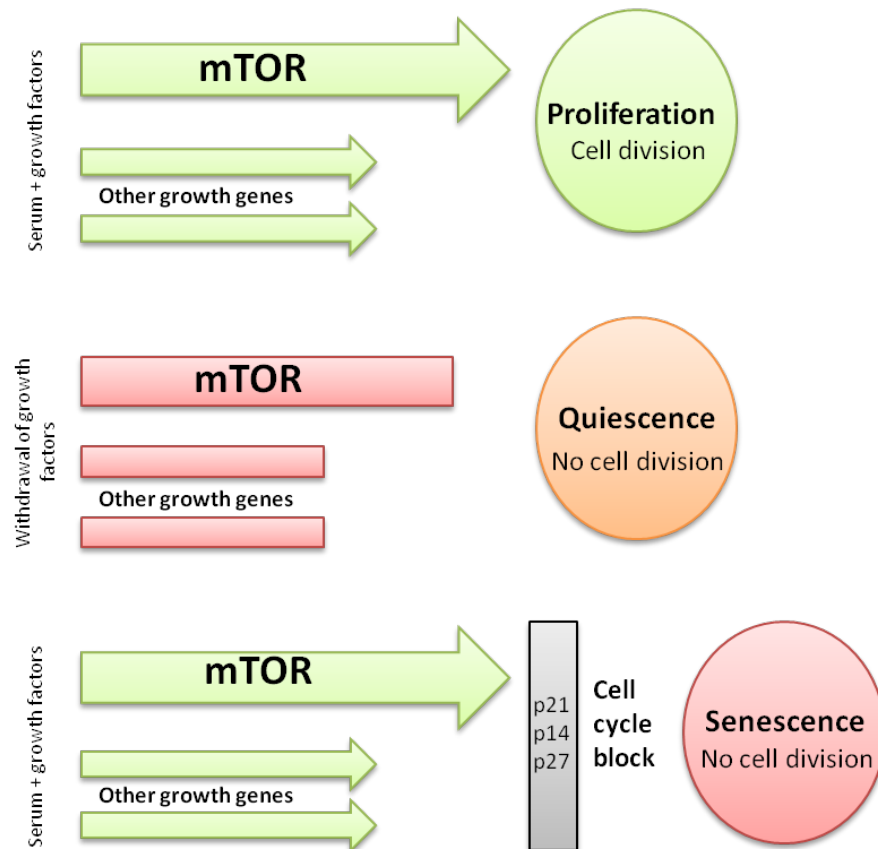


Figure 5.1 Schematic of proliferating vs. quiescent vs. senescent cells.

(A) Proliferating cells respond to serum and growth factors to induce mTOR and other proliferation promoting genes that lead to cell division. (B) Removal of serum/growth factors alongside inhibition of the TOR pathway leads to quiescence. (C) In the presence of serum and growth factors, as well as an active TOR pathway and cyclin dependent kinase inhibitors cells undergo senescence. Adapted from (Blagosklonny, 2011).

5.1.2 Roles of Cellular Quiescence

Quiescence is extremely important in complex multicellular organisms. In humans for instance, the majority of cells are in a quiescent state, i.e. some fibroblasts, lymphocytes, stem and satellite cells (Blagosklonny, 2011; Sousa-Victor *et al.*, 2014). Some further cell types are in a state termed locked/deep quiescence, which involves the silencing of proliferation promoting genes alongside active CDKIs (Blagosklonny, 2011). Some of the cell types in this category include adipocytes, neurons and cardiomyocytes (Blagosklonny, 2011; Lin *et al.*, 2012). Perhaps the most important group of cells on the list above are stem cells. Stem cells are undifferentiated, long-lived cells with the capability to produce differentiated/tissue specific daughter cells (Cheung and Rando, 2013). They are important for tissue regeneration in response to tissue damage, and loss of stem cells is associated with aging phenotypes, including muscle deterioration and immunosenescence (Fulop *et al.*, 2014; Sousa-Victor *et al.*, 2014). Stem cells are often quiescent for prolonged periods (Cheung and Rando, 2013) and loss of quiescence results in stem cell depletion, which compromises tissue regeneration, leading to aging. At the cellular level, aging, or cellular senescence, can be triggered as a result of a number of factors, including an increase in DNA damage, dysfunctional telomeres, decreased mitochondrial function, strong mitogenic signals or changes in chromatin structure (Di Leonardo *et al.*, 1994; Ogryzko *et al.*, 1996; Serrano *et al.*, 1997; Herbig *et al.*, 2004; Campisi and d'Adda di Fagagna, 2007; Benson *et al.*, 2009). As a result, distinguishing senescent and quiescent cells is essential. There has been work carried out on characterizing the transcriptome of different quiescent cell types (Blanpain *et al.*, 2004; Fukada *et al.*, 2007; Forsberg *et al.*, 2010; Martynoga *et al.*, 2013), as well as epigenetic analysis (Martynoga *et al.*, 2013) and while a global view is useful, there is still a limited understanding of the molecular mechanisms, particularly of individual factors, that play a role in the process of quiescence and its maintenance.

Quiescence is also believed to play a role in tumour development (Wells *et al.*, 2013). It is well known that pathogenic proliferation leads to tumorigenesis; however what is less well understood is the role quiescence plays during cancerous transformations. Following metastatic dissemination, metastatic dormancy, which is thought to be a quiescent state, allows cancerous deposits to lie undetected for years after the primary tumours have been removed. These cells maintain the capacity to proliferate, often

leading to further malignancies and death (Wells *et al.*, 2013). It will therefore be important to determine the molecular differences between ‘healthy’ quiescent cells and those of a ‘cancerous’ nature. With that in mind, it is essential to understand the molecular mechanisms regulating quiescence entry, maintenance and exit, in order to fully understand tumorigenesis and to begin the pursuit of differentiating cancerous quiescent cells from healthy ones.

5.1.3 Quiescence in *S. pombe*

As outlined above, quiescence is crucial for the success of complex organisms. It has been highly conserved throughout evolution and plays a key role in not only protecting cells from uncontrollable cell growth, but in unicellular eukaryotes it aids cell survival during harsh environmental conditions, such as nutrient limitation. This is not dissimilar to cultured mammalian cells, whereby serum withdrawal leads to cellular quiescence (Nilausen and Green, 1965; Larsson *et al.*, 1985; Gos *et al.*, 2005). Therefore, the molecular basis of quiescence can be investigated in single celled organisms and indeed they have been exploited due to the ease of genetic manipulation over the years (Roux *et al.*, 2010).

The yeast, *Schizosaccharomyces pombe* provides a good model as it shares key pathways with higher eukaryotes, including humans. G₀ quiescent states in *S. pombe* can be triggered by several methods, most commonly by carbon or nitrogen exhaustion. *S. pombe* cells respond in different ways to nitrogen depletion. If cells of the opposite mating type are available then a program of sexual development can be triggered (conjugation, meiosis, and sporulation) (Masayuki *et al.*, 1997). Alternatively, if only one mating type is present, *S. pombe* cells can enter a G₀ quiescent phase during which cell growth stops, allowing an alternate mechanism for cell survival under environmental duress (Su *et al.*, 1996). Nitrogen starved cells enter the G₀ phase with 1C DNA content from G₁ phase of the cell cycle post two rounds of cell division (Figure 5.2) (Su *et al.*, 1996; Sajiki *et al.*, 2009). These G₀ cells can remain viable for weeks to months, similarly to mammalian cells (Su *et al.*, 1996). They are round in shape and are smaller than actively dividing cells (Su *et al.*, 1996). Furthermore, they have some of the key features of G₀ quiescent cells including a reduction in cell size, chromosomes that are in a pre-replicative state, down regulation of protein synthesis to

a low maintenance mode and diminished ribosome biogenesis (Su *et al.*, 1996; Shimanuki *et al.*, 2007; Sajiki *et al.*, 2009; Yanagida, 2009). In contrast to this, cells that exhaust their carbon supplies during batch culture growth, enter a G₀ state (often called stationary phase) with a 2C DNA content. These cells are elongated rather than round and unlike nitrogen starved G₀ cells do not retain viability for extended periods (Yanagida, 2009; Roux *et al.*, 2010). Nonetheless, this approach has been used as a system for the study of chronological aging (Roux *et al.*, 2010).

Nitrogen starved G₀ cells, have been studied to determine the behaviours and changes of gene expression that occur in quiescence. Some of the molecular changes that happen during early stages of quiescence entry include a major remodelling of the nucleosomes in order to allow differential transcription to take place (Kristell *et al.*, 2010). It has also been shown that the sub nuclear position of specific regions is remodelled (Kristell *et al.*, 2010).

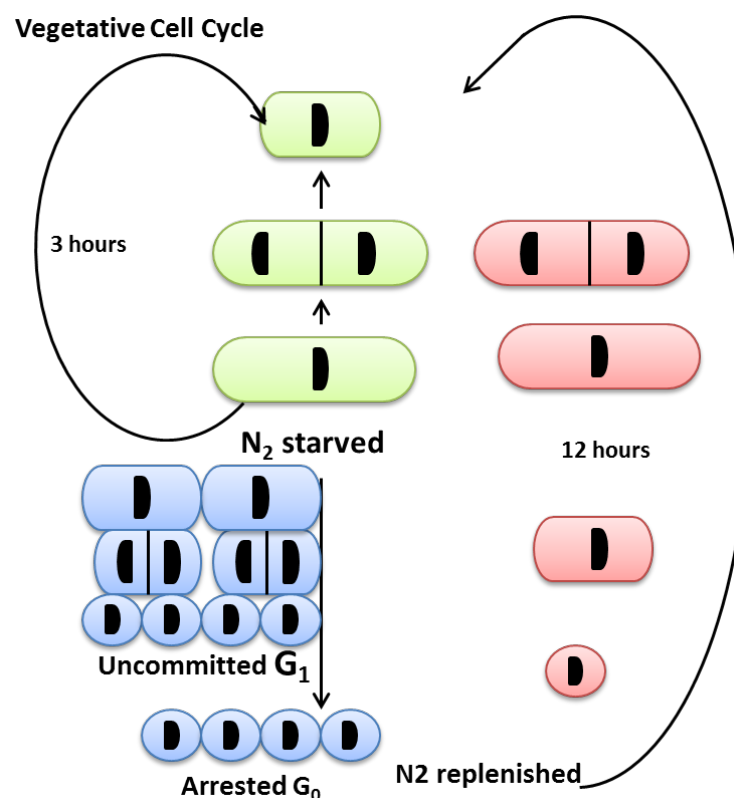


Figure 5.2 Schematic of the vegetative cell cycle and G₀ arrest upon nitrogen removal in *S. pombe*

S. pombe cells enter the quiescent phase with 1C DNA content from G₁ phase of the cell cycle post two rounds of cell division, during which cell size is dramatically reduced. Upon replenishment of nitrogen in the media, cells elongate and re-enter the cell cycle following 8-12 hours. Adapted from (Yanagida, 2009).

Microarray analysis has also been employed to define the relative changes to gene expression. Genes associated with cell cycle progression; growth and proliferation are down regulated while genes that provide resistance against stress, those involved in autophagy and nitrogen recycling are relatively transcriptionally induced (Shimanuki *et al.*, 2007). Notably, genes involved in ribosome biogenesis are almost instantaneously silenced following nitrogen removal, concurrently genes involved in pyrimidine salvage and nucleotide catabolic processes are up-regulated (Shimanuki *et al.*, 2007). More recent work has measured the absolute transcript and protein levels in proliferating and quiescent cells, and has found that the entire transcriptome and proteome shrinks (Marguerat *et al.*, 2012). Thus genes that appeared to be upregulated in quiescence are simply just less down regulated than the majority of genes (Marguerat *et al.*, 2012).

In mammalian quiescent cells nucleosome remodelling at specific sites takes place (Coisy *et al.*, 2004), along with a significant increase in the repressive histone H4K20me2 and H4K20me3 marks (Everitts *et al.*, 2013). Considering the changes to chromatin that take place during quiescence entry, and which will therefore have to be reversed during exit, it is reasonable to consider that histone chaperones may play a role in these processes. Indeed, the HIRA complex, in addition to regulating nucleosome density and recovery following DNA damage repair, has also been associated with senescence in higher eukaryotes (Zhang *et al.*, 2005; Ye *et al.*, 2007; Zhang *et al.*, 2007b), including humans, while other studies have suggested a requirement for the HIRA complex in quiescence (G₀) following nitrogen starvation (Kano and Russell, 2000; Blackwell *et al.*, 2004; Mizuki *et al.*, 2011). However, this remains largely unexplored and therefore, the aim of the work presented in this chapter was to determine the role of the HIRA complex in G₀ cells.

5.2 Results

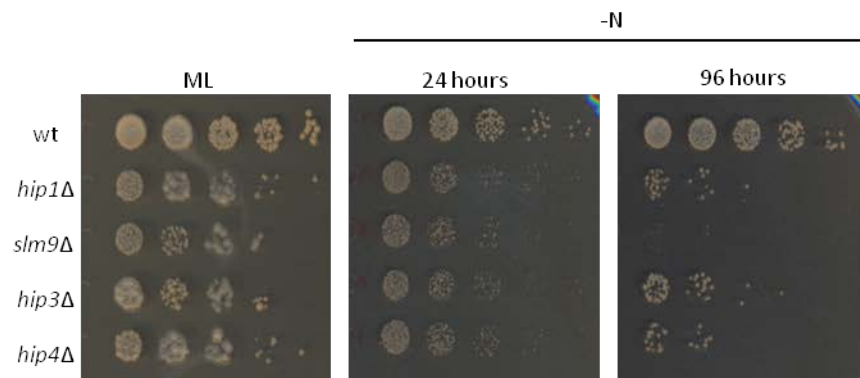
5.2.1 Loss of *HIRA* function leads to diminished viability of *S. pombe* cells following *G*₀ arrest

To induce quiescence, cells were grown in minimal medium (EMM) until OD₅₉₅ ~0.3, washed three times in minimal medium lacking nitrogen (EMM-N) and resuspended in EMM-N. Cell viability was monitored by determining the ability of cells to grow on rich (YE5S) agar. Spot tests of 5-fold serial dilutions showed that deletion of any of the four HIRA subunits, *hip1*⁺, *hip3*⁺, *hip4*⁺ or *slm9*⁺ leads to a reduction in cell viability, which was particularly pronounced by 96 hours in quiescence (Fig 5.3.A). Given that wild type cells retain viability for months this is a striking defect.

In order to determine whether wild type and *hip1*Δ cells arrest appropriately following nitrogen removal, FACS analysis was carried out. As expected, cycling cells presented with 2C DNA content but upon nitrogen depletion arrested with a clear 1C DNA peak. This was also the case in the *hip1*Δ mutant cells (Fig 5.3.B). Therefore, it appears that loss of *hip1*⁺ does not prevent proper cell cycle arrest in *G*₀. Microscopic examination showed that both wild type and *hip1*Δ cells decreased in cell volume and ‘rounded up’ following removal of nitrogen from the media (Fig 5.4). *hip1*Δ mutants were slightly elongated compared to the wild type, as is the case in proliferating cells.

Previous work has demonstrated that autophagy is a key process during nitrogen starvation; in fact autophagy is primarily responsible for providing the nitrogen source for cells during *G*₀ (Kohda *et al.*, 2007). Furthermore, components of the autophagy pathway have been shown to be sensitive to nitrogen starvation (Takeda and Yanagida, 2010; Takeda *et al.*, 2010). Therefore the possibility that autophagy is defective in *hip1*Δ cells was investigated. A method to measure autophagy has recently been implemented which utilizes an Atg8-GFP fusion protein: once nitrogen is removed from the media, Atg8-GFP gets conjugated to the autophagosomal membrane and the GFP molecule is cleaved via proteolysis (Mukaiyama *et al.*, 2009). This cleavage leads to the release of free, and stable, GFP molecules that can be detected by immunochemical assays (Mukaiyama *et al.*, 2009). Therefore, western blotting was employed to determine whether Atg8-GFP cleavage takes place appropriately in *hip1*Δ cells following *G*₀ arrest. Wild type and *hip1*Δ cells presented with comparable levels of free GFP molecules following 24 hours in quiescence (Fig 5.5), suggesting that autophagy is not impaired in *hip1*Δ cells.

(A)



(B)

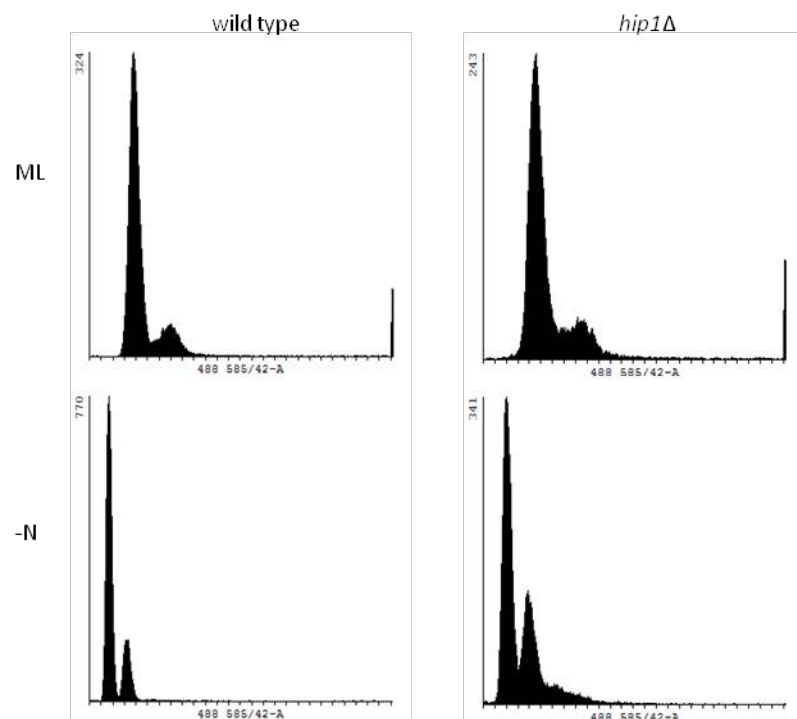


Figure 5.3 Cells lacking HIRA remain slightly elongated following nitrogen starvation induced quiescence.

(A) The indicated strains were grown to midlog phase and then subjected to nitrogen starvation. At the indicated time points cells were subjected to five fold serial dilutions and then spotted onto YE5S. Plates were further incubated at 30°C for 3 nights. (B) ***hip1Δ* cells arrest with 1C DNA content** FACS analysis of wild type and *hip1Δ* cells in midlog phase and following 24 hours in quiescence. Nuclear staining was carried out using Propidium iodide (PI). Data is representative of two independent biological repeats.

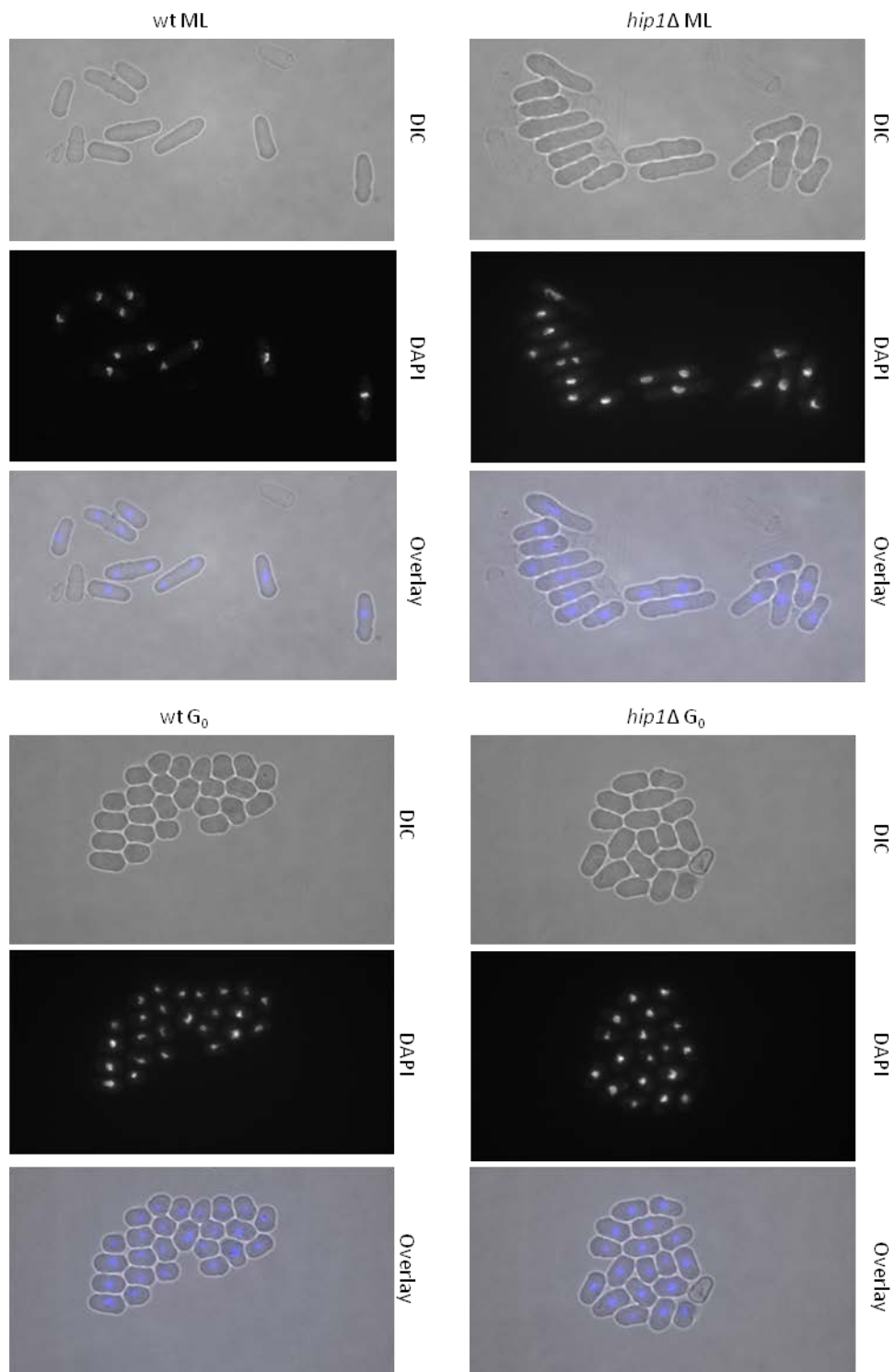


Figure 5.4 Cells lacking HIRA remain slightly elongated following nitrogen starvation induced quiescence.

Midlog and nitrogen starved cells (24 hrs) were stained with DAPI then examined under the microscope. DIC, DAPI and merged images were taken using a Zeiss Axiovert microscope under the 100x oil-immersion lens.

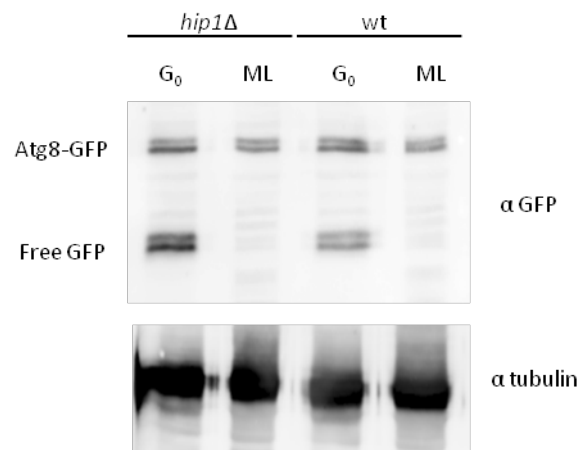


Figure 5.5 Autophagy is induced appropriately upon nitrogen removal from the media.

Atg8-GFP and free GFP levels were measured by western blotting at the indicated conditions. Data is representative of two independent biological repeats.

5.2.2 Cells lacking $hip1^+$ attempt to re-enter the cell cycle following 24 hours in G_0

In order to provide a quantitative measure of viability as a function of time in G_0 , the ability of individual cells to form colonies when seeded onto rich agar plates was monitored. Over 80% of wild type cells formed visible colonies after 24 hours in G_0 and as expected overall viability did not decline after 96 hours. On the other hand, only ~40% of *hip1 Δ* cells managed to form visible colonies following 24 hours in G_0 , a percentage which declined to near ~5% by 48 hours and to 0% by 96 hours (Fig 5.6.A). Cells that did not form visible colonies were subjected to microscopic analysis. These cells were categorized based on their morphology into three groups, ' G_0 ', 'elongated' and those that have managed to form 'microcolonies' (Fig 5.6.B). This revealed that a further ~40% of non-viable *hip1 Δ* cells following 24 hours in G_0 have elongated upon nitrogen replenishment, and a further ~4% have formed microcolonies (Fig 5.6.B). These results suggest, that at least following 24 hours in quiescence, the majority of *hip1 Δ* cells attempt to re-enter the vegetative cell cycle. In contrast, following 96 hours in quiescence *hip1 Δ* cells overwhelmingly remain in a G_0 state, suggesting that these cells have lost the ability to respond to environmental signals and do not attempt to re-enter the cell cycle.

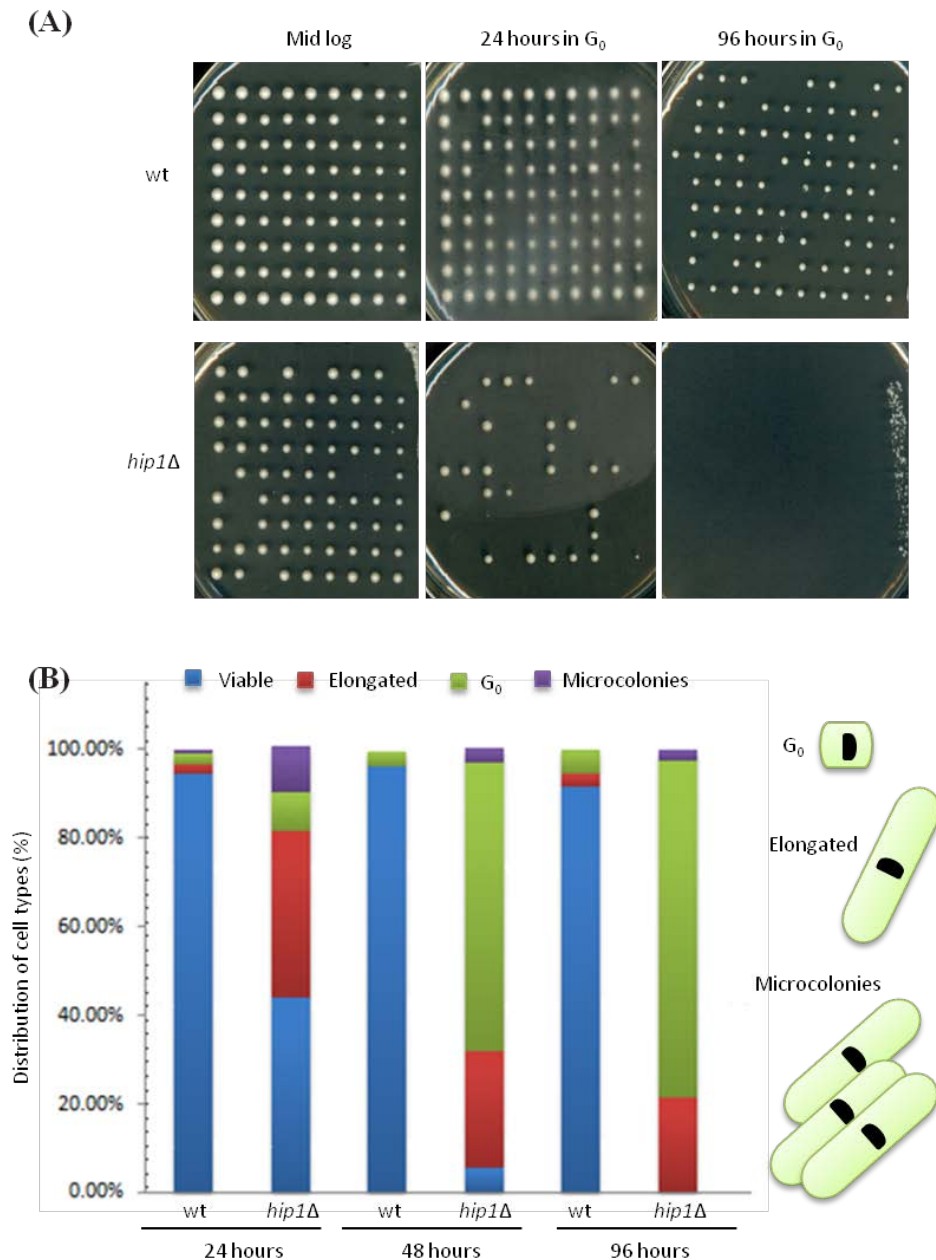


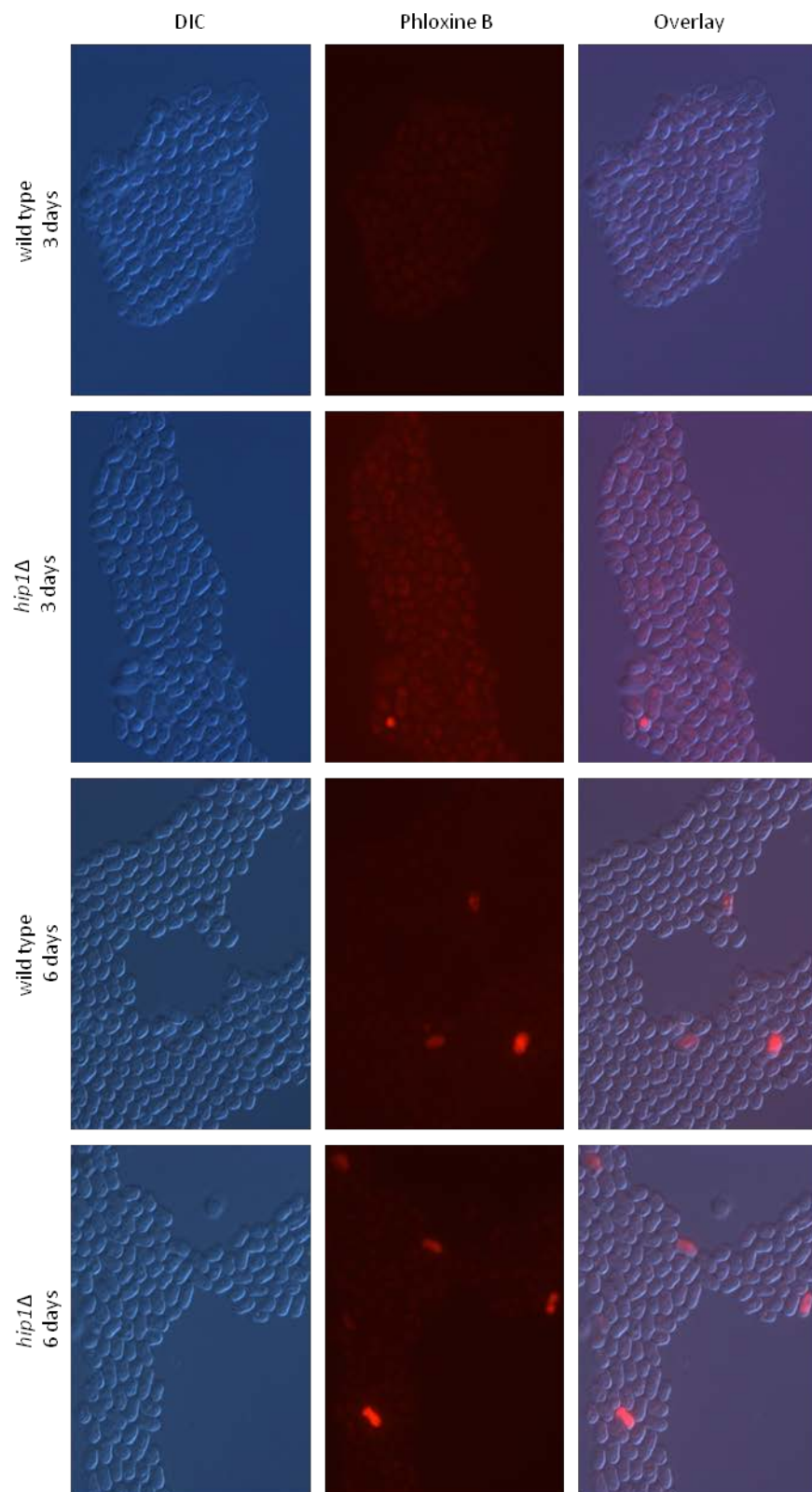
Figure 5.6 The majority of *hip1* Δ cells attempt to re-enter the cell cycle after 24 hours in G_0 .

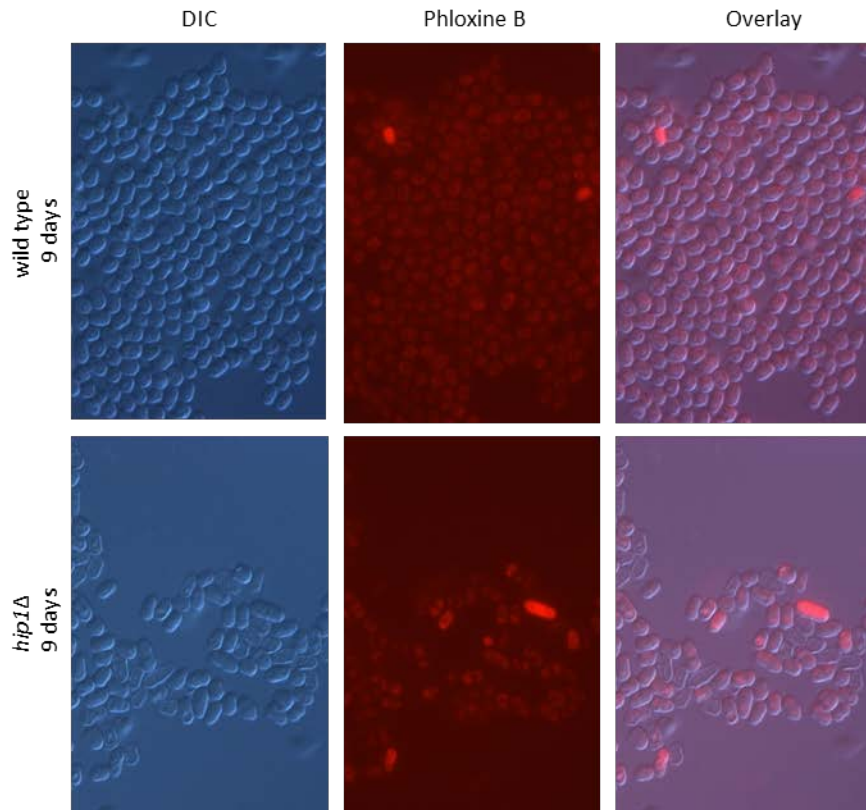
(A) Individual cells were transferred onto YE5S plates during midlog phase and following 24 and 96 hours in quiescence. YE5S plates were incubated at 30°C for 3-4 days in order to allow the formation of visible colonies. Data is representative of four independent biological replicates. **(B)** Percentage viability of cells in (A) and classification of cells, based on morphology, that have failed to enter the vegetative cell cycle. Data are the mean of four biological replicates.

In order to determine whether cells that have failed to re-enter the cell cycle were actually metabolically inactive (dead), Phloxine B staining was implemented. Phloxine B is a dye that stains cells pink/red when they are metabolically inactive/dead, and is commonly used to determine cell viability in yeast (Umeda *et al.*, 2005). Surprisingly, microscopic analysis of cell viability as determined by Phloxine B staining, suggests that the overwhelming majority (89 %) of *hip1Δ* cells are metabolically viable even after 12 days in quiescence (Figure 5.7.A and B). Therefore, it appears that these cells have become prematurely senescent, rather than dead.

Finally, for further confirmation that the immediate growth response to nitrogen replenishment is appropriate, cell length was measured in both wild type and *hip1Δ* cells following 24 hours in quiescence and following 8 hours of nitrogen re-feeding (Fig 5.8.A and B). Wild type cells were similar in length to previously described observations (Shimanuki *et al.*, 2007), while *hip1Δ* cells were slightly elongated both in G₀ and in the vegetative cell cycle, agreeing with the previous observations (Blackwell *et al.*, 2004). Significantly, like wild type, *hip1Δ* mutants enlarged following nitrogen replenishment (Fig 5.8.A and B). This is in agreement with the results described above and suggests that the initial response to nutrients is largely intact in *hip1Δ* cells following 24 hours in quiescence.

(A)





(B)

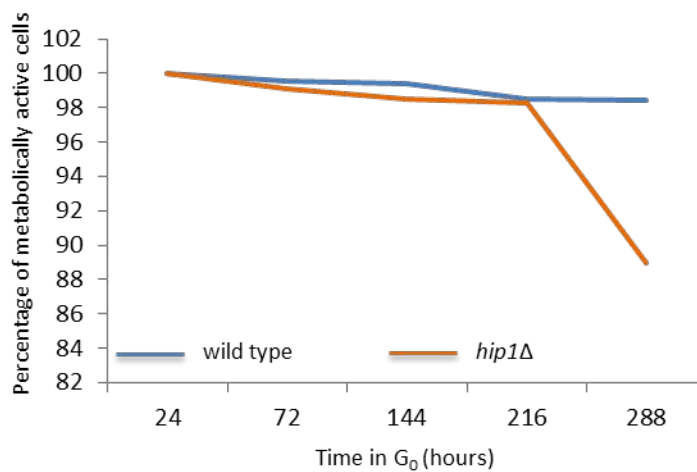


Figure 5.7 Phloxine B staining of *hip1Δ* cells indicates that the majority of these cells are viable even following 9 days in quiescence

(A) Cells were grown to mid-log phase in EMM medium at 30°C then were nitrogen depleted and further incubated in EMM-N media for the indicated times at 30°C. Images were taken of DIC and of Phloxine B stained cells under the 60x oil immersion lens. (B) Cell viability was calculated based on Phloxine B staining.

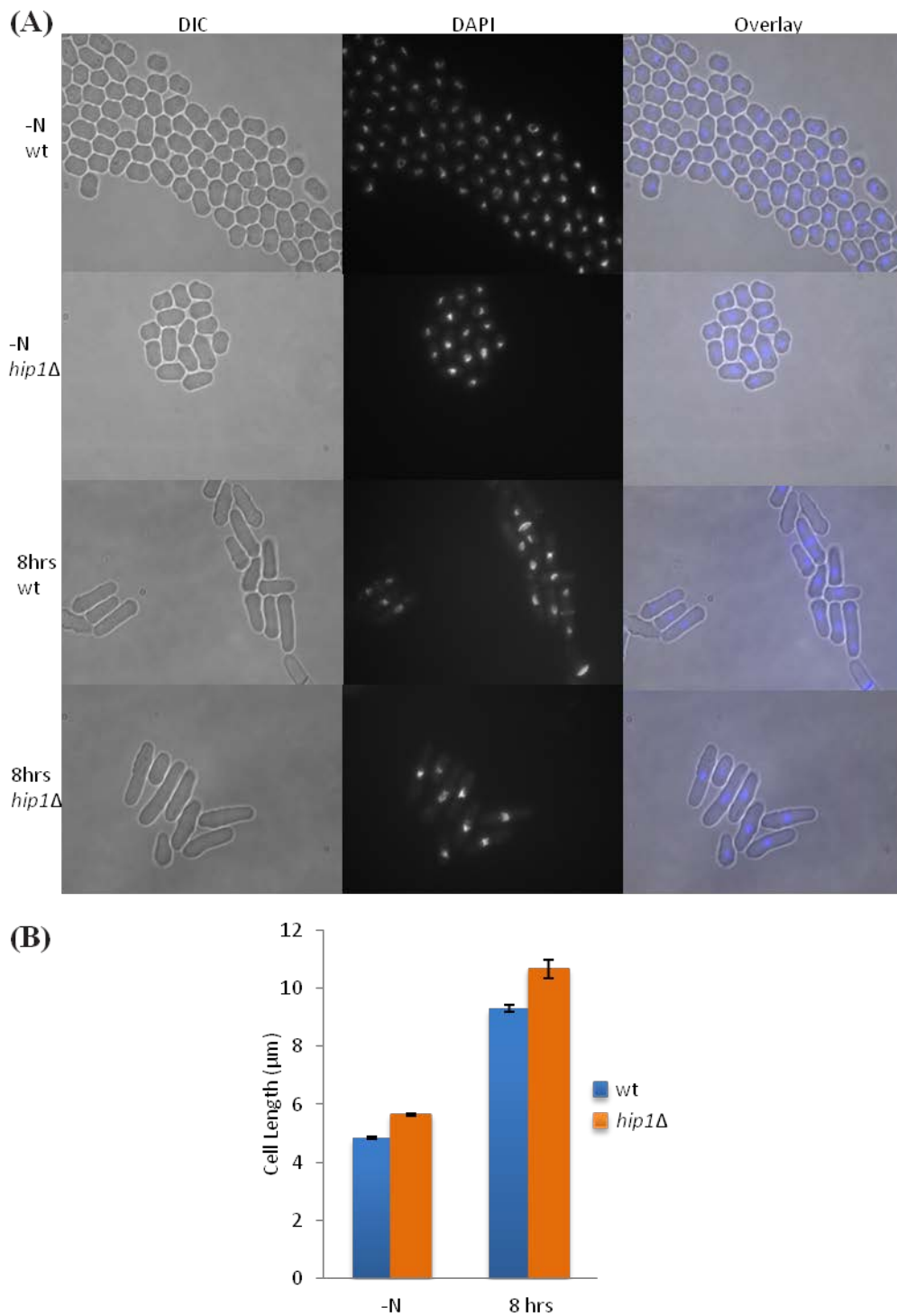


Figure 5.8 Cells lacking HIRA increase in cell length in response to restoration of nitrogen. (A) Cells were grown to mid-log phase in EMM medium at 30°C then were nitrogen depleted and further incubated for 24 hours at 30 °C, following which cells were washed and resuspended in YE5S. DIC, DAPI and merged images were taken at the indicated times using a Zeiss Axiovert microscope under the 100x oil-immersion lens. (B) Cell length in Figure A was measured using Zeiss Axiovision during quiescence and following 8 hours of nitrogen replenishment. Error bars represent \pm SEM.

5.2.3 Chromatin remains intact in cells lacking HIRA

Based on the role of the HIRA complex in replication-independent histone chaperone activity, one possible hypothesis was that *hip1Δ* cells progressively lose nucleosomes as a result of transcription during quiescence, thus disrupting chromatin to a degree that renders large regions of the genome dysfunctional. This seemed like a reasonable possibility due to the fact that the replication-dependent chaperones, like Caf1, would no longer be able to reset the chromatin during replication. Interestingly, the defect in quiescence is specific to HIRA mutants, as none of the other histone chaperone mutants tested, including *nap1Δ*, *pcf2Δ* (CAF subunit), and *rtt106Δ* were sensitive to nitrogen removal. Indeed, the only other chaperone mutant that was particularly sensitive was *asf1-33*. This is not surprising as Asf1 is known to act with the HIRA complex (Malay *et al.*, 2008; Yamane *et al.*, 2011). In order to address the status of the chromatin in *hip1Δ* cells, bulk chromatin DNA was MNase digested as described previously (Section 2.5.3.1). Figure 5.9 shows that both wild type and *hip1Δ* cells presented with clear MNase generated nucleosome ladders, thus suggesting that the integrity of chromatin in *hip1Δ* cells is largely maintained, even after 96 hours in G₀. It should be noted however that bulk DNA digestions do not rule out locus specific nucleosome alterations.

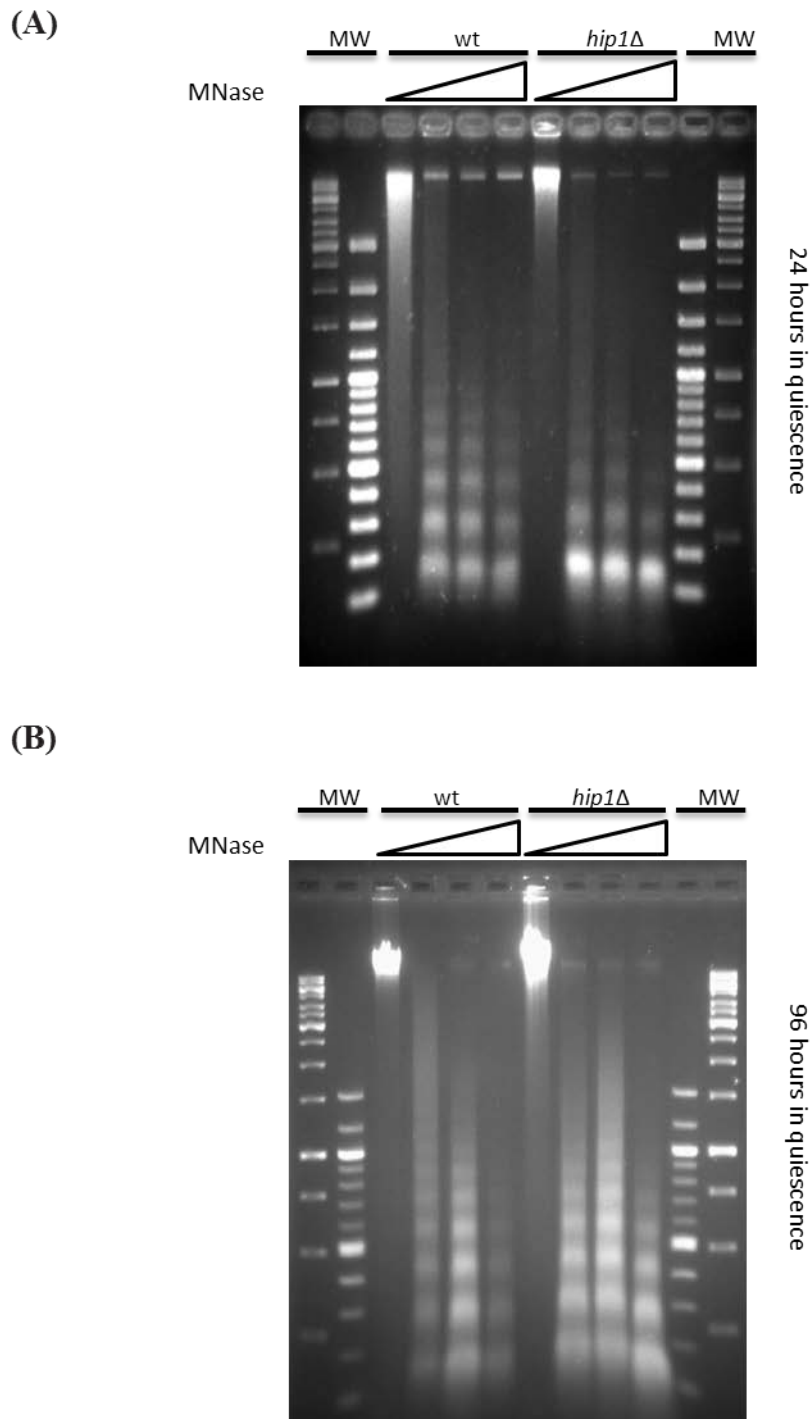


Figure 5.9 MNase digestions of wild type and *hip1Δ* cells following 24 and 96 hours in quiescence.

(A) and (B) Chromatin from the indicated strains under the indicated conditions was treated with increasing concentrations of MNase. DNA was purified and samples were run on 1.5% TAE agarose gels. Data are representative of three biological repeats.

Previous work has shown that HIRA represses histone gene transcription outside of S phase, but total histone H3 protein levels are decreased during vegetative growth in *hip1Δ* cells (Section 4.2.5). However histone levels have not been investigated in *hip1Δ* cells during quiescence. Therefore qRT-PCR analysis was first applied to measure histone mRNA levels in *hip1Δ* cells following 24 hours in quiescence. All histone genes tested (H3, H4, H2A and H2B) showed an increase in transcript levels compared to the wild type (Fig 5.10.A.). Conversely, total histone H3 protein levels were slightly reduced in *hip1Δ* cells compared to the wild type (Fig 5.10.B). Due to time constraints H2A levels have not been measured in quiescent cells. However, overall there does not appear to be a stark decrease or alteration in histone protein levels, nor in chromatin integrity that could by itself warrant the severe phenotype associated with HIRA deficient cells in quiescence.

Genetic analysis was also carried out between the *hip1Δ* allele and combinations of deletions of the histone H3-H4 gene pairs. *hip1Δ* and histone H3-H4 single and double mutants were compared to determine whether these mutants phenocopy the HIRA quiescence phenotype. Deletion of two histone H3-H4 gene pairs (either *hht2Δ hhf2Δ hht1Δ hhf1Δ* or *hht2Δ hhf2Δ hht3Δ hhf3Δ*) did not result in a change in viability compared to the wild type in quiescence (Fig 5.11.A and B). In fact, the only time a clear reduction in viability was observed was when *hht2⁺* and *hhf2⁺* were deleted in combination with *hip1⁺*. These triple mutants had a significantly decreased life span compared to the *hip1Δ* single mutant or to the *hht2Δ hhf2Δ* double mutants (Fig 5.11.C). Thus simply reducing histone dosage does not phenocopy the G₀ defect of HIRA mutants.

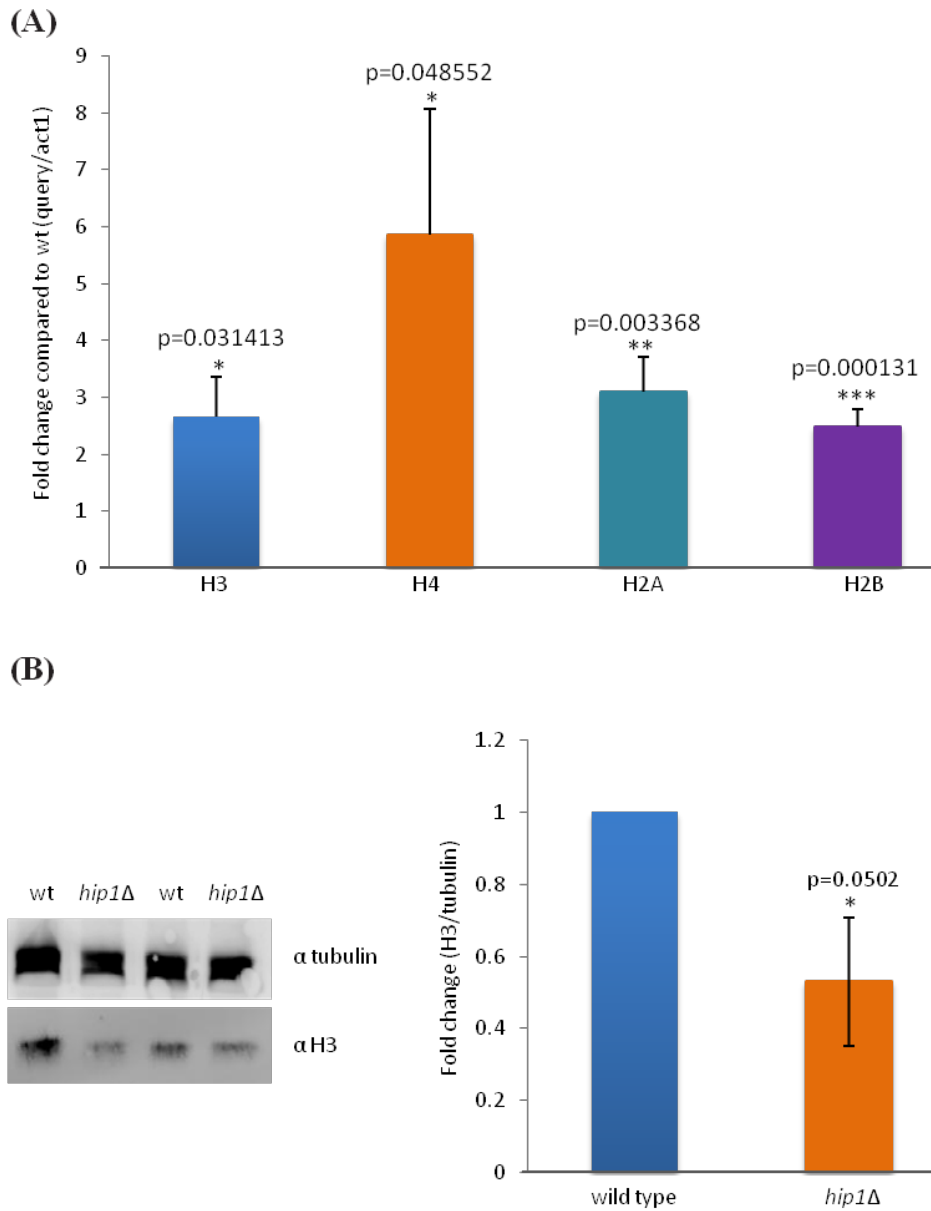


Figure 5.10 Histone gene transcription is upregulated, while histone H3 protein levels are reduced in *hip1Δ* cells compared to the wild type

(A) qRT-PCR analysis of histone gene transcription in G_0 *hip1Δ* cells. Data shown represents fold-change relative to the wild type. Data are the mean of three biological replicates and error bars represent \pm SEM (* $p < 0.05$; ** $p < 0.01$; *** $p < 0.001$). (B) Western blot analysis of histone H3 protein levels in quiescent cells. Quantification of the blots is shown in the right hand panel and data represents fold-change relative to the wild type. Data are the mean of two biological replicates and error bars represent \pm SEM (* $p < 0.05$).

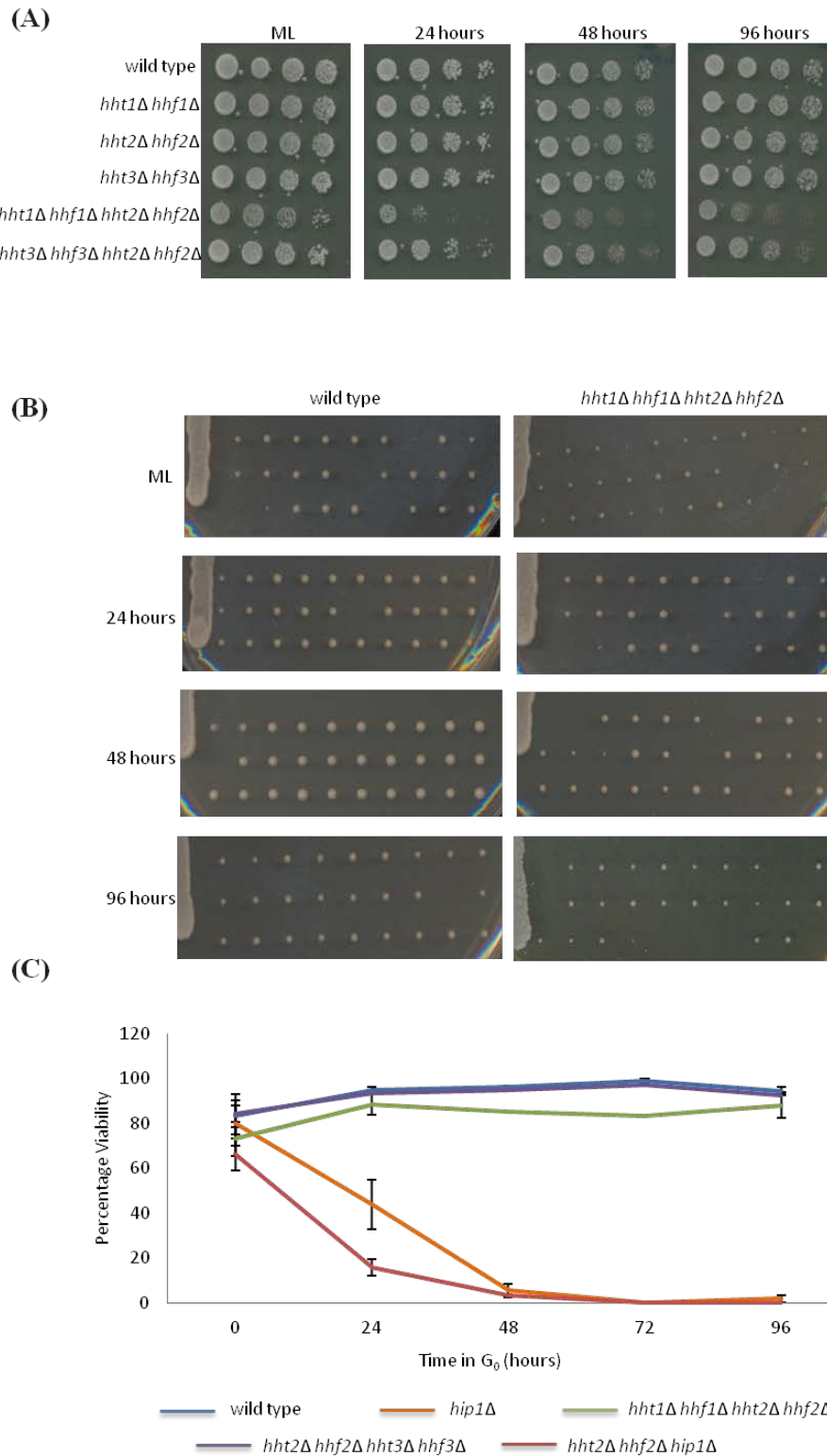


Figure 5.11 Deletion of histone gene pairs does not phenocopy the HIRA quiescence phenotype. (A) Spot tests of wild type and the indicated mutant cells during quiescence. 5-fold serial dilutions were carried out at the indicated times, cells were spotted onto YE5S plates and were further incubated at 30°C for 3 nights. (B) Individual cells were transferred onto rich YE5S agar plates at the indicated times in quiescence. Plates were incubated at 30°C until colonies were visible. The images are representative of three biological replicates. (C) Percentage viability of experiments in Figure B. Data are the mean of three biological replicates and error bars represent \pm SEM.

5.2.4 Over 850 genes are mis-transcribed in *hip1Δ* cells during quiescence

Microarray analysis was carried out in collaboration with Jürg Bähler's group (UCL) to compare the transcriptome of wild type and *hip1Δ* samples following 24 hours in quiescence. Deletion of *hip1*⁺ leads to the upregulation of 598 genes compared to the wild type in G₀. The genes that were upregulated in the absence of *hip1*⁺ are enriched for 'unannotated' gene ontology (GO) terms, with 284 in this category according to the Princeton GO term finder, with a p-value of 1.09e-293. Indeed these genes encode antisense transcripts and non-coding RNAs. Amongst the genes upregulated in the *hip1Δ* are the histone genes, including *hta1*⁺, *htb1*⁺ and *hht2*⁺ encoding histones H2A, H2B and H3 respectively, confirming the previous qRT-PCR results. Also upregulated are components of the RNAi pathway, including *ago1*⁺, *dcr1*⁺ and *hrr1*⁺, possibly as an adjustment to the increase in ncRNAs. Thus, similarly to midlog phase cells, HIRA is primarily required as a repressor of transcription (Kano and Russell, 2000; Blackwell *et al.*, 2004; Greenall *et al.*, 2006; Anderson *et al.*, 2009; Anderson *et al.*, 2010; Mizuki *et al.*, 2011). However, 253 genes were at least two-fold down-regulated in the absence of *hip1*⁺. According to the Princeton GO term finder; these belong to 12 functional categories, with the majority of them unannotated, while the rest are primarily involved in pheromone sensing and conjugation. The GO terms significantly enriched according the GO term finder, in the two-fold down-regulated genes, are listed in Table 5.1. The full list of genes that are at least two fold up or down-regulated in *hip1Δ* cells compared to wild type can be viewed in appendix A. While a large number of genes are mis-transcribed in the absence of *hip1*⁺ their relative contribution to the reduced viability seen in *hip1Δ* cells is not known. It is possible that the transcriptional changes observed here contribute to the reduced fitness of the *hip1Δ* mutant; however proliferating cells experience similar disruption to global transcriptome without compromised viability. Therefore it is unlikely that these changes to the transcriptome are responsible for the 'premature senescence' that is seen in these cells.

Table 5.1. GO terms of genes that are at least 2 fold down-regulated in the absence of *hip1*⁺ relative to the wild type following 24 hours in quiescence

Gene Ontology Term	Number of Genes	p-value
Unannotated	52	3.99e-66
Cellular response to pheromone	12	9.95-e06
Pheromone-dependent signal conjugation with cellular fusion	9	2.46e-05
Response to pheromone	12	3.09e-05
Signal transduction involved in conjugation with cellular fusion	10	5.83e-05
Response to pheromone involved in conjugation with cellular fusion	10	0.00013
Cell surface receptor signalling pathway	11	0.00022
G-protein coupled receptor signalling pathway	10	0.00043
Positive regulation of G-protein coupled receptor protein signalling pathway	5	0.00096
Positive regulation of signal transduction involved in conjugation with cellular fusion	5	0.00096
Positive regulation of pheromone-dependent signal transduction involved in conjugation with cellular fusion	5	0.00096
Cellular response to organic substance	13	0.00936

5.2.5 Restoring HIRA function during quiescence exit rescues cell viability

The conditional *hip1-HBD* allele was once again utilized to address whether HIRA function is required at any particular stage during quiescence (entry, maintenance and/or exit). *hip1-HBD* cells were grown to midlog phase in EMM, nitrogen starved and plated onto YE5S agar at various time points as described previously. The presence of β -estradiol in the media was manipulated to control whether HIRA function was present or absent during proliferation, entry into G_0 , G_0 , and exit from quiescence. The addition of β -estradiol after 96 hours in quiescence partially rescued the viability of *hip1-HBD* cells irrespective of whether HIRA function was present prior to that stage, suggesting that HIRA is important for successful re-entry into the vegetative cell cycle (Fig 5.12) *hip1-HBD* cells also re-entered the cell cycle similarly to wild type cells when HIRA function was active during quiescence and switched off during exit. These results therefore imply that HIRA is required for appropriate maintenance of quiescence, in addition to quiescence exit, but not for entry into quiescence, agreeing with previous observations.

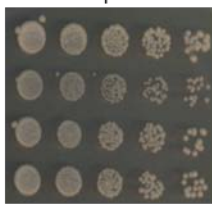
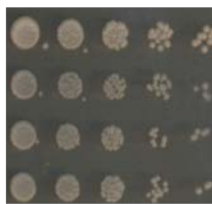
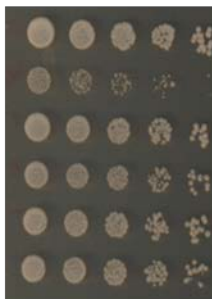
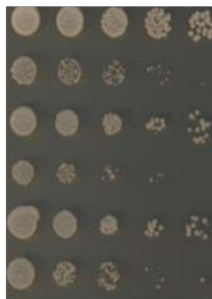
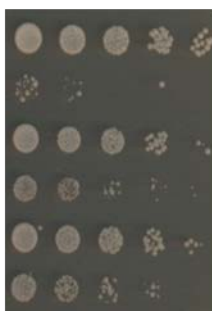
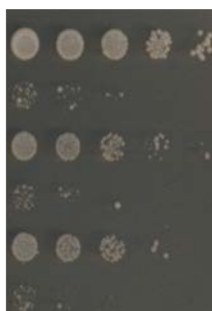
HIRA function					
During Proliferation		During G ₀	During Recovery		
			+	-	
wild type	+	+			Midlog
<i>hip1Δ</i>	-	-			
<i>hip1-HBD</i>	+	+			
<i>hip1-HBD</i>	-	-			
wild type	+	+			24 Hours
<i>hip1Δ</i>	-	-			
<i>hip1-HBD</i>	+	+			
<i>hip1-HBD</i>	+	-			
<i>hip1-HBD</i>	-	+			
<i>hip1-HBD</i>	-	-			
wild type	+	+			96 Hours
<i>hip1Δ</i>	-	-			
<i>hip1-HBD</i>	+	+			
<i>hip1-HBD</i>	+	-			
<i>hip1-HBD</i>	-	+			
<i>hip1-HBD</i>	-	-			

Figure 5.12 Restoring HIRA function during quiescence exit rescues cell viability.

The indicated strains were grown in EMM either in the presence or absence of β -estradiol, then were depleted for the nitrogen source and resuspended in EMM-N media with or without β -estradiol. Cells were incubated at 30°C for up to 96 hours during which five-fold serial dilutions and spot tests were carried out daily onto YE5S plates or YE5S plates supplemented with β -estradiol. Plates were further incubated at 30°C for 3 days, until colonies were visible.

5.2.6 Increased DNA DSBs in *hip1* Δ cells during quiescence exit

It has been shown that cells deleted for *tdp1*⁺, which encodes a tyrosyl-DNA phosphodiesterase, die in quiescence as a result of accumulation of DNA damage (Ben Hassine and Arcangioli, 2009). This manifests as elevated levels of DSBs during the first round of DNA replication. As cells lacking HIRA are sensitive to DNA damaging agents, and have been shown to have defects in repair during G₀ (Section 4.3.4), the possibility that this might be the case in *hip1* Δ cells was addressed. In order to measure DSBs, Rad52 foci formation was monitored. Rad52 is involved in homologous recombination during HR-mediated repair. Here, a Rad52-YFP fusion protein was utilized and the numbers of cells with distinct Rad52-YFP foci were counted as the percentage of the total number of cells. Previous work has shown that in the absence of a functional Asf1 histone chaperone, Rad52 foci levels increase during midlog phase (Tanae *et al.*, 2012). Therefore, Rad52-YFP foci level were measured during midlog, following 24 hours in G₀ and again following 4 hours of nitrogen replenishment. Similarly to *asf1-33* mutants, loss of *hip1*⁺ leads to an increase in Rad52-YFP levels, from ~11% to ~17%, a small but significant increase (Fig 5.13). Moreover, *hip1* Δ cells entered the G₀ state with unrepaired DSBs as evident by the presence of Rad52-YFP foci at around 8%, while Rad52 foci were largely absent in wild type cells. Upon attempted re-entering into the cell cycle, *hip1* Δ cells had increased DSBs compared to the wild type cells. However the level was no more than seen prior to G₀ arrest. This suggests that *hip1* Δ cells do not accumulate large amounts of DNA damage during quiescence. Therefore, the defects of *tdp1* Δ and *hip1* Δ cells are distinct.

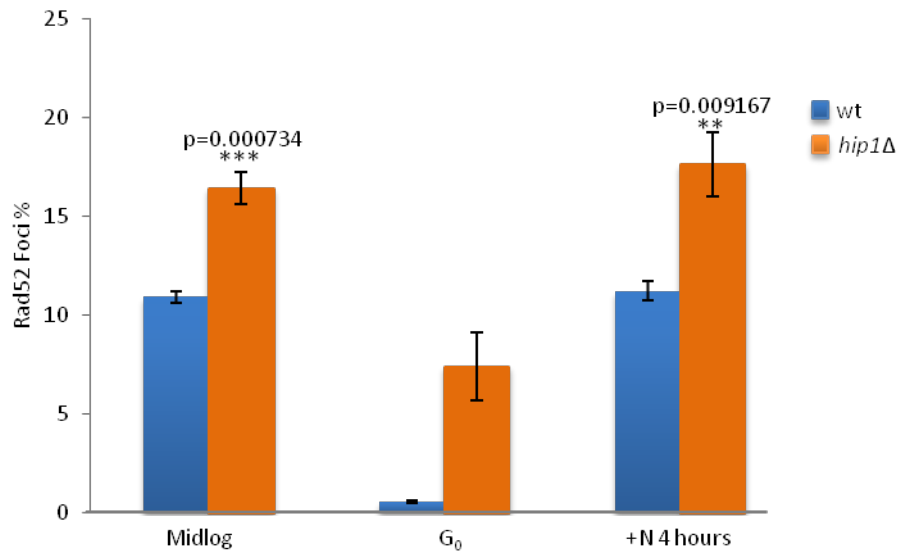


Figure 5.13 Cells lacking HIRA enter and exit quiescence with elevated levels of DSBs.

Rad52 foci were calculated as a percentage of the number of nuclei. Data are the mean of three biological replicates; in each experiment at least 200 nuclei were counted for each strain. Error bars represent \pm SEM (** $p < 0.01$; *** $p < 0.001$).

5.2.7 Loss of *hip1*⁺ leads to diminished activation of cell cycle regulated genes following restoration of a nitrogen source

Next, gene expression during re-entry into the cell cycle was investigated. Upon nitrogen replenishment ribosome biogenesis, along with the induction of metabolic genes takes place almost immediately (Shimanuki *et al.*, 2007). Therefore, mRNA levels of genes involved in metabolism were measured by qRT-PCR to determine whether the induction of growth genes is appropriate in *hip1Δ* cells. *ura3*⁺ and *mis3*⁺ have both been previously characterized as genes that get induced rapidly upon nitrogen replenishment (Shimanuki *et al.*, 2007) and indeed in both wild type and *hip1Δ* cells following 1 day in quiescence their levels increase rapidly, suggesting that induction of 'growth' genes is appropriate in the *hip1Δ* mutants (Fig 5.14.A and B).

Genes involved in cell cycle control are also induced upon nitrogen replenishment. In order to address whether the transcription of these genes gets induced appropriately, *cdc18*⁺ mRNA levels were measured in the first instance. The expression of *cdc18*⁺ is induced prior to S phase via the action of cell cycle regulated MBF transcription factors. *cdc18*⁺ encodes the homologue of the mammalian *CDC6* and along with Cdt1 is required for the assembly of the pre-replicative complex (Kelly *et al.*, 1993; Nishitani *et al.*, 2000; Yanow *et al.*, 2001) during late G₁ phase. In mammalian cells *CDC6* is removed from replication origins during G₀ but not during G₁ and its re-synthesis and loading are important for quiescence exit (Kingsbury *et al.*, 2005; Collier, 2007). In wild type *S. pombe* cells, a significant increase in *cdc18*⁺ mRNA transcript levels was observed following nitrogen replenishment. On the other hand, there was no significant increase in *cdc18*⁺ mRNA levels detected in *hip1Δ* cells following the addition of nitrogen. At all time points measured (except at G₀ and following 120 minutes), there was a significant difference between *cdc18*⁺ mRNA levels in the wild type and *hip1Δ* samples (Fig 5.15.A). *cdt1*⁺ mRNA levels were also measured in independent experiments. Following 90 minutes of nitrogen replenishment *cdt1*⁺ mRNA levels increased several fold in the wild type compared to the G₀ samples and while a small increase was also seen in *hip1Δ* cells, it was significantly lower than the induction seen in the wild type (Fig 5.15.B). Therefore, it appears that transcriptional induction of both *cdc18*⁺ and *cdt1*⁺ is compromised in *hip1Δ* cells. This suggests that HIRA is required for the induction of MBF-dependent genes upon re-entry into the cell cycle.

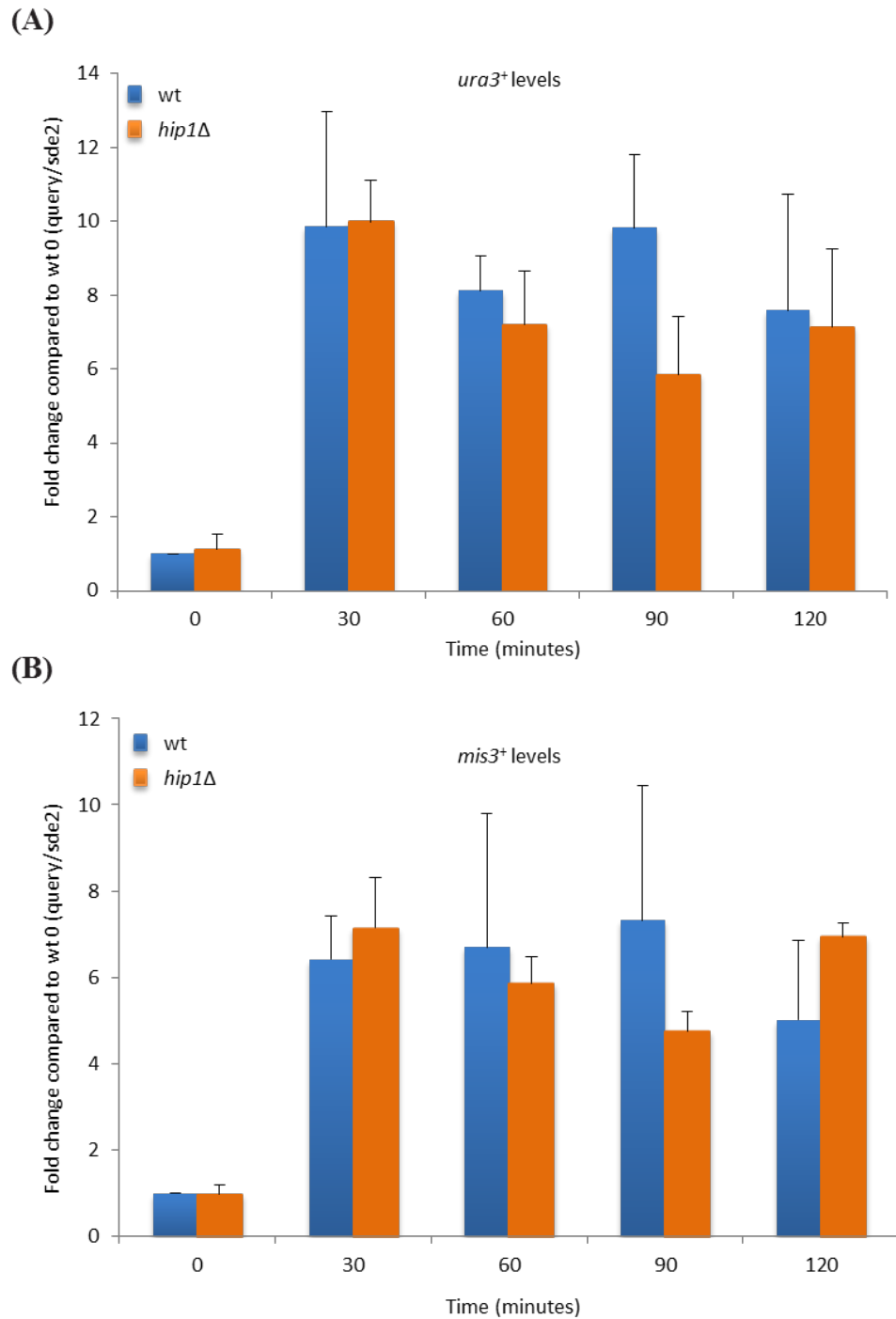


Figure 5.14 Transcriptional induction of growth genes is appropriate in *hip1*Δ cells following exit from G₀.

(A) and (B) qRT-PCR analysis of metabolic gene transcription in wild type and *hip1*Δ cells following nitrogen replenishment of G₀ cells starved for 24 hours. Data shown represents fold-change relative to the wild type time 0 samples. Data are the mean of four biological replicates and error bars represent \pm SEM.

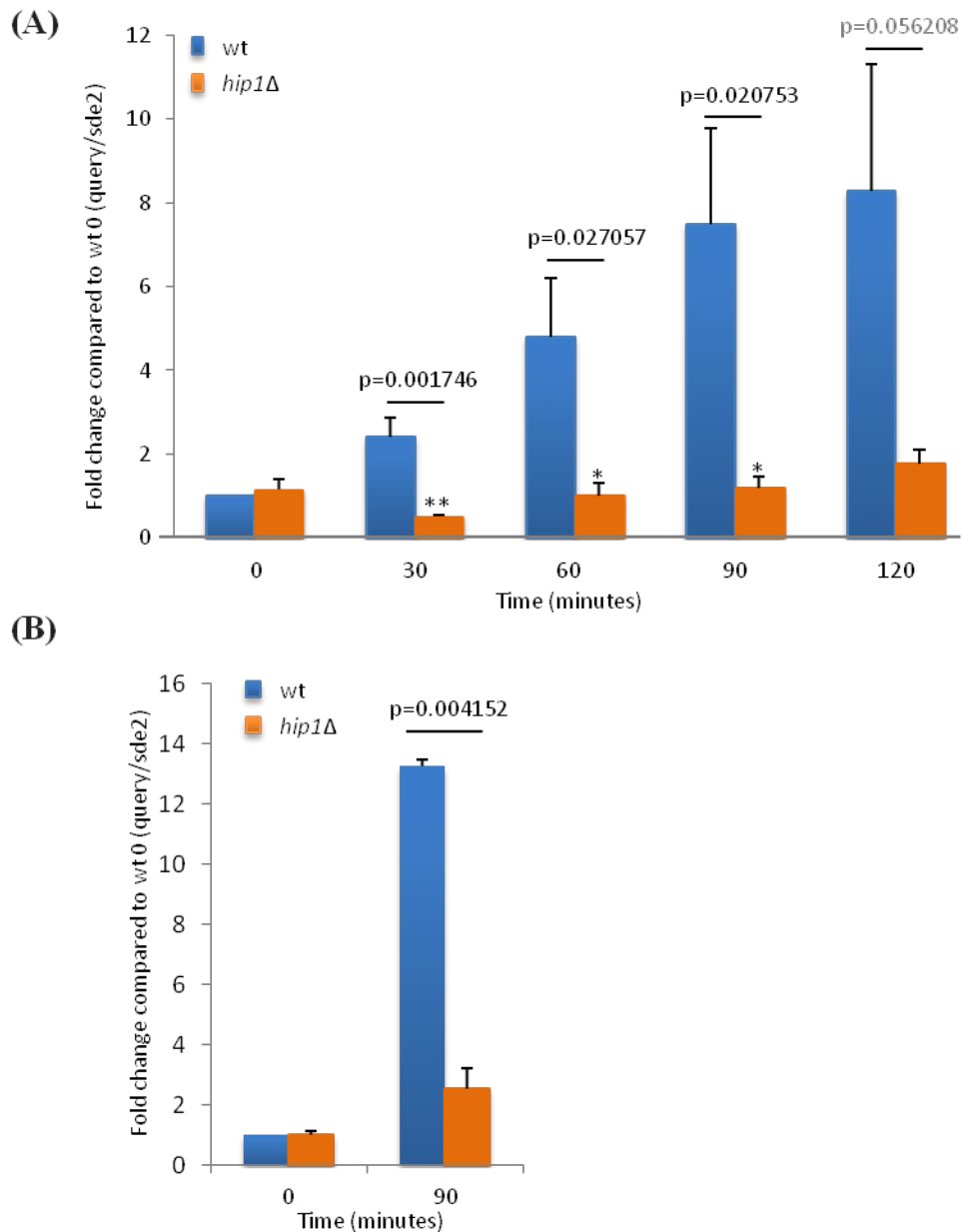


Figure 5.15 Transcriptional induction of *cdc18*⁺ and *cdt1*⁺ is compromised in *hip1*Δ cells following exit from G₀.

(A) qRT-PCR analysis of *cdc18*⁺ gene transcription in wild type and *hip1*Δ cells following nitrogen replenishment of G₀ cells starved for 24 hours. Data shown represents fold-change relative to the wild type time 0 sample. Data are the mean of six biological replicates and error bars represent ± SEM (* p<0.05; **p<0.01). (B) qRT-PCR analysis of *cdt1*⁺ gene transcription in wild type and *hip1*Δ cells following nitrogen replenishment of G₀ cells starved for 24 hours. Data shown represents fold-change relative to the wild type time 0 sample. Data are the mean of two biological replicates and error bars represent ± SEM (**p<0.01).

During quiescence the cyclin dependent kinase inhibitor Rum1 accumulates, blocking the cell cycle (Moreno and Nurse, 1994). Upon nitrogen replenishment, Rum1 is degraded, leading to the accumulation of the cyclin dependent kinase Cdc2, as well as to the downstream transcription and translation of the G₁/S-specific cyclin *cig2*⁺. Increased Cig2 levels help to usher the cells into S-phase (Mondesert *et al.*, 1996). In order to check that the above observed failure to induce *cdc18*⁺ transcription is not a result of the failure of *hip1Δ* cells to degrade Rum1, western blotting was utilized and Rum1 protein levels were measured. Rum1 was present at high levels during quiescence (24 hours), but as expected was degraded within hours following nitrogen replenishment (Shimanuki *et al.*, 2007). Indeed, Rum1 levels were completely undetectable following 3.5 hours in wild type samples (Fig 5.16.A). Rum1 was also degraded in *hip1Δ* cells at a comparable rate. Preliminary data (Fig 5.16.B) also indicates that Rum1 degradation is appropriate following 96 hours in quiescence. Therefore, not surprisingly, defects in the degradation of Rum1 or upstream events are unlikely to be responsible for the HIRA quiescence phenotype.

Next, Cig2 protein levels were measured. Cig2 is a G₁-S phase specific cyclin whose expression is also MBF dependent and is required for appropriate S phase transition (Mondesert *et al.*, 1996). It has previously been demonstrated that deletion of *cig2*⁺ leads to a delay in S phase following quiescence exit (Mondesert *et al.*, 1996), not unlike that seen in the absence of the HIRA complex (Blackwell *et al.*, 2004). Previous work has also demonstrated an inverse relationship between Rum1 and Cig2 levels (Shimanuki *et al.*, 2007); therefore Cig2 protein levels were also measured by western blotting. Agreeing with previous observations, Cig2 protein levels were undetectable during quiescence in both wild type and *hip1Δ* samples, with an increase following 1-2 hours of nitrogen replenishment in wild type cells. *hip1Δ* cells presented with increased Cig2 levels relative to G₀ levels but to a lesser degree than wild type cells (Fig 5.17.A). Preliminary data (Fig 5.17.B) also indicates that following 4 days in quiescence Cig2 levels are not induced in *hip1Δ* cells until 24 hours of nitrogen replenishment, whereas in wild type cells Cig2 induction takes place following 2-3.5 hours, suggesting a severe delay in cell cycle induction. Consequently, it seems highly likely that the HIRA complex is required for the appropriate induction of a subset of cell cycle regulated genes, and it is very possible that a proportion of the phenotypes associated with loss of HIRA are a result of the failure to re-start the transcription of these genes following quiescence.

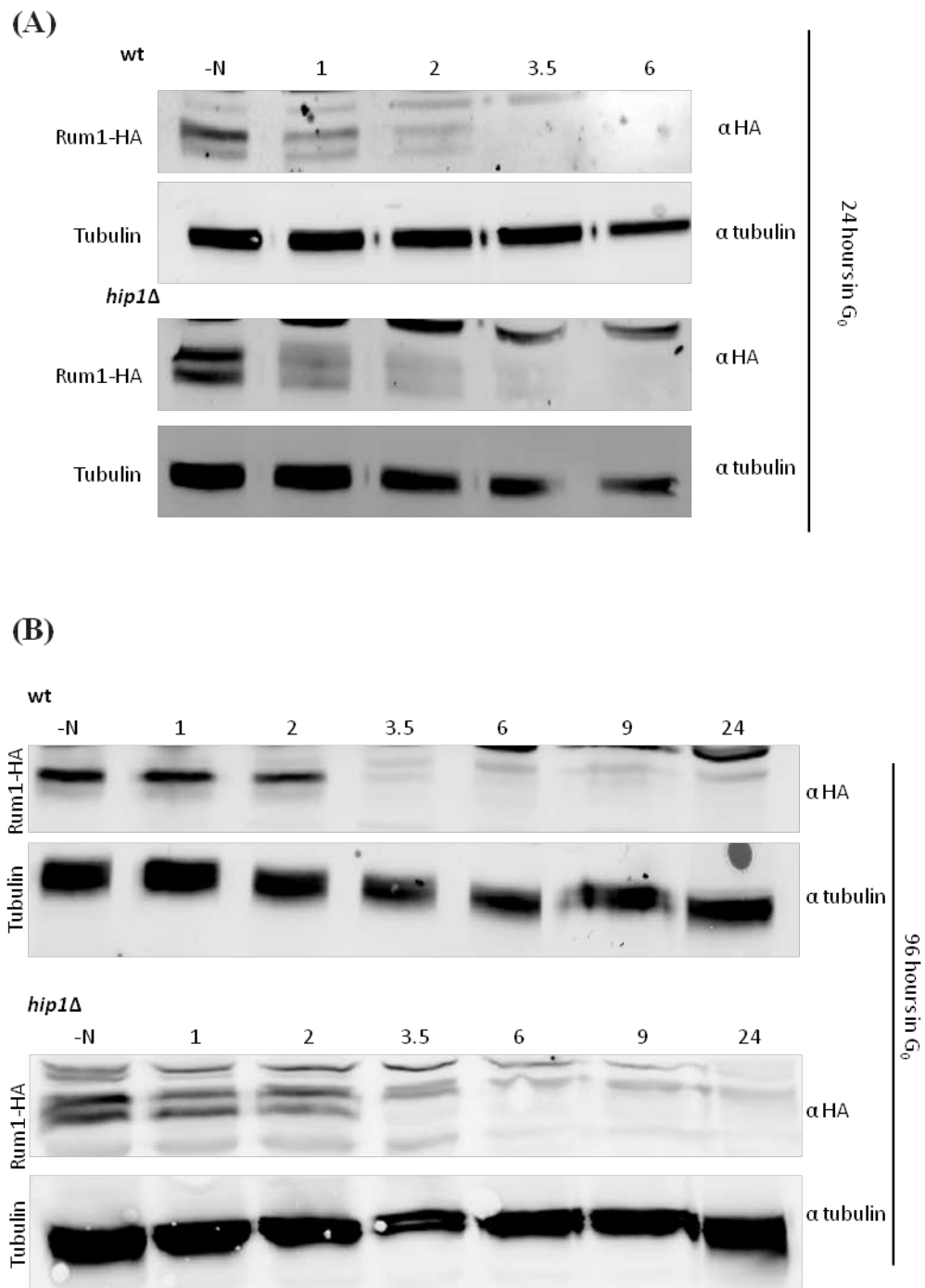


Figure 5.16 Rum1 protein levels are degraded both in wild type and *hip1Δ* cells at comparable rates.

(A) Western blot analysis of Rum1 protein levels in wild type and *hip1Δ* cells following exit from 24 hours in quiescence. Data is representative of three independent biological repeats. **(B)** Western blot analysis of Rum1 protein levels in wild type and *hip1Δ* cells following exit from 96 hours in quiescence. Data is of a single experiment.

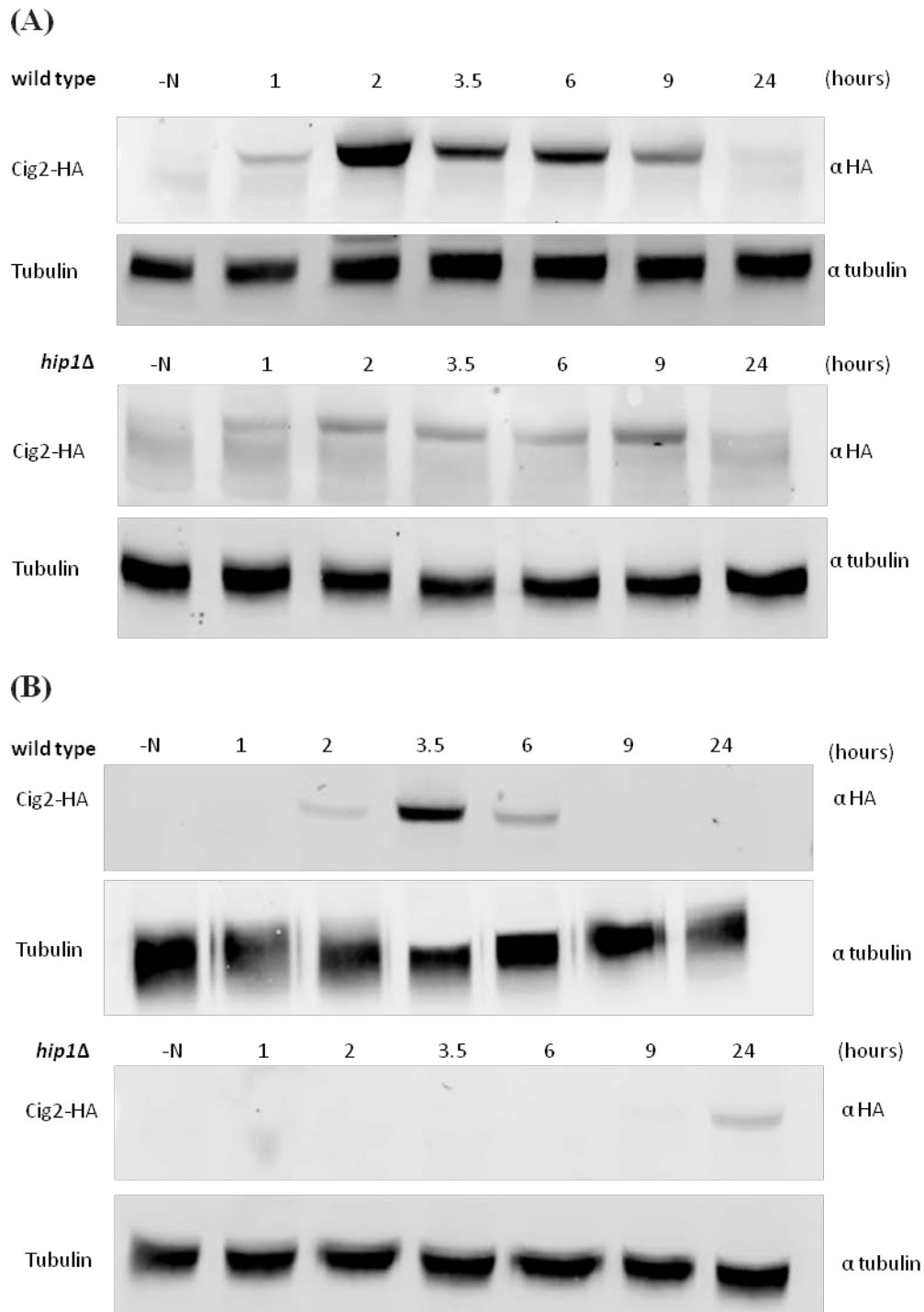


Figure 5.17 Cig2 protein levels are induced to a lesser extent in *hip1* Δ cells than in the wild type.

(A) Western blot analysis of Cig2 protein levels in wild type and *hip1* Δ cells following exit from 24 hours in quiescence. Data is representative of four independent biological repeats. **(B)** Western blot analysis of Cig2 protein levels in wild type and *hip1* Δ cells following exit from 96 hours in quiescence. Data is of a single experiment.

5.3 Discussion

The findings described in this chapter demonstrate a role for the *S. pombe* HIRA complex in the maintenance of nitrogen starvation induced quiescence. Previous work has noted that loss of HIRA subunits leads to a delay in re-entry into the cell cycle following nitrogen depletion as indicated by FACS analysis (Blackwell *et al.*, 2004), but the basis of this remained unexplained. Here is some evidence demonstrating that HIRA deficient cells are severely compromised in their ability to re-enter the cell cycle following quiescence. This is likely to be due to two things; first cells lacking HIRA fail to appropriately induce MBF-dependent genes upon nitrogen replenishment from early G₀, and second these cells are likely entering premature senescence rapidly following G₀ entry. Previous work has characterized a number of mutants that are sensitive to nitrogen starvation induced quiescence, however it should be noted that the *hip1Δ* phenotype is extremely severe.

5.3.1 HIRA deficient cells are unlikely to age rapidly due to a simple reduction in histone levels

One of the key findings in this chapter was that HIRA deficient cells age rapidly upon quiescence entry and apparently enter a permanent senescent state within days. Previous work has demonstrated that reduced histone levels are associated with aging phenotypes, while an increase in histone dosage can lead to life-span extension (Feser *et al.*, 2010). During normal replicative aging in budding yeast, histone transcript levels increase while a drop in histone protein levels is observed. Mutation of the histone chaperone *ASF1* leads to a decrease in histone transcription and histone protein levels and cells age rapidly, while deletion of *HIR1* in *S. cerevisiae* increases both histone mRNA and protein level, and leads to life-span extension (Feser *et al.*, 2010). In light of these results and due to the finding that in *S. pombe* *hip1Δ* cells present with a decrease in both histone H3 protein levels and a drop in nucleosome occupancy, the contribution of histones to the aging phenotype was addressed. Histone H3-H4 gene pairs are encoded by three highly similar genes and two pairs were knocked out in combination and their viability in quiescence was assessed. Surprisingly, it did not appear that loss of two histone H3-H4 gene pairs phenocopied the *hip1Δ* quiescence phenotype, suggesting that while low histone content might contribute to aging, in quiescent *S. pombe* at least, it is not the major determinant in cellular senescence. Also in support of this is the fact that other histone chaperones did not have the same phenotype as HIRA mutants, in fact

loss of the CAF1 subunit, *cac2*⁺, or deletion of *nap1*⁺ and *nap2*⁺ had no obvious effect on cell viability, suggesting that the role of the HIRA complex in quiescence maintenance is more specific than just its ability to maintain histone protein levels. However, it still would be beneficial to investigate whether increasing histone dosage in *hip1*Δ cells helps to rescue the quiescence phenotype at all.

5.3.2 Role for the HIRA complex in regulating MBF genes

A surprising but interesting finding of this work was that loss of *hip1*⁺ did not affect the majority of molecular functions tested, for example Rum1 degradation was normal and so was the induction of growth/metabolism specific genes following nitrogen replenishment after 24 hours in quiescence. However, the HIRA complex is required for the timely induction of at least three MBF-dependent genes; *cdc18*⁺, *cdt1*⁺ and *cig2*⁺. Although the HIRA complex is generally thought of as a repressor of transcription, previous work in *S. pombe* has demonstrated that under specific contexts it is also required for gene activation, for example during low dose stress responses (Chujo *et al.*, 2012). HIRA has also been associated with a cell cycle regulatory role, as it plays a role in S-phase specific regulation of the core histone genes (Blackwell *et al.*, 2004); furthermore HIRA itself gets phosphorylated in a cell-cycle specific manner (Hall *et al.*, 2001) in human cell cultures by a cyclin-Cdk2 kinase (either cyclin A or cyclin E). As expected, this phosphorylation event is confined to cycling cells, as quiescent cells are not phosphorylated (Hall *et al.*, 2001), and, importantly, it coincides with late G₁ to S phase entry (Hall *et al.*, 2001). Moreover, ectopic expression of HIRA leads to S phase arrest, suggesting that the HIRA complex is responsible for progression through S phase (Hall *et al.*, 2001). These findings also agree with the work presented here, which suggests that exit following 24 hours in quiescence is largely but not completely dependent on the HIRA complex. The fact that S phase specific genes are delayed in expression and those HIRA deficient cells still elongate and enter S phase, but then arrest coincide with these previous findings. What is interesting is that *hip1*Δ cells are slightly delayed going through S phase in cycling cells but are viable, while this is not the case following extended periods in quiescence. This strongly suggests that there is a switch in the mechanism behind gene induction and cell cycle regulation following quiescence. However, as to what this may be or how it might be established is currently unknown. It is possible that the HIRA complex is directly involved in activating transcription of *cdc18*⁺, *cdt1*⁺ and *cig2*⁺ possibly by remodelling the nucleosomes

around the promoter regions. It has however not been possible to measure whether this is the case. Hip1-GFP ChIP-qPCR has been carried out over the MCB box of *cdc18*⁺ but there was only a relatively small enrichment to start with that did not increase upon nitrogen replenishment. It is of course possible that HIRA primes these regions but the remodelling event is rapid, and the interaction between HIRA and the chromatin is transient. However, in order to properly address whether HIRA is physically required around these regions it would be essential to optimize the ChIP protocol for components of the HIRA complex. Unfortunately, due to time constraints it was not possible to complete the experiments. An additional way to address whether HIRA plays a role in nucleosome remodelling around these regions would be to generate a nucleosome map of wild type and *hip1Δ* cells in quiescence and following nitrogen replenishment (15-30 minutes) when rapid remodelling is most likely to take place. Alternatively, it would be possible to implement the MNase-qPCR technique to generate a view of a single nucleosome; in this case that would be the nucleosome over the MSB box of *cdc18*⁺ or *cdt1*⁺.

5.3.3 Attempts to isolate suppressor mutations

It could also be useful to determine whether over-expression of *cdc18*⁺, *cdt1*⁺ or a downstream target, like *cig2*⁺, is sufficient to rescue the quiescence phenotype of *hip1Δ* cells. A strain constitutively expressing *cdc18*⁺, *cdc10-4* was crossed with *hip1Δ* to help determine whether this was the case. However, the *cdc10-c4* strain is very slow growing and therefore meaningful analysis of *hip1Δ cdc10-c4* was not possible. It would be more appropriate to perhaps place *cig2*⁺ under an inducible promoter and only express it during the required times. Current work is being carried out to determine whether deleting negative regulators of the MBF genes, *yox1*⁺ and *nrm1*⁺, are able to rescue the HIRA quiescence phenotype.

Another possibility for future work could involve testing a library of deletion mutants to identify knockout alleles that rescue *hip1Δ* cells. Throughout this study a number of genes have been crossed with the *hip1Δ* mutant strain to generate double mutants, which have been tested for quiescence viability. These included *rad3Δ*, *gcn5Δ*, *rtt109Δ*, *abo1Δ* and *abo2Δ*, some of which have previously been indicated to rescue the *hip1Δ* mutant to a degree; however throughout this study *abo1Δ* was the only gene deletion that partially rescued *hip1Δ* viability (Fig 5.18.A, B and C). The basis of this partial

rescue is currently unknown but it hints at a role for Abo1 in quiescence maintenance too, or perhaps suggests that the HIRA complex is important in preventing Abo1 from carrying out certain functions. Due to time constraints it was not possible to follow up this genetic interaction, but it would be interesting to learn more about the function of Abo1 in *hip1* Δ cells and to determine the molecular basis of this rescue.

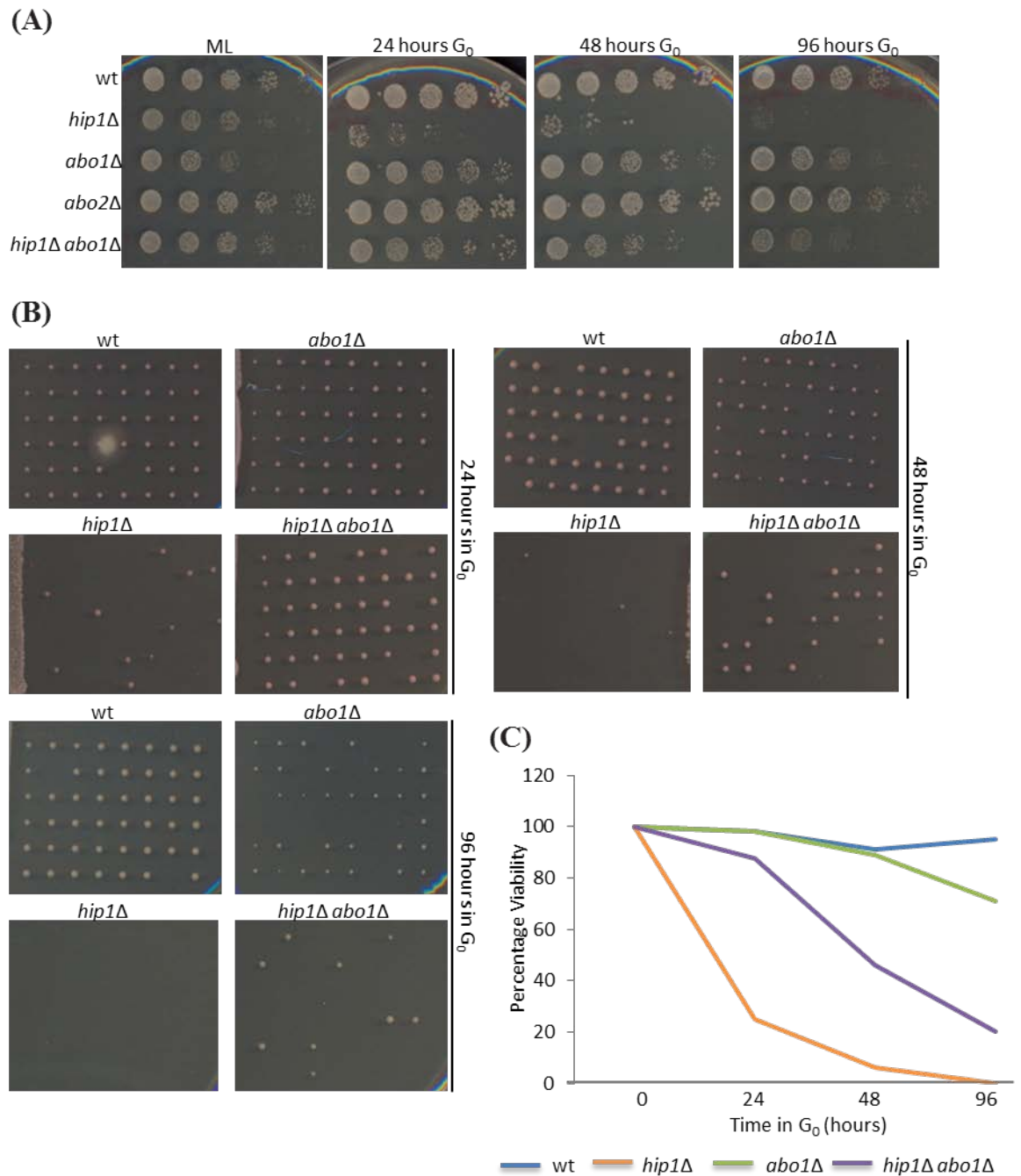


Figure 5.18 Deletion of $abo1^+$ partially rescues $hip1\Delta$ cells in quiescence.

(A) Spot tests of the indicated strains during midlog phase and at the specified times in quiescence at 30°C onto YE5S plates following a 5-fold serial dilution. Plates were further incubated at 30°C for 3 nights. (B) Individual dissections of cells onto YE5S plates during mid-log phase and following 24, 48 and 96 hours in quiescence. Cells were grown at 30°C until colonies were visible. Data is representative of four independent biological replicates. (C) Percentage viability of cells in (B).

5.3.4 HIRA and senescence

In human cells, it has previously been demonstrated that the HIRA complex is also required during senescence (Zhang *et al.*, 2005; Ye *et al.*, 2007; Zhang *et al.*, 2007b; Banumathy *et al.*, 2009). Therefore it is possible that perhaps in *S. pombe*, cells in the absence of the HIRA complex become prematurely senescent. Senescent cells by definition do not enter the cell cycle. Of course whether senescence establishment would be through a direct role of the HIRA complex, i.e. it is actively required to determine quiescence vs senescence or whether HIRA deficient cells are purely deemed too sick to proliferate and so enter senescence as an alternative path is currently not known. Interestingly, recent work has demonstrated that old yeast cells present with an overall nucleosome depleted genome and that the nucleosomes particularly affected are within overwhelmingly silenced or low level transcribed regions (Hu *et al.*, 2014). These findings are strikingly similar to the MNase-seq profiles of *hip1Δ* cells; therefore it is possible that *hip1Δ* cells are generally ‘aged’ and enter quiescence as old cells. Should this be the case further nucleosome loss would be expected along with a continuous increase in mRNA levels. Although MNase digestions of bulk chromatin did not reveal a difference between wild type and *hip1Δ* cells, it is possible that MNase-seq following 24 and 96 hours in quiescence would find a further drop in nucleosome occupancy compared to cycling cells.

In tissue cultures a feature of senescent cells is the down regulation of E2F genes via creation of a heterochromatic environment that includes the recruitment of the retinoblastoma protein (Rb), loss of histone H3 acetylation and an increase in histone H3K9 methylation (Adams, 2007). This recruits HP1 and macroH2A. HIRA and Asf1 have been shown to be required for this process, possibly by removing histone H3-H4 and allowing the incorporation of macroH2A (Zhang *et al.*, 2005; Zhang *et al.*, 2007b; Banumathy *et al.*, 2009). In *S. pombe* a point mutation in the HIRA subunit *hip3*⁺, *hip3-1*, leads to a global increase in histone H3K9me3 levels, a hallmark of heterochromatin (Mizuki *et al.*, 2011). In addition, senescence is often thought to be triggered by DNA damage in cells (Toussaint *et al.*, 2000; Campisi, 2001; Campisi and d'Adda di Fagagna, 2007), and indeed *hip1Δ* mutants enter quiescence with unrepaired DSBs. Also important is that senescent cells remain metabolically active (Di Leonardo *et al.*, 1994; Ogryzko *et al.*, 1996; Serrano *et al.*, 1997; Herbig *et al.*, 2004), although they lose their proliferating potential, as is the case in *hip1Δ* mutants. It might be possible to determine

whether these cells are truly senescent by searching for markers that are conserved between organisms. Furthermore, if *hip1Δ* cells become senescent then controlled over-expression of MBF genes should not be able to rescue the quiescent phenotype following 96 hours. Finally, if these cells indeed just enter senescence prematurely, than mutants that rescue the *hip1Δ* quiescence phenotype might be those that prevent cells from entering into senescence in the first place.

Therefore there are two arguments, which are likely to not be mutually exclusive, that suggest that the HIRA complex plays a role in gene activation following quiescence and that in the absence of the complex senescence is prematurely triggered. If HIRA was only required for re-entry into the cell cycle then one would expect to see an initial drop in cell viability but would not expect that drop to further increase as a function of time, while if the cells become senescent then the number of cells unable to re-enter the cell cycle would increase over time, which is what has been observed in *hip1Δ* cells. It could therefore be postulated that the HIRA complex functions in two different steps, firstly it is amongst the factors required for S-phase specific gene activation, a function that might become prominent during quiescence exit and it is also required for appropriate maintenance of quiescence, possibly through a contribution to chromatin maintenance.

Chapter 6

General Discussion

Proper chromatin maintenance is important in all eukaryotes, as a compromised chromatin structure can lead to highly toxic environments with deregulated transcription, an increase in inter- and intra-chromosomal translocations, and an increase in DNA double strand breaks. All of these alterations lead to unstable genomes, which become highly prone to uncontrolled proliferation and tumour development; in fact genomic instability is the hallmark of cancer. As a consequence of this, proteins that can modulate or alter chromatin structure have long been of interest. Amongst these are ATP-dependent remodelers, histone chaperones, and covalent modifiers of histones.

6.1 Abo1 – A regulator of global chromatin architecture

ATAD2/Yta7 belong to the AAA-ATPase family of proteins, which until recently have been thought of as molecular motors, whose primary function is in protein degradation. ATAD2/Yta7 are unique in that they can directly interact with chromatin and contain a bromodomain, which is traditionally associated with the ability to bind acetylated lysines. While, there is generally a lot of interest in chromatin modifiers, the role of ATAD2/Yta7 to date has not been well characterized. The study presented here aimed to address whether the *S. pombe* homologue, Abo1, has a role in global chromatin maintenance. Indeed, it was possible to demonstrate that Abo1 is necessary for proper nucleosome maintenance, over both eu- and heterochromatic regions. The data suggests that Abo1 facilitates either the stability of nucleosomes during Pol II passage or it plays a role in the re-assembly of any partially/fully disassembled nucleosomes. However, based on the current data available, it is not yet possible to distinguish between the two. It will therefore be important to determine whether Abo1 has *in vitro* nucleosome assembly activity and whether this is dependent upon the AAA-ATPase and bromodomain regions.

It would also be interesting to determine whether the Abo1-FACT interaction is conserved in mammalian cells. FACT is currently a drug target in cancers (Gasparian *et al.*, 2011), therefore determining the nature of the interaction in mammalian cells could be beneficial in drug targeting, perhaps drugs designed to deactivate FACT could also

work on cancers with upregulated ATAD2 levels, and/or vice versa.

There remain a number of further outstanding questions with regards to the regulation of Abo1 itself. For example, Abo1 appears to be removed from the chromatin following replication arrest, which happens to coincide with phosphorylation of Abo1 (by Rad3 and Cds1) (A. J. Whale, personal communications). This is also conserved, as *S. cerevisiae* Yta7 gets phosphorylated by Rad53 (Smolka *et al.*, 2005). Abo1 is also phosphorylated during the cell cycle, and similarly to *S. cerevisiae* it is also phosphorylated by CK2 (A. J. Whale, personal communications) (Kurat *et al.*, 2011). Therefore, determining whether this is conserved in mammalian cells, and if so, then understanding the specific role of these phosphorylation events is likely to be key in the full understanding of Abo1 function. As there have been suggestions that phosphorylation of Yta7/ATAD2 leads to its removal from its target sites, it would be valuable to determine whether this is a general mechanism for controlling ATAD2/Abo1/Yta7 levels and if so then perhaps this mechanism could be exploited in order to reduce ATAD2 binding to its target loci during tumorigenesis.

6.2 Transcription through chromatin

As a result of the link between HIRA and transcriptional control, in this study, the role of HIRA on global chromatin architecture was assessed. It was demonstrated, in agreement with previously attributed functions, that HIRA plays a role in maintaining nucleosome occupancy following transcription, thereby contributing to proper chromatin architecture. In the absence of functional HIRA, global histone H3 protein levels are decreased, overall transcription is increased and the genomes become highly sensitive to DNA damaging agents. *S. pombe* lacking HIRA function present with strong phenotypes that are typically linked to severely compromised chromatin. Yet, sequencing of chromatin revealed only relatively mild changes on a global scale. This could be interpreted to suggest that either HIRA is important at a few sites, where deregulation of transcription leads to the phenotypes associated with cells lacking HIRA, or that it is through small but numerous alterations throughout the genome that add up to compromise chromatin integrity. It would be interesting to determine whether the role for HIRA over transcriptionally active regions is conserved. At this time, there isn't a global nucleosome map available of *HIRA* knockdown mammalian cells, which

could be highly informative.

New evidence is emerging that nucleosomes do not get disassembled during transcription, rather remain as stable but dynamic structures, with only the H2A-H2B dimers removed/remodelled. It is therefore possible that the contributions of H3-H4 histone chaperones like HIRA are only required in the case of the small number of nucleosomes which get completely disassembled. There also appears to be tremendous redundancy amongst chromatin proteins, and so it is also possible that HIRA becomes particularly important when another chromatin protein becomes compromised. Finally, evidence from this study and from others suggests that HIRA becomes critical when transcription is severely perturbed and nucleosomal arrays need to be re-set. Such is the case following DNA damage repair, senescence entry, and quiescence exit, as all of these processes require large-scale remodelling of chromatin.

6.3 HIRA and the DNA damage response pathway

As DNA double strand breaks (DSBs) are highly genotoxic lesions and cells lacking HIRA function are strikingly sensitive to a wide range of DNA damaging agents, the role HIRA plays during the DNA damage response pathway was investigated. It was possible to demonstrate that HIRA, similarly to the CAF-1 histone chaperone, functions independently of the major DSB repair and checkpoint pathways, and that it is likely to exert its role following repair completion. The study presented here illustrates the importance of HIRA during recovery following DNA damage repair, which goes beyond protecting from the genotoxic agents themselves. It has become increasingly clear that HIRA, like other histone chaperones, is essential for the re-start of the cell cycle following arrest and that this is likely through a role in nucleosome assembly over the affected regions, priming the cells for transcriptional restart (Adam *et al.*, 2013; Polo, 2014). This role appears highly conserved, as cells from *S. cerevisiae* to humans lacking HIRA, are sensitive to agents that cause DNA strand breaks. It would be interesting to determine the signals that recruit HIRA to DNA strand breaks, is it simply the presence of naked DNA, or does it, like Asf1, physically associate with some/any of the repair/checkpoint proteins. It would also be interesting to establish whether cells lacking HIRA are able to replace nucleosomes following DNA damage repair in *S. pombe*, for example is CAF-1 able to do this? Could CAF-1 in co-operation with Asf1, Rtt106, and Spt6 be able to deposit H3-H4 tetramers over the repaired lesions, and if so

than what is the role of HIRA that makes it essential for proper recovery? In mammalian cells, it is the ability of HIRA to establish transcriptionally competent chromatin by depositing the histone variant H3.3, but in *S. pombe* no variants of H3 exists, therefore the question remains how does HIRA do this? There is an example in *S. cerevisiae* where FACT and Spt6 are required for the disassembly of the *CLN3* promoter nucleosome, which is required for the START of the cell cycle (Morillo-Huesca *et al.*, 2010). Our findings, which suggest that HIRA is required for the proper induction of *cdc18*⁺, *cdt1*⁺ and *cig2*⁺ following quiescence exit, might also be true for the re-start of the cell cycle following arrest after DNA damage. Should this be the case, then perhaps examining the state of specific nucleosomes could prove to be informative.

6.4 Restart of the cell cycle following quiescence by HIRA

In addition to a role in the DNA damage response pathway, HIRA was found to be sensitive to quiescence arrest. In complex multi-cellular organisms, the majority of differentiated cells, as well as stem cells, spend their life in a quiescent state. Loss of quiescence maintenance can either lead to uncontrolled proliferation, therefore tumorigenesis or to cellular senescence, which is associated with premature aging. In light of the importance of the quiescent state, the mechanism behind quiescence maintenance by HIRA was assessed. Cells lacking HIRA were strikingly sensitive to quiescence and undergo premature senescence within the fraction of the time of the wild type strain. It was possible to demonstrate that HIRA fulfils two key functions during this state; firstly it is required for efficient re-entry into the proliferative cell cycle probably via transcriptional induction of MBF-dependent genes, and secondly it is responsible for preventing the cells from entering senescence. The mechanism behind this second role is still unclear. Its role in the regulation of MBF-dependent genes could be through recruiting factors necessary for transcription initiation or could be by disassembling promoter nucleosomes, thereby creating a permissive environment for binding of MBF transcription factors. However, to date there has been no direct *in vitro* evidence demonstrating that HIRA can disassemble nucleosomes. In mammalian cells it is thought to lead to gene activation by incorporating the histone H3.3 variant, which is more permissible for transcription than other variants. Therefore, addressing this question further could be very exciting and could lead to uncovering a novel role for HIRA.

It would also be interesting to determine the overarching roles of histone chaperones during cell cycle progression. The repression/activation of histone gene expression in *S. cerevisiae* for instance is controlled at the level of promoter assembly/disassembly by a number of factors (Figures 1.9 and 1.15), is it possible that other cell cycle specific genes are regulated in a similar manner? If that is the case, then are the same group of proteins involved? During the course of this work, the effect of loss of *abo1*⁺, *asf1*⁺ and *rtt106*⁺ was determined on quiescence viability. Of the three, loss of *asf1*⁺ presented with severe phenotypes, comparable to that of cells lacking HIRA, while *abo1*Δ cells presented with mild sensitivity to quiescence and *rtt106*Δ mutants grew similarly to wild type. This question therefore remains open, but it wouldn't be entirely surprising if further work on the subject identified a number of chromatin maintenance factors as being required for the proper re-entry into the vegetative cell cycle following quiescence. The question also remains as to whether this is a conserved process. In mammalian cells HIRA primarily localizes to promoter regions and enhancers, and its role in generating a transcriptionally permissive environment is conserved. However, similarly to findings in yeast, a recent study using tissue culture has found that HIRA does not modulate all promoters to the same extent; rather its role in activation is highly specific (Soni *et al.*, 2014). As to what determines this specificity remains unclear and could be of interest for future work.

References

- Adam, M., Robert, F., Larochelle, M. and Gaudreau, L. (2001) 'H2A.Z Is Required for Global Chromatin Integrity and for Recruitment of RNA Polymerase II under Specific Conditions', *Molecular and Cellular Biology*, 21(18), pp. 6270-6279.
- Adam, S., Polo, Sophie E. and Almouzni, G. (2013) 'Transcription Recovery after DNA Damage Requires Chromatin Priming by the H3.3 Histone Chaperone HIRA', *Cell*, 155(1), pp. 94-106.
- Adams, P.D. (2007) 'Remodeling of chromatin structure in senescent cells and its potential impact on tumor suppression and aging', *Gene*, 397(1-2), pp. 84-93.
- Adkins, M.W., Howar, S.R. and Tyler, J.K. (2004) 'Chromatin Disassembly Mediated by the Histone Chaperone Asf1 Is Essential for Transcriptional Activation of the Yeast *PHO5* and *PHO8* Genes', *Molecular Cell*, 14(5), pp. 657-666.
- Adkins, M.W. and Tyler, J.K. (2006) 'Transcriptional Activators Are Dispensable for Transcription in the Absence of Spt6-Mediated Chromatin Reassembly of Promoter Regions', *Molecular Cell*, 21(3), pp. 405-416.
- Akhmanova, A., Miedema, K. and Hennig, W. (1996) 'Identification and characterization of the *Drosophila* histone H4 replacement gene', *FEBS Letters*, 388(2-3), pp. 219-222.
- Amin, A.D., Vishnoi, N. and Prochasson, P. (2012) 'A global requirement for the HIR complex in the assembly of chromatin', *Biochimica et Biophysica Acta (BBA) - Gene Regulatory Mechanisms*, 1819(3-4), pp. 264-276.
- Anderson, H.E., Kagansky, A., Wardle, J., Rappsilber, J., Allshire, R.C. and Whitehall, S.K. (2010) 'Silencing Mediated by the *Schizosaccharomyces pombe* HIRA Complex Is Dependent upon the Hpc2-Like Protein, Hip4', *PLoS ONE*, 5(10), p. e13488.
- Anderson, H.E., Wardle, J., Korkut, Ş.V., Murton, H.E., López-Maury, L., Bähler, J. and Whitehall, S.K. (2009) 'The Fission Yeast HIRA Histone Chaperone Is Required for Promoter Silencing and the Suppression of Cryptic Antisense Transcripts', *Molecular and Cellular Biology*, 29(18), pp. 5158-5167.
- Ardehali, M.B., Mei, A., Zobeck, K.L., Caron, M., Lis, J.T. and Kusch, T. (2011) '*Drosophila* Set1 is the major histone H3 lysine 4 trimethyltransferase with role in transcription', *EMBO J*, 30(14), pp. 2817-28.
- Armstrong, J.A., Papoulas, O., Daubresse, G., Sperling, A.S., Lis, J.T., Scott, M.P. and Tamkun, J.W. (2002) 'The *Drosophila* BRM complex facilitates global transcription by RNA polymerase II', *EMBO J*, 21(19), pp. 5245-5254.
- Askree, S.H., Yehuda, T., Smolikov, S., Gurevich, R., Hawk, J., Coker, C., Krauskopf, A., Kupiec, M. and McEachern, M.J. (2004) 'A genome-wide screen for *Saccharomyces cerevisiae* deletion mutants that affect telomere length', *Proceedings of the National Academy of Sciences of the United States of America*, 101(23), pp. 8658-8663.
- Baber-Furnari, B.A., Rhind, N., Boddy, M.N., Shanahan, P., Lopez-Girona, A. and Russell, P. (2000) 'Regulation of Mitotic Inhibitor Mik1 Helps to Enforce the DNA Damage Checkpoint', *Molecular Biology of the Cell*, 11(1), pp. 1-11.
- Badenhorst, P., Voas, M., Rebay, I. and Wu, C. (2002) 'Biological functions of the ISWI chromatin remodeling complex NURF', *Genes & Development*, 16(24), pp. 3186-3198.
- Balaji, S., Iyer, L.M. and Aravind, L. (2009) 'HPC2 and Ubinuclein define a novel family of histone chaperones conserved throughout eukaryotes', *Molecular BioSystems*, 5(3), pp. 269-275.
- Banaszynski, Laura A., Wen, D., Dewell, S., Whitcomb, Sarah J., Lin, M., Diaz, N., Elsässer, Simon J., Chapgier, A., Goldberg, Aaron D., Canaani, E., Rafii, S., Zheng, D. and Allis, C.D. (2013) 'Hira-Dependent Histone H3.3 Deposition Facilitates PRC2 Recruitment at Developmental Loci in ES Cells', *Cell*, 155(1), pp. 107-120.

- Bannister, A.J. and Kouzarides, T. (2011) 'Regulation of chromatin by histone modifications', *Cell Res*, 21(3), pp. 381-395.
- Banumathy, G., Somaiah, N., Zhang, R., Tang, Y., Hoffmann, J., Andrade, M., Ceulemans, H., Schultz, D., Marmorstein, R. and Adams, P.D. (2009) 'Human UBN1 Is an Ortholog of Yeast Hpc2p and Has an Essential Role in the HIRA/ASF1a Chromatin-Remodeling Pathway in Senescent Cells', *Molecular and Cellular Biology*, 29(3), pp. 758-770.
- Bar-Nun, S. and Glickman, M.H. (2012) 'Proteasomal AAA-ATPases: Structure and function', *Biochimica et Biophysica Acta (BBA) - Molecular Cell Research*, 1823(1), pp. 67-82.
- Barbet, N., Muriel, W.J. and Carr, A.M. (1992) 'Versatile shuttle vectors and genomic libraries for use with *Schizosaccharomyces pombe*', *Gene*, 114(1), pp. 59-66.
- Barski, A., Cuddapah, S., Cui, K., Roh, T.-Y., Schones, D.E., Wang, Z., Wei, G., Chepelev, I. and Zhao, K. (2007) 'High-Resolution Profiling of Histone Methylations in the Human Genome', *Cell*, 129(4), pp. 823-837.
- Batta, K., Zhang, Z., Yen, K., Goffman, D.B. and Pugh, B.F. (2011) 'Genome-wide function of H2B ubiquitylation in promoter and genic regions', *Genes Dev*, 25(21), pp. 2254-65.
- Belotserkovskaya, R., Oh, S., Bondarenko, V.A., Orphanides, G., Studitsky, V.M. and Reinberg, D. (2003) 'FACT Facilitates Transcription-Dependent Nucleosome Alteration', *Science*, 301(5636), pp. 1090-1093.
- Ben-Porath, I., Thomson, M.W., Carey, V.J., Ge, R., Bell, G.W., Regev, A. and Weinberg, R.A. (2008) 'An embryonic stem cell-like gene expression signature in poorly differentiated aggressive human tumors', *Nat Genet*, 40(5), pp. 499-507.
- Ben Hassine, S. and Arcangeli, B. (2009) 'Tdp1 protects against oxidative DNA damage in non-dividing fission yeast', *EMBO J*, 28(6), pp. 632-640.
- Benson, E.K., Zhao, B., Sassoon, D.A., Lee, S.W. and Aaronson, S.A. (2009) 'Effects of p21 deletion in mouse models of premature aging', *Cell Cycle*, 8(13), pp. 2002-2004.
- Berkovich, E., Monnat, R.J. and Kastan, M.B. (2007) 'Roles of ATM and NBS1 in chromatin structure modulation and DNA double-strand break repair', *Nat Cell Biol*, 9(6), pp. 683-690.
- Bjerling, P., Silverstein, R.A., Thon, G., Caudy, A., Grewal, S., and Ekwall, K. (2002) 'Functional Divergence between Histone Deacetylases in Fission Yeast by Distinct Cellular Localization and In Vivo Specificity', *Mol. Cell. Biol.*, 22(7), pp. 2170-2181.
- Black, Joshua C., Van Rechem, C. and Whetstone, Johnathan R. (2012) 'Histone Lysine Methylation Dynamics: Establishment, Regulation, and Biological Impact', *Molecular Cell*, 48(4), pp. 491-507.
- Blackledge, N.P., Farcas, A.M., Kondo, T., King, H.W., McGouran, J.F., Hanssen, L.L., Ito, S., Cooper, S., Kondo, K., Koseki, Y., Ishikura, T., Long, H.K., Sheahan, T.W., Brockdorff, N., Kessler, B.M., Koseki, H. and Klose, R.J. (2014) 'Variant PRC1 complex-dependent H2A ubiquitylation drives PRC2 recruitment and polycomb domain formation', *Cell*, 157(6), pp. 1445-59.
- Blackwell, C., Martin, K.A., Greenall, A., Pidoux, A., Allshire, R.C. and Whitehall, S.K. (2004) 'The *Schizosaccharomyces pombe* HIRA-Like Protein Hip1 Is Required for the Periodic Expression of Histone Genes and Contributes to the Function of Complex Centromeres', *Molecular and Cellular Biology*, 24(10), pp. 4309-4320.
- Blagosklonny, M.V. (2011) 'Cell cycle arrest is not senescence', *Aging (Albany NY)*, 3(2), pp. 94-101.
- Blanpain, C., Lowry, W.E., Geoghegan, A., Polak, L. and Fuchs, E. (2004) 'Self-Renewal, Multipotency, and the Existence of Two Cell Populations within an Epithelial Stem Cell Niche', *Cell*, 118(5), pp. 635-648.
- Boddy, M.N., Furnari, B., Mondesert, O. and Russell, P. (1998) 'Replication Checkpoint

Enforced by Kinases Cds1 and Chk1', *Science*, 280(5365), pp. 909-912.

Boe, C.A., Garcia, I., Pai, C.C., Sharom, J.R., Skjölberg, H.C., Boye, E., Kearsey, S., Macneill, S.A., Tyers, M.D. and Grallert, B. (2008) 'Rapid regulation of protein activity in fission yeast', *BMC Cell Biol*, 9, p. 23.

Bonnefoy, E., Orsi, G.A., Couble, P. and Loppin, B. (2007) 'The Essential Role of *Drosophila* HIRA for *De Novo* Assembly of Paternal Chromatin at Fertilization', *PLoS Genet*, 3(10), p. e182.

Boussouar, F., Jamshidikia, M., Morozumi, Y., Rousseaux, S. and Khochbin, S. (2013) 'Malignant genome reprogramming by ATAD2', *Biochimica et Biophysica Acta (BBA) - Gene Regulatory Mechanisms*, 1829(10), pp. 1010-1014.

Bowen, N.J., Jordan, I.K., Epstein, J.A., Wood, V. and Levin, H.L. (2003) 'Retrotransposons and Their Recognition of Pol II Promoters: A Comprehensive Survey of the Transposable Elements From the Complete Genome Sequence of *Schizosaccharomyces pombe*', *Genome Research*, 13(9), pp. 1984-1997.

Braig, M. and Schmitt, C.A. (2006) 'Oncogene-Induced Senescence: Putting the Brakes on Tumor Development', *Cancer Research*, 66(6), pp. 2881-2884.

Braun, S. and Madhani, H.D. (2012) 'Shaping the landscape: mechanistic consequences of ubiquitin modification of chromatin', *EMBO J*, 31(7), pp. 619-630.

Briggs, S.D., Xiao, T., Sun, Z.W., Caldwell, J.A., Shabanowitz, J., Hunt, D.F., Allis, C.D. and Strahl, B.D. (2002) 'Gene silencing: trans-histone regulatory pathway in chromatin', *Nature*, 418(6897), p. 498.

Bugga, L., McDaniel, I.E., Engie, L. and Armstrong, J.A. (2013) 'The *Drosophila melanogaster* CHD1 Chromatin Remodeling Factor Modulates Global Chromosome Structure and Counteracts HP1a and H3K9me2', *PLoS ONE*, 8(3), p. e59496.

Burgess, R.J. and Zhang, Z. (2013) 'Histone chaperones in nucleosome assembly and human disease', *Nat Struct Mol Biol*, 20(1), pp. 14-22.

Buscaino, A., Allshire, R. and Pidoux, A. (2010) 'Building centromeres: home sweet home or a nomadic existence?', *Current Opinion in Genetics & Development*, 20(2), pp. 118-126.

Cam, H.P., Noma, K.-i., Ebina, H., Levin, H.L. and Grewal, S.I.S. (2008) 'Host genome surveillance for retrotransposons by transposon-derived proteins', *Nature*, 451(7177), pp. 431-436.

Campisi, J. (2001) 'Cellular senescence as a tumor-suppressor mechanism', *Trends in Cell Biology*, 11(11), pp. S27-S31.

Campisi, J. and d'Adda di Fagagna, F. (2007) 'Cellular senescence: when bad things happen to good cells', *Nat Rev Mol Cell Biol*, 8(9), pp. 729-740.

Caron, C., Lestrat, C., Marsal, S., Escoffier, E., Curtet, S., Virolle, V., Barbry, P., Debernardi, A., Brambilla, C., Brambilla, E., Rousseaux, S. and Khochbin, S. (2010) 'Functional characterization of ATAD2 as a new cancer/testis factor and a predictor of poor prognosis in breast and lung cancers', *Oncogene*, 29(37), pp. 5171-5181.

Celona, B., Weiner, A., Di Felice, F., Mancuso, F.M., Cesarini, E., Rossi, R.L., Gregory, L., Baban, D., Rossetti, G., Grianti, P., Pagani, M., Bonaldi, T., Ragoussis, J., Friedman, N., Camilloni, G., Bianchi, M.E. and Agresti, A. (2011) 'Substantial Histone Reduction Modulates Genomewide Nucleosomal Occupancy and Global Transcriptional Output', *PLoS Biol*, 9(6), p. e1001086.

Chagraoui, J., Hébert, J., Girard, S. and Sauvageau, G. (2011) 'An anticlastogenic function for the Polycomb Group gene Bmi1', *Proceedings of the National Academy of Sciences*, 108(13), pp. 5284-5289.

Chang, B.D., Broude, E.V., Fang, J., Kalinichenko, T.V., Abdryashitov, R., Poole, J.C. and Roninson, I.B. (2000) 'p21Waf1/Cip1/Sdi1-induced growth arrest is associated with depletion of mitosis-control proteins and leads to abnormal mitosis and endoreduplication in recovering cells', *Oncogene*, 19(17), pp. 2165-70.

- Chapman, J.R. and Jackson, S.P. (2008) 'Phospho-dependent interactions between NBS1 and MDC1 mediate chromatin retention of the MRN complex at sites of DNA damage', *EMBO Rep*, 9(8), pp. 795-801.
- Cheung, T.H. and Rando, T.A. (2013) 'Molecular regulation of stem cell quiescence', *Nat Rev Mol Cell Biol*, 14(6), pp. 329-340.
- Cheung, V., Chua, G., Batada, N.N., Landry, C.R., Michnick, S.W., Hughes, T.R. and Winston, F. (2008) 'Chromatin- and Transcription-Related Factors Repress Transcription from within Coding Regions throughout the *Saccharomyces cerevisiae* Genome', *PLoS Biol*, 6(11), p. e277.
- Choi, E.S., Strålfors, A., Catania, S., Castillo, A.G., Svensson, J.P., Pidoux, A.L., Ekwall, K. and Allshire, R.C. (2012) 'Factors That Promote H3 Chromatin Integrity during Transcription Prevent Promiscuous Deposition of CENP-A^{Cnp1} in Fission Yeast', *PLoS Genet*, 8(9), p. e1002985.
- Chujo, M., Tarumoto, Y., Miyatake, K., Nishida, E. and Ishikawa, F. (2012) 'HIRA, a Conserved Histone Chaperone, Plays an Essential Role in Low-dose Stress Response via Transcriptional Stimulation in Fission Yeast', *Journal of Biological Chemistry*, 287(28), pp. 23440-23450.
- Ciró, M., Prosperini, E., Quarto, M., Grazini, U., Walfridsson, J., McBlane, F., Nucifero, P., Pacchiana, G., Capra, M., Christensen, J. and Helin, K. (2009) 'ATAD2 Is a Novel Cofactor for MYC, Overexpressed and Amplified in Aggressive Tumors', *Cancer Research*, 69(21), pp. 8491-8498.
- Clapier, C.R. and Cairns, B.R. (2009) 'The Biology of Chromatin Remodeling Complexes', *Annual Review of Biochemistry*, 78(1), pp. 273-304.
- Clements, A., Poux, A.N., Lo, W.-S., Pillus, L., Berger, S.L. and Marmorstein, R. (2003) 'Structural Basis for Histone and Phosphohistone Binding by the GCN5 Histone Acetyltransferase', *Molecular Cell*, 12(2), pp. 461-473.
- Coisy, M., Roure, V., Ribot, M., Philips, A., Muchardt, C., Blanchard, J.-M. and Dantonel, J.-C. (2004) 'Cyclin A Repression in Quiescent Cells Is Associated with Chromatin Remodeling of Its Promoter and Requires Brahma/SNF2 α ', *Molecular Cell*, 15(1), pp. 43-56.
- Coller, H.A. (2007) 'What's taking so long? S-phase entry from quiescence versus proliferation', *Nat Rev Mol Cell Biol*, 8(8), pp. 667-670.
- Collins, R.E., Tachibana, M., Tamaru, H., Smith, K.M., Jia, D., Zhang, X., Selker, E.U., Shinkai, Y. and Cheng, X. (2005) 'In Vitro and in Vivo Analyses of a Phe/Tyr Switch Controlling Product Specificity of Histone Lysine Methyltransferases', *Journal of Biological Chemistry*, 280(7), pp. 5563-5570.
- Cooper, S., Dienstbier, M., Hassan, R., Schermelleh, L., Sharif, J., Blackledge, N.P., De Marco, V., Elderkin, S., Koseki, H., Klose, R., Heger, A. and Brockdorff, N. (2014) 'Targeting polycomb to pericentric heterochromatin in embryonic stem cells reveals a role for H2AK119u1 in PRC2 recruitment', *Cell Rep*, 7(5), pp. 1456-70.
- Corona, D.F.V. and Tamkun, J.W. (2004) 'Multiple roles for ISWI in transcription, chromosome organization and DNA replication', *Biochimica et Biophysica Acta (BBA) - Gene Structure and Expression*, 1677(1-3), pp. 113-119.
- Costanzi, C. and Pehrson, J.R. (1998) 'Histone macroH2A1 is concentrated in the inactive X chromosome of female mammals', *Nature*, 393(6685), pp. 599-601.
- Cuperus, G. and Shore, D. (2002) 'Restoration of Silencing in *Saccharomyces cerevisiae* by Tethering of a Novel Sir2-Interacting Protein, Esc8', *Genetics*, 162(2), pp. 633-645.
- Dainty, S. (2007) *The response of the fission yeast Schizosaccharomyces pombe to zinc deficiency*. Newcastle University.
- Das, C., Lucia, M.S., Hansen, K.C. and Tyler, J.K. (2009) 'CBP/p300-mediated acetylation of histone H3 on lysine 56', *Nature*, 459(7243), pp. 113-117.
- Das, C. and Tyler, J.K. (2013) 'Histone exchange and histone modifications during

transcription and aging', *Biochim Biophys Acta*, 1819(3-4), pp. 332-42.

Davey, M.J., Jeruzalmi, D., Kuriyan, J. and O'Donnell, M. (2002) 'Motors and switches: AAA+ machines within the replisome', *Nat Rev Mol Cell Biol*, 3(11), pp. 826-835.

Deegan, R. (2012) *The role of histone modification in DNA double-strand break repair in Schizosaccharomyces pombe*. University of Oxford.

Del Rizzo, P.A. and Trievel, R.C. (2014) 'Molecular basis for substrate recognition by lysine methyltransferases and demethylases', *Biochimica et Biophysica Acta (BBA) - Gene Regulatory Mechanisms*, 1839(12), pp. 1404-1415.

Delmas, V., Stokes, D.G. and Perry, R.P. (1993) 'A mammalian DNA-binding protein that contains a chromodomain and an SNF2/SWI2-like helicase domain', *Proceedings of the National Academy of Sciences*, 90(6), pp. 2414-2418.

Demidenko, Z.N. and Blagosklonny, M.V. (2008) 'Growth stimulation leads to cellular senescence when the cell cycle is blocked', *Cell Cycle*, 7(21), pp. 3355-3361.

Demidenko, Z.N., Zubova, S.G., Bukreeva, E.I., Pospelov, V.A., Pospelova, T.V. and Blagosklonny, M.V. (2009) 'Rapamycin decelerates cellular senescence', *Cell Cycle*, 8(12), pp. 1888-1895.

Deuring, R., Fanti, L., Armstrong, J.A., Sarte, M., Papoulas, O., Prestel, M., Daubresse, G., Verardo, M., Moseley, S.L., Berloco, M., Tsukiyama, T., Wu, C., Pimpinelli, S. and Tamkun, J.W. (2000) 'The ISWI Chromatin-Remodeling Protein Is Required for Gene Expression and the Maintenance of Higher Order Chromatin Structure *In Vivo*', *Molecular Cell*, 5(2), pp. 355-365.

Dhalluin, C., Carlson, J.E., Zeng, L., He, C., Aggarwal, A.K., Zhou, M.-M. and Zhou, M.-M. (1999) 'Structure and ligand of a histone acetyltransferase bromodomain', *Nature*, 399(6735), pp. 491-496.

Di Leonardo, A., Linke, S.P., Clarkin, K. and Wahl, G.M. (1994) 'DNA damage triggers a prolonged p53-dependent G₁ arrest and long-term induction of Cip1 in normal human fibroblasts', *Genes Dev*, 8(21), pp. 2540-51.

Dimova, D., Nackerdien, Z., Furgeson, S., Eguchi, S. and Osley, M.A. (1999) 'A Role for Transcriptional Repressors in Targeting the Yeast Swi/Snf Complex', *Molecular Cell*, 4(1), pp. 75-83.

Dion, M.F., Kaplan, T., Kim, M., Buratowski, S., Friedman, N. and Rando, O.J. (2007) 'Dynamics of Replication-Independent Histone Turnover in Budding Yeast', *Science*, 315(5817), pp. 1405-1408.

Dlakic, M. (2001) 'Chromatin silencing protein and pachytene checkpoint regulator Dot1p has a methyltransferase fold', *Trends in Biochemical Sciences*, 26(7), pp. 405-407.

Dohke, K., Miyazaki, S., Tanaka, K., Urano, T., Grewal, S.I.S. and Murakami, Y. (2008) 'Fission yeast chromatin assembly factor 1 assists in the replication-coupled maintenance of heterochromatin', *Genes to Cells*, 13(10), pp. 1027-1043.

Drané, P., Ouararhni, K., Depaux, A., Shuaib, M. and Hamiche, A. (2010) 'The death-associated protein DAXX is a novel histone chaperone involved in the replication-independent deposition of H3.3', *Genes & Development*, 24(12), pp. 1253-1265.

Dulić, V., Drullinger, L.F., Lees, E., Reed, S.I. and Stein, G.H. (1993) 'Altered regulation of G1 cyclins in senescent human diploid fibroblasts: accumulation of inactive cyclin E-Cdk2 and cyclin D1-Cdk2 complexes', *Proceedings of the National Academy of Sciences*, 90(23), pp. 11034-11038.

Durut, N., Saez-Vasquez, J. (2015) 'Nucleolin: Dual roles in rDNA chromatin transcription', 556(1), pp. 7-12.

Dutta, D., Ray, S., Home, P., Saha, B., Wang, S., Sheibani, N., Tawfik, O., Cheng, N. and Paul, S. (2010) 'Regulation of Angiogenesis by Histone Chaperone HIRA-mediated Incorporation of Lysine 56-acetylated Histone H3.3 at Chromatin Domains of Endothelial Genes', *Journal of Biological Chemistry*, 285(53), pp. 41567-41577.

- Eirín-López, J.M., Ishibashi, T. and Ausió, J. (2008) 'H2A.Bbd: a quickly evolving hypervariable mammalian histone that destabilizes nucleosomes in an acetylation-independent way', *The FASEB Journal*, 22(1), pp. 316-326.
- Eriksson, P.R., Ganguli, D., Nagarajavel, V. and Clark, D.J. (2012) 'Regulation of Histone Gene Expression in Budding Yeast', *Genetics*, 191(1), pp. 7-20.
- Ernst, T., Chase, A.J., Score, J., Hidalgo-Curtis, C.E., Bryant, C., Jones, A.V., Waghorn, K., Zoi, K., Ross, F.M., Reiter, A., Hochhaus, A., Drexler, H.G., Duncombe, A., Cervantes, F., Oscier, D., Boultonwood, J., Grand, F.H. and Cross, N.C.P. (2010) 'Inactivating mutations of the histone methyltransferase gene EZH2 in myeloid disorders', *Nat Genet*, 42(8), pp. 722-726.
- Evertts, A.G., Manning, A.L., Wang, X., Dyson, N.J., Garcia, B.A. and Collier, H.A. (2013) 'H4K20 methylation regulates quiescence and chromatin compaction', *Molecular Biology of the Cell*, 24(19), pp. 3025-3037.
- Fazly, A., Li, Q., Hu, Q., Mer, G., Horazdovsky, B. and Zhang, Z. (2012) 'Histone Chaperone Rtt106 Promotes Nucleosome Formation Using (H3-H4)₂ Tetramers', *Journal of Biological Chemistry*, 287(14), pp. 10753-10760.
- Fazio, T.G., Kooperberg, C., Goldmark, J.P., Neal, C., Basom, R., Delrow, J. and Tsukiyama, T. (2001) 'Widespread Collaboration of Isw2 and Sin3-Rpd3 Chromatin Remodeling Complexes in Transcriptional Repression', *Molecular and Cellular Biology*, 21(19), pp. 6450-6460.
- Felsenfeld, G. and Groudine, M. (2003) 'Controlling the double helix', *Nature*, 421(6921), pp. 448-453.
- Ferreira, M.E., Flaherty, K. and Prochasson, P. (2011) 'The *Saccharomyces cerevisiae* Histone Chaperone Rtt106 Mediates the Cell Cycle Recruitment of SWI/SNF and RSC to the HIR-Dependent Histone Genes', *PLoS ONE*, 6(6), p. e21113.
- Ferreira, M.G. and Cooper, J.P. (2004) 'Two modes of DNA double-strand break repair are reciprocally regulated through the fission yeast cell cycle', *Genes & Development*, 18(18), pp. 2249-2254.
- Feser, J., Truong, D., Das, C., Carson, J.J., Kieft, J., Harkness, T. and Tyler, J.K. (2010) 'Elevated Histone Expression Promotes Life Span Extension', *Molecular Cell*, 39(5), pp. 724-735.
- Fierz, B., Chatterjee, C., McGinty, R.K., Bar-Dagan, M., Raleigh, D.P. and Muir, T.W. (2011) 'Histone H2B ubiquitylation disrupts local and higher-order chromatin compaction', *Nat Chem Biol*, 7(2), pp. 113-9.
- Filipescu, D., Szenker, E. and Almouzni, G. (2013) 'Developmental roles of histone H3 variants and their chaperones', *Trends in Genetics*, 29(11), pp. 630-640.
- Fillingham, J., Kainth, P., Lambert, J.-P., van Bakel, H., Tsui, K., Peña-Castillo, L., Nislow, C., Figeys, D., Hughes, T.R., Greenblatt, J. and Andrews, B.J. (2009) 'Two-Color Cell Array Screen Reveals Interdependent Roles for Histone Chaperones and a Chromatin Boundary Regulator in Histone Gene Repression', *Molecular Cell*, 35(3), pp. 340-351.
- Fischle, W., Tseng, B.S., Dormann, H.L., Ueberheide, B.M., Garcia, B.A., Shabanowitz, J., Hunt, D.F., Funabiki, H. and Allis, C.D. (2005) 'Regulation of HP1-chromatin binding by histone H3 methylation and phosphorylation', *Nature*, 438(7071), pp. 1116-1122.
- Formosa, T. (2012) 'The role of FACT in making and breaking nucleosomes', *Biochimica et Biophysica Acta (BBA) - Gene Regulatory Mechanisms*, 1819(3-4), pp. 247-255.
- Formosa, T., Eriksson, P., Wittmeyer, J., Ginn, J., Yu, Y. and Stillman, D.J. (2001) 'Spt16-Pob3 and the HMG protein Nhp6 combine to form the nucleosome-binding factor SPN', *EMBO J*, 20(13), pp. 3506-3517.
- Formosa, T., Ruone, S., Adams, M.D., Olsen, A.E., Eriksson, P., Yu, Y., Rhoades, A.R.,

Kaufman, P.D. and Stillman, D.J. (2002) 'Defects in SPT16 or POB3 (yFACT) in *Saccharomyces cerevisiae* Cause Dependence on the Hir/Hpc Pathway: Polymerase Passage May Degrade Chromatin Structure', *Genetics*, 162(4), pp. 1557-1571.

Forsberg, E.C., Passequé, E., Prohaska, S.S., Wagers, A.J., Koeva, M., Stuart, J.M. and Weissman, I.L. (2010) 'Molecular Signatures of Quiescent, Mobilized and Leukemia-Initiating Hematopoietic Stem Cells', *PLoS ONE*, 5(1), p. e8785.

Fouret, R., Laffaire, J., Hofman, P., Beau-Faller, M., Mazieres, J., Validire, P., Girard, P., Camilleri-Broet, S., Vaylet, F., Leroy-Ladurie, F., Soria, J.C. and Fouret, P. (2012) 'A comparative and integrative approach identifies ATPase family, AAA domain containing 2 as a likely driver of cell proliferation in lung adenocarcinoma', *Clin Cancer Res*, 18(20), pp. 5606-16.

Fradet-Turcotte, A., Canny, M.D., Escribano-Diaz, C., Orthwein, A., Leung, C.C.Y., Huang, H., Landry, M.-C., Kitevski-LeBlanc, J., Noordermeer, S.M., Sicheri, F. and Durocher, D. (2013) '53BP1 is a reader of the DNA-damage-induced H2A Lys 15 ubiquitin mark', *Nature*, 499(7456), pp. 50-54.

Froget, B., Blaisonneau, J., Lambert, S. and Baldacci, G. (2008) 'Cleavage of Stalled Forks by Fission Yeast Mus81/Eme1 in Absence of DNA Replication Checkpoint', *Molecular Biology of the Cell*, 19(2), pp. 445-456.

Fukada, S.-i., Uezumi, A., Ikemoto, M., Masuda, S., Segawa, M., Tanimura, N., Yamamoto, H., Miyagoe-Suzuki, Y. and Takeda, S.i. (2007) 'Molecular Signature of Quiescent Satellite Cells in Adult Skeletal Muscle', *Stem Cells*, 25(10), pp. 2448-2459.

Fulop, T., Le Page, A., Fortin, C., Witkowski, J.M., Dupuis, G. and Larbi, A. (2014) 'Cellular signaling in the aging immune system', *Current Opinion in Immunology*, 29(0), pp. 105-111.

Gaillard, P.-H.L., Martini, E.M.D., Kaufman, P.D., Stillman, B., Moustacchi, E. and Almouzni, G. (1996) 'Chromatin Assembly Coupled to DNA Repair: A New Role for Chromatin Assembly Factor I', *Cell*, 86(6), pp. 887-896.

Gallastegui, E., Millán-Zambrano, G., Terme, J.-M., Chávez, S. and Jordan, A. (2011) 'Chromatin Reassembly Factors Are Involved in Transcriptional Interference Promoting HIV Latency', *Journal of Virology*, 85(7), pp. 3187-3202.

Gamble, M.J., Frizzell, K.M., Yang, C., Krishnakumar, R. and Kraus, W.L. (2010) 'The histone variant macroH2A1 marks repressed autosomal chromatin, but protects a subset of its target genes from silencing', *Genes & Development*, 24(1), pp. 21-32.

Ganguli, D., Chereji, R.V., Iben, J.R., Cole, H.A. and Clark, D.J. (2014) 'RSC-dependent constructive and destructive interference between opposing arrays of phased nucleosomes in yeast', *Genome Research*.

Gasparian, A.V., Burkhart, C.A., Purmal, A.A., Brodsky, L., Pal, M., Saranadasa, M., Bosykh, D.A., Commane, M., Guryanova, O.A., Pal, S., Safina, A., Sviridov, S., Koman, I.E., Veith, J., Komar, A.A., Gudkov, A.V. and Gurova, K.V. (2011) 'Curaxins: Anticancer Compounds That Simultaneously Suppress NF- κ B and Activate p53 by Targeting FACT', *Science Translational Medicine*, 3(95), p. 95ra74.

Gatti, M., Pinato, S., Maspero, E., Soffientini, P., Polo, S. and Penengo, L. (2012) 'A novel ubiquitin mark at the N-terminal tail of histone H2As targeted by RNF168 ubiquitin ligase', *Cell Cycle*, 11(13), pp. 2538-2544.

Gayatri, S. and Bedford, M.T. (2014) 'Readers of histone methylarginine marks', *Biochimica et Biophysica Acta (BBA) - Gene Regulatory Mechanisms*, 1839(8), pp. 702-710.

Geng, F. and Tansey, W.P. (2008) 'Polyubiquitylation of histone H2B', *Mol Biol Cell*, 19(9), pp. 3616-24.

Ginjala, V., Nacerddine, K., Kulkarni, A., Oza, J., Hill, S.J., Yao, M., Citterio, E., van Lohuizen, M. and Ganesan, S. (2011) 'BMI1 Is Recruited to DNA Breaks and Contributes to DNA Damage-Induced H2A Ubiquitination and Repair', *Molecular and*

Cellular Biology, 31(10), pp. 1972-1982.

Givens, R.M., Lai, W.K.M., Rizzo, J.M., Bard, J.E., Mieczkowski, P.A., Leatherwood, J., Huberman, J.A. and Buck, M.J. (2012) 'Chromatin architectures at fission yeast transcriptional promoters and replication origins', *Nucleic Acids Research*, 40(15), pp. 7176-7189.

Glozak, M.A., Sengupta, N., Zhang, X. and Seto, E. (2005) 'Acetylation and deacetylation of non-histone proteins', *Gene*, 363(0), pp. 15-23.

Goldstein, M., Derheimer, F.A., Tait-Mulder, J., Kastan, M.B. (2013) 'Nucleolin mediates nucleosome disruption critical for DNA double-strand break repair', *Proc Natl Acad Sci USA*, 110(42), pp. 16874-16879.

Gos, M., Miloszevska, J., Swoboda, P., Trembacz, H., Skierski, J. and Janik, P. (2005) 'Cellular quiescence induced by contact inhibition or serum withdrawal in C3H10T1/2 cells', *Cell Proliferation*, 38(2), pp. 107-116.

Gradolatto, A., Rogers, R.S., Lavender, H., Taverna, S.D., Allis, C.D., Aitchison, J.D. and Tackett, A.J. (2008) '*Saccharomyces cerevisiae* Yta7 Regulates Histone Gene Expression', *Genetics*, 179(1), pp. 291-304.

Gradolatto, A., Smart, S.K., Byrum, S., Blair, L.P., Rogers, R.S., Kolar, E.A., Lavender, H., Larson, S.K., Aitchison, J.D., Taverna, S.D. and Tackett, A.J. (2009) 'A Noncanonical Bromodomain in the AAA ATPase Protein Yta7 Directs Chromosomal Positioning and Barrier Chromatin Activity', *Molecular and Cellular Biology*, 29(17), pp. 4604-4611.

Grant, P.A., Duggan, L., Côté, J., Roberts, S.M., Brownell, J.E., Candau, R., Ohba, R., Owen-Hughes, T., Allis, C.D., Winston, F., Berger, S.L. and Workman, J.L. (1997) 'Yeast Gcn5 functions in two multisubunit complexes to acetylate nucleosomal histones: characterization of an Ada complex and the SAGA (Spt/Ada) complex', *Genes & Development*, 11(13), pp. 1640-1650.

Green, E.M., Antczak, A.J., Bailey, A.O., Franco, A.A., Wu, K.J., Yates 3rd, J.R. and Kaufman, P.D. (2005) 'Replication-Independent Histone Deposition by the HIR Complex and Asf1', *Current Biology*, 15(22), pp. 2044-2049.

Greenall, A., Williams, E.S., Martin, K.A., Palmer, J.M., Gray, J., Liu, C. and Whitehall, S.K. (2006) 'Hip3 Interacts with the HIRA Proteins Hip1 and SIm9 and Is Required for Transcriptional Silencing and Accurate Chromosome Segregation', *Journal of Biological Chemistry*, 281(13), pp. 8732-8739.

Hall, C., Nelson, D.M., Ye, X., Baker, K., DeCaprio, J.A., Seeholzer, S., Lipinski, M. and Adams, P.D. (2001) 'HIRA, the Human Homologue of Yeast Hir1p and Hir2p, Is a Novel Cyclin-cdk2 Substrate Whose Expression Blocks S-Phase Progression', *Molecular and Cellular Biology*, 21(5), pp. 1854-1865.

Hallson, G., Hollebakk, R.E., Li, T., Syrzycka, M., Kim, I., Cotsworth, S., Fitzpatrick, K.A., Sinclair, D.A. and Honda, B.M. (2012) 'dSet1 is the main H3K4 di- and trimethyltransferase throughout *Drosophila* development', *Genetics*, 190(1), pp. 91-100.

Hamada, M., Huang, Y., Lowe, T.M. and Maraia, R.J. (2001) 'Widespread Use of TATA Elements in the Core Promoters for RNA Polymerases III, II, and I in Fission Yeast', *Molecular and Cellular Biology*, 21(20), pp. 6870-6881.

Hammoud, S.S., Nix, D.A., Zhang, H., Purwar, J., Carrell, D.T. and Cairns, B.R. (2009) 'Distinctive chromatin in human sperm packages genes for embryo development', *Nature*, 460(7254), pp. 473-478.

Hansen, K.H., Bracken, A.P., Pasini, D., Dietrich, N., Gehani, S.S., Monrad, A., Rappsilber, J., Lerdrup, M. and Helin, K. (2008) 'A model for transmission of the H3K27me3 epigenetic mark', *Nat Cell Biol*, 10(11), pp. 1291-1300.

Hansen, K.R., Burns, G., Mata, J., Volpe, T.A., Martienssen, R.A., Bähler, J. and Thon, G. (2005) 'Global Effects on Gene Expression in Fission Yeast by Silencing and RNA Interference Machineries', *Molecular and Cellular Biology*, 25(2), pp. 590-601.

Hardy, S., Jacques, P.E., Gevry, N., Forest, A., Fortin, M.E., Laflamme, L., Gaudreau, L. and Robert, F. (2009) 'The euchromatic and heterochromatic landscapes are shaped by antagonizing effects of transcription on H2A.Z deposition', *PLoS Genet*, 5(10), p. e1000687.

Hargreaves, D.C. and Crabtree, G.R. (2011) 'ATP-dependent chromatin remodeling: genetics, genomics and mechanisms', *Cell Res*, 21(3), pp. 396-420.

Harrison, J.C. and Haber, J.E. (2006) 'Surviving the breakup: the DNA damage checkpoint', *Annu Rev Genet*, 40, pp. 209-35.

Harshman, S.W., Young, N.L., Parthun, M.R. and Freitas, M.A. (2013) 'H1 histones: current perspectives and challenges', *Nucleic Acids Research*, 41(21), pp. 9593-9609.

Hassan, A.H., Prochasson, P., Neely, K.E., Galasinski, S.C., Chandy, M., Carrozza, M.J. and Workman, J.L. (2002) 'Function and Selectivity of Bromodomains in Anchoring Chromatin-Modifying Complexes to Promoter Nucleosomes', *Cell*, 111(3), pp. 369-379.

Hayashi, M., Katou, Y., Itoh, T., Tazumi, M., Yamada, Y., Takahashi, T., Nakagawa, T., Shirahige, K. and Masukata, H. (2007) 'Genome-wide localization of pre-RC sites and identification of replication origins in fission yeast', *EMBO J*, 26, pp. 1327-1339.

Heinrichs, A. (2008) 'Cell division: Back and forth', *Nat Rev Cancer*, 8(10), pp. 740-740.

Heintzman, N.D., Stuart, R.K., Hon, G., Fu, Y., Ching, C.W., Hawkins, R.D., Barrera, L.O., Van Calcar, S., Qu, C., Ching, K.A., Wang, W., Weng, Z., Green, R.D., Crawford, G.E. and Ren, B. (2007) 'Distinct and predictive chromatin signatures of transcriptional promoters and enhancers in the human genome', *Nat Genet*, 39(3), pp. 311-318.

Hennig, B.P., Bendrin, K., Zhou, Y. and Fischer, T. (2012) 'Chd1 chromatin remodelers maintain nucleosome organization and repress cryptic transcription', *EMBO J*, 31(11), pp. 997-1003.

Hepp, M.I., Alarcon, V., Dutta, A., Workman, J.L. and Gutiérrez, J.L. (2014) 'Nucleosome remodeling by the SWI/SNF complex is enhanced by yeast High Mobility Group Box (HMGB) proteins', *Biochimica et Biophysica Acta (BBA) - Gene Regulatory Mechanisms*, 1839(9), pp. 764-772.

Herbig, U., Jobling, W.A., Chen, B.P.C., Chen, D.J. and Sedivy, J.M. (2004) 'Telomere Shortening Triggers Senescence of Human Cells through a Pathway Involving ATM, p53, and p21CIP1, but Not p16INK4a', *Molecular Cell*, 14(4), pp. 501-513.

Herz, H.M., Mohan, M., Garruss, A.S., Liang, K., Takahashi, Y.H., Mickey, K., Voets, O., Verrijzer, C.P. and Shilatifard, A. (2012) 'Enhancer-associated H3K4 monomethylation by Trithorax-related, the *Drosophila* homolog of mammalian Mll3/Mll4', *Genes Dev*, 26(23), pp. 2604-20.

Hirota, T., Lipp, J.J., Toh, B.-H. and Peters, J.-M. (2005) 'Histone H3 serine-10 phosphorylation by Aurora B causes HP1 dissociation from heterochromatin', *Nature*, 438(7071), pp. 1176-1180.

Hodawadekar, S.C. and Marmorstein, R. (2007) 'Chemistry of acetyl transfer by histone modifying enzymes: structure, mechanism and implications for effector design', *Oncogene*, 26(37), pp. 5528-5540.

Hong, L., Schroth, G.P., Matthews, H.R., Yau, P. and Bradbury, E.M. (1993) 'Studies of the DNA binding properties of histone H4 amino terminus. Thermal denaturation studies reveal that acetylation markedly reduces the binding constant of the H4 "tail" to DNA', *Journal of Biological Chemistry*, 268(1), pp. 305-314.

Houlard, M., Berlivet, S., Probst, A.V., Quivy, J.-P., Héry, P., Almouzni, G. and Gérard, M. (2006) 'CAF-1 Is Essential for Heterochromatin Organization in Pluripotent Embryonic Cells', *PLoS Genet*, 2(11), p. e181.

Hsieh, F.-K., Kulaeva, O.I., Patel, S.S., Dyer, P.N., Luger, K., Reinberg, D. and Studitsky, V.M. (2013) 'Histone chaperone FACT action during transcription through chromatin by RNA polymerase II', *Proceedings of the National Academy of Sciences*,

110(19), pp. 7654-7659.

Hu, Z., Chen, K., Xia, Z., Chavez, M., Pal, S., Seol, J.H., Chen, C.C., Li, W. and Tyler, J.K. (2014) 'Nucleosome loss leads to global transcriptional up-regulation and genomic instability during yeast aging', *Genes Dev*, 28(4), pp. 396-408.

Huang, H., Yu, Z., Zhang, S., Liang, X., Chen, J., Li, C., Ma, J. and Jiao, R. (2010) '*Drosophila* CAF-1 regulates HP1-mediated epigenetic silencing and pericentric heterochromatin stability', *Journal of Cell Science*, 123(16), pp. 2853-2861.

Huang, S., Zhou, H., Katzmman, D., Hochstrasser, M., Atanasova, E. and Zhang, Z. (2005) 'Rtt106p is a histone chaperone involved in heterochromatin-mediated silencing', *Proceedings of the National Academy of Sciences of the United States of America*, 102(38), pp. 13410-13415.

Huang, S., Zhou, H., Tarara, J. and Zhang, Z. (2007) 'A novel role for histone chaperones CAF1 and Rtt106p in heterochromatin silencing', *EMBO J*, 26(9), pp. 2274-2283.

Hwang, W.W., Venkatasubrahmanyam, S., Ianculescu, A.G., Tong, A., Boone, C. and Madhani, H.D. (2003) 'A conserved RING finger protein required for histone H2B monoubiquitination and cell size control', *Mol Cell*, 11(1), pp. 261-6.

Hyllus, D., Stein, C., Schnabel, K., Schiltz, E., Imhof, A., Dou, Y., Hsieh, J. and Bauer, U.-M. (2007) 'PRMT6-mediated methylation of R2 in histone H3 antagonizes H3 K4 trimethylation', *Genes & Development*, 21(24), pp. 3369-3380.

Ikura, T., Tashiro, S., Kakino, A., Shima, H., Jacob, N., Amunugama, R., Yoder, K., Izumi, S., Kuraoka, I., Tanaka, K., Kimura, H., Ikura, M., Nishikubo, S., Ito, T., Muto, A., Miyagawa, K., Takeda, S., Fishel, R., Igarashi, K. and Kamiya, K. (2007) 'DNA Damage-Dependent Acetylation and Ubiquitination of H2AX Enhances Chromatin Dynamics', *Molecular and Cellular Biology*, 27(20), pp. 7028-7040.

Infante, J., Law, G.L. and Young, E. (2012) 'Analysis of Nucleosome Positioning Using a Nucleosome-Scanning Assay', in Morse, R.H. (ed.) *Chromatin Remodeling*. Humana Press, pp. 63-87.

Ito, T., Bulger, M., Pazin, M.J., Kobayashi, R. and Kadonaga, J.T. (1997) 'ACF, an ISWI-containing and ATP-utilizing chromatin assembly and remodeling factor', *Cell*, 90(1), pp. 145-55.

Ivanovska, I., Jacques, P.-É., Rando, O.J., Robert, F. and Winston, F. (2011) 'Control of Chromatin Structure by Spt6: Different Consequences in Coding and Regulatory Regions', *Molecular and Cellular Biology*, 31(3), pp. 531-541.

Jackson, V. (1990) 'In vivo studies on the dynamics of histone-DNA interaction: evidence for nucleosome dissolution during replication and transcription and a low level of dissolution independent of both', *Biochemistry*, 29(3), pp. 719-31.

Jamai, A., Puglisi, A. and Strubin, M. (2009) 'Histone Chaperone Spt16 Promotes Redeposition of the Original H3-H4 Histones Evicted by Elongating RNA Polymerase', *Molecular Cell*, 35(3), pp. 377-383.

Jambunathan, N., Martinez, A.W., Robert, E.C., Agochukwu, N.B., Ibos, M.E., Dugas, S.L. and Donze, D. (2005) 'Multiple Bromodomain Genes Are Involved in Restricting the Spread of Heterochromatic Silencing at the *Saccharomyces cerevisiae* HMR-tRNA Boundary', *Genetics*, 171(3), pp. 913-922.

Jentsch, S., McGrath, J.P. and Varshavsky, A. (1987) 'The yeast DNA repair gene RAD6 encodes a ubiquitin-conjugating enzyme', *Nature*, 329(6135), pp. 131-4.

Jeong, K.W., Lee, Y.-H. and Stallcup, M.R. (2009) 'Recruitment of the SWI/SNF Chromatin Remodeling Complex to Steroid Hormone-regulated Promoters by Nuclear Receptor Coactivator Flightless-I', *Journal of Biological Chemistry*, 284(43), pp. 29298-29309.

Jin, J., Cai, Y., Li, B., Conaway, R.C., Workman, J.L., Conaway, J.W. and Kusch, T. (2005) 'In and out: histone variant exchange in chromatin', *Trends in Biochemical*

Sciences, 30(12), pp. 680-687.

Kalb, R., Latwiel, S., Baymaz, H.I., Jansen, P.W., Muller, C.W., Vermeulen, M. and Muller, J. (2014) 'Histone H2A monoubiquitination promotes histone H3 methylation in Polycomb repression', *Nat Struct Mol Biol*, 21(6), pp. 569-71.

Kamakaka, R.T. and Biggins, S. (2005) 'Histone variants: deviants?', *Genes & Development*, 19(3), pp. 295-316.

Kanoh, J. and Russell, P. (2000) 'Slm9, a Novel Nuclear Protein Involved in Mitotic Control in Fission Yeast', *Genetics*, 155(2), pp. 623-631.

Kaplan, C.D., Laprade, L. and Winston, F. (2003) 'Transcription Elongation Factors Repress Transcription Initiation from Cryptic Sites', *Science*, 301(5636), pp. 1096-1099.

Kato, H., Okazaki, K., Iida, T., Nakayama, J.-i., Murakami, Y. and Urano, T. (2013) 'Spt6 prevents transcription-coupled loss of posttranslationally modified histone H3', *Sci. Rep.*, 3.

Kaufman, P.D., Cohen, J.L. and Osley, M.A. (1998) 'Hir Proteins Are Required for Position-Dependent Gene Silencing in *Saccharomyces cerevisiae* in the Absence of Chromatin Assembly Factor I', *Molecular and Cellular Biology*, 18(8), pp. 4793-4806.

Kaufman, P.D., Kobayashi, R., Kessler, N. and Stillman, B. (1995) 'The p150 and p60 subunits of chromatin assembly factor I: A molecular link between newly synthesized histories and DNA replication', *Cell*, 81(7), pp. 1105-1114.

Kelly, T.J., Martin, G.S., Forsburg, S.L., Stephen, R.J., Russo, A. and Nurse, P. (1993) 'The fission yeast *cdc18⁺* gene product couples S phase to START and mitosis', *Cell*, 74(2), pp. 371-382.

Kent, N.A., Adams, S., Moorhouse, A. and Paszkiewicz, K. (2011) 'Chromatin particle spectrum analysis: a method for comparative chromatin structure analysis using paired-end mode next-generation DNA sequencing', *Nucleic Acids Research*, 39(5), p. e26.

Kingsbury, S.R., Loddo, M., Fanshawe, T., Obermann, E.C., Prevost, A.T., Stoeber, K. and Williams, G.H. (2005) 'Repression of DNA replication licensing in quiescence is independent of geminin and may define the cell cycle state of progenitor cells', *Experimental Cell Research*, 309(1), pp. 56-67.

Kirov, N., Shtilbans, A. and Rushlow, C. (1998) 'Isolation and characterization of a new gene encoding a member of the HIRA family of proteins from *Drosophila melanogaster*', *Gene*, 212(2), pp. 323-332.

Klose, R.J. and Zhang, Y. (2007) 'Regulation of histone methylation by demethylination and demethylation', *Nat Rev Mol Cell Biol*, 8(4), pp. 307-318.

Kobayashi, J., Fujimoto, H., Sato, I., Hayashi, S., Burma, S., Matsuura, S., Chen, D.J., Komatsu, K. (2012) 'Nucleolin participates in DNA double-strand break-induced damage response through MDC1-dependent pathway', *Plos One*, 7(11), pp. e49245

Kobor, M.S., Venkatasubrahmanyam, S., Meneghini, M.D., Gin, J.W., Jennings, J.L., Link, A.J., Madhani, H.D. and Rine, J. (2004) 'A Protein Complex Containing the Conserved Swi2/Snf2-Related ATPase Swr1p Deposits Histone Variant H2A.Z into Euchromatin', *PLoS Biol*, 2(5), p. e131.

Kohda, T.A., Tanaka, K., Konomi, M., Sato, M., Osumi, M. and Yamamoto, M. (2007) 'Fission yeast autophagy induced by nitrogen starvation generates a nitrogen source that drives adaptation processes', *Genes to Cells*, 12(2), pp. 155-170.

Kornberg, R.D. (1974) 'Chromatin structure: a repeating unit of histones and DNA', *Science*, 184(4139), pp. 868-71.

Kouzarides, T. (2007) 'Chromatin Modifications and Their Function', *Cell*, 128(4), pp. 693-705.

Kristell, C., Orzechowski Westholm, J., Olsson, I., Ronne, H., Komorowski, J. and Bjerling, P. (2010) 'Nitrogen depletion in the fission yeast *Schizosaccharomyces pombe* causes nucleosome loss in both promoters and coding regions of activated genes', *Genome Res*, 20(3), pp. 361-71.

- Kulaeva, O.I., Hsieh, F.-K., Chang, H.-W., Luse, D.S. and Studitsky, V.M. (2013) 'Mechanism of transcription through a nucleosome by RNA polymerase II', *Biochimica et Biophysica Acta (BBA) - Gene Regulatory Mechanisms*, 1829(1), pp. 76-83.
- Kumar, Y. and Bhargava, P. (2013) 'A unique nucleosome arrangement, maintained actively by chromatin remodelers facilitates transcription of yeast tRNA genes', *BMC Genomics*, 14(1), p. 402.
- Kurat, C.F., Lambert, J.P., van Dyk, D., Tsui, K., van Bakel, H., Kaluarachchi, S., Friesen, H., Kainth, P., Nislow, C., Figeys, D., Fillingham, J. and Andrews, B.J. (2011) 'Restriction of histone gene transcription to S phase by phosphorylation of a chromatin boundary protein', *Genes Dev*, 25(23), pp. 2489-501.
- Lantermann, A., Strålfors, A., Fagerström-Billai, F., Korber, P. and Ekwall, K. (2009) 'Genome-wide mapping of nucleosome positions in *Schizosaccharomyces pombe*', *Methods*, 48(3), pp. 218-225.
- Larsson, O., Zetterberg, A. and Engstrom, W. (1985) 'Cell-cycle-specific induction of quiescence achieved by limited inhibition of protein synthesis: counteractive effect of addition of purified growth factors', *Journal of Cell Science*, 73(1), pp. 375-387.
- Le, S., Davis, C., Konopka, J.B. and Sternglanz, R. (1997) 'Two New S-Phase-Specific Genes from *Saccharomyces cerevisiae*', *Yeast*, 13(11), pp. 1029-1042.
- Leachman, N.T., Brellier, F., Ferralli, J., Chiquet-Ehrismann, R. and Tucker, R.P. (2010) 'ATAD2B is a phylogenetically conserved nuclear protein expressed during neuronal differentiation and tumorigenesis', *Development, Growth & Differentiation*, 52(9), pp. 747-755.
- Lee, J.-S., Shukla, A., Schneider, J., Swanson, S.K., Washburn, M.P., Florens, L., Bhaumik, S.R. and Shilatifard, A. (2007) 'Histone Crosstalk between H2B Monoubiquitination and H3 Methylation Mediated by COMPASS', *Cell*, 131(6), pp. 1084-1096.
- Lee, J.H. and Paull, T.T. (2004) 'Direct activation of the ATM protein kinase by the Mre11/Rad50/Nbs1 complex', *Science*, 304(5667), pp. 93-6.
- Lejeune, E., Bortfeld, M., White, S.A., Pidoux, A.L., Ekwall, K., Allshire, R.C. and Ladurner, A.G. (2007) 'The Chromatin-Remodeling Factor FACT Contributes to Centromeric Heterochromatin Independently of RNAi', *Current Biology*, 17(14), pp. 1219-1224.
- Li, B., Gogol, M., Carey, M., Pattenden, S.G., Seidel, C. and Workman, J.L. (2007) 'Infrequently transcribed long genes depend on the Set2/Rpd3S pathway for accurate transcription', *Genes & Development*, 21(11), pp. 1422-1430.
- Li, G., Liu, S., Wang, J., He, J., Huang, H., Zhang, Y. and Xu, L. (2014) 'ISWI proteins participate in the genome-wide nucleosome distribution in *Arabidopsis*', *The Plant Journal*, 78(4), pp. 706-714.
- Li, X. and Heyer, W.-D. (2008) 'Homologous recombination in DNA repair and DNA damage tolerance', *Cell Res*, 18(1), pp. 99-113.
- Liang, G., Klose, R.J., Gardner, K.E. and Zhang, Y. (2007) 'Yeast Jhd2p is a histone H3 Lys4 trimethyl demethylase', *Nat Struct Mol Biol*, 14(3), pp. 243-245.
- Lin, C.-J., Koh, Fong M., Wong, P., Conti, M. and Ramalho-Santos, M. (2014) 'Hira-Mediated H3.3 Incorporation Is Required for DNA Replication and Ribosomal RNA Transcription in the Mouse Zygote', *Developmental Cell*, 30(3), pp. 268-279.
- Lin, G., Xin, Z., Zhang, H., Banie, L., Wang, G., Qiu, X., Ning, H., Lue, T.F. and Lin, C.-S. (2012) 'Identification of active and quiescent adipose vascular stromal cells', *Cytotherapy*, 14(2), pp. 240-246.
- Liu, W.H., Roemer, S.C., Port, A.M. and Churchill, M.E.A. (2012) 'CAF-1-induced oligomerization of histones H3/H4 and mutually exclusive interactions with Asf1 guide H3/H4 transitions among histone chaperones and DNA', *Nucleic Acids Research*, 40(22), pp. 11229-11239.

- Llevadot, R., Marqués, G., Pritchard, M., Xavier, E., Ferrús, A. and Scambler, P. (1998) 'Cloning, Chromosome Mapping and Expression Analysis of the HIRA gene from *Drosophila melanogaster*', *Biochemical and Biophysical Research Communications*, 249(2), pp. 486-491.
- Lombardi, L.M., Ellahi, A. and Rine, J. (2011) 'Direct regulation of nucleosome density by the conserved AAA-ATPase Yta7', *Proceedings of the National Academy of Sciences*, 108(49), pp. E1302–E1311.
- Loppin, B., Bonnefoy, E., Anselme, C., Laurencon, A., Karr, T.L. and Couble, P. (2005) 'The histone H3.3 chaperone HIRA is essential for chromatin assembly in the male pronucleus', *Nature*, 437(7063), pp. 1386-1390.
- Loppin, B., Docquier, M., Bonneton, F. and Couble, P. (2000) 'The Maternal Effect Mutation *sésame* Affects the Formation of the Male Pronucleus in *Drosophila melanogaster*', *Developmental Biology*, 222(2), pp. 392-404.
- Lorenz, A. and Whitby, M.C. (2006) 'Crossover promotion and prevention', *Biochem Soc Trans*, 34(Pt 4), pp. 537-41.
- Loyola, A. and Almouzni, G. (2004) 'Histone chaperones, a supporting role in the limelight', *Biochimica et Biophysica Acta (BBA) - Gene Structure and Expression*, 1677(1–3), pp. 3-11.
- Lu, P.Y.T. and Kobor, M.S. (2014) 'Maintenance of Heterochromatin Boundary and Nucleosome Composition at Promoters by the Asf1 Histone Chaperone and SWR1-C Chromatin Remodeler in *Saccharomyces cerevisiae*', *Genetics*, 197(1), pp. 133-145.
- Luger, K., Mader, A.W., Richmond, R.K., Sargent, D.F. and Richmond, T.J. (1997) 'Crystal structure of the nucleosome core particle at 2.8 Å resolution', *Nature*, 389(6648), pp. 251-260.
- Luk, E., Vu, N.-D., Patteson, K., Mizuguchi, G., Wu, W.-H., Ranjan, A., Backus, J., Sen, S., Lewis, M., Bai, Y. and Wu, C. (2007) 'Chz1, a Nuclear Chaperone for Histone H2AZ', *Molecular Cell*, 25(3), pp. 357-368.
- Lusser, A., Urwin, D.L. and Kadonaga, J.T. (2005) 'Distinct activities of CHD1 and ACF in ATP-dependent chromatin assembly', *Nat Struct Mol Biol*, 12(2), pp. 160-166.
- MacDonald, N., Welburn, J.P.I., Noble, M.E.M., Nguyen, A., Yaffe, M.B., Clynes, D., Moggs, J.G., Orphanides, G., Thomson, S., Edmunds, J.W., Clayton, A.L., Endicott, J.A. and Mahadevan, L.C. (2005) 'Molecular Basis for the Recognition of Phosphorylated and Phosphoacetylated Histone H3 by 14-3-3', *Molecular Cell*, 20(2), pp. 199-211.
- Malay, A.D., Umehara, T., Matsubara-Malay, K., Padmanabhan, B. and Yokoyama, S. (2008) 'Crystal Structures of Fission Yeast Histone Chaperone Asf1 Complexed with the Hip1 B-domain or the Cac2 C Terminus', *Journal of Biological Chemistry*, 283(20), pp. 14022-14031.
- Manning, B.J. and Peterson, C.L. (2013) 'Releasing the brakes on a chromatin-remodeling enzyme', *Nat Struct Mol Biol*, 20(1), pp. 5-7.
- Manolis, K.G., Nimmo, E.R., Hartsuiker, E., Carr, A.M., Jeggo, P.A. and Allshire, R.C. (2001) 'Novel functional requirements for non-homologous DNA end joining in *Schizosaccharomyces pombe*', *EMBO J*, 20, pp. 210-221.
- Marguerat, S., Schmidt, A., Codlin, S., Chen, W., Aebersold, R. and Bähler, J. (2012) 'Quantitative Analysis of Fission Yeast Transcriptomes and Proteomes in Proliferating and Quiescent Cells', *Cell*, 151(3), pp. 671-683.
- Martynoga, B., Mateo, J.L., Zhou, B., Andersen, J., Achimastou, A., Urban, N., van den Berg, D., Georgopoulou, D., Hadjur, S., Wittbrodt, J., Ettwiller, L., Piper, M., Gronostajski, R.M. and Guillemot, F. (2013) 'Epigenomic enhancer annotation reveals a key role for NFIX in neural stem cell quiescence', *Genes Dev*, 27(16), pp. 1769-86.
- Masayuki, Y., Yoshiyuki, I. and Yoshinori, W. (1997) *Mating and Sporulation in Schizosaccharomyces pombe*.

Masumoto, H., Hawke, D., Kobayashi, R. and Verreault, A. (2005) 'A role for cell-cycle-regulated histone H3 lysine 56 acetylation in the DNA damage response', *Nature*, 436(7048), pp. 294-298.

Mattioli, F., Vissers, Joseph H.A., van Dijk, Willem J., Ikpa, P., Citterio, E., Vermeulen, W., Marteijn, Jurgen A. and Sixma, Titia K. (2012) 'RNF168 Ubiquitinates K13-15 on H2A/H2AX to Drive DNA Damage Signaling', *Cell*, 150(6), pp. 1182-1195.

McCabe, M.T., Graves, A.P., Ganji, G., Diaz, E., Halsey, W.S., Jiang, Y., Smitheman, K.N., Ott, H.M., Pappalardi, M.B., Allen, K.E., Chen, S.B., Della Pietra, A., Dul, E., Hughes, A.M., Gilbert, S.A., Thrall, S.H., Tummino, P.J., Kruger, R.G., Brandt, M., Schwartz, B. and Creasy, C.L. (2012) 'Mutation of A677 in histone methyltransferase EZH2 in human B-cell lymphoma promotes hypertrimethylation of histone H3 on lysine 27 (H3K27)', *Proceedings of the National Academy of Sciences*, 109(8), pp. 2989-2994.

McCullough, L., Rawlins, R., Olsen, A., Xin, H., Stillman, D.J. and Formosa, T. (2011) 'Insight Into the Mechanism of Nucleosome Reorganization From Histone Mutants That Suppress Defects in the FACT Histone Chaperone', *Genetics*, 188(4), pp. 835-846.

McKittrick, E., Gafken, P.R., Ahmad, K. and Henikoff, S. (2004) 'Histone H3.3 is enriched in covalent modifications associated with active chromatin', *Proceedings of the National Academy of Sciences of the United States of America*, 101(6), pp. 1525-1530.

Megee, P.C., Morgan, B.A. and Smith, M.M. (1995) 'Histone H4 and the maintenance of genome integrity', *Genes Dev*, 9(14), pp. 1716-27.

Meneghini, M.D., Wu, M. and Madhani, H.D. (2003) 'Conserved Histone Variant H2A.Z Protects Euchromatin from the Ectopic Spread of Silent Heterochromatin', *Cell*, 112(5), pp. 725-736.

Meyer, R.E., Delaage, M., Rosset, R., Capri, M. and Ait-Ahmed, O. (2010) 'A single mutation results in diploid gamete formation and parthenogenesis in a *Drosophila yemanuclein*-a meiosis I defective mutant', *BMC Genet*, 11, p. 104.

Millar, C.B. (2013) 'Organizing the genome with H2A histone variants', *Biochemical Journal*, 449(3), pp. 567-579.

Millar, C.B. and Grunstein, M. (2006) 'Genome-wide patterns of histone modifications in yeast', *Nat Rev Mol Cell Biol*, 7(9), pp. 657-666.

Minsky, N., Shema, E., Field, Y., Schuster, M., Segal, E. and Oren, M. (2008) 'Monoubiquitinated H2B is associated with the transcribed region of highly expressed genes in human cells', *Nat Cell Biol*, 10(4), pp. 483-8.

Mizuguchi, G., Shen, X., Landry, J., Wu, W.-H., Sen, S. and Wu, C. (2004) 'ATP-Driven Exchange of Histone H2AZ Variant Catalyzed by SWR1 Chromatin Remodeling Complex', *Science*, 303(5656), pp. 343-348.

Mizuguchi, G., Tsukiyama, T., Wisniewski, J. and Wu, C. (1997) 'Role of Nucleosome Remodeling Factor NURF in Transcriptional Activation of Chromatin', *Molecular Cell*, 1(1), pp. 141-150.

Mizuki, F., Tanaka, A., Hirose, Y. and Ohkuma, Y. (2011) 'The HIRA Complex Subunit Hip3 Plays Important Roles in the Silencing of Meiosis-Specific Genes in *Schizosaccharomyces pombe*', *PLoS ONE*, 6(4), p. e19442.

Mochida, S. and Yanagida, M. (2006) 'Distinct modes of DNA damage response in *S. pombe* G₀ and vegetative cells', *Genes to Cells*, 11(1), pp. 13-27.

Mondesert, O., McGowan, C.H. and Russell, P. (1996) 'Cig2, a B-type cyclin, promotes the onset of S in *Schizosaccharomyces pombe*', *Molecular and Cellular Biology*, 16(4), pp. 1527-33.

Moreno, S. and Nurse, P. (1994) 'Regulation of progression through the G₁ phase of the cell cycle by the *rum1*⁺ gene', *Nature*, 367(6460), pp. 236-242.

Morillo-Huesca, M., Maya, D., Munoz-Centeno, M.C., Singh, R.K., Oreal, V., Reddy, G.U., Liang, D., Geli, V., Gunjan, A. and Chavez, S. (2010) 'FACT prevents the accumulation of free histones evicted from transcribed chromatin and a subsequent cell

cycle delay in G₁', *PLoS Genet*, 6(5), p. e1000964.

Motamedi, M.R., Hong, E.-J.E., Li, X., Gerber, S., Denison, C., Gygi, S. and Moazed, D. (2008) 'HP1 Proteins Form Distinct Complexes and Mediate Heterochromatic Gene Silencing by Nonoverlapping Mechanisms', *Molecular Cell*, 32(6), pp. 778-790.

Mukaiyama, H., Kajiwar, S., Hosomi, A., Giga-Hama, Y., Tanaka, N., Nakamura, T. and Takegawa, K. (2009) 'Autophagy-deficient *Schizosaccharomyces pombe* mutants undergo partial sporulation during nitrogen starvation', *Microbiology*, 155(12), pp. 3816-3826.

Müller, S. and Almouzni, G. (2014) 'A network of players in H3 histone variant deposition and maintenance at centromeres', *Biochimica et Biophysica Acta (BBA) - Gene Regulatory Mechanisms*, 1839(3), pp. 241-250.

Murakami, H., Ito, S., Tanaka, H., Kondo, E., Koder, Y. and Nakanishi, H. (2013) 'Establishment of New Intraperitoneal Paclitaxel-Resistant Gastric Cancer Cell Lines and Comprehensive Gene Expression Analysis', *Anticancer Research*, 33(10), pp. 4299-4307.

Murton, H.E. (2012) *Regulation of LTR retrotransposons in Schizosaccharomyces pombe*. Newcastle University.

Nabatiyan, A. and Krude, T. (2004) 'Silencing of Chromatin Assembly Factor 1 in Human Cells Leads to Cell Death and Loss of Chromatin Assembly during DNA Synthesis', *Molecular and Cellular Biology*, 24(7), pp. 2853-2862.

Neugeborn, L. and Carlson, M. (1984) 'Genes affecting the regulation of *SUC2* gene expression by glucose repression in *Saccharomyces cerevisiae*', *Genetics*, 108(4), pp. 845-858.

Nelson, C.J., Santos-Rosa, H. and Kouzarides, T. (2006) 'Proline Isomerization of Histone H3 Regulates Lysine Methylation and Gene Expression', *Cell*, 126(5), pp. 905-916.

Ng, H.H., Robert, F., Young, R.A. and Struhl, K. (2002) 'Genome-wide location and regulated recruitment of the RSC nucleosome-remodeling complex', *Genes & Development*, 16(7), pp. 806-819.

Nie, X., Wang, H., Li, J., Holec, S. and Berger, F. (2014) 'The HIRA complex that deposits the histone H3.3 is conserved in *Arabidopsis* and facilitates transcriptional dynamics', *Biology Open*, 3(9), pp. 794-802.

Nilausen, K. and Green, H. (1965) 'Reversible arrest of growth in G₁ of an established fibroblast line (3T3)', *Experimental Cell Research*, 40(1), pp. 166-168.

Nishitani, H., Lygerou, Z., Nishimoto, T. and Nurse, P. (2000) 'The Cdt1 protein is required to license DNA for replication in fission yeast', *Nature*, 404(6778), pp. 625-628.

Nourani, A., Robert, F. and Winston, F. (2006) 'Evidence that Spt2/Sin1, an HMG-Like Factor, Plays Roles in Transcription Elongation, Chromatin Structure, and Genome Stability in *Saccharomyces cerevisiae*', *Molecular and Cellular Biology*, 26(4), pp. 1496-1509.

Ogryzko, V.V., Hirai, T.H., Russanova, V.R., Barbie, D.A. and Howard, B.H. (1996) 'Human fibroblast commitment to a senescence-like state in response to histone deacetylase inhibitors is cell cycle dependent', *Molecular and Cellular Biology*, 16(9), pp. 5210-8.

Ogura, T. and Wilkinson, A.J. (2001) 'AAA+ superfamily ATPases: common structure-diverse function', *Genes to Cells*, 6(7), pp. 575-597.

Onder, T.T., Kara, N., Cherry, A., Sinha, A.U., Zhu, N., Bernt, K.M., Cahan, P., Marcacci, B.O., Unternaehrer, J., Gupta, P.B., Lander, E.S., Armstrong, S.A. and Daley, G.Q. (2012) 'Chromatin-modifying enzymes as modulators of reprogramming', *Nature*, 483(7391), pp. 598-602.

Orphanides, G., LeRoy, G., Chang, C.-H., Luse, D.S. and Reinberg, D. (1998) 'FACT, a

- Factor that Facilitates Transcript Elongation through Nucleosomes', *Cell*, 92(1), pp. 105-116.
- Owen, D.J., Ornaghi, P., Yang, J.C., Lowe, N., Evans, P.R., Ballario, P., Neuhaus, D., Filetici, P. and Travers, A.A. (2000) 'The structural basis for the recognition of acetylated histone H4 by the bromodomain of histone acetyltransferase Gcn5p', *EMBO J*, 19, pp. 6141-6149.
- Pai, C.-C., Deegan, R.S., Subramanian, L., Gal, C., Sarkar, S., Blaikley, E.J., Walker, C., Hulme, L., Bernhard, E., Codlin, S., Bähler, J., Allshire, R., Whitehall, S. and Humphrey, T.C. (2014) 'A histone H3K36 chromatin switch coordinates DNA double-strand break repair pathway choice', *Nat Commun*, 5, p. 4091.
- Papamichos-Chronakis, M., Watanabe, S., Rando, O.J. and Peterson, C.L. (2011) 'Global Regulation of H2A.Z Localization by the INO80 Chromatin-Remodeling Enzyme Is Essential for Genome Integrity', *Cell*, 144(2), pp. 200-213.
- Parthun, M.R. (2007) 'Hat1: the emerging cellular roles of a type B histone acetyltransferase', *Oncogene*, 26(37), pp. 5319-5328.
- Paull, T.T., Rogakou, E.P., Yamazaki, V., Kirchgessner, C.U., Gellert, M. and Bonner, W.M. (2000) 'A critical role for histone H2AX in recruitment of repair factors to nuclear foci after DNA damage', *Current Biology*, 10(15), pp. 886-895.
- Pchelintsev, Nikolay A., McBryan, T., Rai, Taranjit S., van Tuyn, J., Ray-Gallet, D., Almouzni, G. and Adams, Peter D. (2013) 'Placing the HIRA Histone Chaperone Complex in the Chromatin Landscape', *Cell Reports*, 3(4), pp. 1012-1019.
- Phelps-Durr, T.L., Thomas, J., Vahab, P. and Timmermans, M.C.P. (2005) 'Maize rough sheath2 and Its *Arabidopsis* Orthologue ASYMMETRIC LEAVES1 Interact with HIRA, a Predicted Histone Chaperone, to Maintain knox Gene Silencing and Determinacy during Organogenesis', *The Plant Cell Online*, 17(11), pp. 2886-2898.
- Piña, B. and Suau, P. (1987) 'Changes in histones H2A and H3 variant composition in differentiating and mature rat brain cortical neurons', *Developmental Biology*, 123(1), pp. 51-58.
- Pointner, J., Persson, J., Prasad, P., Norman-Axelsson, U., Strålfors, A., Khorosjutina, O., Krietenstein, N., Peter Svensson, J., Ekwall, K. and Korber, P. (2012) 'CHD1 remodelers regulate nucleosome spacing in vitro and align nucleosomal arrays over gene coding regions in *S. pombe*', *EMBO J*, 31(23), pp. 4388-4403.
- Polo, S.E. (2014) 'Reshaping Chromatin after DNA Damage: The Choreography of Histone Proteins', *Journal of Molecular Biology*, S0022-2836(14), pp. 00275-7
- Polo, S.E., Roche, D. and Almouzni, G. (2006) 'New Histone Incorporation Marks Sites of UV Repair in Human Cells', *Cell*, 127(3), pp. 481-493.
- Prezioso, C. and Orlando, V. (2011) 'Polycomb proteins in mammalian cell differentiation and plasticity', *FEBS Letters*, 585(13), pp. 2067-2077.
- Prochasson, P., Florens, L., Swanson, S.K., Washburn, M.P. and Workman, J.L. (2005) 'The HIR corepressor complex binds to nucleosomes generating a distinct protein/DNA complex resistant to remodeling by SWI/SNF', *Genes & Development*, 19(21), pp. 2534-2539.
- Purtill, F.S., Whitehall, S.K., Williams, E.S., McNerny, C.J., Sharrocks, A.D. and Morgan, B.A. (2011) 'A homeodomain transcription factor regulates the DNA replication checkpoint in yeast', *Cell Cycle*, 10(4), pp. 664-670.
- Qian, Z., Huang, H., Hong, J.Y., Burck, C.L., Johnston, S.D., Berman, J., Carol, A. and Liebman, S.W. (1998) 'Yeast Ty1 Retrotransposition Is Stimulated by a Synergistic Interaction between Mutations in Chromatin Assembly Factor I and Histone Regulatory Proteins', *Molecular and Cellular Biology*, 18(8), pp. 4783-4792.
- Radman-Livaja, M., Quan, T.K., Valenzuela, L., Armstrong, J.A., van Welsem, T., Kim, T., Lee, L.J., Buratowski, S., van Leeuwen, F., Rando, O.J. and Hartzog, G.A. (2012) 'A Key Role for Chd1 in Histone H3 Dynamics at the 3' Ends of Long Genes in Yeast',

PLoS Genet, 8(7), p. e1002811.

Raeder, M.B., Birkeland, E., Trovik, J., Krakstad, C., Shehata, S., Schumacher, S., Zack, T.I., Krohn, A., Werner, H.M.J., Moody, S.E., Wik, E., Stefansson, I.M., Holst, F., Oyan, A.M., Tamayo, P., Mesirov, J.P., Kalland, K.H., Akslen, L.A., Simon, R., Beroukhi, R. and Salvesen, H.B. (2013) 'Integrated Genomic Analysis of the 8q24 Amplification in Endometrial Cancers Identifies ATAD2 as Essential to MYC-Dependent Cancers', *PLoS ONE*, 8(2), p. e54873.

Ransom, M., Dennehey, B.K. and Tyler, J.K. (2010) 'Chaperoning Histones during DNA Replication and Repair', *Cell*, 140(2), pp. 183-195.

Ray-Gallet, D., Quivy, J.-P., Scamps, C., Martini, E.M.D., Lipinski, M. and Almouzni, G. (2002) 'HIRA Is Critical for a Nucleosome Assembly Pathway Independent of DNA Synthesis', *Molecular Cell*, 9(5), pp. 1091-1100.

Revenko, A.S., Kalashnikova, E.V., Gemo, A.T., Zou, J.X. and Chen, H.-W. (2010) 'Chromatin Loading of E2F-MLL Complex by Cancer-Associated Coregulator ANCCA via Reading a Specific Histone Mark', *Molecular and Cellular Biology*, 30(22), pp. 5260-5272.

Rhind, N. and Russell, P. (2000) 'Chk1 and Cds1: linchpins of the DNA damage and replication checkpoint pathways', *Journal of Cell Science*, 113(22), pp. 3889-3896.

Ridgway, P. and Almouzni, G. (2000) 'CAF-1 and the inheritance of chromatin states: at the crossroads of DNA replication and repair', *Journal of Cell Science*, 113(15), pp. 2647-2658.

Roberts, C., Sutherland, H.F., Farmer, H., Kimber, W., Halford, S., Carey, A., Brickman, J.M., Wynshaw-Boris, A. and Scambler, P.J. (2002) 'Targeted Mutagenesis of the Hira Gene Results in Gastrulation Defects and Patterning Abnormalities of Mesoendodermal Derivatives Prior to Early Embryonic Lethality', *Molecular and Cellular Biology*, 22(7), pp. 2318-2328.

Robzyk, K., Recht, J. and Osley, M.A. (2000) 'Rad6-dependent ubiquitination of histone H2B in yeast', *Science*, 287(5452), pp. 501-4.

Rogakou, E.P., Pilch, D.R., Orr, A.H., Ivanova, V.S. and Bonner, W.M. (1998) 'DNA double-stranded breaks induce histone H2AX phosphorylation on serine 139', *J Biol Chem*, 273(10), pp. 5858-68.

Roguev, A., Bandyopadhyay, S., Zofall, M., Zhang, K., Fischer, T., Collins, S.R., Qu, H., Shales, M., Park, H.-O., Hayles, J., Hoe, K.-L., Kim, D.-U., Ideker, T., Grewal, S.I., Weissman, J.S. and Krogan, N.J. (2008) 'Conservation and Rewiring of Functional Modules Revealed by an Epistasis Map in Fission Yeast', *Science*, 322(5900), pp. 405-410.

Roux, A.E., Chartrand, P., Ferbeyre, G. and Rokeach, L.A. (2010) 'Fission Yeast and Other Yeasts as Emergent Models to Unravel Cellular Aging in Eukaryotes', *The Journals of Gerontology Series A: Biological Sciences and Medical Sciences*, 65A(1), pp. 1-8.

Rufiange, A., Jacques, P.-É., Bhat, W., Robert, F. and Nourani, A. (2007) 'Genome-Wide Replication-Independent Histone H3 Exchange Occurs Predominantly at Promoters and Implicates H3 K56 Acetylation and Asf1', *Molecular Cell*, 27(3), pp. 393-405.

Ruone, S., Rhoades, A.R. and Formosa, T. (2003) 'Multiple Nhp6 Molecules Are Required to Recruit Spt16-Pob3 to Form yFACT Complexes and to Reorganize Nucleosomes', *Journal of Biological Chemistry*, 278(46), pp. 45288-45295.

Sadeghi, L., Siggins, L., Svensson, J.P. and Ekwall, K. (2014) 'Centromeric histone H2B monoubiquitination promotes noncoding transcription and chromatin integrity', *Nat Struct Mol Biol*, 21(3), pp. 236-243.

Sajiki, K., Hatanaka, M., Nakamura, T., Takeda, K., Shimanuki, M., Yoshida, T., Hanyu, Y., Hayashi, T., Nakaseko, Y. and Yanagida, M. (2009) 'Genetic control of cellular quiescence in *S. pombe*', *Journal of Cell Science*, 122(9), pp. 1418-1429.

Salhia, B., Kiefer, J., Ross, J.T., Metapally, R., Martinez, R.A., Johnson, K.N., DiPerna, D.M., Paquette, K.M., Jung, S., Nasser, S., Wallstrom, G., Tembe, W., Baker, A., Carpten, J., Resau, J., Ryken, T., Sibenaller, Z., Petricoin, E.F., Liotta, L.A., Ramanathan, R.K., Berens, M.E. and Tran, N.L. (2014) 'Integrated genomic and epigenomic analysis of breast cancer brain metastasis', *PLoS One*, 9(1), p. e85448.

Sanematsu, F., Takami, Y., Barman, H.K., Fukagawa, T., Ono, T., Shibahara, K.-i. and Nakayama, T. (2006) 'Asf1 Is Required for Viability and Chromatin Assembly during DNA Replication in Vertebrate Cells', *Journal of Biological Chemistry*, 281(19), pp. 13817-13827.

Santisteban, M.S., Kalashnikova, T. and Smith, M.M. (2000) 'Histone H2A.Z Regulates Transcription and Is Partially Redundant with Nucleosome Remodeling Complexes', *Cell*, 103(3), pp. 411-422.

Saunders, L.R. and Verdin, E. (2007) 'Sirtuins: critical regulators at the crossroads between cancer and aging', *Oncogene*, 26(37), pp. 5489-5504.

Schermer, U.J., Korber, P. and Hörz, W. (2005) 'Histones Are Incorporated in *trans* during Reassembly of the Yeast *PHO5* Promoter', *Molecular Cell*, 19(2), pp. 279-285.

Scully, R. and Xie, A. (2013) 'Double strand break repair functions of histone H2AX', *Mutation Research/Fundamental and Molecular Mechanisms of Mutagenesis*, 750(1-2), pp. 5-14.

Secombe, J., Li, L., Carlos, L. and Eisenman, R.N. (2007) 'The Trithorax group protein Lid is a trimethyl histone H3K4 demethylase required for dMyc-induced cell growth', *Genes & Development*, 21(5), pp. 537-551.

Serrano, M., Lin, A.W., McCurrach, M.E., Beach, D. and Lowe, S.W. (1997) 'Oncogenic ras Provokes Premature Cell Senescence Associated with Accumulation of p53 and p16INK4a', *Cell*, 88(5), pp. 593-602.

Shankaranarayana, G.D., Motamedi, M.R., Moazed, D. and Grewal, S.I.S. (2003) 'Sir2 Regulates Histone H3 Lysine 9 Methylation and Heterochromatin Assembly in Fission Yeast', *Current Biology*, 13(14), pp. 1240-1246.

Sharp, J.A., Fouts, E.T., Krawitz, D.C. and Kaufman, P.D. (2001) 'Yeast histone deposition protein Asf1p requires Hir proteins and PCNA for heterochromatic silencing', *Current Biology*, 11(7), pp. 463-473.

Sharp, J.A., Rizki, G. and Kaufman, P.D. (2005) 'Regulation of Histone Deposition Proteins Asf1/Hir1 by Multiple DNA Damage Checkpoint Kinases in *Saccharomyces cerevisiae*', *Genetics*, 171(3), pp. 885-899.

Shema, E., Kim, J., Roeder, R.G. and Oren, M. (2011) 'RNF20 inhibits TFIIS-facilitated transcriptional elongation to suppress pro-oncogenic gene expression', *Mol Cell*, 42(4), pp. 477-488.

Shen, X., Mizuguchi, G., Hamiche, A. and Wu, C. (2000) 'A chromatin remodelling complex involved in transcription and DNA processing', *Nature*, 406(6795), pp. 541-544.

Shi, J., Zheng, M., Ye, Y., Li, M., Chen, X., Hu, X., Sun, J., Zhang, X. and Jiang, C. (2014) '*Drosophila* Brahma complex remodels nucleosome organizations in multiple aspects', *Nucleic Acids Research*, 42(15), pp. 9730-9739.

Shi, Y., Lan, F., Matson, C., Mulligan, P., Whetstone, J.R., Cole, P.A., Casero, R.A. and Shi, Y. (2004) 'Histone Demethylation Mediated by the Nuclear Amine Oxidase Homolog LSD1', *Cell*, 119(7), pp. 941-953.

Shibahara, K.-i. and Stillman, B. (1999) 'Replication-Dependent Marking of DNA by PCNA Facilitates CAF-1-Coupled Inheritance of Chromatin', *Cell*, 96(4), pp. 575-585.

Shilatifard, A. (2012) 'The COMPASS family of histone H3K4 methylases: mechanisms of regulation in development and disease pathogenesis', *Annu Rev Biochem*, 81, pp. 65-95.

Shim, Y.S., Choi, Y., Kang, K., Cho, K., Oh, S., Lee, J., Grewal, S.I.S. and Lee, D.

- (2012) 'Hrp3 controls nucleosome positioning to suppress non-coding transcription in euchromatin and heterochromatin', *EMBO J*, 31, pp. 4375-4387.
- Shimanuki, M., Chung, S.-Y., Chikashige, Y., Kawasaki, Y., Uehara, L., Tsutsumi, C., Hatanaka, M., Hiraoka, Y., Nagao, K. and Yanagida, M. (2007) 'Two-step, extensive alterations in the transcriptome from G₀ arrest to cell division in *Schizosaccharomyces pombe*', *Genes to Cells*, 12(5), pp. 677-692.
- Shogren-Knaak, M., Ishii, H., Sun, J.-M., Pazin, M.J., Davie, J.R. and Peterson, C.L. (2006) 'Histone H4-K16 Acetylation Controls Chromatin Structure and Protein Interactions', *Science*, 311(5762), pp. 844-847.
- Silva, A.C., Xu, X., Kim, H.-S., Fillingham, J., Kislinger, T., Mennella, T.A. and Keogh, M.-C. (2012) 'The Replication-independent Histone H3-H4 Chaperones HIR, ASF1, and RTT106 Co-operate to Maintain Promoter Fidelity', *Journal of Biological Chemistry*, 287(3), pp. 1709-1718.
- Smith, E. and Shilatifard, A. (2010) 'The Chromatin Signaling Pathway: Diverse Mechanisms of Recruitment of Histone-Modifying Enzymes and Varied Biological Outcomes', *Molecular Cell*, 40(5), pp. 689-701.
- Smith, S. and Stillman, B. (1989) 'Purification and characterization of CAF-I, a human cell factor required for chromatin assembly during DNA replication *in vitro*', *Cell*, 58(1), pp. 15-25.
- Smolka, M.B., Albuquerque, C.P., Chen, S.-h., Schmidt, K.H., Wei, X.X., Kolodner, R.D. and Zhou, H. (2005) 'Dynamic Changes in Protein-Protein Interaction and Protein Phosphorylation Probed with Amine-reactive Isotope Tag', *Molecular & Cellular Proteomics*, 4(9), pp. 1358-1369.
- Smolle, M., Venkatesh, S., Gogol, M.M., Li, H., Zhang, Y., Florens, L., Washburn, M.P. and Workman, J.L. (2012) 'Chromatin remodelers Isw1 and Chd1 maintain chromatin structure during transcription by preventing histone exchange', *Nat Struct Mol Biol*, 19(9), pp. 884-892.
- Snider, J. and Houry, W.A. (2008) 'AAA+ proteins: diversity in function, similarity in structure', *Biochem Soc Trans*, 36(Pt 1), pp. 72-7.
- Soares, Luis M., Radman-Livaja, M., Lin, Sherry G., Rando, Oliver J. and Buratowski, S. (2014) 'Feedback Control of Set1 Protein Levels Is Important for Proper H3K4 Methylation Patterns', *Cell Reports*, 6(6), pp. 961-972.
- Sobhian, B., Shao, G., Lilli, D.R., Culhane, A.C., Moreau, L.A., Xia, B., Livingston, D.M. and Greenberg, R.A. (2007) 'RAP80 Targets BRCA1 to Specific Ubiquitin Structures at DNA Damage Sites', *Science*, 316(5828), pp. 1198-1202.
- Soboleva, T.A., Nekrasov, M., Pahwa, A., Williams, R., Huttley, G.A. and Tremethick, D.J. (2012) 'A unique H2A histone variant occupies the transcriptional start site of active genes', *Nat Struct Mol Biol*, 19(1), pp. 25-30.
- Song, Y., He, F., Xie, G., Guo, X., Xu, Y., Chen, Y., Liang, X., Stagljar, I., Egli, D., Ma, J. and Jiao, R. (2007) 'CAF-1 is essential for *Drosophila* development and involved in the maintenance of epigenetic memory', *Developmental Biology*, 311(1), pp. 213-222.
- Song, Y., Seol, J.-H., Yang, J.-H., Kim, H.-J., Han, J.-W., Youn, H.-D. and Cho, E.-J. (2013) 'Dissecting the roles of the histone chaperones reveals the evolutionary conserved mechanism of transcription-coupled deposition of H3.3', *Nucleic Acids Research*, 41(10), pp. 5199-5209.
- Soni, S., Pchelintsev, N., Adams, P.D. and Bieker, J.J. (2014) 'Transcription factor EKLF (KLF1) recruitment of the histone chaperone HIRA is essential for β -globin gene expression', *Proceedings of the National Academy of Sciences*.
- Sousa-Victor, P., Gutarra, S., Garcia-Prat, L., Rodriguez-Ubreva, J., Ortet, L., Ruiz-Bonilla, V., Jardi, M., Ballestar, E., Gonzalez, S., Serrano, A.L., Perdiguero, E. and Munoz-Canoves, P. (2014) 'Geriatric muscle stem cells switch reversible quiescence

into senescence', *Nature*, 506(7488), pp. 316-321.

Spector, M.S., Raff, A., DeSilva, H., Lee, K. and Osley, M.A. (1997) 'Hir1p and Hir2p function as transcriptional corepressors to regulate histone gene transcription in the *Saccharomyces cerevisiae* cell cycle', *Molecular and Cellular Biology*, 17(2), pp. 545-52.

Stern, M., Jensen, R. and Herskowitz, I. (1984) 'Five SWI genes are required for expression of the HO gene in yeast', *Journal of Molecular Biology*, 178(4), pp. 853-868.

Stevenson, J.S. and Liu, H. (2013) 'Nucleosome Assembly Factors CAF-1 and HIR Modulate Epigenetic Switching Frequencies in an H3K56 Acetylation-Associated Manner in *Candida albicans*', *Eukaryotic Cell*, 12(4), pp. 591-603.

Stracker, T.H. and Petrini, J.H. (2011) 'The MRE11 complex: starting from the ends', *Nat Rev Mol Cell Biol*, 12(2), pp. 90-103.

Straube, K., Blackwell, J.S. and Pemberton, L.F. (2010) 'Nap1 and Chz1 have Separate Htz1 Nuclear Import and Assembly Functions', *Traffic*, 11(2), pp. 185-197.

Stucki, M. and Jackson, S.P. (2006) 'gammaH2AX and MDC1: anchoring the DNA-damage-response machinery to broken chromosomes', *DNA repair*, 5(5), pp. 534-543.

Stuwe, T., Hothorn, M., Lejeune, E., Rybin, V., Bortfeld, M., Scheffzek, K. and Ladurner, A.G. (2008) 'The FACT Spt16 "peptidase" domain is a histone H3-H4 binding module', *Proceedings of the National Academy of Sciences*, 105(26), pp. 8884-8889.

Su, S.S., Tanaka, Y., Samejima, I., Tanaka, K. and Yanagida, M. (1996) 'A nitrogen starvation-induced dormant G₀ state in fission yeast: the establishment from uncommitted G₁ state and its delay for return to proliferation', *Journal of Cell Science*, 109(6), pp. 1347-1357.

Sun, Z.W. and Allis, C.D. (2002) 'Ubiquitination of histone H2B regulates H3 methylation and gene silencing in yeast', *Nature*, 418(6893), pp. 104-8.

Sutton, A., Bucaria, J., Osley, M.A. and Sternglanz, R. (2001) 'Yeast ASF1 Protein Is Required for Cell Cycle Regulation of Histone Gene Transcription', *Genetics*, 158(2), pp. 587-596.

Tackett, A.J., Dilworth, D.J., Davey, M.J., O'Donnell, M., Aitchison, J.D., Rout, M.P. and Chait, B.T. (2005) 'Proteomic and genomic characterization of chromatin complexes at a boundary', *The Journal of Cell Biology*, 169(1), pp. 35-47.

Tagami, H., Ray-Gallet, D., Almouzni, G. and Nakatani, Y. (2004) 'Histone H3.1 and H3.3 Complexes Mediate Nucleosome Assembly Pathways Dependent or Independent of DNA Synthesis', *Cell*, 116(1), pp. 51-61.

Takahata, S., Yu, Y. and Stillman, D.J. (2009a) 'The E2F functional analogue SBF recruits the Rpd3(L) HDAC, via Whi5 and Stb1, and the FACT chromatin reorganizer, to yeast G₁ cyclin promoters', *EMBO J*, 28(21), pp. 3378-89.

Takahata, S., Yu, Y. and Stillman, D.J. (2009b) 'FACT and Asf1 Regulate Nucleosome Dynamics and Coactivator Binding at the HO Promoter', *Molecular Cell*, 34(4), pp. 405-415.

Takayama, Y. and Takahashi, K. (2007) 'Differential regulation of repeated histone genes during the fission yeast cell cycle', *Nucleic Acids Research*, 35(10), pp. 3223-3237.

Takeda, K. and Yanagida, M. (2010) 'In quiescence of fission yeast, autophagy and the proteasome collaborate for mitochondrial maintenance and longevity', *Autophagy*, 6(4), pp. 564-565.

Takeda, K., Yoshida, T., Kikuchi, S., Nagao, K., Kokubu, A., Pluskal, T., Villar-Briones, A., Nakamura, T. and Yanagida, M. (2010) 'Synergistic roles of the proteasome and autophagy for mitochondrial maintenance and chronological lifespan in fission yeast', *Proceedings of the National Academy of Sciences*, 107(8), pp. 3540-3545.

Talbert, P.B. and Henikoff, S. (2010) 'Histone variants - ancient wrap artists of the

epigenome', *Nat Rev Mol Cell Biol*, 11(4), pp. 264-275.

Tanae, K., Horiuchi, T., Matsuo, Y., Katayama, S. and Kawamukai, M. (2012) 'Histone Chaperone Asf1 Plays an Essential Role in Maintaining Genomic Stability in Fission Yeast', *PLoS ONE*, 7(1), p. e30472.

Thoma, F., Koller, T. and Klug, A. (1979) 'Involvement of histone H1 in the organization of the nucleosome and of the salt-dependent superstructures of chromatin', *J Cell Biol*, 83(2 Pt 1), pp. 403-27.

Tjeertes, J.V., Miller, K.M. and Jackson, S.P. (2009) 'Screen for DNA damage responsive histone modifications identifies H3K9Ac and H3K56Ac in human cells', *EMBO J*, 28, pp. 1878-1889.

Touat-Todeschini, L., Hiriart, E. and Verdel, A. (2012) 'Nucleosome positioning and transcription: fission yeast CHD remodellers make their move', *EMBO J*, 31, pp. 4371-4372.

Toussaint, O., Medrano, E.E. and von Zglinicki, T. (2000) 'Cellular and molecular mechanisms of stress-induced premature senescence (SIPS) of human diploid fibroblasts and melanocytes', *Experimental Gerontology*, 35(8), pp. 927-945.

Trojer, P. and Reinberg, D. (2007) 'Facultative Heterochromatin: Is There a Distinctive Molecular Signature?', *Molecular Cell*, 28(1), pp. 1-13.

Tsubota, T., Berndsen, C.E., Erkmann, J.A., Smith, C.L., Yang, L., Freitas, M.A., Denu, J.M. and Kaufman, P.D. (2007) 'Histone H3-K56 Acetylation Is Catalyzed by Histone Chaperone-Dependent Complexes', *Molecular Cell*, 25(5), pp. 703-712.

Tsukada, Y.-i., Fang, J., Erdjument-Bromage, H., Warren, M.E., Borchers, C.H., Tempst, P. and Zhang, Y. (2006) 'Histone demethylation by a family of JmjC domain-containing proteins', *Nature*, 439(7078), pp. 811-816.

Tsukiyama, T., Daniel, C., Tamkun, J. and Wu, C. (1995) 'ISWI, a member of the SWI2/SNF2 ATPase family, encodes the 140 kDa subunit of the nucleosome remodeling factor', *Cell*, 83(6), pp. 1021-6.

Tsukiyama, T. and Wu, C. (1995) 'Purification and properties of an ATP-dependent nucleosome remodeling factor', *Cell*, 83(6), pp. 1011-20.

Tsunaka, Y., Toga, J., Yamaguchi, H., Tate, S.-i., Hirose, S. and Morikawa, K. (2009) 'Phosphorylated Intrinsically Disordered Region of FACT Masks Its Nucleosomal DNA Binding Elements', *Journal of Biological Chemistry*, 284(36), pp. 24610-24621.

Ubersax, J.A., Woodbury, E.L., Quang, P.N., Paraz, M., Blethrow, J.D., Shah, K., Shokat, K.M. and Morgan, D.O. (2003) 'Targets of the cyclin-dependent kinase Cdk1', *Nature*, 425(6960), pp. 859-864.

Umeda, M., Izaddoost, S., Cushman, I., Moore, M.S. and Sazer, S. (2005) 'The fission yeast *Schizosaccharomyces pombe* has two importin-alpha proteins, Imp1p and Cut15p, which have common and unique functions in nucleocytoplasmic transport and cell cycle progression', *Genetics*, 171(1), pp. 7-21.

Valente, L.P., Dehé, P.M., Klutstein, M., Aligianni, S., Watt, S., Bähler, J. and Promisel Cooper, J. (2013) 'Myb domain protein Teb1 controls histone levels and centromere assembly in fission yeast', *EMBO J*, 32, pp. 450-460.

van Deursen, J.M. (2014) 'The role of senescent cells in ageing', *Nature*, 509(7501), pp. 439-446.

VanDemark, A.P., Blanksma, M., Ferris, E., Heroux, A., Hill, C.P. and Formosa, T. (2006) 'The Structure of the yFACT Pob3-M Domain, Its Interaction with the DNA Replication Factor RPA, and a Potential Role in Nucleosome Deposition', *Molecular Cell*, 22(3), pp. 363-374.

Varga-Weisz, P.D., Wilm, M., Bonte, E., Dumas, K., Mann, M. and Becker, P.B. (1997) 'Chromatin-remodelling factor CHRAC contains the ATPases ISWI and topoisomerase II', *Nature*, 388(6642), pp. 598-602.

- Verreault, A., Kaufman, P.D., Kobayashi, R. and Stillman, B. (1996) 'Nucleosome Assembly by a Complex of CAF-1 and Acetylated Histones H3/H4', *Cell*, 87(1), pp. 95-104.
- Voth, W.P., Takahata, S., Nishikawa, J.L., Metcalfe, B.M., Naar, A.M. and Stillman, D.J. (2014) 'A role for FACT in repopulation of nucleosomes at inducible genes', *PLoS One*, 9(1), p. e84092.
- Wagner, T., Brand, P., Heinzel, T. and Krämer, O.H. 'Histone deacetylase 2 controls p53 and is a critical factor in tumorigenesis', *Biochimica et Biophysica Acta (BBA) - Reviews on Cancer*.
- Wan, W.N., Zhang, Y.X., Wang, X.M., Liu, Y.J., Zhang, Y.Q., Que, Y.H. and Zhao, W.J. (2014) 'ATAD2 is highly expressed in ovarian carcinomas and indicates poor prognosis', *Asian Pac J Cancer Prev*, 15(6), pp. 2777-83.
- Wan, Y., Saleem, R.A., Ratushny, A.V., Roda, O., Smith, J.J., Lin, C.-H., Chiang, J.-H. and Aitchison, J.D. (2009) 'Role of the Histone Variant H2A.Z/Htz1p in TBP Recruitment, Chromatin Dynamics, and Regulated Expression of Oleate-Responsive Genes', *Molecular and Cellular Biology*, 29(9), pp. 2346-2358.
- Wang, B., Matsuoka, S., Carpenter, P.B. and Elledge, S.J. (2002) '53BP1, a Mediator of the DNA Damage Checkpoint', *Science*, 298(5597), pp. 1435-1438.
- Wang, M.-Y., Guo, Q.-H., Du, X.-Z., Zhou, L., Luo, Q., Zeng, Q.-H., Wang, J.-L., Zhao, H.-B. and Wang, Y.-F. (2014) 'HIRA is essential for the development of gibel carp', *Fish Physiology and Biochemistry*, 40(1), pp. 235-244.
- Wang, P., Lin, C., Smith, E.R., Guo, H., Sanderson, B.W., Wu, M., Gogol, M., Alexander, T., Seidel, C., Wiedemann, L.M., Ge, K., Krumlauf, R. and Shilatifard, A. (2009) 'Global analysis of H3K4 methylation defines MLL family member targets and points to a role for MLL1-mediated H3K4 methylation in the regulation of transcriptional initiation by RNA polymerase II', *Mol Cell Biol*, 29(22), pp. 6074-85.
- Wang, S.W., Norbury, C., Harris, A.L. and Toda, T. (1999) 'Caffeine can override the S-M checkpoint in fission yeast', *Journal of Cell Science*, 112(6), pp. 927-937.
- Waterborg, J.H. (2001) 'Dynamics of Histone Acetylation in *Saccharomyces cerevisiae*', *Biochemistry*, 40(8), pp. 2599-2605.
- Weber, C.M., Henikoff, J.G. and Henikoff, S. (2010) 'H2A.Z nucleosomes enriched over active genes are homotypic', *Nat Struct Mol Biol*, 17(12), pp. 1500-1507.
- Weber, C.M. and Henikoff, S. (2014) 'Histone variants: dynamic punctuation in transcription', *Genes & Development*, 28(7), pp. 672-682.
- Weber, Christopher M., Ramachandran, S. and Henikoff, S. (2014) 'Nucleosomes Are Context-Specific, H2A.Z-Modulated Barriers to RNA Polymerase', *Molecular Cell*, 53(5), pp. 819-830.
- Wells, A., Griffith, L., Wells, J.Z. and Taylor, D.P. (2013) 'The Dormancy Dilemma: Quiescence versus Balanced Proliferation', *Cancer Research*, 73(13), pp. 3811-3816.
- Weng, M., Yang, Y.U.E., Feng, H., Pan, Z., Shen, W.-H., Zhu, Y.A.N. and Dong, A. (2014) 'Histone chaperone ASF1 is involved in gene transcription activation in response to heat stress in *Arabidopsis thaliana*', *Plant, Cell & Environment*, 37(9), pp. 2128-2138.
- West, A.C. and Johnstone, R.W. (2014) 'New and emerging HDAC inhibitors for cancer treatment', *The Journal of Clinical Investigation*, 124(1), pp. 30-39.
- Whitehouse, I., Stockdale, C., Flaus, A., Szczelkun, M.D. and Owen-Hughes, T. (2003) 'Evidence for DNA translocation by the ISWI chromatin-remodeling enzyme', *Mol Cell Biol*, 23(6), pp. 1935-45.
- Winkler, D.D. and Luger, K. (2011) 'The Histone Chaperone FACT: Structural Insights and Mechanisms for Nucleosome Reorganization', *Journal of Biological Chemistry*, 286(21), pp. 18369-18374.
- Winkler, D.D., Zhou, H., Dar, M.A., Zhang, Z. and Luger, K. (2012) 'Yeast CAF-1

assembles histone (H3-H4)₂ tetramers prior to DNA deposition', *Nucleic Acids Research*, 40(20), pp. 10139-10149.

Wiren, M., Silverstein, R.A., Sinha, I., Walfriddson, J., Lee, H., Laurenson, P., Robyr, D., Grunstein, M., Ekwel, K. (2005) 'Genome wide analysis of nucleosome density histone acetylation and HDAC function in fission yeast' *EMBO J.*, 24, pp. 2906-2918.

Witt, O., Albig, W. and Doenecke, D. (1996) 'Testis-Specific Expression of a Novel Human H3 Histone Gene', *Experimental Cell Research*, 229(2), pp. 301-306.

Wolf, S.S. (2009) 'The protein arginine methyltransferase family: an update about function, new perspectives and the physiological role in humans', *Cell Mol Life Sci*, 66(13), pp. 2109-21.

Wong, H. and Riabowol, K. (1996) 'Differential CDK-inhibitor gene expression in aging human diploid fibroblasts', *Experimental Gerontology*, 31(1-2), pp. 311-325.

Wood, V., Gwilliam, R., Rajandream, M.A., Lyne, M., Lyne, R., Stewart, A., Sgouros, J., Peat, N., Hayles, J., Baker, S., Basham, D., Bowman, S., Brooks, K., Brown, D., Brown, S., Chillingworth, T., Churcher, C., Collins, M., Connor, R., Cronin, A., Davis, P., Feltwell, T., Fraser, A., Gentles, S., Goble, A., Hamlin, N., Harris, D., Hidalgo, J., Hodgson, G., Holroyd, S., Hornsby, T., Howarth, S., Huckle, E.J., Hunt, S., Jagels, K., James, K., Jones, L., Jones, M., Leather, S., McDonald, S., McLean, J., Mooney, P., Moule, S., Mungall, K., Murphy, L., Niblett, D., Odell, C., Oliver, K., O'Neil, S., Pearson, D., Quail, M.A., Rabinowitsch, E., Rutherford, K., Rutter, S., Saunders, D., Seeger, K., Sharp, S., Skelton, J., Simmonds, M., Squares, R., Squares, S., Stevens, K., Taylor, K., Taylor, R.G., Tivey, A., Walsh, S., Warren, T., Whitehead, S., Woodward, J., Volckaert, G., Aert, R., Robben, J., Grymonprez, B., Weltjens, I., Vanstreels, E., Rieger, M., Schafer, M., Muller-Auer, S., Gabel, C., Fuchs, M., Fritze, C., Holzer, E., Moestl, D., Hilbert, H., Borzym, K., Langer, I., Beck, A., Lehrach, H., Reinhardt, R., Pohl, T.M., Eger, P., Zimmermann, W., Wedler, H., Wambutt, R., Purnelle, B., Goffeau, A., Cadieu, E., Dreano, S., Gloux, S., Lelaure, V., et al. (2002) 'The genome sequence of *Schizosaccharomyces pombe*', *Nature*, 415(6874), pp. 871-880.

Woodage, T., Basrai, M.A., Baxevanis, A.D., Hieter, P. and Collins, F.S. (1997) 'Characterization of the CHD family of proteins', *Proceedings of the National Academy of Sciences*, 94(21), pp. 11472-11477.

Wu, G., Liu, H., He, H., Wang, Y., Lu, X., Yu, Y., Xia, S., Meng, X. and Liu, Y. (2014) 'miR-372 down-regulates the oncogene ATAD2 to influence hepatocellular carcinoma proliferation and metastasis', *BMC Cancer*, 14, p. 107.

Wu, L., Zee, B.M., Wang, Y., Garcia, B.A. and Dou, Y. (2011) 'The RING finger protein MSL2 in the MOF complex is an E3 ubiquitin ligase for H2B K34 and is involved in crosstalk with H3 K4 and K79 methylation', *Mol Cell*, 43(1), pp. 132-44.

Wu, M., Wang, P.F., Lee, J.S., Martin-Brown, S., Florens, L., Washburn, M. and Shilatifard, A. (2008) 'Molecular regulation of H3K4 trimethylation by Wdr82, a component of human Set1/COMPASS', *Mol Cell Biol*, 28(24), pp. 7337-44.

Wu, W.-H., Alami, S., Luk, E., Wu, C.-H., Sen, S., Mizuguchi, G., Wei, D. and Wu, C. (2005) 'Swc2 is a widely conserved H2AZ-binding module essential for ATP-dependent histone exchange', *Nat Struct Mol Biol*, 12(12), pp. 1064-1071.

Xhemalce, B. and Kouzarides, T. (2010) 'A chromodomain switch mediated by histone H3 Lys 4 acetylation regulates heterochromatin assembly', *Genes Dev*, 24(7), pp. 647-52.

Xin, H., Takahata, S., Blanksma, M., McCullough, L., Stillman, D.J. and Formosa, T. (2009) 'yFACT Induces Global Accessibility of Nucleosomal DNA without H2A-H2B Displacement', *Molecular Cell*, 35(3), pp. 365-376.

Xu, H., Kim, U.J., Schuster, T. and Grunstein, M. (1992) 'Identification of a new set of cell cycle-regulatory genes that regulate S-phase transcription of histone genes in *Saccharomyces cerevisiae*', *Molecular and Cellular Biology*, 12(11), pp. 5249-5259.

- Yamane, K., Mizuguchi, T., Cui, B., Zofall, M., Noma, K.-i. and Grewal, S.I.S. (2011) 'Asf1/HIRA Facilitate Global Histone Deacetylation and Associate with HP1 to Promote Nucleosome Occupancy at Heterochromatic Loci', *Molecular Cell*, 41(1), pp. 56-66.
- Yanagida, M. (2009) 'Cellular quiescence: are controlling genes conserved?', *Trends in Cell Biology*, 19(12), pp. 705-715.
- Yang, X.J. and Seto, E. (2007) 'HATs and HDACs: from structure, function and regulation to novel strategies for therapy and prevention', *Oncogene*, 26(37), pp. 5310-5318.
- Yanow, S.K., Lygerou, Z. and Nurse, P. (2001) 'Expression of Cdc18/Cdc6 and Cdt1 during G₂ phase induces initiation of DNA replication', *EMBO J*, 20(7), pp. 4648-4656.
- Ye, X., Zerlanko, B., Zhang, R., Somaiah, N., Lipinski, M., Salomoni, P. and Adams, P.D. (2007) 'Definition of pRB- and p53-Dependent and -Independent Steps in HIRA/ASF1a-Mediated Formation of Senescence-Associated Heterochromatin Foci', *Molecular and Cellular Biology*, 27(7), pp. 2452-2465.
- Yen, K., Vinayachandran, V. and Pugh, B.F. (2013) 'SWR-C and INO80 Chromatin Remodelers Recognize Nucleosome-free Regions Near +1 Nucleosomes', *Cell*, 154(6), pp. 1246-1256.
- Zeng, Y., Forbes, K.C., Wu, Z., Moreno, S., Piwnica-Worms, H. and Enoch, T. (1998) 'Replication checkpoint requires phosphorylation of the phosphatase Cdc25 by Cds1 or Chk1', *Nature*, 395(6701), pp. 507-510.
- Zentner, G.E. and Henikoff, S. (2013) 'Regulation of nucleosome dynamics by histone modifications', *Nat Struct Mol Biol*, 20(3), pp. 259-266.
- Zhang, B., Chambers, K.J., Faller, D.V. and Wang, S. (2007a) 'Reprogramming of the SWI/SNF complex for co-activation or co-repression in prohibitin-mediated estrogen receptor regulation', *Oncogene*, 26(50), pp. 7153-7157.
- Zhang, R., Chen, W. and Adams, P.D. (2007b) 'Molecular Dissection of Formation of Senescence-Associated Heterochromatin Foci', *Molecular and Cellular Biology*, 27(6), pp. 2343-2358.
- Zhang, R., Poustovoitov, M.V., Ye, X., Santos, H.A., Chen, W., Daganzo, S.M., Erzberger, J.P., Serebriiskii, I.G., Canutescu, A.A., Dunbrack, R.L., Pehrson, J.R., Berger, J.M., Kaufman, P.D. and Adams, P.D. (2005) 'Formation of MacroH2A-Containing Senescence-Associated Heterochromatin Foci and Senescence Driven by ASF1a and HIRA', *Developmental Cell*, 8(1), pp. 19-30.
- Zhang, X., Yang, Z., Khan, S.I., Horton, J.R., Tamaru, H., Selker, E.U. and Cheng, X. (2003) 'Structural Basis for the Product Specificity of Histone Lysine Methyltransferases', *Molecular Cell*, 12(1), pp. 177-185.
- Zhao, Z.-K., Li, W., Wang, M.-Y., Zhou, L., Wang, J.-L. and Wang, Y.-F. (2011) 'The role of HIRA and maternal histones in sperm nucleus decondensation in the gibel carp and color crucian carp', *Molecular Reproduction and Development*, 78(2), pp. 139-147.
- Zou, J.X., Duan, Z., Wang, J., Sokolov, A., Xu, J., Chen, C.Z., Li, J.J. and Chen, H.W. (2014) 'Kinesin family deregulation coordinated by bromodomain protein ANCCA and histone methyltransferase MLL for breast cancer cell growth, survival, and tamoxifen resistance', *Mol Cancer Res*, 12(4), pp. 539-49.
- Zou, J.X., Guo, L., Revenko, A.S., Tepper, C.G., Gemo, A.T., Kung, H.-J. and Chen, H.-W. (2009) 'Androgen-Induced Coactivator ANCCA Mediates Specific Androgen Receptor Signaling in Prostate Cancer', *Cancer Research*, 69(8), pp. 3339-3346.
- Zou, J.X., Revenko, A.S., Li, L.B., Gemo, A.T. and Chen, H.-W. (2007) 'ANCCA, an estrogen-regulated AAA+ ATPase coactivator for ER α , is required for coregulator occupancy and chromatin modification', *Proceedings of the National Academy of Sciences*, 104(46), pp. 18067-18072.
- Zunder, R.M. and Rine, J. (2012) 'Direct Interplay among Histones, Histone Chaperones, and a Chromatin Boundary Protein in the Control of Histone Gene

Expression', *Molecular and Cellular Biology*, 32(21), pp. 4337-4349.

Appendix A – Microarray analysis of genes misregulated in the absence of *hip1*⁺ following 24 hours in nitrogen starvation induced G₀

2x Up-regulated			
aro1	SPBPB2B2.14c	SPNCRNA.1177	SPCC18B5.02c
tlh1	SPBPB2B2.19c	SPNCRNA.1196	SPAC3H1.02c
SPAC212.12	SPBPB2B2.17c	SPNCRNA.1199	map4
fet4	mug74	SPNCRNA.1195	SPBP18G5.02
htb1	SPNCRNA.1278	SPNCRNA.1193	SPAC1952.01
hta1	SPNCRNA.1271	SPNCRNA.1181	SPBC1289.14
Tf2-10-pseudo	SPNCRNA.1273	SPNCRNA.1187	Tf2-11
wtf12	SPNCRNA.1206	SPNCRNA.1139	SPBC119.17
gal1	SPNCRNA.1213	SPNCRNA.113	ago1
SPBPB2B2.08	SPNCRNA.1212	SPNCRNA.1150	mcp3
saf1	SPNCRNA.1288	SPNCRNA.1153	SPAC1B1.02c
SPAC977.13c	SPNCRNA.256	SPNCRNA.136	hht2
prp5	SPNCRNA.1289	SPAC13G6.08	mok13
nup132	SPNCRNA.1283	mis4	zrt1
pma2	SPNCRNA.1200	SPBPB21E7.06	mug24
cut4	SPNCRNA.1247	SPBPB21E7.09	tpx1
tbp1	SPNCRNA.1230	mug174	SPAPJ695.01c
sib1	SPNCRNA.1242	SPBC3H7.08c	SPBPB21E7.02c
SPAC26F1.07	SPNCRNA.284	mde7	uba5
vps1302	SPNCRNA.1004	SPBC18E5.15	eno102
rec10	SPNCRNA.1002	mse1	Tf2-3
SPCP20C8.03	SPNCRNA.1005	SPNCRNA.1098	SPCC1884.01
mrp20	SPNCRNA.1264	SPNCRNA.1097	SPCC16C4.21
SPCC584.01c	SPNCRNA.1269	SPNCRNA.1094	isp3
cch1	SPNCRNA.240	SPNCRNA.1095	chk1
mok11	SPNCRNA.232	SPNCRNA.1096	nxt2
ssr1	SPNCRNA.231	SPNCRNA.1027	dna2
trs120	SPNCRNA.230	SPNCRNA.1026	trt1
pre3	SPNCRNA.234	SPBC83.19c	SPAC750.01
top2	SPNCRNA.1299	SPBCPT2R1.06c	meu15
orb6	SPNCRNA.1298	cnl2	cut12
SPCC1672.03c	SPNCRNA.293	SPBCPT2R1.05c	dep1
heh2	SPNCRNA.1100	SPBCPT2R1.04c	mug110
SPBPB8B6.02c	SPNCRNA.1126	SPNCRNA.1056	SPBC23G7.06c
SPAC17H9.02	SPNCRNA.1117	SPNCRNA.1046	tra2
SPAC750.05c	SPNCRNA.1123	SPNCRNA.1047	SPAC1002.16c
grt1	SPNCRNA.1135	SPNCRNA.1006	SPCC11E10.01
SPAC750.07c	SPNCRNA.1134	SPNCRNA.1037	meu25
SPAC977.08	SPNCRNA.1105	SPNCRNA.1028	SPAC12G12.16c
SPAC977.02	SPNCRNA.1106	SPNCRNA.1033	SPBC354.11c
SPAC977.03	SPNCRNA.1122	SPNCRNA.1039	SPAC212.08c
SPAC977.01	SPNCRNA.1115	SPCC1450.01c	cbh2
SPAC977.06	SPNCRNA.1114	SPBC1348.07	SPCC330.19c
SPAC977.04	SPNCRNA.1108	SPBC1348.01	SPAC212.06c
SPAC1039.11c	SPNCRNA.1110	SPBC1348.03	gpi10
SPAC24H6.01c	SPNCRNA.1436	SPBC1271.08c	SPAC212.05c
spo2	SPNCRNA.1439	SPBC1348.05	zas1
chp2	SPNCRNA.1410	tim54	akr1
mde4	SPNCRNA.1428	SPNCRNA.1044	bgs1
ppk24	SPNCRNA.1429	tlh2	SPAC23A1.19c
dcr1	SPNCRNA.1434	SPBC19C7.04c	meu27

SPNCRNA.601	SPNCRNA.1498	mug14	SPBCPT2R1.02
SPNCRNA.871	SPNCRNA.1401	alp1	SPAC24H6.08
SPNCRNA.617	SPNCRNA.1423	SPAC513.07	fml1
SPNCRNA.618	SPNCRNA.1421	isp7	Tf2-1
SPNCRNA.619	SPNCRNA.1176	SPAC23D3.05c	cyr1
SPNCRNA.616	SPNCRNA.1174	wtf1	SPBC36B7.04
SPNCRNA.603	SPNCRNA.155	hrr1	SPAC29E6.06c
SPNCRNA.602	SPNCRNA.154	SPNCRNA.747	gcn2
SPNCRNA.900	SPNCRNA.1179	SPNCRNA.742	Tf2-8
SPNCRNA.892	SPNCRNA.1178	SPNCRNA.744	btn1
SPNCRNA.901	SPNCRNA.978	SPNCRNA.729	srb8
SPNCRNA.922	SPNCRNA.977	SPNCRNA.726	deb1
SPNCRNA.883	SPNCRNA.980	SPNCRNA.727	tel2
SPNCRNA.898	SPNCRNA.949	SPNCRNA.732	sap114
SPNCRNA.896	SPNCRNA.986	SPNCRNA.731	cwg2
SPNCRNA.556	SPNCRNA.982	SPNCRNA.734	rdp1
SPNCRNA.555	SPNCRNA.754	SPNCRNA.571	SPBC725.03
SPNCRNA.541	SPNCRNA.773	SPNCRNA.564	tfb4
SPNCRNA.551	SPNCRNA.905	SPNCRNA.560	obr1
SPNCRNA.607	SPNCRNA.942	SPNCRNA.563	SPAC13A11.06
SPNCRNA.507	SPNCRNA.906	SPNCRNA.576	pbi2
SPNCRNA.610	SPNCRNA.928	SPNCRNA.581	skb15
SPNCRNA.515	SPNCRNA.310	SPNCRNA.580	SPCC1529.01
SPNCRNA.510	SPNCRNA.687	SPNCRNA.633	Tf2-13-pseudo
SPNCRNA.972	SPNCRNA.672	SPNCRNA.637	SPAP8A3.05
SPNCRNA.1618	SPNCRNA.325	SPNCRNA.711	cut1
SPNCRNA.1607	SPNCRNA.646	SPNCRNA.652	SPNCRNA.1697
SPNCRNA.1606	SPNCRNA.671	SPNCRNA.705	SPNCRNA.1478
SPNCRNA.1339	SPNCRNA.677	SPNCRNA.706	SPNCRNA.1471
SPNCRNA.1338	SPNCRNA.679	SPNCRNA.707	SPNCRNA.1377
SPNCRNA.1334	SPNCRNA.678	SPNCRNA.712	SPNCRNA.1393
SPNCRNA.1335	SPNCRNA.79	SPNCRNA.1620	SPNCRNA.1456
SPNCRNA.1345	prl67	SPNCRNA.1621	SPNCRNA.1446
SPNCRNA.1664	SPNCRNA.70	SPNCRNA.1307	SPNCRNA.1454
SPNCRNA.1682	SPNCRNA.76	SPNCRNA.1308	SPNCRNA.1460
SPNCRNA.1645	SPNCRNA.307	SPNCRNA.1368	SPNCRNA.1488
SPNCRNA.1648	SPNCRNA.88	SPNCRNA.1363	SPNCRNA.1484
SPNCRNA.1627	SPNCRNA.319	SPNCRNA.1382	SPNCRNA.1450
SPNCRNA.1640	mrp1	SPNCRNA.1383	SPNCRNA.1451
SPNCRNA.1637	SPNCRNA.852	SPNCRNA.1371	SPNCRNA.1300
SPNCRNA.1693	SPNCRNA.855	SPNCRNA.1385	SPNCRNA.1311
SPNCRNA.1694	SPNCRNA.998	SPNCRNA.1320	SPNCRNA.1310
SPNCRNA.1690	SPNCRNA.997	SPNCRNA.1315	SPNCRNA.1301
SPNCRNA.1632	SPNCRNA.829	ec11	SPNCRNA.1590
SPCPB16A4.07	SPNCRNA.828	SPNCRNA.836	SPNCRNA.1591
SPNCRNA.401	SPNCRNA.990	SPNCRNA.838	SPNCRNA.1506
SPNCRNA.469	SPNCRNA.799	SPNCRNA.858	SPNCRNA.1587
SPNCRNA.410	SPNCRNA.796	SPNCRNA.860	SPNCRNA.1673
SPNCRNA.448	SPNCRNA.820	SPNCRNA.373	SPNCRNA.1687
SPNCRNA.483	SPNCRNA.822	SPNCRNA.372	SPNCRNA.1546
SPNCRNA.482	SPNCRNA.761	SPNCRNA.361	SPNCRNA.1529
SPNCRNA.485	SPNCRNA.760	SPNCRNA.360	SPNCRNA.1531
prl28	SPNCRNA.764	SPATRAGLU.02	SPNCRNA.1539
prl31	SPNCRNA.801	SPBTRNAASN.04	SPNCRNA.1535
SPNCRNA.359	SPNCRNA.868	SPATRNALEU.02	SPNCRNA.1577
prl56	SPNCRNA.864	SPBTRNALEU.05	SPNCRNA.1579

SPNCRNA.451	SPNCRNA.818	SPBTRNALEU.10	SPNCRNA.1565
prl15	SPNCRNA.803	SPBTRNAGLY.08	SPNCRNA.1559
prl14	SPCTRNAASN.05	SPBTRNALEU.09	SPNCRNA.499
prl11	SPCTRNAILE.09	snoR69b	snoU14
meu3	arp8	sno12	snR30
SPAC19G12.09	SPAC212.01c	snoR47	sno20
SPBC24C6.08c	rik1	SPATRNAILE.02	snR91
SPBC21C3.19	SPAC1399.01c	SPCTRNAARG.10	snoZ16
SPAC5H10.04	SPAC2E1P3.01	SPBTRNAILE.06	SPNCRNA.402
med13	SPAC4F10.16c	SPCTRNAVAL.10	pck1
grx2	SPAPB24D3.08c	SPCC1450.09c	SPCC70.08c
SPAC4H3.03c	sen1	SPAPB24D3.07c	cid11
mug4	rhp42	SPBC17D1.07c	zym1
SPCC663.14c	SPCC4B3.06c	SPCC663.08c	SPBC56F2.03
clr4	mug132	SPBC1685.05	pho1
pof3	SPCC188.09c	SPAC6C3.03c	SPBC215.11c
SPCC1919.12c	apm4	cta5	ppk31
SPBC530.06c	meu6	SPCC569.03	SPAC22E12.03c
hsp9	dak1	inv1	SPCC13B11.04c
SPAC977.14c	tea2	meu17	exo5
SPAC6F6.04c	SPAC19G12.04	SPBC28E12.02	dak2
SPBPB2B2.18	SPBC800.11	rdh54	SPBPB2B2.09c
mug86	SPCC777.04	SPAC18G6.05c	tae1
SPACUNK4.17	rrg9	gut2	cds1
SPCC663.06c	gal10	myh1	cta3
SPCC777.03c	bgs2	SPBC1198.01	amt3
SPBC8E4.02c	SPAC212.04c	rsv1	SPAC4F10.17
SPCC13B11.03c	meu7	SPAC11D3.01c	spo6
SPCC11E10.07c	hta2	SPBC17G9.12c	mcp5
SPBC800.12c	kap113	SPAC57A7.05	hrp3
ght3	SPAC977.15	SPAC186.06	gst1
SPACUNK4.15	adn3	mde2	mug79
mug97	mok14	SPBPB2B2.11	ssa1
gst2	SPCC320.06	ght7	SPAC212.02
ast1	SPAC1635.01	rga9	whi5
SPBC359.01	ppk6	SPCC417.11c	SPAC12B10.10
mok12	SPBC2A9.02	SPBC685.03	SPAC27F1.05c
SPCC330.06c	SPAC11D3.09	meu8	bud6
SPAC750.06c	SPAC23H3.15c	SPCC794.01c	SPAC5H10.05c
SPAC186.05c	eri1	mug35	ctf18
SPBC1683.12	get4	fft2	gld1
SPBC582.10c	SPCC1281.07c	SPAC5H10.12c	SPAC186.03
crp79	SPAC1F8.04c		

2x Down-regulated

SPNCRNA.1562	psk1	mge1	SPAC227.06
SPNCRNA.1415	cgs1	SPAC15A10.07	mfm2
SPNCRNA.993	vps20	SPAC11D3.17	SPAC513.04
SPNCRNA.1512	SPBTRNAGLY.09	aur1	gpa1
map1	tam6	rrn3	set7
mfm1	fmc1	SPAC18G6.12c	mae2
SPCC24B10.03	gas1	mam2	SPAC1805.02c
SPCC188.05	mug134	tfb5	SPBP4H10.14c
tim11	wsc1	matmc_1	SPCC16C4.22
SPAC4H3.12c	SPAC630.10	dni2	SPNCRNA.1055
mug177	SPAC24H6.11c	SPBC1711.16	ams2
SPNCRNA.1209	SPAC105.02c	SPAC144.01	SPCC1020.08
omt3	SPBC691.04	SPBC21C3.17c	mcs6
SPNCRNA.1232	pab1	snR97	SPBC13A2.04c
sme1	SPCC18.17c	SPBC19F8.03c	cdc18
SPNCRNA.1000	SPAC5D6.13	spe2	SPAC22F8.04
SPNCRNA.217	SPAC15A10.09c	mei2	SPAC22F8.05
SPNCRNA.608	pof4	spk1	SPAC23C11.06c
SPNCRNA.534	SPAPB1A10.08	mug176	SPBC244.02c
SPNCRNA.988	SPAC4A8.07c	rav2	gmh2
SPNCRNA.380	arv1	SPAC227.11c	hip1
SPNCRNA.585	SPCC553.12c	scw1	SPNCRNA.642
SPNCRNA.658	ste11	mis13	rnp24
SPNCRNA.460	SPAC4G9.20c	SPCPB1C11.03	omh1
cdr1	SPAC11D3.03c	snR33	SPNCRNA.775
mlh1	SPAC11D3.04c	apc10	SPNCRNA.1448
pvg5	SPCC737.04	SPBC3E7.11c	SPNCRNA.1378
SPCC4B3.02c	ppk14	SPAC16A10.01	SPNCRNA.1452
SPAC22A12.06c	isp5	uge1	SPNCRNA.863
ogm1	pyk1	ppk1	SPNCRNA.994
SPAC869.04	SPBC25H2.10c	SPBPB21E7.04c	SPNCRNA.1652
SPBC4C3.04c	SPAC19G12.05	sfp1	SPNCRNA.817
csn4	leu2	but2	SPNCRNA.1254
SPAC644.05c	urg1	SPBC3B8.06	pet117
mug103	isp4	mac1	SPAC227.19c
pmp1	mam4	toc1	SPNCRNA.717
bet3	SPBC25B2.08	put4	SPNCRNA.1058
SPBC23E6.10c	SPAC23H4.04	cdt1	SPNCRNA.298
pas1	SPCC1322.09	SPBC27.01c	SPNCRNA.586
SPBC1604.09c	spb1	SPCC70.03c	SPNCRNA.577
fta6	SPAC227.01c	SPAC5H10.03	SPNCRNA.1107
SPBC409.08	SPBC543.02c	dea2	SPNCRNA.945
SPBCPT2R1.10	str3	SPAC922.04	SPNCRNA.111
SPAC869.03c	SPAC1687.08	SPBC1105.18c	cox20
SPCC1795.12c	SPAC1687.07	SPCC594.02c	SPNCRNA.1182
ste6	pop3	gpd2	SPNCRNA.1203
SPBC4F6.14	rrp8	srw1	SPNCRNA.106
dbp3	SPAC56F8.07	SPBC83.13	SPNCRNA.1102
str1	snoZ5	pmr1	SPCC550.15c
SPAP14E8.02	SPBC18A7.01	prz1	SPAC13C5.05c
ppk33	SPCC18.15	gcv2	mpg1
hem13	SPAC977.11	SPBC17G9.06c	cek1
laf2	has1	ibp1	rgs1
sst4	SPNCRNA.454	byr1	SPNCRNA.78
SPBPB8B6.06c	SPCC23B6.02c	pis1	SPNCRNA.77

SPBC16G5.09	gcv3	pac2	SPNCRNA.75
SPAC22A12.16	SPCC330.03c	SPCC757.12	mmd1
SPBC27B12.02	oar2	SPCC757.13	SPAC2H10.01
erg25	SPAC1687.14c	SPBC839.14c	SPBC146.08c
SPAC328.09	sec73	snu23	mph1
mae1	SPBC15C4.06c	SPNCRNA.73	SPNCRNA.71
mam1	SPBP22H7.03	rpc10	SPNCRNA.72
SPAC14C4.01c	SPAC212.10	prl59	frp1
new2			

Appendix B. Datasets used for MNase-sequencing

1. List of solo LTRs used in alignments.

Chromosome Number	Unique identifier	Alignment Start Site (0)	Orientation
chrI	LTR1	28124	F
chrI	LTR2	54499	F
chrI	LTR3	397370	R
chrI	LTR4	617366	F
chrI	LTR5	670131	R
chrI	LTR6	1004892	F
chrI	LTR7	1118434	F
chrI	LTR8	1142619	F
chrI	LTR9	1266166	R
chrI	LTR10	2012006	F
chrI	LTR11	2174235	R
chrI	LTR12	2186786	F
chrI	LTR13	2474583	R
chrI	LTR14	2605356	F
chrI	LTR15	2694225	R
chrI	LTR16	2844091	R
chrI	LTR17	2854057	F
chrI	LTR18	2942286	R
chrI	LTR19	3190954	F
chrI	LTR20	4140896	R
chrI	LTR21	4897866	R
chrI	LTR22	4939621	F
chrI	LTR23	4941720	F
chrI	LTR24	5021560	F
chrI	LTR25	5066762	R
chrI	LTR26	5325497	R
chrI	LTR27	5496655	R
chrII	LTR28	4835	F
chrII	LTR29	93860	R
chrII	LTR30	96619	R
chrII	LTR31	99378	R
chrII	LTR32	102137	R
chrII	LTR33	458478	F
chrII	LTR34	676281	F
chrII	LTR35	847051	R
chrII	LTR36	942476	F
chrII	LTR37	1079189	F
chrII	LTR38	1826267	F
chrII	LTR39	2012648	R
chrII	LTR40	2081276	R
chrII	LTR41	2163463	F

chrII	LTR42	2340297	R
chrII	LTR43	2380161	F
chrII	LTR44	2636814	F
chrII	LTR45	3106180	R
chrII	LTR46	3283208	R
chrII	LTR47	3489651	R
chrII	LTR48	3490610	R
chrII	LTR49	3659390	R
chrII	LTR50	3676727	F
chrII	LTR51	4047404	F
chrII	LTR52	4217977	F
chrII	LTR53	4231522	F
chrII	LTR54	4297025	R
chrII	LTR55	4409793	F
chrII	LTR56	4437498	F
chrII	LTR57	4437850	F
chrII	LTR58	4481842	R
chrII	LTR59	4508064	R
chrIII	LTR60	43111	F
chrIII	LTR61	114382	F
chrIII	LTR62	257531	R
chrIII	LTR63	287053	R
chrIII	LTR64	298890	R
chrIII	LTR65	382003	R
chrIII	LTR66	489396	R
chrIII	LTR67	499951	F
chrIII	LTR68	614910	F
chrIII	LTR69	701782	F
chrIII	LTR70	954537	F
chrIII	LTR71	1176592	R
chrIII	LTR72	1207147	F
chrIII	LTR73	1400870	F
chrIII	LTR74	1530150	F
chrIII	LTR75	1574724	F
chrIII	LTR76	1579526	R
chrIII	LTR77	1582318	R
chrIII	LTR78	1632545	R
chrIII	LTR79	1684578	F
chrIII	LTR80	1716629	R
chrIII	LTR81	1741307	R
chrIII	LTR82	1862384	R
chrIII	LTR83	2017345	R
chrIII	LTR84	2040788	F
chrIII	LTR85	2083919	F
chrIII	LTR86	2108631	R
chrIII	LTR87	2120137	R

chrIII	LTR88	2145096	F
chrIII	LTR89	2148502	R
chrIII	LTR90	2159089	R
chrIII	LTR91	2180475	F
chrIII	LTR92	2210988	R
chrIII	LTR93	2220754	R
chrIII	LTR94	2230688	R
chrIII	LTR95	2422329	F

2. Top 10% highly expressed protein coding genes (Marguerat *et al.*, 2012).

Chromosome Number	Unique identifier	Alignment Start Site (0)	Orientation
chrII	SPBC32F12.11	2807637	F
chrII	SPBC19C2.07	1688332	F
chrII	SPBC1815.01	2201208	F
chrIII	SPCC13B11.01	1591327	F
chrI	SPAC4H3.10c	3846655	R
chrI	SPAC26F1.06	5174638	R
chrIII	SPCC1223.02	1838485	F
chrI	SPAC1F8.07c	103580	R
chrII	SPBC26H8.01	3939420	F
chrII	SPBC14F5.04c	4159425	R
chrIII	SPCC1739.13	2057066	F
chrI	SPAC6F6.07c	2746658	R
chrII	SPBC106.18	413556	F
chrII	SPBC839.15c	627506	R
chrIII	SPCC794.09c	269479	R
chrI	SPAC664.05	1711170	F
chrII	SPBC1709.05	1106447	F
chrI	SPAC1071.10c	3876086	R
chrI	SPAC23A1.10	4095149	F
chrI	SPAC1071.07c	3868989	R
chrII	SPBC32H8.12c	1477314	R
chrII	SPBC16G5.14c	4239336	R
chrIII	SPCC24B10.21	939926	F
chrIII	SPCC576.08c	2096008	R
chrIII	SPCC576.09	2096558	F
chrIII	SPCC622.18	1437153	F
chrI	SPAC6B12.15	2439532	F
chrI	SPAC926.04c	3891098	R
chrI	SPAPB15E9.01c	3991477	R
chrII	SPBC18E5.06	2083868	F
chrII	SPBC14F5.05c	4162528	R
chrIII	SPCC417.08	1685650	F
chrI	SPAC1805.13	2794938	F
chrI	SPAC959.08	3400542	F
chrII	SPBC800.04c	259998	R
chrI	SPAC9.09	1478412	F
chrII	SPBC29A3.04	2045495	F
chrI	SPAC18G6.14c	2242523	R
chrII	SPBC18E5.04	2081514	F
chrIII	SPCC1393.03	798248	F
chrI	SPAC17A5.03	1756109	F
chrI	SPAC6G10.11c	3238362	R
chrI	SPAPB1E7.12	3319260	F

chrI	SPAC26A3.04	3337748	F
chrI	SPAC15E1.03	3722471	F
chrI	SPAPJ698.02c	4037620	R
chrIII	SPCC18.14c	1981891	R
chrI	SPAC22H12.04c	898949	R
chrI	SPAC23A1.08c	4093772	R
chrI	SPAC23A1.11	4097334	F
chrI	SPAC694.05c	4208847	R
chrI	SPAC1F7.13c	4251463	R
chrI	SPAC4F10.14c	4860619	R
chrI	SPAC1006.07	5085532	F
chrII	SPBC354.12	578723	F
chrII	SPBC3D6.02	1268477	F
chrII	SPBC17G9.07	2180906	F
chrII	SPBC365.03c	2503750	R
chrII	SPBC336.10c	2759237	R
chrII	SPBC56F2.12	4088141	R
chrII	SPBC16A3.08c	4283938	F
chrIII	SPCC5E4.07	656625	F
chrII	SPBC1685.02c	499026	R
chrII	SPBC18H10.14	1793928	F
chrII	SPBC685.07c	2780653	R
chrIII	SPCP31B10.08c	540791	R
chrIII	SPCC576.03c	2085722	R
chrI	SPAC8C9.08	3655144	F
chrII	SPBC28F2.03	1576311	F
chrI	SPAC1F12.02c	3810034	R
chrIII	SPCC613.05c	89570	R
chrII	SPBP8B7.06	3643189	F
chrIII	SPCC24B10.09	917864	F
chrII	SPBC3B9.13c	4009384	R
chrIII	SPCC576.11	2099856	F
chrII	SPBC685.06	2778923	F
chrII	SPBC23G7.15c	2128440	R
chrIII	SPCC962.04	553165	F
chrIII	SPCC1183.08c	612565	R
chrI	SPAC8E11.02c	3384221	F
chrIII	SPCC1281.06c	1394865	R
chrI	SPAPB8E5.06c	4918991	R
chrIII	SPCC1682.14	400761	F
chrI	SPAC3G6.13c	5402233	R
chrI	SPAC1A6.04c	1077518	R
chrII	SPBC1685.10	517344	F
chrI	SPAC26H5.10c	4142339	R
chrIII	SPCC330.14c	138575	R
chrI	SPAC589.10c	3108885	R

chrI	SPAC24C9.12c	3071102	R
chrI	SPAC521.05	849486	F
chrI	SPAC23C11.05	2140503	F
chrI	SPAC2C4.16c	4287431	R
chrIII	SPCC16C4.13c	691657	R
chrI	SPAC4G9.16c	2284216	R

3. Top 10% low-level expressed protein coding genes (Marguerat *et al.*, 2012).

Chromosome Number	Unique identifier	Alignment Start Site (0)	Orientation
chrIII	SPCC4F11.05	2010426	F
chrI	SPAC1F8.04c	93871	R
chrII	SPBPB2B2.01	4457742	F
chrI	SPAC2E12.05	5063258	F
chrI	SPAC750.05c	5567565	R
chrII	SPBPB2B2.12c	4487496	R
chrII	SPBPB2B2.19c	4505257	R
chrII	SPBC1348.02	7663	F
chrII	SPBC359.04c	119803	R
chrIII	SPCC576.17c	2113660	R
chrI	SPAC22G7.03	731938	F
chrII	SPBC17D1.07c	3344541	R
chrII	SPBCPT2R1.01c	4507540	R
chrII	SPBCPT2R1.04c	4514667	R
chrI	SPAC2G11.05c	817916	R
chrII	SPBC106.08c	388806	R
chrII	SPBC36.02c	840579	R
chrI	SPAC4H3.08	3841540	F
chrI	SPAC4F10.05c	4838311	R
chrII	SPBC685.05	2777829	F
chrI	SPAPB17E12.10c	1282776	R
chrI	SPAC1805.07c	2786148	R
chrII	SPBC18H10.09	1786501	F
chrII	SPBC18H10.11c	1790736	R
chrII	SPBC1271.01c	371978	F
chrII	SPBC1105.17	3538582	F
chrI	SPAC1B3.11c	4950071	R
chrII	SPBC18H10.10c	1789088	R
chrI	SPAC4G8.11c	783267	R
chrI	SPAC513.02	2911657	F
chrI	SPAC16A10.05c	3089362	R
chrI	SPAC15A10.05c	3686777	R
chrI	SPAC4H3.04c	3836101	R

chrI	SPAC17C9.05c	4490378	F
chrI	SPAC27D7.13c	4536686	R
chrII	SPBC1348.01	5386	F
chrI	SPAC6B12.06c	2420894	R
chrII	SPBC16E9.07	1926374	F
chrI	SPAC22F3.12c	679812	F
chrI	SPAC1556.04c	3801068	R
chrII	SPBC1683.09c	162372	R
chrII	SPBC1773.13	310702	F
chrII	SPBC21B10.12	1649671	R
chrI	SPAC688.06c	3119170	R
chrII	SPBC18E5.08	2088238	F
chrII	SPBC15D4.11c	3031431	R
chrII	SPBC1604.18c	3898065	F
chrII	SPBPB2B2.05	4466651	F
chrIII	SPCC364.01	486011	R
chrIII	SPCPB1C11.02	2072907	F
chrI	SPAC1565.03	1294381	F
chrII	SPBC83.12	1531988	F
chrI	SPAC32A11.01	2445257	F
chrI	SPAC3A11.06	3462098	R
chrIII	SPCC1494.09c	2343890	R
chrI	SPAC20G4.02c	4817740	R
chrI	SPAC23H3.12c	2515985	R
chrI	SPAC19G12.04	4049553	F
chrI	SPAC19G12.13c	4070840	R
chrI	SPAC27D7.03c	4514964	R
chrI	SPAC18B11.03c	311918	F
chrI	SPAC630.07c	359051	R
chrI	SPAC3C7.09	2083358	F
chrII	SPBC36.01c	835352	R
chrII	SPBC16E9.03c	1921745	R
chrII	SPBC3B9.22c	4006355	R
chrIII	SPCC962.05	554379	F
chrI	SPAC7D4.09c	2622466	F
chrI	SPAC11H11.02c	4778521	R
chrII	SPBC3B9.17	4020309	F
chrII	SPBC215.04	4030555	F
chrI	SPAC11D3.05	114026	F
chrI	SPAC1002.01	1798347	F
chrI	SPAC16E8.02	3504068	F
chrI	SPAC11E3.08c	5297733	R
chrII	SPBP35G2.04c	970048	R
chrII	SPBC685.02	2772768	F
chrI	SPAC12G12.16c	315655	F
chrII	SPBC11B10.06	1494857	F

chrII	SPBC21B10.11	1650658	R
chrII	SPBC12D12.06	2316043	F
chrI	SPAC13C5.06c	435996	R
chrI	SPAC823.16c	2610917	R
chrI	SPAC30C2.03	4637119	F
chrI	SPAC186.01	5527572	F
chrII	SPBC800.11	275671	F
chrII	SPBC106.02c	376983	R
chrII	SPBC409.12c	1163209	R
chrII	SPBC16E9.06c	1926201	R
chrII	SPBC609.04	3166458	F
chrIII	SPCC736.02	313147	F
chrI	SPAC343.03	1643082	F
chrI	SPAC3A11.04	3466335	R
chrII	SPBC1703.04	2921241	F
chrII	SPBC2D10.13	2988635	F
chrII	SPBC317.01	3625865	F
chrII	SPBC3B9.09	4002946	F
chrII	SPBC685.04c	2777112	R
chrII	SPBC16C6.10	4349614	F

4. List of genes with particularly disorganized dinucleosome peaks in *abo1Δ* cells

SPAC25B8.03	SPAC16C9.04c	SPAPB24D3.07c	SPAC5H10.05c	SPBC336.14c
SPAC17C9.13c	SPAC1687.03c	SPAC31G5.09c	SPAC1F5.10	SPBC19C7.05
SPAC12B10.03	SPAC1687.15	SPAC26H5.11	SPAC139.04c	SPBC19C7.11
SPAC1834.09	SPAC1687.19c	SPAC25B8.02	SPAC22A12.03c	SPBP4H10.17c
SPAC1B3.06c	SPAC56F8.10	SPAC29E6.01	SPAC607.09c	SPBC25H2.14
SPAC1B3.07c	SPAC22A12.01c	SPAC22F8.11	SPAC18G6.15	SPBC17D11.06
SPAC2E12.03c	SPAC6F12.12	SPAC1952.06c	SPAC13D6.03c	SPBC2G2.15c
SPAC11E3.09	SPAC3H1.14	SPAC890.08	SPAC19A8.15	SPBC16D10.02
SPAC18B11.04	SPAC23H3.05c	SPAC29A4.14c	SPAC23H3.14	SPBC317.01
SPAC31A2.11c	SPAC7D4.03c	SPAC977.10	SPAC31G5.02	SPBC1347.12
SPAC2F7.04	SPAC6F6.05	SPAC1F8.04c	SPAC1B1.02c	SPBC16A3.10
SPAC1D4.13	SPAC1B2.04	SPAC11D3.14c	SPAC1F12.04c	SPBC16C6.03c
SPAC1687.13c	SPAC3G9.09c	SPAC5H10.08c	SPAC4H3.10c	SPCC320.10
SPAC10F6.17c	SPAC3G9.07c	SPAC23C4.14	SPAC1071.13	SPCC548.06c
SPAC57A10.09c	SPAC2F3.01	SPAC5D6.07c	SPAC2F3.05c	SPCC338.16
SPAP27G11.12	SPAC2F3.16	SPAPB1A10.04c	SPAPB15E9.01c	SPCC584.14
SPAC1610.04	SPAC458.04c	SPAPB1A10.15	SPAC26H5.08c	SPCC584.02
SPAC110.04c	SPAPJ691.02	SPAC140.04	SPAC683.02c	SPCC576.03c
SPAC9G1.04	SPAC11E3.15	SPAC4F8.03	SPAC17C9.15c	SPCC830.03
SPAC607.05	SPAC750.07c	SPAC589.06c	SPAC144.14	SPCC613.04c
SPAC732.01	SPAC11D3.06	SPAC589.07c	SPAC4F10.18	SPCC4G3.19
SPAC15F9.03c	SPAC5H10.06c	SPAC3A11.11c	SPAC14C4.15c	SPCC364.01
SPAC6B12.03c	SPAC5H10.11	SPAC926.07c	SPAC1039.08	SPCC1672.01
SPAPB2B4.05	SPAC13G6.03	SPAC926.08c	SPAC977.17	SPCC16C4.05
SPAC2E1P3.02c	SPAC1751.04	SPAC2F3.14c	SPAC5H10.04	SPCC1393.08
SPAC31G5.08	SPAC1751.02c	SPAC25B8.08	SPAC12G12.10	SPCC24B10.21
SPAC16A10.02	SPAC227.14	SPAC23D3.12	SPAC2F7.07c	SPCC550.07
SPAC1071.12c	SPAC4G8.03c	SPAC16.05c	SPAC1296.05c	SPCC417.08
SPAC25G10.01	SPAC1A6.05c	SPAC27D7.04	SPAC139.01c	SPCC1442.05c
SPAC17C9.11c	SPAC30D11.07	SPAC144.18	SPAC20G8.03	SPCC18.07
SPAPYUG7.03c	SPAPB1A10.08	SPAC922.03	SPAC1002.16c	SPCC965.05c
SPAC19B12.02c	SPAC6C3.08	SPAC869.10c	SPAC20H4.02	SPCC330.04c
SPAPB8E5.07c	SPAC23H3.07c	SPAC1F5.07c	SPAC13F5.05	SPCC970.05
SPAC1952.07	SPAC4A8.10	SPAC12G12.09	SPAC18G6.10	SPCC1183.02
SPAC1250.02	SPAC7D4.14c	SPAC3H8.10	SPAC22H10.08	SPCC1183.03c
SPAC3G6.03c	SPAC8F11.04	SPAC22F3.08c	SPAC8F11.09c	SPCC1183.10
SPBC119.09c	SPBC582.04c	SPBP4G3.03	SPAC750.01	SPCC622.05
SPBC216.03	SPBC428.02c	SPBC1773.08c	SPAC57A10.05c	SPCC1223.04c
SPBC1709.05	SPBC1709.10c	SPBC1773.16c	SPAP27G11.03	SPCC1919.06c
SPBC32H8.11	SPBC725.17c	SPBC1271.12	SPAC343.13	SPCC1919.15
SPBC28F2.04c	SPBC3D6.02	SPBC1271.05c	SPAC20H4.07	SPCC790.02
SPBC16E9.03c	SPBC11B10.03	SPBC428.14	SPAC13F5.04c	SPCC1235.17
SPBP23A10.08	SPBC1215.02c	SPBC428.19c	SPAC17G8.07	SPCC4G3.18
SPBC23G7.08c	SPBC17G9.13c	SPBC354.03	SPAC6F6.09	SPCC1672.05c
SPBC24C6.10c	SPBC16H5.03c	SPBC3H7.12	SPACUNK4.19	SPCC645.04
SPBC1921.06c	SPBC36B7.04	SPBC1711.16	SPAC6G9.03c	SPCC965.06

SPBC3E7.05c	SPBC1921.07c	SPBP18G5.02	SPAC926.03	SPCC794.09c
SPBP19A11.07c	SPBC3E7.12c	SPBC32F12.06	SPAC323.05c	SPCC553.05c
SPBP4H10.07	SPBC32F12.02	SPBC17D1.04	SPAC23A1.10	SPCC594.04c
SPBC1703.08c	SPBC19C7.10	SPBC3B8.06	SPAC694.05c	SPCC24B10.05
SPBC30D10.11	SPBC215.09c	SPBC1105.06	SPAC17C9.02c	SPCC13B11.01
SPBC1778.04	SPBC16G5.03	SPBC887.02	SPAC29A4.02c	SPCC18.13
SPBC19F8.07	SPBC1683.06c	SPBC3B9.13c	SPAC4D7.04c	SPCC1739.15
SPBC25H2.18	SPBC800.05c	SPBC1652.01	SPAC186.04c	SPCC830.07c
SPBC3B8.07c	SPBC1271.09	SPBP4G3.02	SPAC750.02c	SPCC613.03
SPBC2G2.05	SPBC947.08c	SPBPB2B2.10c	SPAC977.14c	SPCC794.01c
SPBC1718.03	SPBPJ4664.04	SPBPJ4664.06	SPAC18B11.09c	SPCC1529.01
SPBC887.03c	SPBC119.04	SPBC30B4.01c	SPAC3H8.06	SPCC4B3.12
SPBC19F5.03	SPBC1734.11	SPBC30B4.02c	SPAC1687.10	SPBC1773.01
SPBC1604.07	SPBC1734.12c	SPBC9B6.11c	SPAC30D11.02c	SPBC1685.12c
SPBC215.10	SPBP22H7.03	SPBC3H7.01	SPAC1565.08	SPCC14G10.01
SPBC1289.11	SPBP22H7.09c	SPBC29A3.03c	SPAC9.11	SPCC1393.06c
SPBC1348.05	SPBC3H7.13	SPBC365.09c	SPAC3C7.14c	SPCC1919.11
SPBC359.06	SPBC14C8.05c	SPBC6B1.09c	SPAC23C11.14	SPCP20C8.01c
SPBC1683.11c	SPBC36B7.09	SPBC1703.07	SPAC13D6.01	SPCC569.09
SPBC902.02c	SPBC365.05c	SPBC30D10.05c	SPAC4G9.20c	SPCC569.03
SPBC36.10	SPBC32F12.17	SPBC4B4.02c	SPAC823.14	SPBC1198.08
SPBC83.09c	SPBP4H10.19c	SPBC16D10.03	SPAC1805.01c	SPBC800.13
SPBP16F5.06	SPBC2D10.20	SPBP8B7.13	SPAC1805.08	SPCC31H12.02c
SPBC16E9.01c	SPBC1778.08c	SPBC215.05	SPAC688.13	SPCC31H12.06
SPBP23A10.10	SPBC20F10.04c	SPBC215.11c	SPAC1486.10	SPCC191.09c
SPBC14C8.04	SPBC3B8.04c	SPBC543.10	SPAC3A11.13	SPCC1223.14
SPBC32F12.07c	SPBC13A2.03	SPBC1289.16c	SPAC323.02c	SPCC1494.09c
SPBC1778.07	SPBC887.18c	SPBC1348.14c	SPAC323.03c	SPCC1827.04
SPBC776.16	SPBC21C3.18	SPBC1683.09c	SPAC323.06c	SPBCPT2R1.01 c
SPBC32C12.02	SPBC211.01	SPBC530.02	SPAPB8E5.02c	SPBC1683.07
SPBC56F2.12	SPBC16G5.06	SPBC646.06c	SPAC1B3.15c	SPBC29A10.03c
SPBC3F6.04c	SPBC16G5.07c	SPBP35G2.09	SPAC4D7.02c	SPBC4F6.09
SPBC1289.06c	SPBC16E9.12c	SPBC409.16c	SPAC4D7.10c	SPCC1450.08c
SPBPB2B2.13	SPBC1711.10c	SPBC83.04	SPAC29B12.11c	SPCC330.02
SPBC1348.01	SPBC17G9.05	SPBC83.11	SPAC186.01	SPCC550.02c
SPBPB21E7.02c	SPBC19G7.14c	SPBC18H10.11c	SPBPB21E7.09	SPCC622.21
SPBC1773.15	SPBC12C2.03c	SPBC18H10.17c	SPBC1198.03c	SPBC16D10.09
SPBC106.15	SPBC29A10.14	SPBC18H10.18c	SPBC1198.14c	SPBC365.03c
SPCC1795.06	SPCC550.12	SPBC19G7.06	SPBC15D4.01c	SPCC13B11.02c
SPCC553.10	SPCC1322.02	SPBC19G7.13	SPBC15D4.07c	SPCC1183.08c
SPCC364.02c	SPCC1322.05c	SPBC12C2.09c	SPBC1718.07c	SPCC830.07c



Cell Cycle

Publication details, including instructions for authors and subscription information:

<http://www.tandfonline.com/loi/kccy20>

The impact of the HIRA histone chaperone upon global nucleosome architecture

Csenge Gal^a, Karen M Moore^b, Konrad Paszkiewicz^b, Nicholas A Kent^c & Simon K Whitehall^a

^a Institute for Cell & Molecular Biosciences; Newcastle University; Newcastle upon Tyne, UK

^b Biosciences, College of Life & Environmental Sciences; University of Exeter; Exeter, UK

^c Cardiff School of Biosciences; Cardiff University; Cardiff, UK

Published online: 20 Jan 2015.



[Click for updates](#)

To cite this article: Csenge Gal, Karen M Moore, Konrad Paszkiewicz, Nicholas A Kent & Simon K Whitehall (2015) The impact of the HIRA histone chaperone upon global nucleosome architecture, *Cell Cycle*, 14:1, 123-134, DOI: [10.4161/15384101.2014.967123](https://doi.org/10.4161/15384101.2014.967123)

To link to this article: <http://dx.doi.org/10.4161/15384101.2014.967123>

PLEASE SCROLL DOWN FOR ARTICLE

Taylor & Francis makes every effort to ensure the accuracy of all the information (the "Content") contained in the publications on our platform. Taylor & Francis, our agents, and our licensors make no representations or warranties whatsoever as to the accuracy, completeness, or suitability for any purpose of the Content. Versions of published Taylor & Francis and Routledge Open articles and Taylor & Francis and Routledge Open Select articles posted to institutional or subject repositories or any other third-party website are without warranty from Taylor & Francis of any kind, either expressed or implied, including, but not limited to, warranties of merchantability, fitness for a particular purpose, or non-infringement. Any opinions and views expressed in this article are the opinions and views of the authors, and are not the views of or endorsed by Taylor & Francis. The accuracy of the Content should not be relied upon and should be independently verified with primary sources of information. Taylor & Francis shall not be liable for any losses, actions, claims, proceedings, demands, costs, expenses, damages, and other liabilities whatsoever or howsoever caused arising directly or indirectly in connection with, in relation to or arising out of the use of the Content.

This article may be used for research, teaching, and private study purposes. Terms & Conditions of access and use can be found at <http://www.tandfonline.com/page/terms-and-conditions>

It is essential that you check the license status of any given Open and Open Select article to confirm conditions of access and use.

The impact of the HIRA histone chaperone upon global nucleosome architecture

Csenge Gal¹, Karen M Moore², Konrad Paszkiewicz², Nicholas A Kent^{3,*}, and Simon K Whitehall^{1,*}

¹Institute for Cell & Molecular Biosciences; Newcastle University; Newcastle upon Tyne, UK; ²Biosciences, College of Life & Environmental Sciences; University of Exeter; Exeter, UK;

³Cardiff School of Biosciences; Cardiff University; Cardiff, UK

Keywords: Chromatin, heterochromatin, HIRA, histone chaperone, nucleosome assembly, *S. pombe*

HIRA is an evolutionarily conserved histone chaperone that mediates replication-independent nucleosome assembly and is important for a variety of processes such as cell cycle progression, development, and senescence. Here we have used a chromatin sequencing approach to determine the genome-wide contribution of HIRA to nucleosome organization in *Schizosaccharomyces pombe*. Cells lacking HIRA experience a global reduction in nucleosome occupancy at gene sequences, consistent with the proposed role for HIRA in chromatin reassembly behind elongating RNA polymerase II. In addition, we find that at its target promoters, HIRA commonly maintains the full occupancy of the –1 nucleosome. HIRA does not affect global chromatin structure at replication origins or in rDNA repeats but is required for nucleosome occupancy in silent regions of the genome. Nucleosome organization associated with the heterochromatic (*dg-dh*) repeats located at the centromere is perturbed by loss of HIRA function and furthermore HIRA is required for normal nucleosome occupancy at Tf2 LTR retrotransposons. Overall, our data indicate that HIRA plays an important role in maintaining nucleosome architecture at both euchromatic and heterochromatic loci.

Introduction

Nucleosome assembly is believed to occur in a step-wise manner whereby the deposition of an (H3-H4)₂ tetramer is followed by the assembly of 2 flanking H2A-H2B dimers.^{1,2} This process is regulated by a structurally diverse group of proteins termed histone chaperones.^{1,2} Traditionally, these proteins have been classified as either H3-H4 or H2A-H2B chaperones based upon their histone binding specificity, although some chaperones such as FACT are able to bind both H3-H4 and H2A-H2B.¹ During S-phase nucleosomes are removed ahead of the replication fork and then reassembled onto newly synthesized DNA. However other processes such as transcription, recombination and repair also result in the loss of nucleosomes from DNA which necessitates histone chaperones that mediate replication-independent nucleosome assembly.³ Furthermore, it is now established that in addition to their traditional assembly function, histone chaperones can also mediate nucleosome disassembly and histone exchange. Indeed the central role played by histone chaperones in nucleosome dynamics is becoming increasingly recognized.²

The HIRA (or HIR) complex is an evolutionarily conserved H3-H4 histone chaperone that is implicated in a range of processes including embryonic development, angiogenesis, cellular

senescence and aging.⁴ The human complex is composed of HIRA in association with UBN1 and CABIN1^{5–7} and similarly yeast HIRA proteins (Hir1 and Hir2 in *Saccharomyces cerevisiae* and Hip1 and Slm9 in *Schizosaccharomyces pombe*), are stably associated with orthologs of CABIN1 and UBN1.^{8–11} HIRA co-operates with another H3-H4 chaperone, Asf1 to mediate replication-independent nucleosome assembly.⁴ Consistent with this, in higher eukaryotes HIRA is associated with the histone variant H3.3 which is deposited into chromatin independently of DNA synthesis.⁶

The modulation of chromatin structure by HIRA has been implicated in multiple aspects of transcriptional regulation. In some contexts HIRA is necessary for transcriptional activation. For example the induction of *Vegf1* in human endothelial cells in response to angiogenic signals is HIRA-dependent.¹² Similarly in fission yeast, HIRA subunits are recruited to promoters of specific genes in response to environmental stress. Inactivation of HIRA compromises nucleosome eviction and transcriptional induction at these genes.¹³ Conversely, HIRA has also been shown to be required for transcriptional repression. *S. cerevisiae* Hir1 and Hir2 were initially characterized as repressors of histone gene expression,¹⁴ a role which is conserved in other organisms.^{15,16} Furthermore, HIRA is required for the integrity of

© Csenge Gal, Karen M Moore, Konrad Paszkiewicz, Nicholas A Kent, and Simon K Whitehall

*Correspondence to: Nicholas A Kent; Email: kentn@cardiff.ac.uk; Simon K. Whitehall; Email: simon.whitehall@ncl.ac.uk

Submitted: 06/11/2014; Revised: 09/11/2014; Accepted: 09/12/2014

<http://dx.doi.org/10.4161/15384101.2014.967123>

This is an Open Access article distributed under the terms of the Creative Commons Attribution License (<http://creativecommons.org/licenses/by/3.0/>), which permits unrestricted use, distribution, and reproduction in any medium, provided the original work is properly cited. The moral rights of the named author(s) have been asserted.

silent chromatin in a variety of systems. In fission yeast HIRA/Asf1 spreads across heterochromatic regions via association with the Heterochromatin Protein (HP1) ortholog, Swi6, to maintain a silent state.^{10,15,17} In human fibroblasts HIRA/Asf1a is required for the formation of senescence associated heterochromatin,¹⁸ and furthermore HIRA interacts with PRC2 and is implicated in the maintenance of the repressive H3K27me mark at developmentally regulated genes in mouse embryonic stem cells.¹⁹ HIRA also suppresses the expression of retroelements. Mutation in HIRA components alleviates silencing of *S. pombe* Tf2 LTR retrotransposons^{10,20} and human HIRA was revealed as one of a group of chromatin assembly factors that suppresses HIV-1 proviral expression to maintain latency.²¹ Other studies have also suggested a global role for HIRA in transcriptional elongation and the suppression of cryptic promoters. In *S. cerevisiae* *hir* mutations are synthetically lethal when combined with mutations in the yFACT complex which facilitates transcription elongation.²² Furthermore inactivation of the HIRA complex results in increased levels of spurious transcripts from cryptic promoters in ORFs.^{20,23,24} The genomes of cells defective in HIRA function also exhibit increased accessibility to DNA damaging agents and nucleases.^{20,25} Taken together the data indicate that the HIRA histone chaperone plays an important role in maintaining the global integrity of chromatin.^{20,25} Given this we have identified the impact of the fission yeast HIRA complex on genome-wide nucleosome architecture. Using a chromatin-sequencing approach²⁶ we have mapped changes to nucleosome position and occupancy in cells lacking HIRA function. We find that HIRA is required for normal nucleosome occupancy over ORFs, at some promoters, and also at heterochromatic repeats. As such, HIRA plays an important role in the maintenance of global nucleosomal architecture.

Results

We employed a chromatin sequencing technology²⁶ to determine the impact of the HIRA histone chaperone complex on genome-wide nucleosome occupancy and positioning. With this approach, chromatin is treated with micrococcal nuclease (MNase) to generate ladders of MNase-resistant DNA which is then subjected to sequencing. The resulting datasets are then stratified based on paired read end-to-end distance into ranges representing the expected sizes of MNase resistant DNA species in eukaryotic chromatin. Thus read pairs of 150 bp (+/– 20%) derive primarily from mono-nucleosomes, whereas read pairs of 300 bp (+/– 20%) derive from di-nucleosomes. Frequency distributions of the read midpoints can then be mapped to the genome and the peaks in these distributions used to infer the presence of positioned chromatin particles in the cell population.²⁶ Therefore chromatin derived from fission yeast cells lacking HIRA function (*hip1Δ*) was digested with MNase to generate a DNA ladder with a highly similar molecular weight distribution to our wild type control sample (Fig. 1A and B). Three biological replicate samples were pooled and sequenced which generated data sets for wild type and *hip1Δ* comprising of 56.3 and 49.6 million reads, respectively.

We first compared the average distribution of nucleosomes mapped in our wild-type data-set with that from a previously published study.²⁷ A cumulative frequency distribution of nucleosome position at, and surrounding nucleosome positions was plotted to assess how closely the datasets matched. This revealed that the distribution from our wild-type data set is coincident with the previously published wild-type nucleosome data-set and is distinct from a MNase-digested genomic DNA control²⁷ (Fig. 1C). These control comparisons, suggest that the nucleosome positions we map are accurate and that our wild-type data set agrees well with published work.

HIRA and the integrity of chromatin associated with ORFs

As HIRA has been linked to a variety of aspects of transcriptional control,⁴ we examined the impact of deletion of *hip1*⁺ upon the chromatin surrounding the transcription start-sites (TSS) of protein coding genes. Typically chromatin in these regions is organized with a nucleosome depleted region (NDR) followed by a well ordered nucleosome array that extends from the TSS and packages the transcribed region.²⁸ In comparison, promoter regions are generally associated with lower nucleosome levels. Figure 2A shows a comparison of average nucleosome positions surrounding TSS in wild-type and *hip1Δ* cells. Loss of HIRA did not result in any changes to the NDR or the +1 nucleosome peak indicating that HIRA is not required for the maintenance of chromatin structure around the 5' end of genes, at least at a global level. Nonetheless, the amplitudes of the nucleosome peaks from +4 onwards were reduced indicating that HIRA does contribute to the maintenance of chromatin associated with ORFs.

The reduction in the average peak height in the *hip1Δ* mutant was suggestive of a decrease in nucleosome occupancy and consistent with this view western blotting revealed a significant reduction in histone protein levels in cells lacking HIRA (Fig. 2b). Based upon this finding we predicted that the *hip1Δ* allele would show a strong genetic interaction with mutations in *hrp3*⁺ which encodes a CHD ATP-dependent remodeler that controls nucleosome spacing.^{27,29} Analysis of a *hip1Δ hrp3Δ* double mutant revealed that this strain was extremely slow growing and had severely elongated cell morphology (Fig. 2C; Fig. S1) Therefore as predicted, loss of correct nucleosome spacing exacerbates the growth defects associated with HIRA inactivation.

HIRA suppresses aberrant transcription from the bodies of genes²⁰ and so the global perturbation to genic chromatin that is observed in the *hip1Δ* strain is consistent with this finding. To further investigate this we analyzed the nucleosome profiles of a group of genes which have been shown to produce cryptic transcripts when HIRA function is absent.^{17,20} At the *hrp1*⁺ locus loss of HIRA function resulted in marked changes to the MNase profile which extended throughout the entire gene and into the neighboring genes (*atg12*⁺ and *pap1*⁺) (Fig. 3A; Fig. S2). In contrast, the other genes we inspected exhibited relatively modest changes to their nucleosome profiles in the *hip1Δ* background (Fig. 3B; Fig. S3). An example of this is the *dbp7*⁺ gene, where changes to nucleosome occupancy were mainly observed at the 3'-end of the gene and downstream of the transcription termination site. It therefore appears that relatively small changes to

nucleosome architecture may be sufficient to result in increased levels of cryptic transcripts.

In order to confirm some of the differences in the nucleosome profiles that were observed in Fig. 3A and B, mononucleosomal DNA was isolated from independent pools of MNase-digested DNA and a quantitative PCR (qPCR) approach³⁰ was used to compare the occupancy of some specific nucleosomes in the wild-type and *hip1Δ* samples. Similar to the results from the genome-wide mapping studies, the qPCR analysis also indicated that occupancy of nucleosomes near *hrp1*⁺ (designated *hrp1*₅₁₃₇) and the 3' end of the *dbp7*⁺ gene (*dbp7*₁₉₂₇) were reduced in *hip1Δ* whereas the occupancy of nucleosome located at the 5' (*dbp7*₁₀) was similar in wild type and *hip1Δ*.

Impact of HIRA on chromatin at promoters

In addition to the suppression of spurious transcription initiation, HIRA represses expression from numerous bona fide RNA polymerase II (Pol II) promoters. Indeed the expression of approximately 4% of fission yeast genes is increased by loss of HIRA function.²⁰ We first compared the chromatin organization of these 'HIRA-repressed' genes with the complete set of *S. pombe* coding genes. HIRA-repressed genes were found to have obvious differences in their chromatin organization as average nucleosome peaks associated with the coding sequences of these genes were poorly ordered and the height of the peaks was lower than the global average (Fig. 4A). This suggests that the coding sequences of HIRA-repressed genes are associated with a lower than average nucleosome occupancy. Furthermore, the NDR of the HIRA-repressed gene set was both narrower and shallower when compared to the average promoter. These features are known to be characteristic of genes that have a

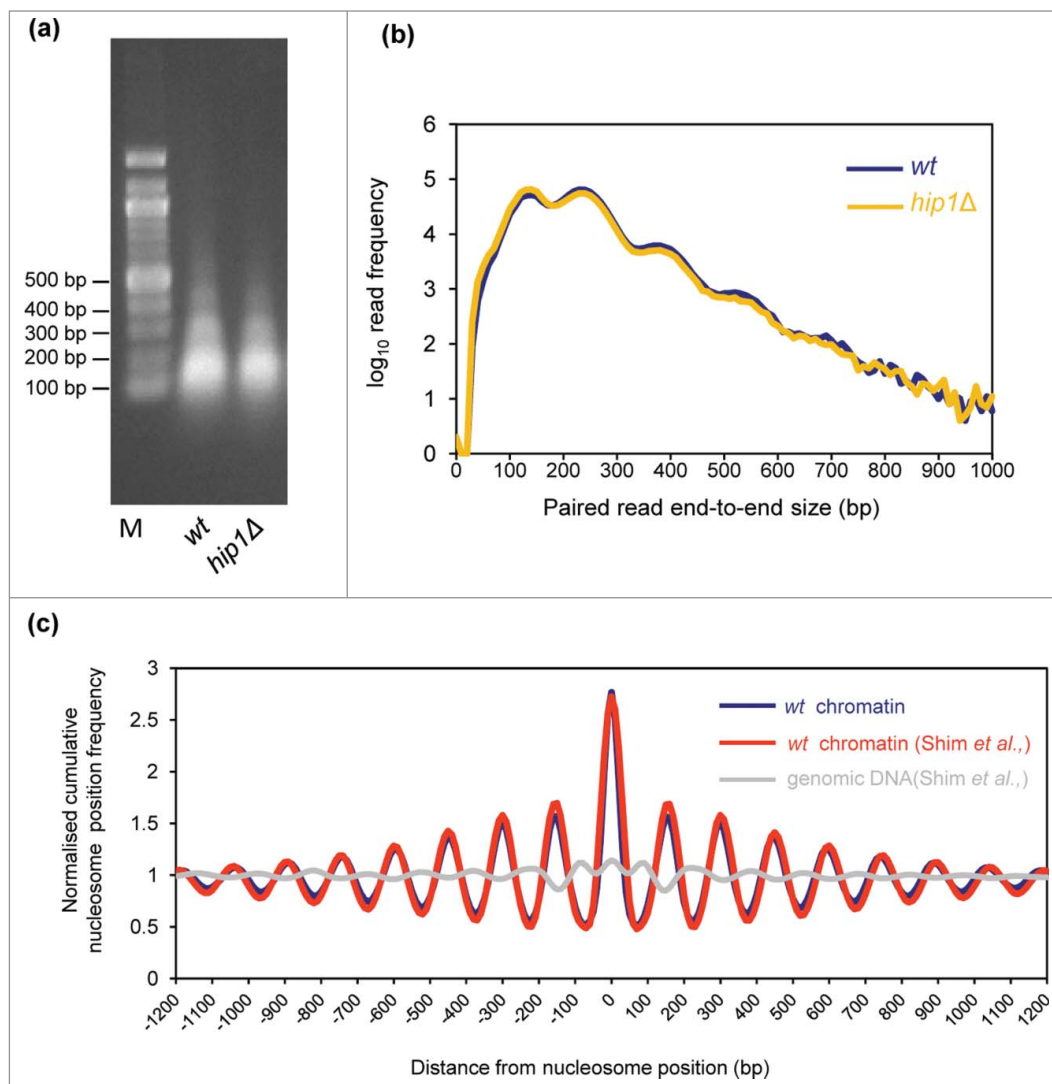


Figure 1. Paired-end mode chromatin-seq of wild type and *hip1Δ* mutant *S. pombe*. (A) Ethidium-stained gel separation of DNA pools extracted from MNase digested *S. pombe* chromatin used for chromatin sequencing in this study. Mono-, di- and tri-nucleosomal bands are visible. (B) Frequency distribution of paired read end-to-end size values after chromatin-seq of DNA shown in (A). (C) Nucleosomes in wild type cells (wt chromatin) were defined as the positions of 150 bp size class particle frequency peak summits (frequency value >25). This procedure marked 60, 658 putative nucleosome positions in the *S. pombe* genome. The 150 bp size class particle frequency distribution centered on, and surrounding (+/-1200 bp) each of these positions was then summed and normalized to the average frequency value occurring in the +/-1200 bp window. The wavelength of the peak pattern should be equal to the *S. pombe* nucleosome repeat length. Comparison to a previously published MNase-treated naked DNA (genomic DNA) dataset and a wt chromatin data set²⁷ is shown.

low level of expression,³¹ a finding which is in agreement with our previous microarray analyses which revealed that HIRA target genes overlap significantly with lowly expressed genes.²⁰ We next determined the impact of *hip1*⁺ deletion upon chromatin architecture of HIRA-repressed genes. Loss of *hip1*⁺ resulted in a reduction in the height of the -1 nucleosome peak and subtle shift in its position which suggests that HIRA promotes the proper occupancy of the -1 nucleosome, a finding which is consistent with the repressive function of HIRA at these promoters (Fig. 4B).

We next examined the histone H3-H4 genes *bht2*⁺-*bhf2*⁺ as their expression outside of S-phase is repressed in a

HIRA is not required for chromatin architecture at Pol I- and Pol III-transcribed genes

As HIRA has a global impact upon the chromatin associated with Pol II-transcribed genes we examined whether it was also required for chromatin organization at Pol I and Pol III genes. We analyzed the chromatin configuration surrounding Pol III-transcribed tRNA genes. In *S. cerevisiae* tRNA genes are typically nucleosome free and flanked by nucleosomes positioned upstream (US) and downstream (DS).³⁴ In comparison, it has been suggested that many tRNA genes in *S. pombe* (like those in resting human CD4+ T cells) are associated with nucleosomes.³⁴ Plots of the average mono-nucleosome (150 bp) profile of 171 *S. pombe* tRNA genes aligned by TSS are consistent with this earlier report as we detected a peak centered at +20 relative to the TSS (Fig. 5A). At this global level we were able to detect an upstream (US) nucleosome peak positioned at -160 bp but we found little evidence of a downstream nucleosome array. Loss of HIRA did not impact upon the US nucleosome although we did note some reduction in the height of the peak located at +20 bp. tRNA genes have internal promoter elements that are binding sites for TFIIC which in turn directs the assembly of TFIIB upstream of the transcription start-site. TFIIB acts as the initiation factor by bringing Pol III to DNA.³⁵ In order to see if HIRA has any global impact upon Pol III transcription factor binding we examined the profile of 75 bp particles as it has been demonstrated that these particles result from the protection of DNA by transcription factors rather than by nucleosomes.²⁶ Comparison of average 75 bp profiles revealed the presence of a prominent peak immediately upstream of the TSS which given its position is likely to result from TFIIB binding (Fig. 5B). Loss of HIRA function did not impact upon this peak suggesting that it does not globally affect TFIIB occupancy at tRNA genes.

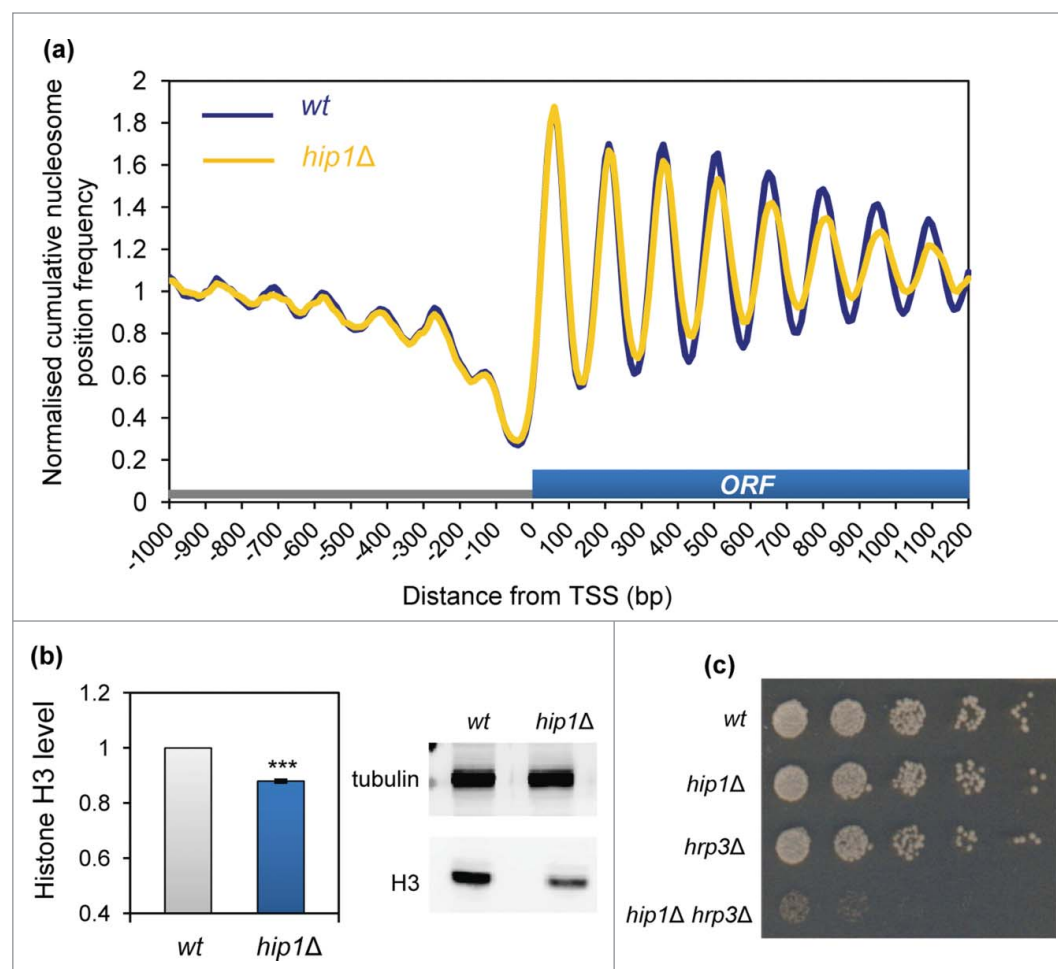


Figure 2. HIRA is required for normal nucleosome occupancy at Pol II transcribed genes. **(A)** Average nucleosome (150 bp size class particle) sequence read frequency profiles for 4013 *S. pombe* genes aligned at the transcription start site (TSS). **(B)** Whole cell extracts were subjected to western blotting with histone H3 (Abcam) and tubulin antibodies. An example of the primary data is shown along with a quantification of histone H3 levels normalized to tubulin (right). Data are the mean of 9 independent repeats and error bars represent \pm SEM. *** indicates $P < 0.001$ t-test. **(C)** Strains, NT5 (*wt*), AW046 (*hrp3Δ*), SW700 (*hip1Δ*), CsG349 (*hip1Δ hrp3Δ*) were grown in YE5S medium until they reached an $OD_{595} = 0.2-0.3$. Cultures were subjected to five-fold serial dilution, spotted onto YE5S agar and incubated for 4 d at 30°C.

HIRA-dependent manner.³² *hht2⁺-hhf2⁺* are divergently transcribed from a short promoter, and analysis of our MNase profiles revealed the presence of a -1 nucleosome peak in the center of this region. Since the majority of fission yeast cells in an asynchronous culture will be in G2, this chromatin configuration is likely to represent a repressed promoter state. Consistent with this hypothesis the promoter nucleosome peak occludes the AACCTT box which is a binding site for the GATA-type factor, Ams2 and the Myb domain protein, Teb1, which activate the transcription of histone genes.^{32,33} Interestingly, both the MNase profiles and qPCR analysis of mononucleosomal DNA indicated that deletion of *hip1⁺* resulted in a marked reduction of this peak, suggesting that HIRA promotes the occupancy of this promoter nucleosome to suppress the inappropriate expression of histone genes (Fig. 4C and D).

stream nucleosome array. Loss of HIRA did not impact upon the US nucleosome although we did note some reduction in the height of the peak located at +20 bp. tRNA genes have internal promoter elements that are binding sites for TFIIC which in turn directs the assembly of TFIIB upstream of the transcription start-site. TFIIB acts as the initiation factor by bringing Pol III to DNA.³⁵ In order to see if HIRA has any global impact upon Pol III transcription factor binding we examined the profile of 75 bp particles as it has been demonstrated that these particles result from the protection of DNA by transcription factors rather than by nucleosomes.²⁶ Comparison of average 75 bp profiles revealed the presence of a prominent peak immediately upstream of the TSS which given its position is likely to result from TFIIB binding (Fig. 5B). Loss of HIRA function did not impact upon this peak suggesting that it does not globally affect TFIIB occupancy at tRNA genes.

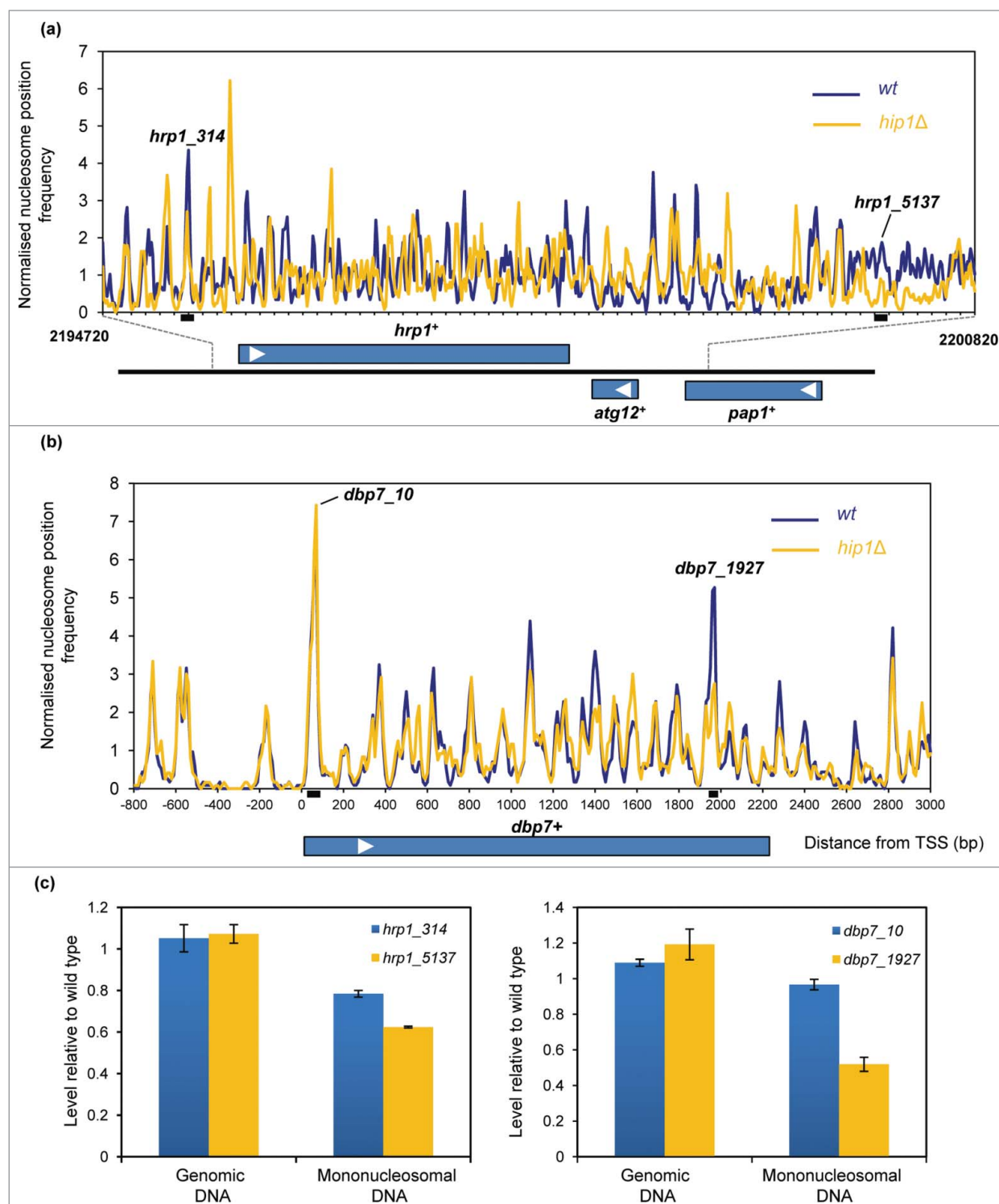


Figure 3. HIRA and nucleosome architecture in gene sequences. **(A)** Nucleosome (150 bp) sequence read frequency profiles of a 6.1 kb region of chromosome 1 (bp 2194720 to 2200820). The positions and orientation of the *hrp1*⁺, *atg12*⁺ and *pap1*⁺ genes are indicated below. **(B)** Nucleosome (150 bp) sequence read frequency profiles of the *dbp7*⁺ gene relative to the TSS. **(C)** The occupancy of specific nucleosomes was estimated by qPCR analysis of mononucleosomal DNA as described in the Materials and Methods. An equivalent amount of genomic DNA was analyzed as a control. The positions of the nucleosome peaks under analysis and the PCR primers are indicated in **(A)** and **(B)**. The level of occupancy in *hip1Δ* relative to wild type is shown. Data is the mean of 2 technical qPCR repeats.

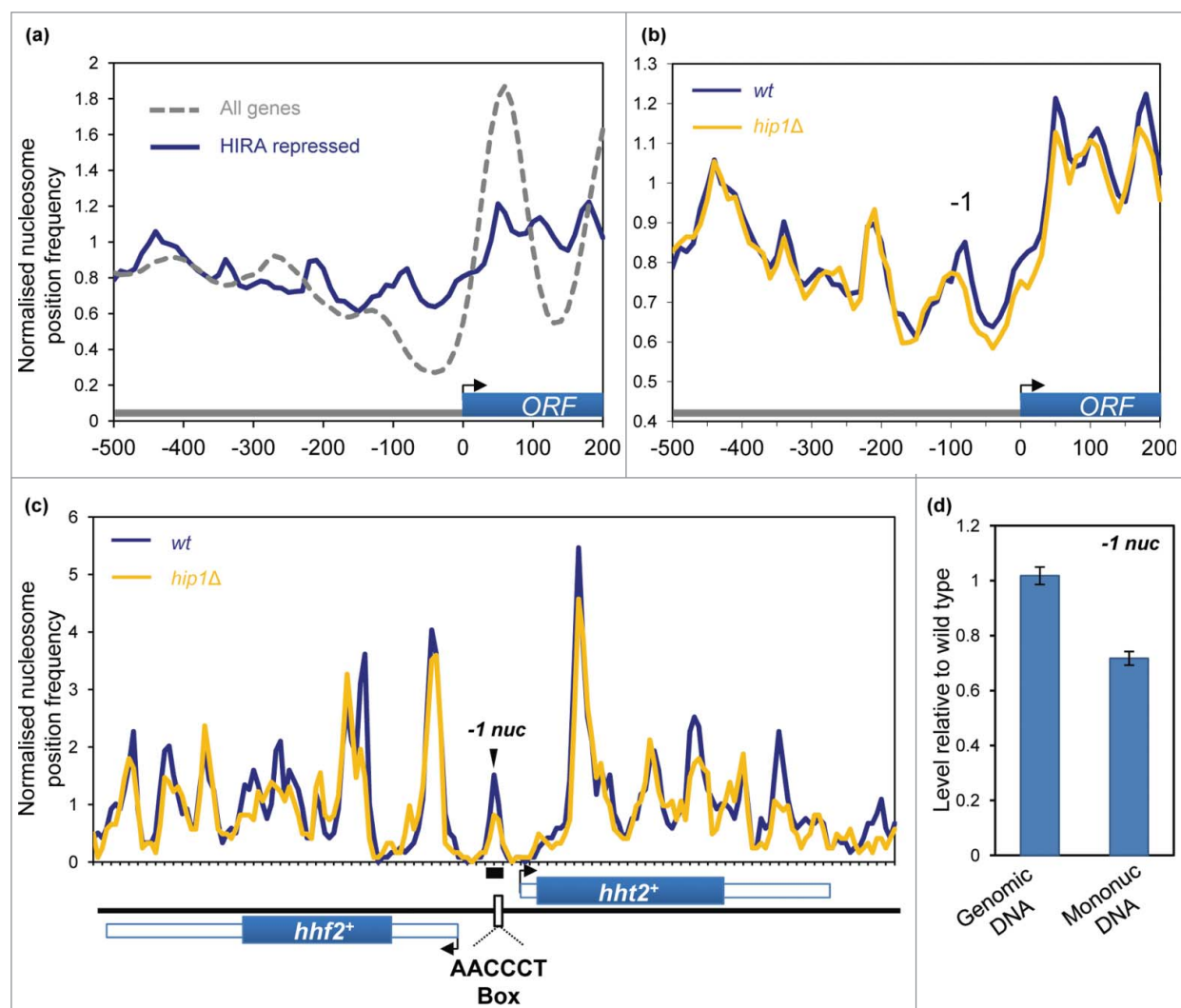


Figure 4. Impact of HIRA on promoter nucleosome profiles. **(A)** Average nucleosome profiles for 4013 *S. pombe* genes aligned at the transcription start site (TSS) compared to the nucleosome sequence read frequency profile of a set of 107 HIRA-repressed protein-coding genes.²⁰ **(B)** Average nucleosome profiles of a set of 107 HIRA-repressed genes in wild type and *hip1Δ* cells. **(C)** Comparison of the nucleosome profile at the *hht2⁺-hhf2⁺* locus in wild type and *hip1Δ* cells. The positions of the coding sequences are indicated by solid blue boxes while 5' and 3' UTRs are represented by open boxes. Positions of *hht2⁺-hhf2⁺* transcription start-sites, termination sites and the AACCCCT box are as described by Takayama and Takahashi.³⁰ **(D)** Occupancy of the *hht2⁺-hhf2⁺* -1 nucleosome (-1 nuc) was determined by qPCR analysis of mononucleosomal DNA. The position of the PCR primers and peak are indicated in **(C)**. The level of occupancy in *hip1Δ* relative to wild type is shown. Data is the mean of 2 technical qPCR repeats.

Recently, the HIR complex has been implicated in the repression of rDNA transcription in *S. cerevisiae*.³⁶ We therefore analyzed the MNase profiles of *S. pombe* rDNA repeat sequences. This suggested that Pol I-transcribed genes are nucleosome free while the intergenic regions are associated with well-positioned nucleosomes. However, loss of HIRA did not have a marked effect upon the MNase profiles of these regions (Fig. 5C) and so we find no evidence to suggest that HIRA is required for the maintenance of nucleosome architecture at Pol I genes in fission yeast. We also examined nucleosome profiles surrounding replication origins which were aligned as described previously.³⁷ In agreement with previous studies,^{31,37} a wide nucleosome

depleted region (NDR) was detectable over the origin center. This feature was also readily detectable in *hip1Δ* cells and indeed the average MNase profile of wild-type and *hip1Δ* cells surrounding origins was strikingly similar (Fig. S4) suggesting that HIRA does not contribute to the global organization of chromatin at replication origins.

Impact of HIRA upon nucleosome organization in silent chromatin

Loss of any one of the subunits of the HIRA complex alleviates heterochromatic silencing at the cryptic mating (*mat*) type locus and also at pericentromeric repeats.^{8,10} These

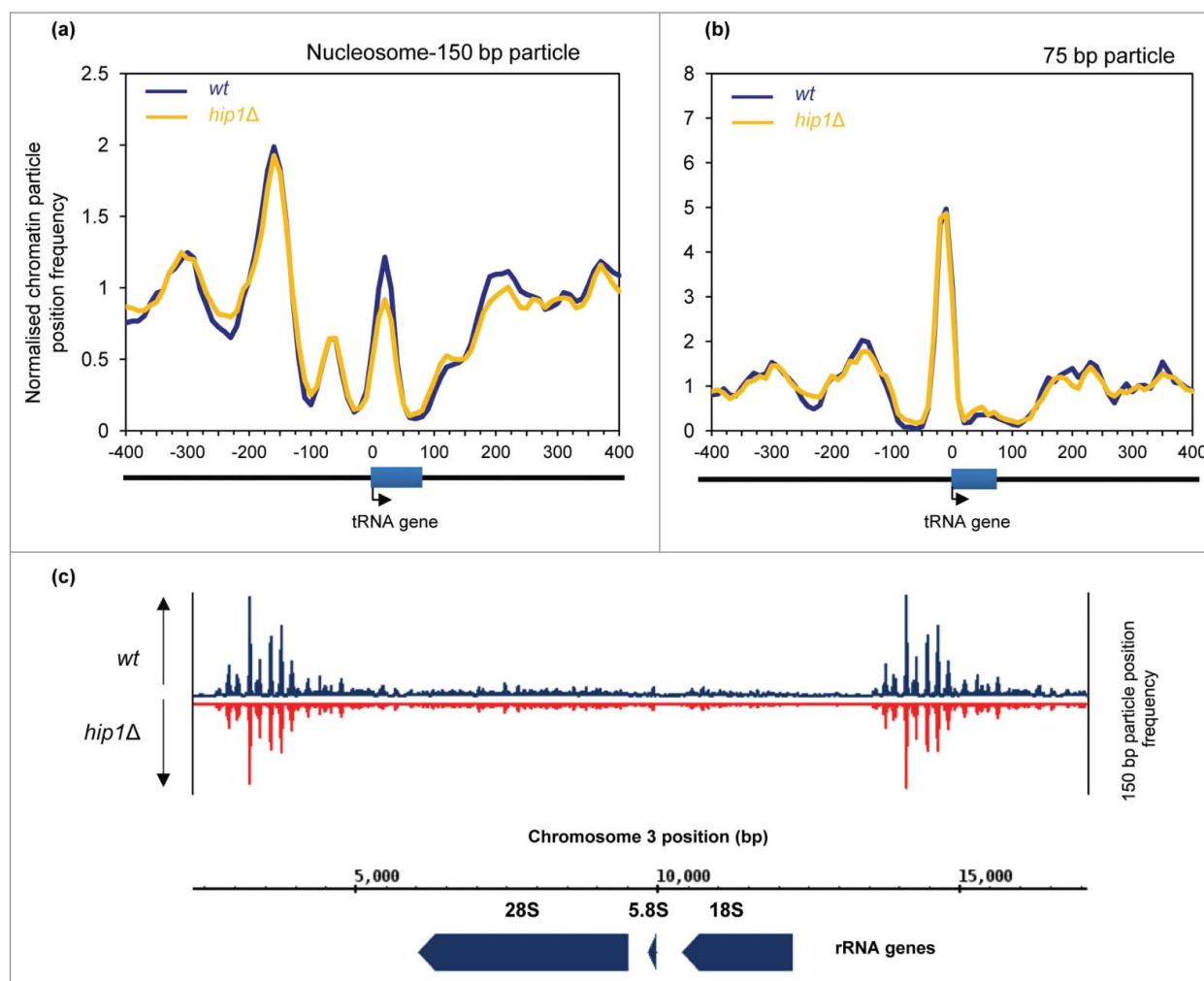


Figure 5. Nucleosome architecture at Pol III and Pol II genes. **(A)** Average nucleosome (150 bp size class particle) sequence read frequency profiles for 171 *S. pombe* tRNA genes aligned at the transcription start site (TSS). **(B)** Average 75 bp size class particle sequence read frequency profiles for 171 *S. pombe* tRNA genes aligned at the transcription start site (TSS). **(C)** Nucleosome (150 bp size class particle) read profile over an rDNA repeat. The positions of the 28S, 5.8S and 18S rRNA genes are indicated.

heterochromatin domains are enriched for methylation of histone H3 lysine 9 (H3K9me) which directs the assembly of chromodomain proteins such as the HP1 ortholog, Swi6.³⁸ Hip1 interacts with Swi6 and also the histone chaperone Asf1, which is required for nucleosome occupancy in heterochromatin.¹⁷ We therefore examined the impact of *hip1⁺* deletion upon the nucleosome profile at pericentromeric *dg-dh* repeats. This revealed that loss of HIRA resulted in changes to specific peaks rather than a uniform reduction in occupancy across the entire repeat region (Fig. 6A and B). Consistent with this, qPCR analysis also indicated that occupancy of specific dg and dh nucleosomes (designated dh_nuc and dg_nuc) were reduced in the absence of HIRA (Fig. 6C). This suggests that HIRA is required to maintain the proper occupancy of a subset of nucleosomes within heterochromatic domains and that this is required for transcriptional silencing in this region.

HIRA is also required for silencing the expression of all 13 intact Tf2 LTR retrotransposons.²⁰ The mechanism of silencing of these elements is distinct from heterochromatin as although it requires HIRA, it is independent of H3K9me.^{10,39} Plots of average nucleosome profiles of these LTR retrotransposons showed that they have a nucleosome architecture which is distinct from typical RNA Pol II-transcribed genes. At Tf2 promoters (5' LTRs), a peak overlapped the TSS and the NDR was located downstream (rather than upstream) of the TSS (Fig. 7A). Interestingly, deletion of *hip1⁺* had very little effect on the nucleosome peak adjacent to the TSS however we noted that *hip1Δ* cells had reduced +1, +2, and +3 nucleosome peaks (relative to the NDR). qPCR analysis also indicated that deletion of *hip1⁺* resulted in a reduction in the occupancy of the +2 nucleosome (Fig. 7B). These findings suggest that the nucleosomes downstream of the TSS may play a role in repression of Tf2 retrotransposons.

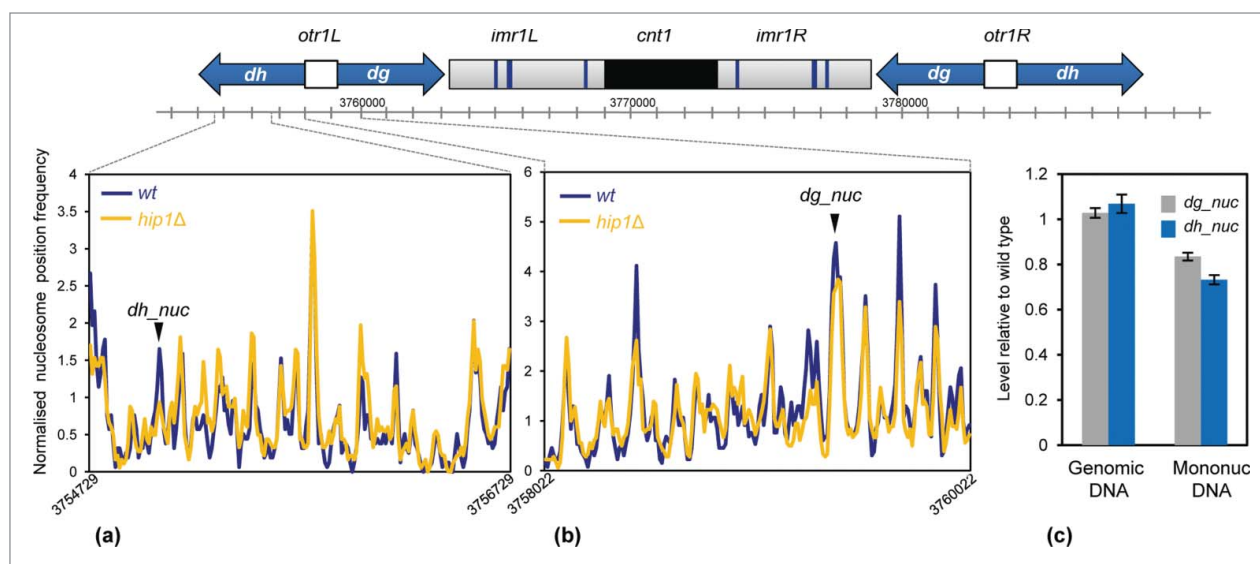


Figure 6. Loss of HIRA perturbs nucleosome architecture at centromeric repeats. **(A and B)** A schematic diagram of centromere 1 is shown along with the average nucleosome (150 bp) sequence read frequency profiles of the indicated regions of the *dg* and *dh* repeats. **(C)** The occupancy of specific *dh* and *dg* repeat nucleosomes was estimated by qPCR analysis of mononucleosomal DNA as described in the Materials and Methods. An equivalent amount of genomic DNA was analyzed as a control. The positions of the nucleosome peaks under analysis are indicated in **(A and B)**. The level of occupancy in *hip1Δ* relative to wild type is shown. Data is the mean of 2 technical qPCR repeats.

Discussion

Here we have determined the global impact of HIRA upon nucleosome architecture and in agreement with previous evidence, find that this histone chaperone plays roles in the maintenance of both euchromatic and heterochromatic regions of the genome. We demonstrate that cells lacking HIRA (*hip1Δ*)

experience a global reduction in nucleosome occupancy. This is consistent with previous studies which revealed that the genomes of fission yeast HIRA mutants are more accessible to DNA damaging agents.²⁰ Similarly in mammalian cells, HIRA depletion results in increased sensitivity of the genome to nucleases.²⁵

The co-ordinated replacement of nucleosomes that are displaced by elongating Pol II is necessary for maintaining the integrity of chromatin structures associated with gene sequences.⁴⁰ The finding that cryptic intragenic transcripts increase in the absence of HIRA²⁰ is consistent with its proposed role in chromatin reassembly in the wake of Pol II. Our data adds further support to this hypothesis, as average MNase profiles revealed that *hip1Δ* cells have a global reduction in nucleosome occupancy which was most pronounced toward the 3' end of gene sequences. Reduced levels of specific nucleosome peaks were also detectable at individual genes where loss of HIRA results in increased cryptic transcription. However there are

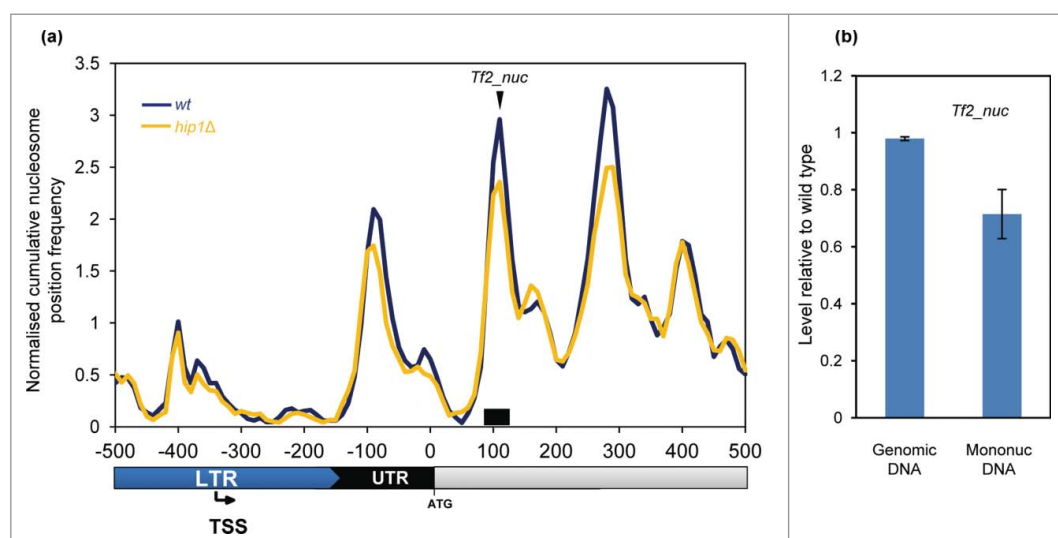


Figure 7. Nucleosome structure of Tf2 LTR retrotransposons. **(A)** Average nucleosome (150 bp) sequence read frequency profile for the 5' region of Tf2 elements aligned relative to the translation start site (ATG). **(B)** The occupancy of a specific Tf2 nucleosome was estimated by qPCR analysis of mononucleosomal DNA as described in the Materials and Methods. An equivalent amount of genomic DNA was analyzed as a control. The position of the nucleosome peak and the PCR primers are indicated in **(A)**. The level of occupancy in *hip1Δ* relative to wild type is shown. Data is the mean of 2 technical qPCR repeats.

also some regions of the genome which are more severely perturbed in the absence of HIRA. Indeed marked changes to both the occupancy and positioning of nucleosome peaks were evident surrounding the *hrp1*⁺ locus. Why specific regions of the genome show a greater dependency upon HIRA than others is currently not clear.

Comparison of average nucleosome plots aligned by TSS in wild-type and *hip1*Δ cells did not reveal a global impact of HIRA upon chromatin at promoters. However when we analyzed the profiles of a set of HIRA repressed genes²⁰ we found that *hip1*⁺ is required for the normal occupancy and positioning of the −1 nucleosome. This set of genes has a chromatin structure that is characteristic of lowly expressed genes³¹ which is consistent with transcript profiling of HIRA mutant cells.²⁰ Taken together this suggests that HIRA commonly functions to maintain a closed/repressive chromatin structure at these genes. This was also evident at the *bht2*⁺-*bhf2*⁺ promoter where HIRA is required for full occupancy of the −1 nucleosome peak. *S. pombe* has 3 H3-H4 gene pairs however HIRA-mediated repression of histone gene expression is believed to operate predominantly through this gene pair.³² Interestingly, the −1 nucleosome peak occludes the proposed binding site for the Ams2 and Teb1 activators suggesting that remodelling of this nucleosome may be required during transcription activation. Reduced occupancy of this nucleosome in the absence of HIRA would be expected to facilitate binding of activating transcription factors. While the expression of *ams2*⁺ is limited to G1/S,⁴¹ the expression of *teb1*⁺ is constitutive.⁴² Therefore the absence of HIRA may allow increased Teb1 binding and thus expression of *bht2*⁺-*bhf2*⁺ outside of S phase. Our results suggest that HIRA is required for a 'closed' chromatin configuration at some promoters and similarly in *S. cerevisiae* Hir1 has been shown to be necessary for chromatin re-assembly at the *PHO5* promoter during the switch from active transcription to repression.⁴³ While these results indicate that HIRA plays roles in promoting nucleosome occupancy, in other contexts it is also involved in mediating nucleosome eviction. HIRA subunits are recruited to specific stress-responsive promoters to facilitate nucleosome removal and gene induction.¹³ Furthermore, the MNase profiles suggested that the occupancy of some nucleosomes is increased in the absence of HIRA. Therefore, in common with other histone chaperones, HIRA seems capable of mediating both nucleosome assembly and disassembly.²

Chromodomain HP1 proteins such as Swi6 are hallmarks of heterochromatin. It has been proposed that these factors provide a platform for the assembly of other chromatin modifying proteins (including HDACs, ATP-dependent remodelers and histone chaperones) which enforce silencing of the underlying repeat sequences.³⁸ HIRA is one of these effectors as its correct localization at heterochromatic repeats is dependent upon Swi6.¹⁷ Previous studies have shown that changes to nucleosome positioning perturb heterochromatin function.⁴⁴ Here we present data which indicates that the changes in nucleosome occupancy associated with loss of HIRA negatively impact upon heterochromatin silencing. Our MNase profiles indicate that loss of HIRA results in changes to

specific nucleosomes rather than a uniform reduction across pericentromeric *dg-dh* repeats. Nonetheless, that cells lacking HIRA have increased levels of centromeric ncRNAs and defective trans-gene silencing,^{10,15,17} implies that these changes are sufficient to impair heterochromatin function and allow increased access of Pol II to repeat sequences. We note that a similar situation has been reported for Hrp3 because loss of this CHD remodeler results in dysfunctional heterochromatin without producing dramatic changes upon nucleosome architecture.²⁷

HIRA has been linked to the regulation of both LTR retrotransposons and retroviruses.^{20,45,46} That loss of HIRA function leads to a dramatic increase in expression of Tf2 LTR retrotransposons prompted comparison of MNase profiles of these elements. Tf2 5'-LTR regions are associated with a single nucleosome which overlaps the TSS. HIRA does not have an effect upon this nucleosome but is required for the full occupancy of the nucleosomes downstream of the transcription start-site. This suggests that chromatin structure in this region is important for maintaining silencing of Tf2 retrotransposons. Interestingly, analysis of HIV-1 expression has demonstrated that a nucleosome downstream of the TSS is important for mediating Pol II pausing and suppressing basal expression.⁴⁷ While the integrity of this region is dependent upon the FACT histone chaperone, other analyses revealed that HIRA is also required for the suppression of HIV-1 proviral expression and the maintenance of latency.⁴⁵ Given the parallels between Tf2 and HIV-1 it will be interesting to determine whether Pol II pausing is required for silencing of Tf2 elements.

Materials and Methods

S. pombe strains

Routine culture and genetic manipulation was performed as previously described.⁴⁸ The strains used in this study were 972 (*h*[−]), SW577 (*h*[−] *hip1::ura4*⁺), NT5 (*h*[−] *ade6*[−] *ura4-D18 leu1-32*), AW046 (*h*⁺ *hrp3::kanMX ade6*[−] *leu1-32 ura4-D18*), SW700 (*h*[−] *hip1::ura4*⁺ *ade6*[−] *ura4-D18 leu1-32*), CsG349 (*h*[−] *hip1::ura4*⁺ *hrp3::kanMX ade6*[−] *ura4-D18 leu1-32*).

Histone levels

Approximately 4×10^7 cells were harvested following addition of trichloroacetic acid (TCA) to a final concentration of 10%. Cells were resuspended in 200 μl 10% TCA and then disrupted using a beadbeater with 0.75 ml of glass beads using 2 pulses of 15 sec with 1 min on ice in between. A 500 μl aliquot of 10% TCA was added, the lysate was recovered from the beads which was then clarified by spinning at 13 000 rpm in a microcentrifuge. The resulting pellet was washed 3 times in acetone, dried and resuspended in 30 μl 100 mM Tris-HCl (pH 8.0), 1% w/v SDS, and 1 mM EDTA. Samples were analyzed on SDS-PAGE gels and subjected to protein gel blotting using anti-histone H3 (Abcam ab1791) and anti-tubulin (TAT-1) antibodies.

MNase digestion of chromatin

Cells (100 ml) were grown to $OD_{595} = 0.75\text{--}8.0$ in YE5S at 30°C , crosslinked for 20 min at 30°C using 1% formaldehyde and quenched by the addition of glycine to 125 mM. Cells were washed once in CES buffer (50 mM citric acid/50 mM Na_2HPO_4 [pH 5.6], 40 mM EDTA [pH 8.0], 1.2 M sorbitol and 10 mM β -mercaptoethanol) and resuspended in 500 μl of CES buffer with 0.5 mg Zymolase 100-T. Cells were spheroplasted at 30°C for up to 1 h and then washed twice with ice cold 1.2 M sorbitol. Spheroplasts were then resuspended in 800 μl NP-S buffer (1.2 M sorbitol, 10 mM CaCl_2 , 100 mM NaCl, 1 mM EDTA pH 8.0, 14 mM β -mercaptoethanol, 50 mM Tris [pH 8.0], 0.075% NP-40, 5 mM spermidine, 0.1 mM PMSF, 1% Sigma Protease inhibitors cocktail [Sigma P8215]). Spheroplasts were then divided into 4 200 μl aliquots and each aliquot was mixed with 300 μl of NP-S buffer. Three aliquots were digested with between 75–187.5 units of MNase (USB) for 10 min at 37°C . The fourth was retained as an undigested control. MNase digestion was terminated by adding EDTA [pH 8.0] to a final concentration of 50 mM and SDS to 0.2%. Reactions were incubated at 65°C overnight with 0.2 mg/ml proteinase K and 10 μg RNase. DNA was purified by extracting twice with phenol:chloroform followed by ethanol precipitation (0.1 volumes of 3 M sodium acetate followed by 2 volumes of ethanol). Pellets were washed in 70% ethanol and resuspended in water containing 10 $\mu\text{g}/\text{ml}$ RNase and incubated at 37°C for 30 min. Triplicate digests were pooled and treated with 100 U unmodified T4 polynucleotide kinase (NEB) for 30 min at 37°C to remove 3'-phosphate groups left by MNase. DNA was extracted once more with phenol:chloroform, re-precipitated with sodium acetate and ethanol, washed with 70% ethanol, dried and re-suspended in TE (pH 7.5).

Chromatin-seq

DNA fragments were end repaired, 3'-adenylated and ligated to indexed adapters without size selection using Nextflex reagents (Newmarket Scientific, UK). Libraries were amplified with 8 cycles PCR using Kapa HiFi PCR master mix (Anachem), primers removed with GeneRead size selection protocol (QIAgen) before quantification by Bioanalyser DNA 7500 assay. Libraries were pooled, denatured, diluted to 6 nM before clustering in a single lane of a high output Illumina flowcell. Sequencing (100 nt) was undertaken on a HiSeq 2500 using TruSeq SBS v3 reagents (Illumina).

Bioinformatics

Paired reads were aligned to the ASM294v1.17 reference genome using Bowtie 0.12.7⁴⁹ with command line flags: `-n 0 -trim 3 75 -maxins 5000 -fr -k 1 -sam`. Aligned read pairs were sorted according to chromosome and then into a range of size classes based on the SAM format ISIZE value (difference between 5' end of the mate read and the 5' end of the first mapped read) plus or minus 20%. Mono-nucleosome-sized reads are, therefore, represented as $150\text{ bp} \pm 30\text{ bp}$. To define the genomic position of MNase-resistant chromatin entities we mapped the mid-point position of the read pairs in a particular size class. Frequency

distributions of the mid-point positions were then calculated using 10 bp bins. Frequency distributions were lightly smoothed by taking a 3-bin moving average. All frequency distributions were output in the zero-referenced, chromosome base, 3-column .sgr format (chromosome number, feature/bin position, mid-point frequency value) for rendering with the Integrated Genome Browser⁵⁰ and for further processing. Average cumulative chromatin particle position frequency distributions at, and surrounding, genomic features were calculated using the script SiteWriterCFD as described previously,^{26,51} with values for each bin normalized to the average cumulative frequency value obtained for all bins within the feature window. To provide the comparison (Fig. 1c) of our data with the smoothed nucleosome position map of Shim and co-workers²⁷ the positions of 33874 unambiguous peak summit bins were marked in our wild type KDE mono-nucleosome data set (using script PeakMarker-EpKDE) and compared with GSM994397_WT.wig replicate and GSM994402_genomicDNA.wig data (converted to 10bp binned .sgr format). Protein-coding gene transcription start sites (TSS) positions were as described by Lantermann et al.³¹ Replication origin positions were as described by Givens et al.³⁷

qPCR analysis of mononucleosomal DNA

MNase digests of wild type and *hip1Δ* cells were performed as described above. For each strain 3 biological replicate samples (independent from those used for sequencing) were pooled and analyzed on 1% TAE agarose gels. Gel slices containing mononucleosomal DNA were excised, frozen at -80°C and spun through 0.45 μM Spin-X columns (Costar). Samples were phenol extracted and ethanol precipitated and resuspended in TE (pH 7.5). dsDNA concentration was measured using a Qubit fluorometer (Life Technologies). 20 ng of mononucleosomal DNA was used in qPCR reactions using the PrimerDesign Mastermix kit. Reactions using the equivalent amount of genomic DNA were included as a control. The primers used for this analysis are listed in Table S1.

Disclosure of Potential Conflicts of Interest

No potential conflicts of interest were disclosed.

Funding

CG was supported by the Medical Research Council and the National Institute for Health Research (NIHR) Newcastle Biomedical Research Center based at Newcastle Upon Tyne Hospitals NHS Foundation Trust and Newcastle University. The views expressed are those of the authors and not necessarily those of the NHS, NIHR, or the Department of Health. KP and SKW acknowledge support from the Wellcome Trust Institutional Strategic Support Fund to the University of Exeter (WT097835MF) and Newcastle University (WT 097823/Z/11/Z), respectively.

Supplemental Material

Supplemental data for this article can be accessed on the publisher's website.

References

- Burgess RJ, Zhang Z. Histone chaperones in nucleosome assembly and human disease. *Nat Struct Mol Biol* 2013; 20:14-22; PMID:23288364; <http://dx.doi.org/10.1038/nsmb.2461>
- Park YJ, Luger K. Histone chaperones in nucleosome eviction and histone exchange. *Curr Opin Struct Biol* 2008; 18:282-9; PMID:18534842; <http://dx.doi.org/10.1016/j.sbi.2008.04.003>
- Ransom M, Dennehey BK, Tyler JK. Chaperoning histones during DNA replication and repair. *Cell* 2010; 140:183-95; PMID:20141833; <http://dx.doi.org/10.1016/j.cell.2010.01.004>
- Amin AD, Vishnoi N, Prochasson P. A global requirement for the HIR complex in the assembly of chromatin. *Biochimica Et Biophysica Acta* 2013; 1819:264-76; PMID:24459729; <http://dx.doi.org/10.1016/j.bbagr.2011.07.008>
- Banumathy G, Somaiah N, Zhang R, Tang Y, Hoffmann J, Andrade M, Ceulemans H, Schultz D, Marmorstein R, Adams PD. Human UBN1 is an ortholog of yeast Hpc2p and has an essential role in the HIRA-ASF1a chromatin-remodeling pathway in senescent cells. *Mol Cell Biol* 2009; 29:758-70; PMID:19029251; <http://dx.doi.org/10.1128/MCB.01047-08>
- Tagami H, Ray-Gallet D, Almouzni G, Nakatani Y. Histone H3.1 and H3.3 complexes mediate nucleosome assembly pathways dependent or independent of DNA synthesis. *Cell* 2004; 116:51-61; PMID:14718166; [http://dx.doi.org/10.1016/S0092-8674\(03\)01064-X](http://dx.doi.org/10.1016/S0092-8674(03)01064-X)
- Balaji S, Iyer LM, Aravind L. HPC2 and ubinuclein define a novel family of histone chaperones conserved throughout eukaryotes. *Mol Biosyst* 2009; 5:269-75.
- Anderson HE, Kagansky A, Wardle J, Rappsilber J, Allshire RC, Whitehall SK. Silencing mediated by the *Schizosaccharomyces pombe* HIRA complex is dependent upon the Hpc2-like protein, Hip4. *PLoS One* 2010; 5:e13488; PMID:20976105; <http://dx.doi.org/10.1371/journal.pone.0013488>
- Green EM, Antczak AJ, Bailey AO, Franco AA, Wu KJ, Yates JR 3rd, Kaufman PD. Replication-independent histone deposition by the HIR complex and Asf1. *Curr Biol* 2005; 15:2044-9; PMID:16303565; <http://dx.doi.org/10.1016/j.cub.2005.10.053>
- Greenall A, Williams ES, Martin KA, Palmer JM, Gray J, Liu C, Whitehall SK. Hip3 interacts with the HIRA proteins Hip1 and Slm9 and is required for transcriptional silencing and accurate chromosome segregation. *J Biol Chem* 2006; 281:8732-9; PMID:16428807; <http://dx.doi.org/10.1074/jbc.M512170200>
- Prochasson P, Florens L, Swanson SK, Washburn MP, Workman JL. The HIR corepressor complex binds to nucleosomes generating a distinct protein/DNA complex resistant to remodeling by SWISNF. *Genes Dev* 2005; 19:2534-9; PMID:16264190; <http://dx.doi.org/10.1101/gad.1341105>
- Dutta D, Ray S, Home P, Saha B, Wang S, Sheibani N, Tawfik O, Cheng N, Paul S. Regulation of angiogenesis by histone chaperone HIRA-mediated incorporation of lysine 56-acetylated histone H3.3 at chromatin domains of endothelial genes. *J Biol Chem* 2010; 285:41567-77; PMID:21041298; <http://dx.doi.org/10.1074/jbc.M110.190025>
- Chujo M, Tarumoto Y, Miyatake K, Nishida E, Ishikawa F. HIRA, a conserved histone chaperone, plays an essential role in low-dose stress response via transcriptional stimulation in fission yeast. *J Biol Chem* 2012; 287:23440-50; PMID:22589550; <http://dx.doi.org/10.1074/jbc.M112.349944>
- Spector MS, Raff A, DeSilva H, Lee K, Osley MA. Hir1p and Hir2p function as transcriptional corepressors to regulate histone gene transcription in the *Saccharomyces cerevisiae* cell cycle. *Mol Cell Biol* 1997; 17:545-52; PMID:9001207
- Blackwell C, Martin KA, Greenall A, Pidoux A, Allshire RC, Whitehall SK. The *Schizosaccharomyces pombe* HIRA-like protein Hip1 is required for the periodic expression of histone genes and contributes to the function of complex centromeres. *Mol Cell Biol* 2004; 24:4309-20; PMID:15121850; <http://dx.doi.org/10.1128/MCB.24.10.4309-4320.2004>
- Hall IM, Noma K, Grewal SI. RNA interference machinery regulates chromosome dynamics during mitosis and meiosis in fission yeast. *Proc Natl Acad Sci U S A* 2003; 100:193-8; PMID:12509501; <http://dx.doi.org/10.1073/pnas.232688099>
- Yamane K, Mizuguchi T, Cui B, Zofall M, Noma K, Grewal SI. Asf1/HIRA facilitate global histone deacetylation and associate with HP1 to promote nucleosome occupancy at heterochromatic loci. *Mol Cell* 2011; 41:56-66; PMID:21211723; <http://dx.doi.org/10.1016/j.molcel.2010.12.009>
- Zhang R, Poustovoitov MV, Ye X, Santos HA, Chen W, Daganzo SM, Erzberger JP, Serebriiskii IG, Canutescu AA, Dunbrack RL, et al. Formation of MacroH2A-containing senescence-associated heterochromatin foci and senescence driven by ASF1a and HIRA. *Dev Cell* 2005; 8:19-30; PMID:15621527; <http://dx.doi.org/10.1016/j.devcel.2004.10.019>
- Banaszynski LA, Wen D, Dewell S, Whitcomb SJ, Lin M, Diaz N, Elsässer SJ, Chapigier A, Goldberg AD, Canaani E, et al. Hira-dependent histone H3.3 deposition facilitates PRC2 recruitment at developmental loci in ES cells. *Cell* 2013; 155:107-20; PMID:24074864; <http://dx.doi.org/10.1016/j.cell.2013.08.061>
- Anderson HE, Wardle J, Korkut SV, Murton HE, Lopez-Maury L, Bahler J, Whitehall SK. The fission yeast HIRA histone chaperone is required for promoter silencing and the suppression of cryptic antisense transcripts. *Mol Cell Biol* 2009; 29:5158-67; PMID:19620282; <http://dx.doi.org/10.1128/MCB.00698-09>
- Gallastegui E, Millan-Zambrano G, Terme JM, Chavez S, Jordan A. Chromatin reassembly factors are involved in transcriptional interference promoting HIV latency. *J Virol* 2011; 85:3187-202; PMID:21270164; <http://dx.doi.org/10.1128/JVI.01920-10>
- Formosa T, Ruone S, Adams MD, Olsen AE, Eriksson P, Yu Y, Rhoades AR, Kaufman PD, Stillman DJ. Defects in SPT16 or POB3 (yFACT) in *Saccharomyces cerevisiae* cause dependence on the HirHpc pathway: polymerase passage may degrade chromatin structure. *Genetics* 2002; 162:1557-71; PMID:12524332
- Cheung V, Chua G, Batada NN, Landry CR, Michnick SW, Hughes TR, Winston F. Chromatin- and transcription-related factors repress transcription from within coding regions throughout the *Saccharomyces cerevisiae* genome. *PLoS Biol* 2008; 6:e277; PMID:18998772; <http://dx.doi.org/10.1371/journal.pbio.0060277>
- Nourani A, Robert F, Winston F. Evidence that Spt2Sin1, an HMG-like factor, plays roles in transcription elongation, chromatin structure, and genome stability in *Saccharomyces cerevisiae*. *Mol Cell Biol* 2006; 26:1496-509; PMID:16449659; <http://dx.doi.org/10.1128/MCB.26.4.1496-1509.2006>
- Ray-Gallet D, Woolfe A, Vassias I, Pellentz C, Lacoste N, Puri A, Schultz DC, Pchelintsev NA, Adams PD, Jansen LE, et al. Dynamics of histone H3 deposition in vivo reveal a nucleosome gap-filling mechanism for H3.3 to maintain chromatin integrity. *Mol Cell* 2011; 44:928-41; PMID:22195966; <http://dx.doi.org/10.1016/j.molcel.2011.12.006>
- Kent NA, Adams S, Moorhouse A, Paszkiewicz K. Chromatin particle spectrum analysis: a method for comparative chromatin structure analysis using paired-end mode next-generation DNA sequencing. *Nucleic Acids Res* 2011; 39:e26; PMID:21131275; <http://dx.doi.org/10.1093/nar/gkq1183>
- Shim YS, Choi Y, Kang K, Cho K, Oh S, Lee J, Grewal SI, Lee D. Hrp3 controls nucleosome positioning to suppress non-coding transcription in eu- and heterochromatin. *EMBO J* 2012; 31:4375-87; PMID:22990236; <http://dx.doi.org/10.1038/emboj.2012.267>
- Jiang C, Pugh BF. Nucleosome positioning and gene regulation: advances through genomics. *Nat Rev Genet* 2009; 10:161-72; PMID:19204718; <http://dx.doi.org/10.1038/nrg2522>
- Pointner J, Persson J, Prasad P, Norman-Axelsson U, Stralfors A, Khorosjutina O, Krietenstein N, Svensson JP, Ekwall K, Korber P. CHD1 remodelers regulate nucleosome spacing in vitro and align nucleosomal arrays over gene coding regions in *S. pombe*. *EMBO J* 2012; 31:4388-403; PMID:23103765; <http://dx.doi.org/10.1038/emboj.2012.289>
- Infante JJ, Law GL, Young ET. Analysis of nucleosome positioning using a nucleosome-scanning assay. *Methods Mol Biol* 2012; 833:63-87; PMID:22183588; http://dx.doi.org/10.1007/978-1-61779-477-3_5
- Lantermann AB, Straub T, Stralfors A, Yuan GC, Ekwall K, Korber P. *Schizosaccharomyces pombe* genome-wide nucleosome mapping reveals positioning mechanisms distinct from those of *Saccharomyces cerevisiae*. *Nat Struct Mol Biol* 2010; 17:251-7; PMID:20118936; <http://dx.doi.org/10.1038/nsmb.1741>
- Takayama Y, Takahashi K. Differential regulation of repeated histone genes during the fission yeast cell cycle. *Nucleic Acids Res* 2007; 35:3223-37; PMID:17452352; <http://dx.doi.org/10.1093/nar/gkm213>
- Valente LP, Dehe PM, Klutstein M, Aligianni S, Watt S, Bahler J, Promislow Cooper J. Myb-domain protein Teb1 controls histone levels and centromere assembly in fission yeast. *EMBO J* 2013; 32:450-60; PMID:23314747; <http://dx.doi.org/10.1038/emboj.2012.339>
- Kumar Y, Bhargava P. A unique nucleosome arrangement, maintained actively by chromatin remodelers facilitates transcription of yeast tRNA genes. *BMC Genomics* 2013; 14:402; PMID:23767421; <http://dx.doi.org/10.1186/1471-2164-14-402>
- Kassavetis GA, Geiduschek EP. Transcription factor TFIIB and transcription by RNA polymerase III. *Biochem Soc Trans* 2006; 34:1082-7; PMID:17073756; <http://dx.doi.org/10.1042/BST0341082>
- Neumuller RA, Gross T, Samsonova AA, Vinayagam A, Buckner M, Founk K, Hu Y, Sharifpour S, Rosebrock AP, Andrews B, et al. Conserved regulators of nucleolar size revealed by global phenotypic analyses. *Sci Signaling* 2013; 6:ra70; PMID:23962978; <http://dx.doi.org/10.1126/scisignal.2004145>
- Givens RM, Lai WK, Rizzo JM, Bard JE, Mieczkowski PA, Leatherwood J, Huberman JA, Buck MJ. Chromatin architectures at fission yeast transcriptional promoters and replication origins. *Nucleic Acids Res* 2012; 40:7176-89; PMID:22573177; <http://dx.doi.org/10.1093/nar/gks351>
- Reyes-Turcu FE, Grewal SI. Different means, same end-heterochromatin formation by RNAi and RNAi-independent RNA processing factors in fission yeast. *Curr Opin Genet Dev* 2012; 22:156-63; PMID:22243696; <http://dx.doi.org/10.1016/j.gde.2011.12.004>
- Hansen KR, Burns G, Mata J, Volpe TA, Martienssen RA, Bahler J, Thon G. Global effects on gene expression in fission yeast by silencing and RNA interference machineries. *Mol Cell Biol* 2005; 25:590-601; PMID:15632061; <http://dx.doi.org/10.1128/MCB.25.2.590-601.2005>
- Li B, Carey M, Workman JL. The role of chromatin during transcription. *Cell* 2007; 128:707-19; PMID:17320508; <http://dx.doi.org/10.1016/j.cell.2007.01.015>
- Chen ES, Saitoh S, Yanagida M, Takahashi K. A cell cycle-regulated GATA factor promotes centromeric localization of CENP-A in fission yeast. *Mol Cell* 2003; 11:175-87; PMID:12535531; [http://dx.doi.org/10.1016/S1097-2765\(03\)00011-X](http://dx.doi.org/10.1016/S1097-2765(03)00011-X)
- Rustici G, Mata J, Kivinen K, Lio P, Penkett CJ, Burns G, Hayles J, Brazma A, Nurse P, Bähler J. Periodic gene expression program of the fission yeast cell cycle. *Nat Genet* 2004; 36:809-17; PMID:15195092; <http://dx.doi.org/10.1038/ng1377>

43. Schermer UJ, Korber P, Horz W. Histones are incorporated in trans during reassembly of the yeast PHO5 promoter. *Mol Cell* 2005; 19:279-85; PMID:16039596; <http://dx.doi.org/10.1016/j.molcel.2005.05.028>
44. Sugiyama T, Cam HP, Sugiyama R, Noma K, Zofall M, Kobayashi R, Grewal SI. SHREC, an effector complex for heterochromatic transcriptional silencing. *Cell* 2007; 128:491-504; PMID:17289569; <http://dx.doi.org/10.1016/j.cell.2006.12.035>
45. Gallastegui E, Marshall B, Vidal D, Sanchez-Duffhues G, Collado JA, Alvarez-Fernandez C, Luque N, Terme JM, Gatell JM, Sánchez-Palomino S, et al. Combination of biological screening in a cellular model of viral latency and virtual screening identifies novel compounds that reactivate HIV-1. *J Virol* 2012; 86:3795-808; PMID:22258251; <http://dx.doi.org/10.1128/JVI.05972-11>
46. Qian Z, Huang H, Hong JY, Burck CL, Johnston SD, Berman J, Carol A, Liebman SW. Yeast Ty1 retrotransposition is stimulated by a synergistic interaction between mutations in chromatin assembly factor I and histone regulatory proteins. *Mol Cell Biol* 1998; 18:4783-92; PMID:9671488
47. Vanti M, Gallastegui E, Respalda I, Rodriguez-Gil A, Gomez-Herreros F, Jimeno-Gonzalez S, Jordan A, Chávez S. Yeast genetic analysis reveals the involvement of chromatin reassembly factors in repressing HIV-1 basal transcription. *PLoS Genet* 2009; 5:e1000339; PMID:19148280; <http://dx.doi.org/10.1371/journal.pgen.1000339>
48. Moreno S, Klar A, Nurse P. Molecular genetic analysis of fission yeast *Schizosaccharomyces pombe*. *Methods Enzymol* 1991; 194:795-823; PMID:2005825; [http://dx.doi.org/10.1016/0076-6879\(91\)94059-L](http://dx.doi.org/10.1016/0076-6879(91)94059-L)
49. Langmead B, Trapnell C, Pop M, Salzberg SL. Ultrafast and memory-efficient alignment of short DNA sequences to the human genome. *Genome Biol* 2009; 10:R25; PMID:19261174; <http://dx.doi.org/10.1186/gb-2009-10-3-r25>
50. Nicol JW, Helt GA, Blanchard SG Jr, Raja A, Loraine AE. The Integrated Genome Browser: free software for distribution and exploration of genome-scale datasets. *Bioinformatics* 2009; 25:2730-1; PMID:19654113; <http://dx.doi.org/10.1093/bioinformatics/btp472>
51. Maruyama H, Harwood JC, Moore KM, Paszkiewicz K, Durley SC, Fukushima H, Atomi H, Takeyasu K, Kent NA. An alternative beads-on-a-string chromatin architecture in *Thermococcus kodakarensis*. *EMBO Rep* 2013; 14:711-7; PMID:23835508; <http://dx.doi.org/10.1038/embor.2013.94>

ARTICLE

Received 14 Oct 2013 | Accepted 12 May 2014 | Published 9 Jun 2014

DOI: 10.1038/ncomms5091

A histone H3K36 chromatin switch coordinates DNA double-strand break repair pathway choice

Chen-Chun Pai^{1,*}, Rachel S. Deegan^{1,*}, Lakxmi Subramanian², Csenge Gal³, Sovan Sarkar¹, Elizabeth J. Blaikley¹, Carol Walker¹, Lydia Hulme¹, Eric Bernhard¹, Sandra Codlin⁴, Jürg Bähler⁴, Robin Allshire², Simon Whitehall³ & Timothy C. Humphrey¹

DNA double-strand break (DSB) repair is a highly regulated process performed predominantly by non-homologous end joining (NHEJ) or homologous recombination (HR) pathways. How these pathways are coordinated in the context of chromatin is unclear. Here we uncover a role for histone H3K36 modification in regulating DSB repair pathway choice in fission yeast. We find Set2-dependent H3K36 methylation reduces chromatin accessibility, reduces resection and promotes NHEJ, while antagonistic Gcn5-dependent H3K36 acetylation increases chromatin accessibility, increases resection and promotes HR. Accordingly, loss of Set2 increases H3K36Ac, chromatin accessibility and resection, while Gcn5 loss results in the opposite phenotypes following DSB induction. Further, H3K36 modification is cell cycle regulated with Set2-dependent H3K36 methylation peaking in G1 when NHEJ occurs, while Gcn5-dependent H3K36 acetylation peaks in S/G2 when HR prevails. These findings support an H3K36 chromatin switch in regulating DSB repair pathway choice.

¹CRUK MRC Oxford Institute for Radiation Oncology, Department of Oncology, University of Oxford, ORCRB, Roosevelt Drive, Oxford OX3 7DQ, UK.

²Wellcome Trust Centre for Cell Biology, Institute of Cell Biology, The University of Edinburgh, Swann Building, Mayfield Road, Edinburgh EH9 3JR, UK.

³Institute for Cell and Molecular Biosciences, The Medical School, Newcastle University, Framlington Place, Newcastle upon Tyne, NE2 4HH, UK. ⁴University College London, Department of Genetics, Evolution and Environment, Darwin Building, Gower Street, London WC1E 6BT, UK. * These authors contributed equally to this work. Correspondence and requests for materials should be addressed to T.C.H. (email: timothy.humphrey@oncology.ox.ac.uk).

DNA double-strand breaks (DSBs) if unrepaired or inappropriately repaired can lead to cell death or genomic instability¹. To prevent such undesirable outcomes, cells employ the evolutionarily conserved non-homologous end joining (NHEJ) or homologous recombination (HR) repair pathways to restore genome integrity. During NHEJ, the broken ends are protected by the Ku70/80 heterodimer, which in mammalian cells facilitates recruitment of the DNA-dependent protein kinase (DNA-PKcs). This facilitates processing of damaged DNA ends and subsequent ligation of the compatible ends through the activity of the conserved DNA ligase 4, XLF, XRCC4 complex². HR is initiated by resection of the 5' end of the DSB to generate a 3' single-stranded DNA (ssDNA) overhang. This is bound by replication protein A (RPA), and, during mitotic recombination, a Rad51 nucleofilament is formed promoting strand invasion of the sister chromatid or homologous chromosome, which is used as a repair template before second end capture³. DSB repair pathway choice is influenced by a number of factors including cell cycle phase. In yeast, NHEJ is restricted to G1, while HR operates in S and G2 phase cells when a sister chromatid is available as a repair template^{4–6}. DSB

resection is a critical determinant of repair pathway choice and is highly regulated as inappropriate pathway deployment can result in pathological consequences¹.

Here we have investigated the role of histone H3 lysine 36 (H3K36) modification in DSB repair pathway choice. H3K36 methylation is associated with numerous functions⁷. In *Saccharomyces cerevisiae*, SET (*Su(var)3-9*, *Ez*, *Trithorax*) domain-containing 2 (*Set2*) is responsible for mono, di and trimethylation of H3K36 (ref. 8). In humans, H3K36 methylation is catalysed through the activities of eight distinct enzymes, while SETD2/HYPB uniquely catalyses the trimethylation of H3K36 (ref. 9). Importantly, SETD2 has recently been classified as a novel tumour suppressor, suggesting a role in genome stability^{10–14}. Links between histone H3K36 methylation and DSB repair have been identified in yeast and human cells^{15–17}. These findings support a role for H3K36 methylation in promoting efficient NHEJ, although the molecular basis of this is unknown. A role for H3K36 methylation in promoting HR has also been recently described¹⁸. Histone H3K36 residues can also be acetylated, which in *S. cerevisiae* is performed by the Gcn5 histone acetyltransferase (HAT)¹⁹. Gcn5 is the catalytic subunit of the SAGA, ADA and SLIK chromatin-modifying complexes that post-translationally modify histones and regulate gene expression²⁰. Gcn5 has also been associated with DSB repair in yeast and human cells, and these data suggest a possible role in HR^{21–24}. Structurally, H3K36 residues can be either methylated or acetylated raising the intriguing possibility that these exclusive marks might drive distinct biological effects within chromatin¹⁹. As NHEJ and HR pathways can exhibit an antagonistic relationship^{25,26}, we have investigated the functional interplay between these H3K36 modifications in regulating DSB repair pathway choice in fission yeast.

Here we identify a role for Set2-dependent H3K36 methylation in facilitating NHEJ. In contrast, we find Gcn5-dependent H3K36 acetylation promotes HR. Together our findings support a role for an H3K36 chromatin switch in coordinating DSB repair pathway choice in fission yeast.

Results

Set2 methyltransferase suppresses homologous recombination.

To determine a possible role for H3K36 modification in DSB repair, we examined the effect of deleting *Set2* on damage sensitivity. *set2Δ* cells were found to exhibit modest sensitivity to both the radiomimetic bleomycin and ionizing radiation (IR) compared with wild-type cells, indicating a role for Set2 in the cellular response to DSBs (Fig. 1a,b). To investigate the role of Set2 methyltransferase activity in the DNA damage response, a highly conserved arginine within the catalytic SET domain was mutated to glycine (*set2-R255G*) within the endogenous *set2⁺* gene, which was predicted to disrupt the methyltransferase activity (Fig. 1c)^{8,27}. No H3K36me3 was observed in *set2Δ* cells, indicating an absolute requirement for Set2 in H3K36 trimethylation in fission yeast, as previously described²⁸ (Fig. 1d). Substantially reduced levels of H3K36me3 were observed in the *set2-R255G* mutant compared with wild type, indicating that this residue is required for optimal H3K36 methylation (Fig. 1d). To investigate a possible role for Set2 in DSB repair, we used a DSB assay to quantitate marker loss profiles and thus repair responses to a site-specific DSB within a non-essential minichromosome²⁹ (Supplementary Fig. 1). This revealed that deletion of *set2⁺* resulted in significantly elevated levels of gene conversion (GC) (72% $P=0.02$), compared with wild type (55%) (Fig. 1e and Table 1). HO induction in a *set2-R255G* background resulted in a very similar DSB repair profile to *set2Δ* with significantly elevated levels of GC

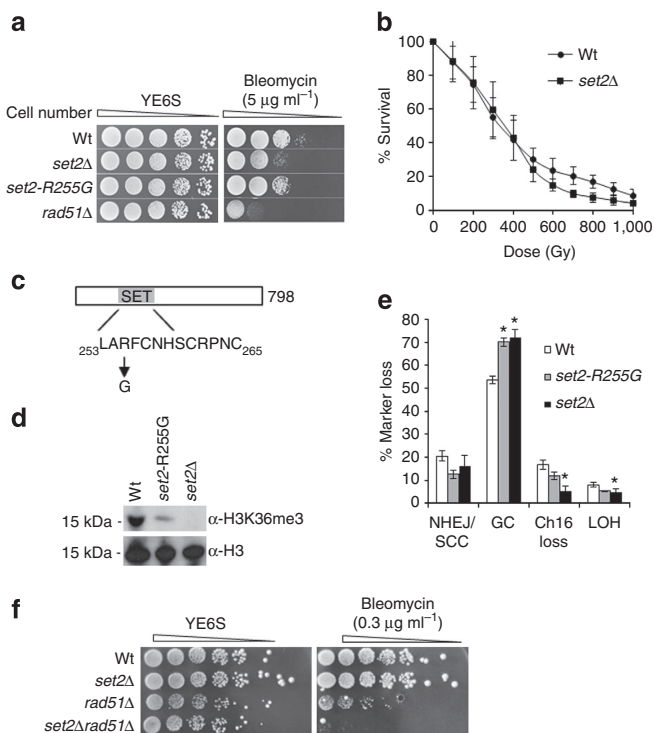


Figure 1 | Set2 is required to suppress HR and for resistance to DNA-damaging agents. (a) 10-fold serial dilutions of wild-type, *set2Δ*, *set2-R255G* and *rad51Δ* strains on YE6S, YE6S + 5 μg/ml bleomycin. Plates were incubated at 32 °C for 3 days. At least two biological replicates were performed. (b) IR survival curve for wild-type (Wt) and *set2Δ* strains. Means ± s.e. of three experiments are shown. (c) A schematic of the structure of Set2 with SET (ASW) domain shown with amino-acid sequences indicating arginine residue mutated in SET domain of the *set2-R255G* mutant. (d) Western blot analysis of H3K36me3 levels in wild-type (Wt), *set2Δ* and *set2-R255G* cells. (e) Percentage DSB-induced marker loss in wild type (Wt), *set2Δ* and *set2-R255G* containing Ch16-RMGAH. The levels of NHEJ/SCC, GC, Ch16 loss and LOH are shown. Means ± s.e. of three experiments are shown. * represents significant difference compared with wild-type ($P < 0.05$, t-test). See also Supplementary Fig. 1 and Table 1. (f) *set2Δ* cells are sensitive to bleomycin in combination with *rad51Δ*. Fivefold serial dilutions of wild-type (Wt), *set2Δ*, *rad51Δ* and *set2Δ rad51Δ* cells were grown on YE6S and YE6S + 0.3 μg/ml⁻¹ bleomycin.

Table 1 | Analysis of DSB repair outcomes in different genetic backgrounds.

Genetic background	% NHEJ/SCC	P-value	% GC	P-value	% Ch ¹⁶ loss	P-value	% LOH	P-value
Wild type (Ch ¹⁶ -RMGAH)	20 ± 2.3	–	55 ± 2.3	–	17 ± 1.4	–	7 ± 1.0	–
<i>set2Δ</i> (Ch ¹⁶ -RMGAH)	16 ± 4.6	0.57	72 ± 3.4	0.02	5 ± 2.2	0.02	5 ± 1.5	0.09
<i>set2-R255G</i> (Ch ¹⁶ -RMGAH)	12 ± 1.8	0.24	70 ± 1.8	<0.01	12 ± 1.7	0.10	5 ± 0.1	<0.01
Wild type (Ch ¹⁶ -RMYAH)	4 ± 0.8	–	67 ± 1.4	–	20 ± 0.8	–	8 ± 0.6	–
<i>gcn5Δ</i> (Ch ¹⁶ -RMYAH)	33 ± 1.6	<0.01	45 ± 3.0	<0.01	14 ± 1.5	0.18	6 ± 0.1	0.04
<i>gcn5Δ lig4Δ</i> (Ch ¹⁶ -RMYAH)	23 ± 1.5	<0.01	56 ± 1.5	0.02	14 ± 2.2	0.07	6 ± <0.01	0.03
<i>set2Δ gcn5Δ</i> (Ch ¹⁶ -RMYAH)	21 ± 1.4	<0.01	71 ± 1.7	0.65	5 ± 0.2	0.01	2 ± 0.3	<0.01

For each genetic background the assay was repeated three times (with independent isolates), such that >1,000 colonies were scored. Mean ± s.e. of the three experiments are shown. A single blank vector control was also analysed in each genetic background to give a spontaneous level of Ch¹⁶ loss, which was subtracted to calculate the break-induced values shown above. P-values (t-test) are against wild type Ch¹⁶-RMYAH unless otherwise stated.

(70% $P < 0.01$), compared with wild type (Fig. 1e and Table 1), thus identifying a role for Set2 methyltransferase activity in suppressing HR repair. Consistent with an HR-independent role for Set2 in DSB repair, a double mutant *set2Δ rad51Δ* exhibited acute sensitivity to bleomycin compared with the single mutants (Fig. 1f), indicating that Set2 is required for survival in the absence of HR.

Set2 methyltransferase is required for canonical NHEJ. As HR and NHEJ can compete during DSB repair^{25,26}, the increased HR observed in the *set2Δ* and *set2-R255G* backgrounds could have arisen from reduced NHEJ, which may have been masked by sister chromatid conversion (SCC) in our DSB assay (Supplementary Fig. 1). Consistent with a role for Set2 in NHEJ, *lig4Δ* was found to be epistatic with *set2Δ* in response to bleomycin (Fig. 2a). Further, quantitating colony survival indicated that the *set2Δ lig4Δ* double mutant phenocopied the sensitivity of *set2Δ* to bleomycin (Fig. 2b). These data support a role for Set2 in canonical NHEJ. However, as *set2Δ* was more sensitive than *lig4Δ*, Set2 must also perform an additional NHEJ-independent function in response to DNA damage. The ability of Set2 to repair a DSB by NHEJ was further assessed using a plasmid-rejoining assay, in which recircularization of linearized *LEU2* plasmids by NHEJ allows stable propagation of *leu*⁺ colonies. *LEU2* plasmids linearized with PstI (3' overhang), EcoRI (5' overhang) or PvuII (blunt) were transformed into wild-type, *lig4Δ*, and *set2Δ* cells and the number of *leu*⁺ colonies quantified. Plasmid rejoining was impaired in *set2Δ* cells compared with wild-type cells (Fig. 2c). Plasmid rejoining was also impaired in the *set2-R255G* strain (Supplementary Fig. 2). These results together define a role for Set2 methyltransferase activity in promoting canonical NHEJ and are consistent with impaired NHEJ in *set2Δ* cells leading to increased HR. No significant changes in gene expression of NHEJ or HR repair genes were observed in *set2Δ* cells in the absence or presence of damage, suggesting a direct role in NHEJ. (Supplementary Fig. 3a,b).

To determine the mechanism by which Set2 promotes NHEJ, we investigated whether H3K36me-interacting proteins (readers) functioned in NHEJ. In *S. cerevisiae*, co-transcriptional methylation of H3K36 by Set2 leads to recruitment of the Rpd3S HDAC complex, which deacetylates histones in the wake of elongating PolII³⁰. However, analysis of *alp13Δ* or *clr6-1*, which disrupt the equivalent deacetylase complex in *S. pombe*^{31,32}, failed to disrupt NHEJ (Supplementary Fig. 4a,b), indicating that Set2 functions independently of the Clr6 HDAC complex to promote NHEJ. To further investigate the role of Set2 in promoting NHEJ and suppressing HR, we considered a possible role for Set2 in protecting DSB ends from resection. To test this, levels of RPA foci were investigated following exposure to 50 Gy IR using a construct in which the large subunit of RPA was GFP-tagged

(Rad11-GFP)³³. As expected, loss of end-protection in *ku70Δ* cells leads to increased Rad11-GFP foci following DSB induction³⁴ (Supplementary Fig. 5). Similarly, an increase in Rad11-GFP foci was observed in a *set2-R255G* mutant background compared with wild type (Fig. 2d), suggesting a role for Set2 methyltransferase activity in preventing break-induced ssDNA formation analogously to Ku70, thus providing an explanation for the increase in HR in the absence of Set2. We also observed increased level of RPA levels in G1-arrested *set2Δ* cells compared with G1-arrested wild-type cells (Supplementary Fig. 6).

We next investigated whether H3K36 methylation was induced in response to a site-specific DSB. Chromatin immunoprecipitation (ChIP) analysis revealed that H3K36me3 levels increase in a Set2-dependent manner following HO-induced DSB induction (Fig. 2e). Given the loss of end protection and increased HR observed following Set2 loss, we examined a possible role for Set2-dependent H3K36 methylation in Ku recruitment to a DSB. ChIP analysis revealed a significant reduction in the levels of Ku80-myc associated with a HO-induced DSB in a *set2Δ* background (Fig. 2f). Together these findings support a role for Set2-dependent H3K36 methylation in Ku recruitment to break-sites thereby facilitating NHEJ.

H3K36 methylation and acetylation are mutually inhibitory.

Lysine residues in proteins can be methylated or acetylated in a mutually exclusive manner. As loss of Set2 led to DSB end deprotection and increased HR, we investigated whether these events were associated with loss of H3K36 methylation and increased H3K36 acetylation. In budding yeast, H3K36 is acetylated by the Gcn5 histone acetyltransferase (HAT)¹⁹. To examine the relationship between H3K36 modifications, levels of H3K36 methylation and acetylation were analysed from nuclear extracts of wild-type, *set2Δ* or *gcn5Δ* cells by western blot analysis. In contrast to wild type, H3K36ac was undetectable in *gcn5Δ* cells, thus defining an evolutionarily conserved role for Gcn5 as the H3K36 HAT in fission yeast, as in budding yeast (Fig. 3a)¹⁹. In the absence of Set2, H3K36ac levels were elevated compared with wild type (Fig. 3a). As expected, no H3K36me3 was observed in *set2Δ* cells, consistent with Set2 being essential for H3K36 methylation (Figs 1d and 3b). Surprisingly, H3K36me3 levels in *gcn5Δ* cells were much higher than that observed in wild-type cells (Fig. 3b). Thus, Gcn5-dependent H3K36ac inhibits H3K36me3, indicating that these H3K36 modifications are mutually inhibitory.

Gcn5 promotes HR and suppresses NHEJ. As Gcn5-dependent H3K36ac inhibits Set2-dependent H3K36me, which our data indicate is required for NHEJ, we investigated whether Gcn5 facilitated HR repair. We found that *gcn5Δ* cells exhibited mild sensitivity to bleomycin (Fig. 3c) consistent with a role for Gcn5

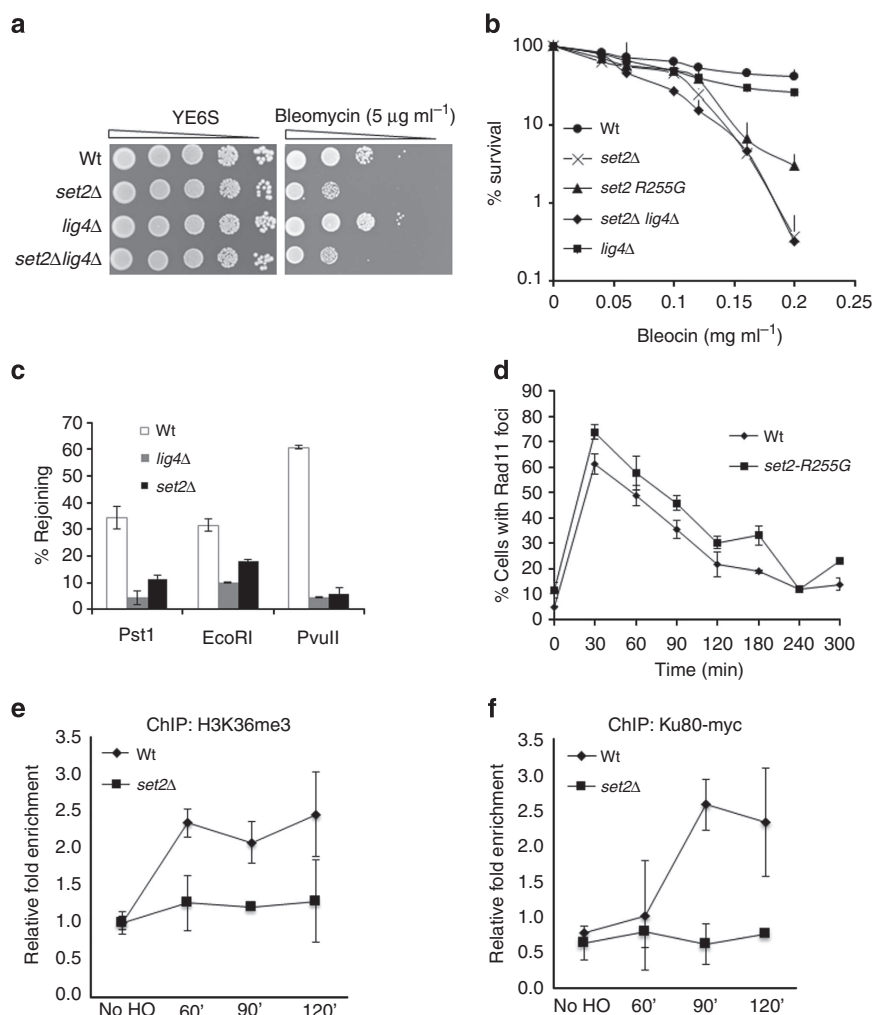


Figure 2 | Set2 is required for C-NHEJ. (a) Serial dilutions of the indicated strains were spotted onto YE6S containing 5 $\mu\text{g ml}^{-1}$ bleomycin or no drug. Plates were incubated at 32 °C for 3 days. (b) Percentage survival of strains indicated compared with wild-type following plating on YE6S +/– the indicated bleocin concentration. Plates were incubated for 3 days at 32 °C and then scored. Means \pm s.e. of four independent experiments are shown. (c) Set2 is required for NHEJ plasmid rejoining. The percentage of leu^+ colonies obtained following transformation rejoining of a *LEU2* plasmid (pAL19) linearized with EcoRI, PstI or PvuII following transformation into wild-type (Wt), *lig4* Δ and *set2* Δ strains compared with uncut plasmid control is shown. Means \pm s.e. of three experiments are shown. See also Supplementary Fig. 2. (d) Quantification of Rpa1(Rad11)-GFP foci in wild-type (Wt) and *set2-R255G* strains following exposure to 50 Gy IR treatment. Mean \pm s.e. of three experiments are shown. See also Supplementary Fig. 5. (e) DSB induction results in a Set2-dependent increase in histone H3K36me3 levels proximal to the HO break. qChIP enrichments of H3K36me3 in wild-type (Wt) or *set2* Δ cells at various times (60, 90 or 120 min) following urg-HO induced DSB induction at the *MATa* site between SPAC3H1.10 and *hsr1* on Chromosome I, as previously described⁵⁹. Enrichment of immunoprecipitated DNA at 50 bp from the break relative to that at *act1* is presented, as a ratio of that observed in a strain expressing no HO endonuclease. Error bars represent s.d. from at least two biological replicates. (f) DSB induction results in a Set2-dependent increase in Ku80 levels proximal to the HO break. qChIP enrichments of Ku80-myc in wild-type (Wt) or *set2* Δ cells at various times (60, 90 or 120 min) following urg-HO induction as described above. Enrichment of immunoprecipitated DNA at 50 bp from the break, relative to that at the *fbp1* locus is presented. Error bars represent s.d. from at least two biological replicates.

in DSB repair³⁵. Microarray analysis previously performed on *gcn5* Δ cells did not identify any alteration in the transcription of DSB repair genes³⁶, suggesting a direct role for Gcn5 in DSB repair. Therefore, a role for Gcn5 in DSB repair was further examined using the DSB assay (Supplementary Fig. 1). DSB induction in a *gcn5* Δ background resulted in significantly increased levels of NHEJ/SCC (33%, $P < 0.01$) and significantly reduced GC (45%, $P < 0.01$) compared with wild-type cells (Fig. 3d and Table 1). These results identified a role for Gcn5 in promoting efficient HR. Further, these results contrasted with those observed following loss of Set2 methyltransferase.

To investigate when Gcn5 acts during HR, the kinetics of Rad51-CFP foci were analysed in *gcn5* Δ cells following treatment with IR. *gcn5* Δ cells exhibited a striking reduction in Rad51-CFP

foci 30–60 min following treatment with 50 Gy IR, compared with wild-type cells (Fig. 3e). Following this initial decline, the percentage of cells with Rad51-CFP foci increased again 120 min after damage. Importantly, Rad51-CFP expression was not affected in *gcn5* Δ cells (Supplementary Fig. 7). These data indicated that *gcn5* Δ cells, although still able to recruit Rad51, did so much less effectively than wild-type cells, indicating a role for Gcn5 in HR before strand invasion (synapsis). To further address the presynaptic role of Gcn5, the recruitment of RPA subunit Rad11-GFP to ssDNA following exposure to 50 Gy IR was examined. In contrast to wild-type cells, the levels of Rad11-GFP foci were reduced in *gcn5* Δ cells at earlier time points (Fig. 3f). Therefore, Gcn5 functions presynaptically during HR to promote ssDNA formation following DSB induction. We noted that again,

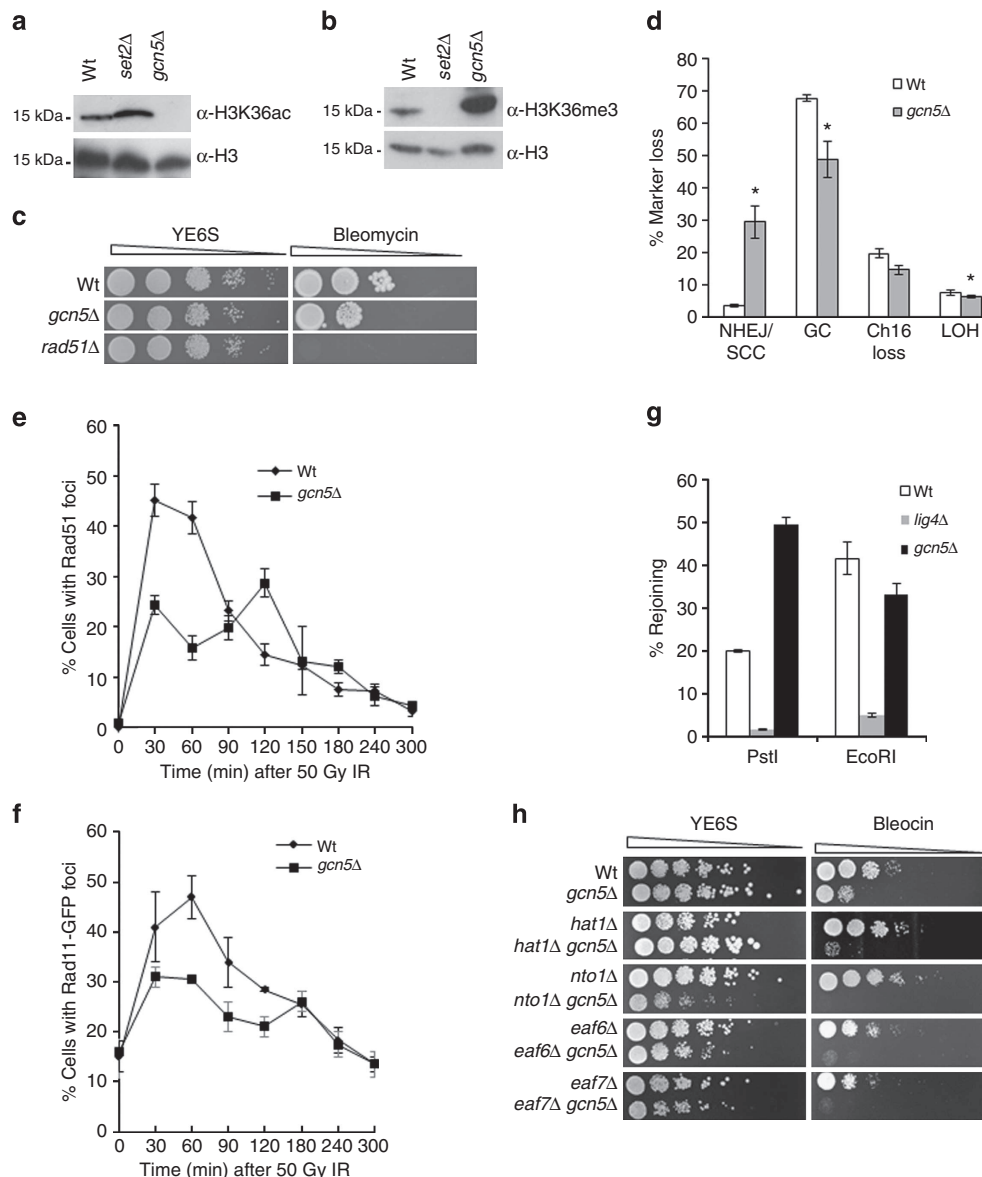


Figure 3 | Gcn5 promotes HR and suppresses NHEJ. (a,b) Methylation and acetylation of H3K36 are mutually inhibitory. (a) Western blot analysis of H3K36me3 in wild type (Wt), *set2Δ* and *gcn5Δ* nuclear extract. (b) Western blot analysis of H3K36ac in wild type (Wt), *set2Δ* and *gcn5Δ* nuclear extract. (c) Fivefold serial dilutions of wild-type (Wt), *gcn5Δ* and *rad51Δ* strains on YE6S and YE6S + 5 μg ml⁻¹ bleomycin. Plates were incubated at 32 °C for 3 days. At least two biological replicates were performed. (d) Percentage DSB-induced marker loss in wild type (Wt) and *gcn5Δ* containing Ch¹⁶-RMYAH. The levels of NHEJ/SCC, GC, Ch¹⁶ loss and LOH are shown. Means ± s.e. of three experiments are shown. * represents significant difference compared with wild type ($P < 0.05$, t -test). See also Table 1. (e) Quantification of Rad51-CFP foci in wild-type and *gcn5Δ* strains following exposure to 50 Gy IR. (f) Quantification of Rpa1(Rad11)-GFP foci in wild-type and *gcn5Δ* strains following exposure to 50 Gy IR treatment. Data are the mean of three experiments and error bars (± s.e.) are shown. (g) Gcn5 suppresses NHEJ plasmid rejoining. The percentage of leu⁺ colonies obtained following transformation and rejoining of a *LEU2* plasmid (pAL19) linearized with EcoRI, PstI into wild-type, *lig4Δ* and *gcn5Δ* strains compared with uncut plasmid control is shown. Means ± s.e. of three experiments are shown. (h) Gcn5 functions redundantly with other HAT complex subunits in the DNA damage response. Fivefold serial dilutions of wild-type (Wt), *gcn5Δ*, *hat1Δ*, *hat1Δ gcn5Δ*, *nto1Δ*, *nto1Δ gcn5Δ*, *eaf6Δ*, *eaf6Δ gcn5Δ*, *eaf7Δ*, and *eaf7Δ gcn5Δ* strains on YE6S and YE6S + 5 μg ml⁻¹ bleocin. At least two biological replicates were performed.

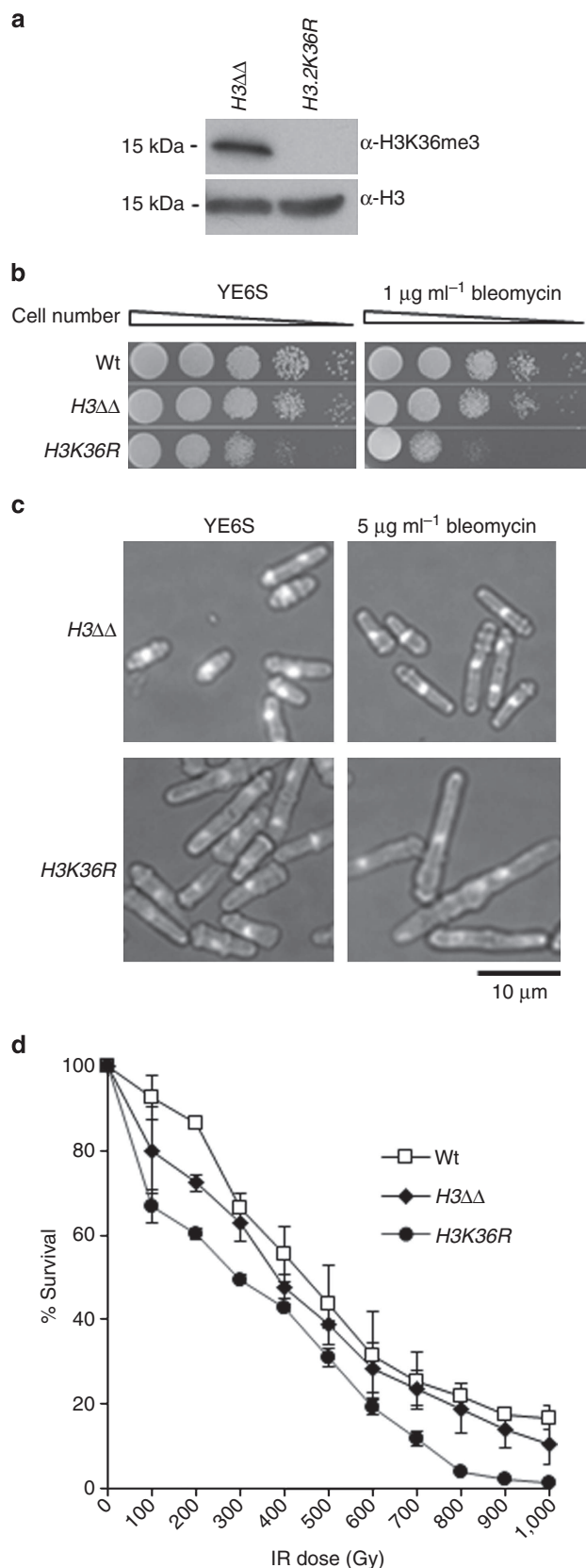
Gcn5 loss exhibited an opposite phenotype to that observed in a *set2-R255G* background (Fig. 2d).

Given the reduced ssDNA formation following DSB induction, we further addressed whether DSB repair was associated with elevated levels of NHEJ in a *gcn5Δ* background. To confirm whether NHEJ was increased following DSB induction in the *gcn5Δ* mutant (Fig. 3d), repair in a *gcn5Δ lig4Δ* double mutant was assessed using the DSB assay (Supplementary Fig. 1). The proportion of NHEJ/SCC colonies was reduced in a *gcn5Δ lig4Δ* background (23%) compared with *gcn5Δ* (33%) consistent with

10% of this population being attributable to NHEJ in a *gcn5Δ* strain (Table 1). This level is significantly greater than the NHEJ/SCC level in wild-type cells (4% $P < 0.01$), and thus represents a significant increase in NHEJ in the *gcn5Δ* mutant. A similar profile was observed in a *gcn5Δ set2Δ* double mutant (Table 1). Further analysis by the plasmid-rejoining assay indicated that *gcn5Δ* cells exhibited consistently increased rejoining of a *PstI* linearized plasmid compared to wild-type cells, although this appeared to depend on the presence of a 3' overhang, as the same was not observed for an *EcoRI*-linearized plasmid (Fig. 3g).

As *gcn5Δ* exhibited mild sensitivity to DNA damage compared with *rad51Δ* (Fig. 3c), we tested whether Gcn5 functioned redundantly with other HAT complexes to facilitate the DNA damage response. We found that deletion of *gcn5⁺* together with

genes encoding the histone acetyltransferase Hat1 (ref. 37), Nto1 (a subunit of the NuA3/Mst2 complex)³⁵, Eaf6 (a subunit of both NuA3 and NuA4)³⁵ or Eaf7 (a subunit of the NuA4 complex)³⁸ resulted in a striking increase in bleomycin sensitivity compared with the single mutants (Fig. 3h). These findings support a key role for Gcn5 in facilitating the DNA damage response in conjunction with other HAT complexes. These findings are consistent with and extend previous observations^{35,37,39}.



Role for H3K36 modification in DSB repair. To test the role of H3K36 modification in DSB repair, we tested the sensitivity of an *H3K36R* mutant to DSB-inducing agents. No H3K36me3 was detected in *H3K36R* cells (Fig. 4a). The *H3K36R* mutant exhibited increased sensitivity to bleomycin (Fig. 4b) compared with wild-type or control cells (*H3.1Δ H3.3Δ*) that retained an intact copy of the *H3.2* gene. *H3K36R* mutant cells were elongated after 6 h exposure to bleomycin, in contrast to wild-type cells, consistent with a checkpoint-dependent cell cycle delay resulting from failed DSB repair (Fig. 4c). Further, the *H3K36R* mutant exhibited increased IR sensitivity compared with wild-type or *H3.1Δ H3.3Δ* controls (Fig. 4d). In addition, the *H3K36R* mutation did not affect total histone H3 levels (Supplementary Fig. 8). These findings are in accordance with a role for H3K36 modification in DSB repair.

H3K36 modification and chromatin accessibility. To address how H3K36 modification might affect DSB repair, we probed chromatin accessibility. Lysine acetylation neutralizes the positive charge on histones and thus weakens interactions between histones and DNA. Thus, more open chromatin arising from lysine acetylation may facilitate resection and subsequent DSB repair by HR. Conversely, lysine methylation might compact chromatin thereby inhibiting resection and promoting NHEJ. We therefore tested the global effect of deleting *set2⁺* or *gcn5⁺* on chromatin accessibility to micrococcal nuclease (MNase) following exposure to bleomycin, as previously described³⁵. We used the percentage of DNA that has a low molecular weight DNA (< tetranucleosome, ~600 bp) as a measure of chromatin accessibility. Deleting *set2⁺* resulted in an increase in the level of low molecular weight DNA fragments, consistent with increased chromatin accessibility following DNA damage. In contrast, deleting *gcn5⁺* resulted in reduced levels of MNase fragments of 600 bp or less, consistent with reduced chromatin accessibility in response to DNA damage (Fig. 5a–c). No obvious difference in DNA accessibility was observed in wild-type, *set2Δ* or *gcn5Δ* backgrounds in the absence of DNA damage (Fig. 5d). These findings are consistent with Set2 and Gcn5 regulating DSB repair pathway choice through modulating H3K36 methylation/acetylation status and subsequently chromatin accessibility to DSB repair factors.

H3K36 modification is cell cycle regulated. In fission yeast, DSB repair pathway choice is cell cycle regulated, with NHEJ being utilized during G1, while HR is employed in S and G2 phases⁶.

Figure 4 | Histone H3K36 is required for survival following exposure to DSB-inducing agents. (a) Western blot analysis of H3K36me3 in wild-type (Wt) and *H3.2K36R H3.1ΔH3.3Δ* (*H3K36R*) cells. α-H3 is shown as a loading control. (b) 10-fold serial dilutions of wild-type (Wt), *H3ΔΔ* and *H3K36R* cells on YE6S, YE6S + 1 μg ml⁻¹ bleomycin. Plates were incubated at 32 °C for 3 days. (c) Methanol-fixed asynchronous wild-type (Wt) and *H3K36R* cells imaged following growth in the presence or absence of 5 μg ml⁻¹ bleomycin for 6 h. Bar, 10 μm. (d) IR survival curve for wild-type (Wt) and *H3K36R* cells. Data are the mean of three experiments and error bars (± s.e.) are shown.

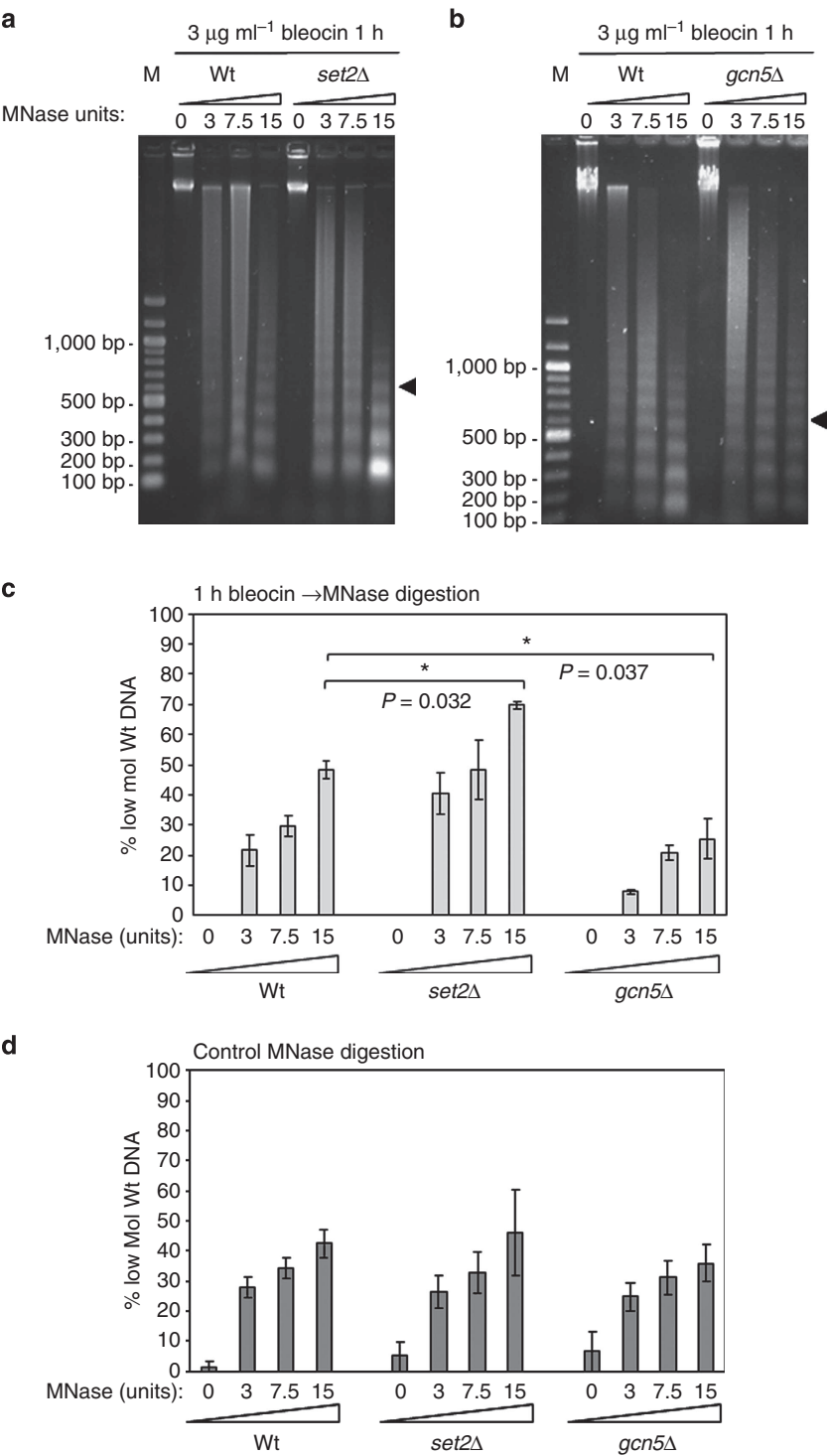


Figure 5 | Chromatin is more accessible to MNase following DNA damage in *set2* Δ cells and less accessible in *gcn5* Δ cells. (a,b) Mid-log phase cells were incubated in 3 $\mu\text{g ml}^{-1}$ bleocin for 1 h followed by MNase digestion for 10 min at the indicated concentrations. Digested chromatin DNA was resolved by gel electrophoresis and detected by ethidium bromide staining. The gels are representative of three independent repeats. (c) MNase digested chromatin DNA resolved on agarose gels were analyzed using Image J. The proportion of low molecular weight DNA (<tetranucleosome) was calculated as a percentage of the total sample. *set2* Δ cells have a significantly higher proportion of low molecular weight particles following digestion with 15U MNase ($P = 0.032$; t -test), while *gcn5* Δ cells have a significantly lower population of low molecular weight particles when compared with wild type ($P = 0.037$; t -test), indicating an increase in *set2* Δ and a decrease in *gcn5* Δ chromatin accessibility. Data are the mean of at least three independent repeats and error bars (\pm s.e.) are shown (* denotes $P < 0.05$; t -test). (d) Control MNase digestions (no bleocin treatment) were analysed as described for c. Data are the mean of at least three independent repeats and error bars (\pm s.e.) are shown. Comparison of *set2* Δ and *gcn5* Δ samples with wild-type revealed no significant change in the proportion of low molecular weight particles (P -value cutoff 0.05; t -test).

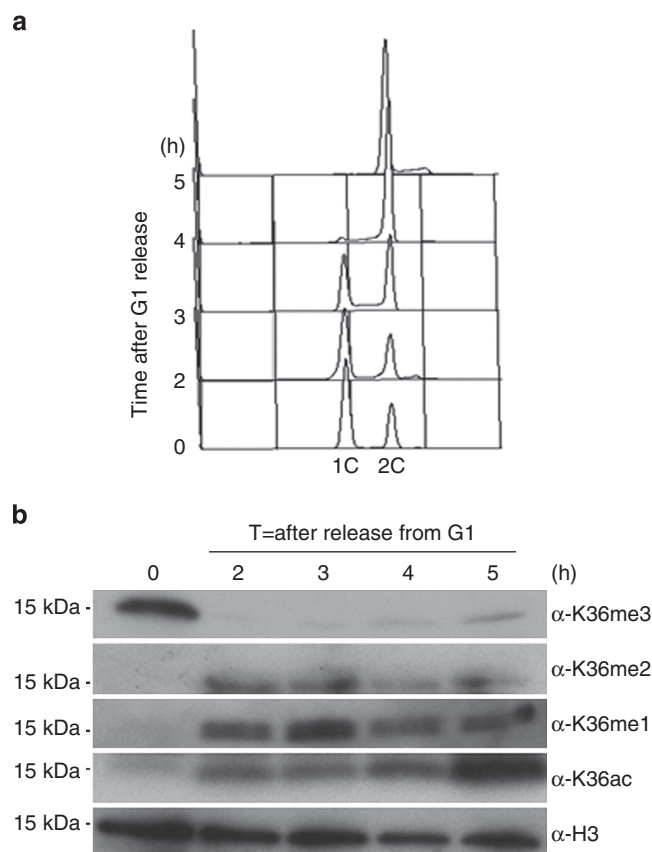


Figure 6 | H3K36 methylation and acetylation are cell cycle regulated.

(a) Flow cytometry analysis of wild-type cells following release from nitrogen starvation. The data shown were performed from at least two biological replicates. (b) Acid-extracted histones prepared from a wild-type strain were resolved on a 4–20% SDS-PAGE gel, transferred to a PVDF membrane and probed for H3K36me3, H3K36me1 and H3K36ac. α -H3 is shown as a loading control. Western blot analysis of H3K36me3, H3K36me2, H3K36me1 and H3K36ac in wild-type nuclear extract at the times shown following release from nitrogen starvation.

This prompted us to investigate whether H3K36 modification was cell cycle regulated. Following arrest in G1 by nitrogen starvation and release into the cell cycle (Fig. 6a), levels of chromatin bound H3K36 methylation and acetylation were determined by western blot. Cells with an increased 1C DNA content exhibited strikingly high H3K36me3 levels, while H3K36ac levels were low (Fig. 6a,b). Cell cycle progression resulted in a significant reduction in H3K36me3 levels after 2 h, whereas levels of H3K36me2 and H3K36me1 increased, consistent with S-phase progression (Fig. 6a). H3K36ac levels also increased with progression through S-phase, peaking at 5 h when the majority of cells were in G2 (Fig. 6b). These results indicate that modification of the H3K36 residue is cell cycle regulated. Further, the peak of methylation in a 1C population and acetylation in S/G2 is consistent with Set2-dependent H3K36 methylation being required for NHEJ, and Gcn5-dependent H3K36 acetylation being required for HR. The protein levels of Set2-myc and Gcn5-myc are constant during the cell cycle (Supplementary Fig. 9).

Discussion

Our findings support an H3K36 modification-mediated switch in coordinating DSB repair pathway choice in fission yeast. We define roles for Set2-dependent H3K36 methylation in reducing

chromatin accessibility, reducing DSB resection and promoting NHEJ through Ku recruitment. In contrast, Gcn5-dependent H3K36 acetylation increases chromatin accessibility, increases DSB resection and promotes HR. Accordingly, loss of Set2 results in increased Gcn5-dependent H3K36Ac, open chromatin, increased resection and increased HR, while loss of Gcn5 results in increased Set2-dependent H3K36me, closed chromatin, reduced resection and increased NHEJ. The role for H3K36 modification in coordinating DSB repair was further confirmed by the observation that H3K36R mutation was sensitive to bleomycin and IR. Moreover, we found H3K36 modification to be cell cycle regulated with chromatin-bound H3K36me3 peaking in G1 where NHEJ occurs while H3K36 acetylation peaked in S/G2 phase when HR predominates. Together these findings support an H3K36 chromatin switch in coordinating DSB repair pathway choice in fission yeast.

How might a switch in chromatin states dictated by H3K36 coordinate DSB repair pathway choice? Here we consider two non-exclusive models suggested by these and other findings. In the first ‘recruitment’ model, Set2-dependent H3K36 methylation is required to recruit the Ku70-Ku80 heterodimer to the break-site thereby promoting NHEJ. In contrast, Gcn5-dependent H3K36 acetylation may be refractory to Ku recruitment and could instead function to recruit HR factors. In this respect, Set2 may promote Ku recruitment through potential readers of the H3K36me mark. However, we found that neither Ctr6, the Rpd3 homologue, nor Alp13, a subunit of the Ctr6 HDAC complex II, exhibited defects in NHEJ. Instead, *alp13 Δ* and the temperature-sensitive *ctr6-1* allele were acutely sensitive to bleomycin^{31,32}, and the *set2 Δ alp13 Δ* double mutant exhibited increased sensitivity, thus indicating a distinct function for the HDAC complex II in the DSB response. Other currently unknown H3K36me readers may promote Ku recruitment. Alternatively, H3K36me may recruit Ku indirectly through other chromatin factors. In this respect, components of the RSC chromatin remodelling complex physically interact with Ku80, and RSC has previously been shown to be required for loading of Ku onto breaks^{40,41}. However, it is possible that Ku, which has a strong affinity for duplex DNA ends *in vitro*⁴², binds DNA ends independently of chromatin or associated factors *in vivo*.

In a second ‘chromatin accessibility’ model, the distinct H3K36 chromatin states control end resection at a break-site via chromatin accessibility. Here, Set2-dependent H3K36me is proposed to promote closed chromatin, protecting ends from resection, thereby facilitating Ku recruitment or retention, and NHEJ. In contrast, Gcn5-dependent H3K36Ac is proposed to promote open acetylated chromatin and/or increased histone exchange, thus facilitating resection, reducing Ku binding or recruitment, and thus increasing HR. Consistent with this model, Set2 has been shown to suppress histone H3 and H4 acetylation by preventing histone exchange during transcription in *S. cerevisiae*. Increased histone exchange in the absence of Set2 facilitates histone acetylation thereby leading to increased cryptic transcripts^{43,44}. In the context of DSB repair, increased histone exchange may facilitate transient nucleosome removal or the dynamic incorporation of histone variants thereby facilitating resection at DSBs. Indeed, a recent study using budding yeast characterizing the impact of chromatin on *in vitro* resection found that efficient resection by Sgs1-Dna2 required nucleosome-free regions adjacent to the DSB, while resection by Exo1 was completely blocked by nucleosomes. Moreover, incorporation of the histone variant H2A.Z was found to enhance resection⁴⁵. Thus, Set2 may promote NHEJ through reducing chromatin accessibility to the resection machinery. The increased levels of Gcn5-dependent H3K36ac and damage-induced nucleosome mobility in a *set2 Δ* background, together with increased ssDNA

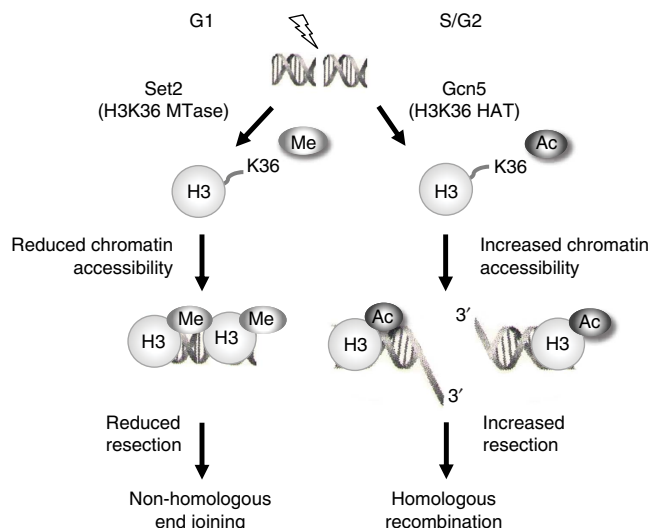


Figure 7 | An H3K36 chromatin switch regulates DSB repair pathway choice in fission yeast. In G1 high levels of Set2-dependent H3K36me (indicated) reduces nucleosome accessibility to repair factors, resulting in reduced resection and increased NHEJ repair of DSBs. In S/G2 high levels of Gcn5-dependent H3K36Ac (indicated) increases nucleosome accessibility to repair factors, resulting in increased resection and increased HR repair of DSBs. See text for details.

formation following IR leading to increased HR compared with wild-type, are consistent with such a model (Fig. 7).

Our findings support an early role for Gcn5-dependent H3K36Ac in facilitating HR. Loss of Gcn5 alone exhibited a modest sensitivity to DNA damaging agents; moreover, both Rad11 and Rad51 foci formation were delayed rather than abrogated in the absence of Gcn5. However, Gcn5 was found to play a critical role in the DNA damage response in conjunction with other HATs, including Hat1, NuA3 and NuA4, which have been previously associated with the DNA damage response and DSB repair^{35,39,46}. Recently, recruitment of chromatin remodelling enzymes to a DSB was found to be dependent on the early steps of HR, while inhibited by NHEJ in budding yeast⁴⁷. We speculate that Gcn5 may function early in HR in conjunction with other HATs to promote recruitment of ATP-dependent remodelers, repair factors and/or to increase DNA accessibility, thus promoting resection and HR.

Importantly, H3K36 methylation is associated with DSB repair in other organisms. Indeed, roles for Set2-dependent H3K36 methylation in transcription-coupled DNA damage checkpoint activation in *S. cerevisiae* are reported in an accompanying manuscript⁴⁸. Moreover, a H3K36 modification switch may help coordinate DSB repair pathway choice in humans. H3K36 dimethylation was reported to be increased at DSBs and to enhance NHEJ through recruiting NBS1 and Ku70 repair factors in a METNASE-dependent manner¹⁷. In contrast, a role for SETD2-dependent H3K36 trimethylation in facilitating HR in actively transcribed regions has recently been described^{49,50}. Here, SETD2-dependent H3K36 trimethylation promotes HR through constitutive recruitment of Lens Epithelial Growth Factor p75 (LEDGF) to chromatin. In response to DNA damage, LEDGF recruits C-terminal binding protein interacting protein (CtIP), which promotes resection, thereby facilitating HR repair¹⁸. However, while LEDGF is present in higher eukaryotes, it is not evolutionarily conserved in budding or fission yeasts. Interestingly, Set1-dependent H3K4 methylation at DSBs also promotes NHEJ through Ku recruitment in budding yeast⁵¹.

Thus, histone methylation plays an important role in facilitating NHEJ. How these methylation events are coordinated, and their functional antagonism through demethylation and acetylation is of considerable interest.

The cell cycle regulation of H3K36 modification is surprising given the wide range of functions associated with H3K36 methylation. However, this finding is consistent with observations recently reported in human cells⁵² and indicates that H3K36 cell cycle modification is evolutionarily conserved. How H3K36 modification is coordinated through the cell cycle and the functional implications for such regulation are currently unknown. The interplay between H3K36 acetylation and methylation has previously been proposed to regulate gene expression¹⁹. Here we show that this H3K36 chromatin switch helps to control DSB repair pathway choice in fission yeast. This chromatin switch, in concert with the complex networks that control DSB repair, ensures that the fidelity of the genome is maintained, preventing deleterious chromosomal rearrangements as a consequence of misuse of repair mechanisms.

Methods

Yeast strains, media and genetic methods. The strains used in this study are listed in Supplementary Tables 1 and 2. Standard media and growth conditions were used throughout this work⁵³. Cultures were grown in rich media (YE5S) or minimal media (EMM) at 32 °C with shaking, unless otherwise stated.

Site-specific DSB assay. Cells were grown exponentially in liquid culture for 48 h in the absence of thiamine (-T) to derepress HO endonuclease expression from the REP81X-HO plasmid. The percentage of colonies undergoing NHEJ/SCC (arg⁺ Hyg^R ade⁺ his⁺), gene conversion (arg⁺ Hyg^S ade⁺ his⁺), minichromosome loss (arg⁻ Hyg^S ade⁻ his⁻) or LOH (arg⁺ Hyg^S ade⁻ his⁻) was calculated (see also Supplementary Fig. 1). To determine levels of break-induced minichromosome loss, background minichromosome loss at 48 h in blank vector assays was subtracted from break-induced minichromosome loss at 48 h in cells transformed with pREP81X-HO. More than 1,000 colonies were scored for each time point, and each experiment was performed three times using three independently derived strains for all mutants tested.

Fluorescent microscopy. Asynchronous cultures were treated with +/– 5 µg ml⁻¹ bleomycin (1 h 26 °C), before being fixed in methanol. Samples were rehydrated and stained with 4',6-diamidino-2-phenylindole (DAPI) before examination using Zeiss Axioplan 2ie microscope, Hamamatsu Orca ER camera and micromanager software. For visualization of Rad11-GFP and Rad51-CFP foci, cells were irradiated with 50 Gy IR using a ¹³⁷Cs source with a dose rate of 2.8 Gy per minute, before being fixed and visualized as above.

Serial dilution assay. A dilution series for the indicated mutants was spotted onto YE6S plates and YE6S with the indicated concentration of MMS, bleomycin or bleocin. Plates were incubated at 32 °C for 2–3 days before analysis.

Ionizing radiation survival curve. Logarithmically growing cells were irradiated by using a ⁶⁰Co source at a dose rate of 31 Gy min⁻¹. Irradiated and unirradiated cells were plated on YE6S and incubated at 32 °C for 4 days before colonies were counted.

Survival analysis. Exponential cultures were obtained in liquid YE6S medium inoculated with a single colony picked from a freshly streaked (YE6S) stock plate and grown overnight at 32 °C with vigorous shaking. Cells were counted microscopically and only cultures with between 2 × 10⁷ and 4 × 10⁷ cells ml⁻¹ were used. Cells were resuspended in YE6S at a density of 2 × 10⁷ cells ml⁻¹, and serial dilutions were made and ~200 cells were plated on YE6S plates with the indicated dose of bleocin as well as an untreated control. Plates were incubated for 3 days at 32 °C and then scored.

Quantitative chromatin immunoprecipitation (qChIP). Chromatin immunoprecipitation (ChIP) was performed as previously described⁵⁴. In brief, cells were grown at 32 °C in Edinburgh Minimal Medium (EMM) supplemented with 0.25 mg/ml uracil, to induce *Purg1*. One hundred millilitres of cells at O.D.₅₉₅ = 0.4 were fixed in 1% formaldehyde (Sigma F8755-25ML) for 20 min at 24 °C with shaking. The reaction was quenched by adding 125 mM glycine for 5 min. Cells were lysed using a bead beater (Biospec Products), and cell lysates were sonicated in a Bioruptor (Diagenode) (15 min, 30 s On and 30 s Off at 'High' (200 W) position). For all ChIPs, 30 µl Protein G Dynabeads (Life Technologies) were used

along with 3.5 μ l ActiveMotif anti-H3K36me3 antibody (cat# 61101) or 1.5 μ l anti-myc 9B11 (Cell Signaling), as appropriate. ChIPs were analysed by real-time PCR using Lightcycler 480 SYBR Green (Roche) with primers specific to the indicated regions. All ChIP enrichments were calculated as % DNA immunoprecipitated at the locus of interest (relative to the corresponding input samples) and normalized to % DNA immunoprecipitated at the *act1* or *fbp1* locus. Data averaged over at least two biological replicates are shown. Error bars represent s.d. values from at least two biological replicates. The primers used for qPCR analysis are listed in Supplementary Table 3.

Micrococcal nuclease digestion of chromatin. One-hundred milliliters of cells were grown to mid-log phase in YE5S at 30 °C, treated with 3 μ g ml⁻¹ bleocin for 1 h, crosslinked with a final concentration of 1% formaldehyde (Sigma F8775) for 20 min at 30 °C and quenched by the addition of glycine to 125 mM. Cells were washed with CES buffer (50 mM citric acid/50 mM Na₂HPO₄ (pH 5.6), 40 mM EDTA (pH 8.0), 1.2 M sorbitol, 10 mM β -mercaptoethanol) and resuspended in 500 μ l CES buffer with 0.5 mg Zymolyase-100T. Cells were spheroplasted by gentle shaking at 30 °C for up to 45 min, washed with ice cold 1.2 M sorbitol and resuspended in 800 μ l NP-S buffer (1.2 M sorbitol, 10 mM CaCl₂, 100 mM NaCl, 1 mM EDTA (pH 8.0), 14 mM β -mercaptoethanol, 50 mM Tris-HCl (pH 8.0), 0.075% NP-40, 5 mM spermidine, 0.1 mM PMSF, 1% Sigma protease inhibitor cocktail (Sigma P8215)). Spheroplasts were divided into four 200 μ l aliquots, each mixed with 300 μ l of NP-S buffer. MNase was added at the indicated concentrations, and samples were digested for 10 min at 37 °C. MNase activity was terminated by the addition of EDTA (pH 8.0) and SDS to the final concentrations of 50 mM and 0.2%, respectively. Samples were incubated at 65 °C overnight with 0.2 mg ml⁻¹ proteinase K and 10 μ g RNase A. DNA was subsequently purified by phenol:chloroform extraction followed by ethanol precipitation.

Plasmid rejoining assay. The plasmid rejoining assay was performed as previously described⁵⁵. In brief, the cohesive-ended substrates for the NHEJ assay were prepared by excision of a ~500 bp *Pst*I fragment or ~700 bp *Pvu*II fragment from PS (p100) or a ~540 bp *Eco*RI fragment from PI (p101) followed by gel purification of the remaining linear vector. Logarithmically growing cells (20 ml of OD₅₉₅ 0.5) were transformed with 1 μ g of undigested control plasmid pAL19 or linear DNA using the lithium acetate method. As the plasmids contain a *LEU2* marker, NHEJ frequency was calculated as the percentage of *leu*⁺ colonies arising from cells transformed with linear plasmid over those transformed with undigested DNA. At least three experiments were performed for each strain, and the average percentage rejoining calculated.

Microarray analysis. Microarray analysis was performed as previously described⁵⁶. In brief, Alexa 555- or 647-labelled cDNA was produced from the RNA, using a Superscript direct cDNA labelling system (Invitrogen) and Alexa 555 and 647 dUTP label mix. The cDNA was then purified using an Invitrogen PureLink PCR Purification system. The cDNA was hybridized to the array using a Gene Expression Hybridization kit (Agilent). The array was an Agilent custom-designed array containing 60-mer oligonucleotides synthesized *in situ* on the array and contained 4 × 44,000 probes. Following hybridization for at least 17 h, the array was washed using a Gene Expression Wash Buffer kit (Agilent) and scanned in an Agilent Array Scanner. The microarray signal was extracted using GenePix.

Analysis of cell cycle-regulated histone modifications. The wild-type yeast strain was arrested in G1 using nitrogen starvation⁵⁷ and released from the block. Samples were taken over a 5-h time course. The samples then underwent the histone acid-extraction method to purify histones for analysis by western blotting as previously described⁵⁸. In brief, one litre of cells were collected by centrifugation. The cell pellet was resuspended in spheroplasting buffer (1.2 M Sorbitol, 20 mM Hepes pH 7.4, 1 mM PMSF, 0.5 μ g ml⁻¹ Leupeptin, 0.7 μ g ml⁻¹ Pepstatin) containing 10 mM dithiothreitol (DTT) and 2 mg ml⁻¹ Zymolyase 20-T (MP Biomedicals) and then incubated in a 32 °C water bath until 90% of cells had lost their cell walls. Cells were centrifuged and resuspended in Nuclei Isolation Buffer (0.25 M Sucrose, 60 mM KCl, 14 mM NaCl, 5 mM MgCl₂, 1 mM CaCl₂, 15 mM MES, pH 6.6, 0.8% Triton X-100, 0.7 μ g ml⁻¹ Pepstatin, 1 mM PMSF, 0.5 μ g ml⁻¹ Leupeptin) on ice water for 20 min. After spinning and washing, most of the chromatin was in the pellet. Histones were extracted by resuspending the pellet in 10 ml of cold 0.4 N H₂SO₄. Protein extracts were made by TCA extraction and analysed by western blotting as previous described⁵⁸. H3 tri-methyl lysine 36 (α H3K36me3) (Abcam 9050), H3 di-methyl lysine 36 (α H3K36me2) (Abcam 9049), H3 mono-methyl lysine 36 (α H3K36me1) (Abcam 9048) and H3 lysine 36 acetylation (Active Motif 39379) were used at a dilution of 1:1,000. An antibody directed against H3 (Abcam1791) was used as a loading control. Anti-rabbit horseradish peroxidase-conjugated secondary antibodies (Amersham Bioscience) were used at a dilution of 1:10,000. For clarity, western blots were cropped to show the band of interest in the main figures. However, corresponding uncropped scans can be found in Supplementary Fig. 10 and Supplementary Fig. 11.

References

- Symington, L. S. & Gautier, J. Double-strand break end resection and repair pathway choice. *Annu. Rev. Genet.* **45**, 247–271 (2011).
- Lieber, M. R. The mechanism of double-strand DNA break repair by the nonhomologous DNA end-joining pathway. *Annu. Rev. Biochem.* **79**, 181–211 (2010).
- Heyer, W. D., Ehmsen, K. T. & Liu, J. Regulation of homologous recombination in eukaryotes. *Annu. Rev. Genet.* **44**, 113–139 (2010).
- Aylon, Y., Liefshitz, B. & Kupiec, M. The CDK regulates repair of double-strand breaks by homologous recombination during the cell cycle. *EMBO J.* **23**, 4868–4875 (2004).
- Ira, G. *et al.* DNA end resection, homologous recombination and DNA damage checkpoint activation require CDK1. *Nature* **431**, 1011–1017 (2004).
- Ferreira, M. G. & Cooper, J. P. Two modes of DNA double-strand break repair are reciprocally regulated through the fission yeast cell cycle. *Genes Dev.* **18**, 2249–2254 (2004).
- Wagner, E. J. & Carpenter, P. B. Understanding the language of Lys36 methylation at histone H3. *Nat. Rev. Mol. Cell Biol.* **13**, 115–126 (2012).
- Strahl, B. D. *et al.* Set2 is a nucleosomal histone H3-selective methyltransferase that mediates transcriptional repression. *Mol. Cell Biol.* **22**, 1298–1306 (2002).
- Edmunds, J. W., Mahadevan, L. C. & Clayton, A. L. Dynamic histone H3 methylation during gene induction: HYPB/Set2 mediates all H3K36 trimethylation. *EMBO J.* **27**, 406–420 (2008).
- Al Sarakbi, W. *et al.* The mRNA expression of SETD2 in human breast cancer: correlation with clinico-pathological parameters. *BMC Cancer* **9**, 290 (2009).
- Dalgliesh, G. L. *et al.* Systematic sequencing of renal carcinoma reveals inactivation of histone modifying genes. *Nature* **463**, 360–363 (2010).
- Newbold, R. F. & Mokbel, K. Evidence for a tumour suppressor function of SETD2 in human breast cancer: a new hypothesis. *Anticancer Res.* **30**, 3309–3311 (2010).
- Zhang, J. *et al.* The genetic basis of early T-cell precursor acute lymphoblastic leukaemia. *Nature* **481**, 157–163 (2012).
- Fontebasso, A. M. *et al.* Mutations in SETD2 and genes affecting histone H3K36 methylation target hemispheric high-grade gliomas. *Acta Neuropathol.* **125**, 659–669 (2013).
- Jazayeri, A., McAnish, A. D. & Jackson, S. P. *Saccharomyces cerevisiae* Sin3p facilitates DNA double-strand break repair. *Proc. Natl Acad. Sci. USA* **101**, 1644–1649 (2004).
- Merkler, J. D. *et al.* The histone methylase Set2p and the histone deacetylase Rpd3p repress meiotic recombination at the HIS4 meiotic recombination hotspot in *Saccharomyces cerevisiae*. *DNA Repair* **7**, 1298–1308 (2008).
- Fnu, S. *et al.* Methylation of histone H3 lysine 36 enhances DNA repair by nonhomologous end-joining. *Proc. Natl Acad. Sci. USA* **108**, 540–545 (2011).
- Daugaard, M. *et al.* LEDGF (p75) promotes DNA-end resection and homologous recombination. *Nat. Struct. Mol. Biol.* **19**, 803–810 (2012).
- Morris, S. A. *et al.* Identification of histone H3 lysine 36 acetylation as a highly conserved histone modification. *J. Biol. Chem.* **282**, 7632–7640 (2007).
- Daniel, J. A. & Grant, P. A. Multi-tasking on chromatin with the SAGA coactivator complexes. *Mutat. Res.* **618**, 135–148 (2007).
- Barlev, N. A. *et al.* Repression of GCN5 histone acetyltransferase activity via bromodomain-mediated binding and phosphorylation by the Ku-DNA-dependent protein kinase complex. *Mol. Cell Biol.* **18**, 1349–1358 (1998).
- Tamburini, B. A. & Tyler, J. K. Localized histone acetylation and deacetylation triggered by the homologous recombination pathway of double-strand DNA repair. *Mol. Cell Biol.* **25**, 4903–4913 (2005).
- Oishi, H. *et al.* An hGCN5/TRRAP histone acetyltransferase complex co-activates BRCA1 transactivation function through histone modification. *J. Biol. Chem.* **281**, 20–26 (2006).
- Lee, H. S., Park, J. H., Kim, S. J., Kwon, S. J. & Kwon, J. A cooperative activation loop among SWI/SNF, gamma-H2AX and H3 acetylation for DNA double-strand break repair. *EMBO J.* **29**, 1434–1445 (2010).
- Lee, S. E. *et al.* *Saccharomyces* Mre11/rad50 and RPA proteins regulate adaptation to G2/M arrest after DNA damage. *Cell* **94**, 399–409 (1998).
- Pierce, A. J., Hu, P., Han, M., Ellis, N. & Jasin, M. Ku DNA end-binding protein modulates homologous repair of double-strand breaks in mammalian cells. *Genes Dev.* **15**, 3237–3242 (2001).
- Rea, S. *et al.* Regulation of chromatin structure by site-specific histone H3 methyltransferases. *Nature* **406**, 593–599 (2000).
- Morris, S. A. *et al.* Histone H3 K36 methylation is associated with transcription elongation in *Schizosaccharomyces pombe*. *Eukaryot. Cell* **4**, 1446–1454 (2005).
- Tinlin-Purvis, H. *et al.* Failed gene conversion leads to extensive end processing and chromosomal rearrangements in fission yeast. *EMBO J.* **28**, 3400–3412 (2009).
- Keogh, M. C. *et al.* Cotranscriptional set2 methylation of histone H3 lysine 36 recruits a repressive Rpd3 complex. *Cell* **123**, 593–605 (2005).
- Nakayama, J. *et al.* Alp13, an MRG family protein, is a component of fission yeast Clr6 histone deacetylase required for genomic integrity. *EMBO J.* **22**, 2776–2787 (2003).

32. Nicolas, E. *et al.* Distinct roles of HDAC complexes in promoter silencing, antisense suppression and DNA damage protection. *Nat. Struct. Mol. Biol.* **14**, 372–380 (2007).
33. Carneiro, T. *et al.* Telomeres avoid end detection by severing the checkpoint signal transduction pathway. *Nature* **467**, 228–232 (2010).
34. Barlow, J. H., Lisby, M. & Rothstein, R. Differential regulation of the cellular response to DNA double-strand breaks in G1. *Mol. Cell* **30**, 73–85 (2008).
35. Wang, Y. *et al.* Histone H3 lysine 14 acetylation is required for activation of a DNA damage checkpoint in fission yeast. *J. Biol. Chem.* **287**, 4386–4393 (2012).
36. Johnsson, A., Xue-Franzen, Y., Lundin, M. & Wright, A. P. Stress-specific role of fission yeast Gcn5 histone acetyltransferase in programming a subset of stress response genes. *Eukaryot. Cell* **5**, 1337–1346 (2006).
37. Benson, L. J. *et al.* Properties of the type B histone acetyltransferase Hat1: H4 tail interaction, site preference, and involvement in DNA repair. *J. Biol. Chem.* **282**, 836–842 (2007).
38. Mitchell, L. *et al.* Functional dissection of the NuA4 histone acetyltransferase reveals its role as a genetic hub and that Eaf1 is essential for complex integrity. *Mol. Cell Biol.* **28**, 2244–2256 (2008).
39. Qin, S. & Parthun, M. R. Histone H3 and the histone acetyltransferase Hat1p contribute to DNA double-strand break repair. *Mol. Cell Biol.* **22**, 8353–8365 (2002).
40. Shim, E. Y., Ma, J. L., Oum, J. H., Yanez, Y. & Lee, S. E. The yeast chromatin remodeler RSC complex facilitates end joining repair of DNA double-strand breaks. *Mol. Cell Biol.* **25**, 3934–3944 (2005).
41. Shim, E. Y. *et al.* RSC mobilizes nucleosomes to improve accessibility of repair machinery to the damaged chromatin. *Mol. Cell Biol.* **27**, 1602–1613 (2007).
42. Blier, P. R., Griffith, A. J., Craft, J. & Hardin, J. A. Binding of Ku protein to DNA. Measurement of affinity for ends and demonstration of binding to nicks. *J. Biol. Chem.* **268**, 7594–7601 (1993).
43. Venkatesh, S. *et al.* Set2 methylation of histone H3 lysine 36 suppresses histone exchange on transcribed genes. *Nature* **489**, 452–455 (2012).
44. Smolle, M. *et al.* Chromatin remodelers Isw1 and Chd1 maintain chromatin structure during transcription by preventing histone exchange. *Nat. Struct. Mol. Biol.* **19**, 884–892 (2012).
45. Adkins, N. L., Niu, H., Sung, P. & Peterson, C. L. Nucleosome dynamics regulates DNA processing. *Nat. Struct. Mol. Biol.* **20**, 836–842 (2013).
46. Bird, A. W. *et al.* Acetylation of histone H4 by Esa1 is required for DNA double-strand break repair. *Nature* **419**, 411–415 (2002).
47. Bennett, G., Papamichos-Chronakis, M. & Peterson, C. L. DNA repair choice defines a common pathway for recruitment of chromatin regulators. *Nat. Commun.* **4**, 2084 (2013).
48. Jha, D. K. & Strahl, B. D. An RNA polymerase II-coupled function for histone H3K36 methylation in checkpoint activation and DSB repair. *Nat. Commun.* **5**, 3965 doi:10.1038/ncomms4965 (2014).
49. Aymard, F. *et al.* Transcriptionally active chromatin recruits homologous recombination at DNA double-strand breaks. *Nat. Struct. Mol. Biol.* **21**, 366–374 (2014).
50. Pfister, S. X. *et al.* ETD2-dependent histone H3K36 trimethylation is required for homologous recombination repair and genome stability. *Cell Reports* (in press, 2014).
51. Faucher, D. & Wellinger, R. J. Methylated H3K4, a transcription-associated histone modification, is involved in the DNA damage response pathway. *PLoS Genet.* **6** pii e1001082 (2010).
52. Li, F. *et al.* The Histone Mark H3K36me3 Regulates Human DNA Mismatch Repair through Its Interaction with MutSalpha. *Cell* **153**, 590–600 (2013).
53. Moreno, S., Klar, A. & Nurse, P. Molecular genetic analysis of fission yeast *Schizosaccharomyces pombe*. *Methods Enzymol.* **194**, 795–823 (1991).
54. Subramanian, L. & Nakamura, T. M. A kinase-independent role for the Rad3(ATR)-Rad26(ATRIP) complex in recruitment of Tel1(ATM) to telomeres in fission yeast. *PLoS Genet.* **6**, e1000839 (2010).
55. Manolis, K. G. *et al.* Novel functional requirements for non-homologous DNA end joining in *Schizosaccharomyces pombe*. *EMBO J.* **20**, 210–221 (2001).
56. Rallis, C., Codlin, S. & Bahler, J. TORC1 signaling inhibition by rapamycin and caffeine affect lifespan, global gene expression, and cell proliferation of fission yeast. *Aging Cell* **12**, 563–573 (2013).
57. Nurse, P. & Bissett, Y. Gene required in G1 for commitment to cell cycle and in G2 for control of mitosis in fission yeast. *Nature* **292**, 558–560 (1981).
58. Shechter, D., Dormann, H. L., Allis, C. D. & Hake, S. B. Extraction, purification and analysis of histones. *Nat. Protoc.* **2**, 1445–1457 (2007).
59. Watson, A. T., Werler, P. & Carr, A. M. Regulation of gene expression at the fission yeast *Schizosaccharomyces pombe* *urg1* locus. *Gene* **484**, 75–85 (2011).

Acknowledgements

We thank the Kearsley lab for the use of their fluorescence microscope and the Carr lab for strains and reagents. We thank Brian Strahl (UNC-Chapel Hill) for communicating results before publication. C.C.P., R.S.D., S.S., E.J.B., C.W., L.H., E.B. and T.C.H. were supported by the Medical Research Council (R06538; R19583); L.S. was supported by an EC FP7 Marie Curie International Incoming Fellowship (PIIF-GA-2010-275280) and an EMBO Long Term Fellowship (ALTF 1491-2010). The Wellcome Trust supported the work of RCA (095021 and 065061) and the Wellcome Trust Centre for Cell Biology (092076); S.C. and J.B. were supported by a Wellcome Trust Senior Investigator Award (095598/Z/11/Z). C.S. and S.W. were supported by the Medical Research Council and the National Institute for Health Research (NIHR) Newcastle Biomedical Research Centre based at Newcastle upon Tyne Hospitals NHS Foundation Trust and Newcastle University. The views expressed are those of the authors and not necessarily those of the NHS, NIHR or the Department of Health.

Author contributions

C.C.P., R.S.D., L.S., S.S., E.J.B., C.W. and L.H. designed and performed experiments with input from T.C.H. in strain engineering. T.C.H. supervised the work and wrote the manuscript with input from all authors. Experiments in Fig. 1 were performed by C.C.P., R.S.D. and C.W.; in Fig. 2 were performed by C.C.P., S.S., R.S.D. and L.S.; in Fig. 3 by C.C.P., R.S.D. and E.J.B.; in Fig. 4 by C.C.P., R.S.D. and C.W. with strain engineering from R.A.; in Fig. 5 were designed by S.W. and performed by C.G.; in Fig. 6 were performed by C.C.P. S.C. and J.B. performed experiments presented in Supplementary Fig. 3.

Additional information

Accession codes: The microarray data have been deposited with ArrayExpress (<https://www.ebi.ac.uk/arrayexpress/>) under accession code E-MTAB-2549.

Supplementary Information accompanies this paper at <http://www.nature.com/naturecommunications>

Competing financial interests: The authors declare no competing financial interests.

Reprints and permission information is available online at <http://npng.nature.com/reprintsandpermissions/>

How to cite this article: Pai, C.-C. *et al.* A histone H3K36 chromatin switch coordinates DNA double-strand break repair pathway choice. *Nat. Commun.* **5**:4091 doi: 10.1038/ncomms5091 (2014).